VOLUME 110 (4) — APRIL 2001

Cwk - HO 3741-54-PO24739

VOL-110
NO. 4-6
2001

ANNALS
OF OTOLOGY, RHINOLOGY & LARYNGOLOGY

Official Organ of
AMERICAN LARYNGOLOGICAL ASSOCIATION
AMERICAN BRONCHO-ESOPHAGOLOGICAL ASSOCIATION

SER CORDOTOMY VERSUS RADIOTHERAPY:
AN OBJECTIVE COST ANALYSIS

ROBOSCOPIC ASSESSMENT OF VOCAL FOLD
KERATOSIS AND GLOTTIC CANCER

SMENT OF VESTIBULAR SCHWANNOMA GROWTH:
ATION OF A NEW MEASURING PROTOCOL TO THE
RESULTS OF A LONGITUDINAL STUDY

54

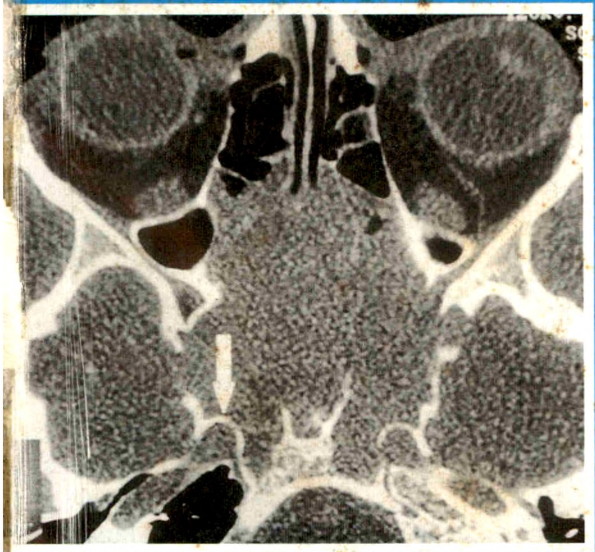

MAKE YOUR DIAGNOSIS. SEE PAGE 332.

ANNALS
PUBLISHING CO.

WEB SITE—http://www.Annals.com

P24739

STROBOCAM

The Alternative to Costly Computer Based Systems*

A video camera/l
source system that
only provides unive
uses in your prac
but will pay for it
through patien
convenience ar
retained fe

SIMPLE AND AFFORDABLE*

As the name implies, revolutionary new technology sets this system apart from all others.

It performs strobovideolaryngoscopy at the touch of a button.

Because StroboCAM does not require an expensive flashing light, its cost and simplicity fit into any practice that encounters laryngeal dysfunction.

*One-third the cost of computer based systems

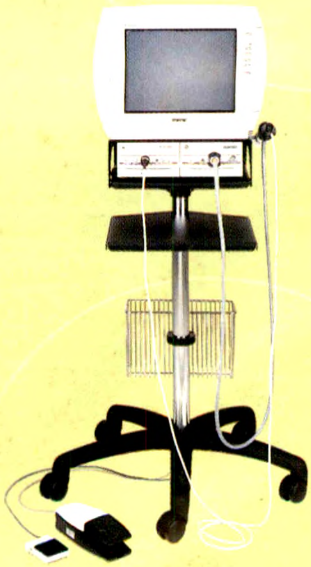

JEDMED
An Employee-Owned Company

Come visit us during the COSM Meeting in booth 401!

5416 JEDMED Ct. | St. Louis, MO 63129 | (314) 845-3770 | Fax: (314) 845-3771
www.jedmed.com | jedmed@worldnet.att.net

ANNALS OF OTOLOGY, RHINOLOGY & LARYNGOLOGY

VOLUME 110 APRIL 2001 NUMBER 4

CONTENTS

54

FROM THE AMERICAN BRONCHO-ESOPHAGOLOGICAL ASSOCIATION

Stroboscopic Assessment of Vocal Fold Keratosis and Glottic Cancer
Darryl Colden, MD; Steven M. Zeitels, MD; Robert E. Hillman, PhD;
John Jarboe, MD; Glenn Bunting, MA; Konstantina Spanou, MD 293

Role of Laryngoscopy, Dual pH Probe Monitoring, and Laryngeal Mucosal Biopsy in the Diagnosis of Pharyngoesophageal Reflux
J. Scott McMurray, MD; Mark Gerber, MD; Yoram Stern, MD; David Walner, MD;
Colin Rudolph, MD; J. Paul Willging, MD; Robin T. Cotton, MD 299

FROM THE AMERICAN LARYNGOLOGICAL ASSOCIATION

Idiopathic Progressive Subglottic Stenosis: Findings and Treatment in 52 Patients
Herbert H. Dedo, MD; Michael D. Catten, MD 305

Laser Cordotomy Versus Radiotherapy: An Objective Cost Analysis
James H. Brandenburg, MD 312

Stellate Cells in the Human Vocal Fold
Kiminori Sato, MD, PhD; Minoru Hirano, MD; Tadashi Nakashima, MD 319

INDEPENDENT CONTRIBUTIONS

Assessment of Vestibular Schwannoma Growth: Application of a New Measuring Protocol to the Results of a Longitudinal Study
Ernestine M. Stipkovits, MD; Kees Graamans, MD, PhD; G. Boudewijn C. Vasbinder, MD;
Johannes E. Van Dijk, MSc, PhD; Frederik J. A. Beek, MD, PhD 326

Aneurysmal Bone Cyst in the Sphenoid Bone: Treatment With Minimally Invasive Surgery
Carlos de Minteguiaga, MD; Frédéric Portier, MD; Jean Pierre Guichard, MD;
Emmanuel Racy, MD; Patrick Heitzmann, MD; Patrice Tran Ba Huy, MD;
Philippe Herman, MD, PhD 331

Transnasal Treatment of Congenital Choanal Atresia With the KTP Laser
Claus Pototschnig, MD; Claudia Völklein, MD; Elisabeth Appenroth, MD;
Walter F. Thumfart, MD 335

Epidermal Inclusion Cyst Versus Thyroglossal Duct Cyst: Sistrunk or Not?
Daniel P. Sullivan, MD; Lisa A. Liberatore, MD; Max M. April, MD;
Jodi Sassoon, MD; Robert F. Ward, MD 340

Pediatric Tracheotomy: Is Postoperative Chest X-ray Necessary?
Daryle Darden, MD; Richard Towbin, MD; Joseph E. Dohar, MD 345

Concurrent Glottic and Tracheal Stenoses: Restoration of Airway Continuity in End-stage Malignant Disease
Klaus Wassermann, MD; Frank Mathen, MD; Hans Edmund Eckel, MD 349

Epidemiological Studies on Hearing Impairment With Reference to Genetic Factors in Sichuan, China
Xue Zhong Liu, MD, PhD; Li Rong Xu, MD; Ying Hu, PhD; Walter E. Nance, MD, PhD; Aristides Sismanis, MD; Si Ling Zhang, MD; Ying Xu, MD 356

Incidence of Pharyngeal Hypophysis in Neonates. A Histologic Study
Bosco E. Noronha, MS, DipNBE; Naresh K. Panda, MS, DipNBE, FRCS(Ed); S. B. S. Mann, MS, FAMS; Y. N. Mehra, FRCSC, DABO; C. K. Banerjee, MD 364

Malignant Melanoma Arising Within a Burn Scar. Case Report and Review of the Literature
Paul M. Spring, MD, MS; Jeffrey N. Myers, MD, PhD; Adel K. El-Naggar, MD, PhD; Howard N. Langstein, MD 369

Fungal Malignant Otitis Externa Due to *Scedosporium apiospermum*
Mike Yao, MD; Anna H. Messner, MD 377

Bilateral Chylothorax Following Neck Dissection: A New Method of Treatment
Khalid Al-Sebeih, MD, FRCS(C); Nader Sadeghi, MD, FRCS(C); Saleh Al-Dhahri, MD 381

Non-inflatable Sterile Sheath for Introduction of the Flexible Nasopharyngolaryngoscope
Harvey D. Silberman, MD 385

IMAGING CASE STUDY OF THE MONTH

Does Cochlear Nerve Aplasia Always Occur in the Presence of a Narrow Internal Auditory Canal?
Hung Thai-Van, MD; Bernard Fraysse, MD; Olivier DeGuine, MD; Annick Sevely, MD; Corinne Berges, MD 388

MISCELLANEOUS

Information for Subscribers 1a
Index to Advertisers 12a

CLINICAL AND RESEARCH FELLOWSHIP IN OTOLOGY AND NEUROTOLOGY

MASSACHUSETTS EYE AND EAR INFIRMARY

Fellowship training is offered for individuals who aspire to a full-time academic career. Two- and three-year fellowships are available. Three-year fellowships provide additional opportunities for basic research training, while the two-year fellowship will provide opportunities for clinical research. Board eligibility or certification is required.

For more information, contact:

Michael J. McKenna, MD
Dept of Otolaryngology
Massachusetts Eye and Ear Infirmary
243 Charles Street
Boston, MA 02114
(617) 573-3654

A2

FELLOWSHIP IN LARYNGOLOGY, PHONOSURGERY AND VOICE DISORDERS

HARVARD MEDICAL SCHOOL

Available July 1, 2003. The Department of Otology and Laryngology is seeking applicants for a one-year clinical fellowship in laryngology, phonosurgery, and management of the professional voice. The curriculum will provide a wide range of experiences, including phonomicrosurgery (cold instruments and lasers), laryngeal framework surgery, laryngeal electromyography, and the use of botulinum toxin injections for spasmodic dysphonia. The fellow will participate in the management of voice disorders as a member of a multidisciplinary team that includes full exposure to state-of-the-art voice laboratory facilities. The curriculum is designed so that upon completion, the fellow will have sufficient background to establish an independent voice disorders program at his or her home institution. There are numerous clinical and basic science research opportunities available as well as the option to work collaboratively with local music conservatories. Certification by the American Board of Otolaryngology or eligibility is a prerequisite.

Direct inquiries to: Steven M. Zeitels, MD, Director, Division of Laryngology, Massachusetts Eye and Ear Infirmary, 243 Charles Street, Boston, MA 02114; Phone: (617) 573-3557, Fax: (617) 573-3068

A136

Physicians' Choice® "Ear Putty"® Ear Plugs provide effective protection against water . . .

- Prevention — helps in the prevention of reoccurring ear problems and patient revisits.
- Inexpensive — costs less than $1.50 per month on average.
- Efficient — with no fitting required.
- Patient Compliance — provides a soft and comfortable seal over the ear canal.
- The Physicians' Choice — "Ear Putty" is the official supplier to the United States Swimming National Team.

For a free sample and information on Physicians' Choice "Ear Putty" Ear Plugs please contact us at:

Santa Barbara Medco, Inc.

P.O. Box 6843
Santa Barbara, CA 93160
805/683-1486
FAX 805/683-4864
e-mail: sbmedco@silcom.com

Visit us at our website www.sbmedco.com

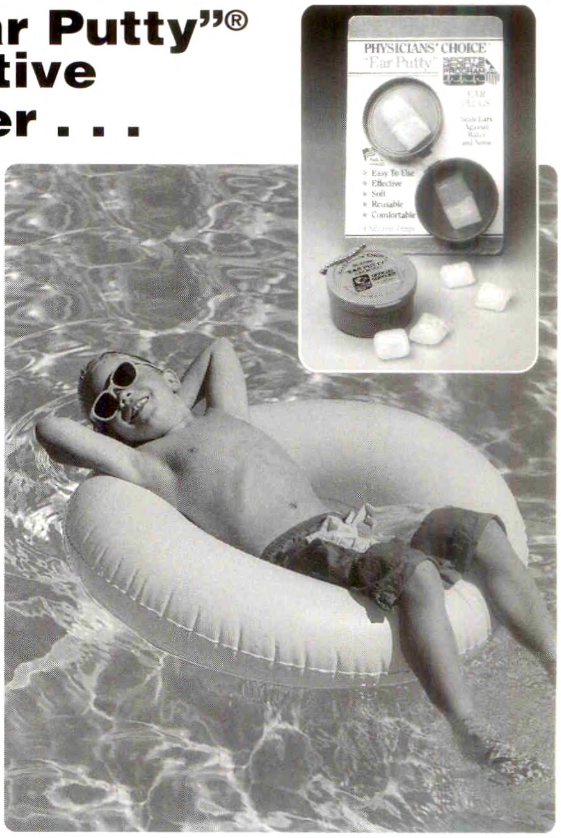

What a Difference 15° Makes

Karl Storz 45° Sinus Telescope

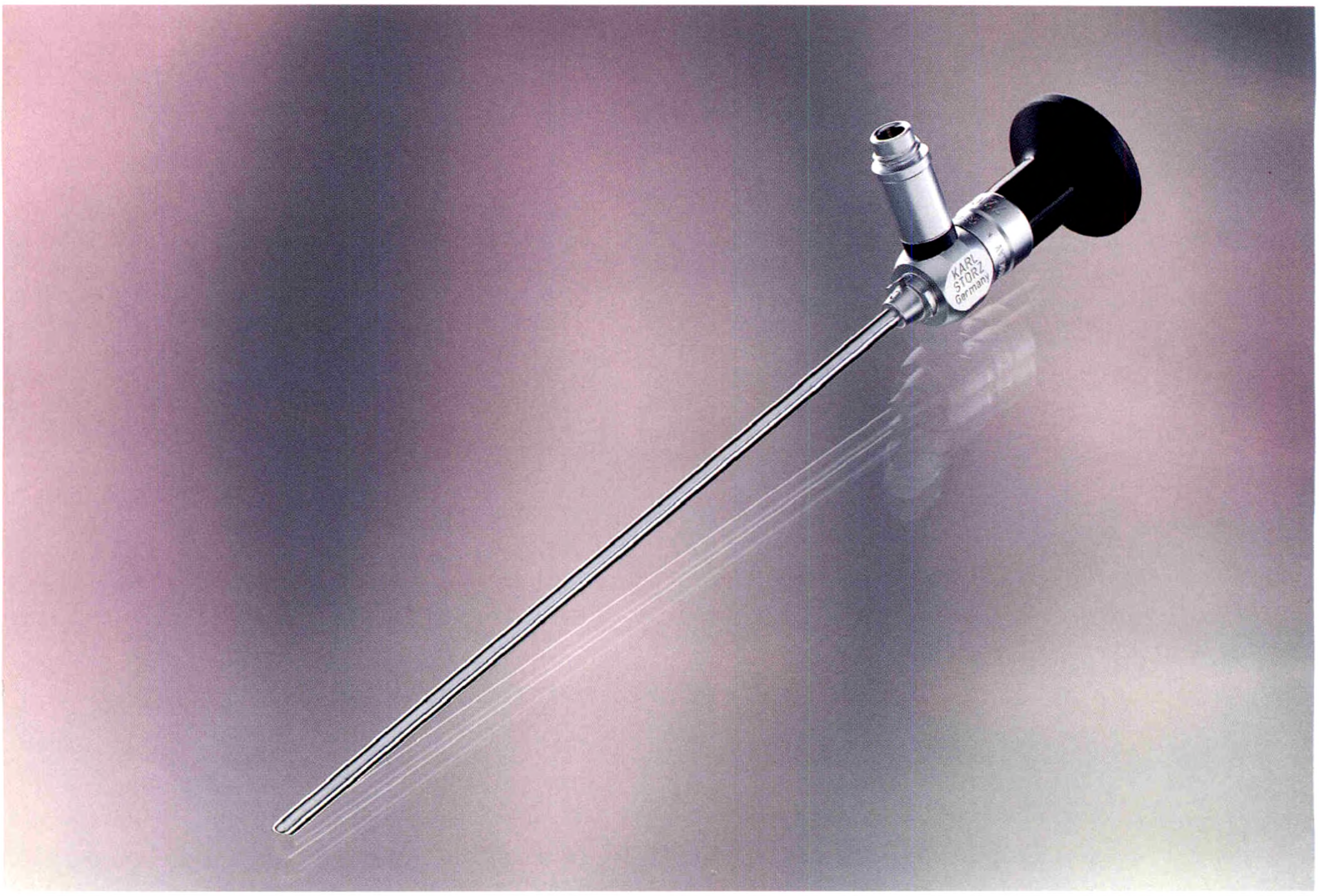

Answer the age-old challenge of "looking around the corner" in the sinus cavities with the new **45° Sinus Telescope** from Karl Storz. The ideal compromise between traditional 30° and 70° telescopes, it provides a unique combination of access and visualization. The 45° line of visualization permits a straight ahead view for orientation as well as increased angulation.

Developed in conjunction with Professor Heinz Stammberger, our 45° Sinus Telescope is ideal for examination of the frontal sinus, frontal recess, maxillary sinus and sphenoid sinus. Optical quality is now better than ever with 30 percent higher light transmission for images of the utmost clarity and resolution.

Improve diagnosis, treatment and postoperative care today with the unique optical capabilities of the 45° Sinus Telescope. Take a look for yourself by calling Karl Storz at **(800) 421-0837** or contacting your local Karl Storz representative.

KARL STORZ GmbH & Co.
Mittelstraße 8, D-78532 Tuttlingen, Germany
Postfach 230, D-78503 Tuttlingen, Germany
Telefon: (07461) 70 80
Telefax: (07461) 70 81 05

KARL STORZ Endoscopy-America, Inc.
600 Corporate Pointe
Culver City, CA 90230-7600
Telephone: (310) 338-8100
(800) 421-0837
Telefax: (310) 410-5530

KARL STORZ Endoscopy-Canada, Inc.
438 University Avenue, Suite 1800
Toronto, Ontario, Canada M5G 2K8
Telephone: (416) 596-9900
(800) 268-4880 (English)
(800) 361-7388 (Francais)
Telefax: (416) 596-9333

KARL STORZ Endoscopia Latino America
815 N.W. 57th Ave., Ste. No. 480
Miami, FL 33126-2042, USA
Telefono: (305) 262-8980
Telefax: (305) 262-8986

E-mail: karlstorz-marketing@karlstorz.de
Internet: http://www.karlstorz.de
http://www.karlstorz.com

STOP BY AND SEE US AT THE COSM MEETING, BOOTH #301.

STORZ
KARL STORZ ENDOSCOPY
THE DIAMOND STANDARD

© 2000 Karl Storz Endoscopy-America, Inc.

Ann Otol Rhinol Laryngol 110:2001

STROBOSCOPIC ASSESSMENT OF VOCAL FOLD KERATOSIS AND GLOTTIC CANCER

DARRYL COLDEN, MD STEVEN M. ZEITELS, MD ROBERT E. HILLMAN, PHD
JOHN JARBOE, MD GLENN BUNTING, MA KONSTANTINA SPANOU, MD
BOSTON, MASSACHUSETTS

Disruption of the normal viscoelastic properties of the superficial lamina propria (SLP) results in aberrant vocal fold vibration and mucosal wave propagation. Therefore, an investigation was performed to determine whether stroboscopy is a reliable method for 1) differentiating invasive glottic carcinoma from intraepithelial atypia or 2) determining the depth of cancer invasion. An analysis was done on the preoperative vocal fold vibration characteristics of 62 keratotic (intraepithelial, 45; cancer, 17) lesions that were subsequently resected by means of microlaryngoscopy. Histopathology and intraoperative mapping were used to specify the depth of invasion. A panel of 4 blinded judges was used to assess the amplitude of vocal fold vibration and the magnitude of mucosal wave activity in the region of the lesion from videostroboscopic recordings. The final comparative data set comprised only those ratings that achieved at least 75% interjudge agreement. Of the 28 intraepithelial lesions that could be reliably evaluated for amplitude of vocal fold vibration, only 2 were normal, with the amplitude reduced in 24 and absent in 2. Of the 30 intraepithelial lesions in which mucosal wave activity could be reliably assessed, only 2 were normal, with the wave reduced in 24 and absent in 4. Furthermore, amplitude of vocal fold vibration and magnitude of mucosal wave propagation were absent in 2 of 4 carcinomas in which the depth of microinvasion did not reach the vocal ligament. According to the findings herein, reduced amplitude of vocal fold vibration and/or mucosal wave propagation associated with keratosis did not reliably predict the presence of cancer or the depth of cancer invasion into the laminae propriae. However, the presence of a flexible mucosal wave probably indicates that there is not extensive vocal ligament invasion. Reductions in the amplitude of vocal fold vibration and in mucosal wave magnitude were usually noted in intraepithelial atypia, despite the fact that there was no invasion into the SLP. The reduced epithelial pliability could be due to bulky keratosis and/or alteration of the SLP occurring as a result of inflammation or fibrovascular scarring.

KEY WORDS — cancer, carcinoma, dysphonia, dysplasia, hoarseness, keratosis, laryngoscopy, leukoplakia, microflap, microlaryngoscopy, phonomicrosurgery, phonosurgery, stroboscopy, vocal cord, vocal fold.

INTRODUCTION

It has long been recognized that glottic cancer is preceded by a precancerous state[1-3] during which there is a window of opportunity to eradicate the disease before malignant degeneration. This concept was developed when vocal fold atypia was recognized with increasing frequency around 10 years after the introduction of mass-produced cigarettes. The first use of laryngeal stroboscopy was reported more than 100 years ago.[4,5] It has been suggested that stroboscopy is a viable method for 1) distinguishing epithelial atypia from glottic cancer[6,7] and 2) determining the depth of invasion of cancer into the laminae propriae.[6,7] These precepts were established by means of pilot data[6] and anecdotal observations.[8] In these two clinical scenarios, the stroboscopic assessment is used to assess the lesion's depth, which is an invisible third dimension (Fig 1A[9]).

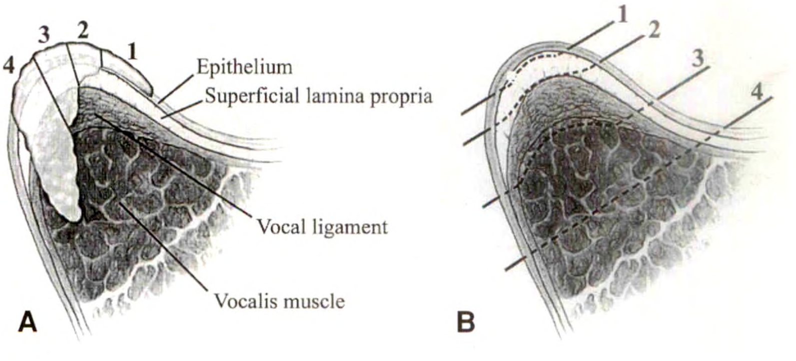

Fig 1. Coronal view of vocal fold's layered microstructure. (Reprinted with permission.[9]) A) Schematic representation displays that surface lesions can have spectrum of patterns of invasion into layered microstructure of vocal fold. B) Diagrammatic demonstration of varied resection techniques that can be performed.

From the Department of Otology and Laryngology, Harvard Medical School (Colden, Zeitels, Hillman, Jarboe, Spanou), and the Division of Laryngology (Colden, Zeitels, Jarboe, Spanou) and the Voice and Speech Laboratory (Hillman, Bunting), Massachusetts Eye and Ear Infirmary, Boston, Massachusetts.

Presented at the meeting of the American Broncho-Esophagological Association, Orlando, Florida, May 15-16, 2000.

CORRESPONDENCE — Steven M. Zeitels, MD, Division of Laryngology, Massachusetts Eye and Ear Infirmary, 243 Charles St, Boston, MA 02114.

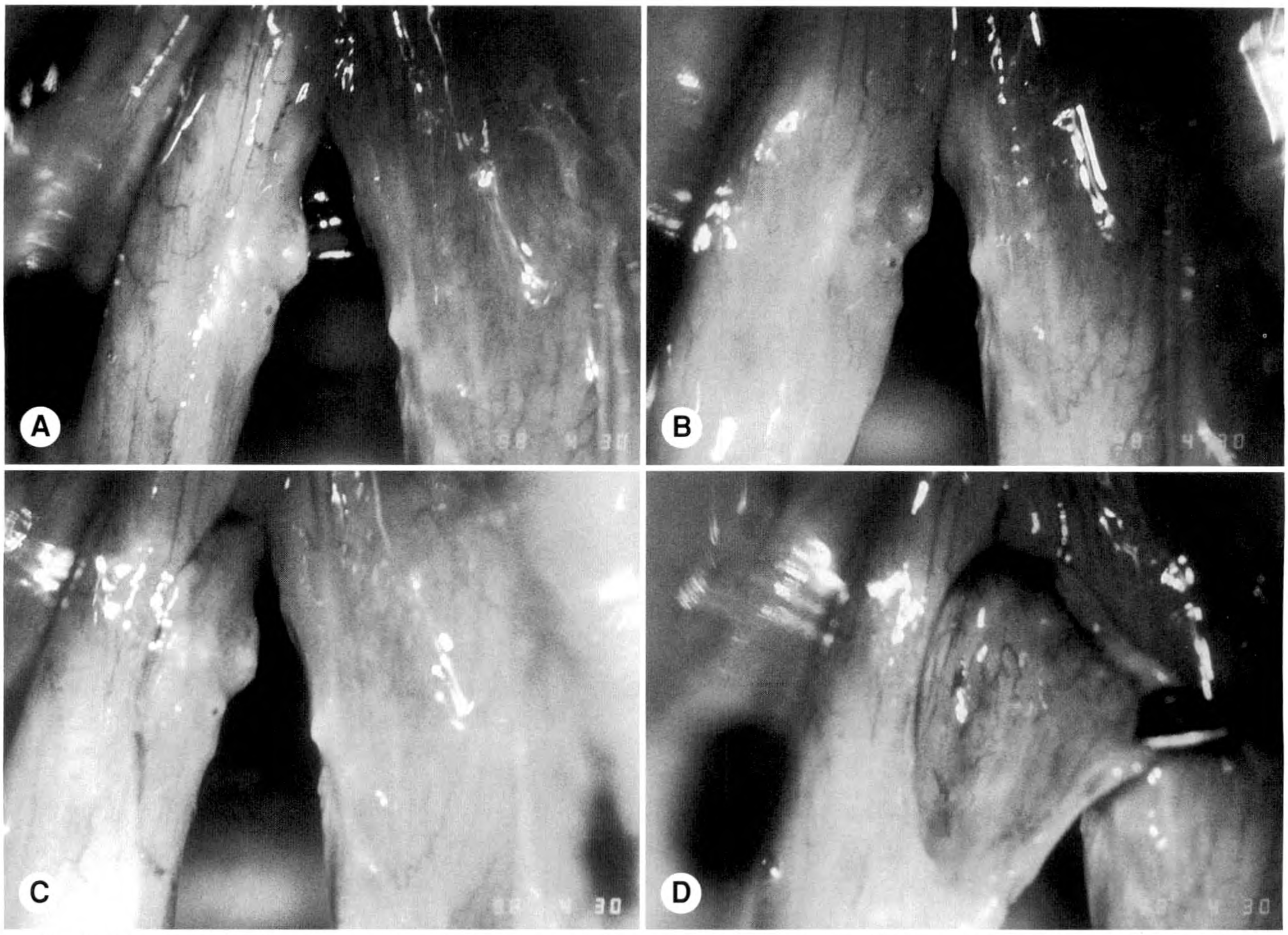

Fig 2. Subepithelial infusion and microflap resection (all views in same patient). A) There is irregular lesion containing microinvasive cancer noted in mid-musculomembranous region on left. There is area of keratosis on right. B) After left subepithelial infusion of saline solution and 1/10,000 epinephrine. C) Perimeter incision is made to perform epithelial cordotomy for exploration and resection. D) Lesion is retracted as microflap. Residual normal superficial lamina propria is easily seen.

The presumption is that premalignant-appearing lesions, which have lost epithelial pliability as reflected by a diminution in vocal fold vibratory (oscillation) behavior and mucosal wave magnitude, harbor occult invasive cancer. Although this thesis is attractive at first glance and is generally accepted, it has never been carefully evaluated. Furthermore, it has been suggested that information derived from stroboscopic examination should be used to guide intraoperative management. This approach has profound implications if a layered phonomicrosurgical resection approach[10-13] (Fig 1B[9]) is used to treat the lesion.

MATERIALS AND METHODS

Subjects. The subjects were 52 patients who underwent microlaryngoscopic resection of 62 lesions. (Ten patients had bilateral lesions.) All patients except 2 (1 patient with videostrobscopy 2 months before surgery and another who was examined 5 months before surgery) had undergone laryngeal videoendoscopy with stroboscopy within 1 month of surgery. A majority of videostroboscopic examinations were performed less than 2 weeks before surgery.

Microsurgical Resection. All patients underwent en bloc phonomicrosurgical microflap resection by means of the subepithelial infusion technique[11-15] (Fig 2). Intraoperative resection maps and associated whole-mount histopathologic analysis were used to specify lesion depth for comparison to the vibratory characteristics found on stroboscopic assessments. The schematic resection map is a derivation of a tumor map, and was designed as a routine clinical tool a number of years ago to portray the 3-dimensional character of vocal edge pathological findings. Each lesion was depicted at the time of the surgery to precisely delineate the involvement of the laminae propriae.

Videostroboscopic Recordings. The videostroboscopic recordings of the 62 vocal fold lesions were randomized into 2 different orders and dubbed onto 2 master study tapes with a tape editing system. This editing system enabled numbering of the video segments and the placement of an arrow on the dubbed video samples to indicate the locations of the lesions being judged. A majority (47/62) of the videostroboscopic recordings were from transoral endoscopic examinations, and the remainder (15/62) were obtained via transnasal flexible endoscopy.

Judges. Two otolaryngologists and 2 clinically certified speech-language pathologists served as judges. All judges had extensive experience in evaluating videostroboscopic recordings and were blinded to the intraoperative lesion mapping and histopathologic results for the study group. Before carrying out their independent evaluations of the videostroboscopic recordings, all of the judges participated as a group in a training session. During this session, videostroboscopic recordings of patients with keratotic lesions similar to those included in the study were shown and discussed so that the judges could reach consensus ratings of amplitude of vocal fold vibration and mucosal wave activity. After this session, a video editing system was used to dub these examples onto a master reference tape along with labeling that represented the group's consensus ratings of each sample. This tape was viewed by each judge before he or she performed independent ratings of the study recordings. The reference tape was also available for each judge to refer to during the evaluation of the study tapes.

Evaluation of Videostroboscopic Recordings. Each judge independently evaluated each of the 2 study tapes with no audio playback (to eliminate the potential confounding influences of auditory perception of voice quality), using standard forms to record his or her responses. The judges were instructed to separately rate the amplitude of vocal fold vibration and the mucosal wave activity at the lesion location by using the following scale: normal, slightly reduced, greatly reduced, absent, or could not rate. Amplitude of vibration was defined as the degree of excursion of the vocal fold from the midline of the glottis that occurred during phonation.[16] Mucosal wave magnitude was defined as the amount of surface wave deformation of the vocal fold that occurred during phonation.[16] The judges were allowed to use the jog shuttle control on the video playback deck to slow down and/or replay each video sample as many times as they wanted to before finalizing their ratings. At least 24 hours elapsed between each judge's evaluations of the 2 randomized study tapes.

A criterion level of at least 75% interjudge agreement was set for accepting the videostroboscopic ratings. Video segments that failed to reach this level of agreement were not used for final comparisons of intraoperative mapping and histopathologic lesion data. Because the highest interjudge variation was observed between the ratings of "slightly reduced" and "greatly reduced," it was subsequently decided to combine these 2 categories into 1 category representing simply "reduced" amplitude of vibration or mucosal wave activity. In addition, video segments were also eliminated from the final comparisons if at least 50% of the judgments (4/8) were "could not rate." Thus, in the final transformed data set, amplitude of vocal fold vibration and mucosal wave activity for each video segment were classified separately as normal, reduced, absent, could not rate, or unreliable rating (ie, less than 75% interjudge agreement).

RESULTS

Surgical Excision. All patients underwent subepithelial infusion, epithelial cordotomy, and en bloc microflap resection of the lesion. Although there were no positive cancer margins that required re-resection, it was not unusual to have atypia at the perimeter margins of the resected specimens. Histopathologic analysis revealed that 45 of the 62 lesions contained intraepithelial atypia or hyperplasia. Cancer was noted in 17 of the 62 lesions. According to the histopathology and intraoperative mapping, the depth of the cancer invasion extended to the superficial lamina propria (SLP) in 6 of the 17, to the vocal ligament in 9, and to the vocalis muscle in 2 (Fig 1).

Amplitude of Vocal Fold Vibration. The intrajudge reliability for the amplitude of vocal fold vibration assessments ranged from 75.8% to 96.8% across the 4 judges. For 6 of the 62 (9.7%) recorded video segments, the amplitude of vocal fold vibration could not be rated on 50% of the judgments (4/8). Thus, these segments were eliminated from further analysis. Of the remaining 56 video segments, 31 (55.4%) were rated with at least 75% interjudge agreement. After the slightly and greatly reduced categories were combined, 43 of the 56 segments (76.8%) were rated with at least 75% interjudge agreement. The Table displays a summary of the final stroboscopic ratings of the amplitude of vocal fold vibration versus depth of lesion.

Magnitude of Mucosal Wave Propagation. The intrajudge reliability for mucosal wave evaluation by the 4 judges ranged from 79.0% to 96.8%. For 6 of the 62 (9.7%) recorded video segments, mucosal wave activity could not be rated on 50% of the judgments (4/8). Thus, these segments were eliminated from further analysis. Of the remaining 56 video segments, 35 (62.5%) were rated with at least 75% interjudge agreement. After the slightly and greatly reduced categories were combined, 45 of the 56 segments (80.4%) were rated with at least 75% inter-

AMPLITUDE OF VOCAL FOLD VIBRATION, AND MAGNITUDE OF MUCOSAL WAVE, VERSUS DEPTH OF LESION

	Lesion Depth				
	1	*2*	*3*	*4*	*Total*
Vibration					
Normal	2	0	1	0	3
Reduced	24	2	3	0	29
Absent	2	2	5	2	11
Not rated	5	1	0	0	6
Unreliable ratings	12	1	0	0	13
Total	45	6	9	2	62
Mucosal wave					
Normal	2	0	1	0	3
Reduced	24	2	2	0	28
Absent	4	2	5	2	13
Not rated	5	1	0	0	6
Unreliable ratings	10	1	1	0	12
Total	45	6	9	2	62

Coding for lesion depth: 1 — intraepithelial atypia; 2 — microinvasive cancer into superficial lamina propria but not into vocal ligament; 3 — cancer invading vocal ligament but not vocal muscle; 4 — cancer progressing through vocal ligament and into vocal muscle.

judge agreement. The Table displays a summary of the final stroboscopic ratings of the magnitude of mucosal wave activity versus lesion depth.

DISCUSSION

In the present study, laryngeal stroboscopy was not a reliable method by which to determine the presence of cancer or the depth of cancer invasion into the laminae propriae. It was remarkable that the vocal folds with intraepithelial atypia were overwhelmingly judged to have impairments in vocal fold vibration amplitude and mucosal wave magnitude. Of the 28 intraepithelial lesions that could be reliably evaluated for amplitude of vocal fold vibration, only 2 were normal, with the amplitude reduced in 24 and absent in 2 (see Table). This tendency has been noted previously by other authors.[7] Of the 30 intraepithelial lesions in which mucosal wave activity could be reliably assessed, only 2 had normal wave motion, while the wave magnitude was reduced in 24. More striking was the fact that the magnitude of the wave was judged as being absent in 4 of the 30 (see Table). It is also worth noting that before the combination of videostroboscopic data into a "reduced" category, a majority of the reliable ratings (ie, ≥75% interjudge reliability) for intraepithelial lesions fell within the subcategory of "greatly reduced" for both amplitude of vibration (11/14) and mucosal wave magnitude (13/16). These findings lend further support to the observation that intraepithelial lesions such as noncancerous keratosis (Fig 3) or papilloma may cause impaired pliability.

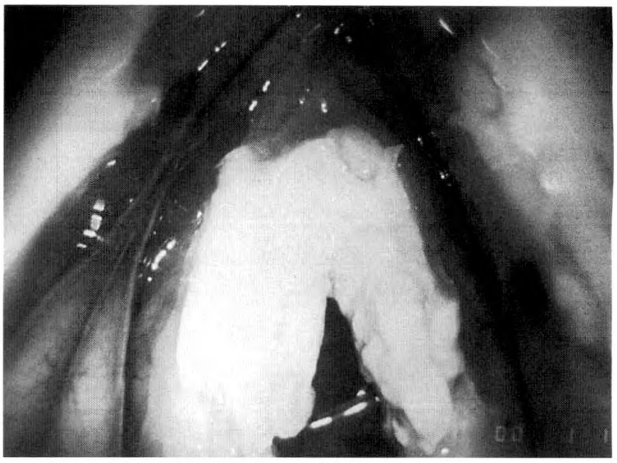

Fig 3. Verrucous keratosis of both vocal folds; there was no mucosal wave noted on stroboscopy. Microflap resection revealed epithelial hyperplasia without atypia.

Furthermore, vocal overusers who develop subsequent epithelial lesions could have had prior loss of normal SLP caused by lifelong phonotrauma (Fig 4).

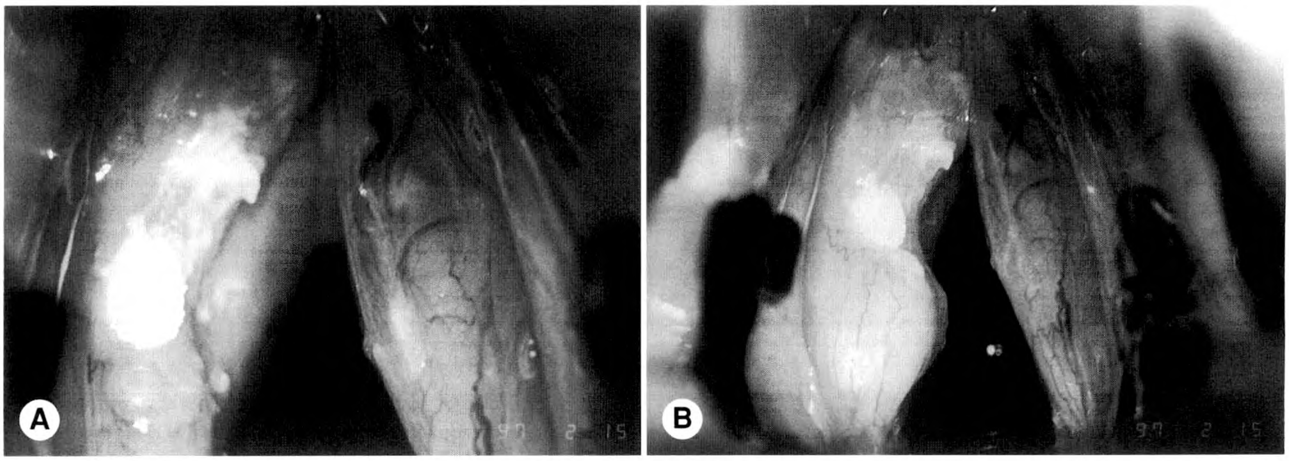

Fig 4. Pop vocalist with long history of vocal abuse. A) There is keratosis overlying sulcus deformity. There is another, more subtle sulcus noted on right vocal fold. There was no mucosal wave progression through lesion. B) After subepithelial infusion on left, depressed area of left sulcus is well seen. Subsequent microflap resection revealed intraepithelial hyperplasia.

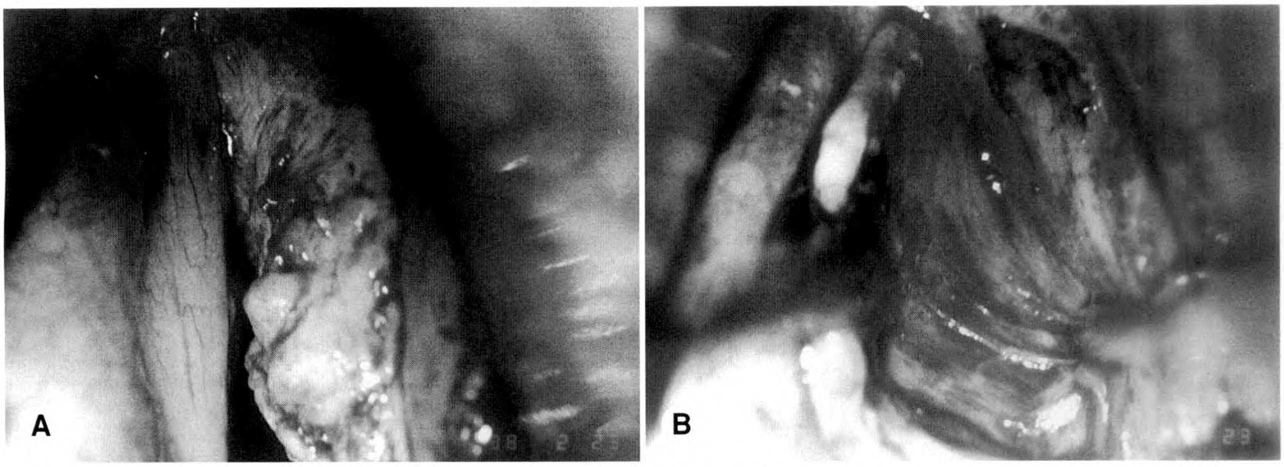

Fig 5. A) Extensive cancer in right vocal fold. Because of size of lesion, subepithelial infusion revealed equivocal information about whether disease was invading vocal ligament. B) After epithelial cordotomy and development of microflap that encompassed lesion, it can be well seen that there was no disease extending into vocal ligament. Note that fibers of superficial lamina propria can be dissected easily with cold instrumentation.

Alternatively, compensatory phonotrauma to the SLP and associated stiffness can result from ongoing vocal overuse after the genesis of the surface epithelial lesion. Finally, the patient could have developed fibrosis of the SLP as a result of prior endolaryngeal instrumentation. One or all of these factors may be present in patients in whom clinical stroboscopy suggests impaired mucosal wave oscillation but in whom histopathology reveals intraepithelial atypia.

These factors also explained the next observation. Even when cancer was present in association with a complete loss of vibration and the mucosal wave, this finding was not a reliable indicator that the disease was invading the vocal ligament. Of the 9 vocal folds with cancer and no amplitude of vibration or magnitude of the mucosal wave, the subepithelial infusion and subsequent resection revealed that 2 had microinvasion confined to the SLP (Fig 5 and Table). The accuracy of the intraoperative assessment of the depth of cancer invasion is supported by the fact that none of these patients underwent resection of the vocal ligament and none developed a local cancer recurrence (after >2.5 years of follow-up in the majority).

A final observation was that 1 of the 3 lesions with normal vibration amplitude and mucosal wave propagation had associated cancer (see Table). Although an area of that lesion reached the vocal ligament, there was enough normal SLP underlying the lesion to allow for the visual impression of normal epithelial pliability and, on stroboscopy, a normal mucosal wave. This situation is encountered routinely when microinvasive cancer occurs in a field of Reinke's edema.

Interestingly, a similar physiological scenario can be observed in the phonatory oscillation characteristics of musical theater performers. These individuals often have various amounts of phonatory-induced fibrous scarring in the superficial aspect of the SLP, just under the epithelial basement membrane. This fibrovascular scarring simulates the epithelial stiffness that occurs with microinvasive cancer. These individuals also have a significantly greater volume of flexible SLP (similar to Reinke's edema) underlying the fibrovascular scarring. We hypothesize that these anatomic findings are the result of elevated subglottal driving pressures associated with long-term use of a "belting" singing voice. The increased volume of flexible SLP facilitates the appearance of normal vocal fold vibration despite the surface stiffness.

The results of this study highlight the subjective nature of evaluating videostroboscopic recordings. Even though all of the judges in this study agreed ahead of time on how to rate representative examples of videostroboscopic recordings, and these examples were then used during the study as reference points (anchors), there was still a relatively high degree of interjudge variation in the ratings. This variation occurred mostly between the "slightly" and "greatly" reduced categories, leading to a combining of ratings within a "reduced" category, and to the elimination of ratings that had less than 75% interjudge agreement. On the basis of this experience, we believe strongly that studies that use videostroboscopic ratings must demonstrate that such ratings attain an acceptable level of reliability across multiple independent judges to be considered valid.

The aforementioned findings regarding vocal fold vibratory amplitude and mucosal wave magnitude associated with surface premalignant and cancerous vocal fold epithelia support the following paradigm. It has been previously shown that normal epithelium is translucent[17] and understandably has little substantive viscoelasticity. Normal vocal fold vibration and mucosal wave activity primarily reflect the viscoelastic properties of the underlying normal SLP. However, hyperplastic or diseased epithelium, especially with overlying thick keratosis, can result in decreased vibration amplitude and mucosal wave pliability. A reduction in these parameters can also result from a loss of SLP. Unfortunately, stroboscopic assessment of the surface does not allow for differentiation between underlying fibrosis and cancer invasion of the SLP. This differentiation is best made by means of a subepithelial infusion and subsequent epithelial cordotomy. Developing a microflap that encompasses the lesion[11-13,15] (Figs 2D and 5B) facilitates visual examination (under high magnification) of the undersurface of the lesion and the residual normal SLP. If the stroboscopic examination reveals that substantial vibration and mucosal wave flexibility are present, it is reasonable to assume that the disease is not invading the vocal ligament (medial and deep laminae propriae)[18-20]; however, it cannot be assumed that the disease is benign.

CONCLUSIONS

1. Laryngeal stroboscopy is not a reliable technique for distinguishing intraepithelial vocal fold atypia from invasive cancer.

2. Laryngeal stroboscopy is not a reliable technique for determining the depth of invasion of vocal fold cancer.

3. A relatively normal mucosal wave suggests that the lesion is not extensively invading the vocal ligament.

4. Because of the subjective nature of videostroboscopic ratings, studies that use them should enhance their dependability by demonstrating that the ratings attain an acceptable level of reliability across multiple independent judges.

REFERENCES

1. Jackson C. Malignant neoplasms of the larynx. In: Jackson C, ed. Peroral endoscopy and laryngeal surgery. St Louis, Mo: Laryngoscope Co, 1915:637.

2. Jackson C. Cancer of the larynx: is it preceded by a recognizable precancerous condition? Trans Am Laryngol Assoc 1922;44:182-201.

3. Pierce NH. Leukoplakia laryngis. Ann Otol Rhinol Laryngol 1920;29:33-56.

4. Oertel M. Ueber eine neues laryngostroboskopische Untersuchungsmethode des Kehlkopfes. Centralbl Med Wiss 1878; 16:81-2.

5. Oertel M. Das Laryngo-stroboskop und die laryngo-stroboskopische Untersuchung. Arch Laryngol Rhinol 1895;3:1-16.

6. Sessions RB, Miller SD, Martin GF, Solomon BI, Harrison LB, Stackpole S. Videolaryngostrobosopic analysis of minimal glottic cancer. Trans Am Laryngol Assoc 1989;110:56-9.

7. Zhao R, Hirano M, Tanaka S, Sato K. Vocal fold epithelial hyperplasia: vibratory behavior versus extent of lesion. Arch Otolaryngol Head Neck Surg 1991;117:1015-8.

8. Woo P, Colton R, Casper J, Brewer D. Diagnostic value of stroboscopic examination in hoarse patients. J Voice 1991;5: 231-8.

9. Hartig G, Zeitels SM. Optimizing voice in conservation surgery for glottic cancer. Oper Techn Otolaryngol Head Neck Surg 1998;9:214-23.

10. Hirano M, Hirade Y. CO2 laser for treating glottic carcinoma. Acta Otolaryngol Suppl (Stockh) 1988(suppl 458):154-7.

11. Zeitels SM. Microflap excisional biopsy for atypia and microinvasive glottic cancer. Oper Techn Otolaryngol Head Neck Surg 1993;4:218-22.

12. Zeitels SM. Premalignant epithelium and microinvasive cancer of the vocal fold: the evolution of phonomicrosurgical management. Laryngoscope 1995;105(suppl 67).

13. Zeitels SM. Phonomicrosurgical treatment of early glottic cancer and carcinoma in situ. Am J Surg 1996;172:704-9.

14. Zeitels SM, Vaughan CW. A submucosal vocal fold infusion needle. Otolaryngol Head Neck Surg 1991;105:478-9.

15. Zeitels SM. Atlas of phonomicrosurgery and other endolaryngeal procedures for benign and malignant disease. San Diego, Calif: Singular Publishing Group (in press).

16. Hillman R. The contemporary clinical voice laboratory — its role in the diagnosis of laryngeal disorders. In: Gluckman JL, ed. American Academy of Otolaryngology: recertification study guide. Dubuque, Iowa: Kendell/Hunt, 1998:365-9.

17. Zeitels SM, Hillman RE, Bunting GW, Vaughn T. Reinke's edema: phonatory mechanisms and management strategies. Ann Otol Rhinol Laryngol 1997;106:533-43.

18. Hirano M. Phonosurgery: basic and clinical investigations. Otologia (Fukuoka) 1975;21:239-442.

19. Hirano M. Structure and vibratory behavior of the vocal fold. In: Sawashima M, Cooper F, eds. Dynamic aspects of speech production. Tokyo, Japan: University of Tokyo, 1977:13-30.

20. Hirano M. Structure of the vocal fold in normal and diseased states: anatomical and physical studies. In: Proceedings of the Conference on the Assessment of Vocal Pathology. The American Speech-Language-Hearing Association, 1981;11:11-27.

Ann Otol Rhinol Laryngol 110:2001

ROLE OF LARYNGOSCOPY, DUAL PH PROBE MONITORING, AND LARYNGEAL MUCOSAL BIOPSY IN THE DIAGNOSIS OF PHARYNGOESOPHAGEAL REFLUX

J. SCOTT MCMURRAY, MD
MADISON, WISCONSIN

MARK GERBER, MD
CHICAGO, ILLINOIS

YORAM STERN, MD
TEL-AVIV, ISRAEL

DAVID WALNER, MD
NILES, ILLINOIS

COLIN RUDOLPH, MD
CINCINNATI, OHIO

J. PAUL WILLGING, MD
CINCINNATI, OHIO

ROBIN T. COTTON, MD
CINCINNATI, OHIO

There is no standard for determining significant pharyngoesophageal reflux. This prospective blind comparison study compared dual pH probe studies, direct laryngoscopy, and mucosal biopsy in children without symptoms of gastroesophageal reflux who underwent airway evaluation. Significant reflux to the lower esophageal probe did not correlate with statistical significance with reflux to the upper probe. In this group of asymptomatic patients, a positive lower pH probe finding did not correlate with upper or lower esophageal mucosal inflammation. Eosinophilia in the esophageal mucosa is diagnostic of gastroesophageal reflux disease, and was seen in 5 of the laryngeal biopsies. A weak correlation was seen between positive findings at laryngoscopy and positive posterior cricoid biopsy in this group. There may be no consistent way to predict significant pharyngoesophageal reflux in asymptomatic patients. Single-probe pH testing will not predict significant pharyngoesophageal reflux with mucosal changes. Laryngoscopy and upper pH probe findings only weakly correlate with significant histologic findings. Laryngeal and posterior cricoid biopsy may be the only sensitive test for mucosal injury. Clinical trials of empiric antireflux therapy should be used to determine whether the laryngeal changes seen in these patients are reversible.

KEY WORDS — intraepithelial eosinophils, laryngoscopy, mucosal biopsy, pH probe, pharyngoesophageal reflux, subglottic stenosis.

INTRODUCTION

The actual incidence and otolaryngological implications of gastropharyngeal reflux are controversial. Investigators have tried to associate diverse disease processes as chronic rhinosinusitis, chronic otitis media, and laryngeal carcinoma to gastropharyngeal reflux.[1-8] Animal models have associated the development of subglottic stenosis with the application of gastric refluxate.[9] Some clinicians emphasize the need for adequate treatment of gastropharyngeal reflux in the perioperative management of patients undergoing laryngotracheal reconstruction.[9] Others report no differences in the outcome of laryngotracheal reconstruction in patients treated for gastroesophageal reflux versus untreated patients.[10]

No gold standard for diagnosis or treatment exists for supraesophageal reflux. Some have reported that there is an overestimation of acid reflux in the development of posterior laryngitis as diagnosed by pH probe study and esophageal biopsy.[11] Normative data have not been collected for gastropharyngeal reflux in either adults or children. Dual-probe pH monitoring is currently the best method available for detecting reflux of acid to the lower or upper esophagus, but the definition of significant reflux to the pharynx has not been determined. Some investigators indicate that any reflux to the level of the pharynx is pathological and should be treated[12]; however, it is well known that about 50% of infants have regurgitant vomiting at least once per day, so this criterion is somewhat illogical in pediatric patients.[13]

Laryngeal findings that were thought to show significant gastropharyngeal reflux have been catalogued.[12,14,15] Posterior glottic edema, hypervascularity, and pseudosulcus are considered important signs of reflux laryngitis. These laryngeal signs may be present even when gastroesophageal reflux cannot be demonstrated by pH probe. These findings have been shown to be reversible in adults, after empiric therapy for gastroesophageal reflux.[15]

Inflammation and especially intraepithelial eosinophilia in the esophageal mucosa is thought to be pathognomonic for reflux esophagitis and is seen in children with symptoms of gastroesophageal reflux who

---

From the Departments of Otolaryngology–Head and Neck Surgery (McMurray, Gerber, Stern, Walner, Willging, Cotton) and Gastroenterology (Rudolph), Children's Hospital Medical Center, Cincinnati, Ohio.

Presented at the meeting of the American Broncho-Esophagological Association, Orlando, Florida, May 15-16, 2000.

CORRESPONDENCE — J. Scott McMurray, MD, Dept of Surgery and Pediatrics, H4-318, University of Wisconsin Medical School, 600 Highland Ave, Madison, WI 53792.

LIBRARY

have positive pH probe studies.[16] It is unknown whether this histologic finding is also seen in the larynx.

Gastropharyngeal reflux is thought to be a predisposing factor leading to complications after laryngotracheoplasty. This study evaluated children without other symptoms of gastroesophageal reflux before surgical repair of their subglottic stenosis. Findings of laryngoscopy, dual-probe pH monitoring, and esophageal and laryngeal histologic examination were assessed in an attempt to find a correlation between physical findings, results of pH probe testing, and histologic findings. We hypothesized that laryngeal appearance or histologic findings would correlate with findings of pharyngeal reflux on pH probe study, even though these children were otherwise asymptomatic.

METHODS

Patients. Consecutive patients under evaluation for airway reconstruction at Children's Hospital Medical Center in Cincinnati were included in the study group. Informed consent was obtained to enter the study as approved by the Institutional Review Board. These patients were undergoing routine laryngoscopy, bronchoscopy, esophagoscopy, and pH probe placement before possible airway reconstruction. Thirty-nine patients entered and completed the study. There were 23 boys and 16 girls. The age range was 0.5 to 11 years, with an average age of 3.5 years. No patient had symptoms of chest pain, vomiting, or excessive regurgitation for his or her age.

Rigid Videomicrolaryngoscopy. During routine airway evaluation under general anesthesia, the rigid endoscopy was videotaped in each patient. A single videotape was then edited to include the laryngoscopic portion of the evaluation. No patient identification was included on this tape. Eight pediatric otolaryngologists reviewed the videotape and rated each larynx for the presence or absence of "reflux laryngitis." Qualities consistent with reflux laryngitis were posterior glottic edema, laryngeal erythema, laryngeal hypervascularity, and laryngeal pseudosulcus. A larynx was considered positive or negative for reflux laryngitis if 6 of the 8 otolaryngologists agreed on the laryngoscopic findings.

Laryngeal and Esophageal Biopsies. During laryngoscopy, full-thickness mucosal biopsy specimens were obtained from the posterior cricoid area and the interarytenoid larynx with a small cupped forceps. Esophageal biopsy specimens were obtained during esophagoscopy. Mucosal biopsy specimens were obtained from the distal esophagus, the area 3 to 4 cm above the lower esophageal sphincter, and the upper third of the esophagus with a standard biopsy forceps. All of the specimens were sent for routine histologic examination. A single pathologist, blinded to the results of the pH probe study and the endoscopic evaluation, scored the biopsy specimens.

The esophageal mucosal biopsy specimens were evaluated by standard histologic criteria for reflux esophagitis.[16] As there are no standards for histologic changes caused by reflux in the larynx, the standards for esophageal inflammation caused by reflux were used in the larynx. A grading scale from 0 to 4 for histologic changes was used, with 0 meaning no alterations and 4 meaning severe changes. Grades for basilar hypertrophy, vascular penetration, and eosinophils in the mucosa were recorded for each specimen. The histologic findings were considered diagnostic of inflammation caused by reflux if all 3 items of the diagnostic cluster received a score of 1 or more. The histologic findings were considered suggestive of inflammation caused by reflux if any 1 item of the diagnostic cluster received a score of 2 or more. The histologic findings were considered consistent with inflammation caused by reflux if intraepithelial eosinophils were present in the mucosa. If the pathologist was unable to adequately evaluate these features because of the quality of the biopsy specimen, the data were considered inadequate.

pH Probe. At the time of laryngoscopy and bronchoscopy, a dual-probe pH monitor was placed. The lower probe was positioned within 3 to 5 cm of the lower esophageal sphincter, and the upper probe was placed just above the cricopharyngeus. The probes' positions were confirmed at placement in the operating room and with subsequent fluoroscopic confirmation. Continuous dual pH probes with intraprobe distances of 5, 10, or 15 cm were used (Medtronic Functional Diagnostics, Shoreview, Minn). Recordings were registered every 8 seconds on the Medtronic recording system. The pH was monitored overnight for a minimum of 16 hours. A single gastroenterologist blinded to the laryngoscopic and histologic findings analyzed the data. The number of individual reflux episodes and the percentage of time the reflux had a pH less than 4 were recorded at the upper and lower probe sites. Reflux to the lower probe was considered significant if the pH was less than 4 for more than 10% of the study time. Gastropharyngeal reflux to the upper probe was considered significant if the pH was less than 4 for more than 3% of the time.

RESULTS

Microlaryngoscopic Evaluation. Reflux laryngitis was determined to be present or absent if 6 of the 8 otolaryngologists agreed on the endoscopic findings. A majority consensus was obtained in 28 of the 39 larynges (72%). With this consensus from the panel of endoscopists, 12 larynges (31%) were consid-

TABLE 1. CONSENSUS OF OTOLARYNGOLOGISTS DURING VIDEOLARYNGOSCOPY

	6/8 Observers Agree (75%)	*7/8 Observers Agree (87%)*	*8/8 Observers Agree (100%)*
No. of patients	28/39 (72%)	18/39 (46%)	11/39 (28%)
Reflux laryngitis	12	6	3
No reflux laryngitis	16	12	8

TABLE 2. FREQUENCY OF SIGNIFICANT REFLUX DURING OVERNIGHT PH STUDY

	No. of Patients
Lower probe pH <4 more than 10% of time Upper probe pH <4 less than 3% of time	6/39 (15%)
Lower probe pH <4 more than 10% of time	11/39 (28%)
Lower probe pH <4 more than 10% of time Upper probe pH <4 more than 3% of time	5/39 (13%)
Upper probe pH <4 more than 3% of time	10/39 (26%)
Upper probe pH <4 more than 3% of time Lower probe pH <4 less than 10% of time	5/39 (13%)

ered positive for reflux laryngitis and 16 (41%) were considered negative by endoscopic criteria. An 87% (7/8) consensus was reached 46% of the time (18/39), with 6 patients considered positive and 12 considered negative for reflux laryngitis. Consensus agreement by all of the observers (8/8) was achieved 28% of the time (11/39), with 3 patients considered positive and 8 considered negative for reflux laryngitis (Table 1).

Laryngeal and Esophageal Biopsies. Of the 39 patients who had biopsy specimens taken, an adequate specimen for histologic analysis was obtained from the lower esophagus in 34, from the upper esophagus in 32, from the posterior cricoid area in 34, and from the interarytenoid area in 31. Fragments that were not thick enough to have their basal mucosal layers evaluated by the pathologist were not included in the data. Sixteen of the 34 lower esophageal biopsies (47%) showed histologic changes consistent with reflux esophagitis. Sixteen of the 32 upper esophageal biopsies (50%) showed histologic changes consistent with reflux esophagitis. Fourteen of the 34 posterior cricoid biopsies (41%) showed histologic changes consistent with inflammation from reflux. Ten of the 31 interarytenoid biopsies (32%) showed histologic changes consistent with inflammation from reflux.

Eosinophilia is one of the important histologic features of esophageal inflammation from reflux. Significant histologic eosinophilic infiltration was seen in 7 of the lower esophageal biopsies, 5 of the upper esophageal biopsies, 5 of the posterior cricoid biopsies, and 2 of the interarytenoid biopsies.

pH Probe. The pH was less than 4 at the lower probe for more than 10% of the study time in 11 of the 39 patients (28%). These patients were considered to have significant reflux to the lower esophagus. The pH was less than 4 at the cricopharyngeal probe for more than 3% of the study time in 10 of the 39 patients (26%). These patients were considered to have significant reflux to the pharynx. Five patients (13%) were found to have significant reflux to both upper and lower pH probes by these criteria. Five patients (13%) were found to have significant reflux to the upper pH probe alone. Significant reflux to the lower pH probe alone was found in 6 patients (15%; Table 2).

There was a general trend toward more frequent episodes of reflux to the lower probe as compared to the upper probe. There was a weak correlation (R = .28, p < .08) between reflux to the upper probe and reflux to the lower probe. This was not found to be statistically significant (Table 3).

Correlation and Relationships. Comparisons were made between the histologic findings from the lower esophagus, upper esophagus, and posterior cricoid and interarytenoid areas; the upper and lower pH probe data; and the laryngoscopy findings. Statistically significant correlations were found between lower esophageal and upper esophageal (R = .44, p < .015), upper esophageal and posterior cricoid (R = .47, p < .015), and upper esophageal and interarytenoid (R = .46, p < .025) histologic findings. A weak correlation that was not statistically significant was found for laryngeal endoscopy and interarytenoid histology (R = .29, p < .075), as well as for lower versus upper pH probe findings (R = .28, p < .08; Table 3).

There was a trend toward fewer episodes of reflux with a pH of less than 4 to the upper probe in patients with normal histologic findings as compared to those with inflammation consistent with reflux in the interarytenoid biopsies. However, this was not statistically significant (see Figure).

DISCUSSION

The diagnosis and treatment of potential laryngeal complications of gastropharyngeal reflux remain controversial. The demonstration in animal models that the infrequent application of gastric contents to the subglottis can induce stenosis, with increased inflammation and scarring after exposure of cricoid cartilage, strongly suggests that even infrequent exposure of the postoperative larynx to gastric contents may be damaging.[9] Hanson et al[15] reported that 96% of patients with reflux laryngitis improved with empiric antireflux therapy. The normal frequency of reflux

TABLE 3. KENDALL TAU BETA CORRELATION COEFFICIENTS, P VALUE, AND SAMPLE SIZE COMPARING UPPER AND LOWER PH PROBES, HISTOLOGIC FINDINGS, AND ENDOSCOPIC FINDINGS

		Upper-Probe pH	*Lower-Probe pH*	*Lower Esophageal Histology*	*Upper Esophageal Histology*	*Posterior Cricoid Histology*	*Interarytenoid Histology*
Lower-probe pH	R	.28441					
	p	.0796*					
	N	39					
Lower esophageal histology	R	.1716	.10214				
	p	.3242	.5574				
	N	32	34				
Upper esophageal histology	R	0	0	.43836			
	p	1	1	.0147†			
	N	32	32	32			
Posterior cricoid histology	R	.18232	.11573	.3077	.47087		
	p	.2949	.5062	.0867	.0112†		
	N	34	34	32	30		
Interarytenoid histology	R	.22384	.0333	.12595	.46156	.18045	
	p	.2202	.8551	.5128	.021†	.3397	
	N	31	31	28	26	29	
Endoscopy	R	.06828	.1147	.04837	0	.29431	.05435
	p	.6558	.4541	.7686	1	.0734*	.7527
	N	39	39	34	32	34	31

*p < .08.
†p < .025.

to the level of the pharynx is not well established, and in infants and children these normative data are simply unavailable. The amount of gastropharyngeal reflux that would be expected to cause a difference in the outcome of laryngotracheoplasty is unknown. Zalzal et al,[10] however, reported that the presence or treatment of reflux did not affect the outcome of laryngotracheal reconstruction. The main problems with current pediatric studies continue to be the difficulty in defining which patients may be at risk from gastropharyngeal reflux, since no studies have established a normal range for pharyngeal reflux or a relationship between any amount of reflux to the esophagus or pharynx and disease. In fact, the pediatric studies available show that upper esophageal pH probe recordings are no better than normal single-probe esophageal recordings for discriminating which pediatric patients are at risk for airway complications of gastroesophageal reflux.[17-19] The current study attempted to correlate esophageal and pharyngeal pH probe recordings with laryngoscopic findings that are thought to be consistent with reflux-associated disease and with biopsy findings from the larynx and esophagus. Findings made at laryngoscopy that are consistent with reflux laryngitis have been catalogued: edema, hypervascularity, and pseudosulcus.[12,15] Subjective analysis of the larynx through laryngoscopy may not give reproducible data, however. Interobserver consistency is required to give reliable parameters for reflux laryngitis for comparisons between patients and for follow-up. Six of the 8 observers agreed upon the presence or absence of laryngeal re-

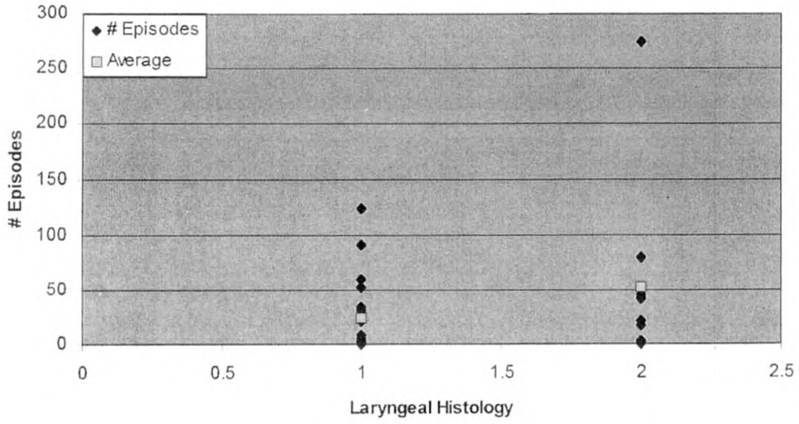

Number of episodes of reflux with pH of <4 at upper pH probe compared to laryngeal histologic findings (combining both posterior cricoid and interarytenoid histologic findings). 1 — normal histologic findings; 2 — histologic findings consistent with reflux inflammation. There is trend toward more frequent reflux in inflammation group, but this carries no statistical significance.

flux changes in 28 of the 39 patients (75%); 7 of the 8 agreed in only 18 of the 39 patients (46%); and there was consensus among all 8 observers in 11 of the 39 patients (28%; Table 1). There was a weak correlation between laryngoscopy and posterior cricoid histology that was not statistically significant ($R = .29$, $p < .07$). Although interobserver reliability was poor, laryngoscopy was a better predictor of abnormalities in laryngeal histologic specimens than were the pH probe measurements.

The pH probe and esophageal mucosal biopsy have been the main diagnostic tools for reflux esophagitis; both have shown abnormal findings in patients with symptomatic esophagitis.[16] Patients with laryngeal pathological changes caused by gastropharyngeal reflux often do not have symptoms of gastroesophageal reflux.[15] Infrequent reflux of gastric contents to the pharynx may be all that is necessary to cause substantial changes in the larynx.[12] It is thought that gastropharyngeal reflux does not need to be a daily event to cause significant changes in the larynx. It should be inherent, then, that 24-hour dual-probe pH studies may not capture meaningful reflux events. Normative data are not available for pediatric patients.

We therefore initially evaluated our data with the supposition that if the pH in the pharynx was less than 4 for more than 3% of the recording time, this likely would discriminate between those patients with a high risk of laryngeal reflux complications and those with less acid exposure in the pharynx. Using this criterion, we found that 26% of our study patients had reflux with a pH of less than 4 to the upper probe more than 3% of the study time, but these patients were not more likely to have changes suggestive of reflux disease on either laryngoscopy or laryngeal histology. Reanalysis of the data to determine whether simply counting episodes of reflux to the larynx would better discriminate patients at risk for laryngeal disease from gastropharyngeal reflux did suggest a weak relationship between the number of episodes of gastropharyngeal reflux and findings of interarytenoid inflammation, but the substantial overlap in numbers of episodes in patients with normal histologic findings versus those with abnormal histologic findings makes the pH probe measurement appear an insensitive clinical tool. Perhaps more significant than visual observation or pH probe findings are the histologic features of the laryngeal mucosa. Esophageal mucosal inflammation has been a hallmark of reflux esophagitis. Esophageal mucosal basilar hypertrophy, vascular penetration, and intraepithelial eosinophilia have been related to inflammation seen in reflux esophagitis.[16] Histologic changes in the laryngeal mucosa have not been described in recent studies of reflux laryngitis. Our study found changes in the laryngeal mucosa similar to those found in reflux esophagitis in 14 of 34 posterior cricoid specimens (41%) and in 10 of 31 interarytenoid specimens (32%). There was a weak correlation ($R = .2$) with a p value of $<.075$ between positive endoscopy for reflux laryngitis and posterior cricoid histologic findings. Changes in the mucosa at the lower esophagus statistically correlated with changes in the upper esophageal biopsy site ($R = .46$, $p < .015$). Changes in the upper esophageal mucosa consistent with reflux esophagitis also statistically correlated with posterior cricoid ($R = .47$, $p < .012$) and interarytenoid ($R = .46$, $p < .02$) changes. Interestingly, changes in the lower esophageal mucosa did not correlate with posterior cricoid ($R = .31$, $p < .09$) or interarytenoid ($R = .23$, $p < .55$) changes. This finding is supported by observations that laryngeal inflammation, reversible through empiric reflux therapy, may not be associated with classic symptoms of reflux esophagitis.

It is apparent that gastropharyngeal reflux occurred in this subset of patients with subglottic stenosis and no reflux symptoms. Clinical criteria suggesting gastropharyngeal reflux were met in 26% of patients by upper pH probe monitoring, in 43% by consensus diagnostic laryngoscopy, and in 41% by histologic findings. Outcomes after laryngotracheoplasty were not measured. The reversibility of these findings by antireflux treatment was also not measured. The findings of pH probe study, visualization, and histologic biopsy did not correlate. It continues to be uncertain which test is best at detecting significant gastropharyngeal reflux. Mucosal biopsy may be the most specific means of detecting inflammation, as it is of detecting reflux esophagitis. Since no correlation among pH probe data, laryngoscopic findings, and histologic findings can be found, trials designed to detect the reversibility of these findings by empiric treatment of gastropharyngeal reflux and prospective blinded outcomes studies in patients requiring laryngotracheoplasty will be required to help resolve this management dilemma.

ACKNOWLEDGMENT — The authors thank Cyndy Daugherty, MD, for her review of the pathology specimens.

REFERENCES

1. Freije JE, Beatty TW, Campbell BH, Woodson BT, Schultz CJ, Toohill RJ. Carcinoma of the larynx in patients with gastroesophageal reflux. Am J Otolaryngol 1996;17:386-90.

2. Olson NR. Aerodigestive malignancy and gastroesophageal reflux disease. Am J Med 1997;103:97S-99S.

3. Contencin P, Maurage C, Ployet MJ, Seid AB, Sinaasappel M. Gastroesophageal reflux and ENT disorders in childhood. Int J Pediatr Otorhinolaryngol 1995;32(suppl):S135-S144.

4. Bothwell MR, Parsons DS, Talbot A, Barbero GJ, Wilder B. Outcome of reflux therapy on pediatric chronic sinusitis. Otolaryngol Head Neck Surg 1999;121:255-62.

5. Ulualp SO, Toohill RJ, Hoffmann R, Shaker R. Possible relationship of gastroesophagopharyngeal acid reflux with pathogenesis of chronic sinusitis. Am J Rhinol 1999;13:197-202.

6. Halstead LA. Role of gastroesophageal reflux in pediatric upper airway disorders. Otolaryngol Head Neck Surg 1999; 120:208-14.

7. Hamilos DL. Gastroesophageal reflux and sinusitis in asthma. Clin Chest Med 1995;16:683-97.

8. Ward PH, Hanson DG. Reflux as an etiological factor of carcinoma of the laryngopharynx. Laryngoscope 1988;98:1195-9.

9. Little FB, Koufman JA, Kohut RI, Marshall RB. Effect of gastric acid on the pathogenesis of subglottic stenosis. Ann Otol Rhinol Laryngol 1985;94:516-9.

10. Zalzal GH, Choi SS, Patel KM. The effect of gastroesophageal reflux on laryngotracheal reconstruction. Arch Otolaryngol Head Neck Surg 1996;122:297-300.

11. Wilson JA, White A, von Haacke NP, et al. Gastroesophageal reflux and posterior laryngitis. Ann Otol Rhinol Laryngol 1989;98:405-10.

12. Koufman JA. The otolaryngologic manifestations of gastroesophageal reflux disease (GERD): a clinical investigation of 225 patients using ambulatory 24-hour pH monitoring and an experimental investigation of the role of acid and pepsin in the development of laryngeal injury. Laryngoscope 1991;101 (suppl 53).

13. Nelson SP, Chen EH, Syniar GM, Christoffel KK. Prevalence of symptoms of gastroesophageal reflux during childhood: a pediatric practice-based survey. Pediatric Practice Research Group. Arch Pediatr Adolesc Med 2000;154:150-4.

14. Koufman J, Sataloff RT, Toohill R. Laryngopharyngeal reflux: consensus conference report. J Voice 1996;10:215-6.

15. Hanson DG, Kamel PL, Kahrilas PJ. Outcomes of antireflux therapy for the treatment of chronic laryngitis. Ann Otol Rhinol Laryngol 1995;104:550-5.

16. Winter HS, Madara JL, Stafford RJ, Grand RJ, Quinlan JE, Goldman H. Intraepithelial eosinophils: a new diagnostic criterion for reflux esophagitis. Gastroenterology 1982;83:818-23.

17. Cucchiara S, Santamaria F, Minella R, et al. Simultaneous prolonged recordings of proximal and distal intraesophageal pH in children with gastroesophageal reflux disease and respiratory symptoms. Am J Gastroenterol 1995;90:1791-6.

18. Gustafsson PM, Tibbling L. 24-Hour oesophageal two-level pH monitoring in healthy children and adolescents. Scand J Gastroenterol 1988;23:91-4.

19. Matthews BL, Little JP, McGuirt WF Jr, Koufman JA. Reflux in infants with laryngomalacia: results of 24-hour double-probe pH monitoring. Otolaryngol Head Neck Surg 1999;120: 860-4.

Ann Otol Rhinol Laryngol 110:2001

IDIOPATHIC PROGRESSIVE SUBGLOTTIC STENOSIS: FINDINGS AND TREATMENT IN 52 PATIENTS

HERBERT H. DEDO, MD MICHAEL D. CATTEN, MD

SAN FRANCISCO, CALIFORNIA

Rarely, patients develop severe idiopathic subglottic stenosis. In 34 years, we have observed this disorder in 52 patients. All but 1 of the patients were female — a finding that suggests a hormonal cause. Without treatment, the airway progressively narrows — in some cases, until the patient requires tracheotomy. Laser submucosal resection and rotation mucosal flaps open and stabilize the airway and provide effective palliation. However, unlike traumatic subglottic stenosis, which has been cured with this technique, the idiopathic form causes submucosal fibrosis that regenerates spontaneously. Thus, treatment helps, but does not cure, the patient. The characteristic pathological finding is of submucosal dense fibrotic tissue with evidence of chronic inflammation. The clinical findings and treatment are here discussed.

KEY WORDS — idiopathic subglottic stenosis, mucosal flap, treatment.

INTRODUCTION

Idiopathic progressive subglottic stenosis (IPSS) is a rare, slowly progressive inflammatory process that is limited to the cricoid cartilage and the first 1 or 2 tracheal rings. The patients are overwhelmingly female (only 2 male cases in nearly 150 found in our review of the literature). There is no recent history of intubation or obvious trauma to the subglottis.

Several studies have attempted to determine the cause of IPSS. Little, Koufman, et al created subglottic stenosis in dogs by application of acid to the subglottis[1] and claimed an above-average incidence of gastric reflux in the IPSS population.[2] Follow-up studies have discussed an association with gastroesophageal reflux disease (GERD),[3-5] but the rarity of IPSS in comparison to the claimed common occurrence of GERD makes a direct association unlikely. Research into an association between IPSS and granulomatous diseases has also been explored without conclusive results.[6] Because of the high female preponderance, a female hormonal cause has been pursued. Stenotic tissue from the subglottis has been tested for estrogen receptors without success.[5] In summary, the cause of IPSS remains unknown.

Many treatment strategies have been tried for IPSS. Steroids, dilation, local resection, laryngotracheal segmental resection and primary anastomosis, resection with stents and mucosal grafting, and micro-trapdoor flaps have all been used. All have achieved only temporary orifice enlargement. The stenosis is progressive, and many patients require tracheotomy.

We here report on 52 patients with IPSS treated over 30 years by the senior author (H.H.D.). We discuss their clinical features and results with surgical management.

MATERIALS AND METHODS

Data Collection. A retrospective chart review was performed of 52 patients with IPSS first seen between 1970 and 2000. Data were collected with regard to age at presentation, gender, nature and duration of symptoms, previous local surgery or trauma, number and type of operations, steroid treatment if received, GERD symptoms and treatment, and presence of other potentially related illness.

The preoperative measurements of the stenosis at first and last operations, the number of operations performed, and the time of follow-up are recorded in the Table. Careful measurements were made with a 2- or 4-mm outside diameter suction tip at the worst level of stenosis in the posterior-anterior and lateral dimensions (the smallest orifice). The vertical length, from the top edge to the bottom edge of the stenosis, was estimated. Tracheotomies that were present at presentation or required during treatment and surgical histopathology reports were also recorded. Eight patients were tested for estrogen receptors in the submucosal connective tissue.

Operative Procedure. A CO_2 laser was used to create mucosal flaps and excise the connective tissue between the cricoid cartilage and the mucosa. Segmental tracheal resection and primary anastomosis was performed in 3 patients with unsatisfactory results. Jet ventilation was used for anesthesia with a

---

From the Department of Otolaryngology–Head and Neck Surgery, University of California at San Francisco, San Francisco, California.

Presented at the meeting of the American Laryngological Association, Orlando, Florida, May 13-14, 2000.

CORRESPONDENCE — Herbert H. Dedo, MD, Dept of Otolaryngology–Head and Neck Surgery, University of California at San Francisco, 350 Parnassus Ave, #501, San Francisco, CA 94117.

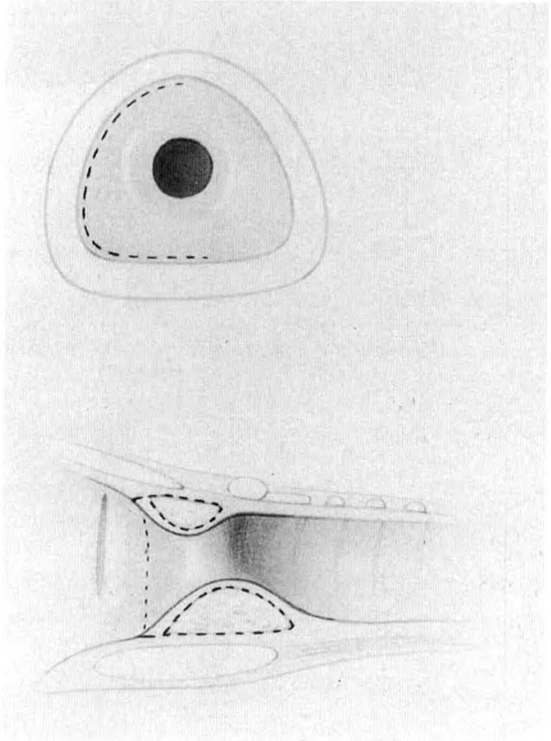

Fig 1. Lateral and top views of stenotic area. Incision is made from 6 to 12 o'clock as viewed from top, thus not exceeding half of tracheal circumference. Area of submucosal resection outlined with dotted line is seen on lateral view.

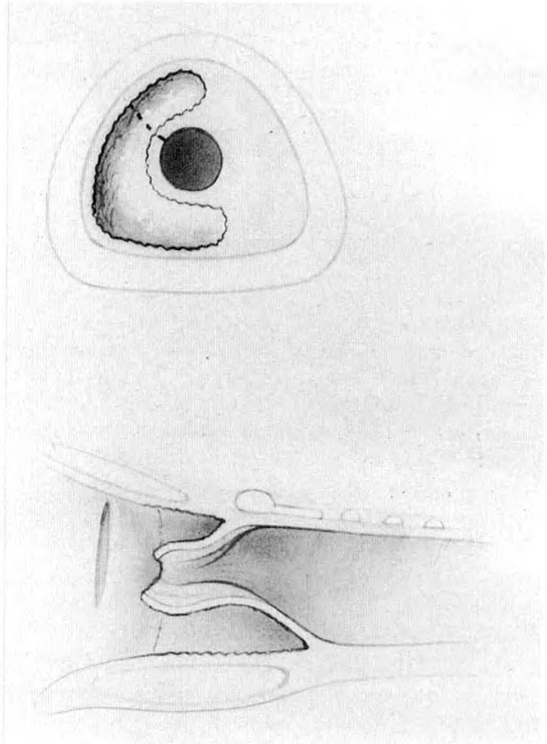

Fig 2. Lateral and top views of stenotic area. Submucosal tissue has been resected while preserving overlying mucosa. Dotted line shows flap incision at 10 o'clock.

Sanders-Venturi system via the ventilation-suction channel on the Dedo-Pilling "laser" laryngoscope (Pilling Co, Fort Washington, Pa). If a tracheotomy was present, a metal-wrapped endotracheal tube was placed through the tracheotomy orifice for ventilation. The operative microscope was used in all cases to visualize the subglottis. Use of an oral-tracheal tube through the larynx was avoided, because it obscures visualization of the stenosis and orifice, distorts the operative field, and, if inserted through the stenosis at the beginning of the procedure, damages the mucosa at the narrowest orifice.

Before presentation at our facility, 9 patients had been treated with dilation, and 4 patients with wedge resections, without lasting improvement. The operative techniques used at our institution included segmental partial cricoid and upper tracheal resection with laryngeal release and anastomosis (3 patients) and use of local mucosal rotation flaps after CO_2 laser submucosal resection (50 patients). Laser submucosal resection with mucosal rotation flaps was the preferred procedure at our institution because it could be done endoscopically, could be repeated when necessary, and had a lower rate of morbidity than open surgical procedures.

First, an incision is made with the CO_2 laser (model 5000C, Coherent Medical Co, Santa Clara, Calif) at the point on the superior surface of the stenosis at which it meets the normal-diameter subglottic airway (1- to 2-mm spot size, 20 W, continuous wave). The incision does not exceed half of the tracheal circumference (Fig 1). The fibrotic tissue is then excised with the laser in the submucosal plane, with preservation of the overlying mucosa (Fig 2). When the submucosal resection is complete, the mucosa is cut with microscissors to create 2 (based at 6 and 12 o'clock) or 3 mucosal flaps. These flaps are rotated into position to cover as much as possible of the raw surface on the adjacent lateral tracheal wall (Fig 3). They usually prevent complete immediate reformation of the stenotic area, but over time (2 to 12 months), the submucosal connective tissue regenerates. No sutures are placed to hold the flap in position, as the raw undersurface adheres to the adjacent raw tracheal wall.

The patients generally returned every 2 months to have the procedure repeated on the opposite side (Fig 4). If the orifice remained over 8 × 8 mm for 2 months, the interval between operations was gradually lengthened to 4 to 12 months, depending on the rate of orifice reduction. Tracheotomy was performed if the diameter of the airway decreased to 3 × 4 mm, or if the patient felt significant dyspnea on exertion.

One patient required tracheotomy in the postoper-

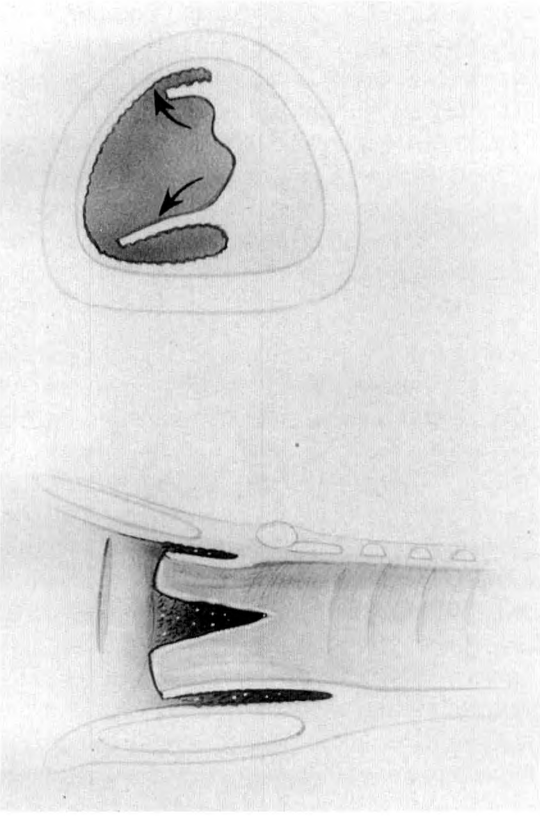

Fig 3. Top drawing is top view of preserved mucosa after resection of submucosal tissue. Incision was made vertically in mucosa, creating 2 flaps that rotate to partially cover raw surface. Bottom drawing is lateral view of rotation flaps created by incision of preserved mucosa. Each flap rotates to partially cover raw surface and speed re-epithelialization.

ative period because of flap swelling. There were no other complications of the procedure.

RESULTS

We have observed IPSS in 52 patients between 1970 and 2000. Two patients were excluded because they did not return after the initial visit, leaving 50 patients in the study. All of the cases, except for 1 questionable case, were in women. (The male patient's subglottic scar is improving so rapidly that we now think it was most likely due to an endotracheal tube injury incurred 10 years earlier. His posterior scar is now gone, and in all the female patients, this is the worst area. Hence, this patient's case is different.) Their ages at presentation to our office ranged from 15 to 77 years (average, 43.5 years). The durations of treatment and follow-up ranged from 6 months to 25 years (average, 71 months), with the ages at last follow-up ranging from 21 to 84 years (average, 50 years). Two patients were related (mother and daughter).

Forty patients presented with dyspnea on exertion as the presenting symptom, and 15 patients presented with noisy breathing. Asthma was the erroneous initial diagnosis in 12 patients, resulting in as much as 18 months' delay in diagnosis. The duration of symptoms before presentation varied between 2 months and 8 years.

None of the patients had a history of cervical trauma or intubation for prolonged periods of time. Six patients were intubated for brief anesthesia between 3 and 15 years before the onset of symptoms. One patient underwent tracheotomy 24 years before the onset of IPSS for an airway emergency of unclear cause at 15 years of age and was decannulated 3 weeks after the event.

Thirty-seven patients were questioned regarding gastroesophageal reflux. Six patients with symptoms were aggressively treated with antireflux medication (omeprazole and cimetidine) without any improvement in their subglottic stenosis course. Another 2 patients had negative pH probe studies. Thirty-one patients had no clinical complaints of reflux.

Indirect and direct laryngoscopy shows 4 types of subglottic stenosis. Type 1 has pink swelling on or just below the undersurface of the vocal cords (6 patients). Type 2 has identical findings to type 1 with the addition of pink swelling on the inner surface of the posterior cricoid cartilage, below the posterior glottis (5 patients). Type 3 is a circular stenosis in the cricoid cartilage that sometimes involves the first tracheal ring (39 patients). This type is always shorter in length anteriorly (usually 1 cm) than posteriorly (2 to 3 cm) and thus on lateral view mimics the shape of the cricoid cartilage. Last, 5 patients presented with type 4 stenosis. This variant is a circumferential stenosis 2 to 3 cm long with 2 levels of narrow orifices:

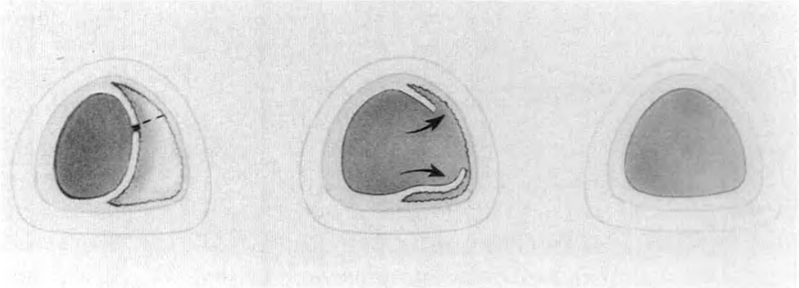

Fig 4. Procedure similar to that in Figs 1-3, repeated on right side, with healed appearance 2 months later.

1 in the cricoid cartilage and the other in the first or second tracheal ring.

All stenoses were noted to start just below the inferior edge of the vocal cords, ie, 1 to 1.5 cm below the free edges of the vocal cords. The maximum stenosis was in the cricoid cartilage. The vocal cord function was usually unimpaired.

Measurements were taken of the stenosis at the narrowest point before the first operation. The average was 4 mm (range, 0 to 8 mm) in the anterior-posterior measurement and 5 mm (range, 0 to 11 mm) in the lateral plane, with an average cross-sectional area of 21 mm^2. At last follow-up, the average measurements were an average of 6 mm posterior-anterior (range, 0 to 10 mm) by 7 mm laterally (range, 0 to 12 mm), with an average cross-sectional area of 46 mm^2 (see Table). One patient had minimal stenosis at first, but progressed to a 12-mm^2 narrowing despite 11 procedures. In 32 patients, the average estimate of the length of the posterior (worst) portion of the stenosis in the superior-inferior plane was 2.3 cm before the first operation and 1.6 cm before the last operation.

Fifteen patients presented with a tracheotomy, and another 10 tracheotomy procedures were performed at our institution. Eight patients were successfully decannulated, and another 4 patients have tracheotomies that are constantly capped but are left in place for ease of giving general anesthesia. Thirteen patients still require open tracheotomy for comfortable breathing. One patient presented with a T-tube that was successfully removed after several operations with mucosal rotation flaps.

DISCUSSION

Most cases of subglottic stenosis occur 4 to 12 weeks after prolonged intubation with an oversized endotracheal tube or an overinflated cuff that results in necrosis of the subglottic mucosa. Other causes include external trauma, granulomatous diseases including Wegener's granulomatosis, tuberculosis, and benign or malignant neoplasms.

Idiopathic subglottic stenosis is a unique form of subglottic stenosis. The cause is truly unknown, despite significant efforts to find one. Gastroesophageal reflux disease has been explored as the source of IPSS.[1,3] Several authors have reported significant reduction or elimination of IPSS by treating GERD.[7,8] Koufman[2] claimed an increased incidence of silent GERD in patients with IPSS. Only 7 of our 38 patients questioned about GERD actually had symptoms. Although no attempt was made to test for "silent" reflux, all patients with symptoms were treated with H2 blockers or proton pump inhibitors without any improvement or slowing of the recurrence of IPSS. Positing GERD as a cause does not explain why almost all patients are female. If GERD were the underlying cause, one would expect many more male patients. Also, GERD is currently a fashionable condition that is diagnosed frequently, whereas IPSS is very rare. The vast difference in incidence between these two conditions makes a causal relationship dubious at best.

Some authors suggest that IPSS is simply an atypical presentation of a granulomatous disease such as Wegener's granulomatosis.[6,9] In a study of 189 patients with Wegener's granulomatosis, subglottic stenosis was found in 43 (23%), with no other areas of granuloma or scar in 21 of those patients.[10] De Vries et al[11] demonstrated an elevated level of antineutrophil cytoplasmic antibodies in 6 patients with presumed idiopathic subglottic stenosis who did not have a diagnosis of granulomatous disease. One patient in our series had a high level of antineutrophil cytoplasmic antibodies without other signs of Wegener's granulomatosis. The other 49 patients all had normal levels of antineutrophil cytoplasmic antibodies. Given the long follow-up of our patients, we would expect to see other manifestations of Wegener's granulomatosis, if this was indeed the underlying cause. No trend of systemic illness, including Wegener's granulomatosis, was identified as a major contributing factor in our series.

A history of intubation is not found in most patients with IPSS. Only 6 of our 50 patients were ever intubated before becoming symptomatic. Each intubation was done for brief anesthesia 3 to 15 years before the onset of symptoms. With the above-mentioned theories excluded by history and testing, we believe our 50 cases are truly idiopathic.

Interestingly, this condition occurs almost exclusively in women (51 of 52 patients in our study). There are only 3 male patients with IPSS described in almost 150 cases in the literature. The reason why men are not affected as frequently remains unknown, but the preponderance of women suggests a female hormonal cause. The presence of sex hormone receptors has been demonstrated in the larynx and other head and neck sites.[12,13] Benjamin et al,[5] however, failed to demonstrate estrogen receptors in 10 samples taken from the stenotic area of patients with IPSS. Using immunohistochemical analysis, we did not find estrogen receptors in the 8 patients we tested. As Benjamin et al indicated, this may reflect a low receptor density or a lack of technique sensitivity. Also in support of a female hormonal cause, we observed that the recurrence of stenosis slowed in wom-

DATA ON PATIENTS WITH IDIOPATHIC PROGRESSIVE SUBGLOTTIC STENOSIS

				Initial Measurement		*Last Measurement*	
Patient	*Age at Presentation (y)*	*Follow-up (mo)*	*No. of Operations*	*Orifice Area (mm²)*	*Vertical Length (cm)*	*Orifice Area (mm²)*	*Vertical Length (cm)*
1*	56	11	3	42	3	90	1
2	48	77	13	64	1.5	81	1.5
3	77	84	7	24	1	24	1
4	56	46	19	4	2	49	2
5	30	15	6	64	1	30	1.5
6	52	50	17	20	2	36	2
7	15	111	17	12.25	2	12	1
8	43	21	9	48	4	42	3
9	46	168	4	30	2	Normal	1
10	51	72	13	12	1	81	0.5
11	49	60	4	20	1.5	110	1
12	72	6	2	44	NA	66	1
13	58	6	3	12	3	28	2
14	27	60	23	16	2	81	1
15	63	34	12	9	3	Normal	1
16	70	26	3	25	2	100	2
17	20	13	1	16	2	NA	1
18	58	192	9	16	2	60	1
19	45	6	3	40	2	64	1
20	26	101	18	56	2	16	2
21	42	192	25	16	2	30	1
22	32	36	4	16	2	20	2
23	32	120	22	21	NA	16	2
24	48	20	2	16	NA	12	2
25	45	27	9	16	1	17.5	1
26	32	156	5	15	NA	20	2
27	75	11	4	24	2.5	48	1
28	25	240	2	8	1	8	1
29	50	22	7	5	NA	9	1
30	48	11	4	48	NA	42	1
31	24	78	3	30	1.5	60	1
32	55	6	2	20	2	Normal	1
33	33	63	3	16	NA	36	1
34	49	108	10	24	1	72	1.5
35	55	9	6	16	1	48	2
36	24	41	8	12	NA	16	2
37	28	39	5	16	3	72	2
38	49	48	5	16	3	0	3.5
39	37	84	5	9	NA	30	2
40	24	247	16	18	3	72	1
41	48	33	8	12	2	72	1
42	40	161	11	NA	NA	12	4
43	41	16	2	36	1.5	72	1
44	55	150	6	16	1	30	1
45	54	19	6	16	3	24	2
46	58	18	7	20	2	36	3
47	37	12	6	6	2	24	1
48	30	86	22	2	NA	15	1.5
49	45	66	10	24	2	100	2
50	43.9	16	3	15	2	90	2

*Only male patient in series. NA — not available.

P24739

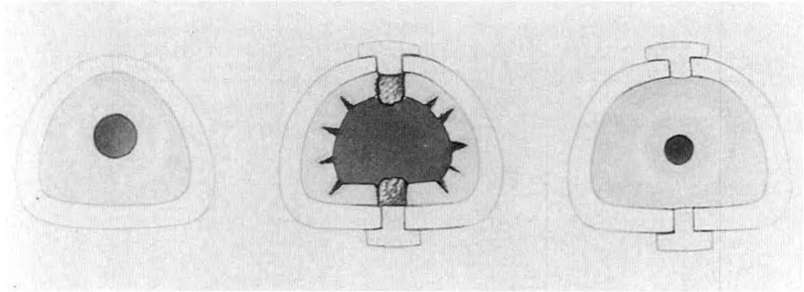

Fig 5. Top view of subglottic stenosis treated with anterior and posterior grafts. This procedure addresses submucosal connective tissue proliferation problem by enlarging outer cartilage framework without removing submucosal scar. In our experience, this procedure has led to worse restenosis in patients with idiopathic progressive subglottic stenosis, because problem of submucosal scar proliferation is not addressed, and grafts stimulate granulation tissue formation.

en as they became older, and especially when they became menopausal. The lack of reported IPSS in the literature before the widespread usage of oral contraceptives made us wonder whether there was a correlation. Despite our search for a possible causal relationship, we could not demonstrate one. The fact that use of oral contraceptives is now commonplace and that IPSS remains rare argues against a direct cause and effect. Although objective data are lacking, we recommended that our patients avoid oral contraceptives and hormonal supplementation, but we have not seen that this slows the recurrence of stenosis.

The other key feature of IPSS, besides its being idiopathic, is the progressive nature of the stenosis. Histologic evaluation of biopsy specimens shows dense submucosal fibrotic tissue. Initially, this may represent an exaggerated extracellular response to a chemical stimulus, and later, it may be partially the result of previous surgery. More detailed histologic analysis found thick fibrotic tissue, poorly cellular, with no evidence of vasculitis or foreign body reaction.[5] Unlike traumatic subglottic stenosis, which usually can be resected and cured, IPSS continues to produce subglottic stenosis, because the presumed chemical stimulus for the fibrotic response is still present. It has been our experience that IPSS is a chronic, lifetime disease, and that multiple surgical treatments are needed for palliation.

Currently, there is no cure for IPSS. The treatment is to maintain an adequate airway without tracheotomy. Medical treatments have included antireflux medications, steroids, and discontinuation of oral contraceptives. In our experience, these treatments have little or no impact. Steroids were used in an attempt to reduce the subglottic stenosis. Although they appeared to slow the recurrence in some of our patients (unpublished observation), they did not prevent recurrence or make the stenosis disappear once it had developed. Because of the serious long-term side effects of chronic steroid use, and the lack of a curative effect, we no longer use them.

Numerous surgical procedures have been proposed for the treatment of IPSS. Mucosal rotation flaps, dilation, segmental resection, stenting, and skin grafting have all been attempted. Grillo et al[9] first reported good to excellent results in 32 of 35 patients with IPSS treated with single-stage reconstruction. Despite their reported long-term success with single-stage resection and that of others, our experience in 7 cases has been that the stenosis returns even after aggressive segmental resection of the cricoid cartilage up to the inferior edge of the thyroid cartilage and down to the second tracheal ring. Conceptually, segmental resection addresses a submucosal connective tissue problem by removing the abnormal airway segment. However, cutting the anterior and posterior cricoid cartilage and installing a bone or cartilage graft enlarges the framework, but does not remove the excess submucosal scar tissue that is the site of the disorder. Cartilage grafts also stimulate granulation tissue formation and lead to restenosis (Fig 5). Other authors have observed this phenomenon.[14] We have attempted resection in 3 patients and were also referred 4 patients who had return of stenosis after aggressive resection at other institutions. Only 1 of our patients, of those treated with resection, experienced long-term patency of the subglottis without revision surgery using mucosal flaps. One patient went on to total stenosis 18 months after the

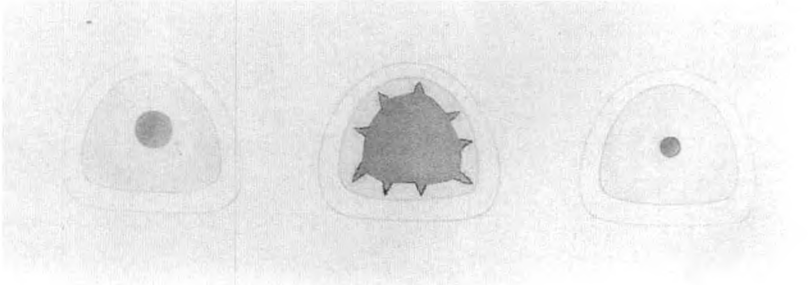

Fig 6. Top view of subglottic stenosis treated with dilation and/or wedge incisions. Mucosa is torn, leaving adjacent areas of exposed connective tissue that scar and contract. In addition, submucosal fibrosis is stimulated and not excised. Result is worse stenosis.

resection. We attribute the failure to cure IPSS with segmental resection to our inability to resect the whole cricoid cartilage, and thus the top of the abnormal connective tissue, and still preserve functional and mobile cricoarytenoid joints. In addition, segmental resection is a major operation with significant morbidity and requires skilled teams of auxiliary hospital personnel and intensive care unit staff that may not be available at every institution.

We have found that dilation and wedge resection with dilation of the orifice rim performed before the patients were referred to us has resulted in worse stenosis. Dilation tears the mucosa and does not reduce the abnormal submucosal tissue (Fig 6). Other authors have reported mixed results with these and other procedures.[5,15]

All current surgical treatments for IPSS are essentially palliative, with complete success (defined as no recurrent stenosis and no tracheotomy) being less than 50% in reported series. Of our 50 patients, 13 still require a tracheotomy, and 16 have required more than 10 revision surgeries. This outcome translates into 21 patients (42%) who were apparently disease-free over the long term. With this consideration, we believe that laser submucosal resection with mucosal rotation flaps provides the best surgical treatment. First, the procedure is performed endoscopically, in contrast to open techniques, which increasingly scar the anterior commissure with each procedure. In addition, it can be done in an outpatient center, in contrast to the intensive care unit–level care required for open techniques. The morbidity and cost are also significantly lower with mucosal rotation flaps than with laryngeal tracheal reconstruction. Last, because all IPSS patients will likely need revision, the least invasive, least morbid procedure should be performed.

CONCLUSION

A rare condition, IPSS is not always recognized early. It is progressive in nature, and treatment is still only palliative. The cause is unknown. Further study is needed to identify the cause and devise a cure. In our experience, repeated endoscopic laser submucosal resection and rotation mucosal flaps provide the least invasive means of maintaining an airway without a tracheotomy.

REFERENCES

1. Little FB, Koufman JA, Kohut RI, Marshall RB. Effect of gastric acid on the pathogenesis of subglottic stenosis. Ann Otol Rhinol Laryngol 1985;94:516-9.

2. Koufman JA. The otolaryngologic manifestations of gastroesophageal reflux disease (GERD): a clinical investigation of 225 patients using ambulatory 24-hour pH monitoring and an experimental investigation of the role of acid and pepsin in the development of laryngeal injury. Laryngoscope 1991;101 (suppl 53).

3. Jindal JR, Milbrath MM, Shaker R, Hogan WJ, Toohill RJ. Gastroesophageal reflux disease as a likely cause of "idiopathic" subglottic stenosis. Ann Otol Rhinol Laryngol 1994;103: 186-91.

4. Zalzal GH, Choi SS, Patel KM. The effect of gastroesophageal reflux on laryngotracheal reconstruction. Arch Otolaryngol Head Neck Surg 1996;122:297-300.

5. Benjamin B, Jacobson I, Eckstein R. Idiopathic subglottic stenosis: diagnosis and endoscopic laser treatment. Ann Otol Rhinol Laryngol 1997;106:770-4.

6. Stolovitzky JP, Todd NW, Cotton RT, Campbell WG. Autoimmune hypothesis of acquired subglottic stenosis: lack of support at time of surgical repair in children. Int J Pediatr Otorhinolaryngol 1997;38:255-61.

7. Halstead LA. Gastroesophageal reflux: a critical factor in pediatric subglottic stenosis. Otolaryngol Head Neck Surg 1999;120:683-8.

8. Walner DL, Stern Y, Gerber ME, Rudolph C, Baldwin CY, Cotton RT. Gastroesophageal reflux in patients with subglottic stenosis. Arch Otolaryngol Head Neck Surg 1998;124: 551-5.

9. Grillo HC, Mark EM, Mathisen DJ, Wain JC. Idiopathic laryngotracheal stenosis and its management. Ann Thorac Surg 1993;56:80-7.

10. Langford CA, Sneller MC, Hallahan CW, et al. Clinical features and therapeutic management of subglottic stenosis in patients with Wegener's granulomatosis. Arthritis Rheum 1996; 39:1754-60.

11. De Vries N, Gans ROB, Donker AJM, Goldschmeding R, Hoorntje SJ, Snow GB. Autoantibodies against constituents of neutrophils in the diagnosis and treatment of (isolated) subglottic stenosis. Arch Otolaryngol Head Neck Surg 1992;118: 1120-3.

12. Virolainen E, Vanharanta R, Carey TE. Steroid hormone receptors in human squamous cell lines. Int J Cancer 1984;33: 19-25.

13. Molteni A, Warpeha RL, Brizio-Molteni L, Fors EM. Estradiol receptor-binding protein in head and neck neoplastic and normal tissue. Arch Surg 1981;116:207-10.

14. Stell PM, Maran AGD, Stanley RE, Murray JAM. Chronic laryngeal stenosis. Ann Otol Rhinol Laryngol 1985;94:108-13.

15. Park SS, Streitz JM, Rebeiz EE, Shapshay SM. Idiopathic subglottic stenosis. Arch Otolaryngol Head Neck Surg 1995;121: 894-7.

Ann Otol Rhinol Laryngol 110:2001

LASER CORDOTOMY VERSUS RADIOTHERAPY: AN OBJECTIVE COST ANALYSIS

JAMES H. BRANDENBURG, MD
MADISON, WISCONSIN

This study presents a cost analysis of and comparison between laser cordotomy and external beam irradiation for the treatment of early glottic carcinoma. It compares the curative results of the two modalities from data of a retrospective study at my institution and a literature review of published cure rates. It also reviews the results of objective voice assessments in cases representing both treatments. The findings of this study indicate that the cure rates are equivalent and that voice quality obtained after laser cordotomy is comparable to that obtained after irradiation, yet the total cost of external beam radiotherapy is significantly higher than that of laser surgery. Hence, the findings of this study provide strong support for initially treating early glottic tumors with laser surgery.

KEY WORDS — cost-benefit analysis, laser surgery, long-term larynx preservation, T1 glottic carcinoma.

INTRODUCTION

Health care costs have risen dramatically in recent years, prompting increasing focus on the delivery of medical care in the United States. As measured by the consumer price index, medical costs have increased at more than twice the average price rise for all goods in general during the past decade.[1] As a result, cost minimization strategies are already becoming necessary to ensure that medical care is accessible to all and at an affordable price. These strategies include choosing the least costly of competing treatments when both the success rate and the quality of life are essentially the same. Such is the case with external beam radiotherapy and endoscopic laser surgery as competing treatments for early glottic cancers. The high cost of radiotherapy is now being challenged, especially when compared to the much lower cost of endoscopic laser cordotomy.

At many institutions, radiotherapy has been considered the preferred treatment option because of the assumption that it can result in a superior voice compared to the surgical options. However, when objective voice analyses are made on patients with early glottic tumors treated with irradiation, the majority exhibit a significant degree of dysphonia, and very few have "normal voices."

The concept of endoscopic removal of early glottic carcinoma is not new. Lynch,[2] in 1920, described his technique of suspension laryngoscopy and reported operating on 9 tumors endoscopically with 6 cures. Lillie and DeSanto,[3] in 1973, published a series of 96 patients with early glottic carcinomas that were removed with endoscopic cordectomy. One patient required total laryngectomy because of recurrence, and 5 other recurrences were treated successfully with another endoscopic resection. No patients died of their early glottic cancer, and none underwent radiotherapy. In 1972, a series of reports on CO_2 laser excision of cordal carcinoma began to be published by a group from Boston University, who stressed the anatomic limitations of this technique and established guidelines for the careful selection of cases for laser surgery.[4-7]

This study presents a comparison between endoscopic laser surgery and radiotherapy in terms of recurrence rates, long-term larynx preservation, and ultimate survival rates for cases of early glottic cancer evaluated and treated initially at the University of Wisconsin Hospital and Clinics. It reviews the results of our previous investigative studies of objective voice analyses of 11 laser cordotomy patients and 20 radiotherapy patients. Last, it compares the average total direct costs of therapy for each modality, and notes to what extent these costs have risen over the past decade.

METHODS AND MATERIALS

Patients. A retrospective review of 74 patients who underwent their initial evaluation and treatment for early glottic cancer (T1N0) at the University of Wisconsin Hospital and Clinics from 1989 to 1999 was undertaken to determine the outcome of patients treated with either radiotherapy or endoscopic laser surgery. The data for this study were gathered by reviewing patients' hospital charts, the Head and Neck

---

From the Division of Otolaryngology–Head and Neck Surgery, University of Wisconsin Hospital, Madison, Wisconsin.

Presented at the meeting of the American Laryngological Association, Orlando, Florida, May 13-14, 2000.

CORRESPONDENCE — James H. Brandenburg, MD, Division of Otolaryngology–Head and Neck Surgery, University of Wisconsin Hospital, 600 Highland Ave, Madison, WI 53792-3236.

Oncology Tumor Board records, and charges obtained from the billing offices of University of Wisconsin Hospital and Clinics and the University of Wisconsin Medical Foundation. Patients with a diagnosis of carcinoma in situ were not included. Patients with any prior primary treatment of their glottic cancer elsewhere were not included. All patients were followed in either the otolaryngology outpatient clinic or the radiotherapy outpatient clinic for 1 to 11 years (median, 5.3 years).

Forty-four patients were treated with radiotherapy at University Hospital and Clinics (41 patients) and its affiliated regional hospitals (3 patients). There were 38 men and 6 women. The median age was 63.2 years (range, 33 to 88 years). The therapy consisted of hyperfractionation (2 treatments per day) with cobalt small field external beam radiation by means of a beam directed shell. The average total dose delivered varied from 65 to 70 Gy. Forty-two patients had T1a cancers, and 2 patients had T1b cancers.

Thirty patients underwent endoscopic laser surgery at University of Wisconsin Hospital and Clinics Outpatient Surgery; 22 of these operations were performed by the author. There were 27 men and 3 women. The median age was 64.5 years (range, 41 to 87 years). Twenty-eight patients had T1a cancers; 6 had the anterior commissure involved, 1 had the posterior vocal cord and vocalis process involved, and 2 patients had T1b cancers.

Surgical Procedure. Direct microlaryngoscopy is performed as an outpatient procedure under general endotracheal anesthesia, and a frozen section of the biopsy specimen is obtained. After the pathologist has confirmed the diagnosis of glottic carcinoma, we then proceed with an en bloc resection of the tumor using a CO_2 laser with a microspot cutting beam. Additional anterior and posterior frozen sections are usually taken to ensure tumor-free margins of the resection. The patient is discharged on the day of surgery.

Voice Analysis. A review of 2 objective voice assessment studies of 20 patients who underwent irradiation of the glottis and 11 patients who were treated with laser cordotomy, the details of which have been reported,[8,9] is analyzed for this study. The objective voice assessments consisted of measures of aerodynamics and duration, laryngovideostroboscopy, and acoustic analysis. The fundamental frequency (F_0) mean and range, maximum duration, airflow, and volume were measured for sustained vowels /i/ and /a/. Acoustic analyses of jitter (frequency perturbation), signal-to-noise ratio, and F_0 were performed with C-Speech 3.0 (Paul Milankovic, University of Wisconsin, Madison, Wis, 1989) from direct recordings of the digitized and inverse filtered waveform.

Cost-Benefit Analysis. The current charges for each modality were determined by taking the average of all charges for 3 patients who underwent endoscopic laser surgery and comparing these with the average of all charges for 3 patients who underwent radiotherapy. The hospital charges for each of the patients were obtained from the billing office of the University of Wisconsin Hospital and Clinics. The professional charges were obtained from the billing office of the University of Wisconsin Medical Foundation.

Diagnostic Evaluation. Since the pretreatment evaluation is identical for both radiotherapy and endoscopic laser surgery, none of the costs incurred in establishing a diagnosis of glottic cancer were figured into the cost for either modality.

Endoscopic Laser Surgery. These charges include additional hospital and professional charges for proceeding to definitive surgery after the diagnosis had been confirmed by direct microlaryngoscopy and biopsy. The hospital costs include charges for the use of laser equipment, 30 to 60 minutes of additional operating room time, and further laboratory expenses. The professional costs include additional charges for the laryngologist, anesthesiologist, and pathologist.

Radiotherapy. The University of Wisconsin Hospital includes charges for computed tomography simulation, treatment simulation, treatment aid block, dosimetry calculation, weekly port x-ray films, weekly in vivo dosimetry, weekly physics quality assurance, and daily complex treatment delivery. The professional costs include charges for consultation, complex teletherapy, treatment device design and construction, complex therapeutic simulation, treatment planning, and weekly megavoltage treatments by the radiation oncologist.

No attempt was made to assess either direct nonmedical costs, such as transportation and lodging of the patient undergoing radiotherapy, or indirect costs, which might include a loss of wages or a decrease in earnings during treatment. Although these costs do have an economic impact, it was impossible to accurately determine these additional expenses retrospectively. Consequently, those factors were considered to be beyond the scope of this study.

RESULTS

Voice Quality. All patients in both the radiotherapy group and the endoscopic laser surgery group experienced some degree of dysphonia after treatment, which varied from a near-normal voice to significant breathiness and hoarseness, depending on the

TABLE 1. PUBLISHED OUTCOMES FOR T1 GLOTTIC TUMORS TREATED WITH RADIOTHERAPY

Authors	*N*	*Tumor Recurrence* *No.*	*Tumor Recurrence* *%*	*Total Laryngectomy for Surgical Salvage*	*Ultimate Survival (%)*
Foote et al[10]	57	3	5.3%	2	100
Morris et al[11]	38	10	26.3%	6	97
Kaiser et al[12]	102	35	34.3%	25	88
Jose et al[13]	81	10	12.3%	9	97
Woodhouse et al[14]	183	37	20.2%	29	97
Mittal et al[15]	147	30	20.4%	23	95
Van Den Bogaert et al[16]	138	22	15.9%	19	90
Minja et al[17]	174	28	16.1%	21	97
Fletcher[18]	332	37	11.1%	36	98
Harwood[19]	571	78	13.7%	72	95
Present study	44	9	20.5%	6	95.5
Total	1,867	299	16.0%	248 (13.3%)	95.3

site and extent of the tumor. In previously published studies from the University of Wisconsin Hospital and Clinics, we compared voice quality, in a comprehensive voice assessment protocol, in 20 radiotherapy patients and 11 laser cordotomy patients.[8,9] We observed the following. The airflow rate of the laser patients was elevated compared to that of the irradiated patients. Both groups demonstrated a reduced phonation time. The frequency range was reduced in both groups, especially in the higher frequencies, and the intensity range was decreased in both groups. The values for jitter, shimmer, and signal-to-noise ratio were elevated in both laser and radiotherapy patients. Breathiness is the predominant vocal feature after laser tumor resection, whereas harshness and raspiness (glottic fry) are the predominant vocal features of irradiated patients. Laryngovideostroboscopy showed a loss of vibration and stiffness at the site of laser resection, with a normal mucosal wave observed on the opposite vocal cord. In the irradiated group of patients, the loss of vibration and stiffness were seen to involve both vocal cords, probably because of submucosal fibrosis occurring as a consequence of radiation damage to the underlying stroma.

Cure Rates. There were 9 recurrences in the group of 44 patients who initially underwent radiotherapy, as shown in Table 1.[10-19] One patient was successfully re-treated with a partial laryngectomy, and 6 patients were salvaged with a total laryngectomy. The long-term larynx preservation rate in this series was 86%. Two patients (5%) ultimately died of their glottic cancer.

There were 5 recurrences in the group of 30 patients who underwent endoscopic laser surgery, as shown in Table 2.[7,20-26] Two patients with small recurrences underwent retreatment procedures with laser that resulted in clear surgical margins. In 1 of these cases, on the advice and encouragement of the radiation oncologist, the patient underwent postoperative irradiation. Two patients with small recurrences were successfully salvaged with radiotherapy. One patient underwent a partial laryngectomy that failed, and a total laryngectomy was subsequently performed. Overall, 29 of the 30 patients (97%) in this series enjoyed larynx preservation. There were no deaths due to glottic tumors.

Cost-Benefit Analysis. In this study, I elected to compare only the actual costs of the two modalities,

TABLE 2. PUBLISHED OUTCOMES FOR T1 GLOTTIC TUMORS TREATED WITH ENDOSCOPIC LASER SURGERY

Authors	*N*	*Recurrence* *No.*	*Recurrence* *%*	*Laser Salvage*	*RT Salvage*	*Surgical Salvage* *Partial Laryngectomy*	*Surgical Salvage* *Total Laryngectomy*	*Ultimate Survival (%)*
Wetmore et al[20]	21	4	19.0	1	3	0	0	100
Koufman[21]	23	1	4.3	1	0	0	0	100
Blakeslee et al[7]	35	4	11.4	0	2	0	2	94.3
Elner and Fex[22]	31	6	19.3	3	3	0	0	100
Steiner[23]	130	10	7.7	6	1	2	1	100
Myers et al[24]	46	4	8.7	0	3	1	0	100
Thomas et al[25]	29	7	24.1	3	0	3	0	100
Wolfensberger and Dort[26]	41	8	19.5	1	7	0	2	100
Present study	30	5	16.7	2	2	0	1	100
Total	386	50	12.9	17 (4.4%)	21 (5.4%)	6 (1.5%)	6 (1.5%)	99.5

TABLE 3. ITEMIZED AVERAGE COSTS FOR ENDOSCOPIC LASER SURGERY (AFTER DIAGNOSIS HAS BEEN CONFIRMED BY BIOPSY)

Hospital charges	
Additional operating room ($8.55/min)	$ 513 (1 h)
Use of laser	$ 414
Clinical laboratory ($57 per frozen section)	$ 114
Average total hospital charges	$1,041
Professional charges	
Laryngologist ($1,598 – $1,423)	$ 175
Anesthesiologist	$ 255
Pathologist	$ 422
Average total professional charges	$ 852
Average grand total for laser surgery	$1,893

TABLE 4. ITEMIZED AVERAGE COSTS FOR RADIOTHERAPY

Hospital charges	
Computed tomography simulation, complex	$ 1,091
Treatment simulation, complex	$ 1,068
Treatment aid block, complex	$ 168
Computed tomography dosage, complex	$ 962
Port film (×6)	$ 58
In vivo dosimetry	$ 284
Physics quality assurance (×7)	$ 171
Treatment delivery complex (per day)	$ 389
Average total hospital charges	$19,809
Professional charges	
Level 4 consultation	$ 265
Therapeutic simulation	$ 379
Therapeutic treatment planning	$ 783
Treatment device design and construction, complex	$ 242
Teletherapy complex	$ 313
Weekly megavoltage treatment management, complex	$ 820
Average total professional charges	$ 9,544
Average grand total for radiotherapy	$29,353

since the cost of confirming a diagnosis of cancer by biopsy is identical for each. Consequently, I did not include any charges for performing the direct laryngoscopy and biopsy. The charges for the laser resection of the tumor are then, in effect, all of the charges for the continuation of the surgery after the direct laryngoscopy and biopsy has established the diagnosis of cancer.

The itemized costs for proceeding to endoscopic laser microresection of the tumor are presented in Table 3. To arrive at the surgeon's charges, the cost for the direct microlaryngoscopy and biopsy (current procedural terminology [CPT] code 31536; $1,423) is deducted from the cost of the direct microlaryngoscopy and cordotomy (CPT code 31541; $1,598). The average total hospital charges, $1,041 (range, $985 to $1,297), and the average total professional charges, $852 (range, $787 to $917), come to a grand total of $1,893.

The itemized costs for radiotherapy as the primary treatment for early glottic cancer are presented in Table 4. The average total professional charges, $9,544 (range, $9,440 to $9,696), and the average total hospital charges, $19,809 (range, $19,653 to $19,965), come to a grand total of $29,353. At our institution, radiotherapy is 15.5 times more costly than endoscopic laser surgery.

Cost Containment. The most revealing aspect of this study is that the cost of radiotherapy has risen dramatically during the past decade, as seen in Table 5.[9] In 1990, we conducted a similar cost study between radiotherapy and laser cordotomy for the treatment of early cordal carcinoma.[9] Table 5 reflects a comparison of the increases in cost for the treatment options over this 10-year period. The professional charges for radiotherapy have risen from $3,029 to $9,544, an increase of 215%. The hospital charges for radiotherapy have also risen dramatically, from $7,634 to $19,809, an increase of 159%. Overall, the total radiotherapy charges from 1990 to 1999 have

TABLE 5. AVERAGE TOTAL COSTS FOR TREATMENT IN 1990 AND 1999

	Laryngologist Charges	*(All) Professional Charges*	*Hospital Charges*	*Total Charges*
Radiotherapy				
1990[9]		$3,029	$ 7,634	$10,663
1999		$9,544	$19,809	$29,353
Difference		$6,515	$12,175	$18,690
% Increase		215%	159%	175%
Endoscopic laser surgery*				
1990[9]	$1,423	$2,322	$3,623†	$5,945
1999	$1,589	$2,936	$3,292§	$6,774
Difference	$ 175	$ 614	(–$331)	$1,172
% Increase	12.3%	26.4%	(–9%)	19.7%

*Includes biopsy and definitive treatment.

†Surgery performed in inpatient surgical suites.

§Surgery performed in ambulatory (outpatient) surgical suites.

increased 175%. In figuring the increase in cost for endoscopic laser surgery from 1990 to 1999, I included the cost of the biopsy together with the definitive treatment, since our calculations in 1990 were done in this manner. The charge by the laryngologist for this surgery (CPT code 31541) has only increased by $175 (12.3%) over the decade. A comparison of hospital charges for 1990 and those for 1999 is impossible, since there was no outpatient surgical facility at our institution in 1990, and all surgery was performed in the inpatient surgical suites, where costs are considerably higher than in the outpatient operating rooms. Operating room charges were subsequently reduced significantly when our ambulatory (outpatient) surgical facility was built in 1992. The total of all professional charges (laryngologist, anesthesiologist, and pathologist) increased 26.4% during this decade.

DISCUSSION

Voice Quality. The rationale given for selecting radiotherapy rather than surgery for the treatment of early glottic cancers is that this modality can restore the voice. This assumption is based on subjective voice assessments made by either the patient or a health care provider. Kaiser et al[12] evaluated the voice quality of 102 patients who had undergone radiotherapy and observed that 59% had good voices, 5% had fair voices, and 36% had poor voices. This report was in contrast to a study by a group of radiation oncologists at Mayo Clinic[10] who reported on their voice assessment of 57 patients treated with radiotherapy. A physician subjectively determined the voice quality to be excellent in 9%, good in 70%, fair in 18%, and poor in 4%. The problems with subjective voice studies are that they may be insensitive to small voice changes and that they may be subject to biases on the part of those who do the judging.

In our study on objective assessment of voice production of 20 patients who had undergone radiotherapy for early glottic cancer,[8] there was a wide variation in the patients' perception of their own voices. When asked about hoarseness, fatigue, dryness, loudness, and pitch, only 2 of the 20 patients reported having no problems. There was also a poor correlation between the self-assessments and the degree of dysphonia as determined by objective measures.

Delsupehe et al[27] conducted a perceptual voice comparison study between 12 patients treated with radiotherapy and 30 patients treated with narrow-margin laser cordotomy for early glottic tumors. In their evaluation of all parameters of voice production, they found no statistical difference between the two groups 24 months after treatment.

McGuirt et al[28] reported similar results when speech pathologists rated both laser cordotomy patients and irradiated patients and found their voices to be indistinguishable and abnormal. They concluded that when strict criteria are met, the voice attained after endoscopic laser surgery, by objective and subjective measurements, is equal to the voice attained after irradiation, in patients with comparable tumors.

My experience has led me to think that the size and site of the cancer may well have greater impact on the voice quality that exists after treatment than does the mode of therapy selected. For example, patients with anterior commissure tumors will experience poor functional voices after treatment, regardless of the modality used.

Cure Rates. Table 1 shows that in 1,867 patients with cordal cancers initially treated with irradiation, the recurrence rate was 16.0% (range among series, 5.3% to 34.3%). Table 2 shows that in 386 patients with similar early glottic tumors initially treated with endoscopic laser surgery, the recurrence rate was 12.9% (range among series, 4.3% to 24.1%).

In our group of 44 patients initially treated with irradiation, 20.5% (9 of 44) developed recurrent cancer (Table 1), and in our group of 30 patients initially treated with laser cordotomy, 16.7% (5 of 30) developed recurrences (Table 2).

A review of the published series shown in Table 1 reveals that when radiotherapy fails, 75% of the surgical salvages require total laryngectomy; 13.3% of the 1,867 patients with early cordal tumors initially treated with radiotherapy eventually lost their larynges to persistent cancer. In contrast, only 1.5% of patients with early cordal tumors initially treated with endoscopic laser surgery eventually had total laryngectomy (Table 2).

In our group of 44 patients treated primarily with irradiation, 13.6% (6 of 44) ultimately underwent total laryngectomy for surgical salvage, whereas in our group of 30 patients initially treated with laser surgery for early glottic cancer, 1 patient (3.3%) was salvaged with total laryngectomy.

The average ultimate survival rate in the radiotherapy series was 95.3% (Table 1), and that in the laser cordotomy series was 99.5% (Table 2).

Cost-Benefit Analysis. The management of health care by managing health care dollars is becoming increasingly popular in the United States, especially when the results of treatment options are equal. Hoffman and Karnell,[29] using data collected by the National Cancer Data Base from 1986-87 and 1992, estimated that there are approximately 12,500 new cases of laryngeal cancer in the United States per year. In that study, 61.2% of the staged laryngeal cancers were of glottic origin. Further extrapolation of the data in that report shows that stage I glottic carcinoma represents 34.8% of all staged laryngeal carcinomas registered with the Data Base. From the data for patients with known clinical staging, we can then estimate that there are 4,350 new cases of early glottic cancers presenting annually. Seventy-six percent of the patients with stage I laryngeal carcinoma underwent radiotherapy. About one third of these cases were recorded as having multimodality therapy (irradiation and surgery), but this was thought to be an artifact of data collection, and the "surgery" most likely represented a laryngeal biopsy followed by single-modality treatment in the form of irradiation.

If one accepts the premise that 76% of patients with early glottic cancer do undergo irradiation as initial single-modality treatment, then approximately 3,300 patients were treated primarily with irradiation in 1999. Using as an average the radiotherapy costs at our institution ($29,353 per patient), I calculate the approximate total cost of radiotherapy throughout the nation for the treatment of early glottic cancers as $96,864,900. As an alternative, if these 3,300 patients were treated with endoscopic laser surgery, using the charges per patient at our institution ($1,893) as the average throughout the nation, I calculate the total cost for laser surgery as $6,246,900 (3,300 times $1,893), representing a cost savings in health care dollars of $90,618,000 ($96,864,000 minus $6,246,000). Clearly, not every patient with an early cordal tumor is a candidate for endoscopic laser surgery. Yet, if even half of these 3,300 patients were to be treated with endoscopic laser surgery rather than with irradiation, the cost savings in health care dollars, $45,309,000, is still significant.

When the results of this study in terms of voice quality, cancer recurrence, long-term larynx preservation, ultimate survival rate, and, finally, cost are compared between the two treatment modalities (radiotherapy and endoscopic laser surgery), endoscopic laser surgery appears to be the single-modality treatment of choice for early-stage glottic carcinoma, and the concept of restricting its use to highly selected cases is no longer valid.

ACKNOWLEDGMENT — The author thanks Kristi Wisniewski, Assistant Director of Business Services, Department of Surgery, University of Wisconsin Medical School, for her assistance in obtaining all of the patients' charges used in this study.

REFERENCES

1. US Bureau of Labor Statistics. Consumer Price Index, December 1997. Washington, DC: US Department of Labor, 1997.

2. Lynch RC. Intrinsic carcinoma of the larynx with a second report of the cases operated on by suspension and dissection. Trans Am Laryngol Assoc 1920;42:119-26.

3. Lillie JC, DeSanto LW. Transoral surgery of early cordal carcinoma. Trans Am Acad Ophthalmol Otolaryngol 1973;77: ORL92-ORL96.

4. Strong MS, Jako GJ. Laser surgery in the larynx. Early clinical experience with continuous CO_2 laser. Ann Otol Rhinol Laryngol 1972;81:791-8.

5. Vaughan DW, Strong MS, Shapshay SM. Treatment of T1 and in situ glottic carcinoma: the transoral approach. Otolaryngol Clin North Am 1980;13:509-13.

6. Davis RK, Jako GJ, Hyams VJ, Shapshay SM. The anatomic limitations of CO_2 laser cordectomy. Laryngoscope 1982; 92:980-4.

7. Blakeslee D, Vaughan CW, Shapshay SM, Simpson GT, Strong MS. Excisional biopsy in the selective management of T1 glottic cancer: a three-year follow-up study. Laryngoscope 1984;94:488-94.

8. Lehman JJ, Bless DM, Brandenburg JH. An objective assessment of voice production after radiation therapy for stage I squamous cell carcinoma of the glottis. Otolaryngol Head Neck Surg 1988;98:121-9.

9. Cragle SP, Brandenburg JH. Laser cordectomy or radiotherapy: cure rates, communication, and cost. Otolaryngol Head Neck Surg 1993;108:648-54.

10. Foote RL, Buskirk SJ, Grado GL, Bonner JA. Has radiotherapy become too expensive to be considered a treatment option for early glottic cancer? Head Neck 1997;19:692-700.

11. Morris MR, Canonico D, Blank C. A critical review of radiotherapy in the management of T1 glottic carcinoma. Am J Otolaryngol 1994;15:276-80.

12. Kaiser TN, Sessions DG, Harvey JE. Natural history of treated T1N0 squamous carcinoma of the glottis. Ann Otol Rhinol Laryngol 1989;98:217-9.

13. Jose B, Calhoun DL, Mohammed A. Recurrences after irradiation in early vocal cord cancer with literature review. J Surg Oncol 1984;27:224-7.

14. Woodhouse RJ, Quivey JM, Fu KK, Sien PS, Dedo HH, Phillips TL. Treatment of carcinoma of the vocal cord: a review of 20 years experience. Laryngoscope 1981;91:1155-62.

15. Mittal B, Rao DV, Marks JE, Perez CA. Role of radiation in the management of early vocal cord carcinoma. Int J Radiat Oncol Biol Phys 1983;9:997-1002.

16. Van Den Bogaert W, Ostyn F, Van Der Schueren E. Glottic carcinoma limited to the vocal cords. Acta Radiol Oncol 1982;21:33-7.

17. Minja BM, van den Broek P, Huygen PL, Kazem I. Primary radiation therapy for T1 glottic cancer. Factors influencing local control. Clin Otolaryngol 1984;9:93-8.

18. Fletcher GH. Textbook of radiotherapy. 3rd ed. Philadelphia, Pa: Lea and Febiger, 1980:330-63.

19. Harwood AR. Cancer of the larynx — the Toronto experience. J Otolaryngol 1982;11(suppl 11):1-21.

20. Wetmore SJ, Key JM, Suen JY. Laser therapy for T1 glottic carcinoma of the larynx. Arch Otolaryngol Head Neck Surg 1986;112:853-5.

21. Koufman JA. The endoscopic management of early squamous carcinoma of the vocal cord with the carbon dioxide surgical laser: clinical experience and a proposed subclassification. Otolaryngol Head Neck Surg 1986;95:531-7.

22. Elner A, Fex S. Carbon dioxide laser as primary treatment of glottic T1S and T1A tumours. Acta Otolaryngol Suppl (Stockh) 1988(suppl 449):135-9.

23. Steiner W. Results of curative laser microsurgery of laryngeal carcinomas. Am J Otolaryngol 1993;14:116-21.

24. Myers EN, Wagner RL, Johnson JT. Microlaryngoscopic surgery for T1 glottic lesions: a cost-effective option. Ann Otol Rhinol Laryngol 1994;103:28-30.

25. Thomas JV, Olsen KD, Neel HB III, DeSanto LW, Suman VJ. Recurrences after endoscopic management of early (T1) glottic carcinoma. Laryngoscope 1994;104:1099-104.

26. Wolfensberger M, Dort JC. Endoscopic laser surgery for early glottic carcinoma: a clinical and experimental study. Laryngoscope 1990;100:1100-5.

27. Delsupehe KG, Zink I, Lejaegere M, Bastian RW. Voice quality after narrow-margin laser cordectomy compared with laryngeal irradiation. Otolaryngol Head Neck Surg 1999;121:528-33.

28. McGuirt WF, Blacock D, Koufman JA, et al. Comparative voice results after laser resection or irradiation of T1 vocal cord carcinoma. Arch Otolaryngol Head Neck Surg 1994;120:951-5.

29. Hoffman HT, Karnell LH. Laryngeal cancer. In: Steele GD, Jessup JM, Winchester DP, Menck HR, Murphy GP, eds. National Cancer Data Base Annual Review of Patient Care 1995. Atlanta, Ga: American Cancer Society, 1995:84-99.

≈

NINTH INTERNATIONAL FACIAL NERVE SYMPOSIUM

The Ninth International Facial Nerve Symposium will be held July 29 to August 1, 2001, in San Francisco, California. For information, contact Office of Continuing Medical Education, University of California, San Francisco; telephone: (415) 476-5808; fax: (415) 502-1795; e-mail: info@ocme.ucsf.edu.

Ann Otol Rhinol Laryngol 110:2001

STELLATE CELLS IN THE HUMAN VOCAL FOLD

KIMINORI SATO, MD, PHD

MINORU HIRANO, MD TADASHI NAKASHIMA, MD

KURUME, JAPAN

Cells have been discovered that are star-like in appearance and that actively synthesize extracellular matrices in the human adult vocal fold mucosa. These cells have no nomenclature and are thus designated as vocal fold stellate cells (VFSC) in this study. Light and electron microscopic investigation of VFSC in the human vocal fold mucosa was carried out on excised human adult larynges. A comparison between VFSC and conventional fibroblasts was made. The results are summarized as follows. 1) The VFSC are distributed in human adult maculae flavae. 2) The VFSC are irregular and stellate in shape, possessing slender cytoplasmic processes. 3) Lipid droplets are present in the cytoplasm. 4) The VFSC have a small nucleus-cytoplasm ratio and well-developed rough endoplasmic reticulum, suggesting active protein synthesis in these cells. 5) No basal lamina is present, and filaments can be seen in the cytoplasm. 6) The VFSC show strong cytoplasm staining with periodic acid–Schiff stain and type III collagen. 7) The VFSC actively synthesize collagenous fibers, including reticular fibers, as well as other extracellular matrices, such as elastic fibers and glycosaminoglycan (hyaluronic acid). 8) The VFSC, first demonstrated in this study, actively synthesize extracellular matrices in the human adult vocal fold mucosa under normal conditions. 9) The VFSC participate in the metabolism of the extracellular matrices essential for the viscoelastic properties of the lamina propria of the human adult vocal fold mucosa as a vibrating tissue.

KEY WORDS — extracellular matrix, larynx, stellate cell, ultrastructure, vocal fold.

INTRODUCTION

The viscoelastic properties of the lamina propria of the human vocal fold mucosa are essential for vibrating behavior and depend on extracellular matrices such as collagenous fibers, elastic fibers, glycoproteins, and glycosaminoglycan (proteoglycan). Fibrillar collagen serves as a stabilizing scaffold in the extracellular matrices. The 3-dimensional structure of the reticular fibers, which are one of the fibrillar collagens, in the vocal fold mucosa is a key component for the structural maintenance and viscoelasticity of the vibrating tissue.[1] The complex of reticular fibers and other extracellular matrices is very important for the viscoelastic properties of the human vocal fold mucosa.[1]

Fibroblasts are among the interstitial cells that produce collagenous fibers and other extracellular matrices. Some fibroblasts in the human vocal fold mucosa were previously found to be star-like cells, and we described them as fibroblasts.[2-7]

Some morphological and functional differences between the star-like nonconventional fibroblasts and conventional fibroblasts are revealed in this report. The presence of star-like cells in the human adult vocal fold is demonstrated here for the first time. These cells have no nomenclature and are thus designated as vocal fold stellate cells (VFSC) for convenience in this report. The morphological and functional characteristics of VFSC were investigated and compared with those of conventional fibroblasts by light and electron microscopy.

MATERIALS AND METHODS

Five normal human adult larynges from autopsy cases ranging in age from 49 to 59 years (3 men and 2 women) were used. For light microscopy, specimens were fixed in 10% formalin, dehydrated in graded concentrations of ethanol, and embedded in paraffin. Hematoxylin and eosin, elastica–van Gieson (EVG), silver, periodic acid–Schiff (PAS), and Alcian blue stainings were used for each section. Elastica–van Gieson staining was done for identification of collagenous and elastic fibers. Silver staining was done for reticular fibers and collagenous fibers, and Alcian blue staining (pH 1.0 and pH 2.5) was done for glycosaminoglycan. For the hyaluronidase digestion study, 50 mg of bovine testes hyaluronidase (Sigma, St Louis, Mo) was diluted in 100 mL of phosphate-buffered saline solution (PBS). Thin sections were incubated in the diluted hyaluronidase solution for 2 hours at 37°C. The thin sections were subsequently stained with Alcian blue (pH 2.5). Type I and type III collagens were detected histologically in formalin-fixed and paraffin-embedded tissue by immunohistochemistry, for which a labeled streptavidin-biotin staining kit (Dako, Carpinteria, Calif) was used. All specimens were sectioned at 5- to 6-μm

---

From the Department of Otolaryngology–Head and Neck Surgery, Kurume University, School of Medicine, Kurume, Japan.

Presented at the meeting of the American Laryngological Association, Orlando, Florida, May 13-14, 2000.

CORRESPONDENCE — Kiminori Sato, MD, PhD, Dept of Otolaryngology–Head and Neck Surgery, Kurume University, School of Medicine, 67 Asahi-machi, Kurume 830-0011, Japan.

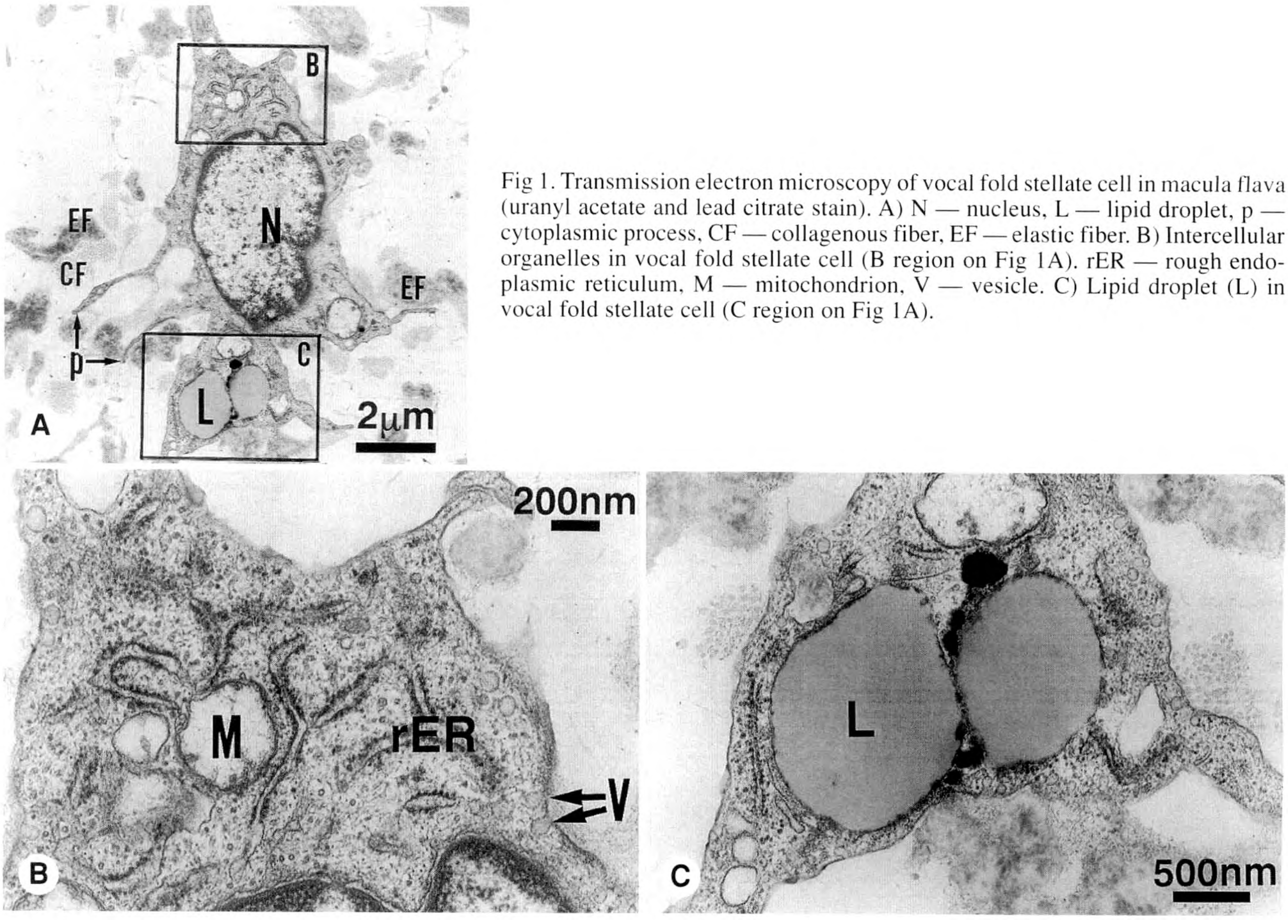

Fig 1. Transmission electron microscopy of vocal fold stellate cell in macula flava (uranyl acetate and lead citrate stain). A) N — nucleus, L — lipid droplet, p — cytoplasmic process, CF — collagenous fiber, EF — elastic fiber. B) Intercellular organelles in vocal fold stellate cell (B region on Fig 1A). rER — rough endoplasmic reticulum, M — mitochondrion, V — vesicle. C) Lipid droplet (L) in vocal fold stellate cell (C region on Fig 1A).

thickness and mounted on glass slides. Deparaffinized and hydrated sections were rinsed with 0.01-mol/L PBS at pH 7.4. The specimens were covered with 3% hydrogen peroxide for 5 minutes and rinsed with 0.01-mol/L PBS, followed by treatment with normal goat serum. The specimens were then incubated with the primary antibody overnight at 4°C. A 1:100 diluted polyclonal antibody against type I and type III collagens (Chemicon International Inc, Temecula, Calif) was used. After rinsing with PBS and labeling with the streptavidin-biotin staining kit, a color reaction was developed with 3,3'-diaminobenzidine for about 10 minutes at room temperature. Immunoreactivity was examined by light microscopy.

For transmission electron microscopy (TEM), the specimens were fixed in 2.5% glutaraldehyde at 4°C for 2 hours, rinsed with cacodylate buffer solution, and postfixed in 2% osmium tetroxide with cacodylate buffer solution at 4°C for 2 hours. After rinsing with cacodylate buffer solution, the specimens were dehydrated in graded concentrations of ethanol and embedded in epoxy resin. Semithin sections were prepared with an ultramicrotome, stained with 1% toluidine blue, and examined with a light microscope. Thin sections were made with an ultramicrotome and stained with uranyl acetate and lead citrate, tannic acid so as to make the glycoprotein and elastin apparent. Observation was conducted with a JEM-2000EX transmission electron microscope (Japan Electron Optic Laboratory Co Ltd, Tokyo, Japan).

RESULTS

MORPHOLOGICAL CHARACTERISTICS OF VFSC IN HUMAN ADULT VOCAL FOLD MUCOSA AND COMPARISON WITH CONVENTIONAL FIBROBLASTS

Many VFSC were distributed in the maculae flavae, but none were found in Reinke's space. Some fibroblasts could be seen throughout the human adult vocal fold mucosa.

Figures 1 and 2 show TEM findings, and Fig 3 shows light microscopic findings of VFSC. The VFSC were irregular and stellate in shape and possessed slender cytoplasmic processes (Figs 1A and 3A).

Lipid droplets were present in the cytoplasm (Figs 1C and 2A,B) and were 1 to 2 μm in diameter. They were distributed not only in the cell body, but also in the cytoplasmic processes, and were of 2 types: membrane-bounded (Fig 2A) and non–membrane-bounded (Fig 2B). The former were each surrounded by a unit membrane. The rough endoplasmic reticulum and membrane-bounded lipid droplets were

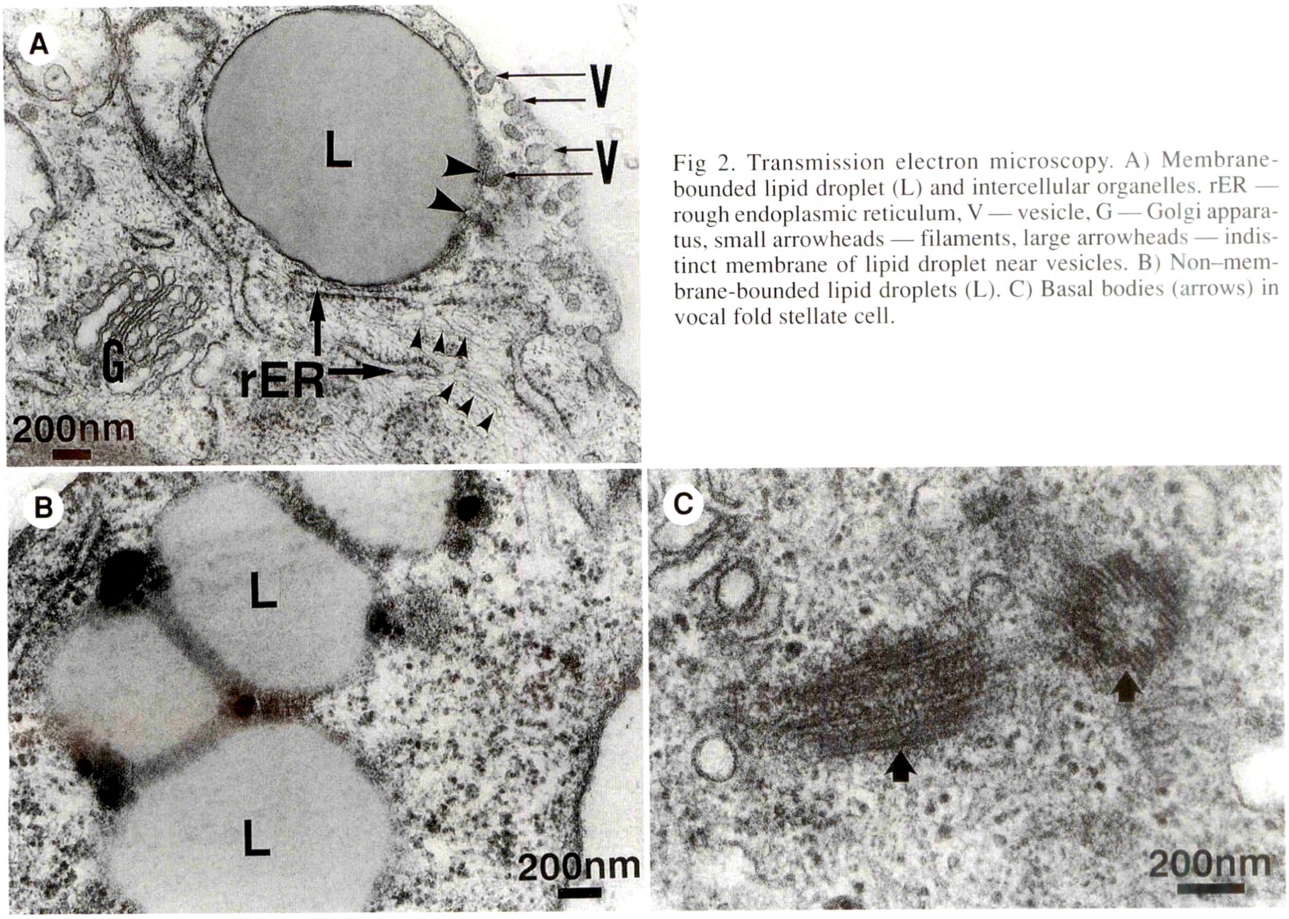

Fig 2. Transmission electron microscopy. A) Membrane-bounded lipid droplet (L) and intercellular organelles. rER — rough endoplasmic reticulum, V — vesicle, G — Golgi apparatus, small arrowheads — filaments, large arrowheads — indistinct membrane of lipid droplet near vesicles. B) Non–membrane-bounded lipid droplets (L). C) Basal bodies (arrows) in vocal fold stellate cell.

closely associated with each other (Fig 2A). Vesicles and lipid droplets were also closely present (Fig 2A). The unit membrane became indistinct near the vesicles (Fig 2A).

The nucleus in VFSC was oval. The nucleus-cytoplasm ratio was small, and a well-developed rough endoplasmic reticulum was present (Figs 1B and 2A). A Golgi apparatus consisting of lamellae associated with vesicles could be seen (Fig 2A). Ten-nanometer-thick filaments were present in the cytoplasm (Fig 2A). Lysosomes were few. Mitochondria were small and few. No basal lamina was found. Along the surface of the VFSC, a number of vesicles were present (Figs 1B and 2A). Occasionally, a basal body was noted in the cytoplasm (Fig 2C).

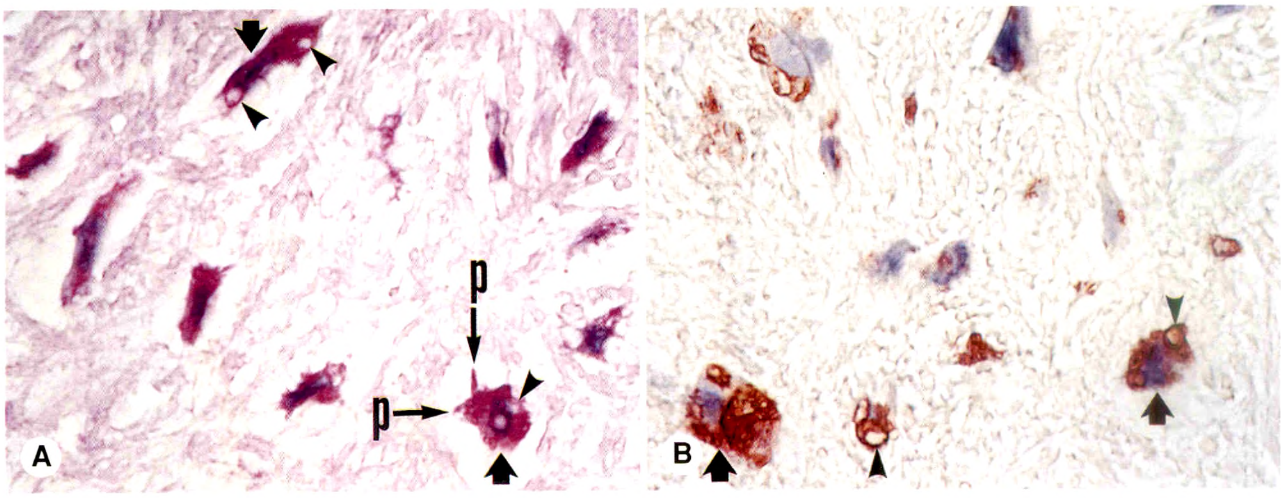

Fig 3. Original ×400. A) Vocal fold stellate cells show strong cytoplasm staining with periodic acid–Schiff stain. Arrows — vocal fold stellate cells, p — cytoplasmic process, arrowheads — lipid droplets. B) Type III collagen in cytoplasm of vocal fold stellate cells, shown by immunohistochemical staining. Arrows — vocal fold stellate cells, arrowheads — lipid droplets.

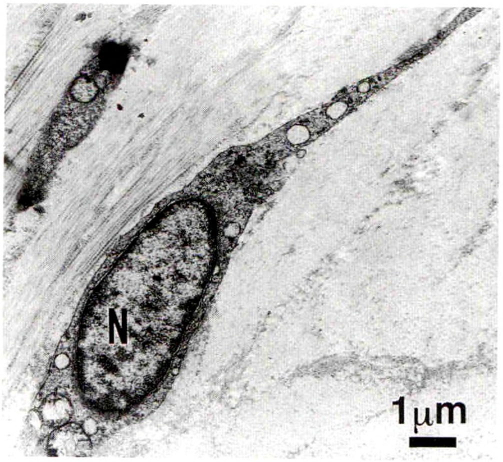

Fig 4. Conventional fibroblast in Reinke's space (transmission electron microscopy). N — nucleus.

The VFSC showed strong cytoplasm staining with PAS (Fig 3A) and type III collagen (Fig 3B), while type I collagen stained few components in the cytoplasm of the VFSC. Lipid droplets were recognized as clear globules in PAS- and type III collagen–precipitated cytoplasm (Fig 3).

The conventional fibroblasts were spindle-shaped or oval (Fig 4), with no processes and few lipid droplets. The fibroblast nuclei were elliptic. The nucleus-cytoplasm ratio was large, and poorly developed rough endoplasmic reticulum and Golgi apparatus were apparent (Fig 4). Filaments were seen in the cytoplasm. There were no basal laminae. Along the surface of the fibroblasts, few vesicles could be seen. The PAS stain and type I and type III collagens stained few components in the cytoplasm of the fibroblasts.

FUNCTIONS OF VFSC IN HUMAN ADULT VOCAL FOLD MUCOSA AND COMPARISON WITH CONVENTIONAL FIBROBLASTS

Collagenous Fibers. There were many collagenous fibers that stained red with EVG (Fig 5A) and silver stain (Fig 5B) around VFSC in human adult maculae flavae. Many reticular fibers, stained black with silver stain, could be detected around the VFSC (Fig 5B). In Fig 6A, an electron microscopic examination was made of the synthesis of collagenous fibers by VFSC. There were many vesicles at the periphery of the cytoplasm, and newly released amorphous materials were present on the cell surface of VFSC. Microfibrils 10 to 15 nm wide were observed around the amorphous materials. Collagenous fibrils were detected near the microfibrils. Thus, the VFSC appear to actively synthesize not only collagenous fibers, but also reticular fibers, in human adult vocal fold mucosa. The electron microscopic study indicated that the conventional fibroblasts synthesized few collagenous fibers (Fig 4).

Elastic Fibers. Many elastic fibers, stained black with EVG staining, were present around VFSC in human adult maculae flavae (Fig 5A). Figure 6B shows electron microscopically the synthesis of elastic fibers by VFSC. There were many vesicles at the periphery of the cytoplasm, and newly released amorphous materials were seen on the cell surface of VFSC. Microfibrils 10 to 15 nm wide were situated around the amorphous materials. There were microfibril assemblies on which elastin appeared to be deposited. The amorphous substance of the elastic fibers may have been produced by fusion of microfibrils. The conventional fibroblasts in the vocal fold mucosa produced few elastic fibers, according to electron microscopy (Fig 4).

Glycosaminoglycan. Maculae flavae were strongly stained light blue with Alcian blue at pH 2.5 (Fig 7), and relatively sparse staining with Alcian blue at pH 1 was noted. The ground substance around VFSC was stained in the same way. Material in the maculae flavae that was strongly stained with Alcian blue (pH

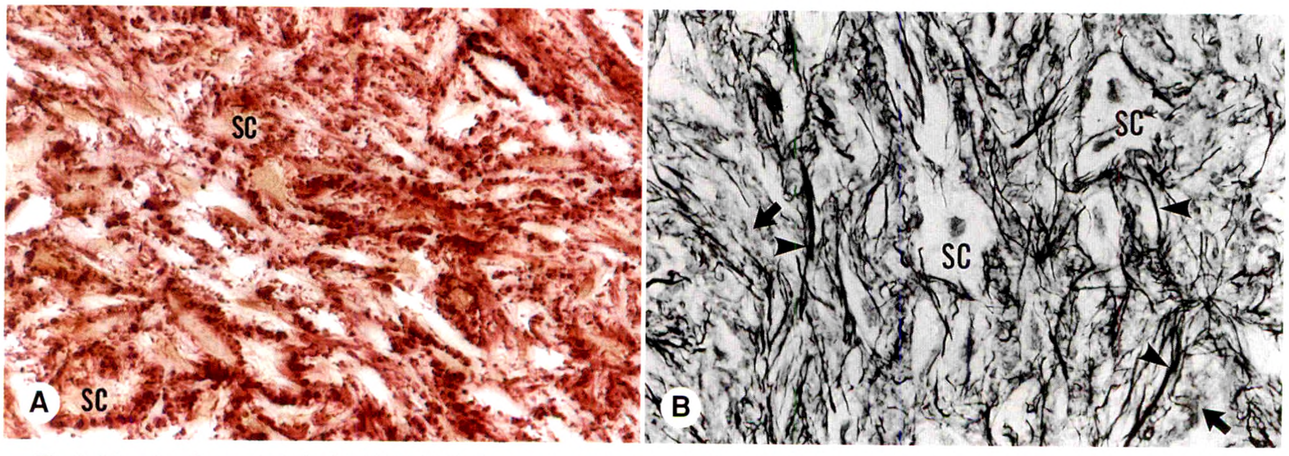

Fig 5. Maculae flavae (original ×400). A) Collagenous (red) and elastic (black) fibers around vocal fold stellate cells (SC) in macula flava (elastica–van Gieson staining). Nuclei of vocal fold stellate cells are shown by yellow color. B) Collagenous (arrows) and reticular (arrowheads) fibers around vocal fold stellate cells (SC) in macula flava (silver staining).

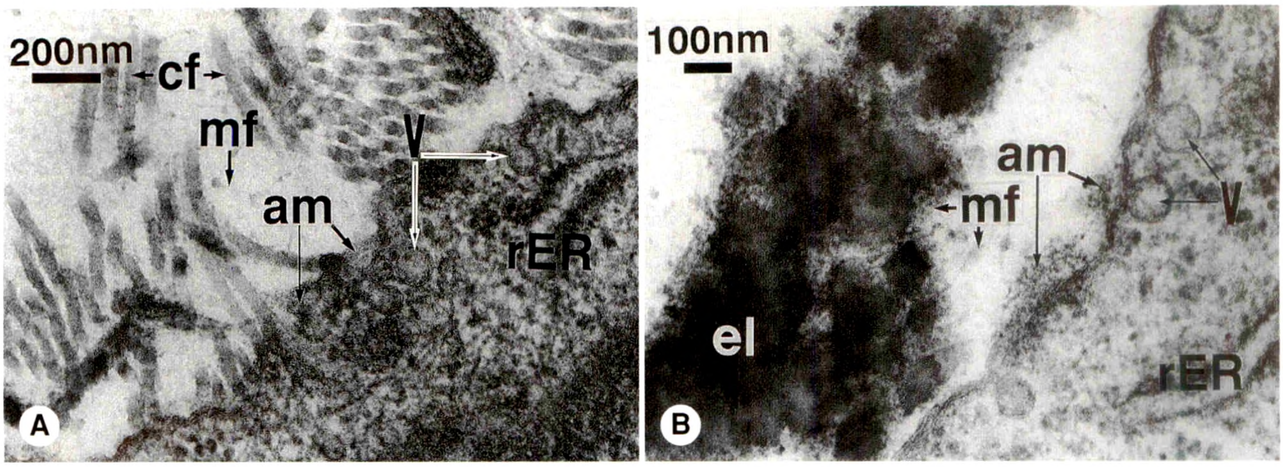

Fig 6. Synthesis of A) collagenous fibers and B) elastic fibers by vocal fold stellate cells (transmission electron microscopy, tannic acid staining). v — vesicle, am — amorphous material, mf — microfibril, cf — collagenous fibril, rER — rough endoplasmic reticulum, el — elastin.

2.5) was digested by hyaluronidase. Much glycosaminoglycan (hyaluronic acid) was situated around the VFSC in the human adult maculae flavae. There was not as much Alcian blue–stained substance around the conventional fibroblasts in the human vocal fold mucosa.

The VFSC located in the human adult maculae flavae and first demonstrated in this study are among the important interstitial cells. They actively synthesize extracellular matrices such as collagenous fibers, including reticular fibers, elastic fibers, and glycosaminoglycan (hyaluronic acid) under normal conditions. The conventional fibroblasts in the human adult vocal fold mucosa synthesize few extracellular matrices under normal conditions.

DISCUSSION

Adult vocal folds have a layered structure consisting of the epithelium; the superficial, intermediate, and deep layers of the lamina propria; and the vocalis muscle.[8,9] These layered structures are very important in vibration.[8] Viscoelasticity of the lamina propria of the vocal fold mucosa (especially the cover, consisting of epithelium and the superficial layer of the lamina propria) is required for vibration and phonation. The viscoelastic properties of the lamina propria are necessary for vibration and depend on extracellular matrices. The 3-dimensional structure composed of extracellular matrices is indispensable to the viscoelastic properties of the human vocal fold mucosa.[1]

The maculae flavae were previously shown to control the synthesis of fibrous components such as the vocal ligaments of human vocal folds.[2] The maculae flavae are essential for the growth, development, and aging of the vocal fold mucosa.[2-4] Some fibroblasts that produce extracellular matrices in the human maculae flavae were previously found to be star-like cells, and we described them as fibroblasts.[2-7] Some morphological and functional differences between nonconventional fibroblasts (star-like cells) and conventional fibroblasts were revealed in this study for the first time.

MORPHOLOGICAL COMPARISON BETWEEN VFSC AND CONVENTIONAL FIBROBLASTS IN HUMAN ADULT VOCAL FOLD MUCOSA

The distribution of fibroblasts differs according to site in the vocal fold mucosa.[6] The cells are dense in the maculae flavae and sparse in Reinke's space.[6,7]

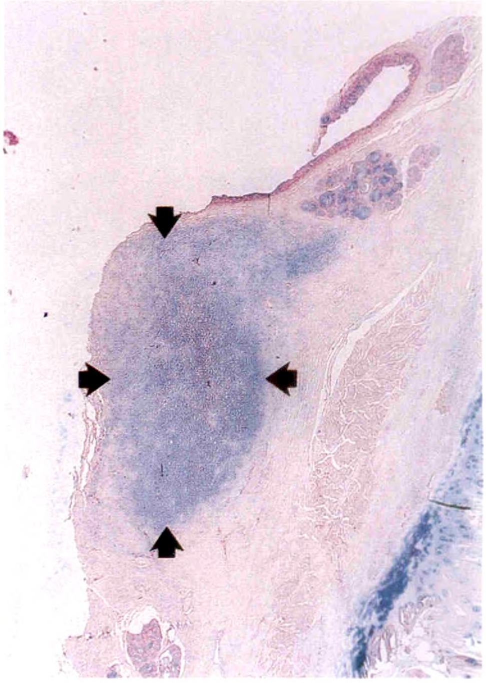

Fig 7. Glycosaminoglycan (hyaluronic acid) around vocal fold stellate cells on coronal section of human vocal fold (Alcian blue staining [pH 2.5], original ×12.5). Posterior macula flava is strongly stained light blue (arrows).

In this study, VFSC were located in the maculae flavae, but were absent in Reinke's space. Conventional fibroblasts were present not only in the maculae flavae, but throughout the vocal fold mucosa.

The VFSC had a fibroblast-like structure essentially the same as that of conventional fibroblasts. The VFSC differed most from conventional fibroblasts in shape, being stellate and possessing slender cytoplasmic processes. Conventional fibroblasts are spindle-shaped or oval.

The VFSC also possessed lipid droplets in the cytoplasm, while fibroblasts had few lipid droplets under normal conditions. Intercellular organelles were also noted in VFSC, in which the nucleus-cytoplasm ratio was small and the rough endoplasmic reticulum was well developed, indicating these cells to be activated and possessing active protein synthesis. The conventional fibroblasts had a large nucleus-to-cytoplasm ratio, less rough endoplasmic reticulum, and fewer Golgi apparatus, and thus are inactive and at rest under normal conditions.

The cell shape on a TEM section is not necessarily the same as that of an entire cell. Some VFSC do not always possess the characteristics specified above. Occasionally, it is difficult to distinguish VFSC from conventional fibroblasts solely on the basis of shape.

The VFSC showed strong cytoplasm staining with PAS, which stained few components in the cytoplasm of conventional fibroblasts. The cytoplasm of VFSC appeared to contain much glycogen and glycoprotein.

The VFSC showed strong cytoplasmic staining with type III collagen, while type I collagen stained few components in the cytoplasm. Type III and type I collagens stained few components in the cytoplasm of conventional fibroblasts under normal conditions. The meaning of these findings is unclear, but possibly may be related to the production of type III collagen and reticular fibers. Type III collagen may become the cell marker of VFSC in human vocal folds.

FUNCTIONAL COMPARISON BETWEEN VFSC AND CONVENTIONAL FIBROBLASTS IN HUMAN ADULT VOCAL FOLD MUCOSA

The VFSC had a well-developed rough endoplasmic reticulum, suggesting active protein synthesis in these cells. The most outstanding functions of VFSC were the active synthesis of collagenous fibers, including reticular fibers, and other extracellular matrices such as elastic fibers and glycosaminoglycan (hyaluronic acid) under normal conditions. These extracellular matrices are dense in the maculae flavae. Conventional fibroblasts produce few extracellular matrices in the human adult vocal fold mucosa under normal conditions.

The predominant collagen in the lamina propria of the vocal folds was previously shown to be type III,[10] a fibrillar collagen traditionally designated as reticular fibers. Fibrillar collagen, such as reticular fibers, serves as a stabilizing scaffold in the extracellular matrices and has been shown to be essential for the structural maintenance and viscoelasticity of vibrating tissue.[1] The delicate 3-dimensional structures of reticular fibers contribute to maintaining the structure of the vocal fold mucosa during vibration without disturbing the vibration.[1] The complex 3-dimensional structure of reticular fibers and other extracellular matrices contributes to maintaining the structure of the vocal fold mucosa and is requisite to the viscoelastic properties of the lamina propria of the vocal fold mucosa, which are very important for the vibratory behavior of the structure.[1]

The VFSC were found here to actively produce extracellular matrices, including reticular fibers, in the vocal fold mucosa under normal conditions. The VFSC may be related to the fibrogenesis that maintains the viscoelastic properties of the human adult vocal fold mucosa. The conventional fibroblasts are inactive and produce few extracellular matrices under normal conditions. The VFSC in the human adult vocal fold mucosa may possibly have some role in the metabolism of the extracellular matrices under normal conditions. The conventional fibroblasts may be activated in a pathological state such as injury of the vocal fold tissue.

As mentioned above, there are many morphological and functional differences between VFSC and conventional fibroblasts in the human adult vocal fold under normal conditions. The VFSC may form an independent cell category that should be considered a new category of cells in the human vocal fold. However, the possibility cannot be excluded that VFSC are a kind of transformed conventional fibroblast.

RELATIONSHIP BETWEEN VFSC AND HEPATIC STELLATE CELLS

Hepatic stellate cells (HSC) resemble VFSC. Stellate cells in the liver were first described by von Kupffer[11] in 1876. However, the true nature of these cells remained unclear until they were rediscovered by Wake[12] in 1971. These cells were formerly known as Ito cells, fat-storing cells, vitamin A–storing cells, lipocytes, perisinusoidal cells, and parasinusoidal cells. The term hepatic stellate cell was established in 1996.[13]

The HSC are important hepatic perisinusoidal cells, are stellate in shape, and have cytoplasmic processes.[12,14] Their most conspicuous feature is the presence of lipid droplets.[12,14,15] Intercellular organelles such as rough endoplasmic reticulum are well developed. The VFSC in the human adult vocal fold mucosa are very similar to HSC.

The storage of vitamin A (retinol) in lipid droplets and fibrogenesis in the liver are the main functions of HSC,[14] and they are correlated.[15] These cells synthesize collagenous fibers, including type III collagen.[15] The retinol contained in lipid droplets controls the fibrogenesis of collagen in HSC, and retinol treatment suppresses collagen synthesis in the liver.[15] Hepatic stellate cells regulate collagen metabolism to produce and digest collagens.[15] The HSC have physiological and pathological functions in the liver.

Whether the lipid droplets in VFSC contain vitamin A could not be determined in this study, since the specimens had been fixed. Rough endoplasmic reticulum and vesicles were closely associated with lipid droplets in the cytoplasm on electron microscopy. The unit membrane of the lipid droplets became indistinct near the vesicles. These findings indicate that the lipid droplets in the VFSC participate in the synthesis of protein and extracellular matrices.

The VFSC actively synthesize extracellular matrices in the human adult vocal fold mucosa under normal conditions. The VFSC in the maculae flavae of human adult vocal folds are involved in the metabolism of extracellular matrices essential for the viscoelastic properties of the lamina propria of the human vocal fold mucosa.

ACKNOWLEDGMENTS — We are grateful to Dr Yuuji Ito and Dr Yasuhiro Nakamura, St Mary's Hospital, Kurume, for providing the cadaver larynges.

REFERENCES

1. Sato K. Reticular fibers in the vocal fold mucosa. Ann Otol Rhinol Laryngol 1998;107:1023-8.

2. Sato K, Hirano M. Histologic investigation of the macula flava of the human vocal fold. Ann Otol Rhinol Laryngol 1995; 104:138-43.

3. Sato K, Hirano M. Histologic investigation of the macula flava of the human newborn vocal fold. Ann Otol Rhinol Laryngol 1995;104:556-62.

4. Sato K, Hirano M. Age-related changes of the macula flava of the human vocal fold. Ann Otol Rhinol Laryngol 1995; 104:839-44.

5. Sato K, Hirano M, Nakashima T. Comparative histology of the maculae flavae of the vocal folds. Ann Otol Rhinol Laryngol 2000;109:136-40.

6. Hirano M, Sato K, Nakashima T. Fibroblasts in human vocal fold mucosa. Acta Otolaryngol (Stockh) 1999;119:271-6.

7. Hirano M, Sato K, Nakashima T. Fibroblasts in geriatric vocal fold mucosa. Acta Otolaryngol (Stockh) 2000;120:336-40.

8. Hirano M. Phonosurgery. Basic and clinical investigation. Otologia (Fukuoka) 1975;21(suppl 1):239-98.

9. Hirano M, Sato K. Histological color atlas of the human larynx. San Diego, Calif: Singular Publishing Group, 1993.

10. Gray SD, Hirano M, Sato K. Molecular and cellular structure of vocal fold tissue. In: Titze IR, ed. Vocal fold physiology. San Diego, Calif: Singular Publishing Group, 1993:1-17.

11. von Kupffer C. Ueber Sternzellen der Leber. Briefliche Mitteilung an Prof Waldeyer. Arch Mikrosk Anat 1876;12:353-8.

12. Wake K. "Sternzellen" in the liver: perisinusoidal cells with special reference to storage of vitamin A. Am J Anat 1971; 132:429-62.

13. Ahern M, Hall P, Halliday J. Hepatic stellate cell nomenclature [Letter]. Hepatology 1996;23:193.

14. Wake K. Perisinusoidal stellate cells (fat-storing cells, interstitial cells, lipocytes), their related structure in and around the liver sinusoids, and vitamin A–storing cells in extrahepatic organs. Int Rev Cytol 1980;66:303-53.

15. Wake K. Liver perivascular cells revealed by gold and silver impregnation methods and electron microscopy. In: Motta PM, ed. Biopathology of the liver. An ultrastructural approach. Dordrecht, the Netherlands: Kluwer Academic Publishers, 1988: 23-36.

Ann Otol Rhinol Laryngol 110:2001

ASSESSMENT OF VESTIBULAR SCHWANNOMA GROWTH: APPLICATION OF A NEW MEASURING PROTOCOL TO THE RESULTS OF A LONGITUDINAL STUDY

ERNESTINE M. STIPKOVITS, MD
KEES GRAAMANS, MD, PHD
G. BOUDEWIJN C. VASBINDER, MD
JOHANNES E. VAN DIJK, MSC, PHD
FREDERIK J. A. BEEK, MD, PHD
UTRECHT, THE NETHERLANDS

This study pertains to a group of 44 patients with unilateral vestibular schwannoma who did not undergo surgery. Prospectively, the dimensions of the tumor were depicted at regular intervals by means of magnetic resonance imaging and then judged independently by an otolaryngologist and a neuroradiologist. Retrospectively, the size of the tumor was quantified by measuring the maximum surface of the lesion in the axial plane. The retrospective surface measurements confirmed the assessments made in the prospective part of the study: growth in 18% of the patients and shrinkage in 7%; 75% remained unchanged. This approach is a pragmatic means to determine whether the size of a tumor has changed over the course of time.

KEY WORDS — follow-up, growth, magnetic resonance imaging, nonoperative management, vestibular schwannoma.

INTRODUCTION

The rationale behind any vestibular schwannoma (VS) operation is that the tumor is presumed to be growing and thereby posing a threat to the patient in the form of further deterioration. Besides hearing loss, VS will eventually lead to serious and progressive neurologic deficits that may have a fatal outcome. The aim of this study was to contribute to the current knowledge about the natural history of VS by reporting on a longitudinal study that we conducted in patients with VS who did not undergo surgery.

Magnetic resonance imaging (MRI) is generally considered the most accurate means of depicting a VS. It can be used to establish the dimensions of a tumor in various ways. It seems practical to take the maximum surface of the lesion in the axial plane as a measure of tumor size; however, this method has not been validated. Therefore, a secondary aim of this study was to determine whether changes in the measured surfaces of a lesion correspond with changes in tumor size as judged by independent observers.

MATERIAL AND METHODS

This longitudinal study pertains to a group of 44 patients with unilateral VS who were referred to the University Hospital Utrecht between 1990 and 1997. The diagnosis of VS in these patients was based on a highly characteristic history, audiovestibular symptoms, and imaging features. The patients' status was followed, and the dimensions of the tumor were recorded prospectively at regular intervals by MRI. This procedure was carried out with T1-weighted pulse sequences. The repetition time was 500 ms, the echo time 30 ms, the number of averages 4, and the slice thickness 3.0 mm, with a gap of 0.3 mm. Sagittal and coronal surveys were used to ensure a scan plane through both internal auditory canals. A transverse scan was made, and no angulation was used. In some patients, this method could have resulted in slightly different scan planes in relation to the tumor. However, a difference of a few degrees is unlikely to result in significant differences in tumor surface. The reasons why these patients were not treated are listed in Table 1. We included only those patients who had been followed for at least 1 year and of whom at least 2 scans had been taken. Two observers (an otolaryngologist and a neuroradiolo-

TABLE 1. PATIENTS WHO DID NOT HAVE THERAPY

Rationale for Conservative Treatment	*Age (y)*			
	<50	*50-59*	*60-69*	*>70*
Decision of patient	11	6	1	1
Refusal despite advice for surgery			2	
Age			10	8
Physical condition			1	3
Tumor in better-hearing ear			1	

From the Departments of Otorhinolaryngology (Stipkovits, Graamans, Van Dijk) and Radiology (Beek), University Hospital Utrecht, and the Department of Otorhinolaryngology, Central Military Hospital (Vasbinder), Utrecht, the Netherlands.

CORRESPONDENCE — Kees Graamans, MD, PhD, Dept of Otorhinolaryngology, University Hospital Utrecht, PO Box 85500, 3508 GA Utrecht, the Netherlands.

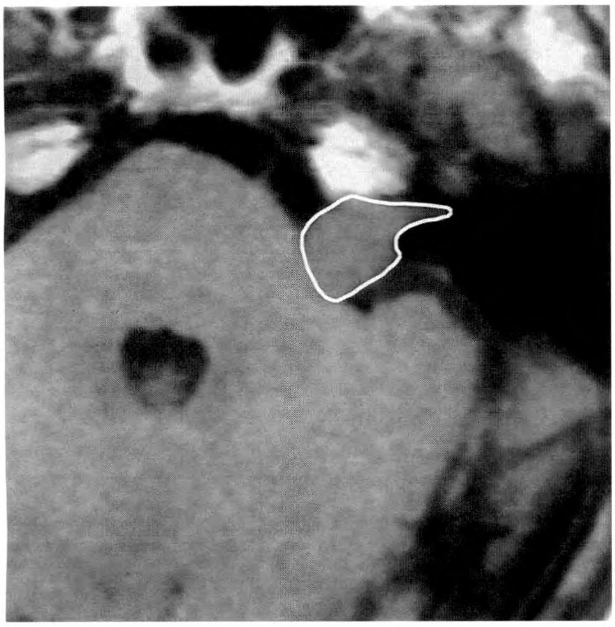

Fig 1. Measurements were performed after manually tracing boundaries of maximum surface of tumor in axial plane.

gist) made independent visual assessments of each MRI print to detect possible changes in tumor size.

The retrospective part of this study consisted of recording the size of each tumor in consecutive MRI scans. To quantify size, the maximum surface of the lesion depicted in the axial plane was measured. This maximum surface was used as a measure of tumor size. Only 1 picture was used from each MRI session: that representing the maximum size. The picture used for the measurement was chosen on the basis of visual inspection. In case of doubt, the picture with the largest lesion surface was selected. The measurement was performed with an IBAS/VIDAS image analysis system (Kontron/Zeiss, Eiching, Germany). Each of the selected pictures was placed on a light box and scanned with a camera (Sony black-and-white charge-coupled device, type XC-77CE, Tokyo, Japan) mounted on a macroscope stand. For each print, the image analysis system was calibrated by aligning the ruler that was included on the picture. The images were subsequently digitized and enhanced (frame size, 768 × 512 pixels; 256 gray levels). The edges of the tumor were manually traced, and the surface was then measured (Fig 1). Each measurement was performed by the 2 observers independently. The average of the 2 observations was taken as the size of the tumor.

For each patient at each test moment, 1 value for the size of the tumor was obtained by averaging the measuring results of the 2 observers. The measurements were repeated during a follow-up period. In this way, we obtained a series of tumor sizes for each patient. We then calculated the mean and the standard deviation (SD) of the tumor size for each patient. Because the length of the follow-up period was different in many patients, the number of measurements of tumor size that were available varied between 2 and 7 per patient (average, 3.7 measurements per patient). The SD was taken as an indicator of growth or shrinkage of the tumor. In other words, the SD will be rather large for a tumor that is either growing or shrinking. A parameter of growth (PG) that equaled the SD was introduced. The parameter was given a negative sign if the tumor was shrinking. Thus, shrinkage could be determined from the consecutive tumor surfaces of the individual subjects. If the tumor hardly changed in size over time, the SD can be interpreted as the reproducibility of the measurements. We introduced an overall threshold for PG whereby patients' lesions with a PG value above the upper threshold can be considered growing tumors. Patients whose lesions had a PG value below the lower threshold were said to have a shrinking tumor. The overall threshold was defined as the average value of 1 SD of all patients.

RESULTS

Twenty-nine male and 15 female patients entered the study. Their mean age was 58 years (range, 29 to 76 years) at the time of the first MRI scan. The prints of 164 scans were examined. An average of 3.7 MRIs were taken of each patient (range, 2 to 7). The mean follow-up period was 3.5 years (range, 12 to 74 months). The time between 2 subsequent scans ranged from 6 to 20 months, with a median of 12 months. There were no discrepancies between the judgments of the 2 observers in the prospective part of this study. Growth was assessed in 8 patients (18%) and shrinkage in 3 (7%), and the size of the tumor remained unchanged in 33 patients (75%).

In the retrospective part of the study, the judgments of the 2 observers appeared to vary only slightly. The pairwise interobserver agreement was excellent; the correlation coefficient was .9978 ($p < .0001$; Fig 2). In Fig 2, the individual patients are represented by their patient number on the x-axis and their PG value on the y-axis. The overall threshold was calculated as described above and equaled 18.2. This value is represented by the horizontal lines at 18.2 and −18.2. The results of the measurements were in accordance with the findings of the otolaryngologist and the neuroradiologist who had visually interpreted the MRI findings. The 8 patients with a PG value above the upper threshold were the same ones identified by these observers as having a growing tumor. Similarly, both procedures — visual inspection and measurement of the lesion on the MRI print — identified the same 3 patients as having a shrinking tumor.

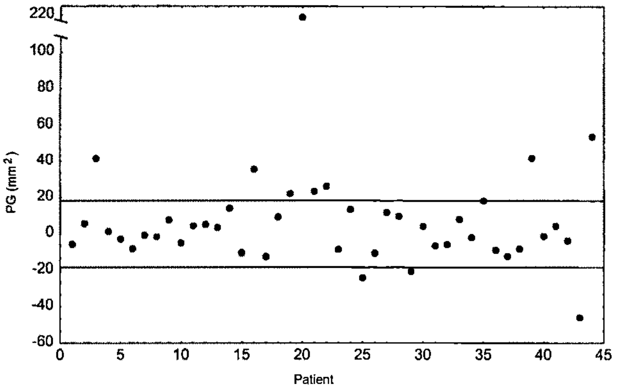

Fig 2. Results of consecutive measurements. Parameter of growth (PG) above upper threshold and that below lower threshold (horizontal lines) represent growth and shrinkage, respectively. When PG lies between these thresholds, tumor size is considered to be unchanged.

DISCUSSION

The body of literature on VS surgical series and operative techniques is extensive. In contrast, few studies have been done on the natural history and growth characteristics of VS, and most of those studies refer to laboratory investigations on histologic specimens obtained at surgery. In that light, any conclusions that have been drawn on the progression of VS must be based on some degree of conjecture. The problem is that the growth of these tumors is determined by various factors that are poorly understood. The only way to obtain definite data on the clinical behavior of VS is to follow patients and record relevant clinical parameters at regular intervals. In particular, the dimensions of the tumor must be noted. However, ethical considerations always impair the composition of a group of patients to be included in a randomized longitudinal study. The present study is no exception. The patients who entered this study might not be representative of all patients with VS, because they were not selected randomly but according to the criteria given in Table 1.

An MRI examination allows for an accurate assessment of the tumor size. In this respect, that method is superior to all previous diagnostic imaging methods. It is hardly possible to relate the numbers presented here to data reported in the literature because the results are difficult to compare. The main reason is that most authors combine the outcomes of several imaging methods and measuring techniques, as illustrated in Table 2.[1-14] Another reason is the inclusion of bilateral and cystic tumors in several studies. Bilateral tumors in patients with neurofibromatosis and cystic tumors have a different natural behavior. Moreover, in patients with bilateral tumors the rationale of a wait-and-see policy is not comparable to the one in patients with VS. Therefore, studies concerning these tumors were excluded from Table 2, which shows the data summarized from the literature. Of the 14 series in the literature shown in this Table, the measurements were restricted to just 1 imaging method in only 5 series. Unlike most of the series from the literature, only 1 imaging method was applied in the present study. Furthermore, a new protocol was used to assess the size of the tumor and any possible changes between consecutive observations.

Studies in the literature express tumor size in diverse ways. The most common procedure is to measure the maximum diameter of the tumor.[15,16] However, this entails gross simplification, because tumors are 3-dimensional structures. Moreover, a change in the diameter implies an exponential change in the

TABLE 2. SERIES IN LITERATURE WITH CONSERVATIVE MANAGEMENT OF VESTIBULAR SCHWANNOMAS

Authors	*No. of Patients*	*Method*	*Follow-up*	*No Growth or Shrinkage (%)*
Bederson et al[1]	70	CT or MRI	24-28 mo (mean, 26 mo)	46
Charabi et al[2]	123	CT or MRI	Mean, 3.4 y	26
Deen et al[3]	68	MRI	Mean, 3.4 y	71
Glasscock et al[4]	34	MRI	5-108 mo (mean, 28.5 mo)	44
Laasonen and Troupp[5]	21	CT	6 mo to 4 y	33
Levo et al[6]	24	MRI	1-6 y (mean, 2 y)	58
Martin et al[7]	39	MRI	6 mo to 14 y	67
Nedzelski et al[8]	50	CT, air CT, or MRI	7-152 mo	52
Sarazin et al[9]	15	MRI volumetry	Mean, 428 d	73
Silverstein[10]	11	CT or MRI	15-108 mo	73
Strasnick et al[11]	51	CT or MRI	6 mo to 11 y (mean, 2.6 y)	78
Thomsen and Tos[12]	21	CT, air CT, or polytomography	1-16 y (mean, 4.2 y)	86
Valvassori and Guzman[13]	35	CT, MRI, or cisternogram	8 mo to 12 y	43
Wiet et al[14]	53	CT or MRI	Mean, 2.13 y	60
Present series	44	MRI	12-72 y (mean, 3.5 y)	82

Series with fewer than 10 patients are not mentioned.

volume of the lesion. For example, when the diameter has doubled, the volume has increased 8 times, assuming that the shape of the tumor has not changed. Thus, it is not sufficient to express growth in terms of diameter alone. To overcome this problem, various solutions have been worked out.

The American Academy of Otolaryngology–Head and Neck Surgery recommends estimating the tumor size by taking the square root of the product of the 2 standardized diameters in the axial plane.[17] This procedure also has some drawbacks. One is that the superior and inferior extents of the tumor are not taken into account. Another is that this procedure is intended to classify VSs in such a manner as to allow comparison of the results of surgery, not to establish changes in tumor size over time.

Charabi et al[2] measured the length and the width of the tumor in a standardized way. Thus, they obtained a numerical value for 2 of the 3 dimensions. They calculated the volume of the tumor with the assumption that it has a spheroid shape. The value of that figure is debatable, because VSs also may take the shape of a globe, pear, dumbbell, or cigar, or even be irregularly lobulated.[18] Moreover, the volume of the intracanalicular part of the tumor is not measured. Only an estimated intracanalicular tumor volume is added to the calculated extrameatal part of the tumor. This may lead to inaccuracies when one tries to determine changes in tumor volume over time. As stated above, many authors describe growth in terms of an increase in diameter. In the method of Charabi et al, the numerical indicators of growth increase up to the third power, because the formula that is used yields the product of the 3 dimensions of the tumor. As a consequence, growth is presented in numbers that are substantially higher than those found with other procedures.

The method described here also has some drawbacks. However, all (potential) errors are presumed to be randomly distributed through the series of measurements. The assessment of changes in tumor size pertains to a series of observations. Minor variations are considered to be an intrinsic part of the method used here. Therefore, only those changes that exceed a certain limit (see above) are considered to be a meaningful and true representation of reality.

Computer-assisted volume calculations, derived from MRI, seem to be the best solution to the problem.[9] Theoretically, volumetric MRI measurements would be optimal if consecutive slices with a maximum thickness of 1 mm were used. With thin slices, the tumor would be depicted on multiple slices. Moreover, the influence of partial volume effects would be marginal. A slice orientation in the sagittal plane would, in the majority of tumors, provide the most slices and lead to the most accurate volume calculation. Also, a volumetric method with thin slices would minimize the influence of different scan angles. Nevertheless, we used 3-mm slices with a 0.3-mm slice gap. The main reason is that this pulse sequence had been used from the start of the study in 1990. It was eventually applied to all patient visits because it remained available on new MRI equipment at our hospital. The slices that can be obtained with this pulse sequence are of limited value for a volumetric measurement. That is especially true for small VSs, because the tumor will be covered by only a few slices. In this study, the possible changes in tumor size as depicted on MRI were initially visually judged by a neuroradiologist and an otolaryngologist. Obviously, their judgments were based on a subjective, visual estimation of tumor size as seen on the consecutive images. The method described here was used in an attempt to objectify their judgments. It entailed outlining the maximum surface of the tumor on an axial slice. This surface was considered to be a parameter of the size of a tumor. The method enabled us to overcome problems that would have arisen if volumetric measurements were used with the pulse sequence as described above. Only the image that showed the maximum size of the lesion was used. The surface measurement appears to be a practical solution to some problems in the assessment of changes in tumor size. It enables us to determine changes in tumor size on images that are obtained through the years with different generations of MRI scanners. As mentioned above, all methods described in the literature have their specific disadvantages and may result in erroneous outcomes. An important conclusion of this study is that the method we used has proven to be as reliable as the judgments of MRI findings by clinicians. This indicates that the figures presented in this study with respect to changes in tumor size are realistic. In future studies, volumetric assessments will certainly be possible with the new sophisticated imaging techniques that are available today. The value of the threshold, being the average of the individual SD values, can be considered as rather arbitrary and needs validation.

The observations presented here give rise to several considerations. Sometimes, in surgery for VSs, minor tumor fragments are left behind deliberately, mainly in order to preserve the continuity of the facial nerve. This is because there is no plane of cleavage between the facial nerve and the tumor.[19,20] It has been demonstrated that this is also likely to occur when hearing conservation is pursued, because the interface between the tumor and the axons of the cochlear nerve is not sharply delineated.[21-23] Nevertheless, recurrences are very rare in these cases. It is conceivable that the natural behavior of VSs is responsible for this lack of demonstrable recurrences after surgical procedures that are obviously not radical. An explanation may be that the tumors have reached a (meta)stable phase, in which the doubling time of the remaining small amount of tumor cells is so long that it is impossible to demonstrate apparent regrowth of a tumor during a patient's lifetime. The result of stereotactic radiosurgery should also be considered in the light of the natural course of the disorder. In view of the observations mentioned above, it does not seem impossible that after radiosurgery, failures might occur in patients in whom pronounced growth of the tumor is an intrinsic part of the disease, whereas radiosurgical success might occur in at least some of the tumors that are not growing.

Finally, our results suggest once again that "watchful waiting" is a realistic and justifiable alternative to treatment, particularly in patients who have small VSs. Follow-up with repeated MRI studies remains mandatory in these cases. Treatment may then be postponed until growth has been definitely established.

REFERENCES

1. Bederson JB, Von Ammon K, Wichmann WW, Yasargil MG. Conservative treatment of patients with acoustic tumors. Neurosurgery 1991;28:646-50.

2. Charabi S, Thomsen J, Mantoni M, et al. Acoustic neuroma (vestibular schwannoma): growth and surgical and nonsurgical consequences of the wait-and-see policy. Otolaryngol Head Neck Surg 1995;113:5-14.

3. Deen HG, Ebersold MJ, Harner SG, et al. Conservative management of acoustic neuroma: an outcome study. Neurosurgery 1996;39:260-4.

4. Glasscock ME, Pappas DG, Manolidis S, Von Doersten PG, Jackson CG, Storper IS. Management of acoustic neuroma in the elderly population. Am J Otol 1997;18:236-41.

5. Laasonen EM, Troupp H. Volume growth rate of acoustic neuromas. Neuroradiology 1986;28:203-7.

6. Levo H, Pyykkö I, Blomstedt G. Non-surgical treatment of schwannoma patients. Acta Otolaryngol Suppl (Stockh) 1997 (suppl 529):56-8.

7. Martin C, Fraysse B, Chelikh L, Cadene MV. Croissance naturelle du neurinome de l'acoustique chez le sujet agé. J Fr Otorhinolaryngol 1994;43:392-7.

8. Nedzelski JM, Schessel DA, Pfleiderer MB, Kassel EE, Rowed DW. Conservative management of acoustic neuromas. Otolaryngol Clin North Am 1992;25:691-705.

9. Sarazin L, Jolivet O, Doyon D. Evaluation informatique du volume tumoral en IRM. Applications à la surveillance des neurinomes de l'acoustique. J Radiol 1993;74:455-60.

10. Silverstein H. The management of acoustic neuromas in a geriatric population. In: Fisch U, Valavanis A, Yasargil MG, eds. Neurological surgery of the ear and skull base. Amsterdam, the Netherlands: Kugler, 1989:197-201.

11. Strasnick B, Glasscock M, Haynes D, McMenomey S, Mior L. The natural history of untreated acoustic neuromas. Laryngoscope 1994;104:1115-9.

12. Thomsen J, Tos M. Acoustic neuromas: diagnostic delay, growth rate and possible non-surgical treatment. Acta Otolaryngol Suppl (Stockh) 1988(suppl 452):26-33.

13. Valvassori GE, Guzman M. Growth rate of acoustic neuromas. Am J Otol 1989;10:174-6.

14. Wiet RJ, Zappia JJ, Hecht CS, O'Connor CA. Conservative management of patients with small acoustic tumors. Laryngoscope 1995;105:795-800.

15. Tos M, Thomsen J. Synopsis on: disagreements in measuring tumor size at the Copenhagen Acoustic Neuroma Conference. In: Tos M, Thomsen J, eds. Acoustic neuroma. Amsterdam, the Netherlands, Kugler, 1991:975-8.

16. Fiirgaard B, Pedersen CB, Lundorf E. The size of acoustic neuromas: CT and MRI. Neuroradiology 1997;39:599-601.

17. Committee on Hearing and Equilibrium. Committee on Hearing and Equilibrium guidelines for the evaluation of hearing preservation in acoustic neuroma. Otolaryngol Head Neck Surg 1995;113:179-80.

18. Russell DS, Rubenstein LJ. Pathology of tumours of the nervous system. London, England: Arnold, 1989:533-55.

19. Schuknecht HF. Pathology of the ear. Philadelphia, Pa: Lea & Febiger, 1993:464.

20. Jääskeläinen J, Paetau A, Pyykkö I, Blomstedt G, Palva T, Troupp H. Interface between the facial nerve and large acoustic neurinomas. J Neurosurg 1994;80:541-7.

21. Ylikoski J, Collan Y, Palva T, Jauhiainen T. Cochlear nerve in neurilemomas. Arch Otolaryngol 1978;104:679-84.

22. Neely JG. Gross and microscopic anatomy of the eighth cranial nerve in relation to the solitary schwannoma. Laryngoscope 1981;91:1512-31.

23. Marquet JF, Forton GE, Offeciers FE, Moeneclaey LL. The solitary schwannoma of the eighth cranial nerve: an immunohistochemical study of the cochlear nerve–tumor interface. Arch Otolaryngol Head Neck Surg 1990;116:1023-5.

Ann Otol Rhinol Laryngol 110:2001

ANEURYSMAL BONE CYST IN THE SPHENOID BONE: TREATMENT WITH MINIMALLY INVASIVE SURGERY

CARLOS DE MINTEGUIAGA, MD
PARIS, FRANCE
FRÉDÉRIC PORTIER, MD
PARIS, FRANCE
JEAN PIERRE GUICHARD, MD
PARIS, FRANCE
EMMANUEL RACY, MD
PARIS, FRANCE
PATRICK HEITZMANN, MD
ORLÉANS, FRANCE
PATRICE TRAN BA HUY, MD
PARIS, FRANCE
PHILIPPE HERMAN, MD, PHD
PARIS, FRANCE

Aneurysmal bone cysts are vascular lesions that destroy and expand bone. We report a recently treated case of an aneurysmal cyst of the sphenoid bone. A 14-year-old girl presented with frontal headaches, bouts of nausea, and vomiting. Computed tomography and magnetic resonance imaging showed typical features of an aneurysmal bone cyst. Arterial embolization was undertaken before surgery. The endoscopic transnasal procedure used allowed the complete removal of the aneurysmal bone cyst. This use of minimally invasive surgery makes this case of interest to surgeons of the skull base and sinuses.

KEY WORDS — aneurysmal bone cyst, endoscopic ethmoidectomy, sphenoid bone.

INTRODUCTION

Aneurysmal bone cysts (ABCs) typically involve the long tubular limb bones, the membranous bones of the thorax and pelvis, and the vertebrae.[1] They rarely occur in the skull (3% to 6% of cases) and facial bones.[1-3] Although ABC is a non-neoplastic condition with no propensity to metastasize, its potential for rapid growth, considerable destruction of bone, and extension into adjacent soft tissue has generally led to aggressive therapy.[1] The conventional therapy has been surgery or radiotherapy. However, direct sclerotherapy has also been used.[4] The following report describes an ABC of the sphenoid bone in a young girl that was treated by minimally invasive surgery and its 3-year follow-up. The rarity of this disease in the ear, nose, and throat area, the vital structures affected by the tumor, the symptoms (a nonrelapsing headache, which revealed the lesion), and the removal of this extradural lesion involving the clivus by minimally invasive surgery make this case of interest to surgeons of the skull base and sinuses.

CASE REPORT

A 14-year-old girl was seen in March 1997 at Orléans Hospital with frontal headaches, bouts of nausea, and vomiting. Computed tomography (CT) showed sphenoid bone erosion that was not compatible with a mucocele, but looked more like a tumor. A biopsy specimen was obtained under general anesthesia by a transnasal approach, and an aneurysmal cyst was diagnosed. The symptoms worsened thereafter, and the girl was given steroids (20 mg methylprednisolone per day) to control the nausea and headache.

A new investigation was done in June 1997, and the girl was sent to our institution. The CT scans (Figs 1 and 2) showed a large tumor centered on the sphenoid bone with extensive bone lysis. The cyst appeared as a blown-out, expansible lesion outlined by paper-thin peripheral ("eggshell") cortical bone. The tumor had spread to involve the optic canals on both sides and the foramen rotundum. There was a very large pneumatization of the sphenoid bone, and the tumor had spread into the roots of the pterygoid processes behind the pterygopalatine pit. Magnetic resonance imaging (MRI; Fig 3) showed the boundaries of the lesion with normal bone and soft tissue extension. The tumor extended to the internal walls of the cavernous sinus and to the clivus. There was no longer a clear posterior limit between the tumor and the sella turcica to the clivus. The tumor had lifted the dura mater of the anterior floor, and the limits of the cribriform plate were not clear. Finally, the tumor had invaded the posterior ethmoid bone up to the basal lamella of the middle turbinate.

Preoperative arterial embolization was undertaken with gelatin sponge particles (250 to 355 µm and 355 to 500 µm, Cordis, Viry-Chatillon, France) after superselective catheterization of both sphenopalatine arteries and the left stylomastoideus artery. A trans-

---

From the Departments of Otorhinolaryngology (de Minteguiaga, Portier, Racy, Tran Ba Huy, Herman) and Neuroradiology (Guichard), Lariboisière Hospital, Paris, and the Department of Otorhinolaryngology, Orléans Hospital, Orléans (Heitzmann), France.

CORRESPONDENCE — Philippe Herman, MD, PhD, Service ORL, Hôpital Lariboisière, 2, rue Ambroise Paré, 75010 Paris, France.

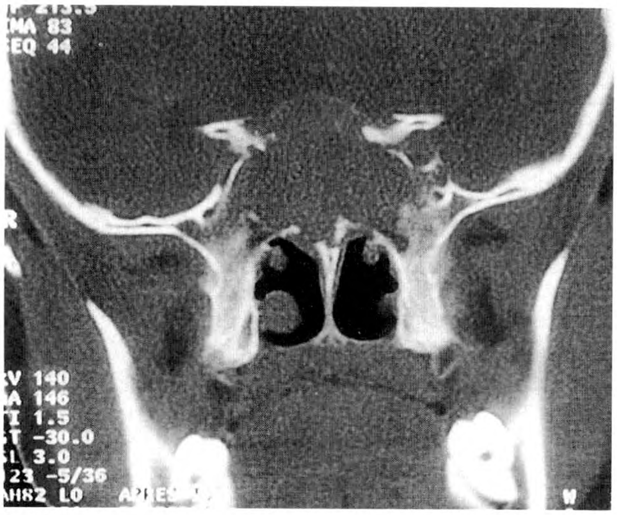

Fig 1. Coronal computed tomography scan with bone windows shows large tumor centered on sphenoid bone with extensive bone lysis. Cyst appears to be outlined by paper-thin peripheral ("eggshell") cortical bone. Tumor has spread to involve optic canals on both sides and roots of pterygoid processes.

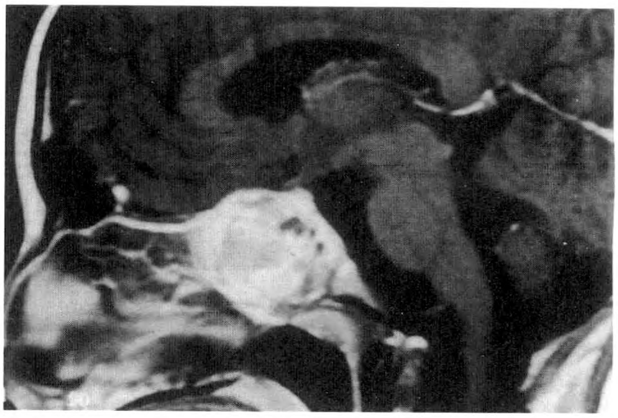

Fig 3. Sagittal gadolinium-enhanced T1-weighted magnetic resonance image shows extension to clivus. There is no longer any clear limit between tumor and sella turcica to clivus. Forward, tumor has invaded posterior ethmoid bone up to basal lamella of middle turbinate.

nasal endoscopic procedure was performed 48 hours after embolization, because the lesion remained extradural. A bilateral ethmoidectomy was performed to completely expose the internal walls of the orbits. The posterior part of the septum was then removed, together with the remnants of the anterior wall of the sphenoid sinus. Most of the tumor could be removed via the midline. Drilling under irrigation with a diamond drill exposed the floor of the sphenoid sinus. The maxillary nerve, the internal walls of the cavernous sinus, the internal carotid arteries, the optic nerves, and the sella turcica could then be gently dissected out, and the dura mater of the posterior fossa was identified. Tumor remnants in the roots of the pterygoid process were removed after drilling out the inner plate of the sphenoid bone.

The follow-up, for 3 years, has remained uneventful. Repeated CT and endoscopic monitoring has shown no sign of residual tumor, but there has been bone reconstruction.

DISCUSSION

We report a case of a sphenoidal ABC treated in our institution with a 3-year follow-up. This lesion is extremely rare, with only 3 published cases in the sphenoid sinuses and 2 in which it extended into the upper nasal fossae or into the ethmoid sinuses.[4-8]

Presently considered to be neither an aneurysm nor a true cyst, ABC is a benign, non-neoplastic bone lesion containing numerous blood-filled, usually non-

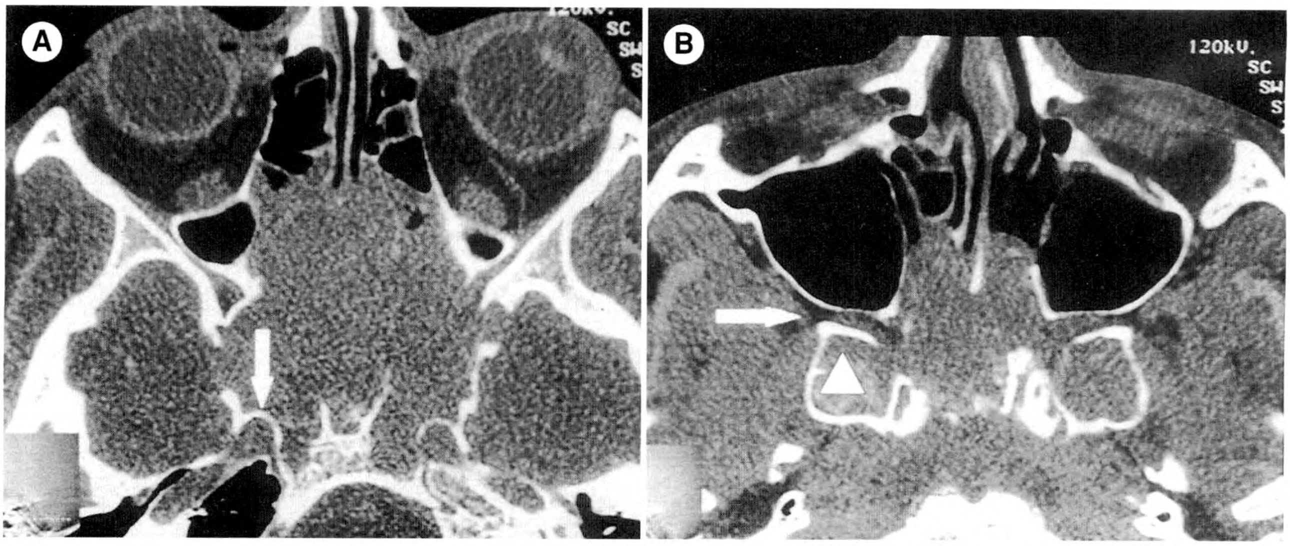

Fig 2. Axial computed tomography scan with bone windows. A) Note very large development of sphenoid sinus with bulging of carotid artery canal (arrow). B) Tumor has spread into roots of pterygoid processes (arrowhead) behind pterygopalatine pit (arrow).

endothelialized cavities.[3] Approximately 95% of ABCs have similar features of blood-filled clefts divided by bony trabeculae, fibrous tissue, and stromal giant cells.[9] The remaining 5% of ABCs are solid tumor variants with features that include fibroblastic or fibrohistiocytic proliferation; osteoid production; osteoblastic differentiation; giant cells; focally degenerate, calcifying fibromyxoid areas; and aneurysmal sinusoids.[10] The cellular nature of the solid variant and its high mitotic index sometimes lead to its being confused with spindle cell malignancies such as osteosarcoma, but no ABCs have atypical cells.[11]

Computed tomography shows a characteristic expansion and thinning of the overlying cortical bone on bone windows. This might be confused with a mucocele, but peripheral enhancement with iodide eliminates this possibility. The CT data may suggest other rare lesions. Then, MRI should be performed. The signal intensities of ABCs vary according to the cyst contents: unclotted blood or bloody fluid gives a strong signal on T1- and T2-weighted images, whereas clear or low-protein fluid gives a weak signal on T1-weighted images and a strong signal on T2-weighted images. Lesions are usually surrounded by a low-intensity rim of fibrocartilage or bone. A fluid-fluid level is a characteristic feature of ABCs (with CT and with MRI), although not diagnostic (occurring also, rarely, in giant cell tumors, fibrous dysplasia, simple bone cysts, chondroblastomas, and telangiectatic osteosarcomas).[1,3,8] Fluid levels in ABCs (and, less commonly, in other lesions) may be solitary or multiple. Nonetheless, the well-defined margins of the ABC usually help to distinguish it from these other lesions.[8]

The ABC is a benign lesion of obscure pathogenesis, usually found in patients less than 20 years old.[1,12] It grows rapidly, with considerable destruction of bone and extension into adjacent soft tissue.[1] Treatment includes wide surgical excision, curettage with or without bone grafting, and irradiation. In the Mayo Clinic series, 19% of primary ABCs treated by curettage recurred, but no patient who had clear surgical margins had a recurrence.[13] Three patients whose ABCs were treated with radiotherapy subsequently developed a sarcoma.[14] Consequently, this treatment can no longer be recommended. Direct intratumoral sclerotherapy has been reported as a treatment for ABCs of the sphenoid bone.[4] The authors concluded that its devascularization of the lesion makes it suitable for treating ABCs, but warn of the risk of intracranial bleeding with this type of vascular lesion. Arterial embolization had failed to produce thrombosis, and the lesion could not be resected surgically. However, the patient treated with this technique had no extension of the tumor that contacted the optic nerve. In our case, the tumor was adhering to the optic nerve, so this technique could not be used because it placed the optic nerve at risk. Preoperative thrombosis was used to reduce the intraoperative bleeding and make the operation smooth and safe. The particles used were large enough to avoid any necrosis. Surgical excision is the treatment of choice for ABCs. Midline skull base lesions can be treated via a transcranial-transbasal approach, a transfacial approach, or an anterior craniofacial approach.[15-17]

This is the first published case in which minimally invasive surgery was used to completely remove an ABC of the sphenoid bone. The treatment consisted of endoscopic transnasal excision, which provided good exposure of the sphenoid bone, sella turcica, optic nerves, pterygoid processes, and cavernous sinus.

REFERENCES

1. Resnick D. Aneurysmal bone cyst. In: Resnick D, ed. Diagnosis of bone and joint disorders. 3rd ed. Vol 6. Philadelphia, Pa: WB Saunders, 1995:3866-78.

2. Ameli NO, Abbassioun K, Azod A, Saleh H. Aneurysmal bone cyst of the skull. Can J Neurol Sci 1984;11:466-71.

3. Barnes L, Peel RL, Verbin RS, Goodman MA, Appel BN. Diseases of bones and joints. In: Barnes L, ed. Surgical pathology of the head and neck. Vol 2. New York, NY: Marcel Dekker, 1985:883-1044.

4. Chartrand-Lefebvre C, Dubois J, Roy D, Mercier C, Raymond J. Direct intraoperative sclerotherapy of an aneurysmal bone cyst of the sphenoid. AJNR Am J Neuroradiol 1996;17:870-2.

5. Delorit GJ, Summers GW. Aneurysmal bone cyst of the sphenoid sinus. Trans Am Acad Ophthalmol Otolaryngol 1975;80:438-43.

6. Kimmelman CP, Potsic WP, Schut L. Aneurysmal bone cyst of the sphenoid in a child. Ann Otol Rhinol Laryngol 1982;91:339-41.

7. Saito K, Fukuta K, Takahashi M, Seki Y, Yoshida J. Benign fibroosseous lesions involving the skull base, paranasal sinuses, and nasal cavity. Report of two cases. J Neurosurg 1998;88:1116-9.

8. Som PM, Schatz CJ, Flaum EG, Lanman TH. Aneurysmal bone cyst of the paranasal sinuses associated with fibrous dysplasia: CT and MR findings. J Comput Assist Tomogr 1991;15:513-5.

9. Kershisnik M, Batsakis JG. Aneurysmal bone cysts of the jaws. Ann Otol Rhinol Laryngol 1994;103:164-5.

10. Sanerkin NG, Mott MG, Roylance J. An unusual intraosseous lesion with fibroblastic, osteoclastic, osteoblastic, aneurysmal and fibromyxoid elements. "Solid" variant of aneurysmal bone cyst. Cancer 1983;51:2278-86.

11. Bertoni F, Bacchini P, Capanna R, et al. Solid variant of aneurysmal bone cyst. Cancer 1993;71:729-34.

12. Morton KS. Aneurysmal bone cyst: a review of 26 cases.

Can J Surg 1986;29:110-5.

13. Vergel De Dios AM, Bond JR, Shives TC, McLeod RA, Unni KK. Aneurysmal bone cyst. A clinicopathologic study of 238 cases. Cancer 1992;69:2921-31.

14. Tillman BP, Dahlin DC, Lipscomb PR, Stewart JR. Aneurysmal bone cyst: an analysis of ninety-five cases. Mayo Clin Proc 1968;43:478-95.

15. Sekhar L, Sen CN. An extended frontal approach to tumors involving the skull base. In: Wilkins RH, Rengachary SS, eds. Neurosurgery update I. Diagnosis, operative technique, and neuro-oncology. New York, NY: McGraw-Hill, 1990:292-301.

16. Bouthillier A, van Loveren HR, Tew JM Jr. Anterior approaches to the clivus: classification and indications. Contemp Neurosurg 1994;16:1-8.

17. Spetzler RF, Herman JM, Beals S, Joganic E, Milligan J. Preservation of olfaction in anterior craniofacial approaches. J Neurosurg 1993;79:48-52.

≈

INTERNATIONAL HEARING AID CONFERENCE

International Hearing Aid Conference VI. Novel Processing and Fitting Strategies will be held in Iowa City, Iowa, June 7-9, 2001. For information, see web site www.medicine.uiowa.edu/otolaryngology/news/news, or contact Rich Tyler by telephone (319-356-2471) or e-mail (rich-tyler@uiowa.edu).

Ann Otol Rhinol Laryngol 110:2001

TRANSNASAL TREATMENT OF CONGENITAL CHOANAL ATRESIA WITH THE KTP LASER

CLAUS POTOTSCHNIG, MD
ELISABETH APPENROTH, MD
CLAUDIA VÖLKLEIN, MD
WALTER F. THUMFART, MD
INNSBRUCK, AUSTRIA

This retrospective analysis presents a minimally invasive method for a transnasal approach to treat bilateral and unilateral choanal atresia and stenosis in infants and children. We describe an advanced surgical technique that applies the use of a KTP laser and give recommendations for preoperative diagnosis and postoperative assessment. We report 13 cases of bilateral and unilateral choanal atresia or stenosis treated over a 3$^1/_2$-year period. We used a transnasal approach and endoscopic control. For bilateral choanal atresia, the operation was performed within the first few days of birth. For unilateral choanal atresia or stenosis, surgery was performed several weeks after birth. In all cases, an intranasal stent was inserted. Our findings demonstrate that this transnasal approach provides significant benefits. A primary advantage is the diminished risk of intraoperative or postoperative complications. Additional benefits include lower rates of re-obstruction and a decreased incidence of subsequent disease, including chronic secretory otitis media.

KEY WORDS — congenital choanal atresia, congenital choanal stenosis, endonasal endoscopic surgery, KTP laser surgery, transnasal approach.

INTRODUCTION

Since Roeder's first description of choanal atresia (Fig 1), made more than 200 years ago, various mechanisms of evolution have been suggested to explain dorsal stenosis of the nose.[1] A dorsal stenosis occurs with the persistence or proliferation of epithelial embryonic cells leading to a complete occlusion of the choana. This condition is more often observed in combination with chromosomal aberrations and craniofacial abnormalities.[2-5]

Fraser[6] reported the incidence of unilateral choanal atresia as 5 times more frequent than bilateral. Of the unilateral cases, 90% involved bone, while the remaining 10% were membranous. In a more recent publication, however, 29% were found to be bony, 71% mixed, and 0% membranous. While dominant heredity is presumed, this relatively rare malformation is described with a frequency rate of 0.82 per 10,000 births (California Birth Monitoring Program), with a slightly higher proportion among whites.[5]

Complete, bilateral, bony atresia is characterized on a computed tomography scan as a triangular posterior vomer (Fig 2). Otherwise known as the "delta deformity," this malformation gives the nasal walls of the choana an hourglass appearance.[2]

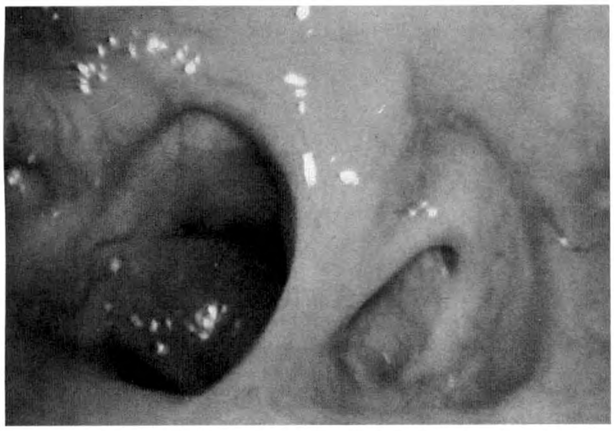
Fig 1. Transoral endoscopic view of unilateral choanal atresia.

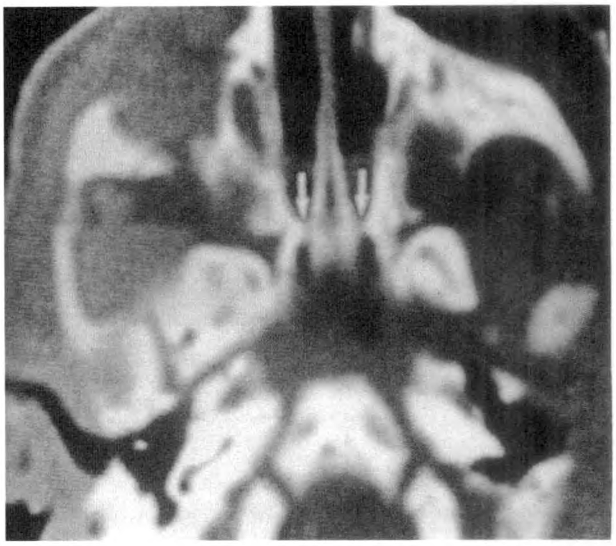
Fig 2. Computed tomography scan shows "hourglass" shape and "delta deformity" (arrows) of choana.

From the Department of Otorhinolaryngology, University of Innsbruck, Innsbruck, Austria.

CORRESPONDENCE — Claus Pototschnig, MD, Dept of Otorhinolaryngology, University of Innsbruck, Anichstrasse 35, A-6020 Innsbruck, Austria.

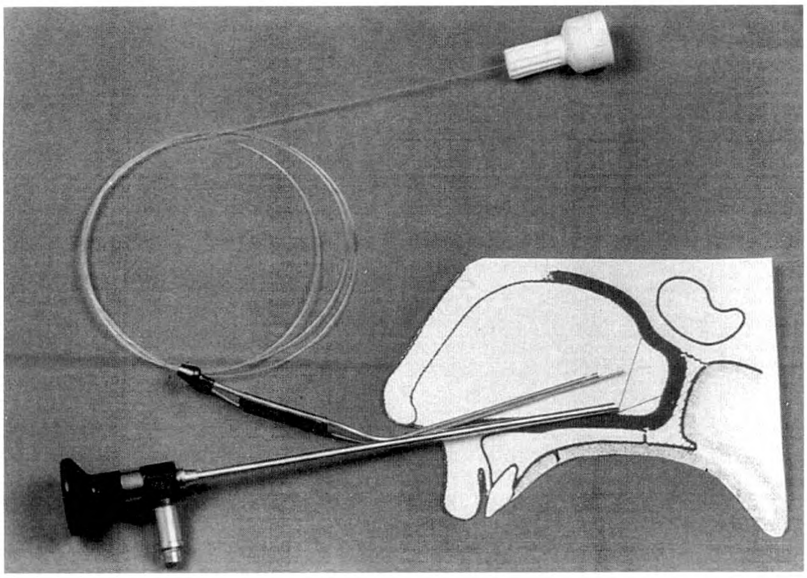

Fig 3. KTP laser fiber with handpiece and 30° angled nasal endoscope.

In the newborn, an obligate nasal breather, bilateral congenital atresia becomes apparent with acute respiratory distress and cyanosis. Intubation is often necessary, as is an orogastral tube for feeding. Because this nasal obstruction constrains swallowing and breathing concurrently, the situation emerges as an acute emergency requiring immediate attention. For unilateral atresia, a delayed operation can be recommended.

A range of surgical approaches, methods, and timetables has been described in the literature.[4,7-15] Previous transpalatal and transmaxillary approaches have been replaced by more current transnasal, endonasal, or transseptal techniques, which conventionally employ a chisel, drill, shaver, or microdebrider, as well as a selection of lasers. Surgical complications may involve lesions to the skull base with injury to the carotid artery, optic nerve, or abducens nerve.

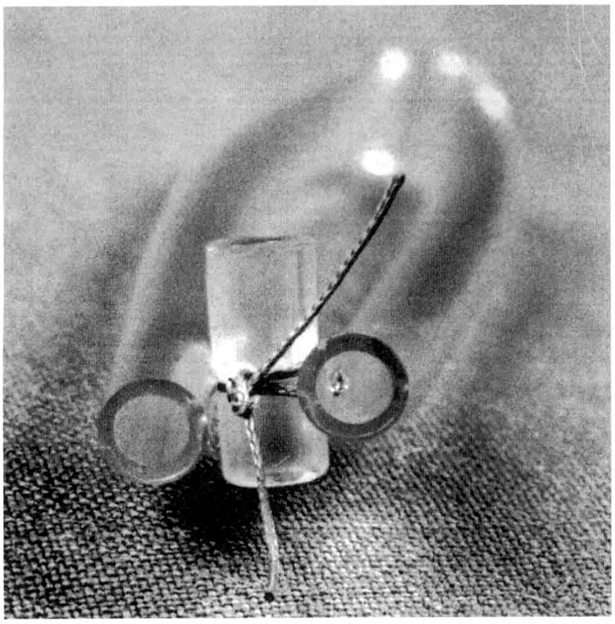

Fig 4. Intranasal silicone stent, which is open at front and back.

The purpose of this report is to introduce a unique, risk-reduced transnasal approach. We present an advanced surgical technique that applies the use of a KTP laser and give recommendations for preoperative diagnosis and postoperative assessment.

PATIENTS, MATERIAL, AND METHODS

Patients. For bilateral choanal atresia or nasal breathing obstruction, stenosis surgery was performed within the first week of birth (n = 7). In patients with unilateral atresia and/or stenosis, we tried to perform surgery within the first weeks or months of birth to avoid subsequent complications (see Table). We did, however, include 2 older patients, 3 and 6 years of age, in this study.

Preparation. To determine the exact location and extent of the atresia or stenosis, we performed a preoperative axial computed tomography scan and endonasal flexible endoscopy of both the nose and the choanal region. Indirect or flexible nasopharyngoscopy was then completed. To evaluate middle ear conditions, we performed otoscopy and tympanometry in all patients and took an additional radiograph of the paranasal sinus in the older children.

Operative Procedure. All surgeries were performed under general anesthesia with oral intubation. In all 13 cases, a KTP laser (model 80/40, Laserscope, San Jose, Calif) was employed with a 0.6-µm fiber in a slim handpiece in contact mode. We used a setting of 3 to 5 W in continuous mode. The operation was performed under visual control of a 30° angled endoscope (Fig 3) with a suction irrigation device (Wigand

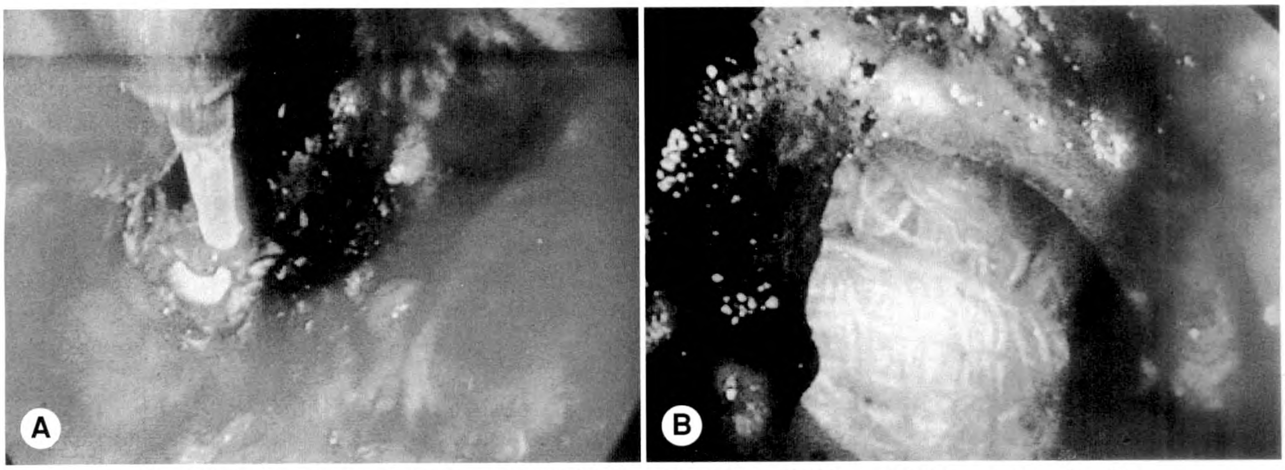

Fig 5. Procedure. A) Intraoperative view of choana with working KTP laser. B) Postoperative situation.

system, Wolf, Knittlingen, Germany). Throughout surgery, the nasopharynx was protected by wet cotton tissues for the absorption of penetrating laser energy. As also applies to procedures performed endonasally, the advantage of the KTP laser is its wavelength, which enables the surgeon to cut the membranous and bony regions of the choanal atresia with simultaneous hemostasis. Under endoscopic control, the resection of the atresia or stenosis is extended to the intraluminal diameter of a reconstructed choana to guarantee a free nasal passage.

Stent. For all patients, an intranasal silicone stent (Fig 4) was placed to allow nasal breathing, to maintain the newly constructed lumen, and to avoid restenosis of the choana.[5,16] The stent was manufactured during the operation from a section of an ordinary silicone tracheal suction tube according to the individual size of each patient. For newborns and small infants, the stent size was about 4 mm. For these patients, the stent required a reserve in length for growth and had to be carefully placed to avoid trauma to the tissues of the nose, particularly the septum and columella. In the older children, the diameter of the stent was about 7 to 8 mm. After the operation and for the first few days, intraluminal suction and cleaning of the stent was necessary to avoid the occurrence of potential obstructions. Well tolerated by the infants and small children, the stent was typically worn for 6 months after surgery.

Control Investigations. After surgery, the parents of the patients were instructed to clean the stent and check its position. Every 6 weeks, the patients were submitted to nasopharyngoscopy, tympanometry, and an examination of the nasal airway while awake. If the stents maintained their correct position, we modified them without exchange every few weeks to accommodate the growth of the child. At the end of 6 months, the stent was removed through one side of the nose without anesthesia. Transnasal, flexible endoscopy should follow to evaluate the lumen of the choana. When there was evidence of either granulation or restenosis, a second surgery under general anesthesia was performed to remove this tissue from the choana.

RESULTS

Operative Procedure. We treated 13 patients exclusively by a unique transnasal approach. Of these 13 patients, 7 were newborns with bilateral choanal atresia, and 6 had unilateral atresia: 2 newborns, a 1-month-old infant, a 3-month-old infant, and 2 children 3 and 6 years of age. All patients were treated with KTP laser surgery (Fig 5). As these patients experienced no complications with wound healing, flaps for the choanal region were not necessary. As with an adenotomy, the tissues, particularly the mucosa, regenerated with spontaneous epithelialization between 10 and 14 days of laser surgery. In all cases, there were no intraoperative complications and no postoperative bleeding.

Stent. An intranasal stent was placed in each pa-

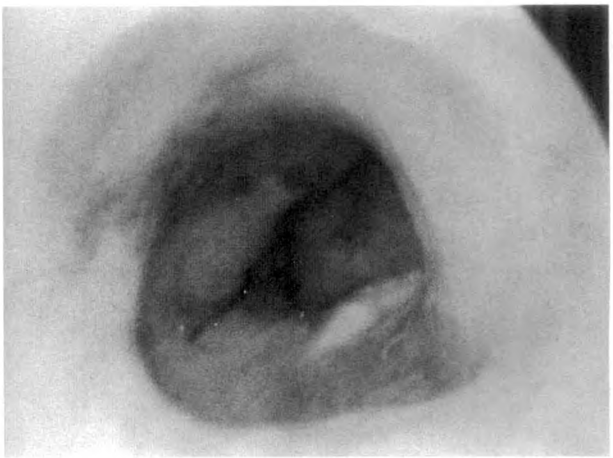

Fig 6. Postoperative result in 1-year-old child, 1 year after surgery. Transnasal view of right choana.

RECOMMENDED TIMETABLE FOR SURGERY

Bilateral choanal atresia	First days after birth
Bilateral choanal stenosis	
Unilateral choanal atresia	First weeks after birth
Unilateral choanal stenosis	

tient as described above. The 6-year-old child removed his stent after 5 months. Younger patients, including infants, tolerated the stent for 6 months without complication. Only 1 patient, a 3-year-old child, required revision surgery for enlarging the choana. He had self-removed the stent 2 months after surgery, and granulation tissue and scars developed in the region of the choana. Revision surgery was completed after 16 months. One newborn, with a very rapid rate of growth, needed a larger stent every 2 months. This child's stent was changed under general anesthesia. Simultaneous endoscopy of the choana showed no tendency to restenosis. On the basis of our experiences in tracheal surgery and surgery of the frontal sinus duct, 6 months seems to be an optimal time for stenting to avoid scarring and restenosis.

Control Investigations. The follow-up was between 6 months and $3^{1}/_{2}$ years after the transnasal laser operation (Fig 6). We often found the development of soft granulation tissue around the newly created choana and along the intranasal localization of the stent without functional stenosis. The granulation tissue could be easily removed without problems while the stent was changed as necessitated by the growth of the patients. Except for the above-noted case of revision operation, we could not perceive any restenosis.

DISCUSSION

A primary advantage of our procedure is the clear visualization it provides the surgeon as he or she maneuvers through the difficult and dangerous area near the skull base. With the unique combination of an endoscope and the KTP laser, the dose of laser energy is optimized for simultaneously removing bone and performing hemostasis during surgery. As a result, the risk of penetration into the skull base or the carotid canal is significantly reduced. As the relatively soft bone of the newborn is easy to treat, the natural transnasal approach imposes no trauma to the sensitive facial structures of the small child. The success with our first 3 cases of infants with bilateral atresia led us to believe that surgery for unilateral choanal stenosis or atresia within the first weeks of birth was achievable (see Table).

In summary, we have established an advanced yet relatively easy approach for a minimally invasive surgery for the treatment of bilateral and unilateral choanal atresia and stenosis. Although the technique has many advantages, the most significant is the diminished risk of both intraoperative and postoperative complications. Furthermore, control investigations may be achieved under local anesthesia. This method minimizes, as well, the development of subsequent diseases, including chronic secretory otitis media, recurrent or chronic otitis media, and paranasal sinus disease. During the follow-up, only 1 patient, with primary bilateral atresia, developed secretory otitis media, 2 years after atresia surgery. Adenotomy and paracenteses were performed. Surprisingly, 3 patients with bilateral atresia and 4 patients with unilateral atresia showed mucociliary problems on the original atretic side with mucus transport to the nasal opening, although they had wide choanas. The substantially lowered rate of re-obstruction further endorses our technique.[1-5,7-17] Last, performing this operation when the patient is at an early age spares the patient and parents the social and physical difficulties often caused by the use of a stent.

REFERENCES

1. Hengerer AS, Strome M. Choanal atresia: a new embryologic theory and its influence on surgical management. Laryngoscope 1982;92:913-21.

2. Ferguson JL, Neel HB III. Choanal atresia: treatment trends in 47 patients over 33 years. Ann Otol Rhinol Laryngol 1989;98:110-2.

3. Weerda H. Abnormalities and malformations [in German]. In: Kastenbauer E, ed. Nase, Nasennebenhöhlen, Gesicht, Mundhöhle und Pharynx, Kopfspeicheldrüsen. Vol 2. New York, NY: Georg Thieme, 1992:125-6, 132-3.

4. Schwartz ML, Savetsky L. Choanal atresia: clinical features, surgical approach, and long-term follow-up. Laryngoscope 1986;96:1335-9.

5. Brown OE, Pownell P, Manning SC. Choanal atresia: new anatomic classification and clinical management applications. Laryngoscope 1996;106:97-101.

6. Fraser JS. Congenital atresia of the choanae. Br Med J 1910;2:1698-701.

7. Josephson GD, Vickery CL, Giles WC, Gross CW. Transnasal endoscopic repair of congenital choanal atresia: long-term results. Arch Otolaryngol Head Neck Surg 1998;124:537-40.

8. Panwar SS, Martin FW. Trans-nasal endoscopic holmium: YAG laser correction of choanal atresia. J Laryngol Otol 1996; 110:429-31.

9. Jung H. The surgical treatment of choanal atresia [in German]. HNO 1987;35:334-41.

10. Jung H. Congenital choanal atresia and its surgical treatment [in German]. Laryngorhinootologie 1994;73:586-90.

11. Miles RJ, Persky MS. Refinement of the transpalatinal exposure of the nasopharynx. Laryngoscope 1992;102:1076-8.

12. Lantz HJ, Birck HG. Surgical correction of choanal atresia in the neonate. Laryngoscope 1981;91:1629-34.

13. Muntz HR. Pitfalls to laser correction of choanal atresia. Ann Otol Rhinol Laryngol 1987;96:43-6.

14. Healy GB, McGill T, Jako GJ, Strong MS, Vaughan CW. Management of choanal atresia with the carbon dioxide laser. Ann Otol Rhinol Laryngol 1978;87:658-62.

15. Metson R. Holmium YAG laser endoscopic sinus surgery. A randomized, controlled study. Laryngoscope 1996;106 (suppl 77).

16. Gleeson MJ, Hibbert J. A stent for the corrective management of bilateral choanal atresia. Laryngoscope 1985;95:1409-10.

17. Nicollas R, Giovanni A, Bonneru JJ, Marti JY, Geigle P, Triglia JM. KTP laser in the upper airways in children: preliminary study on 27 lesions. Ann Otolaryngol Chir Cervicofac 1998; 115:54-8.

≈

MANAGEMENT OF THE TINNITUS PATIENT

The Ninth Annual Conference on the Management of the Tinnitus Patient, for professionals and tinnitus patients, will be held in Iowa City, Iowa, October 4-6, 2001. For information, see web site www.medicine.uiowa.edu/otolaryngology/news/news or contact Rich Tyler by telephone (319-356-2471) or e-mail (rich-tyler@uiowa.edu).

Ann Otol Rhinol Laryngol 110:2001

EPIDERMAL INCLUSION CYST VERSUS THYROGLOSSAL DUCT CYST: SISTRUNK OR NOT?

DANIEL P. SULLIVAN, MD
LISA A. LIBERATORE, MD
MAX M. APRIL, MD
JODI SASSOON, MD
ROBERT F. WARD, MD
NEW YORK, NEW YORK

Epidermal inclusion cyst (EIC) is a recognized cause of an anterior neck mass in children. Controversy exists as to the proper surgical management of an anterior neck EIC: is simple excision adequate treatment, or is a Sistrunk procedure necessary? A retrospective review of the operative logs of the two senior authors (M.M.A., R.F.W.) from 1993 to the present revealed 16 children, ages 6 months to 9 years (mean, 4.5 years), with a diagnosis of anterior neck EIC. An accurate intraoperative diagnosis of an EIC in all cases allowed for a simple excision of the mass rather than a Sistrunk procedure. The final histologic diagnosis was EIC in all 16 patients. Follow-up of these 16 patients for a mean of 4.5 years revealed no recurrences or complications. When the diagnosis of EIC can be made confidently in the operating room, simple excision is an adequate surgical treatment.

KEY WORDS — epidermal inclusion cyst, pediatric neck mass, thyroglossal duct cyst.

INTRODUCTION

A thyroglossal duct cyst (TDC) is the most common midline neck mass in children, but an epidermal inclusion cyst (EIC) is also frequently encountered. Knight et al[1] studied 146 children with midline neck masses that were difficult to diagnose. Of these, 52% were TDCs, 26% were EICs, 16% were lymph nodes, 1.4% were ectopic thyroids, and in 5% no cause was identified. An EIC is a cyst lined with squamous epithelium and keratinaceous debris. Embryologically, it derives from ectoderm only. A dermoid, also called a cutaneous dermoid cyst, is similar to an EIC, but it includes skin appendages such as hair, hair follicles, and sebaceous glands, which are mesodermal derivatives.[2] A teratoma or teratoid cyst contains components of all 3 embryological layers and is very rare in the anterior part of the neck.[3,4] The term "dermoid" is commonly used to describe both true dermoids and EICs.

Although histologically different, an EIC and a dermoid of the anterior part of the neck are similar in their embryological development, and theirs can be contrasted to the embryological development of the TDC. This distinction is important because it forms the basis of the argument for different surgical treatment. The standard surgical approach for the TDC is the Sistrunk procedure, which includes excision of the central portion of the hyoid bone and a portion of the base of the tongue at the foramen cecum.

Knight et al[1] argue that simple excision of an EIC is adequate. The diagnosis must be made during the operation to ensure that the excised mass is an EIC and not a TDC. They recommend always bisecting the mass after it has been removed from the patient to confirm thick cheesy material (keratin) indicative of an EIC. If mucinous material is found, a TDC is more likely and a Sistrunk procedure should be performed. DeMello et al[5] argue that it is frequently difficult to make the diagnosis in the operating room. They report 6 cases in which histologic features of both an EIC and a TDC were found in the same specimen. Thus, during the operation, a surgeon may perform a simple excision on an EIC that also contains a TDC, increasing the chance of a recurrence.

In this report, we examine the embryological basis for using the Sistrunk procedure to treat a TDC or an EIC and seek to demonstrate the feasibility of simple excision in a select group of cases in which a confident diagnosis can be made.

EMBRYOLOGY

Embryologically, thyroglossal duct anomalies can be explained by understanding the development of the thyroid gland (Fig 1). During the fourth week of gestation, the thyroid anlage arises from an invagination of the endodermal cells of the central floor of the pharynx, just below the tuberculum impar of the tongue (the junction between the anterior two thirds and the posterior one third of the tongue).[6] This outpouching enlarges caudally and extends through the

---

From the Department of Otolaryngology, New York University School of Medicine (Sullivan), the Department of Otolaryngology, Lenox Hill Hospital (Liberatore, April, Ward), the Department of Pathology, Manhattan Eye and Ear Hospital (Sassoon), and the Department of Otolaryngology, New York Hospital–Cornell Medical Center (Liberatore, Ward), New York, New York.

CORRESPONDENCE — Robert F. Ward, MD, 186 E 76th St, New York, NY 10021.

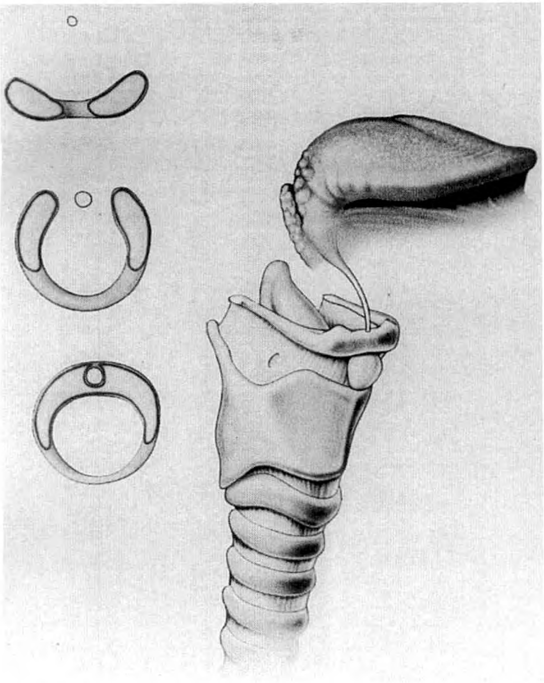

Fig 1. Illustration depicts embryological development of thyroglossal duct cyst. Closure of anterior neck midline results in thyroglossal duct tract extending from foramen cecum to pyramidal lobe of thyroid.

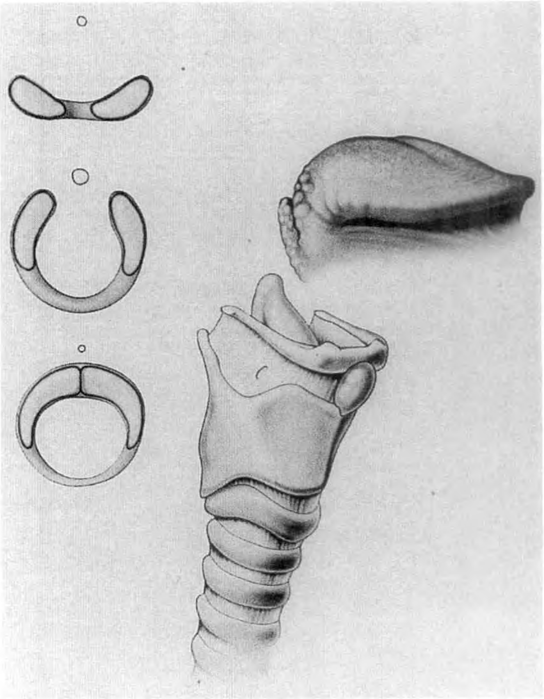

Fig 2. Illustration depicts embryological development of epidermal inclusion cyst. Closure of anterior neck midline traps ectodermal elements in plane anterior to hyoid bone but beneath epidermis.

mesodermal tissues. The foramen cecum lies anterior to the second branchial arch, and therefore, the thyroglossal duct tract runs vertically and anterior to the developing hyoid bone.[7] The thyroid anlage assumes its final position anterior to the trachea by the end of the seventh fetal week, and the tract connecting it to the foramen cecum usually atrophies by 5 to 10 fetal weeks.

If this connecting tract persists, a thyroglossal tract is formed. As the hyoid bone develops, it rotates, thereby drawing the tract posteriorly and cranially at the inferior edge of the hyoid bone. The thyroglossal tract is attached to the undersurface of the hyoid bone and may continue to join the thyroid gland caudally. Ellis and van Nostrand[8] used serial sections of adult and fetal larynges to determine the exact course of the thyroglossal tract in relation to the hyoid bone. They found that the thyroglossal duct is firmly attached to the central aspect of the hyoid bone anteriorly (second branchial arch); then, inferiorly, it hooks under the sharp inferior border of the hyoid bone before arching down anterior to the thyrohyoid membrane. On the basis of their findings, Ellis and van Nostrand conclude that although the thyroglossal duct does not course through the hyoid bone, it is still essential to remove a portion of hyoid bone to ensure that the entire tract is removed.

The embryological explanations for the development of an EIC and of a dermoid in the anterior part of the neck may be similar.[2] Both a dermoid and an EIC may develop from trapping of ectoderm (and mesoderm, in the case of dermoids) at the time of midline fusion of the anterior part of the neck. McAvoy and Zuckerbraun[9] showed that dermoids occur along fusion lines of the first and second branchial arches. The development of a dermoid or an EIC does not involve tissue migrating over and around the hyoid bone; rather, it involves an entrapment of a pocket of tissue as fusion of the branchial arches occurs. Therefore, there is no *embryological* reason for hyoid resection (Fig 2).

PATHOLOGY

Thyroglossal Duct Cysts. A TDC is usually midline and located immediately inferior to the hyoid bone, although sometimes it can be found in lingual, submental, suprahyoid, suprasternal, or mediastinal locations.[10] It may be lined with stratified squamous epithelium when it arises high in the neck. When a TDC arises more inferiorly, it may be lined with epithelium resembling thyroid acinar epithelium. Ciliated, columnar, and transitional epithelia are other possibilities.[4] Other histologic characteristics include an intense lymphocytic infiltration beneath the epithelial lining and a mucinous fluid with or without cholesterol crystals filling the cyst (Fig 3). Sade and Rosen[11] showed that in the region of the foramen cecum, the main cyst may have multiple fingerlike

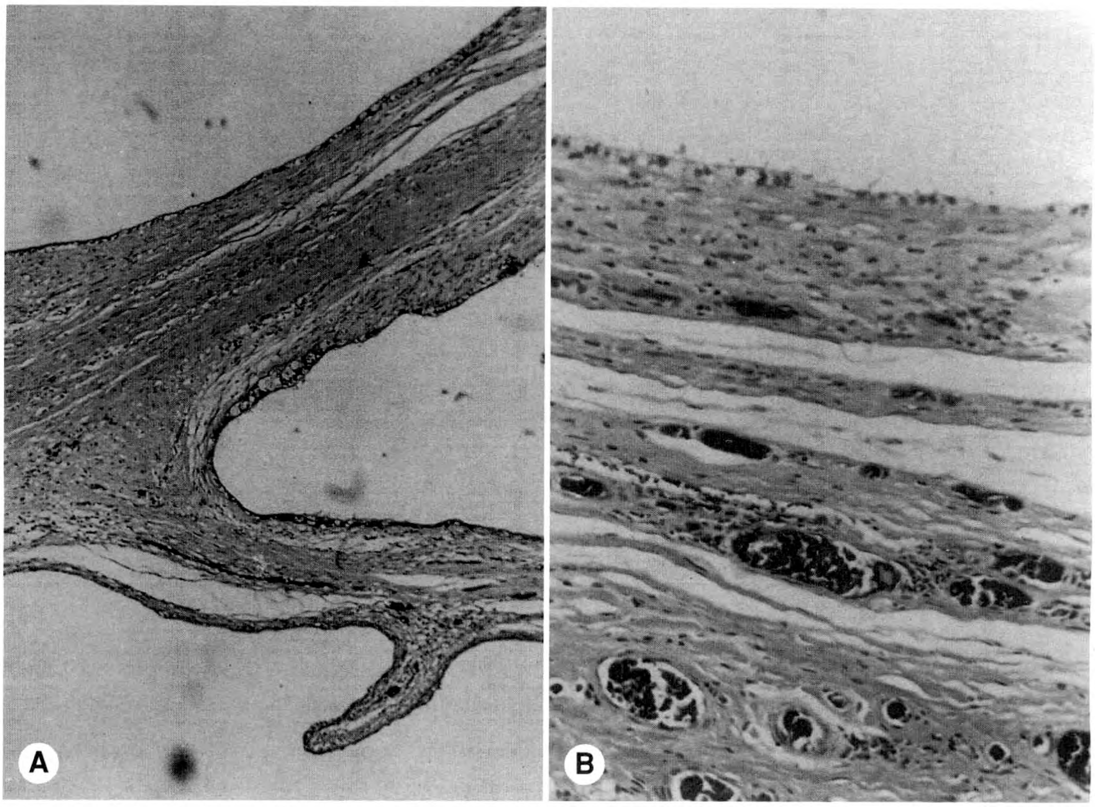

Fig 3. Histopathology of thyroglossal duct cyst. A) Low-power view (original ×40) of thyroglossal duct cyst cavity shows no keratin debris and simple epithelium. B) High-power view (original ×200) of thyroglossal duct cyst wall shows low cuboidal epithelium with rare cilia.

cystic projections that make full excision difficult. Grossly, these fingerlike cysts can easily be mistaken for salivary glands at the base of the tongue. Although it has been theorized that the tract may become trapped within the hyoid body, Ellis and van Nostrand[8] have clearly demonstrated with histopathologic sections that this does not occur. Excised tissue contains thyroid tissue in 35% of cases.[4] Thyroglossal carcinoma can occur within the thyroglossal duct remnant and has been reported in patients ranging from 6 to 81 years old.[12]

Epidermal Inclusion Cysts and Dermoids. An EIC is a dermal cystic enclosure of keratinizing squamous epithelium that is filled with keratin debris (Fig 4).[2] A dermoid cyst also contains skin appendages originating from its walls, including hair, hair follicles, and sebaceous glands, which are mesodermal derivatives.[13] A dermoid differs from a teratoma, which is a mass derived from multipotential germ cells that contains endodermal derivatives as well. A teratoma can contain skin, fat, gastrointestinal epithelium, pancreas, and other tissue components foreign to the neck.[3]

PATIENTS, METHODS, AND MATERIALS

The operative logs of the two senior authors (M.M.A., R.F.W.) were reviewed to find cases of pathologically diagnosed EIC. In the past 6 years, from 1993 to the present, 16 patients were identified. A retrospective chart review of the 16 patients with EICs was performed. The patients ranged in age from 6 months to 9 years (mean, 4.5 years). All had anterior neck masses that were histologically diagnosed as EICs.

The operative logs were also searched for any TDCs that were misdiagnosed as EICs by the surgeon, thus resulting in simple excision rather than a Sistrunk procedure. None were found for the past 6 years.

RESULTS

All 16 patients underwent simple excision on the basis of intraoperative findings. The intraoperative diagnosis was made by detecting a noncystic white mass unattached to the skin and superficial to the strap muscles. The masses were all separate and distinct from the hyoid bone. The cyst was cut open to confirm white cheesy material before it was sent for permanent pathological preparation. Simple excision was performed in all cases. The findings of frozen section biopsy were consistent with EIC in all cases in which it was performed (12/16). The final pathological diagnosis was EIC or dermoid in all 16 cases. All patients required minimal pain medication, started oral intake, and were discharged on the day of opera-

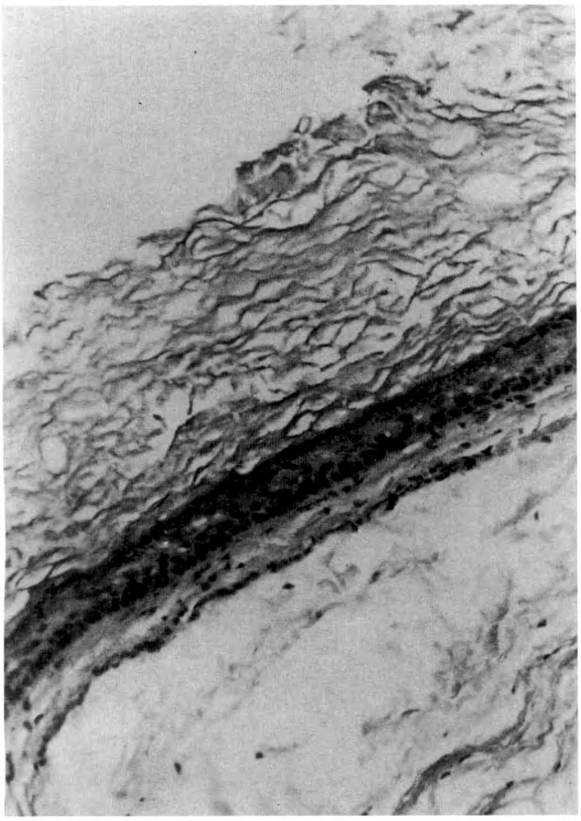

Fig 4. Histopathology of epidermal inclusion cyst. High-power view (original ×200) shows stratified squamous epithelium with keratin debris within cyst. Note absence of skin appendages such as hair, hair follicles, or sebaceous glands.

tion. There were no postoperative complications. Follow-up of 4 months to 6 years, with a mean of 4.5 years, reveals that all wounds have healed well and there have been no recurrences.

DISCUSSION

Thyroglossal duct cyst and EIC are both midline neck masses that typically present in children. It is difficult to differentiate the two solely on the basis of physical examination. The preoperative workup for anterior neck masses may include thyroid function tests, thyroid ultrasound, or a radioactive iodine 131 uptake scan. These are used primarily to rule out an ectopic thyroid mass, which may represent the only functioning thyroid tissue. The differential diagnosis should also include viral or bacterial lymphadenopathy, branchial cleft cyst, and sialadenitis, which, although they do not usually present as midline masses, can be confused with TDC.[1]

A TDC and an EIC arise from different embryological processes. A TDC is derived from the tract that remains after the progenitor thyroid tissue migrates caudally from the foramen cecum over and under the hyoid bone to just below the cricoid cartilage. Sistrunk[14] recognized that in order to ameliorate the 40% to 85% recurrence rate seen with simple excision of a TDC, it was necessary to remove the entire cyst along with the central portion of the hyoid bone and a cuff of foramen cecum in continuity with the tract. Sistrunk reported a recurrence rate of 4% to 8% with this approach. An EIC or a dermoid results from trapping of ectodermal (and mesodermal) elements during anterior neck fusion in the midline. Their development does not involve traveling over and around the hyoid bone as in TDC, and therefore, no embryological rationale exists for performing a Sistrunk procedure in these cases.

Some authors have recommended expanding the indications for the Sistrunk procedure to include all anterior midline neck masses. Sade and Rosen[11] showed that TDC specimens frequently contained multiple ducts connecting to the foramen cecum, and many had mucus-producing glands accompanying the thyroglossal duct. Failure to remove any part of the TDC, including these multiple ducts and mucous glands, results in recurrence. Hoffman and Schuster[15] stressed the importance of thorough primary surgery for TDC, because they found that recurrence rates increased from 6% to 30% when the first operation was inadequate. Pelausa and Forte[7] argue that intraoperative diagnosis is very difficult. They cite several cases in which misdiagnosis by the surgeon during operation led to inadequate surgery and recurrence. DeMello et al[5] report a case in which a specimen contained both an EIC and a TDC and also note several cases in which the specimen had histologic features of both an EIC and a TDC. Additionally, they found 9 EICs that were firmly attached to the hyoid bone. Because of the difficulty of making a definitive diagnosis during operation and because of frequent histologic variants, these authors suggest that all midline neck masses should be removed by the Sistrunk procedure to prevent unnecessary recurrences.

These authors also cite the relatively low rate of postoperative complications from a Sistrunk procedure compared with simple excision. The series of deMello et al[5] on 71 patients reported 1 tracheostomy performed after the operation for edema of the vallecula. Other possible complications include increased pain, swallowing difficulty, reduced oral intake, hematoma, and seroma. Hence, the complications of the Sistrunk procedure, although infrequent, are more serious and more common than those of simple excision. In our series of 16 simple excisions for EIC, none of these complications was seen.

Knight et al[1] advocate cutting all midline neck masses in half before they are sent for permanent pathological preparation. Of the 38 EICs in their series, 9 were submitted to the Sistrunk procedure because of difficulty with diagnosis. None of these 9 were cut open in the operating room, however. Care must be taken not to rupture the cyst while it is still in the patient, as this may lead to increased recurrence; instead, the cyst is opened after it is passed off the field as specimen. Knight et al argue that the Sistrunk procedure involves additional morbidity and is frequently unnecessary if full efforts are made during the procedure to arrive at a diagnosis.

We have followed the recommendations of Knight et al.[1] With this approach, we have not found any recurrences after resection of an intraoperatively diagnosed EIC. The children were spared the additional morbidity of the Sistrunk procedure, with possible swallowing difficulty, drain placement, and overnight admission to the hospital. It is important to note that none of the masses we removed were adherent to the hyoid or deep to the strap muscles. Both of these factors considerably confuse the diagnosis.

Brown and Judd's[16] review of 381 patients with TDCs revealed a recurrence rate of 6% (28/381); 61% (17/28) of the recurrences presented within the first month after removal. Mickel and Calcaterra[17] found that 90% of recurrences from incompletely excised TDCs present within the first postoperative year. Thus, our follow-up range of 4 months to 6 years (mean, 4.5 years) should have detected the majority of recurrences.

A midline neck cyst should always be opened in the operating room. Frozen sections can be examined if the diagnosis is still unclear. If a diagnosis of EIC can be made confidently, simple excision should be performed. If, after making every attempt to arrive at a diagnosis, there is still doubt, a Sistrunk procedure should be performed.

CONCLUSION

An EIC is a recognized cause of anterior neck masses in children. The EIC and the dermoid are embryologically distinct from the TDC. An EIC or dermoid may be diagnosed during removal as a white mass, deep to the skin, superficial to the strap muscles, and more solid than a TDC. We offer a modification to the dictum that all midline neck masses be uniformly removed by the Sistrunk procedure to avoid recurrence. In this series of 16 patients with EIC, simple excision resulted in less morbidity and no recurrences. Thus, when the surgeon can clearly diagnose an EIC, we recommend simple excision for an EIC or a dermoid. For more complicated cases in which the diagnosis is uncertain, a Sistrunk procedure should be performed to avoid simply excising a mass that might be a TDC.

ACKNOWLEDGMENT — The authors thank Richard Larocco at New York Hospital–Cornell Medical Center for the medical illustrations.

REFERENCES

1. Knight PJ, Hamoudi AB, Vassy LE. The diagnosis and treatment of midline neck masses in children. Surgery 1983;93:603-11.

2. Bhansali SA, Chung-Ho C, Hotaling AJ. Clinical and pathologic diagnosis: pathologic quiz case 2. Arch Otolaryngol Head Neck Surg 1989;115:752-5.

3. Abemayor E, Newman A, Bergstrom L. Teratomas of the head and neck in childhood. Laryngoscope 1984;94:1489-92.

4. Guarisco JL. Congenital head and neck masses in infants and children. Ear Nose Throat J 1991;70:75-82.

5. deMello DE, Lima JA, Liapis HL. Midline cervical cysts in children: thyroglossal anomalies. Arch Otolaryngol Head Neck Surg 1987;113:418-20.

6. Hawkins DB, Jacobsen BE, Klatt EC. Cysts of the thyroglossal duct. Laryngoscope 1982;92:1254-8.

7. Pelausa EO, Forte V. Sistrunk revisited: a ten year review of revision thyroglossal duct surgery at Toronto's Hospital for Sick Children. J Otolaryngol 1989;18:325-33.

8. Ellis PD, van Nostrand AW. The applied anatomy of thyroglossal tract remnants. Laryngoscope 1977;87:765-70.

9. McAvoy JM, Zuckerbraun L. Dermoid cyst of the head and neck in children. Arch Otolaryngol 1976;102:529-31.

10. Silimy OE, Bradley PJ. Thyroglossal tract anomalies. Clin Otolaryngol 1985;10:329-34.

11. Sade J, Rosen G. Thyroglossal cysts and tracts. A histological and histochemical study. Ann Otol Rhinol Laryngol 1968;77:139-45.

12. White I, Wilmier T. Squamous cell carcinoma arising in thyroglossal duct remnant cyst epithelium. Otolaryngol Head Neck Surg 1982;90:25-31.

13. Cunningham MJ. The management of congenital neck masses. Am J Otolaryngol 1992;13:78-92.

14. Sistrunk WE. Technique for removal of cysts and sinuses of the thyroglossal duct. Surg Gynecol Obstet 1928;46:109-12.

15. Hoffman MA, Schuster SR. Thyroglossal duct remnants in infants and children: reevaluation of histopathology and methods for resection. Ann Otol Rhinol Laryngol 1988;97:483-6.

16. Brown PM, Judd ES. Thyroglossal duct cysts and sinuses: results of radical (Sistrunk) operation. Ann Surg 1961;102:494-501.

17. Mickel RA, Calcaterra TC. Management of recurrent thyroglossal duct cysts. Arch Otolaryngol 1983;109:34-6.

Ann Otol Rhinol Laryngol 110:2001

PEDIATRIC TRACHEOTOMY: IS POSTOPERATIVE CHEST X-RAY NECESSARY?

DARYLE DARDEN, MD
HOUSTON, TEXAS

RICHARD TOWBIN, MD
PHILADELPHIA, PENNSYLVANIA

JOSEPH E. DOHAR, MD
PITTSBURGH, PENNSYLVANIA

A retrospective study of 101 children who underwent tracheotomy at the Children's Hospital of Pittsburgh from 1993 to 1996 was performed. The following criteria were reviewed in each patient: age, gender, race, prematurity, weight during tracheotomy, presence of preoperative airway support, duration of tracheotomy, nature (emergent versus elective), tracheotomy tube size, reason for tracheotomy, accompanying medical diagnoses, chest x-ray (CXR) findings, surgical service, postoperative symptoms (up to 3 days), and operative mortality rate. Of these criteria, our results show that CXR-screenable complications occurred in patients who underwent emergent recannulation, as well as those who exhibited ventilatory distress (oxygen saturation level of <90%) and specific changes in postoperative symptoms. Pneumothorax developed after tracheotomy in 3 of the 101 patients; each had one of these risk factors. We conclude that CXR of all pediatric patients after tracheotomy may be unnecessary with the use of flexible endoscopy and screening restrictions that are both health-conscious and cost-effective.

KEY WORDS — chest radiography, chest x-ray, child, tracheotomy.

INTRODUCTION

Tracheotomy is used for airway management in a variety of medical conditions. Initially, it was used as a last resort. The earliest procedures were limited primarily to adults. Because of its high mortality rate, many parents initially refused tracheotomy for their children.[1] Improved surgical technique and postoperative care have led to decreased mortality rates.[2] The earliest pediatric application was to relieve airway obstruction due to a foreign body or infection. Presently, tracheotomy is a widely accepted and relatively safe operation. Consequently, its use in children has increased significantly.[3-9]

As with any operation, tracheotomy is not without complications. Table 1 lists the potential complications of tracheotomy in infants and children and identifies those that can be diagnosed by chest x-ray (CXR). A subset of these complications (pneumothorax, pneumomediastinum, and subcutaneous emphysema) is believed to occur more commonly in children. Anatomic differences between adults and children may, in part, be responsible for this. For example, the lung apices may extend into the neck more often in children than adults, leaving them more vulnerable to injury and resultant pneumothorax and subcutaneous emphysema.

Fortunately, clinical experience, cautious observation, CXR, and now, flexible endoscopy can be used to detect and manage these complications.[10] Chest radiography is often recommended in children after tracheotomy to rule out postoperative complications. The disadvantages of CXR include expense and radiation exposure. In an era of cost-conscious health care delivery, expense must be considered when ordering tests. The purpose of this study was to determine the need for routine CXR after tracheotomy in children.

TABLE 1. EARLY COMPLICATIONS OF TRACHEOTOMY AND DETECTABILITY BY CHEST X-RAY

Complication	*Detectable by Chest X-ray*
Hemorrhage	No*
Pneumothorax	Yes
Pneumomediastinum	Yes
Tracheoesophageal fistula	No
Recurrent laryngeal nerve injury	No
Cardiopulmonary arrest	No
Wound infection	No
Subcutaneous emphysema	Yes
Tube obstruction	No*
Tube displacement	Yes
Swallowing problems	No

*May be detected by chest x-ray, but not necessarily specific diagnosis. (Hemorrhage in lung may look like pneumonia, infiltrate, or pleural effusion. Tube obstruction leads to collapse, atelectasis, or hemothorax.)

From the Departments of Radiology (Darden, Towbin) and Pediatric Otolaryngology (Darden, Dohar), Children's Hospital of Pittsburgh, and the Departments of Radiology (Towbin) and Pediatric Otolaryngology (Dohar), University of Pittsburgh School of Medicine, Pittsburgh, Pennsylvania. Dr Darden is currently in the Department of Radiology, University of Texas, Houston Health Science Center, Houston, Texas.

CORRESPONDENCE — Joseph E. Dohar, MD, Dept of Pediatric Otolaryngology, Children's Hospital of Pittsburgh, 3705 Fifth Ave, Pittsburgh, PA 15213.

TABLE 2. DIAGNOSES OF PEDIATRIC PATIENTS WHO UNDERWENT TRACHEOTOMY

Reason for Tracheotomy	*Broad Diagnosis*	*Specific Diagnosis*	*No. of Patients*
Upper airway obstruction	Congenital	Bilateral choanal atresia	1
		Laryngeal cleft	1
		Laryngeal web	3
		Laryngomalacia	7
		Micrognathia	1
		Pierre Robin anomaly	6
		Subglottic stenosis	19
	Degenerative; idiopathic	Vocal cord paralysis	2
	Infection	Laryngotracheitis (croup)	6
		Granular cell tumor	1
		Laryngeal papillomatosis	1
	Neoplasia	Lymphangioma	1
		Neurofibroma	1
		Subglottic hemangioma	3
		Subglottic (post-transplant lymphoproliferative disease)	2
	Trauma	Laryngeal edema	2
Pulmonary toilet; assisted ventilation	Congenital	Severe kyphoscoliosis; restrictive lung disease	1
		Adjunct to craniofacial surgery	4
		Esophageal atresia due to tracheoesophageal fistula	3
		Congenital heart disease	5
		Hypoplastic lung due to diaphragmatic hernia	1
		Central nervous system devastation (microcephaly)	2
		Failure to thrive	1
	Degenerative; idiopathic	Central nervous system failure; cerebral palsy	5
		Central nervous system failure; seizures of unknown cause	2
		Respiratory arrest	4
		Neuromuscular failure (Duchenne's muscular dystrophy)	2
	Metabolic	Respiratory distress syndrome (metabolic)	3
		Cystic fibrosis	1
	Neoplasia	Brain neoplasm	1
	Trauma	Head trauma (shaken baby syndrome)	9
		Total	101

METHODS

The medical records of 101 children who underwent tracheotomy from 1993 through 1996 at the Children's Hospital of Pittsburgh were reviewed. The procedures were performed by an otolaryngology staff surgeon or under his or her immediate supervision. A postoperative portable anterior-posterior radiograph was obtained for each patient. Age, gender, race, prematurity, weight during tracheotomy, presence of preoperative airway support, duration of tracheotomy, nature (emergent versus elective), tracheotomy tube size, reason for tracheotomy, accompanying medical diagnoses, CXR findings, surgical service, postoperative symptoms (up to 3 days), and operative mortality data were recorded.

RESULTS

One hundred one pediatric patient records were reviewed through the fourth postoperative day. Forty-four patients were male, and 57 were female. The patients ranged in age from 0 to 22 years (mean, 4.36 years; SD, 5.94 years; SE, 0.59 years). The patients' weights ranged from 1.4 to 91 kg (mean, 16.58 kg; SD, 19.12 kg; SE, 1.90 kg). Four patients weighed less than 2 kg and had no postoperative complications. The duration of the procedure, including any other procedures performed in conjunction with the tracheotomy, such as endoscopy, averaged 1.8 hours (SD, 1.90 hours; SE, 0.19 hours). Nineteen of the 101 patients had been born prematurely; pneumomediastinum developed in 2 after the operation. Tracheotomy was performed electively in 94 patients and emergently in 7 patients, 1 of whom had a pneumomediastinum before operation. No patients died in the perioperative period or up to 4 days after undergoing operation. Six of the 101 patients had postoperative complications that were diagnosed by CXR. Two had pneumothorax, 3 had pneumomediastinum, and 1 had both. Five patients were not intubated; none of them had complications. There were no statisti-

TABLE 3. SIGNS AND SYMPTOMS OF PNEUMOTHORAX

Signs	*Symptoms*
Respiratory distress	Chest pain (initially sharp and pleuritic, then dull and constant)
Decreased chest wall motion (on affected side)	Dyspnea
Subcutaneous emphysema to palpation	Tachypnea
Tracheal deviation (away from affected side)	Orthopnea
Hyperresonance on percussion	Nonproductive cough
Decreased fremitus	Hemoptysis
Decreased or absent breath sounds on auscultation	Pleural rub
Pleural rub	
Tachycardia	

cally significant relationships between postoperative complications and sex, age, weight, procedure length, prematurity, or the nature of the procedure. All 6 complications were in patients with diagnoses of upper airway obstruction, as opposed to ventilator dependence. These data are summarized in Table 2.

DISCUSSION

Cost-effective health care delivery is a priority for clinicians. The challenge is to achieve it without compromising patient care. Omission of unnecessary tests is one way to decrease costs. As a result, the role of routine postoperative CXR has come into question. A study by Barlow et al[10] examined the cost-effectiveness of CXR after tracheotomy in adults. This study concluded that limiting CXR to patients with certain risk factors and clinical evidence of pneumothorax can result in a significant savings. One risk factor identified in that study was tracheotomy in children. This risk factor was identified on the basis of conventional practice; however, the study did not include patients younger than 19 years of age. The question in children, therefore, remains unanswered.

In the past, the mortality rate in pediatric patients with tracheotomies was reported to be as high as 40%.[11] The reported death rates directly attributable to tracheotomy, however, range from 0% to 3.4%. Further, the number of perioperative deaths from complications of tracheotomy that may be diagnosed by CXR is extremely small. For example, Dutton et al[11] reported a tracheotomy-related mortality rate of 1.4%. In 286 pediatric tracheotomy patients reviewed, 4 deaths occurred and were caused by accidental decannulation, tracheotomy tube plugging, or vascular hemorrhage, all of which developed after standard post-tracheotomy CXR. Ward et al[12] reported 5 deaths of intraoperative or postoperative complications in 103 children. No deaths resulted from tracheotomy in this series.

Only a small subset of complications of tracheotomy can be screened for by postoperative CXR. For example, in the study by Ward et al,[12] the overall complication rate was 36%, whereas the rate of complications that can be screened for by CXR was 2%. We examined complications that can be identified by CXR after operation (pneumothorax, pneumomediastinum, subcutaneous emphysema, and tube displacement). In this study, we found that CXR identified complications in 6% of children, and all of these were clinically obvious: 2 patients with pneumothorax, 3 with pneumomediastinum, and 1 with both. Further, an even smaller subset of postoperative pneumothoraces occur before CXR screening. The literature suggests that some cases of pneumothorax occur well after both the operation and postoperative CXR, during episodes of emergent recannulation.[13]

Complications diagnosable by CXR include pneumothorax, pneumomediastinum, subcutaneous emphysema, and tube displacement. Routine CXR screening for these is often irrelevant and has little impact on treatment decisions. Improper tube placement is a rare complication, and with the advent of smaller-caliber flexible fiberoptic endoscopes, proper tube placement can most often be confirmed during the procedure. In a study of 996 tracheotomy procedures, Futran et al[14] reported only 1 intraoperative complication: tube displacement through the posterior tracheal wall that was identified and corrected during the procedure. Other complications, such as subcutaneous emphysema and pneumomediastinum, can most often be treated conservatively with careful observation.[15] Indeed, airflow restriction caused by a pneumomediastinum can enhance the development of a tension pneumothorax, and CXR detection of a pneumomediastinum may heighten a clinician's concern over a new-onset pneumothorax. The symptoms that accompany pneumothorax, however, should alone lead a clinician to proceed with the same workup regardless of a preexisting pneumomediastinum. This was our experience in this study. It seems, therefore, that screening with postoperative CXR may only have a significant impact in cases of pneumothorax, with a lesser impact on pneumomediastinum.

Is routine postoperative CXR necessary to detect pneumothoraces caused by tracheotomy? As stated above, only a small percentage of pneumothoraces occur during operation. Considering that iatrogenic pneumothoraces may develop up to 24 hours after the procedure, one may question the utility of immediate postoperative CXR.[16] The risk of pneumothoraces' developing after tracheotomy increases even further in the significant number of patients who undergo artificial ventilation. Patients with mechanical ventilation have a 5% overall incidence of pneumothorax, which increases to 35% with the coexistence of inflammatory pulmonary disease.[16] Under this circumstance, pneumothorax fails to develop before routine postoperative CXR and must be identified later through corresponding changes in signs and symptoms, which are usually obvious on examination. Considering the broad span of time in which tracheotomy-related pneumothoraces can develop, we think that individual CXR screening based on physical examination and clinical suspicion is a more accurate and useful method than routine screening of all patients.

Certainly, there are instances in which post-tracheotomy CXR is appropriate. It is indicated after pediatric tracheotomy when the patient shows clinical evidence of a preexisting pneumothorax or has any risk factors that would predispose him or her to a new pneumothorax. Table 3 lists the postoperative signs and symptoms of pneumothorax. This study failed to confirm additional risk factors suggested by the literature to be associated with increased risk for pneumothorax: emergent tracheotomy, prematurity, and weight less than 2 kg. In addition, at least 2 cases of postoperative pneumothorax in pediatric patients with laryngeal papillomatosis have been reported.[10,12] Patients with pulmonary nodules secondary to papillomatosis are more prone to pneumothorax. This is an independent variable and remains separate from the issue of tracheotomy. This study included 1 patient with laryngeal papillomatosis in whom pneumothorax did not develop.

Our sample size was too small to evaluate which patients should undergo CXR screening after tracheotomy. Our complications occurred in children who had emergent recannulation, ventilatory difficulty (oxygen saturation level of <90%), or signs or symptoms of respiratory distress. The decision of when to obtain postoperative CXR must be left to individual clinical judgment.

CONCLUSION

Since the advent of artificial ventilation in the 1960s, the number of tracheotomy procedures performed in children has increased; therefore, one must take a closer look at the costs incurred.[17] Flexible endoscopy permits visualization of the tracheotomy tube position during the procedure, negating the need to confirm the tube position by CXR. Only 3 of 101 patients required treatment on the basis of CXR findings, and these patients had clear signs and symptoms of pneumothorax. This study suggests that routine CXR screening after tracheotomy may be unnecessary, and omitting it would result in a significant cost savings. With good clinical observation and judgment, CXR screening may be reserved for infants and children who are at increased risk according to the clinical observation and individual judgment of an experienced otolaryngologist.

REFERENCES

1. Goodal EW. The story of tracheotomy. Br J Child Dis 1934;31:167.

2. Jackson C. High tracheotomy and other errors: the chief causes of chronic laryngeal stenosis. Surg Gynecol Obstet 1921; 32:392.

3. Myers EN, Carrau MR. Early complications of tracheostomy. Clin Chest Med 1991;12:589-95.

4. Oliver P, Richardson JF, Clubb RW, Flake CG. Tracheotomy in children. N Engl J Med 1962;267:631-7.

5. Tucker JA, Silberman HD. Tracheotomy in pediatrics. Ann Otol Rhinol Laryngol 1972;81:818-24.

6. Line WS Jr, Hawkins DB, Kahlstrom EJ, MacLaughlin EF, Ensley JL. Tracheotomy in infants and young children: the changing perspective 1970-1985. Laryngoscope 1986;96:510-5.

7. Gerson CR, Tucker GF Jr. Infant tracheotomy. Ann Otol Rhinol Laryngol 1982;91:413-6.

8. Benjamin B, Curley JW. Infant tracheotomy: endoscopy and decannulation. Int J Pediatr Otorhinolaryngol 1990;20:113-21.

9. MacRae DL, Rae RE, Heeneman H. Pediatric tracheotomy. J Otolaryngol 1984;13:309-11.

10. Barlow DW, Weymuller EA Jr, Wood DE. Tracheotomy and the role of postoperative chest radiography in adult patients. Ann Otol Rhinol Laryngol 1994;103:665-8.

11. Dutton JM, Palmer PM, McCulloch TM, Smith RJH. Mortality in the pediatric patient with tracheotomy. Head Neck 1995;17:403-8.

12. Ward RF, Jones J, Carew JF. Current trends in pediatric tracheotomy. Int J Pediatr Otorhinolaryngol 1995;32:233-9.

13. Hotaling AJ, Robbins WK, Madgy DN, Belenky WM. Pediatric tracheotomy: a review of technique. Am J Otolaryngol 1992;13:115-9.

14. Futran ND, Dutcher PO, Roberts JK. The safety and efficacy of bedside tracheotomy. Otolaryngol Head Neck Surg 1993;109:707-11.

15. Wetmore RF. Tracheotomy. In: Bluestone CD, Stool SE, Kenna MA, eds. Pediatric otolaryngology. 3rd ed. Philadelphia, Pa: WB Saunders, 1996:1425-40.

16. Fishman AP, ed. Fishman's pulmonary diseases and disorders. 3rd ed. New York, NY: McGraw-Hill, 1998.

17. Palmer PM, Dutton JM, McCulloch TM, Smith RJ. Trends in the use of tracheotomy in the pediatric patient: the Iowa experience. Head Neck 1995;17:328-33.

Ann Otol Rhinol Laryngol 110:2001

CONCURRENT GLOTTIC AND TRACHEAL STENOSES: RESTORATION OF AIRWAY CONTINUITY IN END-STAGE MALIGNANT DISEASE

KLAUS WASSERMANN, MD
FRANK MATHEN, MD
HANS EDMUND ECKEL, MD
COLOGNE, GERMANY

Six patients known to have inoperable esophageal carcinoma presented with stridor due to both malignant tracheal stenosis (with additional respiratory-digestive tract fistula in 2 patients) and bilateral vocal cord paralysis. Patency was restored by endotracheal stenting plus unilateral cordotomy. Four patients had immediate relief. Two patients required enlargement of the vocal cord incision. One of them declined reoperation and underwent tracheostomy. The stent function was uneventful, with no dislodgment or mucus impaction. The fistula seal was complete, with no aspiration through the newly shaped glottic orifice. The peak expiratory flow increased from 24.4% ± 9.7% of predicted normal before the procedure to 40.5% ± 13.7% after the procedure. Restoration of airway continuity in serial laryngotracheal stenoses by a combined approach is a feasible technique in end-stage cancer patients. It effectively relieves respiratory distress and ensures voice preservation. In addition, it may avoid the risks of tracheotomy.

KEY WORDS — malignant airway obstruction, tracheal stenting, unilateral laser cordotomy.

INTRODUCTION

Acute onset of respiratory distress or gradually worsening dyspnea in patients with known esophageal cancer is often due to high-grade tracheal stenosis caused by the invading malignancy. It may also reflect bilateral vocal cord paralysis (BVCP).[1] Not infrequently, the vocal cord lesion precedes or succeeds the tracheal occlusion by a short delay. Every now and then, however, both the glottis and the trachea are severely obstructed at the same time. Because in this case the relative contribution of either site to the increased airflow resistance is difficult to assess,[2] both obstructions need urgent treatment.

Airway stenting has become an established palliative endoscopic measure for restoration of sustained patency in malignant tracheobronchial obstruction. The current literature underscores that prompt symptomatic and functional improvement is brought about by all available endoprostheses.[3] Early and late complications are minimal and, if present, are easy to overcome. There is virtually no incidence of procedure-related mortality, and median survival times of up to 10.5 months have been documented.[4]

Bilateral vocal cord paralysis in the paramedian position after thyroid gland surgery is now being treated successfully with the use of laser-assisted microlaryngoscopic interventions.[5-11] In particular, laser cordotomy seems to be favorable for the therapy of this complication.[12] The incidence of associated morbidity is usually low, and temporary tracheostomy is no longer required.

Hitherto, no data have been published on cordotomy in conjunction with central airway stenting for the management of concomitant glottic and tracheobronchial stenoses in oncology patients. Therefore, this retrospective study seeks to evaluate the surgical technique, feasibility, complication rate, and efficiency of a combined laryngobronchologic approach for the symptomatic relief of concomitant central airway stenoses in 6 patients with locally advanced esophageal carcinoma. To ease the patients' symptoms and to preserve their voice, we undertook laser-assisted unilateral cordotomy and endoscopic tumor coring followed by the insertion of stents in 2 subsequent sessions. We believe that in this particular group of individuals with tumors, restoration of the normal airway passage is superior to bypassing it by a tracheostomy, which is a different and, it may seem, more straightforward way to circumvent the obstacle.[1] But, given malignant tissue growth adjacent to the larynx and trachea, tracheostomy is liable to cause complications in the form of delayed wound closure and subsequent relapsing local infection. Also, permanent tracheal cannulation may be an additional cause of life-threatening mucus impaction and asphyxiation.

CASE REPORTS

Case 1: A 50-year-old woman presented in whom esophageal cancer had first been diagnosed in March

---

From the Third Medical Department (Wassermann, Mathen) and the Department of Otorhinolaryngology (Eckel), University of Cologne, Cologne, Germany.

CORRESPONDENCE — Klaus Wassermann, MD, Klinik III für Innere Medizin der Universität zu Köln, Gebäude 0/D, Raum 409, Josef-Stelzmann-Strasse 9, 50924 Köln, Germany.

PATIENT CHARACTERISTICS AND CLINICAL AND FUNCTIONAL DATA

Patient No.	*Sex*	*Age (y)*	*ID*	*Pretreatment*	*AcPro*	*Tracheal Lesion*	*PEF*		*PIF*		*Survival*
							Before	*After*	*Before*	*After*	
1	F	50	3/97	RC, S, RC	5/98	Comp, infiltr	0.77 (12.2)	2.06 (32.7)	0.71	1.25	2 mo
2	M	50	5/96	RC, B, S	4/98	Comp	2.10 (20.5)	2.60* (25.4)	0.95	1.92*	1 mo
3	M	55	4/98	None	6/98	Comp	1.91 (21.4)	3.54 (39.5)	1.03	1.01	LTF
4	F	64	9/95	S, RC	5/99	Comp, infiltr	2.25 (36.4)	3.33 (54.1)	1.91	1.89	2.5 mo
5	M	67	6/98	RC	4/99	Fist, comp	1.70 (20.0)	2.51 (30.5)	0.81	0.86	2 mo
6	M	73	10/98	RC, B	8/99	Fist, comp	3.63 (36.0)	4.75 (60.0)	1.25	1.68	Alive after 2 mo

Means ± SD of 6 patients: PEF before, 2.06 ± 0.93 L/s; PEF after, 3.13 ± 0.96 L/s; PEF% (percentage of predicted value,[16] in parentheses) before, 24.4 ± 9.7; PEF% after, 40.5 ± 13.7; PIF before, 1.11 ± 0.43 L/s; PIF after, 1.44 ± 0.46 L/s.

ID — time of initial diagnosis (mo/y); RC — radiochemotherapy; S — surgery; B — brachytherapy; AcPro — time of actual procedure (mo/y); comp — compression; infiltr — infiltration; fist — fistula; PEF — peak expiratory flow ("before" and "after" double intervention; absolute values in L/s; percentages of predicted values[16] are in parentheses); PIF — peak inspiratory flow (no reference values available); LTF — lost to follow-up (after 1 mo).

*Preoperative spirometry in this patient was performed after stent insertion but before cordotomy.

1997 as stage T3N0M0.[13] After 2 courses of radiochemotherapy, transthoracic esophagectomy was performed in September 1997. A third course of radiochemotherapy followed in December 1997. In May 1998, she presented to the bronchology unit in respiratory distress and stridor. Bronchoscopy showed BVCP in addition to high-grade rigid compression of the distal trachea (residual lumen, 3 to 5 mm) with substantial malignant infiltration of the carina. Treatment consisted of stent insertion plus right-sided laser cordotomy. The bifurcated silicone-hybrid stent that would have seemed most suitable[14] could not be passed through the narrowed tracheal segment. Even dilation with a rigid bronchoscope was only partly successful. Further bougienage was thought to be quite risky because of imminent tracheal rupture. Therefore, 2 nested 12-mm Palmaz stents[15] (Cordis GmbH, Haan, Germany) were chosen because of their maximal resistance to compressive forces and their elegant insertion technique using a thin catheter as a carrier. The next day, posterior laser cordotomy was performed. The patient showed immediate symptomatic and functional improvement (see Table[16] and Fig 1). She died of cachexia and pneumonia secondary to metastatic lung disease 2 months later.

Case 2. A 50-year-old man had esophageal carcinoma, stage T3N0M0, that had been known since May 1996. Radiochemotherapy had been performed, applying a total dose of 56 Gy in addition to 5-fluorouracil and cisplatin. A subsequent course of esophageal brachytherapy was reported. In January 1997, the patient underwent surgical resection. In April 1998, he presented with dyspnea that had rapidly progressed over 2 weeks. Because of the emergency intervention, no lung function test could be performed at baseline. Bronchoscopy showed impaired motility of both vocal cords, but no complete paralysis in a paramedian position. There was, however, high-grade compression of the trachea over its whole length (residual lumen, 2 to 4 mm). On April 17, 1998, a 13-mm bifurcated Dynamic stent (Willy Rüsch AG, Kernen, Germany) was placed. Because of tracheal distortion, proper stent positioning proved quite difficult. On the fifth postoperative day, stridor reappeared. Bronchoscopy revealed that the vocal cords were now

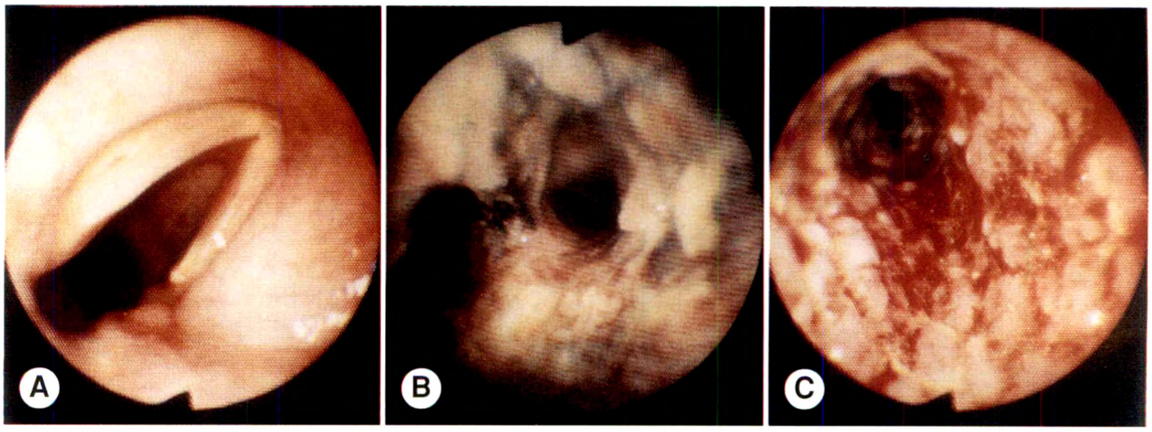

Fig 1. (Case 1) A) Glottis 1 month after unilateral cordotomy. B) Distal trachea with open-mesh Palmaz stent. View of carina. C) Midtrachea. Stent mesh is within necrotic infiltrated mucosa.

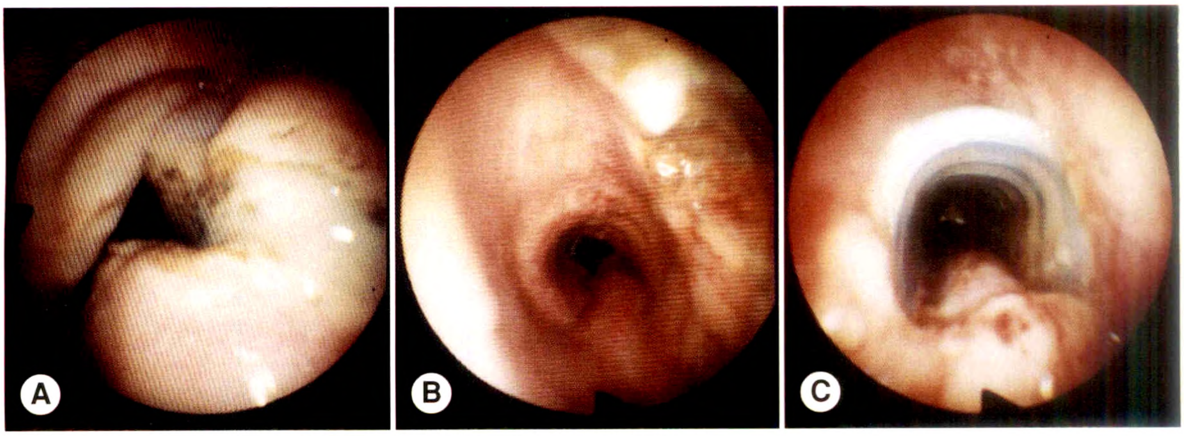

Fig 2. (Case 3) A) Glottis 2 days after cordotomy; note edema of resection wound. B) Subglottic level. Trace of resection wound is visible. Proximal stent border is seen in background behind cricoid. C) Proximal circumference of Dynamic stent.

in a paramedian position. Left-sided posterior cordotomy was performed at once (April 22, 1998) and led to definitive respiratory improvement. The patient died 1 month later of fatal hemorrhage caused by malignant destruction of the vascular wall (see Table).

Case 3. A 55-year-old man had received a diagnosis of esophageal cancer in April 1998, staged as inoperable T4N2M0 cancer. He presented with swallowing difficulties, dyspnea, and stridor on May 1, 1998. Bronchoscopy revealed BVCP and compressive stenosis of the distal trachea. The orifices of both main bronchi were involved in the stenosis. Left-sided posterior cordotomy was performed on June 7, 1998, and placement of a bifurcated Dynamic 13-mm stent followed 1 week later. The tumor-induced esophageal obstruction was effectively treated by balloon dilation. The patient improved, but after 1 month he was lost to follow-up (see Table and Fig 2).

Case 4. A 64-year-old woman presented who had received a diagnosis of esophageal cancer in September 1995 (pT1pN0M0). Surgical resection had been performed, but postoperative chemotherapy had been declined by the patient. In July 1998, local tumor relapse in conjunction with tracheal infiltration necessitated 6 courses of radiochemotherapy. Since February 1999, progressive tumor growth with concomitant gradually deteriorating dyspnea at rest had been reported. In May 1999, when stridor appeared, bronchoscopy revealed BVCP plus 60% midtracheal compression and mucosal infiltration. The stenotic segment was approximately 3 cm long. On May 18, 1999, 2 serial nested Polyflex stents[17] (Willy Rüsch AG) were implanted. Right unilateral posterior cordotomy was performed on the following day. Although the tracheal stent had been placed uneventfully and was functioning with no mucus impaction whatsoever, formation of massive fibrin deposits on the cordotomy wound resulted in secondary stenosis; therefore, the patient's dyspnea did not improve substantially. Bronchoscopic suction and removal of the material by flexible forceps was necessary every other day. Because no real breakthrough to normal respiration was achieved, we decided to perform subtotal cordectomy with preservation of the anterior third of the vocal cord on May 21, 1999. The patient's dyspnea was relieved. She died on August 2, 1999, of hemorrhage (see Table and Fig 3).

Fig 3. (Case 4) A) Glottis subsequent to enlarged unilateral resection. B) Two overlapping tracheal Polyflex stents.

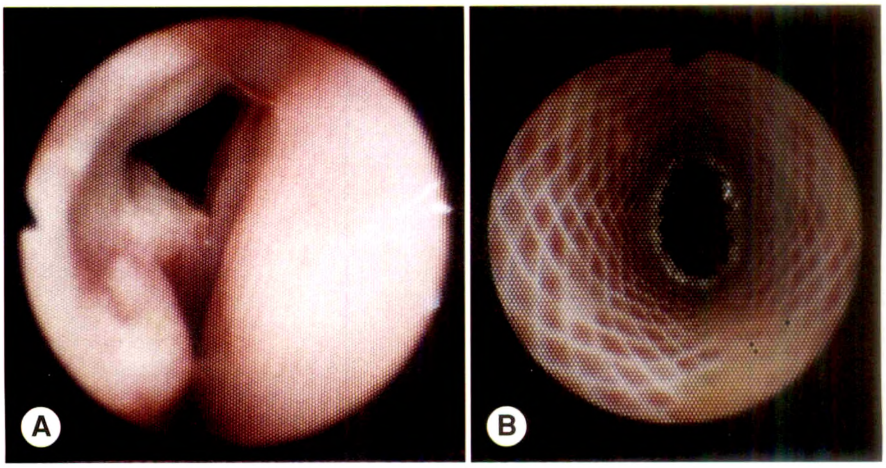

Case 5. A 67-year old man had received a diagnosis of esophageal cancer (stage T3N0M0) in June 1998. Subsequently, radiochemotherapy had been applied, and an endogastric catheter was advanced because of intractable high-grade esophageal stenosis at the level of the cervicothoracic transition. The patient complained of increasing dyspnea and relapsing purulent bronchitis. Flexible bronchoscopy showed BVCP with the vocal cords in a paramedian position. In addition, a subcricoid posterior tracheal compression accompanied by a 60% luminal decrease was visible. Distal to that stenosis, there was a large (7 cm) tracheoesophageal fistula. In order to seal the fistula and dilate the tracheal stenosis, we inserted a Polyflex stent. Later, a left posterior cordotomy was undertaken (May 11, 1999). Respiratory improvement ensued, but was short-lived because of vocal cord edema in conjunction with a relatively narrow glottic entrance. The stent function remained excellent. Because the patient refused further surgery at the level of the glottis, tracheostomy and intubation were undertaken after stent removal. The patient left the hospital in good respiratory condition. He died at home. His reported symptoms were consistent with asphyxia subsequent to mucus impaction of the tracheostomy tube (see Table).

Case 6. A 73-year-old man had a striking medical history of arterial hypertension, 2 ischemic cerebral infarcts, laryngeal carcinoma, and subsequent radiochemotherapy. He had received a diagnosis of inoperable esophageal carcinoma T3N1M1 (cerebral) in October 1998. Radiochemotherapy led to partial remission. Relapsing local malignancy was treated with brachytherapy and the additional placement of an esophageal stent. Endoscopic control in August 1999 demonstrated a midtracheal respiratory-digestive tract fistula 2 cm long. The esophageal stent was visible within the orifice of the fistula. Tumor tissue overgrowth resulted in secondary stenosis of the esophagus and moderate compression of the tracheal lumen. There was near-complete BVCP with minor residual vocal cord motility. The initial presentation was with hoarseness, but without significant dyspnea at rest. Polyflex stent placement for fistula seal was performed on August 18, 1999. Within the subsequent 2 weeks, complete paralysis of the vocal cords in a paramedian position developed. Acute stridor was the presenting symptom. Right-sided posterior cordotomy was then performed, resulting in good respiratory function and fistula seal. The patient was still alive and in good respiratory condition 2 months after the initial intervention (see Table).

SUMMARY OF FINDINGS

The majority of patients had undergone prior treatment consisting of surgery, palliative radiochemotherapy, or both. They now presented with far-advanced, incurable local tumor growth, and all of them deliberately chose to undergo the combined laryngobronchoscopic approach instead of tracheostomy. Their main reason was voice preservation.

Four patients had simultaneous complete BVCP and tracheal obstruction, and 2 more had tracheal stenosis and fistula and incomplete BVCP at first presentation. However, complete paralysis associated with a paramedian cord position developed within 2 weeks of endotracheal stenting. This was signaled by stridor reappearing after transient relief. Given the initial glottic aspect, which was one of immotile cords standing somewhat apart, we think that complete paralysis was the result of progressing tumor growth and by no means an adverse effect of the rigid bronchoscopy that had been necessary for stent placement.

The stent function proved satisfactory and uneventful. There was no dislodgment, mucus impaction, or major granulation. The fistula seal was effective. Aspiration subsequent to cordotomy was not noticed in any of the patients. All could resume their normal diet on the first day after surgery. Two patients were thought to require surgical revision of the larynx either because of secondary obstruction by fibrin deposits on the cordotomy wound or because the incision was too small. In 1 patient, the debris was removed by repeated bronchoscopies, and a more extended (subtotal) cordectomy was carried out thereafter. The further healing process was uncomplicated, and the final respiratory and phonatory results were good. The other patient declined repeat cordectomy. He underwent tracheostomy and died at home after a short period of relief.

Preoperative and postoperative spirometry was performed with standard equipment (MasterLab, Jäger, Würzburg, Germany). Normal values were derived from a report by Quanjer.[16] The mean best peak expiratory flow (PEF), including tests of patient 5 before tracheostomy, increased from 24.4% of the predicted normal before the procedure to 40.5% afterward. The mean best peak inspiratory flow (PIF) did not show any substantial change from 1.11 L/s to 1.44 L/s, although 3 of 6 patients improved slightly (see Table and Fig 4). Some mentioned minor expectoration difficulties and shortness of breath while climbing stairs, but except for patient 5, they experienced respiratory improvement. They could speak clearly, though in a whispering tone. Two patients died of fatal hemorrhage. The duration of survival attained by the deceased patients was 1 to 2.5 months.

DISCUSSION

Bilateral vocal cord paralysis is potentially life-threat-

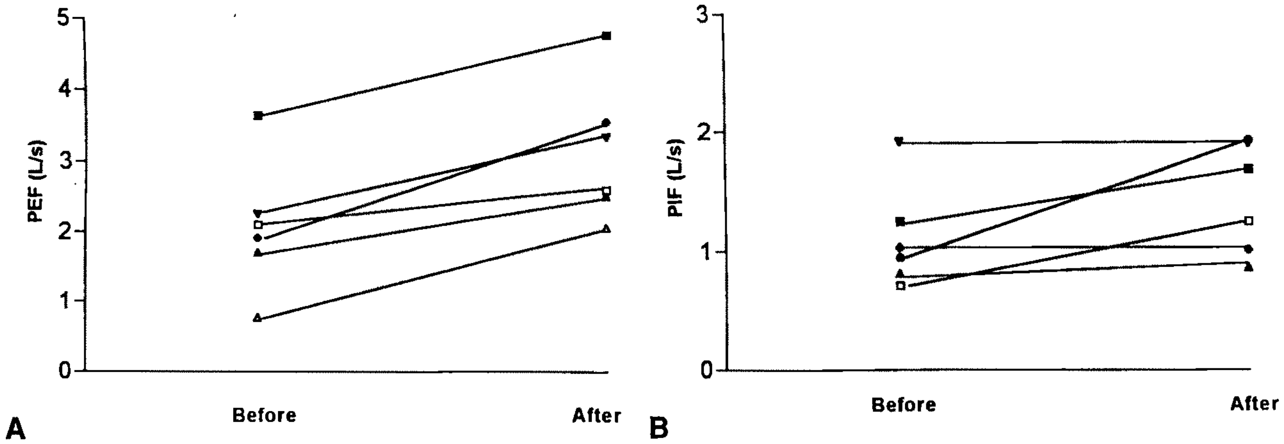

Fig 4. Test data from before and after endoscopic microsurgical procedure. A) Peak expiratory flow (PEF). B) Peak inspiratory flow (PIF). Symbols denote individual patients.

ening and requires some kind of surgical intervention to prevent acute asphyxiation. It sometimes develops during the natural course of esophageal carcinoma and may then significantly contribute to these patients' morbidity. If recognized in time, such glottic stenoses can now be treated with minimally invasive endoscopic procedures. The patients in the present series underwent unilateral posterior cordotomy according to the method of Dennis and Kashima.[7] A surgical CO2 laser was used coupled to an operating microscope. All patients were intubated transorally for surgery. In manipulating the tube, care was taken not to dislodge previously inserted tracheal stents. The procedure included transection of the vocal process of the arytenoid cartilage, followed by resection of a minor portion of the posterior part of the vocalis muscle and the lateral thyroarytenoid muscle. As described by Ossoff et al,[6,8] the conus elasticus was carefully transected from the vocal process of the arytenoid cartilage down to the inner surface of the cricoid cartilage. The anterior portion of the vocal cord, however, was not included in the resection, because its removal would have contributed little to the desired airway enlargement. Extubation was performed 30 to 60 minutes after the end of the intervention. No patient had a tracheotomy at the time of surgery or during the postoperative recovery period. In the long run, unilateral posterior cordectomy was successful for 4 patients, but required enlargement in 2 because of continuing breathlessness. In a recent analysis of 25 patients who underwent unilateral or bilateral laser cordotomy, Laccourreye et al[18] also found insufficient airway restoration after the unilateral approach. Eight of 15 such patients needed revision, whereas all bilateral procedures were immediately successful.

As might have been expected, the findings of lung function tests performed after the interventions were far from normal. Although the PEF results were within the realm of postcordectomy values reported in a previous article,[12] PIF was essentially unchanged. This finding may be best explained by the patients' poor physical condition, rather than as a reflection of insufficient inspiratory glottic patency, because PIF depends on respiratory muscle strength and motivation more than PEF does. Eventually, the leading central resistance became the "new" vocal cords, because voice preservation requires a certain degree of glottic closure. The stented trachea no longer contributed to residual obstruction. It is true that any surgical widening of the glottis for the treatment of BVCP trades voice for airway. A related problem is the potential risk of aspiration after surgical procedures on the larynx for glottic airway rehabilitation. This risk is of particular concern in patients with coexisting tracheal, pulmonary, or cardiac disease and may lead to severe aspiration pneumonia. Therefore, a compromise must be found between retaining voice quality and restoring an adequate translaryngeal airway. Tissue-sparing resections like the one described in this report generate superior phoniatric results associated with only minor airway stenosis.[12] Furthermore, with the arytenoid cartilages left intact, no aspiration will result from such a procedure. Bilateral cordotomy may also be feasible. An absence of aspiration together with a good voice quality on subjective rating has been reported.[18]

The placement of the stents used in this series has been described elsewhere.[4,15,17] In short, orolaryngeal intubation was performed with an operating laryngoscope attached to a chest support (Karl Storz, Tuttlingen, Germany). It was positioned to expose the entire circumference of the vocal cords. Ventilation was sustained by a low-frequency jet through a nozzle fixed to the outer orifice of the instrument. A rigid bronchoscope was used to dilate the narrowed trachea and to peel off the congested or infiltrated mucosa. If necessary, the main stem bronchi were pretreated in a similar way.

Stent insertion seems to be of immediate and sustained benefit whenever the tracheobronchial tree is compromised by extrinsic tumor compression or respiratory-digestive tract fistula. Most patients (77% to 100%) experience prompt symptomatic and functional improvement. According to published data,[3] the main serious side effects are stent dislodgment, mucus impaction within the device, and granulation at both ends of the device. The complication rates vary between 5% and 25% irrespective of the particular material or shape. Stent location within the central airways (trachea and bifurcation) is associated with median survival durations of 4 to 10.5 months. Whether survival is prolonged in comparison to that of nonstented patients with similar tumor growth remains a matter of debate.[4] Compared with data from the pertinent literature, our patients' duration of survival was distinctly shorter. One reason may have been a more advanced cancer stage, as evidenced by the additional damage of the laryngeal nerves. Second, esophageal carcinoma, once it infiltrates the trachea and adjacent structures, may grow more aggressively than lung cancer with concomitant tracheal involvement. Two of our 6 patients died of fatal hemorrhage, which is a higher rate than that found in other study groups, in which lung cancer is a frequent cause of tracheal stenosis. The relatively short observation period may have contributed to the total lack of noted stent complications, which tend to increase with indwelling time. Even tumor growth through the open mesh of the Palmaz stent, as has occasionally been reported, was missing in the present series.

CONCLUSIONS

Palliative measures in end-stage tumor patients should provide effective long-standing relief from distressing conditions such as pain, dyspnea, and recurrent pneumonia without being too invasive, painful, or risky by themselves. In no case should they be associated with any substantial morbidity, let alone mortality. In our experience, cordotomy plus tracheal stenting reliably provided prompt and adequate palliation for cancer patients with serial tracheal occlusion and BVCP. However, there were some drawbacks that necessitated reintervention: occasional massive fibrin deposits on the resection wound, and a vocal cord incision that proved to be too narrow to be of real benefit. There happened to be no major stent problems such as dislocation or mucus impaction, which have been described elsewhere.

Whereas stent insertion can be performed on an outpatient basis, given a sufficiently long postoperative surveillance period (6 hours), laser cordotomy often leads to transient edema, fibrin deposits, and debris that would cause serious restenosis unless instantly removed. Hence, hospitalization of at least 2 days is necessary.

In light of our experience, unilateral posterior cordotomy may sometimes be insufficient for an adequate enlargement of the glottic airway in end-stage cancer. Therefore, bilateral posterior cordotomy or subtotal cordectomy will be chosen whenever necessary for the treatment of future patients. In addition, we will try to improve our interdisciplinary emergency airway management protocol in such a way that both interventions (cordotomy and tracheal stenting) can consistently be carried out during one single session of anesthesia, thereby obviating multiple airway procedures.

Whether the presented approach is a true advantage over tracheostomy in terms of survival rate, reduced respiratory emergencies, lower infection rates, etc, will be elucidated further. It seems unquestionable, however, that quality-of-life issues are better addressed in end-stage cancer patients with central airway stenosis if endoscopic techniques are applied to restore the airway and tracheostomy is avoided. These are preliminary data. Clearly, more research will be needed to elaborate criteria for individual treatment selection, given the choice of different endolaryngeal procedures that are readily available.

REFERENCES

1. Strauss A, Pinder M, Lipman J, Conidaris M. Acute stridor as a presentation of bilateral abductor vocal cord paralysis. Anaesthesia 1996;51:1046-8.

2. Wassermann K, Koch A, Warschkow A, Mathen F, Müller-Ehmsen J, Eckel HE. Measuring in situ central airway resistance in patients with laryngotracheal stenosis. Laryngoscope 1999;109:1516-20.

3. Wassermann K. Atemwegsstents. Ein skeptisches Plädoyer für die Palliativmedizin. Dtsch Med Wochenschr 2000;125:429-35.

4. Wassermann K, Eckel HE, Michel O, Müller RP. Emergency stenting of malignant obstruction of the upper airways: long-term follow-up with two types of silicone prostheses. Ann Otol Rhinol Laryngol 1998;107:149-54.

5. Eskew JR, Bailey BJ. Laser arytenoidectomy for bilateral vocal cord paralysis. Otolaryngol Head Neck Surg 1983;91:294-8.

6. Ossoff RH, Sisson GA, Duncavage JA, Moselle HI, Andrews PE, McMillan WG. Endoscopic laser arytenoidectomy for the treatment of bilateral vocal cord paralysis. Laryngoscope 1984;94:1293-7.

7. Dennis DP, Kashima H. Carbon dioxide laser posterior cordectomy for treatment of bilateral vocal cord paralysis. Ann Otol Rhinol Laryngol 1989;98:930-4.

8. Ossoff RH, Duncavage JA, Shapshay SM, Krespi YP, Sisson GS. Endoscopic laser arytenoidectomy revisited. Ann

Otol Rhinol Laryngol 1990;99:764-71.

9. Crumley RL. Endoscopic laser medial arytenoidectomy for airway management in bilateral laryngeal paralysis. Ann Otol Rhinol Laryngol 1993;102:81-4.

10. Remacle M, Lawson G, Mayné A, Jamart J. Subtotal carbon dioxide laser arytenoidectomy by endoscopic approach for treatment of bilateral cord immobility in adduction. Ann Otol Rhinol Laryngol 1996;105:438-45.

11. Bigenzahn W, Hoefler H. Minimally invasive laser surgery for the treatment of bilateral vocal cord paralysis. Laryngoscope 1996;106:791-3.

12. Eckel HE, Thumfart M, Wassermann K, Vössing M, Thumfart WF. Cordectomy versus arytenoidectomy in the management of bilateral vocal cord paralysis. Ann Otol Rhinol Laryngol 1994;103:852-7.

13. Spiessl B, Beahrs OH, Hermanek P, et al. TNM-Atlas. Illustrierter Leitfaden zur TNM/pTNM-Klassifikation maligner Tumoren. Berlin, Germany: Springer, 1993:119-20.

14. Freitag L, Eicker R, Linz B, Greschuchna D. Theoretical and experimental basis for the development of a dynamic airway stent. Eur Respir J 1994;7:2038-45.

15. Müller C, Dienemann H, Hoffmann H, et al. Expandierbare Metallmaschenstents zur Behandlung von Trachealstenosen und Tracheomalazie. Zentralbl Chir 1993;118:543-8.

16. Quanjer PH. Clinical respiratory physiology. Bull Eur Physiopathol Respir 1983;19(suppl 5):49-50.

17. Wassermann K, Koch A, Müller-Ehmsen J, Reuter M, Michel O, Eckel HE. Clinical and laboratory evaluation of a new thin-walled self-expanding tracheobronchial silicone stent: progress and pitfalls. J Thorac Cardiovasc Surg 1997;114:527-34.

18. Laccourreye O, Paz Escovar MI, Gerhardt J, Hans S, Biacabe B, Brasnu D. CO2 laser endoscopic posterior partial transverse cordotomy for bilateral paralysis of the vocal fold. Laryngoscope 1999;109:415-8.

Ann Otol Rhinol Laryngol 110:2001

EPIDEMIOLOGICAL STUDIES ON HEARING IMPAIRMENT WITH REFERENCE TO GENETIC FACTORS IN SICHUAN, CHINA

XUE ZHONG LIU, MD, PHD
RICHMOND, VIRGINIA

LI RONG XU, MD
CHENGDU, CHINA

YING HU, PHD
WASHINGTON, DC

WALTER E. NANCE, MD, PHD
RICHMOND, VIRGINIA

ARISTIDES SISMANIS, MD
RICHMOND, VIRGINIA

SI LING ZHANG, MD
CHENGDU, CHINA

YING XU, MD
CHENGDU, CHINA

Hearing impairment is the most common disorder of sensorineural function and is an economically and socially important cause of human morbidity. A large-scale epidemiological survey of hearing loss was conducted with 126,876 unselected subjects (63,741 male and 63,135 female) from Sichuan, China. The overall prevalence of hearing loss was 3.28% (4,164 of 126,876), and the prevalence increased with age, reaching 12.8% (1,465 of 11,421) at 60 years of age. In 73.03% of all cases (3,041 of 4,164), the hearing loss was sensorineural, and in 20.39% (849 of 4,164), it was conductive; the remaining cases (6%) were mixed hearing loss. Bilateral loss was found in 74.5% of cases (3,103 of 4,164). In 63.79% of cases (2,656 of 4,164), the degree of hearing loss was less than 55 dB hearing level (HL), and in 5.67% of cases (236 of 4,164), it was greater than 90 dB HL. The prevalence of hearing loss in childhood (<15 years of age) was 0.67% (227 of 34,157), of which 57.7% of cases were conductive and 38.8% were sensorineural. The prevalence of genetic hearing loss was 0.28% (349 of 126,876). Persons who lived in the flatlands appeared to have a higher prevalence than those who lived in the hills. Several ethnic groups, including Tibetans, the Yi, and the Lisu, had a higher prevalence of hearing loss. Presbycusis, otitis media, and genetic factors were the most commonly recognized causes of hearing impairment overall, but otitis media and genetic factors were the main causes of hearing loss in children. Causes for the observed differences in prevalence and etiologic factors between China and industrialized countries will be discussed. In China, infections and genetic factors appear to be of major importance as causes of hearing loss.

KEY WORDS — Chinese, epidemiology, etiology, genetic deafness, hearing loss.

Hearing loss is a major community health problem and a serious medicosocial problem. There have been many investigations on population prevalence and causes of hearing loss in industrialized countries,[1-5] but few such studies have been conducted in developing nations, including China. However, such knowledge about the frequency and causes of hearing loss is an essential prerequisite to the rational planning of research and the provision of health care.

Sichuan is the most populous province in China, with 104 million people (1987). It is quite representative of all China in its economic, cultural, and demographic aspects. During 1986 and 1987, a large-scale epidemiological survey of more than 100 genetic diseases was carried out.[6] The survey covered 100 million people, a sampling frame population of 11,168,000, and a study group of 126,876 people. More than 400 doctors, paramedical personnel, epidemiologists, statisticians, and computer workers collaborated on the field, clinical, or laboratory work. As part of this project, subjects with hearing impairment were surveyed, and the prevalence and causes of hearing loss in the general population were estimated.

METHODS

Selection of Population and Sampling. Sichuan is a large province in southwestern China. Ninety-seven percent of its population is Chinese (Han). The rest are Yi, Tibetan, Qiang, Lisu, and others. The referral sites were selected on the basis of a stratified random sampling method considering the density and geographic and urban-rural distribution of the population, so that the results would be as representative of the whole province as possible. The area of Sichuan is 570,000 km^2, about 6% of the total area of China.

From the Departments of Human Genetics (Liu, Nance) and Otolaryngology (Liu, Sismanis), Medical College of Virginia, Richmond, Virginia, the Laboratory of Population Genetics, Division of Cancer Epidemiology and Genetics, National Cancer Institute, National Institutes of Health, Washington, DC (Hu), and the Department of Otolaryngology, West China University of Medical Sciences (Liu, L. R. Xu), and the Department of Epidemiological Survey, Sichuan Family Planning Research Institute (Zhang, Y. Xu), Chengdu, China. This work is part of the project Genetico-Epidemiological Surveys of the General Population in Sichuan. The data analysis of this work was partly supported by the National Institute on Deafness and Other Communication Disorders (NIDCD R03 DC04530), the Deafness Research Foundation, the National Institutes of Health (NIH DC02530), and the Foundation Fighting Blindness.

CORRESPONDENCE — Xue Zhong Liu, MD, PhD, Dept of Human Genetics, Medical College of Virginia, Sanger Hall, 1101 E Marshall St, PO Box 980033, Richmond, VA 23298-0033.

TABLE 1. PROTOCOL OF HEARING SCREENING USED IN THIS SURVEY

Stage	*Methods Used*	*Aims*
First	Questionnaires	To screen subjects for hearing loss
	Whispered voice	
	Behavioral test	
Second	History-taking otolaryngological examinations	To confirm diagnosis of hearing loss
	Otoscopy	
	Tuning fork tests	
	Pure tone audiometry	
	Otoimmittance if available	
	Examination by other specialists	To identify causes of hearing loss
	Nonaudiological tests if necessary	
Third	Establish pedigrees of unknown cases	To ascertain genetic cases
	Repeat examinations used at second stage for available family members	
	Population genetic analysis	To determine inheritance modes

Geographically, Sichuan consists of the West Sichuan Plateau, with an average altitude of more than 3,000 m, and the Sichuan Basin, below which lies Chengdu Plain. The land slopes gradually downward from northwest to southeast. Three land types — mountainous, hilly, and flat — can be distinguished. Its population distribution is uneven, with the urban-rural ratio about 1:4. Each referral site consisted of 2 to 4 neighboring villages or residents' committees (in towns) with about 3,000 people or 500 to 600 families. Selected population groups, such as army units, schools, colleges, and sites with massive emigration in the past 20 to 30 years, were excluded. Forty-two villages or towns were chosen to be referral sites and were compatible with the above requirements.

Screening Procedure. A 3-stage protocol was adopted in the current survey (Table 1). In the first stage, all inhabitants of a referral site were questioned and examined by means of a standardized comprehensive questionnaire and examination scheme by one of the team of doctors and secondary medical personnel.[6] The questionnaire used in this stage included medical and family history of all conditions investigated in this survey. In terms of hearing loss, special emphasis was placed on 1) identifying the presence or absence of hearing loss and 2) ascertaining the age at which the hearing deficit was noticed by the patient or by his or her parents, as well as the age at which the problem was diagnosed. The questionnaire used for hearing screening is shown in Table 2. The examinations designed to screen for hearing loss in this stage included whispered voice testing (>6 years of age) and behavioral tests (<6 years of age).

TABLE 2. QUESTIONNAIRE FOR SCREENING OF HEARING LOSS AT FIRST STAGE

For adults:
- Do you have any hearing impairment?
- How old were you when you noticed your hearing problem?
- Is there a history of hearing loss in your family?

For parents with children:
- Do you think your child has normal hearing?
- Does your child seem startled if there is a loud noise (such as thunder or a car horn)?
- If you speak normally to your child, does he or she turn to look at you?
- Does any family member have a hearing problem?

If any question above is answered positively for hearing loss, subject goes to second stage.

In the second stage, patients in whom hearing loss was suspected were referred to otologists and other specialists (including a pediatrician, an obstetrician, an ophthalmologist, a dermatologist, a neurologist, a surgeon, and an internist) to evaluate the causes of hearing loss and to identify associated organ abnormalities. This entailed a careful history-taking, clinical investigations, and laboratory tests that would indicate exogenous factors or identify a genetic cause. A detailed history regarding age at onset and knowledge of pathogenesis (infection, drugs, etc) was obtained. Nonaudiological examinations included triiodothyronine and thyroxine levels, urine tests for proteinuria and hematuria, electrocardiography, skull radiography, and chromosomal analysis.

The last stage involved investigating patients in whom no environmental factors were identified that would be responsible for hearing impairment. A detailed medical history was obtained, with an emphasis on a family history of hearing loss and other associated congenital anomalies, and a pedigree including at least 3 generations was established. Routine otologic examinations (including pure tone and oto-immittance audiometry) and physical examinations were carried out on all available family members. Finally, a segregation analysis as described by Vogel and Motulsky[7] was applied to determine the inheritance modes of hearing loss in these patients. In our study,

TABLE 3. DISTRIBUTION OF HEARING LOSS BY AGE IN 4,164 CASES

		Patients With Hearing Loss		
Age (y)	*Total No. Examined*	*No. of Cases*	*Percentage*	*Prevalence (%)*
0-4	8,915	20	0.48	0.22
5-9	8,826	57	1.37	0.65
10-14	16,416	150	3.60	0.91
Total children	34,157			
15-29	38,231	511	12.27	1.34
30-44	26,613	953	22.89	3.58
45-59	16,454	1,008	24.21	6.12
60+	11,421	1,465	35.18	12.83
Total adults	92,719			
Total	126,876	4,164	100.00	3.28

the proportion of autosomal recessive (AR) to autosomal dominant (AD) nonsyndromic cases in the genetic group was determined by segregation analysis. This statistical technique estimates the segregation ratio, proportion of sporadic cases, and ascertainment probability. This method assumes complete ascertainment, which is appropriate because all affected individuals in the referral sites were ascertained. Analysis of multiplex sibships (more than 1 affected sibling) with unaffected parents gave a segregation ratio of 0.27±0.07, compatible with AR inheritance. The proportion of nongenetic cases was estimated from the proportion of simplex (1 affected) to multiplex families.[8]

Audiological Assessment. Pure tone audiometry (Danplex AS 72 audiometer, air conduction and bone conduction with masking, if necessary) was undertaken whenever possible. Air conduction thresholds were measured at 250 and 500 Hz and at 1, 2, 6, and 8 kHz. Bone conduction thresholds were determined to identify the type of hearing loss. Oto-immittance measurements were carried out in some patients, and all were examined otoscopically. Individuals with a hearing loss averaging 27 dB hearing level (HL) or more in the better ear across 500, 1,000, 2,000, and 4,000 Hz were regarded as affected. The degree of hearing loss was examined in terms of mean values across the frequency range. The degree of loss was divided into the following categories: less than 55 dB HL, 56 to 90 dB HL, and more than 90 dB HL. Sensorineural hearing loss was defined as an air-bone gap of less than 15 dB averaged over 0.5, 1, and 2 kHz. Conductive hearing loss was defined as normal bone conduction thresholds (<20 dB) and an air-bone gap of greater than 15 dB averaged over 0.5, 1, and 2 kHz. Mixed hearing loss was diagnosed if there was a more than 20–dB HL bone conduction threshold, together with a 15-dB air-bone gap averaged across 0.5, 1, and 2 kHz.

TABLE 4. PREVALENCE OF HEARING LOSS IN DIFFERENT GEOGRAPHIC AREAS

Geographic Area	*Total Subjects Examined*	*No. With Hearing Loss*	*Prevalence (%)*
Flatlands	33,597	1,291	3.84
Hills	52,107	1,541	2.96
Mountains	41,172	1,332	3.24

TABLE 5. PREVALENCE OF HEARING LOSS IN DIFFERENT ETHNIC GROUPS

Ethnic Group	*Total No. Examined*	*No. With Hearing Loss*	*Prevalence (%)*
Han (Chinese)	116,534	3,726	3.20
Yi	2,964	164	5.53
Tibetan	2,933	129	4.40
Lisu	1,968	95	4.83
Others	2,477	50	2.02

RESULTS

In total, 126,876 persons (63,741 male and 63,135 female) were investigated, representing 96% of the population in the referral sites. To evaluate the first stage of the screening protocol, we invited all subjects from the first referral site to undergo all of the tests from the first stage to the third stage.[6] Analysis of the resulting data showed that the initial screening test for hearing loss had a sensitivity of 87.5% and a specificity of 93.3%. Among the 126,876 people screened at the first stage, 4,164 were identified as having hearing loss. The overall prevalence was 3.28% of the general population, with no significant difference between male (3.34% or 2,191 of 63,741) and female (3.13% or 1,973 of 63,135; p > .05) subjects. The distribution of various ages for the 4,164 cases is shown in Table 3. The prevalence of hearing loss increases with age. The prevalences in various geographic areas and different ethnic groups are shown in Tables 4 and 5, respectively.

The hearing loss was sensorineural in 73.03% of patients (3,041 of 4,164), conductive in 20.39% (849), and mixed conductive and sensorineural in 6.58% (274). The hearing loss was bilateral in 74.5% (3,103) and unilateral in 25.5% (1,061). The distribution and prevalences of degrees of hearing loss can be seen in Table 6. The prevalence of hearing loss was 0.67%

TABLE 6. DISTRIBUTION OF HEARING LOSS BY SEVERITY IN 4,164 CASES

Hearing Threshold (dB)	*No. of Cases*	*Percentage*	*Prevalence (%)*
<55	2,656	63.79	2.09
56 to 90	1,272	30.54	1.00
>90	236	5.67	0.19
Total	4,164	100.00	3.28

TABLE 7. DISTRIBUTION OF CAUSES IN 4,164 PATIENTS

Cause	*No. of Cases*	*Percentage*	*Prevalence (%)*
Environmental	3,156	75.80	2.49
Presbycusis	1,563	37.54	1.23
Sequelae of otitis media	1,034	24.83	0.82
Noise-induced	227	5.45	0.19
Ototoxicity	121	2.91	0.10
Infections	84	2.02	0.07
Trauma	47	1.13	0.04
Sudden onset	17	0.41	0.01
Ear malformation	15	0.36	0.01
Others	48	1.15	0.04
Genetic	349	8.38	0.28
Autosomal recessive (nonsyndromic)	216	5.19	0.17
Autosomal dominant (nonsyndromic)	105	2.52	0.08
Otosclerosis	10	0.24	0.008
Familial ototoxicity	9	0.22	0.007
X-linked	5	0.12	0.004
Usher's syndrome	2	0.05	<0.001
Waardenburg's syndrome	1	0.02	<0.001
Pendred's syndrome	1	0.02	<0.001
Chromosomal defects	3	0.07	0.002
Unknown	656	15.75	0.52
Total	4,164	100.00	3.28

in children younger than 15 years of age (227 of 34,157), in whom the hearing loss was conductive in 57.7%, sensorineural in 38.8%, and mixed in 3.5%. The prevalence of hearing loss was 4.25% in adults (3,937 of 92,719), in whom the hearing loss was conductive in 17.78%, sensorineural in 75.01%, and mixed in 6.76%. Profound deafness (defined as a hearing loss of greater than 90 dB HL) was found in 17.2% of the children (39 of 227), for a prevalence of 0.114%.

In 84.25% of cases, a causative factor could be identified, whereas in 15.75%, the cause of the hearing impairment was unknown, as shown in Table 7. The distribution of causes of hearing loss in children and adults is presented in Table 8.

DISCUSSION

Prevalence of Hearing Loss. Hearing impairment is the most common sensorineural impairment. Some population-based surveys on hearing have been undertaken in industrialized countries, and existing information about prevalences was obtained from them.[1-5] Estimates of the prevalence of hearing impairment in China are not accurate. In previous studies,[9,10] the authors selected groups of people in schools for the deaf or in certain geographic locations. Therefore, their sampling represents a biased view that is not representative of the population as a whole. To estimate the actual prevalence of hearing loss in a general population, it is necessary that people be examined and tested from different geographic regions. In addition, the audiological tests must be standardized to encompass all ages and degrees of hearing loss. The present survey aims to provide an accurate measure of the prevalence of hearing loss in the general population of Sichuan.

TABLE 8. DISTRIBUTION OF CAUSES OF HEARING LOSS IN CHILDREN AND ADULTS

Cause	*Children*		*Adults*	
	No.	*%*	*No.*	*%*
Presbycusis			1,563	39.70
Otitis media	123	54.19	911	23.14
Genetic factors	42	18.50	307	7.80
Noise	15	6.61	212	5.38
Ototoxicity	18	7.93	103	2.62
Infections	14	6.17	70	1.78
Trauma	7	3.08	40	1.01
Others	8	3.52	731	18.57
Total	227	100.00	3,937	100.00

The overall prevalence of hearing loss in the general population of Sichuan obtained from the present survey was 3.82%, which is lower than that of industrialized countries. A national survey in the United Kingdom suggested that 20% of the population had a hearing impairment exceeding 25 dB HL in the better-hearing ear.[1] A similar survey in the US population based on household interviews of civilians found that approximately 4% of people younger than 45 years of age and 29% of those 65 years or older had a hearing loss.[2] Population-based surveys on hearing from England and Denmark reported an overall 15% to 20% prevalence of hearing loss (>25 dB HL for the average across 0.5 to 4 kHz in the better ear).[4,11] The difference in prevalence between China and Western countries may be explained by the following factors: 1) there may be a true difference between the countries; 2) different criteria and different screening methods for hearing loss were used; 3) the individuals in the developed countries might have more noise exposure, in light of the low prevalence of noise-induced hearing loss in China; and 4) there may be a demographic difference in age between China and the Western countries. The results of the investigation (Table 3) also indicated that the prevalence of hearing impairment increased with age, so that approximately 12.8% of the population were affected by 60 years of age — similar to the prevalence in the US population.[2]

There are numerous surveys of hearing impairment in childhood throughout the world, with the prevalence ranging from 0.5 to 4.2 per 1,000.[3,12] The data on the prevalence in childhood are often obtained from clinical samples that are ill-defined from an epidemiological perspective. An appropriate study based on identical birth cohorts (1983 to 1988) from England and Denmark showed that the prevalence of bilateral sensorineural or mixed hearing loss in childhood was 127 per 100,000 (>40 dB for the average across the audiometric frequencies 0.5 to 4 kHz).[5] In our survey, the overall prevalence of hearing impairment in childhood (<15 years) and the prevalence of sensorineural or mixed hearing loss (>27 dB for the average across the frequencies 0.5 to 4 kHz) are 665 per 100,000 and 281 per 100,000, respectively. That these prevalences are much higher than those of Western countries can be attributed to different criteria for hearing loss and to a higher prevalence in China of hearing loss due to otitis media.

In the present series, there was a difference in prevalence among various types of hearing loss, with the highest prevalence being 2.4%, for sensorineural hearing loss. In the child group, the prevalence of conductive hearing loss (3.84%) was significantly higher than that of sensorineural hearing loss (2.58%; $p < .05$). Conductive hearing loss was identified in only 17.6% of adult cases, but was identified in 61.2% of child cases. These differences may reflect the fact that children are more susceptible to the factors that can cause damage to the middle ear and that conductive hearing loss is the main type of hearing impairment in children in China. For most patients (63.79%), the degree of hearing loss is less than 55 dB HL. Only 5.67% of patients had a hearing loss of more than 90 dB HL.

There have been many population-based surveys concerning the prevalence of hearing loss as a function of age, gender, hearing levels, and social class, but few reports offer the prevalence of genetic hearing impairment. In the current survey, special attention was focused on identifying genetic hearing loss at the time the data were collected and during their analysis (see Methods). The overall prevalence of genetic hearing loss was 275 per 100,000, with a high prevalence of nonsyndromic AR hearing loss (170 per 100,000; Table 7). This high prevalence may be explained in part by the high incidence of consanguinity in some population groups. Overall, consanguinity was documented in 7.4% of the AR group in this study. An estimate of the incidence of genetic hearing loss in childhood of 123 per 100,000 was obtained from this survey, which is somewhat higher than the prevalence of 88 per 100,000 claimed in the first decade of life in an age-matched population-based study.[12] To our knowledge, no epidemiological information is available on the prevalence of genetic hearing loss in adult populations, largely because of the lack of large-scale genetic-epidemiological surveys. In this study, the prevalence of genetic hearing impairment in the adult population (≥15 years) was 335 per 100,000, which is higher than that in children. This result is not surprising, because genetically determined hearing impairment can develop at any age throughout life, either as the sole manifestation of the mutant genes or as part of an inherited syndrome.[13] Among syndromic hearing losses, only Waardenburg's, Usher's, and Pendred's syndromes were identified (Table 7) — compatible with the fact that they are the most frequent syndromes that include deafness.[14] In terms of chromosomal defects, Down syndrome was diagnosed in 3 cases, for a prevalence of 2.37 per 100,000.

Presently, there are few reports on the prevalence of hearing impairment in different geographic areas and among different ethnic groups in China. Our results showed that the population located in the flat area appeared to have a higher prevalence of hearing impairment than did people who lived in the hills and mountains (Table 4). There also appeared to be differences in the prevalence of hearing loss among different ethnic groups in Sichuan. The 3 main minorities (Tibetan, Yi, and Lisu) presented a higher prevalence than did the Chinese Han (Table 5). The reasons for the differences between geographic areas and between ethnic groups are unclear.

Causes of Hearing Loss. A number of reports appearing over the years have addressed the causes of hearing impairment in populations throughout the world.[1,3,13] However, most of the studies were carried out in industrialized countries, and there is little information on the causes of hearing loss in the developing nations. In many surveys throughout the world, the proportion of various causes of hearing impairment varies among populations.[15] Probably the most important reason is the difficulty of obtaining appropriate etiologic data, arising from a lack of worldwide consensus on protocols for investigation and diagnosis. In addition, making accurate judgments about the etiologic effect of genetic factors in hearing impairment is not easy, because there is no uniform clinical terminology or set of criteria for genetic hearing loss.

In our investigation, the cause of hearing impairment was clarified in 84.25% of cases; in 15.75%, the etiologic factors were unknown. As shown in Table 7, the most common causes of hearing impairment in the general population of China are presbycusis, otitis media, and genetic factors. An etiologic analysis of a profoundly deaf group has been published showing genetic factors (43%) and infectious diseases (31%) as the main causes.[16]

Most conductive or mixed hearing loss (94.2% in children, 92.58% in adults) results from chronic suppurative otitis media and otitis media with effusion, from which most adult patients suffered in childhood. Among other infectious diseases, high fever (defined as hearing loss without identified cause after high fever), meningitis, and measles were other significant causes (Table 7). The proportion of middle ear infection in various age groups may reflect etiologic differences between developed countries and developing countries. In China, there is surprisingly little mention of the etiologic effect on hearing of viral factors such as congenital rubella, which is cited as a significant cause of congenital deafness.[14,15] One of the probable reasons is that few deaf children take routine serologic tests for the virus in China. However, as shown in a study on the prevalence of congenital profound deafness in this population, certain environmental factors (such as rubella) would contribute to the differences in prevalence related to different ages and seasons.[17] In our survey, presumably, cases that resulted from congenital viral infections might have been placed in the "unknown" category.

It is hard to carry out a direct comparative analysis of the proportion of genetic hearing loss between 2 studies because of the wide range in criteria, definition of samples, age of subjects, and hearing levels. The estimates of the proportion of cases with genetic hearing impairment vary widely, from 3% to 78% in adults and children[15] and from 9% to 54% in childhood.[18] The wide variation in the percentage of hereditary hearing loss may reflect true differences in genetic expression within the various target populations. However, it is possible that the etiologic effect of genetic factors in hearing impairment has been underestimated in the literature because of 1) a lack of valid epidemiological data on genetic hearing loss; 2) difficulties in distinguishing genetic hearing impairment from acquired impairment audiologically[19]; and 3) the poor specificity and low sensitivity of routine audiological methods for screening the carriers of genes that cause hearing impairment.[20,21]

There have been few surveys in China to evaluate the etiologic effects of genetic factors. In the present study, inherited hearing impairment accounted for 20.98% of the adults with sensorineural hearing loss (excluding presbycusis) and 42.6% of the children with sensorineural hearing loss. The most common forms of genetic hearing impairment were the AR forms, accounting for 62.75% of cases, and AD forms, accounting for 33.24%. X-linked inheritance was found in 1.43%, and mitochondrial transmission in 2.58%. In another study, only 5.94% of genetically determined profound hearing loss was the AD form.[16] The high proportion of the AD mode in the current study can be attributed to the fact that cases of hearing loss ranging from mild to profound were included. Recent advances in molecular biology and genetics have made possible the isolation, sequencing, and characterization of genes that cause hearing impairment. This will provide a basis for better understanding of the molecular biochemistry and development of the auditory system. The genes for several of the most common genetic syndromes that include deafness (Waardenburg's, Usher's, and Pendred's syndromes) have been identified.[22] There has been substantial recent progress in nonsyndromic hearing loss, with more than 50 loci having been mapped from various populations around the world.[23] Moreover, 2 forms of genetic deafness are much more frequent than the others, accounting for at least 30% of all genetic cases in many populations. One of these genes, the connexin 26 locus (Cx26), has been found to be a major cause of nonsyndromic AR deafness in many populations.[23] Most interestingly, a single mutation in the connexin 26 gene, 35delG, accounts for the majority (60% to 80%) of mutant Cx26 alleles in families with nonsyndromic deafness in the United Kingdom, France, Italy, Spain, Tunisia, Lebanon, Australia, Russia, and New Zealand. The second most common form of genetic deafness is the A1555G substitution in a mitochondrial ribosomal RNA gene, which causes increased susceptibility to aminoglycoside antibiotic–induced deafness, as well as nonsyndromic hearing loss.[24] The mitochondrial DNA (mtDNA) A1555G mutation has been reported in many ethnic groups, with more than 20% of deaf individuals carrying this mutation in some populations.[23] So far, there have been no reports regarding Cx26 mutations and mtDNA A1555G mutation or the prevalence of the 35delG mutation in large samples of Chinese patients with nonsyndromic hearing loss. At least 8 different loci were responsible for AR profound deafness in the present population on the basis of the calculation of heterogeneity.[17] Recently, 2 Chinese families with nonsyndromic AR deafness from the current population were identified as carrying mutations in the myosin VIIA gene.[25] More recently, we have started to perform mutation analysis of the 2 most common mutations in a large number of probands with nonsyndromic hearing loss from this population. We found that 30% of the probands carried the mtDNA A1555G mutation. Surprisingly, the 35delG mutation in Cx26 was not found in any of these cases (Liu et al, unpublished data).

A variety of commonly used drugs have ototoxic properties. The most common ototoxic drugs in China are aminoglycoside antibiotics (such as streptomycin, kanamycin, and gentamicin). The incidence of aminoglycoside-induced deafness has increased in recent years and is one of the major causes of hearing impairment in China. Some investigations based in schools for the deaf have indicated that 12.8% to 66.1% of cases of profound deafness resulted from aminoglycoside antibiotics, with a population prevalence of 0.035%.[9] In our survey, the prevalence of drug-induced deafness was 0.103% and accounted for 8.8% of sensorineural hearing loss (excluding presbycusis) and for 20.45% of sensorineural hearing loss in children. Among the 130 cases of pharmacological ototoxicity, 6.92% had a positive family history, yielding a prevalence of recognizable familial cases of 0.007%. The matrilineal transmission of aminoglycoside-induced deafness in the Chinese population was first reported in isolated pedigrees in the early 1990s, and mutations in the mtDNA were suggested as the likely cause.[26,27] The identification of the mtDNA A1555G mutation in a large proportion of families with nonsyndromic deafness in our sample provides a molecular explanation for the high prevalence of aminoglycoside-induced hearing loss in the Chinese population.

Presbycusis, the hearing loss associated with aging, is the most common etiologic form of hearing loss in all studied populations. It affects more than 27% of persons over the age of 65 years and 50% of those 80 years of age or older.[2,4] Because of the lack of worldwide diagnostic criteria for presbycusis and different socioeconomic conditions, we defined cases as presbycusis using the following criteria: 1) age of hearing impairment greater than 55 years; 2) symmetric bilateral sensorineural hearing loss without known causes; and 3) negative family history of hearing loss. In the present study, presbycusis accounted for 37.54% of all cases, and affected 9.99% of those more than 55 years of age.

CONCLUSION

Individuals with hearing impairment were investigated in the general population of Sichuan. The total prevalence (3.28%) of hearing impairment obtained from this study is significantly lower than that in industrialized nations, but the prevalence in children (0.665%) is significantly higher than that in reports from Western countries, mainly because of a higher prevalence of otitis media in China. There is a significant difference in the proportion of the types of hearing loss between children and adults. The prevalences of genetic hearing loss in children (0.11%) and in adults (0.33%) were higher than those in previous reports. The high proportions of infections in the middle ear and aminoglycoside-induced hearing loss reflect differences in causes of hearing impairment between developed countries and developing ones. Presbycusis and sequelae of otitis media were the main causes of hearing impairment in adults; otitis media and genetic factors were the main causes in children. It is suggested that the effect of genetic factors in the general population should be emphasized.

ACKNOWLEDGMENTS — We thank all of the medical personnel from the 11 prefectures of Sichuan who aided in the field, clinical, and laboratory work.

REFERENCES

1. Davis AC. Hearing disorders in the population: first phase findings of the MRC National Study of Hearing. In: Lutman ME, Haggard MP, eds. Hearing, science and hearing disorders. New York, NY: Academic Press, 1983:35.

2. Dawson DA. National Center for Health Statistics: current estimates from the National Health Interview Survey, 1989. Vital and Health Statistics, Series 10. No. 176.

3. Davidson J, Hyde ML, Albert PW. Epidemiology of hearing impairment in childhood. Scand Audiol 1988;30:13-20.

4. Davis AC. The prevalence of hearing impairment and reported hearing disability among adults in Great Britain. Int J Epidemiol 1989;18:911-7.

5. Davis AC, Parving A. Towards appropriate epidemiology data on childhood hearing disability: a comparative European study of birth-cohorts 1982-1988. J Audiol Med 1994;3:35-47.

6. Zhang SL, Tang XD, Zhang SZ. Genetico-epidemiological survey of the general population in Sichuan. Chengdu, China: CST University Press, 1990:10-58.

7. Vogel F, Motulsky AG. Human genetic problems and approaches. New York, NY: Springer-Verlag, 1979:530-98.

8. Liu XZ, Xu LR. Sensorineural hearing loss: a segregation analysis. J Chin Med Genet 1988;5:193-5.

9. Hu DN, Qiu WQ, Wu BT, et al. Prevalence and genetic aspects of deaf mutism in Shanghai. J Med Genet 1987;24:589-92.

10. Jiang SZ, Wang SL, Liu PI. The survey of hearing loss in Nangton County, China. Chin J Otolaryngol 1988;23:282-3.

11. Parving A, Hein HO, Suadicani P, Ostri B, Gyntelberg F. Epidemiology of hearing disorders: some factors affecting hearing. The Copenhagen male study. Scand Audiol 1993;22:101-7.

12. Parving A. Hearing disability in childhood — a cross-sectional and longitudinal investigation of causative factors. Int J Paediatr Otorhinolaryngol 1993;27:101-11.

13. Gorlin RJ. Genetic hearing loss with no associated abnormalities. In: Gorlin RJ, Toriello HV, Cohen MM, eds. Hereditary hearing loss and its syndromes. Oxford, England: Oxford University Press, 1995:43-61.

14. Fraser GR. The causes of profound deafness in children. Baltimore, Md: Johns Hopkins University Press, 1976.

15. Williamson I, Steel K. The aetiology of hearing impairment. Hereditary Deafness Newsletter 1990;5:7-16.

16. Liu XZ, Xu LR, Zhang SL, Xu Y. Prevalence and aetiology of profound deafness in the general population of Sichuan, China. J Laryngol Otol 1993;107:990-3.

17. Liu XZ, Xu LR, Zhang SL, Xu Y. Epidemiological and genetic studies of congenital profound deafness. Am J Med Genet 1994;53:192-5.

18. Parving A. Epidemiology of genetic hearing impairment. In: Martini A, Read A, Stephens D, eds. Genetics and hearing impairment. London, England: Whurr Publishers, 1996:73-81.

19. Liu X, Xu L. Nonsyndromic genetic deafness: an analysis of audiograms. Ann Otol Rhinol Laryngol 1994;103:428-33.

20. Meredith R, Stephens D, Sirimanna T, Meyer-Bisch C, Reardon W. Audiometric detection of carriers of Usher's syndrome type II. J Audiol Med 1992;1:11-9.

21. Liu XZ, Newton VE. Distortion product emissions in normal-hearing and low-frequency hearing loss carriers of genes for Waardenburg's syndrome. Ann Otol Rhinol Laryngol 1997; 106:220-5.

22. Steel K, Brown SDM. Genetics of deafness. Curr Opin Neurobiol 1996;6:520-5.

23. Van Camp G, Smith RJH. Hereditary hearing loss homepage. Available at: http:dnalab-www.uia.ac.be/dnalab/hhh/. Accessed 1999.

24. Prezant TR, Agapian JV, Bohlmann MC, et al. Mitochondrial ribosomal RNA mutation associated with both antibiotic-induced and non-syndromic deafness. Nat Genet 1993;4:289-94.

25. Liu XZ, Walsh J, Mburu P, et al. Mutations in the myosin VIIA gene cause non-syndromic recessive deafness. Nat Genet 1997;16:188-90.

26. Liu XZ, Xu LR, Yang S. Aminoglycoside-induced hearing loss: a mitochondrial inheritance. Hereditary Deafness Newsletter 1991;6:18.

27. Hu DN, Qiu WQ, Wu BT, et al. Genetic aspects of antibiotic induced deafness: mitochondrial inheritance. J Med Genet 1991;28:79-83.

Ann Otol Rhinol Laryngol 110:2001

INCIDENCE OF PHARYNGEAL HYPOPHYSIS IN NEONATES

A HISTOLOGIC STUDY

BOSCO E. NORONHA, MS, DIPNBE
NARESH K. PANDA, MS, DIPNBE, FRCS(ED)
S. B. S. MANN, MS, FAMS
Y. N. MEHRA, FRCSC, DABO
C. K. BANERJEE, MD
CHANDIGARH, INDIA

The presence of adenohypophysial tissue in the nasopharynx is no longer disputed. This study was performed in 50 neonatal cadavers subjected to medical autopsy within 6 hours of death. The aim was to study the incidence of extrasellar pituitary tissue in the nasopharynx and its various histologic cell types. The transpalatal approach was used to obtain the specimens. The specimens were stained with hematoxylin and eosin and periodic acid-Schiff–orange G for selective demonstration of adenohypophysial cells. Histopathologic evaluation led to the detection of pituitary tissue in 16% of the examined specimens. Selective staining demonstrated a 6% positive incidence of adenohypophysial cells. The pharyngeal hypophysis exists in 2 forms: a typical adenohypophysial collection of cells and an atypical subepithelial cluster. The incidence of hypophysial tissue was higher in the older neonates, perhaps because of hormonal stimulation of the caudal remnant of Rathke's pouch.

KEY WORDS — histology, neonate, pharyngeal pituitary tissue.

INTRODUCTION

The collection of adenohypophysial tissue with functional potential in the mucoperiosteum of the nasopharynx was first described by Erdheim and Stumme[1] in 1909. Many studies[1-4] have demonstrated and documented the presence of extrasellar pituitary tissue. Melchionna and Moore[2] detected pharyngeal gland tissue in 51 of 54 cases, present constantly in the midline submucosa or the periosteum adjacent to the vomerosphenoidal articulation. It occurred most frequently as a single well-circumscribed and encapsulated structure. Richards and Evans[5] noted in their series that the pharyngeal hypophysis is an elongated structure approximately 5 mm long, 0.5 mm wide, and 0.3 mm deep. After a study of 133 hypophyses, McGrath[6] reported the length, width, and depth as 9.6 mm, 1.5 mm, and 1 mm, respectively.

The pharyngeal pituitary tissue is histologically very similar to the corresponding adenohypophysis. The appearance is of a glandular tissue with a poorly defined capsule. Chromophobes, acidophils, and basophils are present in approximately the same proportions as in the adenohypophysis.[6]

The functional significance of the pharyngeal hypophysis is in doubt, even after its histologic demonstration by many authors. There have been some studies wherein adenohypophysial hormones have been extracted from the pharyngeal hypophysis of embalmed cadavers.[7] Tumors of the pharyngeal hypophysis have also been reported in literature,[5,8,9] thereby enhancing the surgical significance of this entity. The present study was undertaken in neonatal cadavers, first to highlight the incidence of extrasellar adenohypophysial tissue in the roof of the nasopharynx, and then to study the various histologic cell types in the specimens.

MATERIAL AND METHODS.

This study was performed on 50 neonatal cadavers (less than 1 month of age) that were subjected to medical autopsy at the Postgraduate Institute of Medical Education and Research, Chandigarh, India, in collaboration with the Department of Pathology. All cadavers were dissected for the tissue specimens within 6 hours of death. A lawful familial consent was obtained before the dissection of study material.

Mode of Obtaining Specimens. The pharyngeal pituitary tissue is normally located over the vomerosphenoidal articulation and adjacent roof of the nasopharynx. A transpalatal approach was used to obtain the tissue specimen. After a Boyle-Davis mouth gag was applied, a curvilinear incision was made along the hard and soft palate just inside the gingival margins, extending onto the posterior extremity of the alveolar margins on both sides. The mucosa along with the periosteum was elevated over the entire area of the hard palate. The soft tissue over the hard palate along with the soft palate was removed so as to provide partial exposure of the nasopharyn-

---

From the Departments of Otolaryngology (Noronha, Panda, Mann, Mehra) and Morbid Anatomy (Banerjee), Postgraduate Institute of Medical Education and Research, Chandigarh, India.

CORRESPONDENCE — Naresh K. Panda, MS, DipNBE, FRCS(Ed), Dept of Otolaryngology, PGIMER, Chandigarh-12, India 160012.

TABLE 1. AGE DISTRIBUTION

Group	*Age (d)*	*No.*	*%*
1	1-5	4	8
2	6-10	5	10
3	11-15	9	18
4	16-20	10	20
5	21-25	11	22
6	26-30	11	22
	Total	50	100

geal vault. The exposure of the vomerosphenoidal articulation was accomplished by removing the bone of the entire hard palate.

After exposure of the biopsy site, a horizontal periosteum-deep incision was made along the posterior third of the vomerine part of the nasal septum. The mucoperiosteum from the posterior third of the vomer and adjacent vomerosphenoidal articulation and nasopharyngeal vault was then elevated off the osseous base. The final specimen was a rectangular piece of tissue measuring 15 × 10 mm with its long axis in the midsagittal plane and centered on the vomerosphenoidal articulation.

Processing and Staining. The specimen was stored in a 4% solution of formalin. Subsequently, the tissue was processed routinely, and paraffin blocks were prepared. Thin sections of 5 to 8 µm were then made from the blocks. One set of sections was stained with hematoxylin and eosin dye, and a second set was stained with periodic acid–Schiff (PAS)–orange G. The slides were then studied under high- and low-power magnification. The primary intention of microscopy was to identify the presence of pituitary tissue, the types of cells (chromophobes, acidophils, and basophils), and subepithelial cell rests, which are thought to be a remnant of Rathke's pouch. In the hematoxylin and eosin preparation, the following features were looked for in the nonpituitary tissue: 1) type of surface epithelium, 2) presence of adenoid and/or lymphoid collection, 3) vascularity of the tissue, and 4) presence of fibrous and cellular infiltrates and associated features such as cyst formation and colloid aggregates.

The study material was divided into 6 subgroups (Table 1) based on the age of the cadavers in days: group 1 (1 to 5 days), group 2 (6 to 10 days), group 3 (11 to 15 days), group 4 (16 to 20 days), group 5 (21 to 25 days), and group 6 (26 to 30 days).

TABLE 2. OBSERVATIONS IN NONPITUITARY TISSUE

	% of Specimens
Adenoid tissue	92
Cellular infiltrates	
Diffuse	32
Neuronal tissue	40
Salivary gland tissue	
Seromucinous	60
Mucinous	40

Surface epithelium was pseudostratified.

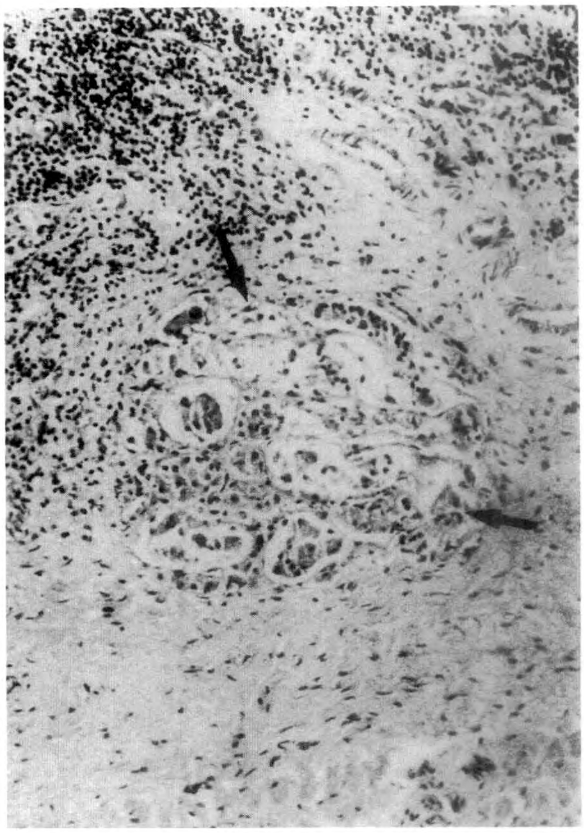

Fig 1. Rests of pharyngeal pituitary cells (arrows) beneath lymphoid tissues of adenoid (H & E, original ×155).

RESULTS

Age and Sex Distribution. The age distribution in the study population is shown in Table 1. The sex distribution was nearly equal, with a slight female preponderance of 28 cadavers as opposed to 22 male cadavers.

Observations in Nonpituitary Tissue. The type of surface epithelium, adenoid tissue, cellular infiltrates, and salivary gland tissue were seen as shown in Table 2.

Pituitary Tissue and Subepithelial Cell Rests. After evaluation of tissue sections under a microscope, sections with features suggestive of typical or atypical pituitary tissue constituted a total of 16% of the tissue specimens (8 of 50). Sections with tissue identical to an adenohypophysis in morphology accounted for an incidence of 6% (3 of 50). They appeared as solid clumps of cells surrounded by a well-defined fibrous stroma. With hematoxylin and eosin, the cells appeared to have a pinkish cytoplasm with a basophilic nuclear staining. These solid clusters of cells were situated in deeper layers of the sections, closer

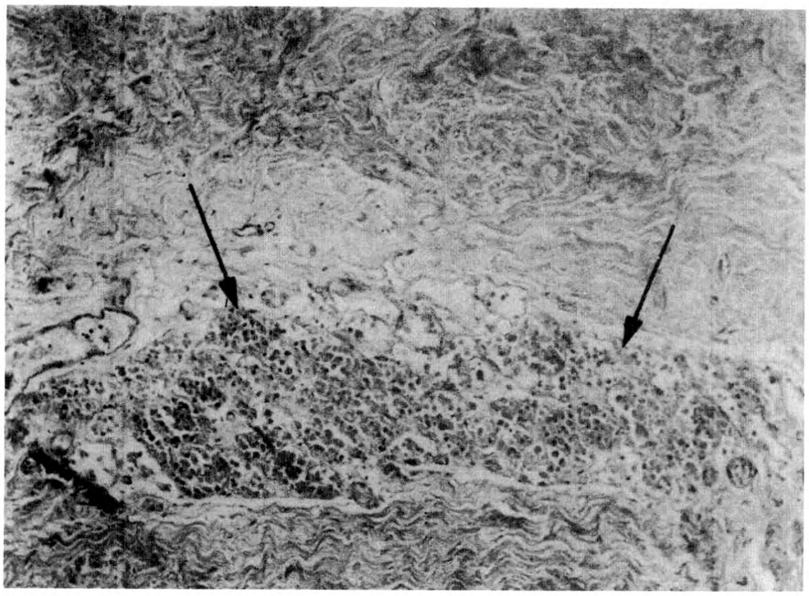

Fig 2. Pharyngeal pituitary cell rests (arrows) embedded in fibrous tissue (periodic acid–Schiff–orange G, original ×155).

to the vomerosphenoidal articulation than to the epithelial lining (Fig 1). Apart from the cells of adenohypophyses, findings of epithelial cell rests were noted in the subepithelial plane and also close to the vomerosphenoidal articulation, and were considered as atypical pituitary cells in this study. The morphology of these cells was of 2 types, namely, the squamous cell rests, which were made up of moderate-sized cells with basophilic cytoplasm and intercellular bridges, and the undifferentiated cell rests, which were small cells with scanty cytoplasm interspersed with minute capillaries. This atypical pituitary tissue accounted for 10% (5 of 50) of the positive specimens in this study.

PAS–Orange G Sections. A second batch of sections were stained with PAS–orange G. This was for selective demonstration of cells with the morphology of adenohypophysial tissue (Fig 2). It revealed a positive rate of 6% (3 of 50 sections). In 2 of the 3 sections, there was an equal proportion of acidophils and basophils. No chromophobes were seen. The third positive section showed 2 solid cell clusters producing a neuroendocrine pattern with a predominance of acidophils in comparison to basophils (Fig 3).

Relation of Age to Tissue Positivity. In group 2 (6 to 10 days), group 3 (11 to 15 days), and group 4 (16 to 20 days), there was 1 positive specimen in each group, ie, 12.5% positive specimens in each group. There were 2 (25%) positive specimens in group 5 (21 to 25 days) and 3 (37.5%) positive specimens in group 6 (26 to 30 days). In total, 8 of the 50 (16%) neonates showed histologic evidence of typical or atypical pituitary tissue.

DISCUSSION

The pharyngeal hypophysis is a remnant of Rath-

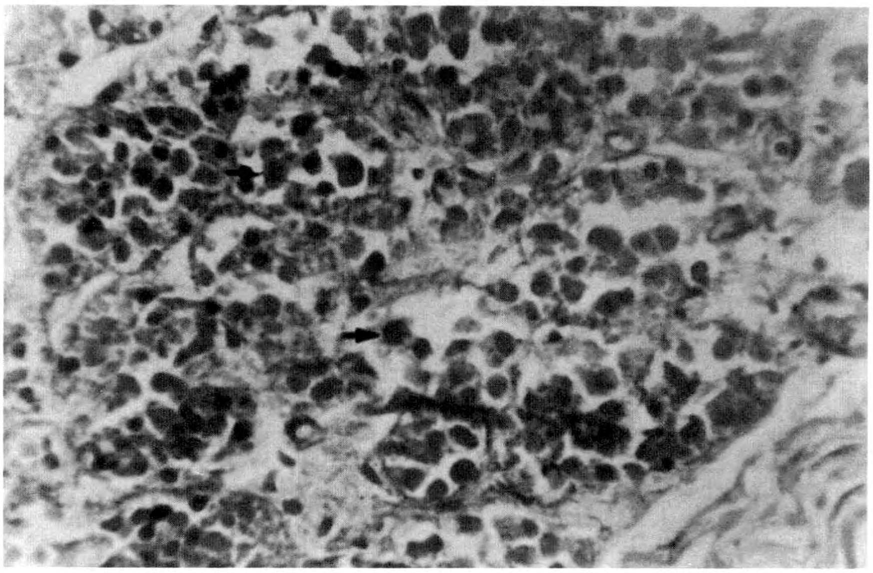

Fig 3. Pharyngeal pituitary cells show predominance of acidophil cells (arrows; periodic acid–Schiff–orange G, original ×550).

ke's pouch. A portion of persistent Rathke's pouch forms the pharyngeal hypophysis, which retains its continuity with the pharyngeal epithelium. The distal end persists to form the future adenohypophysis.

This study was undertaken on neonatal cadavers that were subjected to medical autopsy with the objective of determining the incidence of hypophysial tissue in the nasopharyngeal vault and documenting the histologic differentiation in the specimens. This study, undertaken in neonates, is to our knowledge the first of its kind to address the problem of extrasellar hypophysis. The earliest report of pharyngeal pituitary tissue was by Erdheim and Stumme,[1] who demonstrated pituitary tissue in the nasopharyngeal roof with an incidence of 35%. In our study, histopathologic evaluation led to the detection of pituitary tissue in 16% of the examined specimens. In contrast, Melchionna and Moore,[2] Boyd,[10] and McGrath[11] have shown a high incidence of positivity. McGrath's inclusion of all age groups in her studies could account for such a high incidence.

Melchionna and Moore[2] obtained pharyngeal tissue from the nasopharyngeal vault and vomerosphenoidal area, which were sectioned at 10-µm intervals after fixation in 6% formaldehyde solution. They noted that the pharyngeal pituitary tissue was composed essentially of undifferentiated cells and differentiated cells similar to those found in the anterior lobe of the pituitary gland. It is interesting to note that in 25% of their cases, there were no chromophobe cells, and in 35%, either acidophils or basophils were absent. Even when chromophobe cells were present, they were few in number and constituted less than 1% of the total number of cells. In our study, there was an equal proportion of acidophils and basophils. No chromophobes were seen. The absence of chromophobe cells and the small size of the gland render it unlikely that the pharyngeal pituitary tissue makes any significant contribution to the overall function of the endocrine system.

In this study, we noted 2 histologic types of adenohypophysis: an adenohypophysial or cellular group and subepithelial cell rests. The rests were of 2 types, namely, squamous rests and undifferentiated cells. These epithelial rests accounted for 10% of the 50 specimens that were examined (5 positive specimens). McGrath (1971),[8] on the other hand, divided the pharyngeal hypophysis into 3 histologic groups: a cellular group, a mixed group containing both epithelial and pituitary elements, and a squamous group.

Melchionna and Moore,[2] Boyd,[10] and McGrath[8] have all considered the subepithelial rests that lie adjacent to the surface epithelium to be atypical pituitary tissue. In contrast, we considered the deeply placed epithelial cell rests adjacent to the vomerosphenoidal articulation to be atypical pituitary tissue. This probably explains the low incidence of positivity in our study compared to other studies.

The use of PAS–orange G has been advocated as a staining procedure specifically for demonstrating the cells of adenohypophyses. In the staining of anterior pituitary tissue with PAS–orange G, the ultimate principle revolves around the knowledge that basophils contain mucoprotein and are PAS-positive. In the final result, nuclei stain black, mucoid cells magenta, acidophils orange, and chromophobes pale gray.

Using this staining, we noted that the adenohypophysial tissues, which accounted for 6% overall positivity, were arranged in solid clusters of cells. All 3 types of cellular components were seen. Melchionna and Moore[2] reported the presence of fibrous tissue with colloid material in the intercellular spaces, which was not seen in our cases.

The incidence of hypopharyngeal hypophysis varies in different case studies. The variance can probably be attributed to the method of interpretation of subepithelial atypical cell clusters. Many studies[2,6,9] have quoted a higher incidence in older age groups, which may be due to hormonal stimulation of the caudal remnant of Rathke's pouch. This idea could also explain the increased incidence of pharyngeal hypophysis in the older neonates (26- to 30-day) seen in our study.

It is apparent from the present study that pharyngeal hypophysis is an entity that should not be considered a hypothetical issue. An incidence of 16% in the nasopharyngeal epithelium in neonates suggests that its existence is more frequent than is thought. The presence of pituitary tissue in the nasopharynx brings us to the important question of whether this tissue has any functional significance. Under normal conditions of growth and activity, pharyngeal pituitary tissue may not contribute any significant physiological function. However, in cases of altered structure or activity of the pituitary gland, pharyngeal pituitary tissue may undergo structural alterations and may serve as an endocrine organ.

Conclusive evidence of the functional potential of the pharyngeal pituitary tissue could be demonstrated by estimation of various adenohypophysial hormones with a radioimmunoassay technique. In addition, staining the tissue for prolactin, growth hormone, and adrenocorticotropin hormone granules would provide additional evidence that there are endocrine-active rests. In those few cases of acromegaly and Cushing's disease that do not respond to hypophysectomy, the pharyngeal pituitary tissue may well be the source of excessive secretion. Surgical exploration and excision of glandular tissue should receive serious consideration in the future.

REFERENCES

1. Erdheim J, Stumme E. Uber die schwanger Schaftsneranderung der Hypophyse. Beitr Z Pathol Allerg Pathol 1909;46: 1-132.

2. Melchionna RH, Moore RA. The pharyngeal pituitary gland. Am J Pathol 1938;14:736-71.

3. Frazer JE. The anatomy of the human skeleton. 4th ed. London, England: Churchill, 1946:182.

4. Willis RA. Borderland of embryology and pathology. London, England: Butterworths, 1958:269.

5. Richards SH, Evans ITG. The pharyngeal hypophysis and its surgical significance. J Laryngol Otol 1974;88:937-46.

6. McGrath P. The volume of the human pharyngeal hypophysis in relation to age and sex. J Anat 1971;110:275-82.

7. McGrath P. Prolactin activity and human growth hormone in pharyngeal hypophysis from embalmed cadavers. J Endocrinol 1968;42:205-12.

8. McGrath P. Cysts of sellar and pharyngeal hypophysis. Pathology 1971;3:123-31.

9. Warner DO, Barry A, Richard J, Stanten I, Robert BR. Growth hormone and prolactin secretion by a tumor of the posterior pharyngeal pituitary. Ann Intern Med 1982;13:65-6.

10. Boyd JD. Observations in the human pharyngeal hypophysis. J Endocrinol 1956;14:66-7.

11. McGrath P. Volume and histology of the human pharyngeal hypophysis. Aust N Z J Surg 1967;37:16-27.

Ann Otol Rhinol Laryngol 110:2001

MALIGNANT MELANOMA ARISING WITHIN A BURN SCAR

CASE REPORT AND REVIEW OF THE LITERATURE

PAUL M. SPRING, MD, MS
LEXINGTON, KENTUCKY
ADEL K. EL-NAGGAR, MD, PHD
HOUSTON, TEXAS
JEFFREY N. MYERS, MD, PHD
HOUSTON, TEXAS
HOWARD N. LANGSTEIN, MD
HOUSTON, TEXAS

Burn scar carcinomas, also called Marjolin's ulcers, are uncommon tumors that arise from an antecedent burn. Most burn scar carcinomas are diagnosed about 30 years after the burn, and most are well-differentiated squamous cell carcinomas. We report a case in which a squamous cell carcinoma developed within a burn scar on the cheek and then a malignant melanoma arose within the burn scar after the squamous cell carcinoma had been excised. We also review the available literature on burn scar carcinoma, covering the demographics, pathogenesis, diagnosis, prognosis, and treatment of the disease. Given the multifocality of this disease process, we advocate aggressive resection of the entire burn scar, as well as the tumor, to prevent the development of further cancers within the wound.

KEY WORDS — burn scar carcinoma, Marjolin's ulcer.

CASE REPORT

A 67-year-old woman was referred to The University of Texas M. D. Anderson Cancer Center for further evaluation and treatment of a rapidly growing, painless nodule on the skin of her right cheek. A biopsy of the nodule performed 2 months earlier at another institution had demonstrated a malignant neoplasm with "an unusual spindle cell proliferation." Pathological review at our institution confirmed the spindle cell characteristics, and a diagnosis of desmoplastic spindle cell melanoma with an osteoclastic giant cell response was rendered. The patient had suffered severe thermal burns over her right arm and cheek at age 5. She was treated at the time with debridement and split-thickness skin grafting. At age 65, she had had a squamous cell carcinoma excised from her right cheek. The surgical margins of excision at that time were negative, and the site was covered with a split-thickness skin graft. Soon afterward, another lesion of the right cheek developed, and the patient underwent Mohs surgery that yielded tumor-negative margins. A full-thickness skin graft was used to repair the defect from that surgery.

The patient's medical history was significant for a benign thyroid mass removed at age 22. She did not take medications, and she was not allergic to any medications. She denied alcohol or tobacco use, but admitted to a history of significant sun exposure. There was no family history of skin cancer. Physical examination revealed a 2 × 1-cm firm, erythematous nodule sitting on a plateau of injured skin located on the patient's right cheek near the margin of the recent skin graft (Fig 1). This area corresponded to the area of the burn injury that the patient had sustained as a child and extended from the zygoma caudally to the inferior border of the mandible. Lymphadenopathy was not noted by palpation of the head and neck. The remainder of the findings on examination were unremarkable.

Preoperative evaluation included an axial computed tomography scan of the head and neck, a chest radiograph, and hematologic studies, including liver

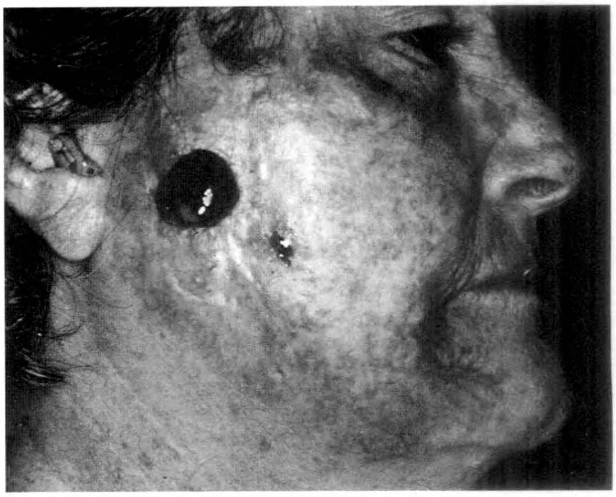

Fig 1. Preoperative view of burn scar lesion. Note previously skin-grafted area around lesion.

From the Departments of Head and Neck Surgery (Spring, Myers), Pathology (El-Naggar), and Plastic Surgery (Langstein), The University of Texas M. D. Anderson Cancer Center, Houston, Texas. Dr Spring is currently in the Division of Otolaryngology–Head and Neck Surgery, University of Kentucky, Lexington, Kentucky.

CORRESPONDENCE — Jeffrey N. Myers, MD, PhD, Dept of Head and Neck Surgery, M. D. Anderson Cancer Center, Box 069, 1515 Holcombe Blvd, Houston, TX 77030-4009.

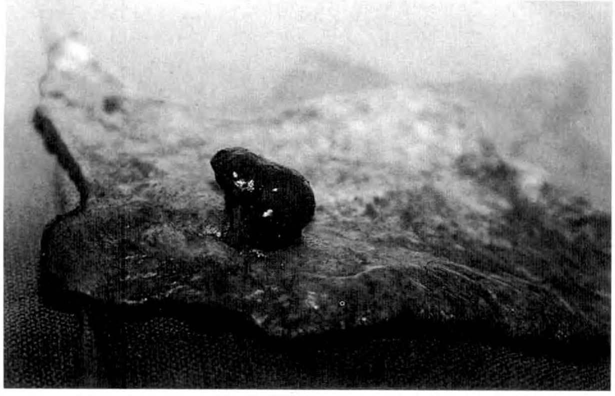

Fig 2. Wide local excision of lesion.

function tests. These studies revealed no evidence of regional or distant metastases. Surgery consisted of a wide local excision of the entire right facial burn scar, encompassing the lesion, along with a superficial parotidectomy and a supraomohyoid neck dissection (Figs 2 and 3). The skin defect was repaired with a full-thickness skin graft obtained from the lower abdomen and a cervical advancement flap (Fig 4). The patient tolerated the procedure well and had an unremarkable postoperative course.

The final diagnosis was malignant melanoma, Clark's level V, Breslow thickness 12 mm. Spindle cells, osteoclasts intermingled with osteoid material, and numerous giant cells were present on microscopy. Parotid tissue, parotid lymph nodes, cervical lymph nodes, and facial lymph nodes were negative for tumor. The margins of the excision were also negative for tumor. The patient received postoperative radiotherapy. The primary site was treated by a right lateral field with 12-MeV electrons, and the right side of the neck was treated with 9-MeV electrons to a total dose of 30 Gy administered in 6-Gy fractions twice weekly over $2^1/2$ weeks. At the time of this report, 2 years have passed since the surgery, and the patient has a well-healed skin graft and no evidence of recurrence. Figure 5 shows her appearance at 3 months after surgery.

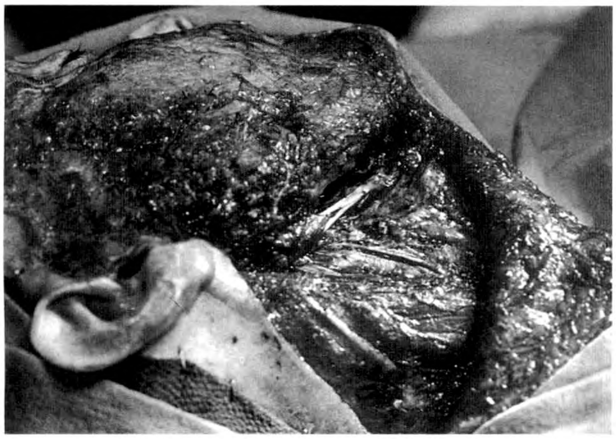

Fig 3. Intraoperative view of excision. Neck dissection and parotidectomy also performed. Note degree of excision beyond burn scar lesion.

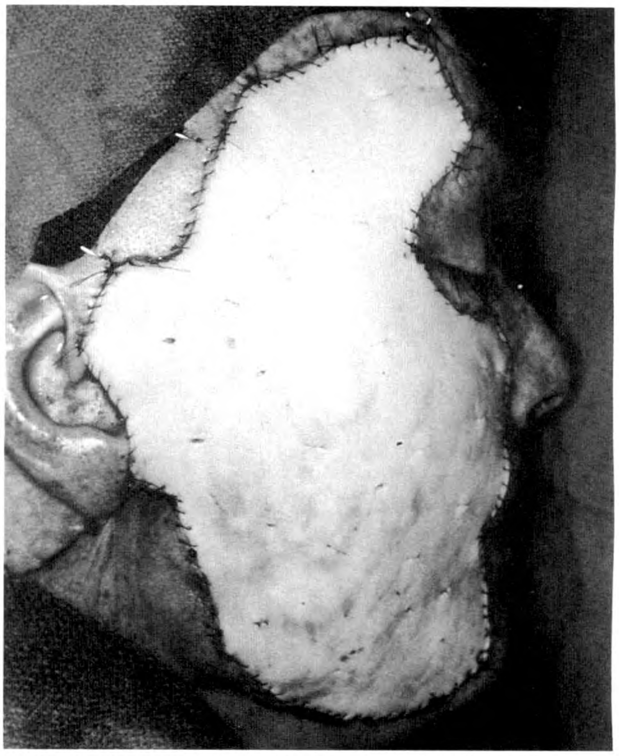

Fig 4. Reconstruction of defect with full-thickness skin graft from lower abdomen and cervical advancement.

DISCUSSION

Skin cancer is the most common form of malignant tumor. Approximately 600,000 new skin cancers are diagnosed and reported in the United States each year. Of those, 80% arise in the head and neck

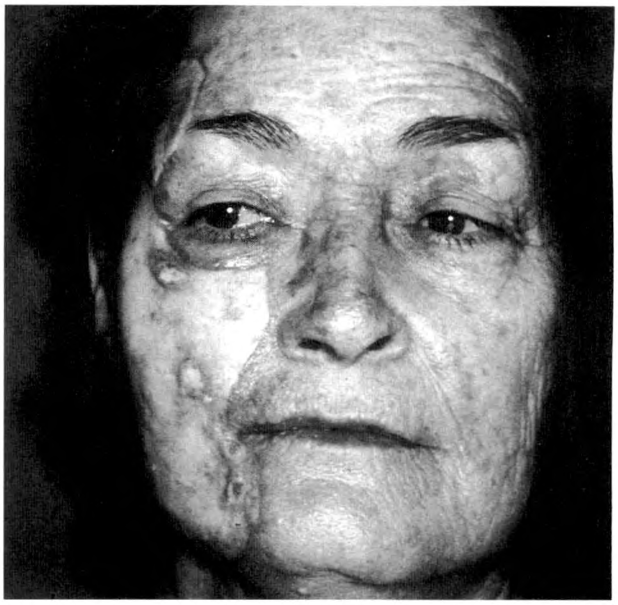

Fig 5. Three months after reconstruction.

CLINICAL FEATURES OF ACUTE VERSUS CHRONIC BURN SCAR CARCINOMAS

Feature	*Acute*	*Chronic*
Average lag period (burn to cancer development)	3 months	32.5 years
Type of burn	Superficial	Intermediate to deep
Presentation	Nonhealing ulcer	Nonhealing ulcer
Most common histologic subtype	Basal cell carcinoma	Squamous cell carcinoma
Locoregional lymph node metastasis	Infrequent	Common
Prognosis	Good	Fair to poor

area.[1] The majority of these head and neck skin cancers are basal cell carcinoma. The next most common histologic subtype is squamous cell carcinoma. Head and neck skin cancers are usually ascribed to a combination of solar damage, use of tobacco products, and genetic or racial predisposition. A small percentage of these lesions arise within skin that has been traumatized or is chronically inflamed.

Published reports have documented cancer development in discoid lupus erythematosus lesions, osteomyelitic scars, amputation stumps, x-ray burns, insect bites, chronic fistulae, vaccination sites, frostbitten areas, and other chronic wounds. Burns are the most common wounds or scars within which carcinomas arise. Although burn scar carcinomas are more common on the extremities, approximately 20% to 30% of these tumors occur within the head and neck area.[2]

Origin of Eponym "Marjolin's Ulcer." Credit for the earliest written description of burn scar carcinoma is given to Celsus, who in the first century AD described a cancerous ulceration of chronic scar tissue. The condition does not appear to be mentioned again in the medical literature until 1825, when the English surgeon Caesar Hawkins described war wound burns that later became cancerous in 2 English soldiers in India. In 1850, the Irish physician Robert William Smith described burn scars that had undergone neoplastic transformation, and he referred to the resulting cancers as "Marjolin's ulcers." This term was a reference to an article in the 1828 edition of *Dictionnaire de Médecine* by a Paris surgeon named Jean-Nicolas Marjolin, titled "*Ulcère*." Marjolin wrote extensively on the subject of trauma- and burn-induced skin lesions. Of interest, however, Marjolin never mentioned the progression from ulcer to cancer. Nevertheless, after Smith's article appeared, the term "Marjolin's ulcer" became a synonym for carcinomas arising from burn scars and other wounds. The interested reader is encouraged to review 2 articles by Dr Charles Steffen[3,4] for a detailed and learned description of the origin of the Marjolin eponym.

In 1866, Broca reported the development of ulceration and malignant degeneration in a man who had sustained a burn 51 years earlier.[5] To date, the series from Memorial Hospital in New York City reported by Treves and Pack[2] in 1930 represents one of the best treatises on burn scar carcinoma.

Acute and Chronic Burn Scar Carcinomas. Two classes of burn scar carcinomas exist: acute burn scar carcinomas and chronic burn scar carcinomas (see Table). Acute burn scar carcinomas are those that occur in wounds within 1 year of the injury, as described by Treves and Pack.[2] (Others have suggested that a lag period of 5 years or less is required for a wound to be classified as acute.[6]) Acute carcinomas account for approximately 13% to 22% of burn scar carcinomas in the relatively large series from Treves and Pack. Acute burn scar carcinomas tend to occur in superficial burns that involve a small surface area, and they are usually basal cell carcinomas. Superficial thermal burns affect only the epidermal layer and spare the skin adnexa, such as the hair follicles and sweat glands. Chronic burn scar carcinomas, which account for approximately 78% to 87% of burn scar carcinomas, tend to be well-differentiated squamous cell carcinomas. In the series of Treves and Pack, the average lag period (burn to cancer diagnosis) for chronic burn scar carcinomas was 32.5 years. Later studies by Lawrence,[7] Giblin et al,[5] and Novick et al[8] reported mean lag periods of 32, 34, and 42 years, respectively.

Pathological Features. Grossly, burn scar carcinomas are often multiple in the case of extensive scarring. In large ulcers, the carcinomas will be demarcated by the margins of the ulcer. Two major pathological subtypes of burn scar carcinoma exist: infiltrative (also called ulcerative) and a type with an exophytic or papillary growth pattern. The ulcerative subtype, which occurs far more often than the exophytic type, is associated with invasion through the subcutaneous fat, fascia, muscle, and, rarely, bone. Ulcerative tumors may also metastasize. The epidermoid cancer that develops is keratinizing and demonstrates the characteristic keratin pearls seen in differentiated epithelial cancer, as well as intercellular cross-bridging and mitotic figures. In addition, an initial lymphocytic reaction occurs that eventually yields to a polymorphonuclear process indicative of the local infection commonly associated with ulcer formation.

Treves and Pack[2] reported 28 cases of burn scar carcinoma: 21 epidermoid carcinomas and 7 basal cell carcinomas. They estimated that squamous cell carcinomas arising from burn scars accounted for 2%

of the epidermoid skin cancers seen in their practice and that basal cell carcinomas arising from burn scars accounted for 0.3% of the epidermoid skin cancers they saw.

The reported rates of regional metastasis at initial presentation range from 15% to 35%.[2,8-10] Metastasis in burn scar carcinoma appears to be a function of the degree of differentiation of the tumor and the degree of scar bed formation. For the tumor to metastasize, it must first break through the thick fibrosis created by the scarring process. Then, once the tumor has broken through the avascular fibrosis of the scar, it must engage the lymphatics, whose network has been destroyed by the scarring. Nothing indicates that these tumors have an inherently greater tendency than other epidermoid carcinomas of the skin to metastasize once they have gained access to the lymphatics. Therefore, the regional lymphatics are the expected drainage level for these cancers. Distant metastases are very rare.

Nearly 95% of burn scar carcinomas are squamous cell carcinomas, and about 2% to 3% are basal cell carcinomas; burn scar melanomas and sarcomas are rare. While melanomas are mentioned often in the literature as being the third most common histologic diagnosis associated with burn scar carcinomas, we have identified only 2 cases of melanoma arising within a burn scar in the literature.[5,11] Novick et al[8] reported a lesion with both squamous cell carcinoma and malignant melanoma arising within a burn scar carcinoma.

Sarcomas have been reported arising from a previous burn. Fleming and Rezek[10] reported the finding of a spindle cell sarcoma arising from an old burn scar and surmised that the mesenchymal structures that approximate the burn are susceptible to malignant degeneration. After further pathological review, the lesion was determined to be a malignant fibrous histiocytoma. Another burn scar sarcoma, a high-grade malignant fibrous histiocytoma, was described as originating from a long-standing ulcer of the greater trochanter of the femur in a patient who had sustained burns to her waist.[11] One case of liposarcoma from an untreated neck burn has also been reported.[12]

Race, Gender, and Age Distribution. Malignant changes in burn scars may occur in patients of all ages. In the classic article of Treves and Pack,[2] of the burn scars that developed into squamous cell carcinomas, 76% were in men and 24% were in women. Of the burn scars that developed into basal cell carcinomas, 86% were in men and only 14% were in women. These gender distributions are interesting, because burn injuries are more common in women than in men. These distributions are also interesting because they are more heavily skewed toward men than is the distribution of epithelial carcinomas of the skin.[2]

In the series reported by Treves and Pack,[2] the mean ages of the 28 patients with burn scar development were 53.5 and 56 years for chronic and acute burn scar cancers, respectively. However, the authors also found patients with childhood burns who developed cancers in their teens and twenties. The authors concluded that the age of the scar is more important than the age of the individual in determining whether cancer will develop. In the relatively modern series of Novick et al,[8] the average age at onset of burn scar carcinoma was 58 years.

Prognosis. The prognosis of burn scar carcinoma is directly related to the stage at which the cancer is detected. In general, the acute variety of burn cancer has a better prognosis owing to the smaller size of the tumor, the shallower depth of invasion, and the fact that superficial burns tend to transform into basal cell carcinomas rather than squamous cell carcinomas.[2] The most significant prognostic factor is the development of lymph node metastasis.[8]

Phillips et al[6] recently published an article that tabulates the prognostic factors in burn scar carcinoma. Among the factors associated with a good prognosis are 1) an acute latency, versus chronic, 2) cancer located in head and neck and upper extremities, versus trunk and lower extremities, 3) exophytic versus ulcerative growth pattern, 4) well-differentiated versus poorly differentiated histopathology, 5) dense versus scant peritumoral T-lymphocyte infiltration, and 6) absence of metastases.[6]

Locoregional recurrences are a relatively common event in Marjolin's ulcers, especially squamous cell carcinomas. Edwards et al[13] reported a 52% recurrence rate in their burn scar patients, which is consistent with rates in other reports. These data, when compared to those on actinic-induced skin cancer, also indicated a much higher rate of recurrence after 5 years. The survival data from the Edwards et al article indicated a 53% 5-year survival rate for burn scar carcinoma patients.

Pathogenesis. Heat or thermal injury has been cited as the cause of burn scar carcinoma. The 2 most frequently mentioned examples of heat-related carcinomas are those arising from the traditional Kashmiri custom of "*kangri*" and the traditional Japanese custom of "*kairo.*" A *kangri* is an earthenware bowl surrounded in basketwork that is heated by wood or charcoal and worn under a thin garment against the skin by the northern Indians and Pakistani of Kashmir to keep warm. The *kangri*, which is worn against the lap area, causes a chronic dermatitis that may degenerate into malignant epithelial carcinoma. The *kairo* is a tin box worn under a kimono and against a shirt that contours to the abdomen of the wearer (usually a woman). The *kairo* contains powdered charcoal, which when ignited generates heat that lasts for hours. The heat in turn can cause a skin cancer that originates in the area of the *kairo*. The *kangri* and *kairo* burn scar carcinomas share a common causation, which is the thermal burn and irritation of the skin in the area of the particular utensil.[2] The custom of *kairo* use has changed with the advent of chemical, disposable *kairos*. Whether the newer *kairos* produce burn scar carcinoma has not been determined.

Edwards et al,[13] at M. D. Anderson Cancer Center, compared 2 groups of patients who had suffered skin tissue injury secondary to either burns or irradiation. The hypothesis was that injured skin that undergoes malignant transformation does so independently of the mechanism of injury. While the results indicated similar natural histories and survival rates for burn scar carcinomas and skin cancers induced by radiation, the study fell short of providing conclusive evidence that these processes are pathogenically identical. Interestingly, this same study examined nodal disease at initial presentation and found that the incidence was 27% in burn scar carcinoma but only 0.5% to 3.3% in actinic-induced carcinomas. This implies a different pathogenesis based on the mechanism of injury.

It is often asked whether a burn scar carcinoma would have developed in a particular site even without an antecedent burn. The answer appears to lie in the fact that the distribution of burn scar carcinomas does not sufficiently approximate that of normally appearing skin cancers. This implies a separate or, at the very least, a contributory effect from the thermal insult. In 1928, Ewing[14] formulated a set of postulates that can be used to establish the relationship between trauma and cancer; these may be applied to burn scar carcinomas. The modification of Ewing's postulates states that there must exist incontrovertible evidence of the burn, that the cancer must originate within the boundaries of the burned area, that there must be no precursory or similar neoplasm on the site of the burn before the development of the cancer, that the histologic variety of the cancer must be compatible with that of the tissues found in thermal wounds and scars, and that the interval between the date of burning and the onset of the cancer must be proper.

Burn scar carcinomas develop because of the unique physiology of scar formation and the external pressures exerted on scars. Burn scars differ from other wound scars in that the scar is located on the surface of the skin, not beneath it. Also, the amount of epithelialization that occurs in a burn scar is greater, and the neoepithelium that is formed is perturbed easily by minor trauma. Virchow's theory of chronic irritation holds that the continual cycle of damage and repair and persistent wounding may increase the likelihood of malignant transformation.[2] This theory fits the initiator-and-promoter model of carcinogenesis, whereby the burn acts as the initiator and the repetitive injury serves as the promoter.[15]

Burns around the joints and other flexion and extension points tend to ulcerate more often than burns in other sites because of the tensions generated from the scar contractures and the repetitive movement. The tendency to ulcerate is further promoted by the lack of organization that exists in the scar. The fibroproliferative response in a colonized, if not infected, area of tissue with poor vascularization and compromised nutritional supply creates a chronic ulcer with degenerative changes. In addition, cytokines and growth factors may further contribute to a selective growth advantage of cells with extensive alterations of growth or survival regulatory genes. In the series of Treves and Pack,[2] the 6 patients with acute burn scar carcinomas never experienced complete wound healing before the appearance of the cancers, and in certain instances of the chronic burn scar carcinomas as well, the wound never healed before the cancers appeared. None of the 28 patients in the series had had skin grafts.[2] A hallmark of ungrafted burns is the presence of microbial colonization and possible invasive infection. The infection impedes the healing process by a prolonged inflammatory response, which prevents epithelialization and leads to a chronic unstable wound.

It has been hypothesized that the local environment surrounding a burn scar carcinoma represents an immunologically privileged area not accessible to normal immunosurveillance.[16] This hypothesis holds that as a result of the dense fibrous scar tissue and the altered lymphatic structure, the tumor-specific antigens cannot reach the regional nodes, and once the tumor reaches the host's system, the local immune system becomes overwhelmed.[17] Bostwick et al[18] provide support for this theory of immunologic privilege by citing 6 cases of Marjolin's ulcer (none in the head and neck area) that recurred rapidly and aggressively with nodal metastasis after excision. Bostwick et al also reference a paper by Arons et al[19] that describes 11 of 15 Marjolin's ulcers of the extremities that had adequate treatment but recurred aggressively at both local and regional sites and eventually resulted in death.

An interesting article by Crawley et al[17] presented qualitative evidence that patients with burn scar carcinoma who had a brisk lymphocytic infiltrate had prolonged survival compared with patients whose tumors lacked lymphocytic infiltration. The authors examined 10 patients with burn scar carcinoma with at least 1-year follow-up. Eight individuals had had a significant immunologic response and were alive; the 2 who had lacked a significant response were dead; and 4 patients with non–scar-related squamous cell carcinoma of the skin who had had a significant response were alive. The authors surmised that this lymphocyte response was a direct reflection of the competence of the host's cancer surveillance system.[17]

Given the long lag periods for chronic burn scar carcinomas, some have suggested that in fact only acute burn carcinomas may be attributable to the heat effect and that metagenetic changes may account for the development of chronic burn scar carcinoma. Lawrence[7] purports that the lag period is inversely proportional to the age of the patient at the time of burn, such that the younger the patient at the time of the burn, the longer the delay until onset of the cancer.

Prevention. A useful classification system described by Goldblatt recognizes the difference between burns that will develop scar formation (type 1) and those that will not develop scar formation (type 2).[2] This simple, practical scheme distinguishes burns that will need further treatment such as skin grafting and those that will not require further treatment from burns that ultimately will not form scars. Burn scar carcinomas result from type 1 burns only. The other recognized scheme for classifying burns is the Dupuytren classification, which focuses on burn depth. Burns are classified from first-degree to fifth-degree, progressing from superficial to deep. In this classification, a first-degree burn is one that does not scar, and a second-degree burn is one that produces only superficial pitting of the skin. Third-degree burns are superficial and do not demonstrate significant contraction of the wound. Burns that cause thick scarring and severe contraction are classified as fourth- and fifth-degree burns as a matter of degree.[2] Scar thickness and degree of contraction are the two factors that ultimately predispose burns to the development of carcinoma.[2]

Proper management of burn wounds is the cornerstone of prevention of burn scar squamous cell carcinoma. Treves and Pack[2] enumerate 5 measures to take to prevent burn scar carcinoma: burn prevention, local wound care of the burn scar, promulgation of epithelialization, early skin grafting of the burned area, and radical excision of a suspicious wound. A case can be made that all burn wounds are infected or at least colonized with multiple microbial pathogens. Therefore, every effort must be made to promote a good bed of granulation at the wound site that is acceptable for full-thickness skin grafting. Pus and chronic inflammation encourage the formation of fibrosis, which delays healing of the wound and increases the risk of cancer development. Cultures of the wound should be performed, and the appropriate antimicrobial therapy should be used. Skin grafting, which approximates early epithelialization, is a profound deterrent to cancer development following burns. In fact, none of the 28 patients treated by Treves and Pack who developed burn scar carcinomas had skin grafts. It must be noted, however, that Novick et al[8] reported 5 cases of burn scar carcinoma occurring in sites that had been primarily grafted. The details of the grafting technique and success rate were not reported.

Diagnosis. Cancer arising within chronic scar typically manifests as a nonhealing ulcer. The malignant degeneration usually begins at the margin of the ulcer. The carcinoma will grow slowly and insidiously, eccentrically and deeply. Symptoms of chronic burn scar carcinoma include pruritis and hyperesthesia. Once the ulcer has formed, a burning sensation may develop that is associated with lancinating pain. A cheesy, malodorous discharge accompanies the ulcer when it is infected. Hemorrhage is an uncommon manifestation until the deeper soft tissue structures of the muscle, tendon, etc, are invaded. Cancers that evolve from burn scars are rarely multiple. Because of the focal nature of the disease, only a portion of the ulcer is malignant, and the rest remains as a nonhealing wound.

Ulcers that develop from other disease entities are readily distinguished from burn scar carcinoma. However, because the chronic ulcers of burn scar carcinomas are frequently associated with infections, biopsy of an infected ulcer may be required to exclude the diagnosis of cancer. It is important that biopsies be performed at both the margin and the center of the lesion to minimize false-negative results. Skin manifestations of tuberculosis are rare today and usually occur in children, but tuberculosis must always be considered in the differential diagnosis of burn scar carcinoma. Pseudoepitheliomatous hyperplasia, which is a benign, noninvasive, nonmetastasizing tumorlike process delimited by a defined basement membrane, must be excluded diagnostically, because it is considered a premalignant condition in the progression of traumatic carcinoma.[9]

Treatment. As mentioned, wide local excision followed by full-thickness skin grafting is the treatment of choice for burn scar carcinoma. The recommended margins of excision are 2 cm.[8] Treatment of lesions in the head and neck may be complicated by the need for resection of functional or cosmetically important structures to achieve adequate margins of excision. Cervical lymph node dissection should be reserved for palpable disease. Prophylactic or elective lymph node dissection is not supported for burn scar carcinoma of the head and neck.

Primary radiotherapy is discouraged for the following reasons: well-differentiated cancers are predisposed to radioresistance; a fibrotic, infected, macerated tissue bed prevents normal repair of the radiodamaged tissue; and radionecrosis, even in the setting of low-dose orthovoltage and supervoltage, still occurs at an unacceptable rate. Adjuvant radiotherapy is feasible and is particularly appropriate in the case of positive margins or extracapsular spread of lymph node disease.[13]

Ryan et al[20] reported 3 cases of Marjolin's ulcer (squamous cell carcinoma) treated effectively with topical and injected forms of 5-fluorouracil. These authors also report 5 cases of advanced cutaneous melanoma (non–Marjolin's ulcer) successfully treated with 5-fluorouracil alone and in combination with surgery.[21] Their theory asserts that 5-fluorouracil produces a round cell infiltration that changes the environment of the immunologically privileged area around the Marjolin's ulcer and sensitizes the host immune system.

SUMMARY

Burn scar carcinomas are uncommon lesions. Most burn scar carcinomas appear around 30 years after the burn, and most are squamous cell carcinomas. The occurrence of melanoma is very rare. We presented a case of malignant melanoma that arose from a burn scar 2 years after a squamous cell carcinoma had been removed from the same scar. Ulcer formation appears to be integral to malignant transformation in burn scars, and scar fibrosis of the wound appears to be at least partly responsible for the long lag period normally seen between the burn and diagnosis of the cancer. When these lesions metastasize, they do so late and very aggressively to regional nodes. The most interesting clinical observation to date regarding burn scar carcinomas is the rapid development of regional metastases with persistent disease that can occur after adequate resection of the carcinoma.

Early intervention in burn wounds can help prevent burn scar carcinoma. Wound debridement, antimicrobial measures, and early wound coverage with viable biomaterial will protect against the progression of malignant transformation. Burn scar carcinomas are aggressive lesions and must be diagnosed and treated without delay. Once a malignancy has developed, wide local resection of the tumor and the burn scar is mandatory. Prompt coverage of the wound with a skin graft is important in halting the inflammatory phase of healing. Coverage can include excision and closure, skin grafting, and tissue transfers to achieve the most functional outcome. Lymph node dissection is recommended if there is a high degree of suspicion of nodal involvement; lymph node dissection is mandatory in the face of palpable disease. Primary irradiation does not appear to be indicated. Topical and injectable 5-fluorouracil may be considered.

REFERENCES

1. Renner GJ, Clark D. Facial skin malignancies. Otolaryngol Clin North Am 1993;26:ix-x.
2. Treves N, Pack GT. The development of cancer in burn scars: an analysis and report of thirty-four cases. Surg Gynecol Obstet 1930;51:749-82.
3. Steffen C. The man behind the eponym. Jean-Nicolas Marjolin. Am J Dermatopathol 1984;6:163-5.
4. Steffen C. Marjolin's ulcer. Report of two cases and evidence that Marjolin did not describe cancer arising in scars of burns. Am J Dermatopathol 1984;6:187-93.
5. Giblin T, Pickrell K, Pitts W, Armstrong D. Malignant degeneration in burn scars: Marjolin's ulcer. Ann Surg 1965;162: 291-7.
6. Phillips TJ, Salman SM, Bhawan J, Rogers GS. Burn scar carcinoma. Diagnosis and management. Dermatol Surg 1998;22: 561-5.
7. Lawrence EA. Carcinoma arising in the scars of thermal burns. Surg Gynecol Obstet 1952;95:579-88.
8. Novick M, Gard DA, Hardy SB, Spira M. Burn scar carcinoma: a review and analysis of 46 cases. J Trauma 1977;17: 809-17.
9. Fleming MD, Hunt JL, Purdue GF, Sandstad J. Marjolin's ulcer: a review and reevaluation of a difficult problem. J Burn Care Rehabil 1990;11:460-9.
10. Fleming RM, Rezek PR. Sarcoma developing in old burn scar. Am J Surg 1941;54:457-65.
11. Gargan TJ, Mitchell L, Plaus W. Burn scar sarcoma. Ann Plast Surg 1988;20:477-80.
12. Horton CE, Crawford HH, Lower HG, Loettler RA. The malignant potential of burn scars. Plast Reconstr Surg 1958;22: 348-53.
13. Edwards MJ, Hirsch RM, Broadwater JR, Netscher DT, Ames FC. Squamous cell carcinoma arising in previously burned or irradiated skin. Arch Surg 1989;124:115-7.
14. Ewing J. Neoplastic diseases: a treatise on tumors. 3rd ed. Philadelphia, Pa: WB Saunders, 1928:862.

Ann Otol Rhinol Laryngol 110:2001

FUNGAL MALIGNANT OTITIS EXTERNA DUE TO *SCEDOSPORIUM APIOSPERMUM*

MIKE YAO, MD
HOUSTON, TEXAS

ANNA H. MESSNER, MD
STANFORD, CALIFORNIA

Malignant otitis externa (MOE) is an infection of the external auditory canal that invades the skull base. *Aspergillus* species fungi were the pathological organism in 21 of 23 reported cases of fungal MOE. We report on a 21-year-old man with end-stage acquired immunodeficiency syndrome (AIDS) and fungal MOE caused by *Scedosporium apiospermum*. Fungal MOE is most common in patients with end-stage AIDS and hematologic malignancies. Granulation tissue is not a common finding in these patients, and the infectious process often starts in the mastoid air cells or middle ear space, as opposed to the external auditory canal. Surgical debridement and amphotericin B are the mainstays of therapy; resolution of the infection depends greatly on the severity of the underlying disease.

KEY WORDS — human immunodeficiency virus, malignant otitis externa, mastoiditis, *Pseudallescheria, Scedosporium.*

INTRODUCTION

Certain unusual infections are becoming more common because of an increasing number of patients with compromised immune function as a result of hematologic malignancies and end-stage acquired immunodeficiency syndrome (AIDS). These immunocompromised patients have been recognized to be at risk for malignant otitis externa (MOE), an infection of the external auditory canal that invades the skull base, although this infection is usually described in patients with diabetes mellitus. *Pseudomonas aeruginosa* is the most common infecting organism in MOE, but a wider spectrum of organisms appears to infect immunocompromised patients, including some fungal organisms.

Fungal MOE was first described in a granulocytopenic patient with acute myelogenous leukemia by Petrak et al[1] (see Table,[1-18] case 1). A review of the literature shows 23 patients with MOE caused primarily by a fungal organism (see Table), with 21 of these patients infected by *Aspergillus* species fungi. In this report, we describe a patient with fungal MOE infection due to *Scedosporium apiospermum*, which to our knowledge has only been reported twice previously (cases 19 and 23).[15,18]

CASE REPORT

A 21-year-old man with a history of hemophilia A, human immunodeficiency virus (HIV), and hepatitis C presented with a 2-day history of increasing left ear pain and swelling. He had a diagnosis of AIDS with a CD4 count of 90 cells per microliter of blood and a history of multiple opportunistic infections, including *Pneumocystis carinii* pneumonia, *Nocardia* pneumonia, *Pseudomonas* pneumonia, and invasive pulmonary aspergillosis. Over the previous 6 weeks, the patient had complained of left external auditory canal discomfort and bleeding; cultures from the ear during this period revealed *P aeruginosa*, *Aspergillus fumigatus*, and *S apiospermum*. The patient had just finished a 2-week course of ceftazidime and tobramycin sulfate for a *Pseudomonas* pneumonia and had been treated for 4.5 months for invasive pulmonary aspergillosis with liposomal amphotericin B. He also reported nasal congestion.

Examination revealed mastoid tenderness and swelling causing protrusion of the ear. A granulation polyp was present in the posterior superior quadrant of the external auditory canal, adjacent to the tympanic membrane.

The patient was admitted to the hospital, placed on a regimen of intravenous imipenem, tobramycin, amphotericin B, and itraconazole, and taken to the operating room with a presumptive diagnosis of acute suppurative mastoiditis. A simple mastoidectomy and nasal endoscopy with culture were performed. Operative findings showed devitalized bone, bony erosion of the tegmen tympani and the posterior external auditory canal wall, inflammation of the exposed dura mater, multiple pockets of inspissated pus, and granulation tissue filling the mastoid antrum. A potassium hydroxide preparation of the mastoid material showed hyphae consistent with a fungal infection.

Macroscopic and microscopic morphology identified *S apiospermum* as the infecting organism in the

---

From the Division of Otolaryngology–Head and Neck Surgery, Stanford University Medical Center, Stanford, California. Dr Yao is currently in the Department of Head and Neck Surgery, M. D. Anderson Cancer Center, Houston, Texas.

CORRESPONDENCE — Anna H. Messner, MD, Stanford University Medical Center, Division of OTO/HNS, Stanford, CA 94305-5328.

FUNGAL MALIGNANT OTITIS EXTERNA CASES REPORTED IN LITERATURE

Case	*Authors*	*Year*	*Underlying Disease*	*Organism*	*Antifungal Rx*	*Infection Status*	*Outcome*
1	Petrak et al[1]	1985	AML	*A fumigatus*	Ampho	Cured	Survivor
2	Stanley et al[2]	1988	CLL	*A fumigatus*	Ampho + Flucyt	Cured	Septicemia + GI
3	Cunningham et al[3]	1988	Aged	*A fumigatus*	Ampho	Cured	CHF
4	Bickley et al[4]	1988	Myelodysplasia	*Aspergillus* species	Ampho	Cured	Pneumonia
5	Menachof and Jackler[5]	1990	AML	*A flavus*	Ampho	Cured	AML relapse
6			COM	*A fumigatus*	None	Persistent	MI
7	Phillips et al[6]	1990	AML, DM	*Aspergillus*	Ampho → Itra	Cured	AML relapse
8	Strauss and Fine[7]	1991	AIDS	*A fumigatus*	Ampho → Itra	Persistent	DOD
9	Reiss et al[8]	1991	AIDS	*A fumigatus*	Ampho → Itra	Cured	Survivor
10			AIDS	*A fumigatus*	Ampho → Itra	Cured	Septicemia
11	Hall and Farrior[9]	1993	COM	*A fumigatus*	Ampho	Cured	Lost to F/U
12			COM	*A fumigatus*	Ampho	Cured	Survivor
13	Hanna et al[10]	1993	DM	*A flavus, C ciferri*	Ampho	Cured	Survivor
14	Gordon and Giddings[11]	1994	DM	*A flavus*	Ampho → Itra	Cured	Survivor
15			Aged	*A flavus*	Ampho → Itra	Cured	Survivor
16	Harley et al[12]	1995	ALL	*A flavus*	Ampho	Persistent	DOD
17	Bryce et al[13]	1997	AIDS	*A fumigatus*	Ampho → Itra	Cured	Survivor
18	Ress et al[14]	1997	AIDS	*A fumigatus*	None	Persistent	DOD
19	Busaba and Poulin[15]	1997	AIDS	*P boydii*	Ampho → Itra	Cured	Survivor
20	Munoz and Martinez-Chamorro[16]	1998	AIDS	*A fumigatus*	Itra → Ampho	Persistent	DOD
21	Diop et al[17]	1998	AIDS	*A fumigatus*	Ampho	Persistent	DOD
22	Slack et al[18]	1999	ALL	*A flavus, A fumigatus, A niger*	Ampho → Itra	Persistent	GVHD, DOD
23			AIDS	*S apiospermum*	Ampho + Itra	Persistent	LWD
24	This report	1999	AIDS	*S apiospermum*	Ampho + Itra → Ampho + Keto → Mic	Persistent	DOD

Rx — drugs prescribed, AML — acute myelogenous leukemia, *A fumigatus* — *Aspergillus fumigatus*, Ampho — amphotericin B, CLL — chronic lymphocytic leukemia, Flucyt — flucytosine, GI — gastrointestinal hemorrhage, CHF — congestive heart failure, *A flavus* — *Aspergillus flavus*, COM — chronic otitis media, MI — myocardial infarction, DM — diabetes mellitus, Itra — itraconazole, AIDS — acquired immunodeficiency syndrome, DOD — dead of disease, F/U — follow-up, *C ciferri* — *Candida ciferri*, ALL — acute lymphoblastic leukemia, *P boydii* — *Pseudallescheria boydii*, *A niger* — *Aspergillus niger*, GVHD — graft-versus-host disease, *S apiospermum* — *Scedosporium apiospermum*, LWD — living with disease, Keto — ketoconazole, Mic — miconazole.

majority of the cultures. Left mastoid cultures grew *S apiospermum*; right nasal cavity cultures grew *S apiospermum* and *Staphylococcus aureus*; left nasal cavity cultures grew *S aureus*; sputum cultures grew *S apiospermum* and *Candida glabrata*; and blood cultures had no growth. Eight months before the current admission, the patient had had a sputum culture that also grew *S apiospermum*. Experimental susceptibility testing was performed, and the fungus was found to be susceptible to ketoconazole and amphotericin B but resistant to itraconazole, fluconazole, and 5-flucytosine. Miconazole was not tested. With these results, the patient was continued on amphotericin B and ketoconazole.

After the operation, the patient's pain improved to a manageable level, and he was discharged home on postoperative day 5. On postoperative day 6, he developed a 50% weakness of his left facial nerve, mental status changes, and left ear pain. He returned to the hospital on postoperative day 7. Magnetic resonance imaging showed no brain invasion, but dural enhancement was noted in the region overlying the mastoid cavity. Because of the patient's somnolence and facial nerve weakness, a reexploration of the mastoid cavity with facial nerve decompression was considered. After extensive discussion, it was decided that aggressive surgical intervention was not in the patient's best interest because of the advanced stage of his disease.

With the progression of the infection and reports that miconazole was effective against *S apiospermum*,[19] the patient was started on a regimen of intravenous miconazole imported from Japan, as it is not available in the United States. The patient developed intractable pain in his left ear despite use of fentanyl patches and intravenous morphine. The patient was taken back to the operating room on postoperative day 8 in an attempt to palliate his pain. Operative findings showed extensive blood clot and debris filling the mastoid cavity, but no anatomic evidence of infection progression. After the second procedure, the patient reported continued left facial nerve palsy and left ear pain. The miconazole caused intolerable nausea and vomiting. As a result of the severe pain and nausea, the patient's family elected to stop the miconazole and take him home. The patient died of his infection approximately 2 weeks later.

Standardized sensitivity regimens have been developed for testing yeast; however, no standard exists for filamentous fungi such as *S apiospermum*. Our patient's fungal specimen was sent to the Institute for Medical Research at the Santa Clara Valley Medical Center in San Jose, California, for experimental sensitivity testing. This testing required 12 days and showed this patient's strain of *S apiospermum* to be susceptible to miconazole and resistant to itraconazole, fluconazole, amphotericin B, and ketoconazole. At the time that this information became available, the patient had already failed a trial of miconazole, so no further interventions were taken.

REVIEW OF LITERATURE

In the 23 reports in the literature of fungal MOE, 21 of the fungal organisms identified were *Aspergillus* species (see Table). *Aspergillus fumigatus* was present in 13 cases, *Aspergillus flavus* in 5 cases, *A flavus*, *A fumigatus*, and *Aspergillus niger* in 1 case, unidentified *Aspergillus* species in 2 cases, *Pseudallescheria boydii* in 1 case, and *S apiospermum* in 1 case. *Scedosporium apiospermum* is commonly found in the soil and is the most frequent organism isolated from mycetoma in Europe and the Americas.[20] *Scedosporium apiospermum* is the asexual or anamorphic state of *P boydii*.[20]

In these case reports, the primary therapy included debridement of the infected mastoid cavity and treatment with antifungal agents. Amphotericin B was the primary antimicrobial agent. In 10 cases, however, amphotericin B was changed to oral itraconazole because of the toxicity of amphotericin B (cases 7, 8, 14, 15, and 17), the sensitivity of the organism to itraconazole (cases 19 and 23), or the need for prolonged therapy (cases 9, 10, and 22). Seven of these 10 patients were cured with the itraconazole regimen (see Table). *Scedosporium apiospermum* has been shown to be resistant to amphotericin B in vitro, but has shown sensitivity to itraconazole and miconazole.[19]

Fungal MOE differs in many ways from bacterial MOE. Diabetes mellitus is not as prevalent in the fungal MOE patients; only 3 of the 23 patients had a history of diabetes (see Table). The most common underlying diseases were AIDS (8 of 23 patients) and hematologic malignancies such as leukemia and myelodysplasia (7 of 23 patients; see Table).

In most bacterial MOE patients, granulation tissue is found at the floor of the external auditory canal at the bony cartilaginous junction, but in fungal MOE patients, granulation tissue was noted in only 8 of the 23 patients (cases 3, 4, 7, 14, 15, 19, 20, and 23). Previous reports have shown that granulation tissue is not prevalent in AIDS patients with MOE.[14] The presence of granulation tissue in fungal MOE appears to be a favorable prognostic indicator. Six of the 8 patients with granulation tissue in the external auditory canal were cured of their infections (cases 3, 4, 7, 14, 15, and 19); 1 of the 8 is living with disease (case 23); and only 1 of the 8 died of the fungal MOE (case 20). Interestingly, the 7 patients cured or living with disease were less immunocompromised than the patient in case 20, who had end-stage AIDS and died of the fungal MOE. One patient had acute myelogenous leukemia and diabetes mellitus (case 7), 1 had myelodysplasia (case 4), 2 had AIDS (cases 19 and 23), 1 had diabetes mellitus only (case 14), and 2 had no history of compromised immune status (cases 3 and 15). Granulation tissue may represent an ability to mount an immunologic response, thus inhibiting the growth of the fungal organism.

Bacterial MOE appears to start in the external auditory canal, whereas fungal MOE often occurs without evidence of infection in the external auditory canal; it has been presumed to originate in the mastoid air cells or middle ear. Only 10 of the 23 patients with fungal MOE initially presented with otitis externa without signs of middle ear or mastoid involvement (cases 1, 4, 7, 13, 15, 16, 19, 20, 22, and 23).

Six patients died of uncontrolled fungal infection. All 6 of these patients were young (14, 20, 21, 27, 27, and 41 years of age in cases 22, 16, 21, 8, 20, and 18, respectively) and were severely immunocompromised (4 with end-stage AIDS, 1 with severe neutropenia from chemotherapy for acute lymphoblastic leukemia, and 1 with graft-versus-host disease following bone marrow transplantation). An additional 7 patients died of other causes within a year of their fungal MOE. Three succumbed to opportunistic infections (cases 2, 4, and 9), 2 to leukemic relapses (cases 5 and 7), and 2 to cardiac disease (cases 3 and 6). All 13 patients who died were either severely immunocompromised or had significant comorbid disease. Overall, survival appeared to be correlated with the severity of the underlying disease, rather than with any particular therapeutic regimen.

Our case of *S apiospermum* infection in the mastoid air cells is consistent with the data from other fungal MOE cases. Our patient had end-stage AIDS, succumbed to his disease at a young age (21 years), and had an infection that we suspect originated from his mastoid air cells. Contrary to the other fungal MOE cases, our patient had granulation tissue in his mastoid air cells, but was not able to mount a sufficient immunologic response to rid himself of the infection. Overall, our patient's death was probably related more to the severity of his immunocompromised status than to his particular infection.

CONCLUSION

Fungal MOE has been reported in 23 patients in the literature, and most of these patients were infected by fungi from the *Aspergillus* genus. Fungal MOE occurs most commonly in end-stage AIDS patients and patients with hematologic malignancies. With fungal MOE patients, granulation tissue is not as common a finding as in bacterial MOE, and the infectious process often starts in the mastoid air cells or middle ear space as opposed to the external auditory canal. Surgical debridement and amphotericin B are the mainstays of therapy, but long-term survival depends greatly on the severity of the underlying disease. We have described the 24th patient in the literature with fungal MOE, and reported on the third case of fungal MOE due to *S apiospermum.*

REFERENCES

1. Petrak RM, Pottage JC Jr, Levin S. Invasive external otitis caused by *Aspergillus fumigatus* in an immunocompromised host [Letter]. J Infect Dis 1985;151:196.
2. Stanley RJ, McCaffrey TV, Weiland LH. Fungal mastoiditis in the immunocompromised host. Arch Otolaryngol Head Neck Surg 1988;114:198-9.
3. Cunningham M, Yu VL, Turner J, Curtin H. Necrotizing otitis externa due to *Aspergillus* in an immunocompetent patient. Arch Otolaryngol Head Neck Surg 1988;114:554-6.
4. Bickley LS, Betts RF, Parkins CW. Atypical invasive external otitis from *Aspergillus*. Arch Otolaryngol Head Neck Surg 1988;114:1024-8.
5. Menachof MR, Jackler RK. Otogenic skull base osteomyelitis caused by invasive fungal infection. Otolaryngol Head Neck Surg 1990;102:285-9.
6. Phillips P, Bryce G, Shepherd J, Mintz D. Invasive external otitis caused by *Aspergillus*. Rev Infect Dis 1990;12:277-81.
7. Strauss M, Fine E. *Aspergillus* otomastoiditis in acquired immunodeficiency syndrome. Am J Otol 1991;12:49-53.
8. Reiss P, Hadderingh R, Schot LJ, Danner SA. Invasive external otitis caused by *Aspergillus* fumigatus in two patients with AIDS [Letter]. AIDS 1991;5:605-6.
9. Hall PJ, Farrior JB. *Aspergillus* mastoiditis. Otolaryngol Head Neck Surg 1993;108:167-70.
10. Hanna E, Hughes G, Eliachar I, Wanamaker J, Tomford W. Fungal osteomyelitis of the temporal bone: a review of reported cases. Ear Nose Throat J 1993;72:532, 537-41.
11. Gordon G, Giddings NA. Invasive otitis externa due to *Aspergillus* species: case report and review. Clin Infect Dis 1994; 19:866-70.
12. Harley WB, Dummer JS, Anderson TL, Goodman S. Malignant external otitis due to *Aspergillus* flavus with fulminant dissemination to the lungs. Clin Infect Dis 1995;20:1052-4.
13. Bryce GE, Phillips P, Lepawsky M, Gribble MJ. Invasive *Aspergillus* tympanomastoiditis in an immunocompetent patient. J Otolaryngol 1997;26:266-9.
14. Ress BD, Luntz M, Telischi FF, Balkany TJ, Whiteman ML. Necrotizing external otitis in patients with AIDS. Laryngoscope 1997;107:456-60.
15. Busaba NY, Poulin M. Invasive *Pseudallescheria boydii* fungal infection of the temporal bone. Otolaryngol Head Neck Surg 1997;117:S91-S94.
16. Munoz A, Martinez-Chamorro E. Necrotizing external otitis caused by *Aspergillus fumigatus*: computed tomography and high resolution magnetic resonance imaging in an AIDS patient. J Laryngol Otol 1998;112:98-102.
17. Diop EM, Schachern PA, Paparella MM. Acquired immunodeficiency syndrome with massive *Aspergillus fumigatus* infection. Otolaryngol Head Neck Surg 1998;118:283-5.
18. Slack CL, Watson DW, Abzug MJ, Shaw C, Chan KH. Fungal mastoiditis in immunocompromised children. Arch Otolaryngol Head Neck Surg 1999;125:73-5.
19. Hennequin C, Benailly N, Silly C, et al. In vitro susceptibilities to amphotericin B, itraconazole, and miconazole of filamentous fungi isolated from patients with cystic fibrosis. Antimicrob Agents Chemother 1997;41:2064-6.
20. Bloom SM, Warner RR, Weitzman I. Maxillary sinusitis: isolation of *Scedosporium (Monosporium) apiospermum*, anamorph of *Petriellidium (Allescheria) boydii.* Mt Sinai J Med 1982;49:492-4.

Ann Otol Rhinol Laryngol 110:2001

BILATERAL CHYLOTHORAX FOLLOWING NECK DISSECTION: A NEW METHOD OF TREATMENT

KHALID AL-SEBEIH, MD, FRCS(C)
NADER SADEGHI, MD, FRCS(C)
SALEH AL-DHAHRI, MD
MONTREAL, CANADA

Chylothorax is a serious condition with a high rate of morbidity that may lead to death. Although it is encountered more frequently with certain thoracic procedures, it is considered to be a rare complication of neck dissection. Different forms of management have been postulated; however, no consensus of treatment has been achieved. A case of severe bilateral chylothorax that developed after bilateral neck dissection in a patient with laryngeal carcinoma is presented. Somatostatin injection was successful after total parenteral nutrition failed to control the chylothorax. On the basis of this case and the review of the literature discussed here, we advocate the use of somatostatin with other conservative measures in the management of chylothorax.

KEY WORDS — chylothorax, neck dissection, somatostatin.

INTRODUCTION

Chylous fistula is a well-known complication of neck dissection that occurs in 1% to 2% of cases. Chylothorax, on the other hand, is a serious complication that occurs very rarely after neck dissection.[1,2] Chylothorax was first described in 1907 by Stuart.[3] Since then, fewer than 20 cases have been reported in the literature. Many mechanical, nutritional, and immunologic complications can develop secondary to chyle effusion in the pleural space.[4]

The key to understanding the pathophysiology of chylothorax is to know the anatomy of the thoracic duct,[5] which is the final common pathway for most of the lymphatic drainage of the body. It arises from a triangular dilation called the cisterna chyli at the level of the second lumbar vertebra, then enters the thorax through the aortic hiatus and extends extrapleurally. The course continues superiorly into the posterior mediastinum to the right of midline between the aorta and the azygos vein. At the level between the fourth and the sixth thoracic vertebrae, the duct crosses to the left behind the esophagus and enters the left posterior mediastinum, where it lies behind the aortic arch and the subclavian vein. The duct exits the chest through the superior thoracic aperture and enters the root of the neck. As the duct enters the base of the neck, it lies behind the left common carotid artery. From this deep position, the duct arches upward, forward, and laterally and emerges between the left common carotid and left subclavian arteries. Here, it arches above the level of the subclavian artery and passes between the internal jugular vein and the anterior scalene muscle to terminate at the junction between the left internal jugular and subclavian veins.[6] In more than 40% of individuals, there are 2 or more divisions in the thoracic duct prior to its termination.[5,7-10] The duct may loop high into the neck and then downward, or may not rise above its level of termination.

CASE REPORT

A 70-year-old man who was a heavy smoker and an ex-alcoholic presented to our head and neck tumor clinic with a 6-month history of dysphonia and progressive shortness of breath. A full workup and a biopsy of a laryngeal lesion revealed squamous cell cancer of the larynx (T3N2cM0). Because of the obstructive tumor and progressive shortness of breath, the patient underwent an emergency tracheotomy before the total laryngectomy and bilateral modified neck dissection. During the left neck dissection, inadvertent injury to the thoracic duct resulted in leakage of a milky fluid. This was managed during the procedure by identifying and ligating the duct with a 2-0 silk suture. The site was reinforced by suturing the sternocleidomastoid muscle to the underlying paravertebral muscles. At the end of the procedure, the site of the leak was inspected, and positive pressure ventilation was used to confirm its closure. Two closed suction drainage systems were inserted into the neck, one on each side. The patient was transferred to the intensive care unit for monitoring, and spent an uneventful 24 hours. A chest radiograph taken within the first 24 hours of surgery did not reveal any abnormality. Feeding through a nasogastric tube was introduced on the second postoperative day. On the third postoperative day, the patient complained

---

From the Department of Otolaryngology–Head and Neck Surgery, Royal Victoria Hospital, McGill University, Montreal, Canada.

CORRESPONDENCE — Nader Sadeghi, MD, FRCS(C), Royal Victoria Hospital, ENT–Room E4.46, 687 Pine Ave W, Montreal, Quebec, Canada H3A 1A1.

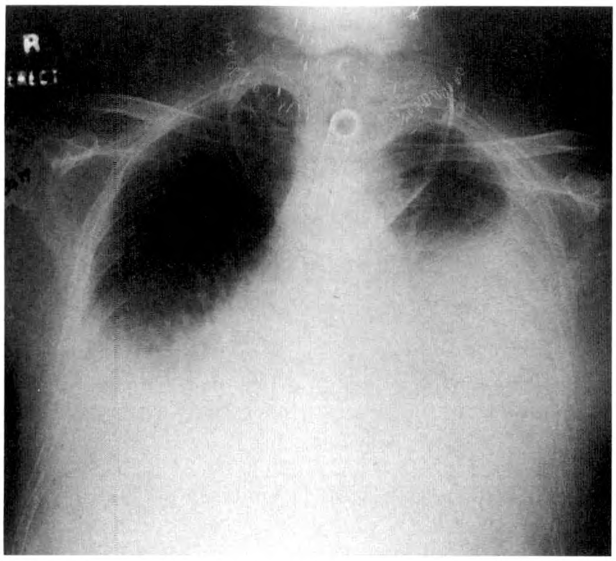

Fig 1. Chest radiograph of patient shows large bilateral pleural effusion on third postoperative day.

of breathing difficulty, and O_2 desaturation was noted. The heart rate was raised to 100 to 200 pulses per minute, and the blood pressure to 170/100 mm Hg. A chest radiograph revealed extensive bilateral pleural effusion (Fig 1). The patient was returned to the intensive care unit, where bilateral chest tubes were inserted. The left chest tube drained 1,800 mL of milky fluid, and the right, 1,500 mL. The vital signs of the patient normalized shortly after the drainage of the pleural effusion. Laboratory analysis of a sample of the drained fluid confirmed its chylous nature. The patient was kept fasting for 2 days and was then introduced to total parenteral feeding with no fat constituents.

Close monitoring of the chyle leak showed an initial decrease in the leakage, but it increased on the 12th postoperative day. The patient never had any chyle accumulation in or drainage from the neck. We decided to start somatostatin injection as a last attempt for conservative treatment of the chylothorax before surgical exploration. Somatostatin was introduced on the 13th postoperative day as 100-mg subcutaneous injections given 3 times a day. Soon there was a drastic improvement and a decrease in chyle leakage (Fig 2). On the 16th postoperative day, the total parenteral nutrition was discontinued and a regular diet was introduced without any noticeable increase in chylothorax. The chest tubes were removed on the 20th postoperative day. One week later, chest radiography showed no evidence of chyle in the pleural space (Fig 3).

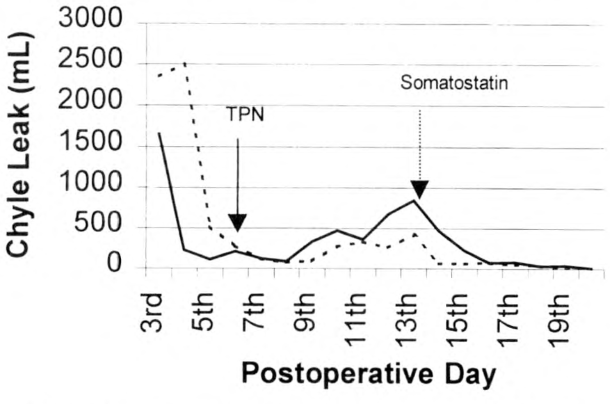

Fig 2. Daily amounts of chyle drainage from left (dotted line) and right (solid line) chest tubes. Note starting day of total parenteral nutrition (TPN) and starting day of somatostatin.

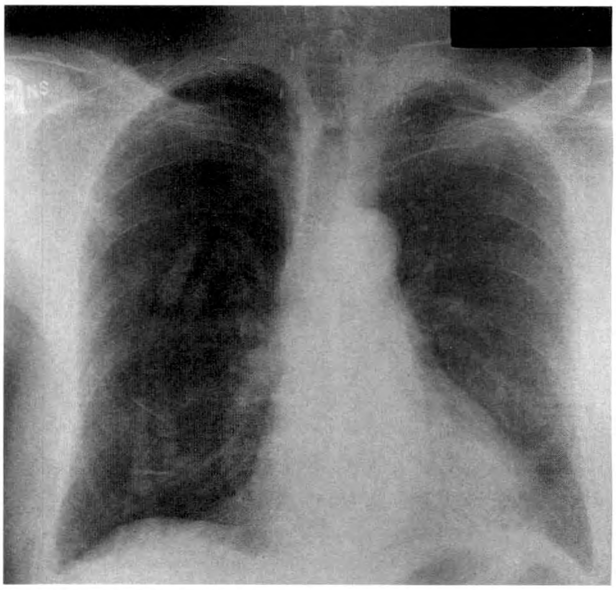

Fig 3. Follow-up chest radiograph taken 1 week after removal of chest tubes reveals no pleural effusion.

DISCUSSION

The causes of chylothorax can be classified as traumatic, obstructive, or congenital. Traumatic causes are considered to be the most common and can be accidental or iatrogenic.[11,12] Iatrogenic chylothorax is a potential risk in procedures involving the thorax, but is less common in radical neck dissection. Twenty percent of traumatic chylothoraces are secondary to penetrating or blunt injuries to the neck or chest.[13] Obstruction of the thoracic duct lumen can be intrinsic or extrinsic. An enlarged lymph node or tumor mass can compress the duct externally and obstruct the lymph flow.[14-17] Infiltration of the thoracic duct by neoplastic cells can also cause obstruction of the duct with subsequent chylous effusion. In either case, intraductal pressure increases. This renders lymphatic valves incompetent, resulting in regurgitation of the lymph flow that ultimately drains into the pleural space.[18] Congenital chylothorax is a very rare entity. It is usually idiopathic, but may be associated with Down syndrome and Noonan's syndrome.[18]

In the case reported, the exact pathophysiology of the chylothorax is unknown. It could have been due to direct leakage from the injured thoracic duct at the base of the neck, or the complete obstruction of lymph flow from the thoracic duct ligation and secondary extravasation of lymph into the pleural space. The latter mechanism is, however, highly likely, given no leakage from the neck despite a suction drain and no chylothorax on the first postoperative day. In addition to the increase in the intraductal pressure, the negative pressure during inspiration makes the extravasation lower, in the mediastinum rather than in the neck. This factor may explain the absence of a chyle leak in the neck.[19] The chylous accumulation in the mediastinum soon penetrates into the pleura through the high hydrostatic pressure and the inflammation that the chyle has induced.[19] Alternatively, the chyle can also extravasate directly through the dilated intrapulmonary lymphatic vessel and enter the pleural space, resulting in chylothorax.[17,20]

The first step in the management of chylothorax is to establish the proper diagnosis.[18,21-24] This requires a high index of suspicion in postoperative cases in which a high level of fluid output from the neck is noted. Certain tests can confirm the diagnosis of chylothorax on the basis of its constituents. Sudan III is a stain that has a high affinity for fat globules and can be used to confirm the nature of the chyle.[25] Lipoprotein electrophoresis of a sample of the effusion will demonstrate a chylomicron band and is indicative of chyle.[26] Measurement of triglycerides in the chyle will reveal a higher level than in the corresponding plasma.[26] A triglyceride level of >110 mg/dL strongly suggests chylous effusion.[18,26] Additionally, the cholesterol-to-triglycerides ratio will be <1.[26] Enteral administration of cream induces an increase in chyle flow and hence causes an increase in the chyle leak.[21,27]

Pleural chylous effusion can compress the vital structures within the thoracic cage, such as the lungs and the heart. If the effusion exceeds a certain limit, the patient will have symptoms and perhaps signs such as hypoxia and cardiac arrhythmias. If the patient is symptomatic or decompensated, a chest tube or multiple thoracenteses can be used to decompress the pleural cavity.

The loss of nutritional elements, such as proteins and fat-soluble vitamins, with drainage of chylous effusion can result in severe nutritional depletion with a negative impact on healing. Management should be aimed at monitoring and replacing fluids, electrolytes, and other nutritional requirements. A medium-chain triglyceride diet is an invaluable fat source that can be used to nourish a patient with chylothorax.[28] These triglycerides are absorbed directly in the portal system without being absorbed into the splanchnic vessels.[18] However, since enteral rest per se is also required to decrease the chyle flow and leak, the success rate of the medium-chain triglyceride diet is variable. Alternatively, total parenteral nutrition with a low-fat formula usually allows spontaneous cessation of the chyle drainage.[29]

Because chyle contains large numbers of leukocytes (400/mm^3 to 6,800/mm^3), chylothorax may reduce the count of inflammatory cells to very low levels and result in severe immunodeficiency.[18,21,24] In this situation, infectious surveillance should be maintained.[4] Intrapleural infections are infrequent, because of the bacteriostatic properties of the chyle.[30]

Some authors recommend surgical correction of chylothorax, especially in malnourished and debilitated patients. Thoracotomy with ligation of the duct at the site of injury or at the hiatus was the standard procedure for many years.[31,32] Some reports have described the success of injection of fibrin glue into the pleural cavity.[33,34] Thoracoscopic ligation has also been used with encouraging results.[35] There is no consensus on the timing of surgical correction. In general, a chyle leak of more than 1 L/d for 5 days,[21,27,36] a chyle leak that persists for 2 weeks in spite of conservative management,[5] loculated chylothorax,[5] an incarcerated lung,[5] and development of severe metabolic complications[37,38] are all indications for surgical correction of chylothorax.

Somatostatin has been used in the conservative treatment of chylothorax.[39] Somatostatin reduces the lymph flow within the thoracic duct in animals.[40] It also causes a decrease in the hepatic venous pressure gradient and a mild but sustained decrease in the splanchnic blood flow without interfering with systemic hemodynamics.[31,41] In the case reported here, somatostatin caused a drastic improvement in the chylous effusion in a short period of time, and no side effects developed from its use for 1 week. This outcome is consistent with the literature regarding the role of somatostatin in the treatment of chylothorax.

REFERENCES

1. El Zawahry MD, Sayed NM, El-Awady HM, Abdel-Latif A, El-Gindy M. A study of the gross, microscopic and functional anatomy of the thoracic duct and the lympho-venous junction. Int Surg 1983;68:135-8.

2. Miller JI. Diagnosis and management of chylothorax. Chest Surg Clin N Am 1996;6:139-48.

3. Stuart W. Operative injury of the thoracic duct in the neck. Edinburgh Med J 1907;22:301-6.

4. Marts BC, Naunheim KS, Fiore AC, Pennington DG.

Conservative versus surgical management of chylothorax. Am J Surg 1992;164:532-5.

5. Merrigan BA, Winter DC, O'Sullivan GC. Chylothorax. Br J Surg 1997;84:15-20.

6. Hollinshead WH. Anatomy for surgeons, the head and neck. 3rd ed. Philadelphia, Pa: JB Lippincott, 1982:475-7.

7. Pernis V. Variation of the thoracic duct. Surgery 1949;26:806-9.

8. Cha EM, Sirijintakarn P. Anatomic variation of the thoracic duct and visualization of mediastinal lymph nodes: a lymphographic study. Radiology 1976;119:45-8.

9. Kinnaert P. Anatomical variations of the cervical portion of the thoracic duct in man. J Anat 1973;115:45-52.

10. Orringer MB, Bluett M, Deeb GM. Aggressive treatment of chylothorax complicating transhiatal esophagectomy without thoracotomy. Surgery 1988;104:720-6.

11. Ramzy AI, Rodriguez A, Cowley RA. Pitfalls in the management of traumatic chylothorax. J Trauma 1982;22:513-5.

12. Engevik L. Traumatic chylothorax. Scand J Thorac Cardiovasc Surg 1976;10:77-8.

13. Robinson CL. The management of chylothorax. Ann Thorac Surg 1985;39:90-5.

14. Breaux JR, Marks C. Chylothorax causing reversible T-cell depletion. J Trauma 1988;28:705-7.

15. Tan KL, Lim LC, Hsu AA, Eng P, Ong YY. Chylothorax: case report and review of literature. Ann Acad Med Singapore 1997;26:225-8.

16. Bruneau R, Rubin P. The management of pleural effusion and chylothorax in lymphoma. Radiology 1965;85:1085-92.

17. Roy P, Carr D, Payne W. The problem of chylothorax. Mayo Clin Proc 1967;42:457-67.

18. Ross J. A review of the surgery of the thoracic duct. Thorax 1961;16:12-8.

19. Weidner WA, Steiner RM. Roentgenographic demonstration of intrapulmonary and pleural lymphatics during lymphangiography. Radiology 1971;100:533-9.

20. Abdul Jabbar AS, Al-Abdulkareem A. Bilateral chylothorax following neck dissection. Head Neck 1995;17:69-72.

21. Cevese PG, Vecchioni R, D'Amico DF, et al. Postoperative chylothorax. Six cases in 2,500 operations, with a survey of the world literature. J Thorac Cardiovasc Surg 1975;69:966-71.

22. Teba L, Dedhia HV, Bowen R, Alexander JC. Chylothorax review. Crit Care Med 1985;13:49-52.

23. Higgins CB, Reinke RT. Postoperative chylothorax in children with congenital heart disease. Clinical and roentgenographic features. Radiology 1976;119:409-13.

24. Valentine VG, Raffin TA. The management of chylothorax. Chest 1992;102:586-91.

25. Sassoon CS, Light RW. Chylothorax and pseudochylothorax. Clin Chest Med 1985;6:163-71.

26. Denborough M, Nestel P. Milky effusion. Med J Aust 1964;2:874-9.

27. Staats BA, Ellefson RD, Budahn LL, Dines DE, Prakash UB, Offord K. The lipoprotein profile of chylous and nonchylous pleural effusions. Mayo Clin Proc 1980;55:700-4.

28. Schulman A, Fataar S, Dalrymple R, Tidbury I. The lymphographic anatomy of chylothorax. Br J Radiol 1978;51:420-7.

29. Hashim S, Roholt H, Babayan V, et al. Treatment of chyluria and chylothorax with medium-chain triglycerides. N Engl J Med 1964;270:56-61.

30. Bozzetti F, Arullani A, Baticci F, Terno G, Ammatuna M, Cappello G. Management of lymphatic fistulas by total parenteral nutrition. JPEN J Parenter Enteral Nutr 1982;6:526-7.

31. Erbas T, Usman A, Erbas B, Varoglu E, Aras T, Bekdik C. Short-term effects of somatostatin analogue (SMS 201-995) on left ventricular function in healthy persons: a scintigraphic study. J Endocrinol Invest 1993;16:857-61.

32. Ferguson MK, Little AG, Skinner DB. Current concepts in the management of postoperative chylothorax. Ann Thorac Surg 1985;40:542-5.

33. Rubin JW, Moore HV, Ellison RG. Chylothorax: therapeutic alternatives. Am Surg 1977;43:292-7.

34. Nguyen D, Tchervenkov CI. Successful management of postoperative chylothorax with fibrin glue in a premature neonate. Can J Surg 1994;37:158-60.

35. Akaogi E, Mitsui K, Sohara Y, Endo S, Ishikawa S, Hori M. Treatment of postoperative chylothorax with intrapleural fibrin glue. Ann Thorac Surg 1989;48:116-8.

36. Janssen JP, Joosten HJ, Postmus PE. Thoracoscopic treatment of postoperative chylothorax after coronary bypass surgery. Thorax 1994;49:1273.

37. Patterson GA, Todd TR, Delarue NC, Ilves R, Pearson FG, Cooper JD. Supradiaphragmatic ligation of the thoracic duct in intractable chylous fistula. Ann Thorac Surg 1981;32:44-9.

38. Selle JG, Snyder WH III, Schreiber JT. Chylothorax: indications for surgery. Ann Surg 1973;177:245-9.

39. Rimensberger PC, Muller-Schenker B, Kalangos A, Beghetti M. Treatment of a persistent postoperative chylothorax with somatostatin. Ann Thorac Surg 1998;66:253-4.

40. Nakabayashi H, Sagara H, Usukura N, et al. Effect of somatostatin on the flow rate and triglyceride levels of thoracic duct lymph in normal and vagotomized dogs. Diabetes 1981;30:440-5.

41. Cirera I, Feu F, Luca A, et al. Effects of bolus injections and continuous infusions of somatostatin and placebo in patients with cirrhosis: a double-blind hemodynamic investigation. Hepatology 1995;22:106-11.

Ann Otol Rhinol Laryngol 110:2001

NON-INFLATABLE STERILE SHEATH FOR INTRODUCTION OF THE FLEXIBLE NASOPHARYNGOLARYNGOSCOPE

HARVEY D. SILBERMAN, MD
PHILADELPHIA, PENNSYLVANIA

Since the inception of the flexible nasopharyngolaryngoscope, sterility has been a primary concern. The increased incidence of hepatitis, tuberculosis, and acquired immunodeficiency syndrome has raised the fear of cross-contamination. Sterilization requires the use of ethylene oxide, which is economically disadvantageous, forcing most practitioners to disinfect rather than sterilize their nasopharyngolaryngoscopes. A presterilized, disposable sheath was designed in 1993. The system was cumbersome, because it required an air pump. Thus, it was not adopted by the majority of physicians. As a result, the manufacturer developed a new system, which I evaluated. It is cost-effective, smoother-surfaced, 70% thinner-walled, and much simpler to use. The disposable, single-use sheath is sterile, with no need for a pump or any additional device, and can be used anywhere at any time. I believe it will become the standard method for sterile introduction of the nasopharyngolaryngoscope.

KEY WORDS — endoscope, flexible scope, nasopharyngolaryngoscope, sterile sheath.

In an otolaryngology office, the nasopharyngolaryngoscope is an indispensable diagnostic tool. The constant use of this instrument engenders the risk of cross-contamination. Few studies have been undertaken to measure the degree of transference of infection. Because of this lack and the fact that the nasopharyngolaryngoscope has no operating channel, many are lulled into a false sense of security.

Some otolaryngologists use only a cursory wash of the nasopharyngolaryngoscope between patients. Endoscopes come into contact with blood, mucus, and tissue debris. Fortunately, the majority of otolaryngologists realize that a higher level of cleansing is necessary and rely on disinfection or true sterilization.

Disinfection techniques have major drawbacks. The scopes are washed thoroughly and then soaked for 30 minutes in glutaraldehyde or similar solutions. Over the years, constant cleaning and soaking of nasopharyngolaryngoscopes causes the covering to slowly degrade, resulting in cracks and crevices that potentiate destruction of the scope, specifically at the distal flexing portion. The cracks and crevices can act as collecting points for bacteria and viruses, much as a channel will in other types of flexible endoscopes. Kaczmarek et al[1] have shown that indeed, there can be a breakdown in disinfecting techniques, with persistent contamination of endoscopes. Without question, this poses a great potential threat to our patients.

The time demands of the glutaraldehyde technique cause the nasopharyngolaryngoscope to be out of service, thus requiring multiple instruments. In truth, the technique only provides high-level disinfection, and not sterilization.[2] Working with glutaraldehyde can also be hazardous to health workers. In fact, there have been reports of allergic reactions such as asthma and rhinitis with exposure to glutaraldehyde.[3] Another option is the Steris system, which also claims sterilization. In the final analysis, however, this may only provide disinfection for the practitioner.[4]

True sterilization is the goal for all physicians. Indeed, ethylene oxide does provide a truly sterile nasopharyngolaryngoscope, but the downtime of the instrument is prohibitive. Frequently, the scope is unavailable for an entire practice day because of the aeration requirements.

In 1993, we introduced a new method of sterile introduction of the flexible nasopharyngolaryngoscope.[5] The technique used a presterilized plastic sheath that was designed to fit over the flexible nasopharyngolaryngoscope. This sheath had to be preinflated so that the scope could be slipped into and out of it. A small pump performed the inflation and deflation of the sheath. In their extensive study of universal precautions for the otolaryngologist, Murr and Lee[6] recommended the use of the flexible scope with the EndoSheath cover.

Some problems arose with the use of the sheath. Difficulties were encountered in using the pump. The requirement of the pump made performing bedside upper endoscopy with the flexible nasopharyngolaryngoscope logistically difficult. It was necessary to carry not only the scope and a light source, but also

---

From the Department of Otolaryngology–Head and Neck Surgery, Temple University Hospital, Philadelphia, Pennsylvania. Supported by Vision Sciences, Inc, Natick, Massachusetts.

CORRESPONDENCE — Harvey D. Silberman, MD, 156 Serrill Rd, Elkins Park, PA 19027.

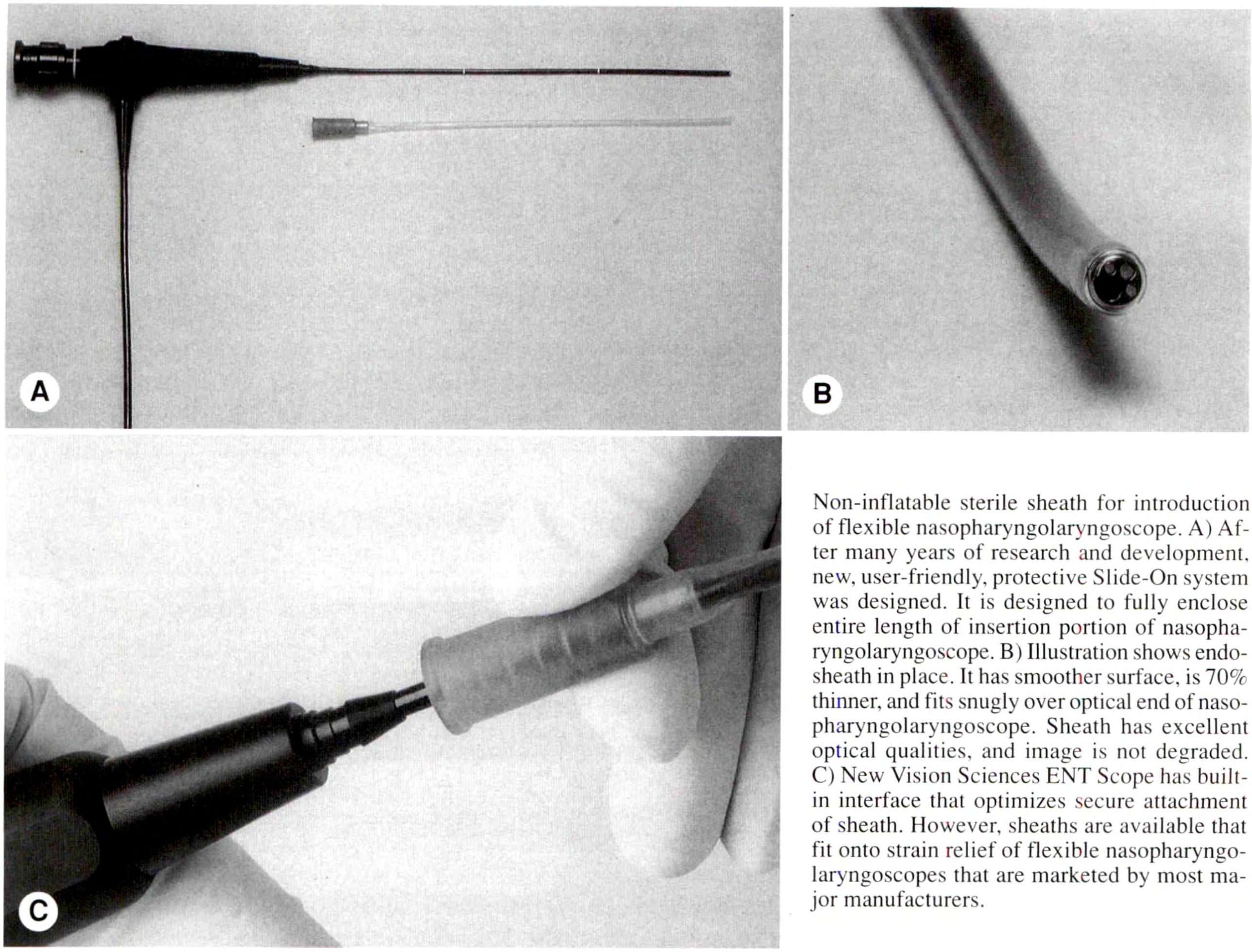

Non-inflatable sterile sheath for introduction of flexible nasopharyngolaryngoscope. A) After many years of research and development, new, user-friendly, protective Slide-On system was designed. It is designed to fully enclose entire length of insertion portion of nasopharyngolaryngoscope. B) Illustration shows endosheath in place. It has smoother surface, is 70% thinner, and fits snugly over optical end of nasopharyngolaryngoscope. Sheath has excellent optical qualities, and image is not degraded. C) New Vision Sciences ENT Scope has built-in interface that optimizes secure attachment of sheath. However, sheaths are available that fit onto strain relief of flexible nasopharyngolaryngoscopes that are marketed by most major manufacturers.

the pump, which was the heaviest and most cumbersome part of the equipment. Occasionally, the sheath was difficult to remove because of problems with the seal. Despite these disadvantages, the EndoSheath system was the simplest and best way to maintain both sterility and rapid turnaround time for the otolaryngologist.

The use of the pump to inflate the EndoSheath was deemed to be the biggest problem of the EndoSheath system. The manufacturer was aware of the limitations of the original EndoSheath system, but strongly believed in the importance of the sterile EndoSheath.

After several years of research and development, the new, user-friendly, protective Slide-On system was designed. I clinically evaluated the new sheath. It is designed to fully enclose the entire length of the insertion portion of the nasopharyngolaryngoscope (see Figure, A). It is more cost-effective because of its short downtime, has a smoother surface, is 70% thinner, and fits snugly over the optical end of the nasopharyngolaryngoscope. The sheath is constructed from non-latex materials and is compatible with commonly used water-based lubricants and topical anesthetics. It has excellent optical qualities, and the image is not degraded (see Figure, B). The disposable, single-use sheath is sterile, is individually prepackaged, and easily slides on and off the flexible scope, with no need for a pump or any additional device. The sheaths can be used anywhere at any time.

The sheath was tested by an independent laboratory according to the US Food and Drug Administration Guidance Document for ENT Endoscope Sheaths with Protective Barrier Claims (October 21, 1996) and was proved to be an effective barrier to microorganisms as small as 27 nm.

The new Vision Sciences ENT Scope has a built-in interface that optimizes the secure attachment of the sheath (see Figure, C). However, sheaths are available that fit onto the strain relief of flexible nasopharyngolaryngoscopes that are marketed by most major manufacturers.

Beginning on April 6, 1999, a study was performed on 50 volunteer subjects to evaluate the safety, ease of use, and comfort obtained with the new non-inflatable EndoSheath. Having used the nasopharyngolaryngoscope both without a sheath and with the in-

NASOPHARYNGOLARYNGOSCOPY WITH NEW, NON-INFLATABLE STERILE ENDOSHEATH

Parameters Studied	*Poor*	*Below Average*	*Average*	*Above Average*	*Excellent*
Image clarity through sheathed nasopharyngolaryngoscope				13	37
Illumination during procedure			1	14	35
Uniformity of illumination during procedure			1	13	36
Lack of fogging of distal tip of sheathed scope versus unsheathed scope			3	17	30
Ease of passage and feel of sheathed nasopharyngolaryngoscope	1	1	1	18	29
Flexibility of sheathed scope during procedure		1	1	14	34
Ease of distal tip angulation during procedure		1	2	16	31
Ease of EndoSheath installation and removal	2	1	2	5	40
Overall impression of new EndoSheath system		1	1	12	36

Based on author's evaluation of procedure in 50 volunteers, none of whom had to withdraw because of discomfort.

flatable sheath for some time, I basically wanted to evaluate its use with the new non-inflatable EndoSheath. The parameters evaluated during this study are noted in the Table.

As one can see from the results of the tests, the noninflatable EndoSheaths worked extremely well. There were few unfavorable experiences. There were 3 instances of difficulty in removing the sheaths, resulting in ratings of "poor" or "below average." They all occurred early in the study and happened when the tester mishandled the sheath on its removal from the scope. The 2 cases of difficulty in passing the nasopharyngolaryngoscope were in patients who had extremely dry mucosa as a result of systemic disease or radiotherapy. This problem can occur with or without a sheath. I have found that simply wetting the instrument with water resolves the problem. There were no instances of sheath rupture during use. According to the sheath manufacturer's instructions, if a rupture is suspected, or moisture is observed on the insertion portion of the scope upon removal, the scope must be disinfected or sterilized according to the scope manufacturer's instructions. The use of non–petroleum-based lubricants should be avoided, if possible, since they frequently are wiped over the optical end of the scope, blurring vision.

The results of the study make true sterility of the nasopharyngolaryngoscope a viable option for the physician. The new, non-inflatable EndoSheath system is a vast improvement over its predecessor. It took, on average, 15 seconds to install and 5 seconds to remove. I have found the new protective Slide-On EndoSheath easy to work with in the office. The use of the sheath did not impinge upon the diagnostic parameters of the nasopharyngolaryngoscope. It also provided for a convenient, portable, sterile system in the hospital setting. This is especially important in view of the mounting incidence of methicillin-resistant organisms. I recommend the new Slide-On, sterile, disposable EndoSheath as the simplest method for true sterilization of the nasopharyngolaryngoscope.

REFERENCES

1. Kaczmarek RG, Moore RM Jr, McCrohan J, et al. Multistate investigation of the actual disinfection/sterilization of endoscopes in health care facilities. Am J Med 1992;92:257-61.

2. Urayama S, Kozarek RA, Sumida S, Raltz S, Merriam L, Pethigal P. Mycobacteria and glutaraldehyde: is high-level disinfection of endoscopes possible? Gastrointest Endosc 1996;43:451-6.

3. Corrado OJ, Osman J, Davies RJ. Asthma and rhinitis after exposure to glutaraldehyde in endoscopy units. Hum Toxicol 1986;5:325-8.

4. Rutala WA, Gergen MF, Weber DJ. Comparative evaluation of the sporicidal activity of new low-temperature sterilization technologies: ethylene oxide, 2 plasma sterilization systems, and liquid peracetic acid. Am J Infect Control 1998;26:393-8.

5. Silberman HD, Hampel A, Kominsky AH. New technique for the sterile introduction of flexible nasopharyngolaryngoscopes. Ann Otol Rhinol Laryngol 1993;102:687-9.

6. Murr AH, Lee KC. Universal precautions for the otolaryngologist: techniques and equipment for minimizing exposure risk. Ear Nose Throat J 1995;74:338, 341-6.

Ann Otol Rhinol Laryngol 110:2001

IMAGING CASE STUDY OF THE MONTH

DOES COCHLEAR NERVE APLASIA ALWAYS OCCUR IN THE PRESENCE OF A NARROW INTERNAL AUDITORY CANAL?

HUNG THAI-VAN, MD
LYON, FRANCE

BERNARD FRAYSSE, MD
TOULOUSE, FRANCE

OLIVIER DEGUINE, MD
TOULOUSE, FRANCE

ANNICK SEVELY, MD
TOULOUSE, FRANCE

CORINNE BERGES, MD
TOULOUSE, FRANCE

INTRODUCTION

The current approach to management of deafness in childhood is to identify the cause of the auditory deficit and its exact location. It then becomes necessary for otolaryngologists and audiologists to assess cochlear nerve integrity before selecting any therapeutic options. To date, cochlear nerve hypoplasia or aplasia has been known to occur concomitantly with an internal auditory canal (IAC) whose diameter is below normal limits, ie, 4 mm.[1] This association has been strongly supported by several studies that reported cochlear implant failure in the presence of a stenotic IAC.[2-4]

This report describes a case of unilateral total deafness related to cochlear nerve aplasia. The findings described contradict some recognized opinions. The radiologic findings are discussed and compared to the electrophysiological data.

CASE REPORT

A 7-year-old boy, referred by the neurosurgery department, had received a diagnosis of Dandy-Walker syndrome and had undergone operation for hydrocephalus 1 year earlier. He recovered completely from all of his neurologic symptoms, but reported unexplained hearing disorders.

At the physical examination, the otologic and head and neck status was unremarkable. The facial nerve function was unimpaired and symmetric. There were neither syndromic deafness stigmas nor a family history of hereditary sensorineural hearing loss. The child had never had mumps. No more gait disturbance or vertigo had occurred since the surgery. A perilymph fistula test was negative. No symptoms of ear fullness or pressure were reported, and the boy was free of tinnitus. The child's only complaint was that he continued to experience some degree of hearing impairment; however, he could not identify on which side the impairment was located.

The results of audiological testing were as follows: pure tone audiometry and speech testing showed total deafness on the right side, but normal hearing thresholds in the left ear. Objective auditory measures confirmed the unilateral deafness. However, they attested that outer hair cell function was present and normal on both sides. Although brain stem auditory evoked potential testing failed to elicit any identifiable waveforms in the right ear (Fig 1A), transiently evoked otoacoustic emission testing demonstrated the existence of normal cochlear emissions with an excellent response reproducibility across the frequency spectrum between 1.0 and 5.0 kHz (Fig 1B). The overall average transiently evoked otoacoustic emission amplitude (root mean square amplitude) corresponding to the sum of echo power in the whole frequency range of the power spectrum was of 14.6 dB sound pressure level. Audiological assessments therefore provided 2 possible explanations for the right-sided hearing loss. First, the hearing impairment could have been of retrocochlear origin. Second, there could have been a total loss of inner hair cells with a normal auditory nerve.

The child's medical examination was completed with vestibular laboratory tests. The findings of ocular motor testing, which included saccadic testing,

---

From the Departments of Otorhinolaryngology (Thai-Van, Fraysse, DeGuine, Berges) and Pediatric Neuroradiology (Sevely), Purpan University Hospital, Toulouse, France.

CORRESPONDENCE — Hung Thai-Van, MD, Service d'Explorations Fonctionnelles ORL et Audiophonologiques, Pavillon U, CHU Edouard Herriot, Place d'Arsonval, 69437 Lyon Cedex 03, France.

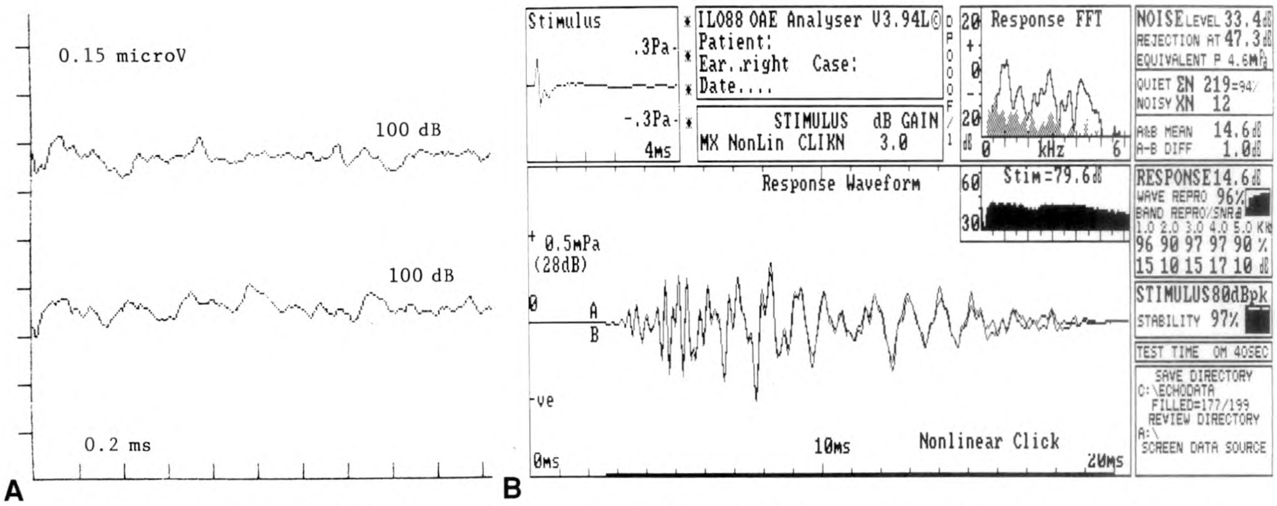

Fig 1. Electrophysiological testing performed on right ear. A) Brain stem auditory evoked potentials are absent on 2 successive recordings performed with stimulus intensity of 100 dB normal hearing level. B) Transiently evoked otoacoustic emissions clearly demonstrate existence of cochlear emissions.

sinusoidal pursuit tracking, and optokinetic testing, were entirely normal. Neither spontaneous nor positional nystagmus was recorded. Rotational testing of the vestibulo-ocular reflex (VOR) did not show any directional preponderance, and showed a VOR gain within normal limits. In addition, bithermic caloric testing indicated that the vestibular function was symmetric, without any vestibular paresis.

To assess the inner ear morphology, we performed a computed tomography (CT) scan of the temporal bones with 1-mm-thick slices (GE High Speed CT/i, Milwaukee, Wis). Computed tomography allowed verification of the cochlea's integrity, ruling out the hypothesis of a right-sided inner ear malformation. A well-developed IAC was clearly visualized on both sides (Fig 2). Magnetic resonance imaging (MRI) studies, performed on Magnetom Vision at 1.5 T (Siemens, Erlangen, Germany), were used to investigate the child's unilateral, presumably retrocochlear, deafness. No labyrinthitis, neuritis, or enhancing lesion of the posterior fossa was detected on either T1- or T2-weighted spin echo studies. The endolymphatic duct and sac were not enlarged. Selective (0.7-mm) 3-dimensional Fourier transformation–constructive interference in steady state slices were also acquired, providing the best existing MRI sequence for study of the cochleovestibular nerve.[5] Surprisingly, the right eighth nerve was severely hypoplastic, despite the presence of a well-developed IAC. If the vestibular branch was delineated, no cochlear branch could be individualized (Fig 3). Conversely, the left cochleovestibular nerve was normal (Fig 4). Since the child's hearing impairment was strictly unilateral, no social or cognitive consequences were detected.

DISCUSSION

It is commonly accepted that cochlear nerve agen-

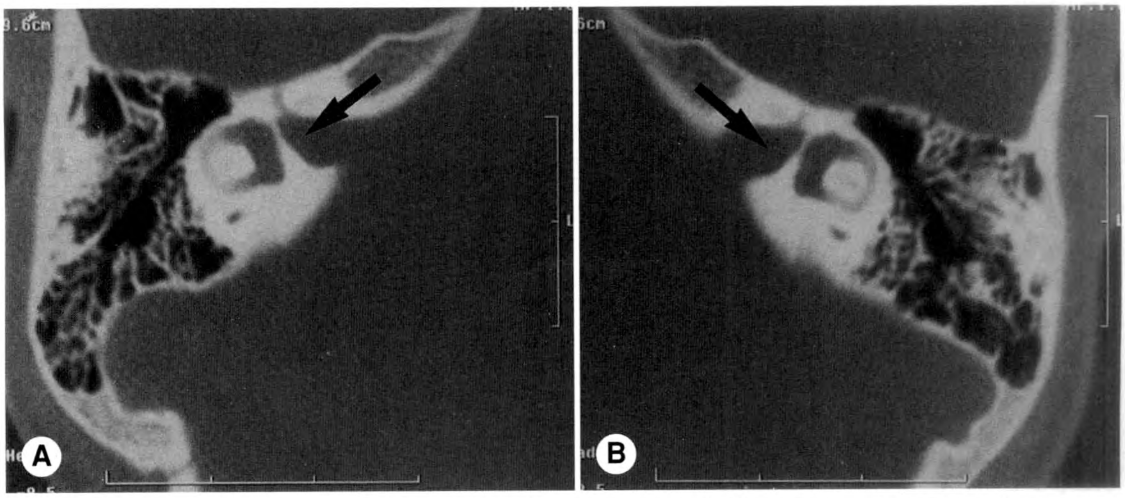

Fig 2. Axial 1-mm-thick computed tomography slices obtained on A) right side and B) left side. Note that dimensions of internal auditory canal are within normal limits (arrows).

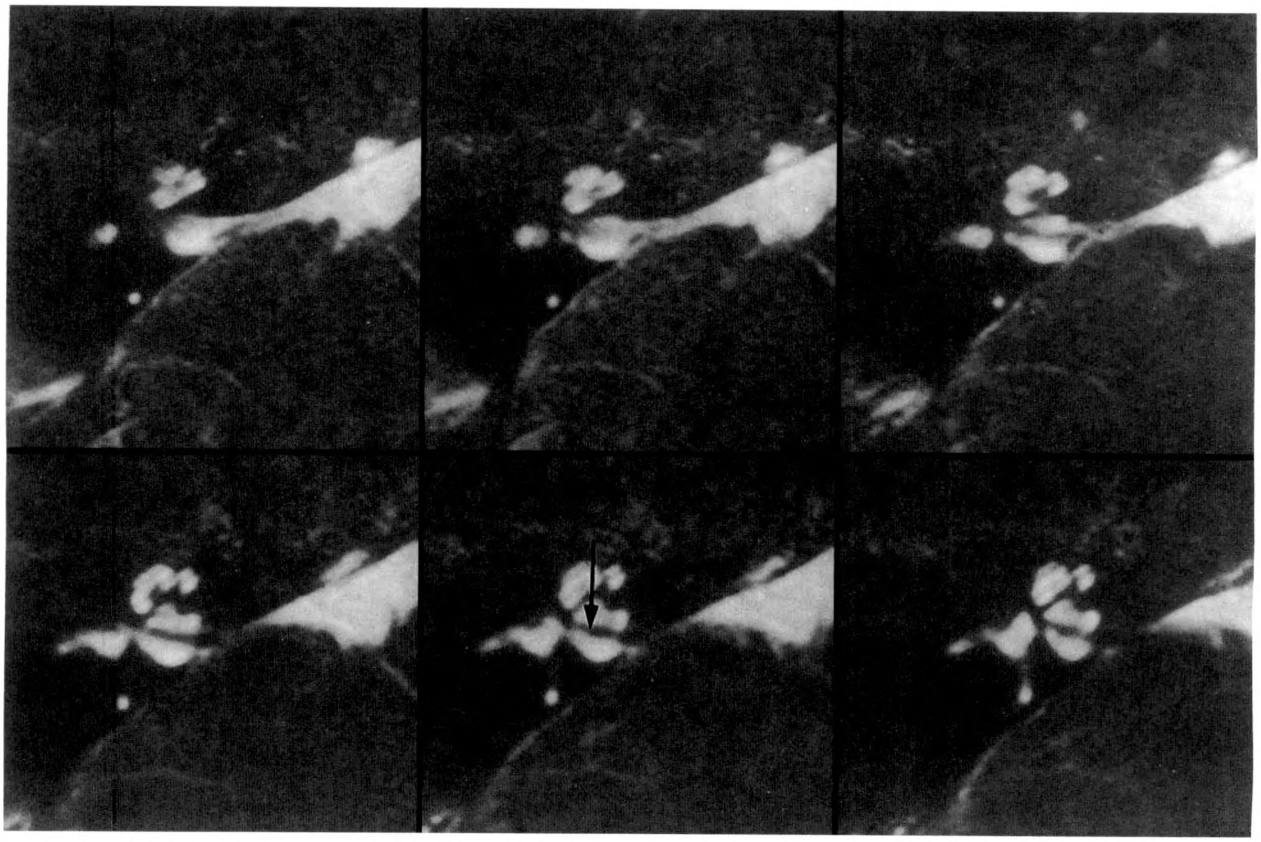

Fig 3. Axial 0.7-mm-thick 3-dimensional Fourier transformation–constructive interference in steady state consecutive sections acquired at level of right cerebellopontine angle. There is neither inner ear malformation nor small internal auditory canal syndrome in this case of monaural right deafness. Image of eighth nerve delineates single vestibular branch (arrow).

esis occurs in the presence of a narrow IAC. This belief is based on the fact that atresias of the facial canal and optic foramen are associated with atresia of their respective nerves.[6] From a developmental point of view, atresia of the IAC has been thought to result from an inhibition subsequent to a delayed embryological maturation of the cochleovestibular nerve. A lack of chemotactic mechanisms directing nerve growth from the statoacoustic ganglion to the labyrinthine end organs, by the sixth week of gestation, may indeed indirectly interrupt the chondrification of the mesoderm surrounding the acousticofacial bun-

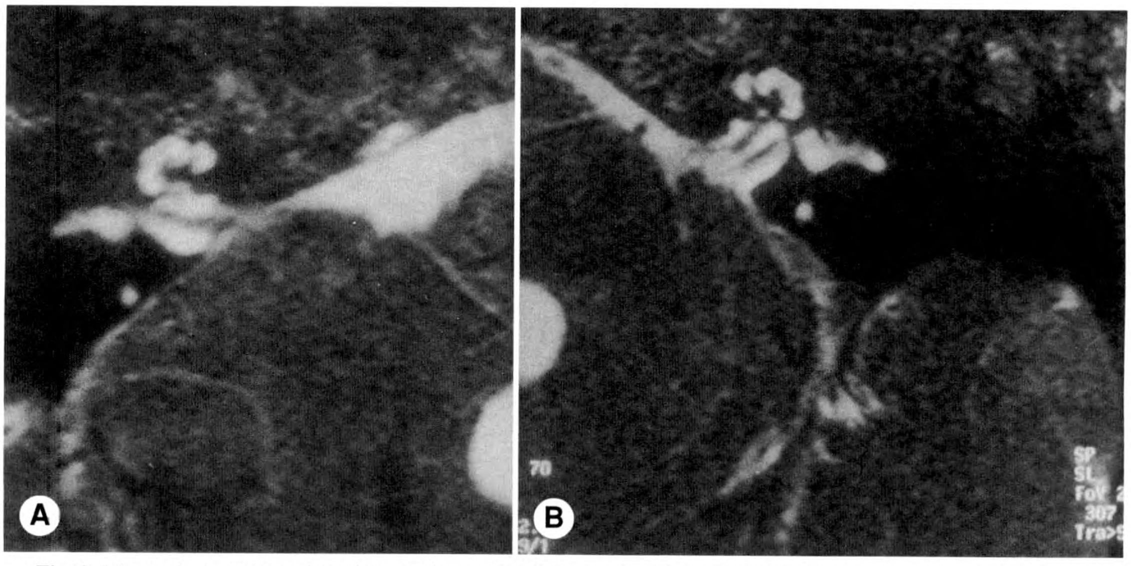

Fig 4. Magnetic resonance imaging sections with 3-dimensional Fourier transformation–constructive interference in steady state. A) Right eighth nerve is hypoplastic. B) Left eighth nerve is normal.

dle.[3] Involvement of neuronotrophic processes in acoustic nerve growth has been experimentally demonstrated in vitro.[7-10] On the basis of this finding, physicians were implicitly advised to suspect hypoplasia or aplasia of the cochlear nerve only when facing a narrow IAC on a CT scan.[11,12]

The clinical features of cochleovestibular nerve dysplasia need to be investigated. We previously reported the case of a congenitally deaf child, followed from the age of 22 months, who exhibited both measurable hearing and a normal VOR despite a narrow IAC with aplasia of the cochleovestibular nerve bilaterally suggested by neuroradiologic investigation.[13] Functional MRI of the auditory cortex confirmed that some acoustic fibers effectively projected into Brodmann's areas 41 and 42.[13] The main contribution of the present report is to demonstrate that cochlear nerve aplasia or severe hypoplasia may occur together with an apparently well-developed IAC. To our knowledge, such an association has not yet been described. Furthermore, this report introduces a novel and atypical presentation of retrocochlear deafness in which the electrophysiological findings correlate well with the neuroradiologic data.

In our observation, evidence of preserved cochlear outer hair cell function on the impaired side was proven by acquisition of reproducible otoacoustic emissions. It is noteworthy that this finding is consistent with the diagnosis of auditory neuropathy. This audiological, electrophysiological syndrome has been defined as absent or markedly distorted auditory brain stem responses with normal distortion product otoacoustic emissions and cochlear microphonics.[14,15] Consequently, it is thought to reflect an auditory dysfunction involving the eighth nerve.[16,17] However, damage and/or dysfunction of the inner hair cells could also explain this entity.[18] The present case suggests that the auditory neuropathy syndrome may be caused, at least occasionally, by cochlear nerve aplasia. It would be of great interest to investigate the radiologic anatomy of the eighth nerve in a case of suspected auditory neuropathy syndrome, especially one in which pure tone thresholds or speech discrimination skills are severely altered. Recently, a case of IAC atresia with cochlear nerve agenesis was reported, in which recordings of cochlear microphonics contrasted with the absence of brain stem auditory evoked potentials.[19]

The case presented illustrates that a normal-sized IAC on CT is not sufficient to rule out the risk of aplasia or hypoplasia of the acoustic nerve. Because of the lack of information provided by CT, diagnosis of such congenital abnormalities requires the use of MRI studies. When suspecting "neural" deafness, it is important to look for the bifurcation of the eighth nerve into its cochlear and vestibular branches on consecutive MRI slices, obtained through the inferior half of the IAC and at the middle third of the canal. In our case, no bifurcation was visualized at this level — a finding suggestive of an agenesis of the cochlear branch.

To explain these findings, we need to consider that the sole development of the facial nerve, with part of the vestibular nerve, could be sufficient to structure a nonstenotic IAC. The resulting IAC might contain both a superior part for the facial nerve and an inferior part for the vestibular nerve, exhibiting a normal diameter on CT. Detection of such an uncommon syndrome appears to benefit from objective audiological testing.

CONCLUSION

Malformations of the eighth nerve may occur even when the IAC dimensions appear normal on CT. This finding may be of use to specialized deafness management teams in assessing the potential benefits of a cochlear implant, as well as the benefits of a conventional hearing aid. Normal outer hair cell function in the absence of auditory brain stem responses is a strong argument for using complementary neuroradiologic studies to test the cochlear nerve integrity. Reciprocally, detection of cochlear nerve aplasia or hypoplasia may considerably clarify an unexplained auditory neuropathy.

ACKNOWLEDGMENTS — The authors thank Prof Lionel Collet for his constructive comments and Dr France Bui for her assistance in manuscript preparation.

REFERENCES

1. Valvassori GE, Pierce RH. The normal internal auditory canal. Am J Radiol 1964;92:1232-41.

2. Jackler RK, Luxford WM, House WF. Sound detection with the cochlear implant in five ears of four children with congenital malformations of the cochlea. Laryngoscope 1987;97 (suppl 40):15-7.

3. Shelton C, Luxford WM, Tonokawa LL, Lo WW, House WF. The narrow internal auditory canal in children: a contraindication to cochlear implants. Otolaryngol Head Neck Surg 1989;100:227-31.

4. Maxwell AP, Mason SM, O'Donoghue GM. Cochlear nerve aplasia: its importance in cochlear implantation. Am J Otol 1999;20:335-7.

5. Casselman JW. Temporal bone imaging. Neuroimaging Clin N Am 1996;6:265-89.

6. Everberg G, Ratjen E, Sorensen H. Unilateral atresia of the auditory meatus, confirmed by radiography. Br J Radiol 1963;36:568-73.

7. Van de Water TR. Determinants of neurons–sensory re-

ceptor cell interaction during development of the inner ear. Hear Res 1986;22:265-77.

8. Hemond SG, Morest DK. Tropic effects of otic epithelium on cochleo-vestibular ganglion fiber growth in vitro. Anat Rec 1992;232:273-84.

9. Lefebvre PP, Leprince P, Weber T, Rigo JM, Delree P, Moonen G. Neuronotrophic effect on developing otic vesicle on cochleo-vestibular neurons: evidence for nerve growth factor involvement. Brain Res 1990;507:254-60.

10. Jimenez C, Gireldez F, Represa J, Garcia-Diaz JF. Calcium currents in dissociated cochlear neurons from the chick embryo and their modification by neurotrophin-3. Neuroscience 1997;77:673-82.

11. Casselman JW, Offeciers FE, Govaerts PJ, et al. Aplasia and hypoplasia of the vestibulocochlear nerve: diagnosis with MR imaging. Radiology 1997;202:773-81.

12. Yates JA, Patel PC, Millman B, Gibson WS. Isolated congenital internal auditory canal atresia with normal facial nerve function. Int J Pediatr Otorhinolaryngol 1997;41:1-8.

13. Thai-Van H, Fraysse B, Berry I, et al. Functional magnetic resonance imaging may avoid misdiagnosis of cochleovestibular nerve aplasia in congenital deafness. Am J Otol 2000;21:663-70.

14. Deltenre P, Mansbach AL, Bozet C, Clercx A, Hecox KE. Auditory neuropathy: a report on three cases with early onsets and major neonatal illnesses. Electroencephalogr Clin Neurophysiol 1997;104:17-22.

15. Deltenre P, Mansbach AL, Bozet C, et al. Auditory neuropathy with preserved cochlear microphonics and secondary loss of otoacoustic emissions. Audiology 1999;38:187-95.

16. Starr A, Picton TW, Sininger Y, Hood LJ, Berlin CI. Auditory neuropathy. Brain 1996;119:741-53.

17. Doyle KJ, Sininger Y, Starr A. Auditory neuropathy in childhood. Laryngoscope 1998;108:1374-7.

18. Konradsson KS. Bilaterally preserved otoacoustic emissions in four children with profound idiopathic unilateral sensorineural hearing loss. Audiology 1996;35:217-27.

19. O'Leary SJ, Gibson WP. Surviving cochlear function in the presence of auditory nerve agenesis. J Laryngol Otol 1999;113:1008-10.

CII Bionic Ear™ System

CII BTE™

Platinum Sound Processor™

The high resolution CLARION® CII Bionic Ear™ is a **NEW** generation cochlear implant technology that delivers **MORE SOUND** information for **BETTER HEARING**. Advancements in cochlear implant technology over the past twenty years have demonstrated that the ability to provide more sound information to the hearing nerve has resulted in increased patient **PERFORMANCE**. Conventional cochlear implants have been limited in their ability to deliver a full or complete sound signal. The CII Bionic Ear System* can deliver sound information to the hearing nerve up to 1,000,000 times per second through 31 distinct audio processing channels. Special state-of-the-art safeguard electronics are designed to ensure that the high resolution CII Bionic Ear delivers the **FULL BROADBAND** sound information to the hearing nerve safely and effectively. The system utilizes the latest advances in focusing electrode technology and powerful miniature sound processor electronics to provide the **HIGHEST FIDELITY** to its users.* To learn more about the possibilities please contact us.

PLEASE VISIT US AT BOOTH 311.

*CAUTION: High Resolution broadband information delivery is limited to investigational use only

CLARION®

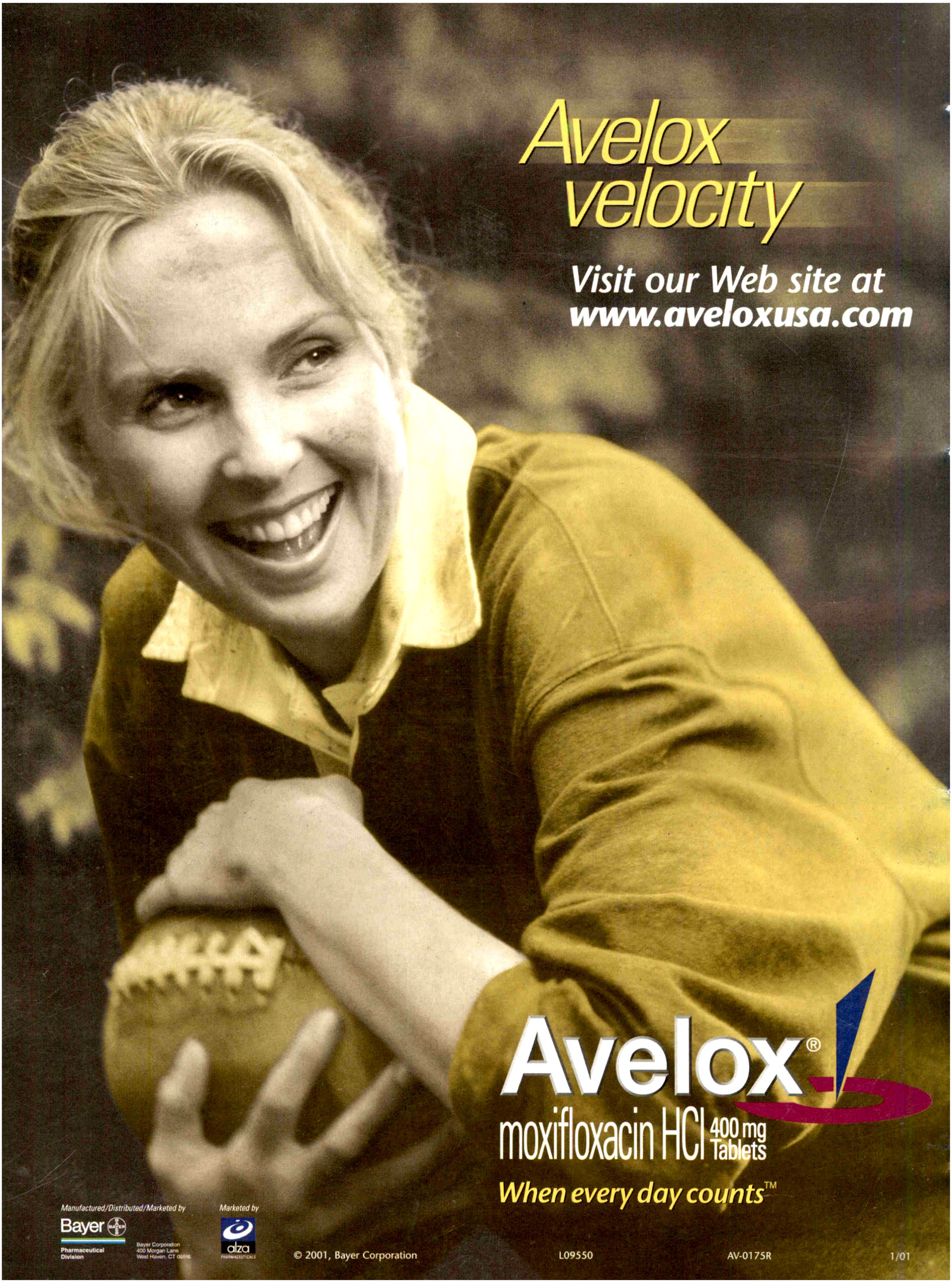

Manufactured/Distributed/Marketed by
Bayer
Pharmaceutical Division
Bayer Corporation
400 Morgan Lane
West Haven, CT 06516

Marketed by
alza
PHARMACEUTICALS

© 2001, Bayer Corporation L09550 AV-0175R 1/01

VOLUME 110 — MAY 2001
Number 5, Part 1 (Issued in 2 Parts)

— Founded in 1892 —

ANNALS

OF OTOLOGY, RHINOLOGY & LARYNGOLOGY

Official Organ of the
AMERICAN LARYNGOLOGICAL ASSOCIATION
AMERICAN BRONCHO-ESOPHAGOLOGICAL ASSOCIATION

PRESENCE OF AUTOANTIBODIES IN THE SERA OF MENIERE'S DISEASE

DURATION OF STENTING IN SINGLE-STAGE ARYNGOTRACHEAL RECONSTRUCTION WITH ANTERIOR COSTAL CARTILAGE GRAFTS

RITICAL ROLE OF CENTRAL FACILITATION IN THE GLOTTIC CLOSURE REFLEX

PERILYMPHATIC FISTULA AND MENIERE'S DISEASE. CLINICAL SERIES AND LITERATURE REVIEW

BONE CONDUCTION IMPAIRMENT IN CHRONIC EAR DISEASE

HISTOPATHOLOGY OF SUBMANDIBULAR GLANDS REMOVED FOR SIALOLITHIASIS

ANNALS
PUBLISHING CO.

WEB SITE — http://www.Annals.com

CII Bionic Ear™ System

CII BTE™

Platinum Sound Processor™

The high resolution CLARION® CII Bionic Ear™ is a **NEW** generati cochlear implant technology that delivers **MORE SOUN** information for **BETTER HEARING**. Advancements in cochle implant technology over the past twenty years have demonstrat that the ability to provide more sound information to the heari nerve has resulted in increased patient **PERFORMANC** Conventional cochlear implants have been limited in their ability deliver a full or complete sound signal. The CII Bionic Ear System* c deliver sound information to the hearing nerve up to 1,000,000 tim per second through 31 distinct audio processing channels. Spec state-of-the-art safeguard electronics are designed to ensure that t high resolution CII Bionic Ear delivers the **FULL BROADBAN** sound information to the hearing nerve safely and effectively. T system utilizes the latest advances in focusing electrode technolo and powerful miniature sound processor electronics to provi the **HIGHEST FIDELITY** to its users.* To learn more about t possibilities please contact us.

PLEASE VISIT US AT BOOTH 311.

*CAUTION: High Resolution broadband information delivery is limited investigational use only

CLARION

ANNALS OF OTOLOGY, RHINOLOGY & LARYNGOLOGY

VOLUME 110 MAY 2001 NUMBER 5

CONTENTS

PART 1

FROM THE AMERICAN LARYNGOLOGICAL ASSOCIATION

Transforming Growth Factor and Neutralizing Antibodies in Subglottic Stenosis
David G. Dillard, MD; Anthony A. Gal, MD; Jesse Roman-Rodriguez, MD;
Stephen White, MD; Ian N. Jacobs, MD 393

Critical Role of Central Facilitation in the Glottic Closure Reflex
Clarence T. Sasaki, MD; Steven Ho, MD; Young-Ho Kim, MD 401

Assessment of Posterior Cricoarytenoid Botulinum Toxin Injections in Patients With Abductor Spasmodic Dysphonia
Steven Bielamowicz, MD; Shrita Squire; Kimberly Bidus, MS; Christy L. Ludlow, PhD 406

FROM THE AMERICAN BRONCHO-ESOPHAGOLOGICAL ASSOCIATION

Duration of Stenting in Single-Stage Laryngotracheal Reconstruction With Anterior Costal Cartilage Grafts
Benjamin E. J. Hartley, MBBS, FRCS; L. Mark Gustafson, MD; James H. Liu, MD;
Christopher J. Hartnick, MD; Robin T. Cotton, MD 413

Fine Structure of the Human Newborn and Infant Vocal Fold Mucosae
Kiminori Sato, MD, PhD; Minoru Hirano, MD; Tadashi Nakashima, MD 417

INDEPENDENT CONTRIBUTIONS

Presence of Autoantibodies in the Sera of Meniere's Disease
T. J. Yoo, MD, PhD; John Shea, Jr, MD; Xianxi Ge, MD; Soon Seog Kwon, MD, PhD;
Yoshiro Yazawa, MD, PhD; Osman Sener, MD; Francesco Mora; Renzo Mora;
Massimilliano Mora; Marco Barbieri, MD; Xiaoping Du 425

Perilymphatic Fistula and Meniere's Disease. Clinical Series and Literature Review
Dennis C. Fitzgerald, MD 430

Bone Conduction Impairment in Chronic Ear Disease
Christopher J. Linstrom, MD; Carol A. Silverman, PhD; Arie Rosen, MD;
Lawrence Z. Meiteles, MD 437

Detection of Intracytoplasmic Cytokines by Flow Cytometry in Adenoids and Peripheral Blood Lymphocytes of Children
Joel M. Bernstein, MD, PhD; Mark Ballow, MD; Gary Rich 442

Immunopathologic Study of Chronic Sinusitis: A Proposal for Atopic and Non-Atopic IgE-Activated Mast Cell Allergic Inflammation
Lawrence S. Loesel, MD 447

Ludwig's Angina: Report of a Case and Review of Management Issues
Michael S. Barakate, BSc(Med), MBBS; Michael J. Jensen, FRACS, FACS;
Jonathan M. Hemli, MBBS(Hons); Antony R. Graham, FRACS, FRCS(Eng) 453

Effect of Macrolides on the Expression of HLA-DR and Costimulatory Molecules on Antigen-Presenting Cells in Nasal Polyps
Yukiko Iino, MD, PhD; Yukako Sasaki, MD; Chie Kojima, MD, PhD;
Tetsuo Miyazawa, MD 457

Histopathology of Submandibular Glands Removed for Sialolithiasis
Francis Marchal, MD; Anne-Marie Kurt, MD; Pavel Dulguerov, MD;
Minerva Becker, MD; Michaela Oedman, BS; Willy Lehmann, MD 464

Characterization of the Medial Surface of the Vocal Folds
David A. Berry, PhD; Martyn J. O. Clark, MS; Douglas W. Montequin, MA;
Ingo R. Titze, PhD 470

Mass Loading on the Ossicles and Middle Ear Function
Rong Z. Gan, PhD; Robert K. Dyer, MD; Mark W. Wood, MD; Kenneth J. Dormer, PhD 478

Volume of Mastoid Pneumatization: Three-Dimensional Reconstruction With Ultrahigh-Resolution Computed Tomography
Michal Luntz, MD; Shelton Malatskey, MD; Mark Tan, MD; Elisha Bar-Meir, MD;
David Ruimi, PhD 486

IMAGING CASE STUDY OF THE MONTH

Petrous Internal Carotid Artery Pseudoaneurysm Due to Gunshot Injury
Juha-Pekka Vasama, MD; Hans Ramsay, MD; Antti Markkola, MD 491

MISCELLANEOUS

Letter to the Editor 494
Book Review 494
Information for Subscribers 1a
Index to Advertisers 10a

PART 2

Analysis of the Suprabullar and Retrobullar Recesses for Endoscopic Sinus Surgery
William E. Bolger, MD; LCDR Christopher B. Mawn, MC, USN .... Supplement 186

Ann Otol Rhinol Laryngol 110:2001

TRANSFORMING GROWTH FACTOR AND NEUTRALIZING ANTIBODIES IN SUBGLOTTIC STENOSIS

DAVID G. DILLARD, MD
ATLANTA, GEORGIA

ANTHONY A. GAL, MD
ATLANTA, GEORGIA

JESSE ROMAN-RODRIGUEZ, MD
ATLANTA, GEORGIA

STEPHEN WHITE, MD
ATLANTA, GEORGIA

IAN N. JACOBS, MD
PHILADELPHIA, PENNSYLVANIA

Transforming growth factor beta 1 (TGF-β1), which is implicated in the pathogenesis of fibrotic diseases such as interstitial fibrosis, may be associated with subglottic stenosis. To study this hypothesis, we measured TGF-β1 expression sequentially in 28 rats after posterior cricoid injury, using both standard immunohistochemistry and reverse transcriptase–polymerase chain reaction. In addition, an osmotic pump infused TGF-β1 in 18 rats, normal saline solution in 9 rats, and neutralizing antibodies in 9 rats. Specimens were stained for fibronectin and procollagen at 1, 7, and 21 days and underwent optical density analysis. In the injured airway, TGF-β1 expression peaked at 1 day and returned to baseline by 21 days. The TGF-β1 infusion led to an increase in the expression of extracellular matrix proteins relative to controls. In contrast, neutralizing antibodies led to a decrease in extracellular matrix protein expression. These findings suggest that TGF-β1 may possibly play a role in the pathogenesis of subglottic stenosis.

KEY WORDS — subglottic stenosis, transforming growth factor beta 1.

INTRODUCTION

Endotracheal intubation for long-term ventilatory support has been responsible for the survival of premature infants smaller than those surviving heretofore. Acquired subglottic stenosis occurs in a small percentage (1% to 9%) of premature infants who require long-term ventilatory support.[1-4] Endotracheal tube injury to the mucosal surface of the airway may result in cartilage exposure and subsequent chondritis, which leads to submucosal gland proliferation, cartilage necrosis, abnormal collagen expression, and increased scar formation.[5,6] Scar tissue will narrow the subglottic airway, resulting in airway compromise.

Wound repair involves complex interactions among epidermal cells, monocytes, fibroblasts, cytokines, enzymes, and extracellular matrix (ECM) proteins such as fibronectin and procollagen. Polypeptide growth factors regulate wound healing on a molecular and cellular level and cause target cells to either replicate or migrate. Growth factors activate target cells by binding to high-affinity cell surface receptors, and the activation leads to an enzymatic cascade resulting in cell replication or migration.[7]

Polypeptide growth factors can be categorized into 6 major families based on their type of activity. These include epidermal growth factors, fibroblast growth factors, platelet-derived growth factors, insulin-like growth factors, interleukins, and transforming growth factor beta (TGF-β).[7] There is substantial evidence to indicate that TGF-β is an essential multifunctional mediator of scar tissue formation, as it promotes monocyte infiltration, fibroblast proliferation, and ECM expression.[8] Increased production of TGF-β has been associated with normal and pathological repair processes, such as interstitial pulmonary fibrosis and glomerulonephritis.[9,10] TGF-β is produced by platelets and macrophages. TGF-β exists as 3 distinct subtypes in humans and most mammals: TGF-β1, TGF-β2, and TGF-β3. TGF-β1 is the predominant form in humans. TGF-β is a protein made up of 2 identical polypeptide chains. The precursor form contains an N-terminal segment, which is cleaved off in an acidic environment.[11,12]

Although it has not been studied extensively in

From the Departments of Otolaryngology (Dillard, White), Pathology (Gal), and Medicine (Roman-Rodriguez), Atlanta Veterans Administration Medical Center and Emory University School of Medicine, Atlanta, Georgia, and the Division of Pediatric Otolaryngology, The Children's Hospital of Philadelphia and University of Pennsylvania School of Medicine, Philadelphia, Pennsylvania (Jacobs). This study was performed in accordance with the PHS Policy on Humane Care and Use of Laboratory Animals, the NIH *Guide for the Care and Use of Laboratory Animals,* and the Animal Welfare Act (7 U.S.C. et seq.); the animal use protocol was approved by the Institutional Animal Care and Use Committee (IACUC) of Emory University.

Presented at the meeting of the American Laryngological Association, Palm Desert, California, April 24-25, 1999. This project was funded by a grant from the American Laryngological Association.

CORRESPONDENCE — Ian N. Jacobs, MD, Division of Pediatric Otolaryngology, The Children's Hospital of Philadelphia, 34th St and Civic Center Blvd, First Floor, Wood Center, Philadelphia, PA 19104.

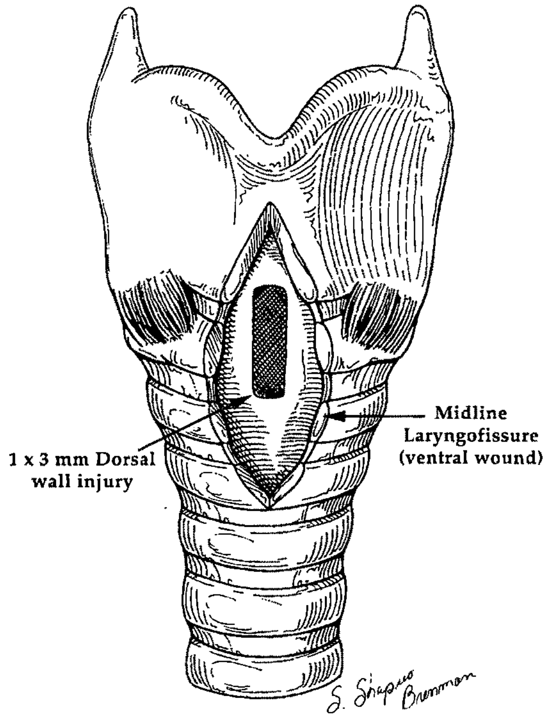

Fig 1. Ventral laryngofissure in rat larynx shows dorsal wall injury (1 × 3-mm area). Osmotic infusion pump was implanted at laryngofissure site.

the airway, numerous experimental studies have suggested that TGF-β1 is a potent mediator of scar tissue formation in other organ systems. For example, exogenous administration of TGF-β1 increases ECM formation.[8] Furthermore, fetal wounds, which heal in a "scarless" manner, have a deficiency of TGF-β1 relative to adult wounds. Addition of TGF-β1 to fetal wounds induces scar tissue formation.[13-15] This may reflect differences that exist at the tissue receptor level during development. To better understand the role of TGF-β1 in subglottic stenosis, we studied the expression of endogenous TGF-β1 in wounded rat laryngotracheal airways and the effect of exogenous administration of TGF-β1 on healing airway wounds of rats.

MATERIALS AND METHODS

This study was completed in 2 parts. The first was the immunohistochemical detection of TGF-β1 in injured and uninjured rat larynges. The second was the measurement of ECM proteins after exogenous administration of TGF-β1 and neutralizing antibodies to TGF-β1 to the injured rat airway. The ECM proteins were used as markers of scar tissue formation in this model. Our techniques were as follows.

Laryngeal Injury Technique. Adult male Sprague-Dawley rats (450 to 600 g) were anesthetized with methoxyflurane by inhalation and then ketamine hydrochloride 87 mg/kg and xylazine hydrochloride 13 mg/kg by intraperitoneal injection. The rats then underwent a midline laryngofissure to expose the larynx and the posterior wall of the cricoid cartilage as follows. In a sterile fashion, a transverse cervical incision was made and the laryngotracheal complex was exposed with sharp dissection. The lower third of the thyroid cartilage, the cricoid cartilage, and the first 2 tracheal rings were divided with a midline longitudinal incision. A rectangular area (1 × 3 mm) of mucosa, submucosa, and perichondrium was removed from the posterior luminal wall of the cricoid cartilage under the microscope with a microsurgical blade and an otologic microscopic Tabb knife (Fig 1). The laryngofissure incision was then closed, and the rats were allowed to recover.

Twenty-eight injured rats and 4 normal control rats were euthanized by lethal injection of 100 mg/kg of pentobarbital sodium. Four rats were sacrificed at each time period (0, 1, 2, 4, 7, 14, and 21 days after injury). Their larynges were harvested, sectioned, and fixed in formalin for at least 24 hours. They were embedded in paraffin blocks by standard histologic techniques. Five-micron-thick sections were cut on a microtome. Cross sections were cut from the midpoint of the injury. The sections were placed on slides and underwent immunohistochemical staining for latent TGF-β1 by standard immunohistochemical techniques as outlined by Hsu et al.[16] Polyclonal rabbit anti–TGF-β1 LC (1 through 30) antibodies were used at a 1:72 dilution. Anti–TGF-β1 LC has a high binding affinity to amino acids 1 through 10 and 21 through 30 of the N-terminal end of latent TGF-β1.[17] The antibodies were a generous gift of Dr Kathleen Flanders, National Institutes of Health.

Osmotic Pump Infusion of TGF-β1 and Neutralizing Antibodies. Thirty-six additional rats, which underwent the same posterior cricoid wall injury, underwent implantation of an Alzet osmotic pump device (ALZA Corp, Palo Alto, Calif). Dr S. Hanson of Emory University developed an implantable drug delivery system for continuous infusion. Its performance has been documented previously in an arteriovenous polytetrafluoroethylene (PTFE) fistula model.[18] The osmotic pump delivers drug to the device through silicone tubing that empties into a reservoir and delivers the drug evenly to the attached PTFE membrane and subsequently to the tissue adjacent to the PTFE. The pumps were primed with TGF-β1 at a concentration of 1.25 ng/μL (R & D Systems, Minneapolis, Minn). The device was oriented so that the PTFE strip was adjacent to the ventral wound site and secured with 6.0 Prolene sutures (Ethicon, Somerville, NJ). The pump was buried subcutaneously in the chest. The TGF-β1 was infused continuously at a rate of 10 ng/h for 24 hours. In the control group, the pump delivered phosphate buffered saline solu-

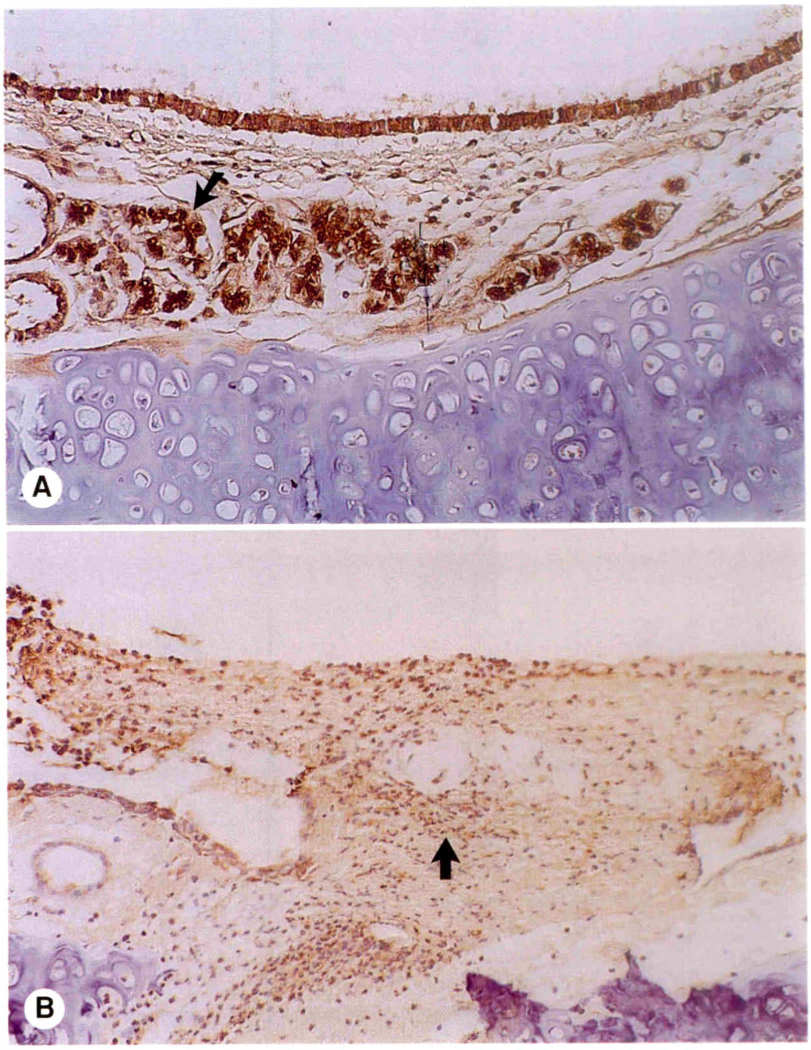

Fig 2. Cross sections stained for latent transforming growth factor beta 1 (TGF-β1; original ×20). **A)** Uninjured rat larynx reveals staining of normal epithelial cells and submucous glands (arrow). **B)** Dorsal wall injury site 1 day after injury shows increased expression of TGF-β1 in fibrocellular matrix (arrow). **(Continued on next page.)**

Calcutta University College of Medicine C.U.
LIBRARY

tion (pH 7.4, 0.1% bovine serum albumin) at the same rate for 24 hours. To ensure that the cytokine reached the intraluminal larynx, we closed the ventral laryngofissure site loosely, leaving a small gap. Another 9 rats underwent osmotic pump implantation in identical fashion, but with infusion of chicken anti-human neutralizing antibodies to TGF-β1 at 2 μg/h (R & D Systems). Six rats were sacrificed at each of 3 time periods (1, 7, and 21 days) for the TGF-β1 group, and 3 at each time period for the blocking antibody group and control group. The rats were all humanely euthanized by lethal injection of 100 mg/kg of pentobarbital sodium.

Tissue Processing and Immunohistochemistry. The larynges were harvested from all rats, the sutures were removed from the ventral wall to facilitate microscopic processing, and the specimens were fixed in formalin for 24 hours and embedded in paraffin blocks. Five-micron-thick sections were cut on a microtome from the midpoint of the injury. The sections were placed on glass slides and stained for hematoxylin-eosin, fibronectin, and type I procollagen by standard immunohistochemical techniques[16] with the following antibodies and dilutions: 1) mouse anti-human procollagen I carboxy-terminal monoclonal antibody 1:100 (Chemicon International, Inc, Temecula, Calif) and 2) polyclonal rabbit anti-human serum fibronectin 1:50 (Dako, Carpinteria, Calif).

Optical Density Analysis. The tissues were placed on a CAS computer system (Cell Analysis Systems, Inc, Palo Alto). In the region of the ventral and dorsal wounds, 5 high-power (40× magnification) noncontiguous, nonoverlapping fields per animal were measured for optical density of percent staining area and percent staining intensity. These measurements were then averaged. Regions from the cricoid ring, which were uninjured, were also measured and averaged. The average measurements for the percent staining intensity and area for the injured regions were divided by the same measurements for uninjured regions within that specimen. This provided an internal control for background staining intensity and provided an index of injured to uninjured region staining.

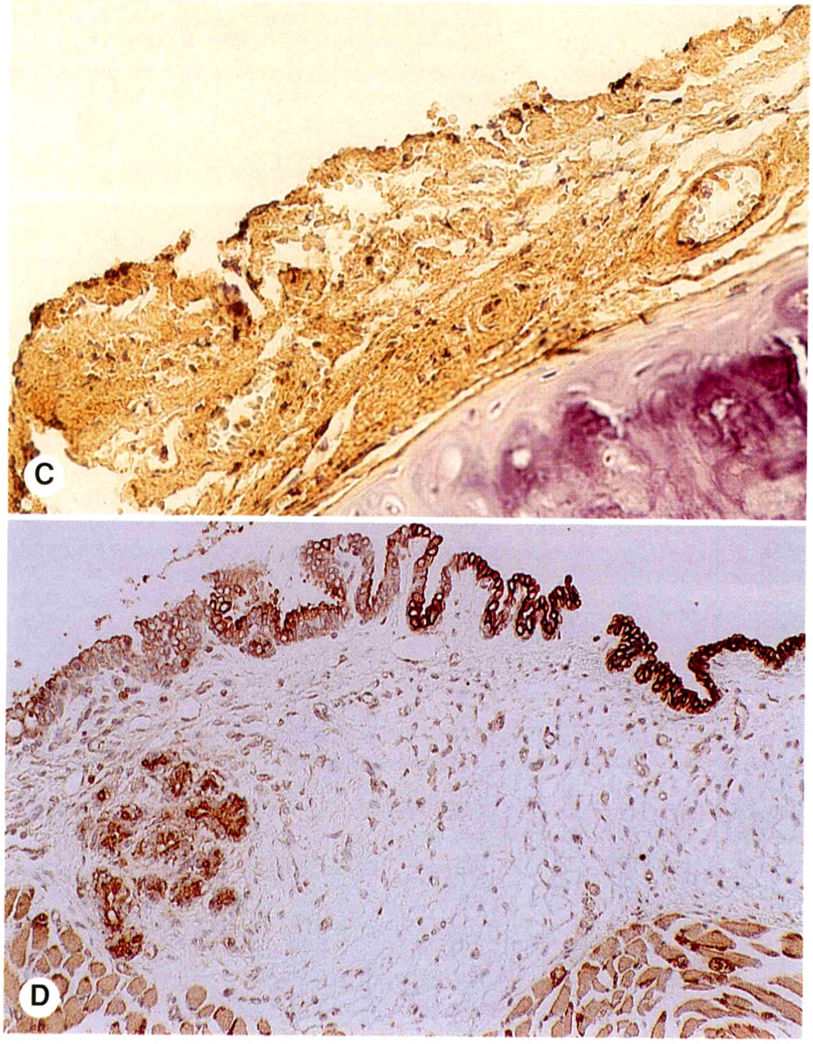

Fig 2, continued. C) Dorsal wall injury site 2 days after injury reveals highest intensity of staining. **D)** Dorsal wall of injured rat larynx 21 days after injury shows baseline staining and reepithelialization.

Reverse Transcriptase–Polymerase Chain Reaction. The RNA was extracted from the tissue of 3 saline infusion control samples at 0.5, 1, 7, and 21 days. The procedure for quantitative bioluminescent detection of TGF-β1 messenger RNA (mRNA) was performed as previously described.[19,20] Comparison and standardization were made to the housekeeping gene β-actin.

RESULTS

TGF-β1 Expression. The normal controls showed expression of latent TGF-β1 in the respiratory epithelium and submucosal glands. TGF-β1 was also identified in the endothelial cells of blood vessels. In the injured specimens, increased intensity of TGF-β1 staining was detected in the submucosal fibrocellular matrix near both anterior (laryngofissure) and posterior injury sites. The staining was most intense in the early time periods (1 or 2 days after injury) and returned to the level of the uninjured control specimens by day 21 (Fig 2). The reverse transcriptase–polymerase chain reaction revealed a quantitative peak of TGF-β1 mRNA expression at 1 day, followed by a slight decrease at 7 days and a return to baseline at 21 days (Fig 3).

TGF-β1 Infusion. By histologic analysis, all TGF-β infusion specimens revealed a marked increase in fibrosis and inflammation relative to the saline infusion control specimens (Fig 4). The immunohistochemical staining for cellular fibronectin and type I procollagen revealed an increase in expression at 1, 7, and 21 days relative to controls (Fig 5). The optical density analysis verified these findings. There was a significant inflammatory response to the infusion device, but the response in the specimens with TGF-β1 infusion far exceeded that in the controls.

Anti–TGF-β1 Neutralizing Antibodies. The infusion of neutralizing antibodies to TGF-β1 resulted in a decrease in the intensity of fibronectin and type I procollagen staining at the laryngofissure site relative to the saline infusion control and the posterior wound (internal control specimens). The optical density analysis revealed a significant decrease in the expression of fibronectin and type I procollagen at 1 and 7 days (Fig 6).

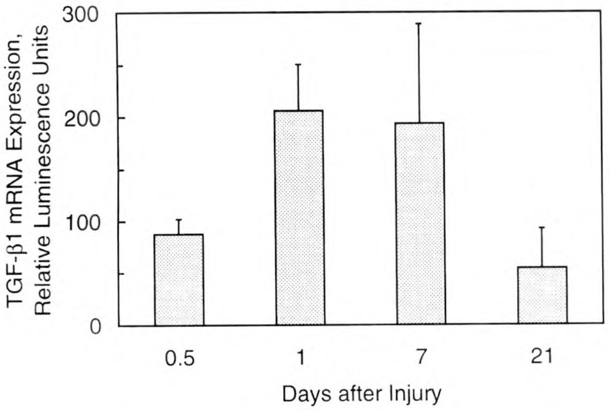

Fig 3. Tracheal tissue samples were obtained from ventral laryngofissure site at 0.5 (12 hours), 1, 7, and 21 days after injury in saline infusion controls and were processed for reverse transcriptase–polymerase chain reaction to detect TGF-β1 messenger RNA (mRNA). Ventral laryngofissure site of saline infusion had increase in TGF-β1 mRNA expression at days 1 and 7, followed by decrease to baseline levels at day 21.

DISCUSSION

We chose to study TGF-β1 in the larynx because of its potent role as a mediator of fibrosis and scarring in other organ systems. Moreover, blockade of TGF-β1 activity may reduce scarring. There are several ways to block TGF-β1 activity, including neutralizing antibodies, blockade at the receptor level, down-regulation of TGF-β1 mRNA expression, and the blockade of some other by-product of the cytokine. Shah et al[21] were successful at decreasing fibrosis in cutaneous wounds by blockade of TGF-β1 activity with neutralizing antibodies to TGF-β1, as well as down-regulation with TGF-β3. TGF-β3 may competitively inhibit TGF-β1 expression. Furthermore, TGF-β1 is largely absent in fetal wounds, which heal in a scarless manner.

This study demonstrated a potential role for TGF-β1 in the evolution of subglottic stenosis. The latent precursor form of TGF-β1 was found initially in epithelial and endothelial cells of the larynx, as well as the submucosal glands, and increased in the early period after injury. TGF-β1 then returned to baseline levels after active healing was complete (21 days). The absolute production of TGF-β1, as reflected by the increase in TGF-β1 mRNA levels within 24 hours after injury, increased and then returned to baseline. This finding is supported by the observations of Kane et al,[22] who studied TGF-β1 expression in human and porcine cutaneous wounds. They found that inactive TGF-β1 is present in all suprabasal keratinocytes of normal human skin. Five minutes after injury, activated TGF-β1 is rapidly induced in the epidermis and progresses outward from the site of injury. As wound healing resolves, the active TGF-β1 disappears, but the inactive form remains. This pattern reflects rapid activation by the local wound environment after injury.[22]

Nevertheless, TGF-β1, as a single cytokine, is part of a large, complex system. There are other, poorly understood factors and complex interactions that control the healing process and deserve further study. Moreover, in order to elucidate more of these interactions, we need to rectify several major shortcomings of this model in future studies. The most important is the qualitative nature of immunohistochemical detection of cytokines, which needs to be backed up with quantitative data. Nevertheless, the stains

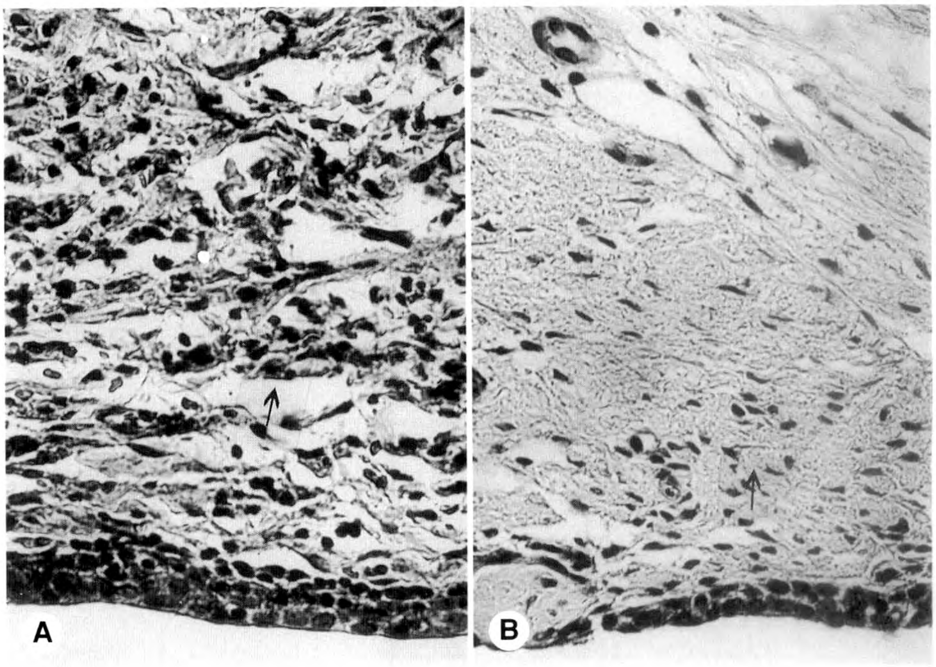

Fig 4. Luminal epithelial surface of ventral laryngofissure site near infusion pump at 7 days after injury (H & E, original ×50). **A)** TGF-β1 infusion. Arrow points to submucosa of ventral laryngofissure site with increase in fibrosis and with inflammatory cell infiltration. **B)** Normal saline control shows less inflammation and less inflammatory cell infiltration (arrow).

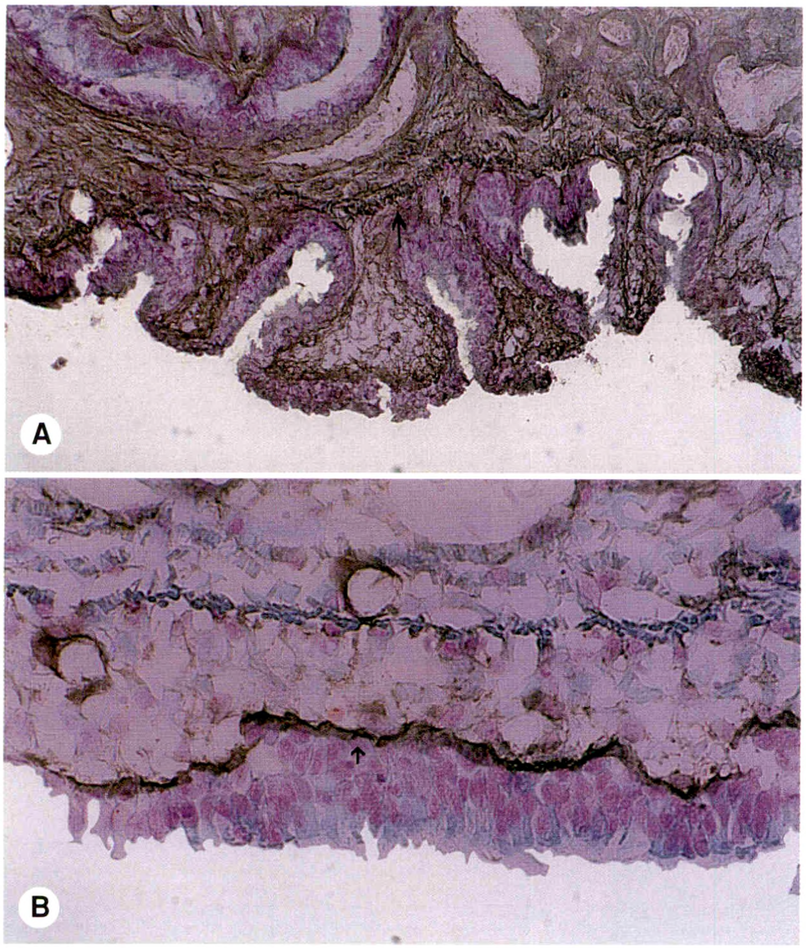

Fig 5. Immunohistochemical stain for fibronectin 7 days after surgery (original ×50). **A)** TGF-β1 infusion at ventral site reveals highest intensity of fibronectin staining (arrow) with increased submucosal glands and fibrosis consistent with early subglottic stenosis. **B)** Normal saline infusion (ventral site) reveals less intense fibronectin staining (arrow) and less inflammation.

were quite consistent, and optical density analysis quantified the immunohistochemical results.

Second, the osmotic pump itself induces a significant background inflammatory response and therefore is not intended to become a useful delivery system for clinical use. The biological activity of growth factors such as TGF-β1 is determined by dose, timing of delivery, and local environmental factors. The osmotic pump was used to test the in vitro biological activity of TGF-β1 in the airway at a concentration used by Shah et al[21] in cutaneous wound healing. It appears that TGF-β1 is critical in the very early phases of wound healing at concentrations similar to those in skin wounds in rats.

A more optimal delivery system for potential clinical use might include direct injection, coated endo-

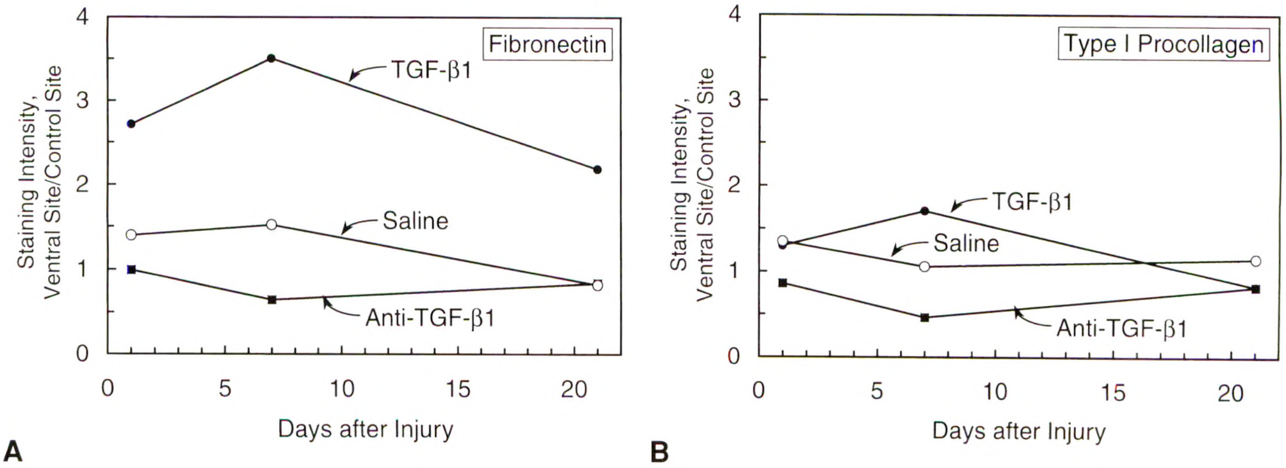

Fig 6. Computerized analyses show ratios of staining intensity in ventral injury site to that in internal control site for infusions of TGF-β1, normal saline solution, and neutralizing antibodies at 1, 7, and 21 days. **A)** Fibronectin. **B)** Type I procollagen.

tracheal tubes, or direct gene transfer. Gene transduction perhaps may allow for the continuous delivery of growth factors during the critical phases of healing. For instance, adenovirus-mediated transduction of laryngotracheal tissue would result in gene expression for relatively short periods of time (7 to 10 days).[23] The expression of the cytokine would be temporary and promote down-regulation of fibrosis during the critical phases of wound healing. Needless to say, there are potential problems, such as the background inflammatory response, even with short periods of transduction, and these problems need to be worked out.

A third limitation of our animal model study was the fact that the degree of stenosis or scar tissue formation was quite minimal. Most of the animals survived the experiments without distress. A more substantial injury, such as the result of topical application of sodium hydroxide, would result in a more severe grade of stenosis and thus a better "signal-to-noise" ratio for studying the effects of cytokines on wound healing.

Nevertheless, the study demonstrated a potential role for TGF-β1 in laryngeal wound healing in an animal model. We found that TGF-β1 is expressed early during the course of laryngeal wound healing and returns to baseline levels within 21 days. We also found that TGF-β1, which leads to fibrosis in several organ systems, is capable of enhancing scar tissue formation in the subglottic airway. Potential "antiscarring" strategies may involve blockade of TGF-β1 activity. Further study is necessary to clarify the exact role of TGF-β1 in human subglottic stenosis and in wound healing in general. Future studies will involve staining for activated TGF-β1 in specimens from human larynges that are actively developing subglottic stenosis.

CONCLUSIONS

1. Endogenous TGF-β1 was detected in the epithelial cells and submucosal glands of normal rat larynges.
2. Endogenous TGF-β1 expression increased in early time periods after an injury to the subglottic airway and returned to baseline within 21 days, as documented by immunohistochemistry and reverse transcriptase–polymerase chain reaction.
3. Infusion of exogenous TGF-β1 led to an increase in the expression of ECM proteins and to inflammatory changes in the airway consistent with early subglottic stenosis.
4. Infusion of neutralizing antibodies led to a decrease in the expression of ECM proteins that was specific for the ventral infusion site.
5. Further study is needed to elucidate the role of TGF-β1 and its complex interactions in normal and pathological wound healing in the airway.

ACKNOWLEDGMENTS — We are grateful for the technical assistance of J. David Rackley, BSE, and for the generous donation of anti–TGF-β1 antibodies by Dr Kathleen Flanders from the National Institutes of Health.

REFERENCES

1. Parkin JL, Stevens MH, Jung AL. Acquired and congenital subglottic stenosis in the infant. Ann Otol Rhinol Laryngol 1976;85:573-81.

2. Papsidero MJ, Pashley NRT. Acquired stenosis of the upper airway in neonates. An increasing problem. Ann Otol Rhinol Laryngol 1980;89:512-4.

3. Sherman JM, Lowitt S, Stephenson C, Ironson G. Factors influencing acquired subglottic stenosis in infants. J Pediatr 1986;109:322-7.

4. Orlowski JP, Ellis NG, Amin NP, Crumrine RS. Complications of airway intrusion in 100 consecutive cases in a pediatric ICU. Crit Care Med 1980;8:324-31.

5. Alexander KJ, Schuller DE. Ferret model for acquired subglottic stenosis. Ann Otol Rhinol Laryngol 1989;98:910-5.

6. Whited RE. A prospective study of laryngotracheal sequelae in long-term intubation. Laryngoscope 1984;94:367-77.

7. Hom DB. Growth factors in wound healing. Otolaryngol Clin North Am 1995;28:933-53.

8. Roberts AB, Sporn MB, Assoian RK, et al. Transforming growth factor type beta: rapid induction of fibrosis and angiogenesis in vivo and stimulation of collagen formation in vitro. Proc Natl Acad Sci USA 1986;83:4167-71.

9. Border WA, Okuda S, Languino LR, Sporn MB, Ruoslahti E. Suppression of experimental glomerulonephritis by antiserum against transforming growth factor β1. Nature 1990;346:371-4.

10. Broekelmann TJ, Limper AH, Colby TV, McDonald JA. Transforming growth factor β1 is present at sites of extracellular matrix gene expression in human pulmonary fibrosis. Proc Natl Acad Sci USA 1991;88:6642-6.

11. Graycar JL, Miller DA, Arrick BA, Lyons RM, Moses HL, Derynck R. Human transforming growth factor-β3: recombinant expression, purification, and biological activities in comparison with transforming growth factors-β1 and β2. Mol Endocrinol 1989;3:1977-86.

12. Roberts AB, Sporn MB. The transforming growth factors. In: Sporn MB, Roberts AB, eds. Peptide growth factors and their receptors. Berlin, Germany: Springer Verlag, 1990:419-72.

13. Sullivan KM, Lorenz HP, Meuli M, Lin RY, Adzick NS. A model of scarless human fetal wound repair is deficient in transforming growth factor beta. J Pediatr Surg 1995;30:198-203.

14. Krummel TM, Michna BA, Thomas BL, et al. Transforming growth factor beta (TGF-β) induces fibrosis in a fetal wound model. J Pediatr Surg 1988;23:647-52.

15. Lin RY, Sullivan KM, Argenta PA, Meuli M, Lorenz HP,

Adzick NS. Exogenous transforming growth factor–beta amplifies its own expression and induces scar formation in a model of human fetal skin repair. Ann Surg 1995;222:146-54.

16. Hsu SM, Raine L, Fanger H. Use of avidin-biotin-peroxidase complex (ABC) in immunoperoxidase techniques: a comparison between ABC and unlabeled antibody (PAP) procedures. J Histochem Cytochem 1981;29:577-80.

17. Flanders KC, Thompson NL, Cissel DS, et al. Transforming growth factor-β1: histochemical localization with antibodies to different epitopes. J Cell Biol 1989;108:653-60.

18. Chen C, Ku DN, Kikeri D, Lumsden AB. Tenascin: a potential role in human arteriovenous PTFE graft failure. J Surg Res 1996;60:409-16.

19. Svetic A, Finkelman FD, Jian YC, et al. Cytokine gene expression after in vivo primary immunization with goat antibody to mouse IgD antibody. J Immunol 1991;147:2391-7.

20. Wynn TA, Eltoum I, Cheever AW, Lewis FA, Gause WC, Sher A. Analysis of cytokine mRNA expression during primary granuloma formation induced by eggs of *Schistosoma mansoni*. J Immunol 1993;151:1430-40.

21. Shah M, Foreman DM, Ferguson MWJ. Neutralisation of TGF-β1 and TGF-β2 or exogenous administration of TGF-β3 to cutaneous rat wounds reduces scarring. J Cell Sci 1995; 108:985-1002.

22. Kane CJM, Hebda PA, Mansbridge JN, Hanawalt PC. Direct evidence for spatial and temporal regulation of transforming growth factor β1 expression during cutaneous wound healing. J Cell Physiol 1991;148:157-73.

23. Sylvester KG, Yang EY, Cass DL, Crombleholme TM, Adzick NS. Fetoscopic gene therapy for congenital lung disease. J Pediatr Surg 1997;32:964-9.

Ann Otol Rhinol Laryngol 110:2001

CRITICAL ROLE OF CENTRAL FACILITATION IN THE GLOTTIC CLOSURE REFLEX

CLARENCE T. SASAKI, MD

STEVEN HO, MD

YOUNG-HO KIM, MD

NEW HAVEN, CONNECTICUT

The sphincteric function of the larynx, essential to lower airway protection, is most efficiently achieved through strong reflex adduction by both vocal cords. We hypothesize that central facilitation is an essential component of a bilateral adductor reflex and that its disturbance could result in weakened sphincteric closure. Six adult 50-kg pigs underwent evoked response laryngeal electromyography under 0.5 to 1.0 minimal alveolar concentration (MAC) isoflurane anesthesia. The internal branch of the superior laryngeal nerve was stimulated through bipolar platinum-iridium electrodes, and recording electrodes were positioned in the ipsilateral and contralateral thyroarytenoid muscles. Consistent threshold responses were obtained ipsilaterally from 0.5 to 1.0 MAC anesthesia. However, the contralateral reflex responses approached 0% in successive trials as anesthetic levels approached 1.0 MAC. Alteration of central facilitation by deepening anesthesia abolishes the crossed adductor reflex, predisposing to a weakened glottic closure response. A precise understanding of this effect may improve the prevention of aspiration in patients emerging from prolonged sedation or under heavy psychotropic control.

KEY WORDS — anesthesia, aspiration, central facilitation, glottic closure reflex, laryngeal sphincter.

INTRODUCTION

The most important and basic function of the larynx is to provide sphincteric protection of the lower airway, which is most efficiently achieved by simultaneous adduction of both vocal cords. Such action serves to close the glottis by involving the activation of both thyroarytenoid muscles, among other groups of adductors. In this regard, reflexive glottic closure is reliably elicited by stimulating the internal branch of the superior laryngeal nerve (iSLN).

Three categories of protective laryngeal responses have been observed after stimulation of one iSLN. First, an early response involves adduction of the *ipsilateral* vocal cord with a latency of approximately 10 to 18 ms in anesthetized cats,[1] dogs,[1] and pigs.[2] This short-latency R1 evoked response has also been consistently noted in anesthetized humans.[1] A second category of short-latency evoked R1 response involves simultaneous *contralateral* adduction, also known as the crossed adductor reflex. Although this crossed response with a latency of 10 to 18 ms has been found to be consistently present in anesthetized cats, it is less consistently found in dogs and is rarely observed in anesthetized human subjects.[1] Still a third category of adductor response involving a longer-latency reflex, termed R2, has been observed to produce bilateral vocal cord responses, but its presence appears to be most readily noted in awake human subjects; it has a latency of 50 to 80 ms.[3]

TABLE 1. LEFT iSLN STIMULATION

	Minimal Alveolar Concentration				
	<0.5	*0.5*	*0.75*	*1.0*	*>1.0*
Ipsilateral R1					
Efficiency	9/9 (100%)	12/12 (100%)	18/18 (100%)	15/15 (100%)	20/20 (100%)
Latency (ms; average ± 1 SD)	14.7 ± 1.3	15.2 ± 0.2	15.0 ± 1.1	17.7 ± 2.3	17.0 ± 1.3
Contralateral R1					
Efficiency	9/9 (100%)	12/12 (100%)	12/18 (67%)	3/15 (20%)	0/20 (0%)
Latency (ms; average ± 1 SD)	14.7 ± 1.3	15.4 ± 0.8	15.7 ± 0.8	18.2 ± 0.7	

iSLN — internal branch of superior laryngeal nerve.

From the Section of Otolaryngology, Department of Surgery, Yale University School of Medicine, New Haven, Connecticut. Supported in part by the Charles W. Ohse Endowment and the Christopher McFadden Endowment. This study was performed in accordance with the PHS Policy on Humane Care and Use of Laboratory Animals, the NIH *Guide for the Care and Use of Laboratory Animals*, and the Animal Welfare Act (7 U.S.C. et seq.); the animal use protocol was approved by the Institutional Animal Care and Use Committee (IACUC) of Yale University School of Medicine (protocol 99-07921).

Presented at the meeting of the American Laryngological Association, Orlando, Florida, May 13-14, 2000.

CORRESPONDENCE — Clarence T. Sasaki, MD, Section of Otolaryngology, Dept of Surgery, Yale University School of Medicine, 333 Cedar St, PO Box 208041, New Haven, CT 06520-8041.

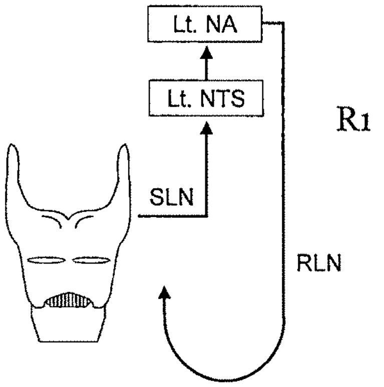

Fig 1. Ipsilateral R1 reflex. Lt. NA — left nucleus ambiguus; Lt. NTS — left nucleus tractus solitarius; SLN — superior laryngeal nerve; RLN — recurrent laryngeal nerve.

From these observations, we note that prior studies conducted in fully anesthetized dogs, pigs, and humans failed to consistently demonstrate the presence of either the crossed R1 or the R2 adductor reflex. Despite species differences, the presence of crossed reflexes in awake non-anesthetized human subjects suggests the possibility that the crossed evoked response may be anesthesia-dependent.

In the present study, we attempted to examine crossed adductor reflexes by electromyographic (EMG) recordings from the thyroarytenoid muscles under various levels of anesthesia in a pig model. We hypothesized that the crossed reflex represents a facilitated response dependent on supramedullary influences that, when abolished by general anesthesia, also abolishes the crossed response. The presence of central facilitation may be an essential component of a bilateral adductor reflex, and its disturbance could result in conversion to a unilateral reflex response, overall resulting in a weakened sphincteric closure. A precise understanding of this effect may improve the prevention of aspiration in patients at risk while emerging from prolonged sedation[4,5] or while under heavy psychotropic control.[6]

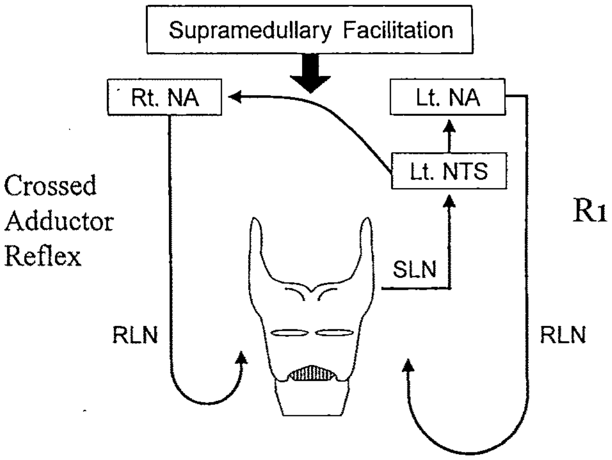

Fig 3. Contralateral R1 reflex under light anesthesia.

MATERIALS AND METHODS:

Six adult Yorkshire male pigs were each studied at 5 different depths of isoflurane anesthesia (<0.5, 0.5, 0.75, 1.0, and >1.0 minimal alveolar concentration [MAC]). The subjects were approximately 5 to 8 months of age, and their weights ranged from 43 to 50 kg (95 to 110 lb). The pig larynx was selected as a model because of its anatomic and physiological similarities to the human larynx.[2,7]

Ketamine hydrochloride (30 mg/kg) and xylazine hydrochloride (5 mg/kg) were administered together intramuscularly as induction agents. Anesthesia was maintained with inhalational isoflurane through a nose cone while each subject maintained spontaneous respiration. A sufficient amount of time was allowed (at least 90 minutes) for the pharmacological effects of the induction agents to clear before initiation of the study protocol. Each subject was exposed to various levels of general anesthesia, with 1 MAC defined as 1.50% inhaled isoflurane concentration.[8] At 1 MAC, periods of electroencephalographic suppression[9] are expected to occur, characterized by an increase in delta wave activity,[10] whereas at 2 MAC, electrical silence is expected to predominate.[9,10] No

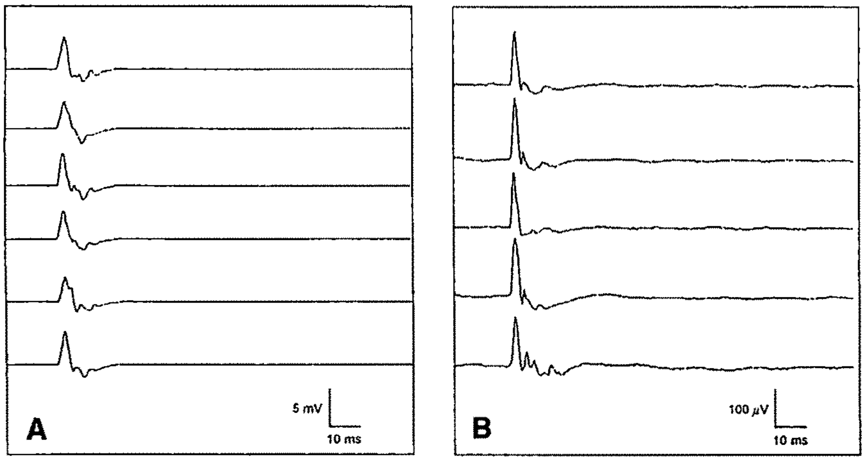

Fig 2. Stimulation of left internal branch of SLN. Compound muscle action potential (CMAP) recordings obtained from ipsilateral thyroarytenoid muscle at **A)** 0.5 minimal alveolar concentration (MAC) and **B)** 1 MAC.

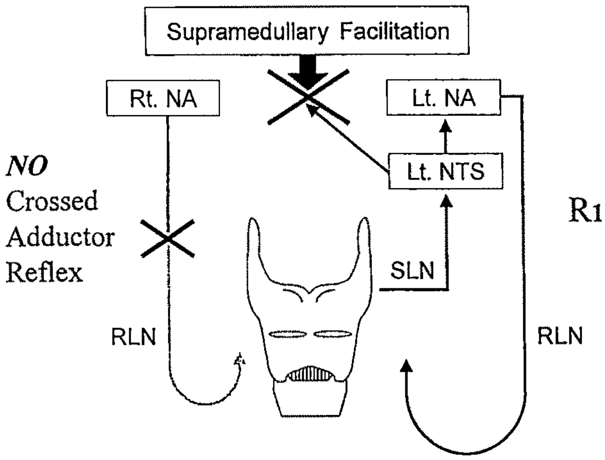

Fig 4. Loss of contralateral R1 reflex under deep anesthesia.

other pharmacological agent was used during the period of data collection. At least 20 minutes of equilibration was allowed after each incremental increase in anesthetic level.

A DataScope was used to monitor the electrocardiogram, respiratory rate, pulse oximetry, and core body temperature. The arterial oxygen saturation was maintained above 95% at all times by adjusting the inhaled oxygen concentration as necessary. The core body temperature was normothermically maintained between 37.8°C and 38.6°C (100°F and 101.5°F) with a heating pad.

After antiseptic preparation and draping of the operative site, a midline neck incision was made extending from the hyoid bone to the sternal notch. Tracheotomy was performed below the fourth tracheal ring, allowing an endotracheal tube (inside diameter, 6 mm) to be inserted into the trachea and secured to the skin. Subsequent inhalational anesthesia was maintained through the tracheotomy. Both the right and left iSLNs were identified. Sufficient thyroid cartilage was removed to allow full access to and visualization of both vocal cords.

TABLE 2. SUMMARY OF LEFT iSLN STIMULATION

	Minimal Alveolar Concentration	
	<1.0	*>1.0*
Ipsilateral R1		
% Efficiency	100 (39/39)	100 (35/35)
Latency (ms; average ± 1 SD)	15.0 ± 0.8	17.2 ± 1.9
Contralateral R1		
% Efficiency	85 (33/39)*	8 (3/35)*
Latency (ms; average ± 1 SD)	15.4 ± 1.1	18.2 ± 0.7

*$p < .01$ (Student's *t*-test).

An XLTEK NeuroMax provided nerve stimulation and EMG recording capability. Bipolar 200-mΩ platinum-iridium stimulating electrodes were applied to the proximal end of each severed iSLN. Monopolar platinum-iridium recording electrodes were inserted into the mid-portion of the thyroarytenoid muscles bilaterally. Reference electrodes were placed in the ipsilateral strap muscles, and a ground electrode was placed in the sternocleidomastoid muscle. Although simultaneous bilateral iSLN stimulation is perhaps more physiologic, sequential unilateral stimulation was used to allow an accurate analysis of the crossed components of the evoked adductor response that would otherwise be obscured by bilateral iSLN stimulation.

With each subject sequentially under various depths of anesthesia as described earlier, the left iSLN was electrically stimulated with a single rectangular pulse of 0.1 mA/0.1 ms. The stimulation intensity was incrementally increased by 0.1 mA until a consistent EMG response was seen in the thyroarytenoid muscle or until a maximum stimulation intensity of 12.0 mA was attained. An average of 6 trials was performed in each experimental paradigm. The procedures were identically repeated on the right side.

RESULTS

The average latencies of the ipsilateral and contra-

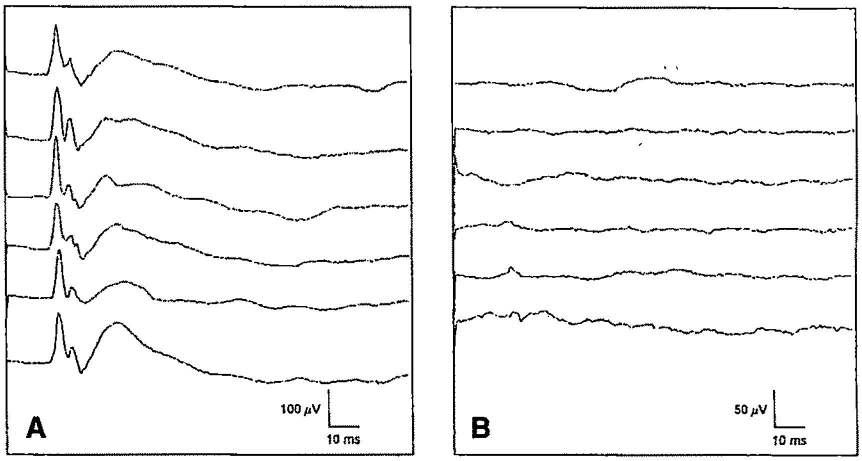

Fig 5. Stimulation of left iSLN. CMAP recordings obtained from contralateral thyroarytenoid muscle at **A)** 0.5 MAC and **B)** 1 MAC.

TABLE 3. RIGHT iSLN STIMULATION

	Minimal Alveolar Concentration				
	<0.5	*0.5*	*0.75*	*1.0*	*>1.0*
Ipsilateral R1					
Efficiency	15/15 (100%)	15/15 (100%)	6/6 (100%)	18/18 (100%)	20/20 (100%)
Latency (ms; average ± 1 SD)	13.3 ± 0.4	13.7 ± 0.8	13.2 ± 1.3	15.0 ± 2.0	17.0 ± 1.3
Contralateral R1					
Efficiency	9/9 (100%)	15/15 (100%)	3/6 (50%)	0/18 (0%)	0/20 (0%)
Latency (ms; average ± 1 SD)	14.9 ± 1.0	13.7 ± 1.0	13.0 ± 0.0		

lateral evoked responses with their standard deviations for left iSLN stimulation are summarized in Table 1. The number of evoked responses compared to the number of stimulus presentations under each level of anesthesia allows us to calculate the percentage of responses achieved within each level of anesthesia. We note that *ipsilateral* R1 evoked responses occur at all depths of anesthesia with 100% efficiency (Figs 1 and 2). However, the number of contralateral R1 responses undergoes a dramatic decline with anesthesia levels over 0.75 MAC. By 1 MAC, only 1 out of 5 stimulations results in *contralateral* R1 evoked responses. Above 1 MAC, no contralateral responses can be elicited (Figs 3-5). When the percentage of contralateral responses obtained below 1.0 MAC is compared to the percentage of responses obtained above 1.0 MAC, the difference is statistically significant ($p < .01$; Table 2). No R2 evoked responses are noted.

The results of right iSLN stimulation are shown in Table 3. Again, the number of contralateral evoked responses undergoes a marked decline with anesthesia levels above 0.75 MAC. No contralateral response can be elicited with anesthesia levels at or above 1 MAC. When the percentage of contralateral responses obtained below 1.0 MAC is compared to the percentage of responses obtained above 1.0 MAC, the difference is again statistically significant ($p < .01$; Table 4).

DISCUSSION

The rationale for our hypothesis is based on the following historical considerations. Prior observations conducted in fully anesthetized dogs, pigs, and humans failed to consistently show a contralateral evoked response. The presence of crossed R1 or R2 adductor reflexes in the awake state suggests that the contralateral reflex may be anesthesia-dependent. The variable observation by Ludlow et al[3] of crossed R1 response in 2 awake human subjects underscores their variable susceptibility to higher-order central control. The pig model appears to support the notion that a facilitated adductor reflex is likely responsible for a crossed R1 response in the awake state, whereas the sensitivity of the crossed R1 response to pharmacological sedation would imply that relevant facilitatory mechanisms are located central to motor neurons of the nucleus ambiguus. Furthermore, that the latencies of ipsilateral and contralateral evoked responses are nearly equal suggests that each circuit involves equivalent numbers of interneurons. As well, the longer latency of the left as compared to the right ipsilateral evoked response understandably reflects the longer course of the left recurrent laryngeal nerve. On the assumptions that nerve conduction velocity approximates 5 cm/ms,[11] that the average length of the neural circuitry from the larynx to the brain stem is 20 cm, and that each synaptic delay is 1.5 ms,[11] the data support the following organizational model (Fig 6). In our model, we propose that the iSLN projects to motor neurons of the nucleus ambiguus

TABLE 4. SUMMARY OF RIGHT iSLN STIMULATION

	Minimal Alveolar Concentration	
	<1.0	*>1.0*
Ipsilateral R1		
% Efficiency	100 (36/36)	100 (38/38)
Latency (ms; average ± 1 SD)	13.5 ± 0.8	14.5 ± 1.7
Contralateral R1		
% Efficiency	90 (27/30)*	0 (0/38)*
Latency (ms; average ± 1 SD)	13.7 ± 1.0	

*p < .01 (Student's *t*-test).

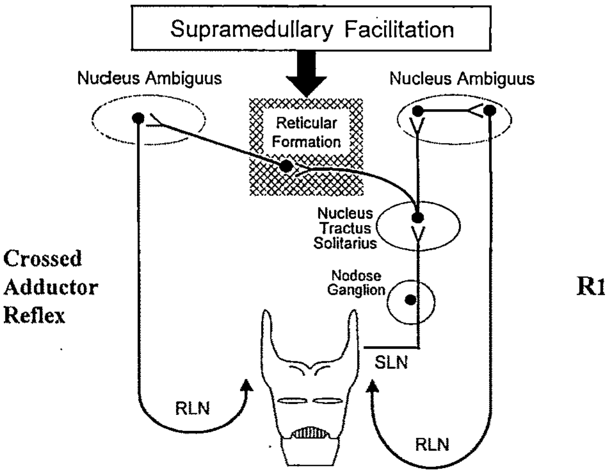

Fig 6. Organizational model of crossed adductor reflex pathway.

through at least 2 synapses: the first, within the ipsilateral nucleus tractus solitarius, and the second, likely within the nucleus ambiguus ipsilaterally and within the reticular formation contralaterally in a manner supported by Sessle's observations.[12]

In summary, whereas a contralateral R1 response is supported by central facilitation in the awake state, anesthetic suppression of facilitative mechanisms restricts the response to an ipsilateral response. Therefore, in the pig model, the anesthesia-dependent loss of the crossed R1 response is expected to weaken the summated closure response even under conditions of physiologic stimulation, in which stimuli are delivered bilaterally and concurrently to each iSLN. Despite the observation that the crossed R1 response appears variably in awake human subjects,[3] its complete suppression under anesthesia may exert a clinically important, but perhaps lesser, effect than would have been observed in the pig model. Pharmacological suppression of supramedullary facilitation offers a unified explanation for several interesting and important clinical findings, including the increased incidence of life-threatening aspiration among sedated patients in an intensive care setting and among institutionalized psychiatric patients under heavy psychotropic control, in whom death from aspiration represents a highly significant risk. The results of this study should provide the neurophysiological basis for preventive measures in high-risk patients and could, for example, alter dosing schedules of psychotropic medications, improve respiratory monitoring, or institute lifesaving dietary modifications. They may also stimulate the search for alternative agents with pharmacological properties that preserve or augment facilitation of the glottic closure response without altering the agents' specific psychotropic or sedative properties.

REFERENCES

1. Sasaki CT, Suzuki M. Laryngeal reflexes in cat, dog, and man. Arch Otolaryngol 1976;102:400-2.
2. Goding GS, Richardson MA, Trachy RE. Laryngeal chemoreflex: anatomic and physiologic study by use of the superior laryngeal nerve in the piglet. Otolaryngol Head Neck Surg 1987;97:28-38.
3. Ludlow CL, Van Pelt F, Koda J. Characteristics of late responses to superior laryngeal nerve stimulation in humans. Ann Otol Rhinol Laryngol 1992;101:127-34.
4. Shifrin RY, Choplin RH. Aspiration in patients in critical care units. Radiol Clin North Am 1996;34:83-96.
5. Vincent MT, Goldman BS. Anaerobic lung infections. Am Fam Physician 1994;49:1815-20.
6. Roy TM, Ossorio MA, Cipolla LM, Fields CL, Snider HL, Anderson WH. Pulmonary complications after tricyclic antidepressant overdose. Chest 1989;96:852-6.
7. Cohen S, Esclamado RM, Telian S, Aloe L, Kileny P. Laryngeal brain stem evoked response in the porcine model. Ann Otol Rhinol Laryngol 1993;102:28-34.
8. Lerman J, Oyston JP, Gallagher TM, Miyasaka K, Volgyesi GA, Burrows FA. The minimum alveolar concentration (MAC) and hemodynamic effects of halothane, isoflurane, and sevoflurane in newborn swine. Anesthesiology 1990;73:717-21.
9. Blitt CD, ed. Monitoring in anesthesia and critical care medicine. 2nd ed. New York, NY: Churchill Livingstone, 1990: 450-1.
10. Drummond JC, Patel PM. Cerebral physiology and the effects of anesthetics and techniques. In: Miller RD, ed. Anesthesia. 5th ed. New York, NY: Churchill Livingstone, 2000:695-733.
11. Waxman SG, ed. Correlative neuroanatomy. 23rd ed. Appleton and Lange, Stamford, Conn: 1996:25-6.
12. Sessle BJ. Excitatory and inhibitory inputs to single neurones in the solitary tract nucleus and adjacent reticular formation. Brain Res 1973;53:319-31.

Ann Otol Rhinol Laryngol 110:2001

ASSESSMENT OF POSTERIOR CRICOARYTENOID BOTULINUM TOXIN INJECTIONS IN PATIENTS WITH ABDUCTOR SPASMODIC DYSPHONIA

STEVEN BIELAMOWICZ, MD
WASHINGTON, DC
KIMBERLY BIDUS, MS
BETHESDA, MARYLAND
SHRITA SQUIRE
BETHESDA, MARYLAND
CHRISTY L. LUDLOW, PHD
BETHESDA, MARYLAND

In this study, we compared 2 techniques for injection of botulinum toxin type A (Botox) into the posterior cricoarytenoid (PCA) muscle for the treatment of abductor spasmodic dysphonia (ABSD). Fifteen patients with ABSD were enrolled in a prospective randomized crossover treatment trial comparing the 2 injection techniques. The PCA muscle was injected with 5 units on each side, with the injections staged 2 weeks apart, via either a percutaneous posterior-lateral approach or a transnasal fiberoptic approach. Eleven patients reported some benefit with the injections; however, the patient-perceived benefits were not related to changes in symptoms on blinded counts by speech pathologists. No significant reductions in the numbers of breathy breaks occurred with either technique, and no differences were found between techniques. Although patients perceived a benefit, blinded symptom counts did not substantiate these benefits. Thus, PCA muscle injections of Botox provided limited benefits to patients with ABSD, demonstrating the need for a more effective therapy for these patients.

KEY WORDS — Botox, botulinum toxin, electromyography, larynx, posterior cricoarytenoid muscle, spasmodic dysphonia, voice.

INTRODUCTION

Abductor spasmodic dysphonia (ABSD) is a rare focal dystonia affecting the larynx, characterized by breathy breaks during prolonged voice production following voiceless consonants and an overall breathy voice quality in some cases.[1,2] Fiberoptic laryngeal examination confirms persistent abduction of the vocal folds during prolonged voiceless consonants. The movement abnormalities may be due to either bursting activity within the posterior cricoarytenoid (PCA) muscle or cricothyroid (CT) muscle or underactivity of the thyroarytenoid (TA) muscle (a negative dystonia).[2] Treatment of ABSD has been aimed at reducing tone in the PCA muscle by means of botulinum toxin type A (Botox) injections, although 1 report found benefit with CT injections in a subgroup of ABSD patients with CT muscle spasms.[2] In contrast with adductor spasmodic dysphonia (ADSD), the symptom response with PCA Botox in patients with ABSD may not be as robust.[3] Explanations for this difference in treatment response include difficulty in placement of the Botox within the PCA muscle, the inability to deliver enough Botox into the PCA muscle due to the risk of airway obstruction, and fundamental differences in the pathophysiology of the 2 types of spasmodic dysphonia.

Patient response to Botox injections into the PCA muscle may depend in part on the accuracy of the injection technique. Two techniques have been employed in this study: the percutaneous posterior-lateral approach described by Blitzer et al[4] and an adaptation of a fiberoptic endoscopic approach described by Rhew et al.[5] Both approaches have potential advantages and disadvantages. The percutaneous approach uses physiological verification to ensure that the toxin is being injected into a muscle active for vocal fold opening during sniffing and for voiceless sound production during speech. The difficulties with this technique are possible discomfort during manual rotation of the larynx and possible pain with needle insertion near the pyriform sinus. This technique also requires considerable experience to accurately detect the PCA activation pattern during speech. On the other hand, the endoscopic technique uses visual verification for PCA insertion. However, some patients find nasoendoscopy with a 5-mm fiberoptic scope uncomfortable, and approximately 50 units of Botox is required to prime the injection catheter, with only a small amount injected and the remainder wasted.

Studies have looked at patient satisfaction with PCA Botox, and the majority of patients perceive a benefit.[2,6] Meleca et al[6] evaluated subjective com-

---

From the Laryngeal and Speech Section, National Institute of Neurological Disorders and Stroke, National Institutes of Health, Bethesda, Maryland. The research was supported by National Institutes of Health Intramural Program Z01 DC 00004.

Presented at the meeting of the American Laryngological Association, Orlando, Florida, May 13-14, 2000.

CORRESPONDENCE — Steven Bielamowicz, MD, Division of Otolaryngology–Head and Neck Surgery, The George Washington University Medical Center, 2150 Pennsylvania Ave NW, Washington, DC 20037.

TABLE 1. DEMOGRAPHICS OF STUDY POPULATION

Subject	*Sex*	*Age at Disease Onset (y)*	*Age at Botox Injection (y)*	*Presence of Tremor*
1	F	24	51	No
2	F	33	38	No
3	F	27	35	No
4	F	43	48	No
5	F	32	47	No
6	F	26	34	No
7	F	29	33	No
8	M	40	62	Yes
9	F	40	48	No
10	F	39	74	Yes
11	M	44	48	No
12	F	35	43	No
13	M	46	60	No
14	F	39	46	No
15	F	22	57	No

fort and technique preference by using either the external posterior-lateral technique or an anterior transcricoid cartilage technique. Regardless of technique, all patients reported benefit, and all preferred the transcricoid technique. While benefit occurred in the majority of patients using a nonblinded subjective rating scale, the amount of improvement for patients with ABSD was much less than that reported for patients with ADSD[4] and of shorter duration of benefit.[7] Objective blinded counts of voice breaks were significantly improved after TA Botox injection in patients with ADSD.[8] An objective assessment of speech symptom reduction in ABSD would help to further substantiate the patients' perceived benefit with Botox injections into the PCA muscle. Also, a blinded measurement of symptom frequency effects would eliminate rater bias. In this study, we evaluated the treatment effects on blinded symptom counts and ratings of change in severity in subjects enrolled in a randomized crossover treatment comparison of PCA Botox. Our purpose was to compare changes in symptoms following different injection techniques that might vary in placement accuracy.

METHODS

Subjects. Twelve women and 3 men (Table 1) with ABSD were enrolled for study. The subjects ranged in age from 33 to 74 years at the time of enrollment in the study, with a mean of 48 years. The procedures were reviewed and approved by the Institutional Review Board of the National Institutes of Health as part of protocol number 85-N-195. Some of these subjects had previously been treated with Botox. A minimum of 1 year had elapsed from the last Botox injection to participation in this study for each subject. The average time from onset of disease to participation in the study was 12 years (Table 1). The subjects had no other signs of neurologic or speech disorders, and the diagnosis of ABSD was based upon findings from a flexible fiberoptic examination performed during various speech and phonatory tasks. The criteria for diagnosis included breathy breaks after voiceless consonants (/k/, /h/, /p/, /s/, and /t/) during connected speech either with or without an overall breathy voice quality. The voice interruptions were associated with prolonged abduction of the vocal folds following the voiceless consonant production when observed on fiberoptic laryngoscopy. No laryngeal movement abnormalities or asymmetries were noted during nonspeech tasks such as whistling and singing. Two subjects had concomitant vocal fold tremor. The patients received a "series" of Botox injections, 1 injection into each PCA muscle (spaced 2 weeks apart) by 1 injection technique and returned 6 months later for a second series of PCA injections by the other technique. Either the endoscopic technique or the external approach technique was used for each series of 2 Botox injections.

Protocol. For Botox injection into the PCA muscles, 2 injection techniques were used on each subject in random order. We followed the external PCA injection technique of Blitzer et al[4] and a modification of the endoscopic technique of Rhew et al[5] for this study. The external PCA injection technique involves rotating the posterior aspect of the larynx toward the surface and passing a 27-gauge, 37-mm Teflon-coated needle immediately posterior to the free edge of the thyroid lamina, at the junction of the lower third and the upper two thirds of the lamina. The needle is passed through the inferior constrictor muscle and into the PCA muscle, and confirmation is obtained by recruitment with a sniff gesture and recruitment during the /s/ sound of the /si/ syllable. A second confirmation is obtained by palpating the cricoid cartilage with the tip of the needle. The endoscopic technique required the use of an Olympus ENF-T3 (Olympus Corp, Lake Success, NY) fiberoptic laryngoscope with a 5-mm outer diameter and a 2.2-mm working channel. The larynx is visualized after adequate topical anesthesia, and a disposable Mill-Rose sclerotherapy injection needle (Mill-Rose Laboratories, Inc, Mentor, Ohio) is passed through the working channel of the fiberoptic scope. Under fiberoptic visualization, the PCA muscle is injected at the level of the cricoid cartilage.

Our protocol for data collection and Botox injections was the same for both the endoscopic and external techniques. Initially, each patient received a pretreatment speech recording and fiberoptic laryngeal examination. Five mouse units of Botox were then injected into the PCA muscle under fiberoptic visualization for the endoscopic technique and under electromyographic guidance for the external approach. The patient returned in 2 weeks and was asked to assess his or her symptomatic response and report his or her side effects, particularly any shortness of breath and/or stridor. If the patient noted symptomatic benefit after the first injection, no additional Botox was given. Posttreatment speech recording and fiberoptic laryngeal examination were performed. If the patient had no difficulty with airway obstruction and had no symptomatic benefit after the first Botox injection on 1 side, the opposite PCA muscle was injected with an additional 5 units of Botox by the same technique used in the initial injection of this series. The patient returned 2 weeks after injection and again reported side effects and his or her symptomatic response. Posttreatment speech recording and fiberoptic laryngeal examination were performed. The patient returned for a second series of PCA Botox injections after any residual benefit from the first injection had resolved and a minimum of 6 months had passed since the last injection. A fiberoptic laryngeal examination was repeated to confirm no residual impairment of abductor PCA activity. Pretreatment speech recordings were made before both the endoscopic and external injection series. The second series of Botox injections and data collection was performed in the same manner as the first series; only the injection technique varied.

Analysis of Abductor Impairment. Transnasal fiberoptic examinations were performed before the PCA Botox injections and 2 weeks after each injection. These examinations included quiet breathing, deep inhalation, sniff gestures, sniff-/i/ gestures, and prolonged /i/. In addition, the patients performed repeated /i/, /mi/, /si/, /pi/, and /i/-/si/, as well as repeating 3 sentences: "We eat eels every day," "She speaks pleasingly," and "Peter will keep at the peak." All fiberoptic examinations were dubbed onto a coded rating tape and were randomized across subjects and treatment conditions. A Board-certified otolaryngologist experienced in fiberoptic evaluations of laryngeal function rated the impairment of abduction for each fiberoptic laryngeal examination. The criteria for abduction impairment included evidence of abduction impairment, especially for the maximum-abduction gestures, ie, sniff, sniff-/i/, and deep inhalation. Each side was rated individually. The rater was blinded to treatment condition and subject identity. The rater identified a unilateral abduction movement impairment in 8% of the pretreatment evaluations. After the first PCA Botox injection, 81% of the evaluations demonstrated an abduction movement impairment on the side of the injection, and 15% on the side opposite the injection. After the second (ie, contralateral) PCA Botox injection, a unilateral abduction movement impairment on the side of the injection was identified in 47% of the evaluations. After the second PCA Botox injection, a residual unilateral abduction movement impairment on the side of the first injection was identified in 35% of the evaluations.

Speech Symptom Recording and Measurement. A head-mounted microphone was positioned 2 inches (5 cm) from the mouth, and speech was recorded onto a digital audiotape. The speech recordings performed in the pretreatment and posttreatment periods were identical. The subjects listened to a prerecorded instruction tape that presented several tasks to be repeated. Five were sentences: "We mow our lawn all year," "A dog dug a new bone," "The puppy bit the tape," "Did he go to the right or to the left?" and "When he comes home we'll feed him." A prolonged vowel /i/ lasting for 5 to 7 seconds was also recorded. The pretreatment and posttreatment speech samples for each patient were dubbed onto a digital audiotape for listener measurement and rating. The pretreatment and posttreatment speech samples were randomly ordered within each pre-post pair of speech samples for each injection technique. The pre-post sets were further randomized by patient and by injection type and coded without subject identification. Two speech-language pathologists experienced in the diagnosis and rating of symptoms of ABSD performed comparative ratings for the speech samples and counted symptoms within each of the 5 sentences for each sample. The raters were blind to injection type, preinjection-postinjection status, and subject identity. The raters also judged symptom severity on 3 scales for "breathiness," "harshness," and "tremor" using a 4-point scale for each: "0" was within normal limits, "1" was mild with occasional deviation from normal only intermittently noticeable to others, "2" was a moderate deviation from normal that draws attention to itself, and "3" was a severe deviation from normal that would significantly impair speech intelligibility for communication. Ratings of breathiness and harshness were made from the sentence productions and the prolonged /i/ vowel, while the ratings of tremor were made only from the prolonged vowel. For the pre-post randomly ordered pairs, the raters compared the second speech sample to the first. A rating of "0" means no appreciable difference, "+1" represents a mild to moderate improvement in the second sample, "−1" represents a mild to moderate decrement in the second sample, and +2 represents normalization of symptoms. In addition to ratings, the number of noticeable vowel breaks, breathy breaks, and tremors within the sentences were counted. The mean count of the 2 raters for each sam-

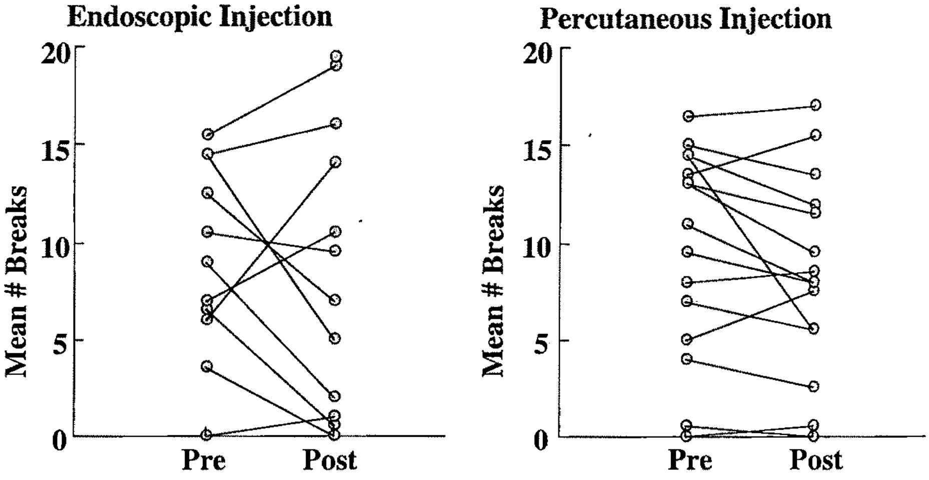

Fig 1. Mean number of counted breaks in pretreatment condition versus posttreatment condition by injection type.

ple was used for the statistical analyses. The patients reported their symptom change at the time of their posttreatment speech recording. They provided ratings of either "no improvement," "some improvement," or "significant improvement."

Statistical Analyses. Paired *t*-tests were performed to compare the numbers of breaks occurring before and after treatment within subjects, separately for each treatment technique. A paired *t*-test also compared the changes in the number of breaks following the 2 injection approaches. The 95% confidence interval with a Bonferroni correction for 3 comparisons resulted in a criterion p value of .017. A χ^2 analysis was used to compare the frequencies of the raters' judgments of change in symptom severity following each injection type. Also, a possible relationship between the patients' ratings and the speech pathologists' ratings of benefit was examined with a χ^2 analysis. A third χ^2 analysis compared the patient ratings of symptom change by injection type.

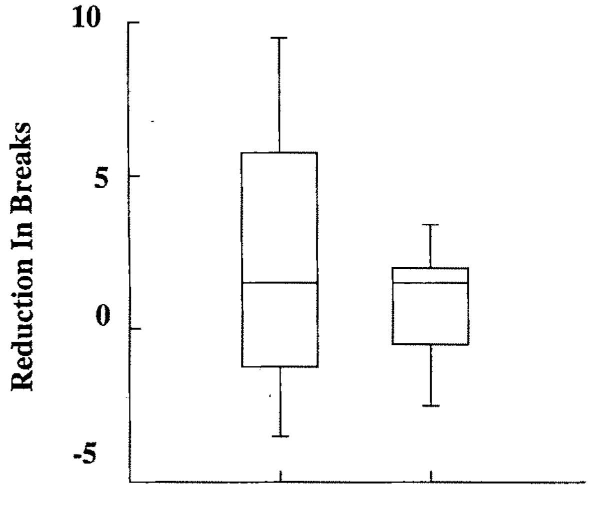

Fig 2. Box plots show median, distribution of mean, and standard error for reduction in voice breaks.

RESULTS

The randomized assignment to injection type resulted in 7 patients' receiving the percutaneous injection type first, followed by the endoscopic technique, and 4 patients' receiving the endoscopic approach first, followed by the percutaneous type. Four subjects received injections only via the external approach because of difficulties in introducing the Olympus ENF T-3 scope through the nasal cavity of subjects with narrow nasal airways. Only 1 patient developed stridor, which resolved without medical intervention within 1 week of injection (her first injection, using the endoscopic technique). No other side effects were reported.

Of the 15 patients treated in this study, 11 reported some benefit from at least 1 of the series of PCA injections. The only patient who developed stridor, beginning 2 days after the first of a series of Botox injections, had a significant reduction in symptoms following the unilateral injection. The stridor episode precluded injection on the opposite side. The remainder of the patients received bilateral injections 2 weeks apart. Four of the 11 patients reporting benefit reported no benefit after the first PCA side was injected and only received subjective benefit after the second side was injected.

The ratings of the speech pathologists were examined for agreement. The counts of the numbers of breaks in sentences were within 1 break of agreement on 84.4% of the ratings. The 2 sets of counts had a Pearson correlation coefficient of .957. The judgments of change in symptoms were the same between the 2 raters 85% of the time, and all were within 1 interval of agreement.

While the average number of breathy breaks decreased from 10 to 8 after treatment with either injection technique, the paired *t*-test comparisons were not statistically significant for the endoscopic (*t* =

TABLE 2. FREQUENCY DISTRIBUTION OF PATIENT RATINGS AND SPEECH PATHOLOGIST RATINGS OF BENEFIT

Speech-Language Pathologist Ratings	*Patient Ratings*		
	No Improvement	*Some Improvement*	*Significant Improvement*
−1.0	1	1	1
−0.5	1	0	0
0.0	7	3	4
0.5	0	1	0
1.0	2	3	1
1.5	0	0	1
Total	11	8	7

Speech-language pathologist ratings were averaged across raters, with rating of 0 meaning no appreciable difference, +1 representing mild to moderate improvement, −1 representing mild to moderate decrement, and +2 representing normalization of symptoms.

–.928; p = .37) or the percutaneous approach (*t* = –1.892; p = .08; Fig 1). An average decrease of 1.4 breaks followed the endoscopic approach, and a decrease of 1.3 breaks followed the percutaneous approach (Fig 2). The ratings of symptom change made by the speech pathologists did not reveal any statistical differences by injection type on χ^2 analyses (p = .5). Table 2 is a frequency distribution table of the relationship between patient and speech pathologist ratings for both injection types. The χ^2 analysis of these data showed no statistical relationship between patient ratings and speech pathologist ratings of benefit (p = .75). The χ^2 analysis for patient rating of symptom change by injection type showed no statistically significant differences (p = .72). The patients with perceived treatment benefits did not differ on the speech pathologists' breathy break counts (F = .149; p = .86). However, patients who perceived some benefit had a greater reduction in number of breaks than subjects who perceived no benefit (Fig 3).

DISCUSSION

The movement analysis performed after the first PCA Botox injection demonstrated an 81% abduction movement impairment on the side of the first injection. Rating asymmetric movement impairment after the second injection was difficult because of residual abduction impairment from the first injection. Possible explanations for the 19% who failed to develop movement impairment include inaccurate placement of Botox outside the PCA muscle, injection of an inadequate amount of Botox to achieve movement impairment, errors in the rating technique, and a return of abduction activity within the first 2 weeks after the injection. Inaccurate placement was limited by use of electromyographic guidance for the external Botox injections and visual guidance for the endoscopic technique. As with Botox injections into the TA muscle in patients with ADSD, a wide range of dosages can be injected. Injection doses of 5 units separated 2 weeks apart were chosen for this study on the basis of the experience of Blitzer et al.[4] This dosage was chosen to minimize severe impairment of PCA function and thus avoid airway obstruction symptoms. Despite our attempts to prevent this complication, 1 patient developed stridor after her first unilateral Botox injection, and this was the only patient who perceived a benefit after a unilateral PCA injection. While surgical intervention is not usually required for airway obstruction symptoms due to PCA impairment after Botox injection, patients are often uncomfortable with exertion and while lying down. Airway obstruction may be the primary limiting factor for the utility of Botox for symptom control in patients with ABSD.

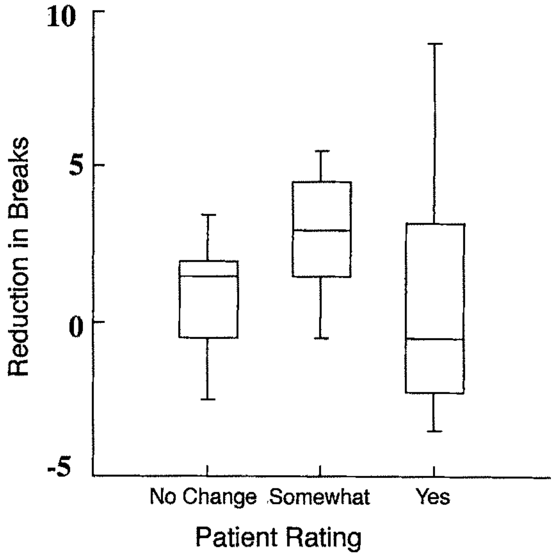

Fig 3. Box plots show median, distribution of mean, and standard error for reduction in voice breaks when subjects are grouped according to their perceived degree of benefit following completion of Botox treatment series.

In evaluating the 2 methods of placement of Botox into the PCA muscle, we found no significant differences between the techniques in treatment benefit. Patients with a small nasal airway often found the endoscopic approach more uncomfortable. However, placement of the Botox into the PCA muscle was accomplished with visual certainty. Placement of Botox into the PCA muscle by the percutaneous technique is less certain. Electromyographic identification is difficult because of surrounding muscular activity from the strap and inferior constrictor muscles. Also, the need to rotate the larynx while the verification gestures are performed makes this technique less reliable. Some patients found the percutaneous approach uncomfortable because of stimulation of the pyriform sinus mucosa with referred pain to the ear.

Additional techniques have been developed, but were not evaluated in this study, including an anterior approach and a transoral approach.[9,10] All of these techniques appear adequate for allowing for placement of Botox into the PCA muscles. From this study, we found no difference in benefit that was related to the injection technique. We recommend, therefore, that the choice of technique be directed by either the comfort of the patient or the physician's familiarity with the technique.

Botox has been established as an effective treatment for patients with ADSD through controlled treatment trials.[11] Previous trials of PCA Botox injections for patients with ABSD have been limited to analysis of patient-perceived benefit.[3,4,7] In a study of the effects of CT Botox injection in ABSD, no significant change was found in acoustic measures of voiceless consonant duration, although 6 of the 10 patients reported benefit.[2] In this study, we evaluated the treatment response of Botox delivered into the PCA muscles using 2 different assessment techniques: 1 blinded and quantitative, the other based on subjective patient report. The subjective treatment response of the patients was that 73% reported benefit with at least 1 injection, which compares favorably with the literature.[3,4,7] However, we found little correlation between blinded measures of breathy breaks or speech pathologist ratings of benefit and the patients' subjective treatment response. In a previous study using a similar rating scale for ADSD, the ratings were significantly improved after TA Botox injection, and the changes in the speech pathologist ratings correlated significantly with changes in the number of TA muscle bursts after treatment.[8] In addition, breathy breaks were not significantly reduced after Botox injection in this study of ABSD using a quantification technique similar to that previously shown to demonstrate significant improvements in patients with ADSD.[8]

The differences in patient versus speech pathologist subjective ratings of benefit may be explained by a placebo effect or by a true benefit perceived by the patient that cannot be perceived by others. The major complaint of patients with either ADSD or ABSD is excessive effort required while speaking. Benefit may be related to a perception of diminished effort following muscle injection. Diminished effort was not measured in this study. Measures of diminished effort may be related to adductory strength, which is reflected in part by computation of laryngeal resistance with an airway interrupter.[12] Laryngeal resistance is dependent, however, upon both adductory force and subglottal pressure.[13] The perception of effort may also depend upon several additional factors, such as proprioceptive feedback from the laryngeal muscles and joints experienced by patients during speech. A quantitative assessment of perceived effort would be difficult to develop.

Another possible explanation for the limited benefits from PCA Botox injections found in this study is a possible subject selection bias. Some patients had been previously treated with Botox for ABSD at the National Institutes of Health in the past, and a minimum of 1 year had elapsed since the last Botox injection. This time period was established to minimize contamination of the data by previous injections. These patients were not enrolled in this study because of a previous failure to receive benefit from Botox injections. Rather, these patients were involved in our protocol because of limited access to a facility that could administer Botox into the PCA muscles in their area. Most patients traveled by airplane to participate in this study.

Additionally, the limited benefit in ABSD may also be explained by differences in the pathophysiology of these 2 forms of spasmodic dysphonia. The pathophysiology of ABSD may not necessarily be due to excessive activity of the PCA muscle. Previous studies have demonstrated bursting activity in the TA muscles coincident with voice interruptions in patients with ADSD.[14] Studies of the PCA muscle in ABSD have not shown abnormal activity levels of this muscle as compared to those of normal controls.[15,16] In some patients, an imbalance in TA muscle activity between the 2 sides occurs during a breathy voice break.[2,17] Therefore, using a technique that reduces muscle activity in a disorder that is not always characterized by excessive muscle activity may explain the more limited benefit of Botox in ABSD as compared to ADSD.

If ABSD is a negative dystonia, therapy may be better aimed at effecting vocal fold closure during the vocalization following a voiceless consonant. A static medialization procedure has been employed and has resulted in limited benefit in some patients.[4,18] A dynamic medialization technique could be effected by functional electrical stimulation. Partial success with such an approach was reported by Friedman et al,[19,20] and the technique is currently under investigation in our laboratory.

REFERENCES

1. Merson RM, Ginsberg AP. Spasmodic dysphonia: abductor type. A clinical report of acoustic, aerodynamic and perceptual characteristics. Laryngoscope 1979;89:129-38.

2. Ludlow CL, Naunton RF, Terada S, Anderson BJ. Successful treatment of selected cases of abductor spasmodic dysphonia using botulinum toxin injection. Otolaryngol Head Neck

Surg 1991;104:849-55.

3. Blitzer A, Brin MF, Stewart CF. Botulinum toxin management of spasmodic dysphonia (laryngeal dystonia): a 12-year experience in more than 900 patients. Laryngoscope 1998; 108:1435-41.

4. Blitzer A, Brin M, Stewart C, Aviv JE, Fahn S. Abductor laryngeal dystonia: a series treated with botulinum toxin. Laryngoscope 1992;102:163-7.

5. Rhew K, Fiedler DA, Ludlow CL. Technique for injection of botulinum toxin through the flexible nasolaryngoscope. Otolaryngol Head Neck Surg 1994;111:787-94.

6. Meleca RJ, Hogikyan ND, Bastian RW. A comparison of methods of botulinum toxin injection for abductory spasmodic dysphonia. Otolaryngol Head Neck Surg 1997;117:487-92.

7. Ludlow CL, Bagley JA, Yin SG, Koda J. A comparison of different injection techniques in the treatment of spasmodic dysphonia with botulinum toxin. J Voice 1992;6:380-6.

8. Bielamowicz S, Ludlow CL. Effects of botulinum toxin on pathophysiology in spasmodic dysphonia. Ann Otol Rhinol Laryngol 2000;109:194-203.

9. Rontal M, Rontal E, Rolnick M, Merson R, Silverman B, Truong DD. A method for the treatment of abductor spasmodic dysphonia with botulinum toxin injections: a preliminary report. Laryngoscope 1991;101:911-4.

10. Bastian RW, Delsupehe KG. Indirect larynx and pharynx surgery: a replacement for direct laryngoscopy. Laryngoscope 1996;106:1280-6.

11. Truong DD, Rontal M, Rolnick M, Aronson AE, Mistura K. Double-blind controlled study of botulinum toxin in adductor spasmodic dysphonia. Laryngoscope 1991;101:630-4.

12. Bard MC, Slavit DH, McCaffrey TV, Lipton RJ. Noninvasive technique for estimating subglottic pressure and laryngeal efficiency. Ann Otol Rhinol Laryngol 1992;101:578-82.

13. McHenry MA, Kuna ST, Minton JT, Vanoye CR. Comparison of direct and indirect calculations of laryngeal airway resistance in connected speech. J Voice 1996;10:236-44.

14. Shipp T, Izdebski K, Reed C, Morrissey P. Intrinsic laryngeal muscle activity in a spastic dysphonic patient. J Speech Hear Res 1985;50:54-9.

15. Watson BC, Schaefer SD, Freeman FJ, Dembowski J, Kondraske G, Roark R. Laryngeal electromyographic activity in adductor and abductor spasmodic dysphonia. J Speech Hear Res 1991;34:473-82.

16. Van Pelt F, Ludlow CL, Smith PJ. Comparison of muscle activation patterns in adductor and abductor spasmodic dysphonia. Ann Otol Rhinol Laryngol 1994;103:192-200.

17. Cyrus C, Bielamowicz S, Ludlow CL. Decreased adductor muscle activity in abductor spasmodic dysphonia [Abstract]. Otolaryngol Head Neck Surg 1999;121:144.

18. Postma GN, Blalock PD, Koufman JA. Bilateral medialization laryngoplasty. Laryngoscope 1998;108:1429-34.

19. Friedman M, Toriumi DM, Grybauskas V, Applebaum EL. Treatment of spastic dysphonia without nerve section. Ann Otol Rhinol Laryngol 1987;96:590-6.

20. Friedman M, Toriumi DM, Grybauskas VT, Applebaum EL. Implantation of a recurrent laryngeal nerve stimulator for the treatment of spastic dysphonia. Ann Otol Rhinol Laryngol 1989;98:130-4.

Ann Otol Rhinol Laryngol 110:2001

DURATION OF STENTING IN SINGLE-STAGE LARYNGOTRACHEAL RECONSTRUCTION WITH ANTERIOR COSTAL CARTILAGE GRAFTS

BENJAMIN E. J. HARTLEY, MBBS, FRCS
LONDON, ENGLAND

L. MARK GUSTAFSON, MD
CINCINNATI, OHIO

JAMES H. LIU, MD
HOUSTON, TEXAS

CHRISTOPHER J. HARTNICK, MD
CINCINNATI, OHIO

ROBIN T. COTTON, MD
CINCINNATI, OHIO

In single-stage laryngotracheal reconstruction (ss-LTR), the endotracheal tube is used as a stent. The optimal duration of stenting is not known. The stenting period requires a stay in the intensive care unit, as the patient is intubated. Sedation and, rarely, paralysis may be required. An analysis from a prospectively collected database was performed to investigate the effect of length of stenting on the outcome of ss-LTR. The outcomes used were reintubation rate and postoperative tracheostomy rate. Patients with anterior costal graft ss-LTR were selected, as they had undergone similar procedures and have similar stenosis types and grades. In 101 patients, the duration of stenting ranged from 2 to 14 days (mean, 7 days; SD, 2.6 days). No significant correlation was found between the number of days stented and the reintubation rate or the postoperative tracheostomy rate. Patients stented for longer than 1 week were an average of 15 months younger than those stented for less than 1 week; however, the stenosis grades for the two populations were equivalent. The differences in rates of reintubation ($p = .68$) and postoperative tracheostomy ($p = .52$) in these 2 groups were not significant. For patients undergoing ss-LTR with anterior costal cartilage grafts, no correlation was found between the number of days stented (intubated) and the reintubation rate or the postoperative tracheostomy rate.

KEY WORDS — pediatric laryngotracheal reconstruction, stenting, subglottic stenosis.

INTRODUCTION

The past 3 decades have seen many advances in the surgical management of laryngotracheal stenosis in children. The number of surgical procedures available for treatment of pediatric laryngotracheal stenosis has steadily risen.[1-3] The single-stage approach utilizes the endotracheal tube as a stent for the reconstruction in the postoperative period. It also secures the airway, enabling the tracheostomy to be excised at the time of reconstruction.

In 1980, Cotton and Seid[4] described the anterior cricoid split procedure as an alternative to tracheostomy in intubated neonates who could not be extubated because of subglottic edema and granulation tissue. It was demonstrated that the endotracheal tube could serve as a stent and also as a temporary airway. Application of this technique to older children gave rise to the single-stage laryngotracheoplasty.[5] This approach has been used with anterior cartilage grafts alone, posterior cartilage grafts alone, and combined anterior and posterior cartilage grafts. Variations on grafting techniques have included the posterior split technique, which may be combined with an anterior graft. Lateral cuts have been made in the cricoid cartilage, and combinations of these techniques, such as the 4-quadrant split technique, have been used. These operations are now considered together under the combined heading of single-stage laryngotracheal reconstruction (LTR).[6]

The proportion of LTR procedures performed with the single-stage approach has progressively risen. As a general principle, the single-stage approach has been reserved for children with normal pulmonary function, as they cope better with the prolonged intubation period. The technique was initially reserved for mild stenoses, but with time, more severe stenoses have come to be treated this way.

The optimal duration of stenting with the endotracheal tube in single-stage LTR is not known. A long period has many risks, including those of sedation, laryngeal edema secondary to the tube, and even subglottic stenosis. There are important cost implications in keeping patients in intensive care. A short period of stenting is preferred, as long as the ultimate success of the procedure is not compromised.

The goal of this study was to retrospectively analyze the results of 101 patients with subglottic steno-

---

From the Department of Pediatric Otolaryngology, The Children's Hospital Medical Center, Cincinnati, Ohio.

Presented at the meeting of the American Broncho-Esophagological Association, Orlando, Florida, May 15-16, 2000.

CORRESPONDENCE — Benjamin E. J. Hartley, MBBS, FRCS, The Royal National Throat Nose and Ear Hospital, Gray's Inn Road, London WC1X 8DA, England.

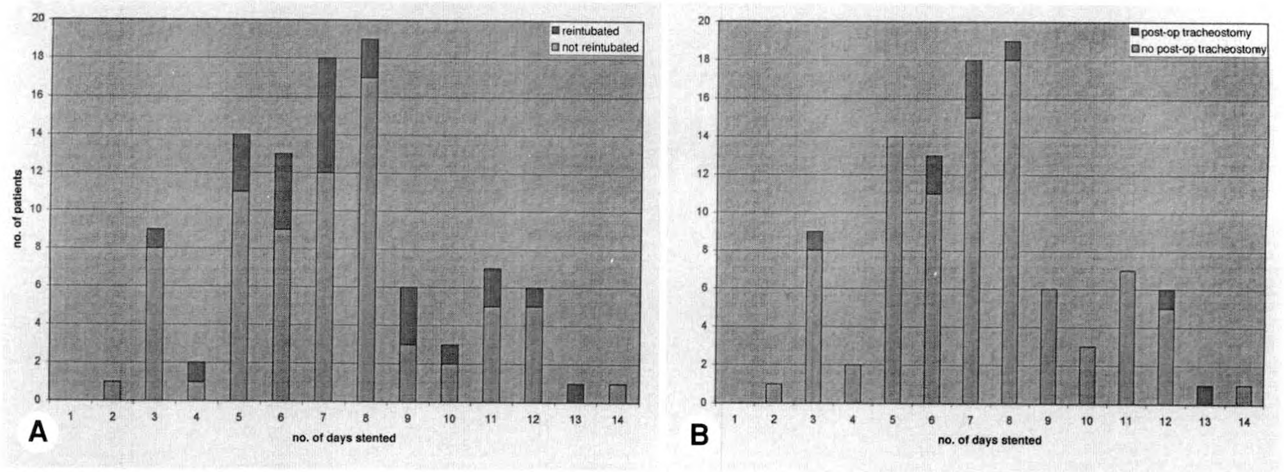

Duration of stenting in 101 patients with single-stage laryngotracheal reconstruction with anterior costal cartilage graft. **A)** Rate of postoperative reintubation. **B)** Rate of postoperative tracheostomy.

sis who underwent single-stage LTR with anterior costal cartilage grafts to determine whether the duration of stenting influenced the outcome. The principal outcome measures used were reintubation rate and postoperative tracheostomy rate.

MATERIALS AND METHODS

In this institution, a prospective database of all airway surgery has been kept since 1974. It includes more than 1,000 LTR procedures. We identified 206 patients as having undergone single-stage LTR between 1986 and 1998. This group had a variety of different procedures, including anterior costal cartilage grafts, posterior costal cartilage grafts, combined anterior and posterior costal cartilage grafts, anterior grafts with posterior cricoid splits, auricular cartilage grafts, and thyroid alar cartilage grafts. The heterogeneity of the surgical procedures used made the total group inappropriate for analysis as to the effect of length of stenting. Within the total group were 101 patients who had undergone LTR with anterior costal cartilage grafts only. These were selected for further analysis as a large group of patients with similar stenoses who had undergone the same operative procedure.

The ages of the 101 children ranged from 7 months to 18 years (mean, 52 months). There were 67 boys and 34 girls. Associated airway disease was present in 18 patients: 17 had tracheomalacia and 1 had laryngomalacia. The tracheomalacia was assessed by an experienced otolaryngologist as mild in 9 cases, moderate in 7 cases, and severe in 1 case. Three patients had Down syndrome. Four patients had cerebral palsy.

All patients had subglottic stenosis without glottic involvement. The vast majority of patients had acquired stenosis due to previous intubation, but 4 had congenital stenosis. The stenoses were graded on the Myer-Cotton scale[7]: 17 patients had grade 1 stenosis, 43 patients had grade 2 stenosis, 18 patients had grade 3 stenosis, and 1 patient had grade 4 stenosis.

The original decision as to how long to leave the stent in place was based on experience with the anterior cricoid split procedure for failed extubation in neonates. Around 1 to 2 weeks was used, and was successful in the majority of cases. Over a 10-year period, shorter stenting times have been introduced with varying success. No comprehensive analysis of the outcomes of these experiments with shorter stenting times had been performed, and this was the reason for this study. In theory, younger patients and those with more severe stenosis might be stented for longer times. In this study, the grade of stenosis was found to be equivalent in those intubated into the second week, and the age was only slightly different (58 months in those intubated less than 1 week and 43 months in those intubated more than 1 week).

The goal of this study was to examine the effect of length of stenting on rates of reintubation and postoperative tracheostomy.

RESULTS

One hundred one children underwent single-stage LTR with anterior costal cartilage grafts between January 1987 and September 1998. The length of stenting (duration of intubation) ranged from 2 to 14 days (median, 8 days). The day-by-day distribution of the length of stenting is illustrated in the Figure. The Figure also shows the number of patients reintubated and the number of patients undergoing postoperative tracheostomies as a function of the number of days stented.

Overall, 24 patients (24%) required reintubation, and 9 patients (9%) required postoperative tracheostomy. With further reconstructive surgery, 4 of these 9 patients were decannulated, for an ultimate decannulation rate of 95% for these patients.

DATA ANALYSIS

Patients with a longer duration of stenting were compared with those who had a shorter duration of stenting. Spearman's test was used to assess the correlation between the number of days stented and the postoperative tracheostomy rate and reintubation rate. No significant correlation was found between the duration of stenting and the reintubation rate ($r = .284$) or the postoperative tracheostomy rate ($r = .367$).

The patients were then divided into 2 approximately equal-size groups for comparison: those stented for less than 1 week (57 patients; mean age, 58 months) and those stented for more than 1 week (44 patients; mean age, 43 months). The stenosis grades in the 2 groups were equivalent. In the group stented for 1 week or less, 15 patients required reintubation (26%) and 6 required postoperative tracheostomy. In the group stented into the second week, 10 patients required reintubation (26%) and 3 required postoperative tracheostomy.

The χ^2 test was used to examine the frequency distribution of reintubation and postoperative tracheostomy in the 2 groups (group 1 being those stented for less than 1 week and group 2 being those stented for 8 to 14 days). The null hypothesis was that it makes no difference to the occurrence of reintubation or postoperative tracheostomy whether the patient is intubated for more than 1 week or less than 1 week. The p values of .68 and .51 were obtained for reintubation and postoperative tracheostomy, respectively, and the null hypothesis is upheld.

DISCUSSION

When assessing a child with laryngotracheal stenosis before and during operation, the surgeon now has to make a number of decisions. First, the type of procedure must be decided on, and cricotracheal resection is now an established alternative to LTR for selected stenoses.[8-12] If LTR is preferred, decisions must be made as to the type of graft, the position of the graft, the method of stenting, and the duration of stenting. A further consideration is the use of antireflux medication, antibiotics, or steroids, or the possible postoperative use of mitomycin-C to prevent restenosis. At the current time, randomized, controlled trials to help the surgeon make these decisions have not been performed. In view of the rarity of pediatric laryngotracheal stenosis and the large variation in type and severity of stenoses, we cannot expect guidance from controlled trials in matched patients with equivalent disease in the near future.

The next-best option is to use information from prospectively collected databases to guide our surgical decision-making. Large numbers enable us to select patients with equivalent disease and compare variations in treatment and their effect on selected outcome measures.

In this study, we examine 1 aspect of the practice of LTR in detail. We have selected a specific group of patients undergoing anterior costal cartilage graft LTR, as this group are likely to have similar stenosis types and grades and to have had similar surgical interventions. The choice of the duration of stenting has been based on the initial descriptions of the procedure supplemented by experience. Over a 10-year period, shorter stenting periods have been tried. No overall analysis of the effect of shortening the stenting period has, however, previously been made. In this study, no significant correlation was found between the duration of stenting and the reintubation rate ($r = .284$) or the postoperative tracheostomy rate ($r = .367$). The χ^2 test was used to examine the frequency of reintubation and tracheostomy in the 2 groups of patients (group 1 being those stented for 1 week or less and group 2 being those intubated for 8 to 14 days). The p values of .68 and .51 were obtained for the occurrence of reintubation and postoperative tracheostomy, respectively.

Therefore, the differences in reintubation rate and postoperative tracheostomy rate between the 2 groups are not statistically significant. This statement should be qualified with the acknowledgment that the decision as to how long to keep the stent was not randomized. Patients selected to be stented for longer periods may have had more severe problems. Against this qualification is the observation that the stenosis grades were no higher in the patients stented for more than 1 week. The ages in the 2 groups differ slightly, with the group stented for 1 week or less being an average of 15 months older. This difference reflects the clinical practice of stenting younger children for slightly longer periods.

Overall, the patients who have longer stenting periods have reintubation and postoperative tracheostomy rates similar to those of patients with shorter stenting periods. The likely explanation is that long stenting periods do not give extra benefit. The next step is to try shorter stenting periods and carefully audit the results. Since this study was carried out, 2 patients were successfully extubated on postoperative day 3, and 1 patient underwent a single-stage LTR with an anterior costal cartilage graft and was extubated successfully the following day. With time, our experience with a shorter stenting period in this selected group of patients will increase, but the initial results are encouraging.

One might ask the question, why use stents at all? It is likely that some form of structural support for the reconstruction in the initial stages of healing is helpful. For an anterior costal cartilage graft single-stage LTR, a stent is probably only required for a short time, as a stable reconstruction is usually created. If the cartilage is carved into a shape such that it does not tend to prolapse into the lumen, then the stent is less important. Anterior costal cartilage grafts have been used successfully without stents as part of a 2-stage procedure, and it is possible that in certain circumstances they could be used in a single-stage procedure. This procedure would, however, leave the patient totally dependent on the newly reconstructed airway. Graft prolapse could lead to acute airway obstruction, which could be fatal. If reintubation were required, then a tube would need to be passed through the newly reconstructed airway, with potential disruption. For these reasons, we have not extubated patients at the end of the operation, but rather, have waited until the surgeon feels confident that sufficient healing has occurred for the graft to be stable. If anterior and posterior grafts are used, the reconstruction is less stable, as the cricoid ring is split in 2 places, and it would be expected that stenting is more important. The surgeon has to make a decision about stenting type and duration in all cases on the basis of the unique structure of the reconstruction in an individual patient.

CONCLUSION

For patients undergoing single-stage LTR with a single anterior costal cartilage graft, no significant correlation was found between the duration of stenting and the reintubation rate or the postoperative tracheostomy rate. The implication is that shorter periods of stenting may be appropriate, with reduced morbidity and cost. No added advantage was found in stenting patients with anterior costal cartilage graft single-stage LTR for more than 1 week.

REFERENCES

1. Cotton RT, Gray SD, Miller RP. Update of the Cincinnati experience in laryngotracheal reconstruction. Laryngoscope 1989;99:1111-6.
2. Ochi JW, Evans JNG, Bailey CM. Pediatric airway reconstruction at Great Ormond Street: a ten-year review. Laryngotracheoplasty and laryngotracheal reconstruction. Ann Otol Rhinol Laryngol 1992;101:465-8.
3. Maddalozzo J, Holinger LD. Laryngotracheal reconstruction for subglottic stenosis in children. Ann Otol Rhinol Laryngol 1987;96:665-9.
4. Cotton RT, Seid AB. Management of the extubation problem in the premature child. Anterior cricoid split as an alternative to tracheotomy. Ann Otol Rhinol Laryngol 1980;89:508-11.
5. Seid AB, Pransky SM, Kearns DB. One-stage laryngotracheoplasty. Arch Otolaryngol Head Neck Surg 1991;117:408-10.
6. Cotton RT, Myer CM III, O'Connor DM, Smith ME. Pediatric laryngotracheal reconstruction with cartilage grafts and endotracheal tube stenting: the single-stage approach. Laryngoscope 1995;105:818-21.
7. Myer CM III, O'Connor DM, Cotton RT. Proposed grading system for subglottic stenosis based on endotracheal tube sizes. Ann Otol Rhinol Laryngol 1994;103:319-23.
8. Monnier P, Savary M, Chapuis G. Partial cricoid resection with primary tracheal anastomosis for subglottic stenosis in infants and children. Laryngoscope 1993;103:1273-83.
9. Monnier P, Lang F, Savary M. Partial cricotracheal resection for severe pediatric subglottic stenosis: update of the Lausanne experience. Ann Otol Rhinol Laryngol 1998;107:961-8.
10. Monnier P, Lang F, Savary M. Cricotracheal resection for pediatric subglottic stenosis. Int J Pediatr Otorhinolaryngol 1999;49(suppl 1):S283-S286.
11. Stern Y, Gerber ME, Walner DL, Cotton RT. Partial cricotracheal resection with primary anastomosis in the pediatric age group. Ann Otol Rhinol Laryngol 1997;106:891-6.
12. Walner DL, Stern Y, Cotton RT. Margins of partial cricotracheal resection in children. Laryngoscope 1999;109:1607-10.

Ann Otol Rhinol Laryngol 110:2001

FINE STRUCTURE OF THE HUMAN NEWBORN AND INFANT VOCAL FOLD MUCOSAE

KIMINORI SATO, MD, PHD

MINORU HIRANO, MD TADASHI NAKASHIMA, MD

KURUME, JAPAN

This study was carried out to determine the fine structure of the membranous portion of the human newborn and infant vocal fold mucosae and to clarify how the human vocal fold mucosa begins to grow after birth. Light and electron microscopic observations were made on the vocal fold mucosae excised from human newborn and infant larynges. Our findings are summarized as follows. 1) Reinke's space of the newborn vocal fold is a loose structure composed of ground substance and sparse fibers. 2) Ground substance is abundant and glycoproteins (fibronectin) are present in the lamina propria. 3) In the maculae flavae of newborn vocal folds, fibroblasts begin to form collagenous, reticular, and elastic fibers. 4) In the infant maculae flavae, fibroblasts are activated to become stellate in shape and synthesize extracellular matrices such as collagenous and reticular fibers. 5) After birth, the collagenous and reticular fibers synthesized in the maculae flavae extend toward the middle of the membranous portion of the vocal fold mucosa. 6) Glycoprotein (fibronectin) determines the orientation of collagenous and reticular fiber deposition. 7) Glycoprotein (fibronectin) decreases with the increase of the fibrous components in Reinke's space. 8) Elastic fibers increase after collagenous and reticular fibers appear in Reinke's space. 9) Much hyaluronic acid (glycosaminoglycan) is actively produced in the infant maculae flavae. 10) The collagenous and reticular fibers serve as stabilizing scaffolds for the other extracellular matrices, such as elastic fibers and glycosaminoglycan. During infancy, the extracellular matrices synthesized in the maculae flavae appear in the membranous portion of the vocal fold, each at a different time, so as to initiate the 3-dimensional formation of the vocal fold mucosa.

KEY WORDS — extracellular matrix, histology of larynx, infant, larynx, newborn, vocal fold.

INTRODUCTION

In adults, the vocal fold has a layered structure consisting of the epithelium, the lamina propria (superficial, intermediate, and deep layers), and the vocalis muscle.[1,2] These structures are required for phonation.[1]

Hirano et al[2,3] have reported light microscopic studies of newborn vocal folds. The structures were found to differ from those of adults. In newborn vocal folds, the entire lamina propria appears as a uniform structure with no vocal ligament.[2,3] The layered structure of the vocal fold matures during adolescence.[3] The maculae flavae of the mucosa of human newborn vocal folds, situated at the anterior and posterior ends of the vocal folds, have been examined by electron microscopy.[4] The newborn maculae flavae are considered important for the growth and development of the vocal ligament.[4]

The growth and development of the layered structure of the human vocal fold mucosa have not been adequately examined. Our study investigated the fine structure of the lamina propria, the most important vibrating structure, of human newborn and infant vocal fold mucosae so as to clarify how the growth of the human vocal fold mucosa is initiated.

MATERIALS AND METHODS

Eight normal human newborn (4) and infant (4) vocal folds from autopsy cases were examined. Four were from boys and 4 from girls.

For light microscopy, the specimens were fixed in 10% formalin, dehydrated in graded concentrations of ethanol, and embedded in paraffin. Hematoxylin and eosin, elastica–van Gieson, silver, periodic acid–Schiff, and Alcian blue stains were employed for each section. Elastica–van Gieson staining was used for the identification of collagenous and elastic fibers. Silver staining was done for reticular fibers and collagenous fibers, and Alcian blue staining (pH 1.0 and pH 2.5) for glycosaminoglycan. For the hyaluronidase digestion study, 50 mg of bovine testis hyaluronidase (Sigma, St Louis, Mo) was diluted in 100 mL of phosphate-buffered saline (PBS) solution. Thin sections were incubated in the diluted hyaluronidase solution for 2 hours at 37°C. The thin sections were subsequently stained with Alcian blue (pH 2.5). Type I collagen, type III collagen, and fibronectin were detected histologically in formalin-fixed and paraffin-embedded tissue by immunohistochemical study, for which a labeled streptavidin-biotin staining kit (Dako, Carpinteria, Calif) was used. All specimens were sectioned at 5- to 6-µm thickness and mounted

---

From the Department of Otolaryngology–Head and Neck Surgery, Kurume University, School of Medicine, Kurume, Japan.

Presented at the meeting of the American Broncho-Esophagological Association, Orlando, Florida, May 15-16, 2000.

CORRESPONDENCE — Kiminori Sato, MD, PhD, Dept of Otolaryngology–Head and Neck Surgery, Kurume University, School of Medicine, 67 Asahi-machi, Kurume 830-0011, Japan.

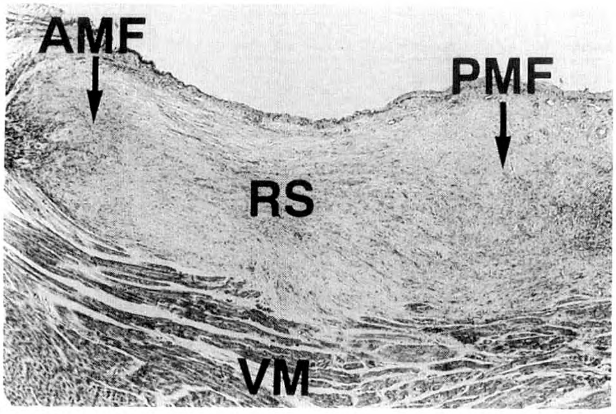

Fig 1. Horizontal section of newborn vocal fold (elastica–van Gieson stain, original ×25). AMF — anterior macula flava, PMF — posterior macula flava, RS — Reinke's space, VM — vocalis muscle.

on glass slides. Deparaffinized and hydrated sections were rinsed with 0.01-mol/L PBS solution at pH 7.4. The specimens were covered with 3% hydrogen peroxide for 5 minutes and rinsed with 0.01-mol/L PBS solution, then treated with normal goat serum. The specimens were then incubated with the primary antibody overnight at 4°C. A 1:100 diluted polyclonal antibody against type I and type III collagens (Chemicon International Inc, Temecula, Calif) was used. A 1:50 diluted polyclonal antibody against fibronectin (ICN Pharmaceuticals Inc, Aurora, Ohio) was used. After rinsing with PBS solution and labeling with the streptavidin-biotin staining kit, a color reaction was developed with 3,3'-diaminobenzidine at room temperature. Immunoreactivity was examined by light microscopy.

For transmission electron microscopy, the specimens were fixed in 2.5% glutaraldehyde at 4°C for 2 hours, rinsed with cacodylate buffer solution, and postfixed in 2% osmium tetroxide with cacodylate buffer solution at 4°C for 2 hours. After rinsing with cacodylate buffer solution, the specimens were dehydrated in graded concentrations of ethanol and embedded in epoxy resin. Semithin sections were prepared with an ultramicrotome, stained with 1% toluidine blue, and examined with a light microscope. Thin sections were made with an ultramicrotome and stained with uranyl acetate and lead citrate, tannic acid so as to make the glycoprotein and elastin apparent. Observations were conducted with a JEM-2000EX transmission electron microscope.

RESULTS

NEWBORN VOCAL FOLD MUCOSA

In newborns, the entire lamina propria of the vocal fold mucosa was loose, and no structure corresponding to the vocal ligament could be found (Fig 1).

The maculae flavae of the newborn vocal fold were formed by relatively dense masses of cells (Fig 1). The maculae flavae were composed of fibroblasts, ground substance, elastic fibers, reticular fibers, and collagenous fibers. Cellular components were abundant, and fibrous components were sparse. More collagenous fibers were present than elastic fibers.

Reinke's space of the newborn vocal fold was a loose structure (Fig 1) chiefly composed of ground substance, fibroblasts, reticular fibers, collagenous fibers, and elastic fibers. Fibrous components were sparse.

Fibroblasts. In the newborn maculae flavae, many fibroblasts were present; the density was great. The fibroblasts were oval or stellate in shape, with a large nucleus-cytoplasm ratio (Fig 2A). The rough endoplasmic reticulum and Golgi apparatus in the cytoplasm were not well developed. Free ribosomes were well developed in the cytoplasm (Fig 2B). A basal

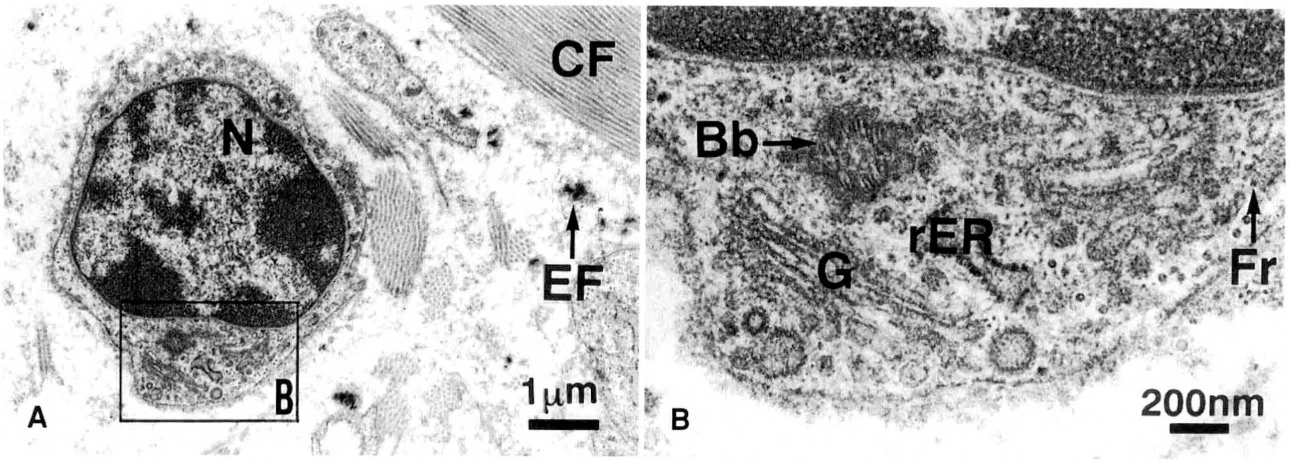

Fig 2. Transmission electron micrograph of newborn macula flava (tannic acid stain). **A)** N — nucleus of fibroblast, CF — collagenous fiber, EF — elastic fiber. **B)** Intracellular organelles of fibroblast (B region on **A**). rER — rough endoplasmic reticulum, G — Golgi apparatus, Bb — basal body, Fr — free ribosome.

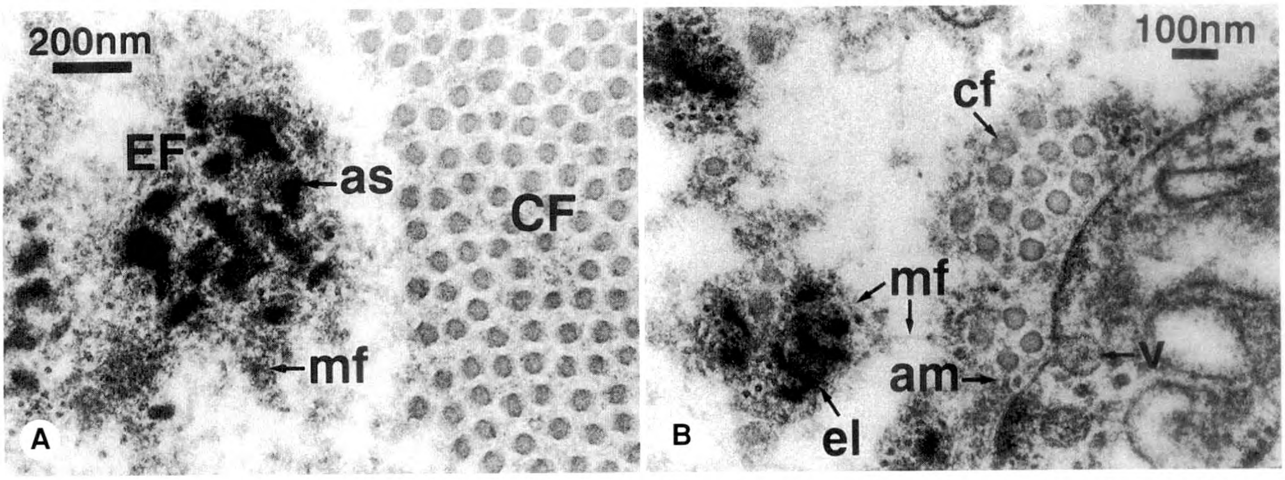

Fig 3. Transmission electron micrographs (tannic acid stain). **A)** Fibers in newborn Reinke's space. CF — collagenous fiber, EF — elastic fiber, as — amorphous substance, mf — microfibril. **B)** Synthesis of collagenous fibers and elastic fibers by fibroblasts in newborn macula flava. v — vesicle, am — amorphous material, mf — microfibril, cf — collagenous fibril, el — elastin.

body was seen in the cytoplasm (Fig 2B). The fibroblasts were immature and possessed some features of mesenchymal cells. In the cytoplasm of some fibroblasts, rough endoplasmic reticulum and Golgi apparatus could be seen (Fig 2B). Newly released amorphous material was present on the cell surfaces. Some fibers were seen close to fibroblasts. Some fibroblasts had started to synthesize extracellular matrices, such as collagenous fibers, reticular fibers, and elastic fibers. Periodic acid–Schiff stain, type I collagen, and type III collagen stained few components in the cytoplasm of the fibroblasts.

Fibroblasts were sparse in Reinke's space of the newborn vocal fold mucosa (Fig 1), but their density was greater than it is in adults. The fibroblasts were not spindle-shaped, but oval. The nucleus-cytoplasm ratio was large, and the cytoplasm occupied a small area around the nucleus. The rough endoplasmic reticulum and Golgi apparatus were not well developed — a finding indicating that these cells were in the resting phase. Few vesicles were present along the periphery of the cytoplasm. Newly released amorphous material was scarce on the cell surface. Few fibers could be seen close to fibroblasts. Periodic acid–Schiff stain, type I collagen, and type III collagen stained few components in the cytoplasm of fibroblasts in Reinke's space.

Collagenous and Reticular Fibers. Collagenous and reticular fibers were fewer in either the maculae flavae or Reinke's space of the newborn vocal fold mucosa than in that of adults. The collagenous fibers were made up of numerous collagenous fibrils approximately 40 to 50 nm in width (Fig 3A). The collagenous fibers were almost mature.

The collagenous fibers were synthesized by the fibroblasts in the maculae flavae (Fig 3B). There were vesicles along the periphery of fibroblasts in the maculae flavae. Newly released amorphous materials were seen on the fibroblast surfaces. Microfibrils 10 to 15 nm in width were near the amorphous materials, and collagenous fibrils were close to the microfibrils.

Elastic Fibers. The number of elastic fibers was small compared to the number of collagenous fibers. The elastic fibers were composed of microfibrils and amorphous substances (Fig 3A). The former were abundant, and the latter were sparse and reticular in shape (Fig 3A), indicating that the elastic fibers were immature.

Synthesis of elastic fibers had taken place in the maculae flavae (Fig 3B). There were vesicles along the periphery of the cytoplasm of the fibroblasts. Newly released amorphous materials were seen on the cell surface. Microfibrils 10 to 15 nm in width were situated around the amorphous materials. The microfibrils were assembled, and elastin was deposited on them.

Ground Substance. Much glycoprotein (fibronectin) was present in the newborn vocal fold mucosa (Fig 4). The ground substance contained a flocculent material that stained with tannic acid and was abundant in the lamina propria of the newborn vocal fold mucosa (Fig 4A). Thus, much glycoprotein could be seen by electron microscopy. Reinke's space of the newborn vocal fold mucosa stained with fibronectin immunohistochemically (Fig 4B).

INFANT VOCAL FOLD MUCOSA

The maculae flavae of the infant vocal folds were also relatively dense masses of cells. The maculae flavae were composed of collagenous fibers, reticular fibers, fibroblasts, ground substance, and elastic

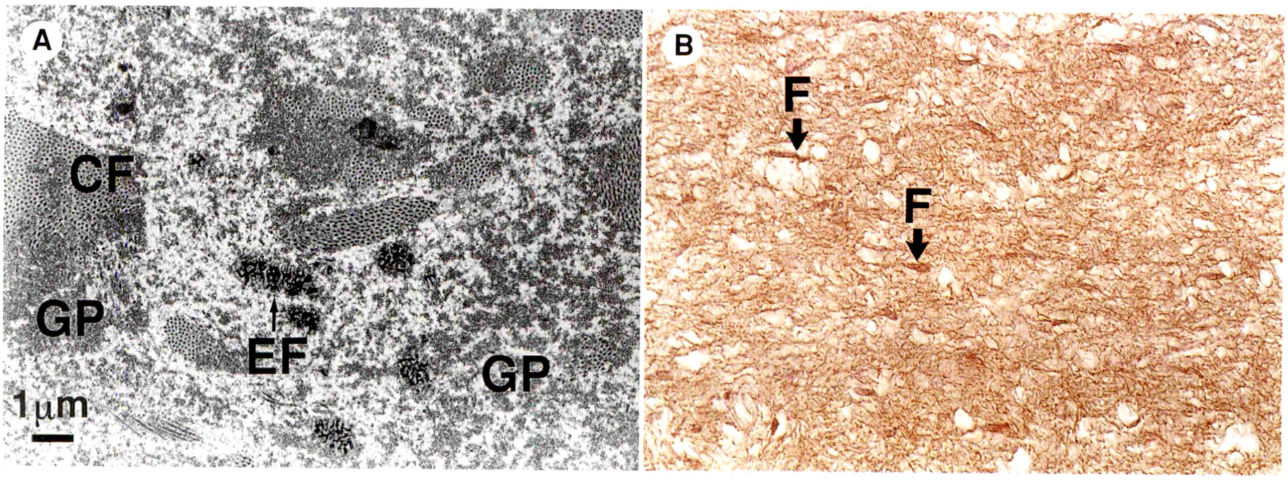

Fig 4. Reinke's space in newborn. **A)** Transmission electron micrograph shows glycoprotein (GP; tannic acid stain). CF — collagenous fiber, EF — elastic fiber. **B)** Immunohistochemical staining shows fibronectin (brown color; original ×200). F — fibroblast.

fibers. Cellular components were more abundant than fibrous components. The fibrous components had increased by comparison to those of the newborn maculae flavae (Fig 5). More reticular and collagenous fibers were present than elastic fibers (Fig 5).

Many reticular and collagenous fibers extended from the maculae flavae toward the middle of Reinke's space of the infant vocal fold mucosa (Fig 6). No structure corresponding to the vocal ligament could be found. Reticular and collagenous fibers were seen throughout the entire lamina propria, running roughly parallel to the vocal fold edge (Fig 6). There were elastic fibers in Reinke's space, but their density was sparse (Fig 6A).

Fibroblasts. In infant maculae flavae, many fibroblasts were noted, and their density was also high (Fig 7). Many fibroblasts were stellate in shape (Fig 7) and had a small nucleus-cytoplasm ratio. The rough endoplasmic reticulum and Golgi apparatus in the cytoplasm were developed. Newly released amorphous material was present on the cell surfaces. Some fibers were seen close to fibroblasts. Stellate fibroblasts showed strong cytoplasmic staining with periodic acid–Schiff stain (Fig 7A) and type III collagen (Fig 7B). Type I collagen stained few components in the cytoplasm.

Fibroblasts were sparse in Reinke's space of the infant vocal fold mucosa. Many fibroblasts were spindle-shaped. The nucleus-cytoplasm ratio was large, and the cytoplasm occupied a small area around the nucleus. The rough endoplasmic reticulum and Golgi apparatus were not well developed, indicating that the fibroblasts were in the resting phase. Few vesicles were present along the periphery of the cytoplasm. Newly released amorphous material was scarce on the surfaces of the fibroblasts. Few fibers were situated close to fibroblasts. Periodic acid–Schiff stain, type I collagen, and type III collagen stained few components in the cytoplasm of fibroblasts in Reinke's space.

Collagenous Fibers and Reticular Fibers. Reticular and collagenous fibers were increased through-

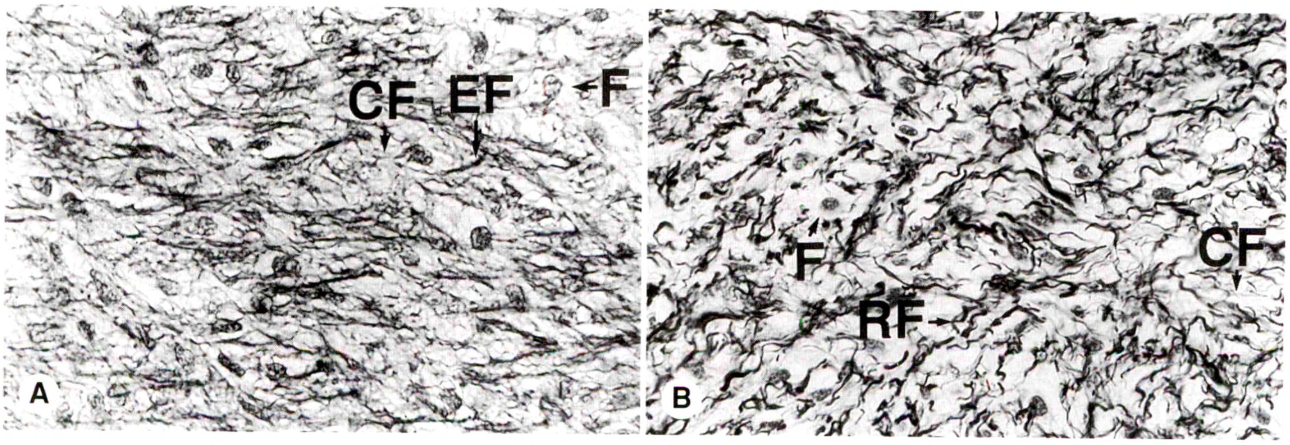

Fig 5. Infant maculae flavae (original ×400). CF — collagenous fiber, F — fibroblast. **A)** Elastica–van Gieson stain. EF — elastic fiber. **B)** Silver stain. RF — reticular fiber.

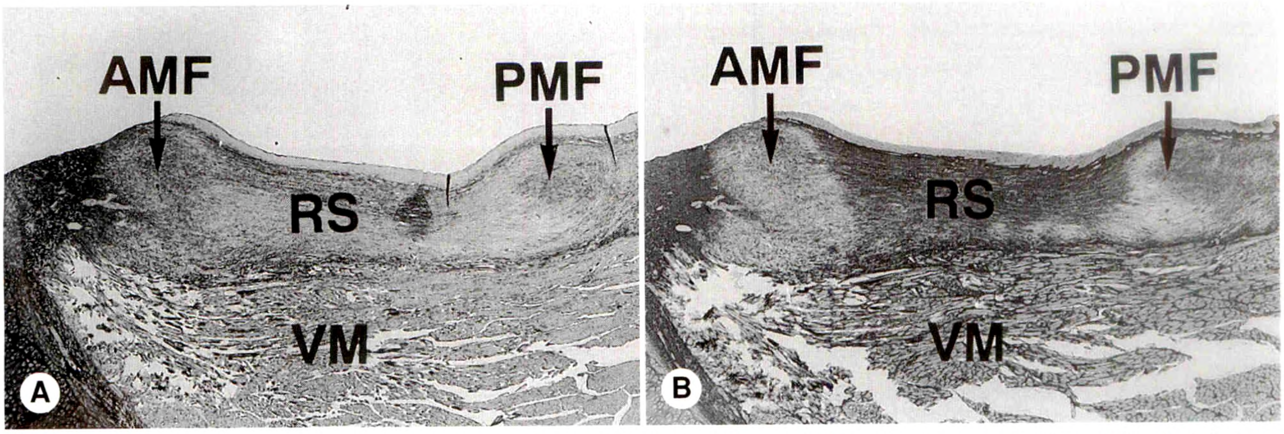

Fig 6. Horizontal sections of vocal fold from 6-month-old girl (original ×12.5). AMF — anterior macula flava, RS — Reinke's space, PMF — posterior macula flava, VM — vocalis muscle. **A**) Elastica–van Gieson stain. **B**) Silver stain.

out the entire Reinke's space of the infant vocal fold mucosa as compared to that of newborns, and ran roughly parallel to the vocal fold edge (Fig 8A). The collagenous fibers were made up of numerous collagenous fibrils approximately 50 nm in width. Their structure was nearly mature morphologically. The reticular fibers were made up of unit fibrils, were about 40 nm in diameter, and had cross-bands with a periodicity of about 67 nm (Fig 8B). The slender fibrils did not form bundles (Fig 8B). Stellate fibroblasts in the infant maculae flavae were synthesizing collagenous and reticular fibers.

Elastic Fibers. Elastic fibers could be seen in the lamina propria of the infant vocal fold mucosa at low density and were composed of abundant microfibrils and sparse and reticular amorphous substances. The elastic fibers were immature, but increased in amount over time in Reinke's space after collagenous and reticular fibers appeared in the space. Stellate fibroblasts in the infant maculae flavae were synthesizing elastic fibers.

Ground Substance. The ground substance showed some flocculent material stained with tannic acid in the lamina propria. The glycoprotein (fibronectin) in Reinke's space decreased over time with the increase of fibrous components immunohistochemically.

The infant maculae flavae were heavily stained light blue with Alcian blue at pH 2.5 (Fig 9), but were relatively weakly stained with Alcian blue at pH 1. The material that strongly stained in the maculae flavae with Alcian blue (pH 2.5) was digested by hyaluronidase. Much glycosaminoglycan, especially hyaluronic acid, was actively produced in the infant maculae flavae.

PERIOD OF GROWTH INITIATION OF HUMAN VOCAL FOLD MUCOSA

In infancy, many fibroblasts in the maculae flavae had become stellate in shape and actively synthesized extracellular matrices, especially reticular and collagenous fibers. Glycoproteins (fibronectin) in Reinke's space appeared to determine the orientation of deposition of reticular and collagenous fibers synthesized in the maculae flavae. Many reticular

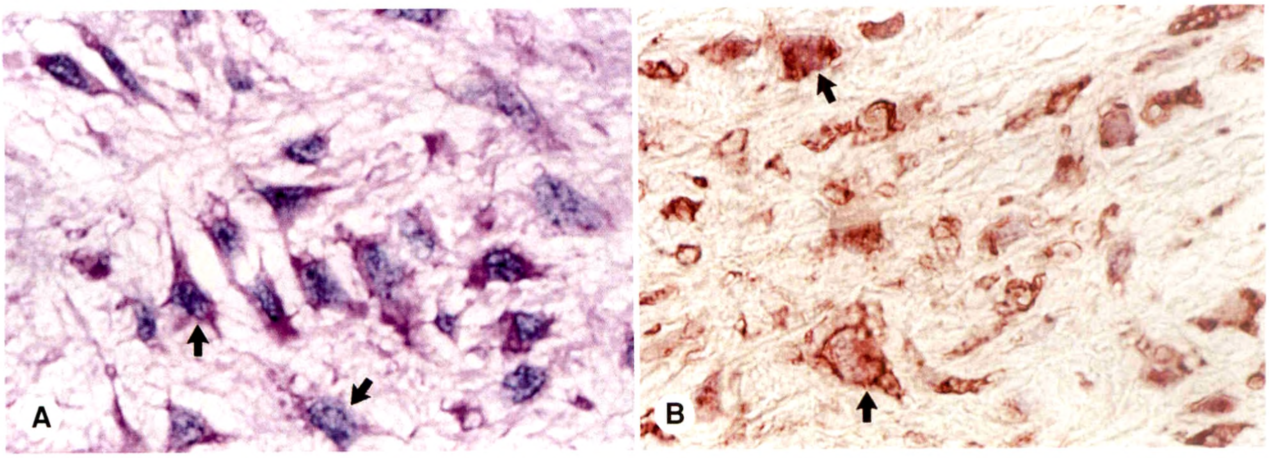

Fig 7. Infant maculae flavae (original ×400). **A**) Stellate fibroblasts (arrows) show heavy cytoplasm staining with periodic acid–Schiff stain. **B**) Type III collagen in cytoplasm of stellate fibroblasts (arrows) is shown with immunohistochemical staining.

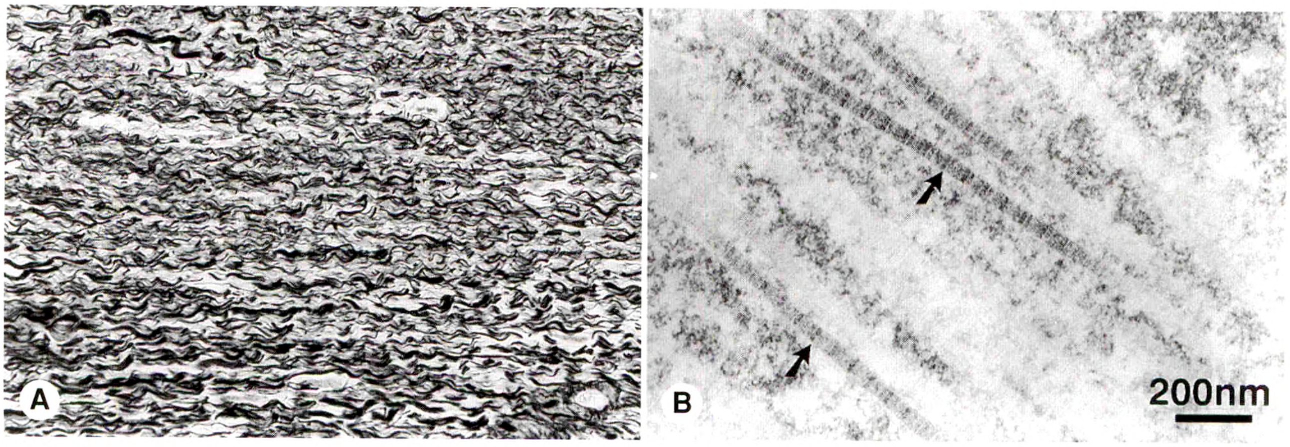

Fig 8. Infant Reinke's space. **A)** Horizontal section (6-month-old girl, silver stain, original ×200). Reticular and collagenous fibers run parallel to vocal fold edge. **B)** Transmission electron micrograph of reticular fibers (arrows; uranyl acetate and lead citrate stain).

and collagenous fibers extended from the maculae flavae toward the middle of Reinke's space. Fibrillar collagen, such as reticular and collagenous fibers, served as a stabilizing scaffold and possessed innumerable potential spaces. The extracellular interstitial spaces were made up of minute chambers or compartments occupied by other extracellular matrices, such as elastic fibers and glycosaminoglycan (hyaluronic acid).

During infancy, extracellular matrices, synthesized in the maculae flavae, appeared in Reinke's space of the vocal folds at different times to initiate 3-dimensional structural formation of the vocal fold mucosa.

DISCUSSION

In adults, the superficial layer of the lamina propria vibrates most markedly during phonation, and its viscoelasticity is essential for vibration. The delicate 3-dimensional structure of reticular fibers in the vocal fold mucosa is essential for the structural maintenance and viscoelasticity of vibrating tissues.[5] The complex of reticular fibers and other extracellular matrices, such as elastic fibers and glycosaminoglycan (proteoglycan), is required for the viscoelasticity of the vocal fold mucosa.[5]

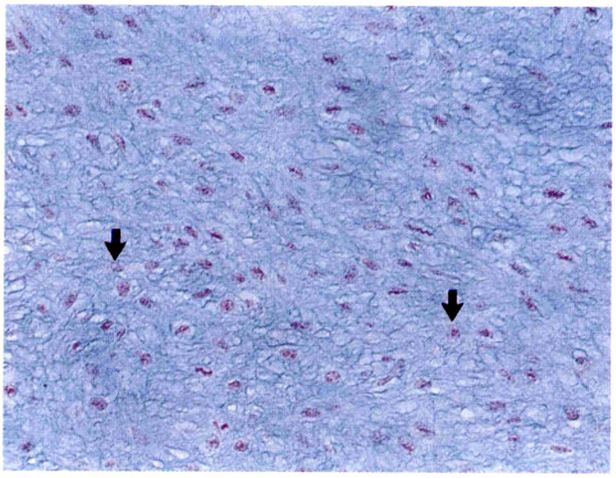

Fig 9. Hyaluronic acid (glycosaminoglycan) in infant macula flava shown by Alcian blue staining (pH 2.5; 6-month-old girl; original ×200). Hyaluronic acid (glycosaminoglycan) is detected by light blue color. Arrows — stellate fibroblasts.

The fine structure of the maculae flavae of the adult vocal fold has been described.[6] Adult maculae flavae control the synthesis of fibrous components such as the vocal ligament.[6,7] In adult maculae flavae, there are many stellate cells (nonconventional fibroblasts) with the following morphological characteristics[7]: 1) stellate in shape; 2) lipid droplets and well-developed endoplasmic reticulum present in their cytoplasm; 3) strong cytoplasmic staining with periodic acid–Schiff stain and type III collagen; 4) active synthesis of extracellular matrices, such as reticular fibers, collagenous fibers, elastic fibers, and glycosaminoglycan (hyaluronic acid); and 5) involvement in the metabolism of extracellular matrices in the vocal fold mucosa.

At birth, there is no structure to be found corresponding to the vocal ligament or the layered structure of the adult vocal fold.[2,3] Under a light microscope, the entire lamina propria appears as a roughly uniform structure,[2,3] and Reinke's space of the newborn vocal fold resembles the superficial layer of the lamina propria of the adult vocal fold.[3]

Electron microscopy and immunohistochemical investigation showed Reinke's space of the newborn vocal folds to be abundant in glycoprotein, especially fibronectin. Fibrous components, such as reticular fibers, were not well developed. Reinke's space of the newborn vocal fold mucosa had no special structure such as that noted in adults. The delicate 3-dimensional structure of reticular fibers seen in the adult vocal fold mucosa was not present. No complex of reticular fibers and other extracellular matrices, such as elastic fibers and glycosaminoglycan (proteoglycan), could be detected. Collagenous fibers were sparse and essentially mature, but elastic fibers were immature. Collagenous fibers have supportive functions, and elastic fibers have sufficient resilience to return to their original state.[8] The viscoelasticity of the newborn vocal fold mucosa was morphologically seen not to be sufficient for phonation. The lamina propria of the newborn vocal folds lacked not only a vocal ligament and a layered structure, but also the characteristic complex of extracellular matrices seen in the adult, and therefore the viscoelasticity for vibration was inadequate.

Fibroblasts are sparse in Reinke's space of the newborn vocal fold mucosa, but the density is greater than in adults.[2,9] The fibroblasts in the membranous portion of the newborn vocal folds are not in the active phase, but rather, in the resting phase.[9]

Newborns already have maculae flavae at the same sites as in adults.[2-4] The fibroblasts in newborn maculae flavae are immature and possess some features of mesenchymal cells.[4] Some fibroblasts are already synthesizing collagenous and elastic fibers.[4] Phonation (vocal fold vibration) following birth may stimulate the fibroblasts in the maculae flavae and activate them to form fibrous components.[4] The maculae flavae in newborn vocal folds are important structures that are essential to the growth and development of the vocal ligament.[4]

The basic functions of the larynx are to act as a protective sphincter, as a passageway for air, and in sound production. The posterior glottis is important for respiration.[10] In the newborn, the area of the intercartilaginous portion (posterior glottis) relative to the entire glottic area is greater than in adults.[2] The newborn vocal fold mucosa has no layered structure. The newborn vocal fold mucosa appears morphologically not to have adequate viscoelasticity for phonation. From a functional point of view, the glottis of the newborn serves more for respiration than phonation.

In the infant maculae flavae, the fibroblasts had become stellate in shape and actively synthesized extracellular matrices such as reticular fibers, collagenous fibers, elastic fibers, and glycosaminoglycan (hyaluronic acid). In the maculae flavae of infant vocal folds, the fibrous components had increased as compared to the newborns. The number of elastic fibers was small compared with the numbers of reticular and collagenous fibers. The elastic fibers were immature morphologically. Much hyaluronic acid was produced.

Fibronectin is a glycoprotein that serves as a template for the oriented deposition of collagen.[11] It acts as an interfibrillar stabilizing factor between collagen fibrils and as a skeleton for elastic tissue formation and is involved with aggregation of proteoglycans.[11]

Reticular and collagenous fibers synthesized in infant maculae flavae extended toward the middle of the membranous portion of the vocal folds, in which glycoprotein (fibronectin) was abundant. Glycoproteins (fibronectin) in Reinke's space appeared to direct the oriented deposition of reticular and collagenous fibers. Reticular and collagenous fiber formation may be induced in Reinke's space of infant vocal folds with growth. Glycoprotein (fibronectin) decreased with the increase of the fibrous components in Reinke's space. Fibronectin acts as an interfibrillar stabilizing factor between collagen fibrils and is involved in the aggregation of elastic fibers and glycosaminoglycan (proteoglycan). Glycoprotein plays the role of a skeleton for elastic tissue formation in the infant vocal fold mucosa.

To summarize, fibrillar collagen, such as reticular and collagenous fibers, serves as a stabilizing scaffold in extracellular matrices[12] and possesses innumerable potential spaces.[5] These extracellular interstitial spaces are made up of minute chambers or compartments occupied by other extracellular matrices, such as elastic fibers and glycosaminoglycan (proteoglycan).[5] In this manner, the complex of reticular fibers and other extracellular matrices important for the viscoelasticity of the vocal fold mucosa[5] is formed.

The extracellular matrices of human adult vocal folds are collagenous fibers, reticular fibers, elastic fibers, glycoprotein, and glycosaminoglycan (proteoglycan).[5] During infancy, extracellular matrices synthesized in the maculae flavae appear in the membranous portion of the vocal fold at different times to initiate the formation of the 3-dimensional extracellular matrix structure of the vocal fold mucosa that has the viscoelastic properties of a vibrating structure.

ACKNOWLEDGMENTS — We are grateful to Dr Yasuhiro Nakamura and Dr Yuuji Ito, St Mary's Hospital, Kurume, for providing the cadaver larynges.

REFERENCES

1. Hirano M. Phonosurgery. Basic and clinical investigations. Otologia (Fukuoka) 1975;21(suppl 1):239-60.

2. Hirano M, Sato K. Histological color atlas of the human larynx. San Diego, Calif: Singular Publishing Group, 1993:18-21.

3. Hirano M, Kurita S, Nakashima T. Growth, development and aging of human vocal folds. In: Bless DM, Abbs JH, eds. Vocal fold physiology. San Diego, Calif: College-Hill Press,

1983:22-43.

4. Sato K, Hirano M. Histologic investigation of the macula flava of the human newborn vocal fold. Ann Otol Rhinol Laryngol 1995;104:556-62.

5. Sato K. Reticular fibers in the vocal fold mucosa. Ann Otol Rhinol Laryngol 1998;107:1023-8.

6. Sato K, Hirano M. Histologic investigation of the macula flava of the human vocal fold. Ann Otol Rhinol Laryngol 1995; 104:138-43.

7. Sato K, Hirano M, Nakashima T. Stellate cells in the human vocal fold. Ann Otol Rhinol Laryngol 2001;110:319-25.

8. Fawcett DW. A textbook of histology. Philadelphia, Pa: WB Saunders, 1986:136-51.

9. Hirano M, Sato K, Nakashima T. Fibroblasts in human vocal fold mucosa. Acta Otolaryngol (Stockh) 1999;119:271-6.

10. Hirano M, Kurita S, Kiyokawa K, Sato K. Posterior glottis. Morphological study in excised human larynges. Ann Otol Rhinol Laryngol 1986;95:576-81.

11. Anderson JC. Glycoproteins of the connective tissue matrix. In: Hall DH, Jackson DS, eds. International review of connective tissue research. Vol 7. New York, NY: Academic Press, 1976:251-322.

12. Kreis T, Vale R. Guidebook to the extracellular matrix and adhesive proteins. Oxford, England: Oxford University Press, 1993.

≈

NINTH INTERNATIONAL FACIAL NERVE SYMPOSIUM

The Ninth International Facial Nerve Symposium will be held July 29 to August 1, 2001, in San Francisco, California. For information, contact Office of Continuing Medical Education, University of California, San Francisco; telephone: (415) 476-5808; fax: (415) 502-1795; e-mail: info@ocme.ucsf.edu.

Ann Otol Rhinol Laryngol 110:2001

PRESENCE OF AUTOANTIBODIES IN THE SERA OF MENIERE'S DISEASE

T. J. Yoo, MD, PhD
Memphis, Tennessee

John Shea, Jr, MD
Memphis, Tennessee

Xianxi Ge, MD
Memphis, Tennessee

Soon Seog Kwon, MD, PhD
Memphis, Tennessee

Yoshiro Yazawa, MD, PhD
Otsu, Japan

Osman Sener, MD
Memphis, Tennessee

Francesco Mora
Genoa, Italy

Renzo Mora
Genoa, Italy

Massimilliano Mora
Genoa, Italy

Marco Barbieri, MD
Genoa, Italy

Xiaoping Du
Memphis, Tennessee

We examined the sera of patients with Meniere's disease for the presence of antibodies against 8 inner ear antigens by enzyme-linked immunosorbent assay (ELISA). One hundred eight patients with Meniere's disease and 28 control subjects were studied. The antibodies against chicken type II collagen, bovine type II collagen, the cyanogen bromide cleaved peptide 11 (CB11) of each, type IX and XI collagens, C-Raf, and tubulin were measured by ELISA. The sensitivity of each antigen was between 37% and 60% individually, and was 91% when all 8 inner ear antigens were combined. These results showed that 91% of Meniere's disease sera have antibody activities to 1 or more of these inner ear antigens. The results suggest that performing ELISA for these 8 inner ear antigens was useful as a diagnostic tool for Meniere's disease. Further study is required for elucidating the role of these antigens in the pathogenesis of Meniere's disease, which might eventually result in better therapy.

KEY WORDS — autoantibody, enzyme-linked immunosorbent assay, Meniere's disease, serum.

INTRODUCTION

Since McCabe[1] first described autoimmune sensorineural hearing loss, now accepted as autoimmune inner ear disease,[2] a number of experimental and clinical studies have been reported in the field of otoimmunology.[3-7] These reports presented evidence that the pathogenesis of Meniere's disease might be related to autoimmunity, but they have not fully confirmed the autoimmune pathological mechanisms. One of the main reasons is that the inner ear antigens targeted by the immune system have not been identified, although attempts to find the antigens have been promising. Our laboratory has reported that type II collagen might have a key role as the inner ear antigen in Meniere's disease and otosclerosis.[3,8] Helfgott et al[9] suggested that type II collagen may be important in the pathogenesis of bilateral progressive sensorineural hearing loss (PSNHL).

In a previous investigation with Western blotting, we found that 3 of 6 patients with Meniere's disease had antibodies directed against a 30 kd protein extracted from the human inner ear.[8] Using guinea pig inner ear extract, Cao et al[10] demonstrated that a 30 kd band was detected in sera from patients with various forms of hearing loss, including PSNHL, in accordance with the findings of our study.

A 28 kd protein in the membranous fraction of the inner ear of guinea pigs positively reacted with sera from patients with Meniere's disease.[11] This 28 kd protein has been purified, microsequenced, and identified as one of the signal transduction proteins, Raf-1.[12]

We have just sequenced another inner ear antigen from guinea pigs and found it to be a β-tubulin that binds sera from Meniere's disease.[13] This study examines the presence of antibodies in the sera of patients with Meniere's disease against 8 antigens: chicken and bovine type II collagens and the cyanogen bromide cleaved peptide (CB11) of each, type IX and XI collagens, C-Raf, and tubulin.

MATERIALS AND METHODS

Sera from 108 patients with Meniere's disease were supplied courtesy of Dr John Shea of the Shea Clinic. The diagnosis of Meniere's disease was based on the criteria of the American Academy of Otolaryngol-

---

From the Division of Allergy and Immunology, Department of Medicine, University of Tennessee, Memphis, Tennessee (Yoo, Kwon, Sener, Du), the Department of Otolaryngology, Shiga University of Medical Science, Otsu, Japan (Yazawa), and the Department of Otolaryngology, University of Genoa, Genoa, Italy (F. Mora, R. Mora, M. Mora, Barbieri). This study was supported in part by grant DC RO-1-00652 from the National Institutes of Health, Biotec 2000, the Republic of Korea Ministry of Science and Technology, and The Shea Foundation.

CORRESPONDENCE — T. J. Yoo, MD, PhD, Division of Allergy and Immunology, Dept of Medicine, University of Tennessee, Memphis, TN 38163.

RESULTS OF ENZYME-LINKED IMMUNOSORBENT ASSAY (N = 108)

	Positive		*Negative*	
Antigen	*No.*	*%*	*No.*	*%*
C CB11	46	41	62	59
B CB11	41	38	67	62
CII	44	41	64	59
BII	48	44	60	56
IX	41	38	67	62
XI	45	42	63	58
C-Raf	59	55	49	45
Tubulin	66	61	42	39
A (C CB11 + B CB11 + CII + BII)	72	67	36	33
IX + XI	59	55	49	45
A + (IX + XI)	83	77	26	23
C-Raf + tubulin	86	80	22	20
All antigens	98	91	10	9

C CB11 — cyanogen bromide fragment of chicken type II collagen, B CB11 — cyanogen bromide fragment of bovine type II collagen, CII — chicken type II collagen, BII — bovine type II collagen, IX — type IX collagen, XI — type XI collagen.

ogy–Head and Neck Surgery,[14] and sera from 28 healthy normal controls were obtained.

Type II collagens and their CB11 peptide and type IX and XI collagens were obtained as previously described.[15-18] C-Raf was obtained as described,[12] and tubulin was obtained commercially (ICN, Irvine, Calif).

The specific antibodies from the sera from patients with Meniere's disease and those from the 28 control subjects were examined with an enzyme-linked immunosorbent assay as follows: 50 μL of 8 antigens (4 to 5 μg/mL) were dispensed in each well of a polystyrene microtiter plate and incubated overnight at 4°C. After washing with 0.05% phosphate-buffered saline solution–Tween buffer, the plate was incubated with sera (1:20, 1:40, 1:80, or 1:160 dilution), or normal goat serum as a control, overnight at 4°C. The plates were washed with 0.05% phosphate-buffered saline solution–Tween buffer and incubated overnight with heavy-chain–specific anti-human IgG antibodies at 4°C. The plates were washed 5 times before the addition of a citric acid–phosphate buffer (pH 5.0) containing 0.15 mg/mL of *o*-phenylenediamine. The color was developed at room temperature, and the reaction was stopped by 2.5-mol/L sulfuric acid. The color was measured at 492 nm.

RESULTS

The results of the enzyme-linked immunosorbent assay are summarized in the Table. The antibodies against type II collagens (chicken and bovine, respectively) were present in 41% and 44% of the sera from patients with Meniere's disease.

Respectively, 41% and 38% of the sera from patients with Meniere's disease reacted to the CB11 peptides of chicken and bovine type II collagens. Type IX collagen showed 38% binding activity with Meniere's sera and type XI collagen showed 42%. C-Raf and tubulin showed 55% and 61% binding activity, respectively.

If type II collagens and their CB11 peptides are all combined, binding activity was present in 67% of the sera from patients with Meniere's disease (72 of 108). The combined type IX and XI collagen binding activity was 55% (59 of 108). The binding activity for the combination of types of collagen II, their CB11 fragments, and collagens IX and XI was 77% (83 of 108).

The combination of C-Raf and tubulin binding activities was 80% (86 of 108). If all 8 antigens are combined, 91% of sera specimens showed binding activity to 1 or more of the 8 antigens. The control sera showed universally low binding activity: 1 of 28 sera with CB11 or C-Raf protein, 2 with bovine type II collagen, 3 with chicken type II collagen, 1 with type IX collagen, and none with tubulin or type XI collagen.

DISCUSSION

Meniere's disease is an idiopathic inner ear disease with the triad of fluctuating hearing loss, episodic vertigo, and tinnitus. Since McCabe coined the term "autoimmune sensorineural hearing loss," it has been recognized that some cases of Meniere's disease could be caused by an autoimmune response to inner ear tissues. The immune mechanisms of Meniere's disease have yet to be fully defined. The weight of recent evidence strongly implicates immunologic or chronic inflammatory processes, or both, as contributing to the pathogenesis of this illness. Several key factors, such as TH cells, B cells, MHC antigen, and cytokines, contribute to the immune response in inner ear diseases.

An increase in anti–type II collagen antibodies from sera of patients with Meniere's disease, otosclerosis, idiopathic PSNHL, or sudden deafness has been identified.[3,8,9] In an animal model study, immunization of type II collagen or CB11 (a cyanogen bromide–digested type II collagen fragment) induced autoimmune ear disease.[19] In other studies, diseased animals suffered spiral ganglion cell degeneration, atrophy of Corti's organ, cochlear vasculitis and atrophy of the stria vascularis, endolymphatic hydrops with atrophy of the surface epithelium of the endolymphatic duct, otospongiotic changes of the bone of the external meatus and otic capsule, hearing loss, and vestibular dysfunction.[20-28] Chicken type II collagen is distributed widely in the inner, middle, and external ear.[29-31]

In 1982, Yoo et al[3] reported that levels of antibodies to type II collagen were significantly higher (41.7%) in patients with Meniere's disease and otosclerosis. Since then, several investigators have reexamined type II collagen antibody in Meniere's disease, and some obtained the same positive results,[8,9,32,33] although some showed negative results.[34,35] Type IX collagen seems to be another candidate for autoimmunity in the inner ear.[8] Type XI collagen could also be another autoantigen.

TH cells have been shown to play a pivotal role in several autoimmune diseases. The discovery by Guild[36] in 1927 that endolymph flows from the cochlear duct to the endolymphatic sac (ES) has led to proposals that the ES acts as an immunodefensive organ in the inner ear. Rask-Andersen and Stahle[37] identified immune cells, including lymphocytes and macrophages, in the ES and adjacent tissue in the inner ear of guinea pigs. The distribution of these immunocompetent cells is Thy 1+ (TH cells) within the ES epithelium and in the perisaccular region, and macrophages in the lumen of the distal portion of the ES.[38,39] The ES is surrounded by a rich network of lymphatic capillaries and blood vessels. It has the necessary immunologic components for antigen processing and for being the active site for a local immunodefense.[40] However, several studies indicate that the inner ear is not an immunoprivileged site for the initial antigen stimulation.[37,41,42] It is proposed that the immune cells initially activated in the periphery migrate from the systemic circulation to the ES and subsequently develop a response to antigen in the inner ear.[43] In animal studies, TH usage is restricted to the Vb8 subfamily (TCRBV8) in type II collagen–induced ear disease.[44]

A number of extracted proteins from bovine, guinea pig, or human inner ear had reactivity with sera from patients with inner ear disease.[8,10,11,45-48] Harris and Sharp[7] showed that 35% of sera specimens from patients with PSNHL reacted with a 68 kd protein from bovine inner ear extract proteins. This 68 kd protein was later identified as a 70 kd heat shock protein (hsp70).[49,50] The 68 kd inner ear antigen from Carey's group does not have any sequence homology with hsp70.[51] Their 68 kd protein binds to supporting cells in the organ of Corti, whereas hsp70 antibody does not bind to any site in the inner ear. They also showed that the hsp70 antibody level is the same in autoimmune inner ear disease as in the normal population, and they concluded that hsp70 does not play any role in autoimmune inner ear disease. Trune et al[52] could not induce hearing loss in experimental animals when they used hsp70 as an immunizing antigen. The Harris group also was not able to induce any ear lesions with hsp70 in animal models (Jeffrey Harris, personal communication, 1998). The human hsp70 does not bind Meniere's disease or autoimmune hearing loss patients' sera that bind other inner ear antigens (Yoo et al, unpublished observations). Furthermore, the patient's sera still bind 68 kd bovine inner ear antigen after the sera have been extensively absorbed with bovine hsp70 (Jeffrey Harris, personal communication, 1998).

A 30 kd protein extracted from the human inner ear has been reported by us to react with sera from patients with Meniere's disease.[8] Cao et al[53] reported that patients with PSNHL and those with Meniere's disease have an antibody against a 30 kd protein from the guinea pig inner ear. They have identified this 30 kd protein as a myelin PO protein derived from the acoustic nerve and spiral ganglion. Further study showed that a 28 kd protein in the membranous fraction of the inner ear of guinea pigs reacted positively with sera from patients with Meniere's disease.[11] This 28 kd protein has been purified and microsequenced. It has been identified as one of the signal transduction proteins: Raf-1.[12] So far, antigens for which human antibodies have been found in PSNHL or Meniere's disease are bovine 32-34 kd,[54] porcine 27, 45, 50, 68, and 80 kd,[55] guinea pig 42 and 58 kd,[10] bovine 220, 60, 58, 35, 33, 32 kd,[46,47] and guinea pig 25, 28, 30, 32, 40, 42, 46, 52, 67, 79 kd.[11] Thus, 32-35 kd, 42-46 kd, 52-58 kd, 67-68 kd, and 79-80 kd could be important antigens for autoimmune ear disease. These results suggest that multiple antigens are involved in autoimmune ear diseases. Among those, the 4 antigens Raf-1, PO, CII, and tubulin are so far the only antigens with defined molecular characteristics.

Raf-1 protein is highly conserved in mice, rats, chickens, *Xenopus laevis*, *Drosophila melanogaster*, and *Caenorhabditis elegans*. Raf is a serine/threonine-specific protein kinase that functions in a signal transduction pathway(s) between the cell membrane and the nucleus. The Raf-1 protein is a 74 kd protein that includes 3 conserved regions (CR). The CR1 (approximately 53 to 200 amino acids) and CR2 (a short sequence in the N terminal half) are considered to be critical for regulation of Raf-1 activity. The mutation of these regions activates the oncogenic potential of Raf-1.[56] On mitogen stimulation of resting cells, Raf-1 undergoes hyperphosphorylation, which correlates with an increase of Raf-1 kinase activity. Raf-1 then phosphorylates and activates MAP kinase kinase, which activates MAP kinase (Erk1/2), leading to transactivation of transcription from promoters bearing AP-1 (Jun/Fos), Ets, and other response elements. Raf-1 is required for activation of c-Jun via phosphorylation in the transactivation domain.[56] This sequence we identified here is not matched to A-Raf protein, a member of the Raf family that is highly expressed in the urogenital tissues, including the epididymus, ovary, prostate, kidney, and bladder. Because of the structural similarity of membrane tissue in the inner ear and urogenital tissue, we have suspected that A-Raf protein is highly expressed in the inner ear tissue. However, findings suggest that the expression of A-Raf protein in the inner ear tissue is much lower than that of Raf-1 protein.[12]

β-Tubulin is a molecule found in the microtubule and inner ear tissue. The amino acid sequence of a 55 kd protein from guinea pig inner ear membranes was a β-tubulin sequence. Combining the protein sequence data and the complementary DNA library cloning data, we were convinced that indeed, β-tubulin is an inner ear autoantigen in Meniere's disease.[13]

Further study of the level of antibody to 68 kd antigen and 30 kd PO antigen and the relationship of the above antibodies to the 8 antigens we studied would also be beneficial for further understanding of the autoimmunity of Meniere's disease. This study shows the presence of multiple autoantibodies in patients with Meniere's disease, which suggests that Meniere's disease may be an autoimmune disorder. The sensitivity for the antigens was between 38% and 61% individually, and 91% when all 8 antigens were combined. The specificity was 79%.

However, this carefully performed enzyme-linked immunosorbent assay for the measurement of autoantibodies to these 8 antigens could provide us with useful information. Further study is required to define the role of these autoantibodies in the pathogenesis of Meniere's disease.

REFERENCES

1. McCabe BF. Autoimmune sensorineural hearing loss. Ann Otol Rhinol Laryngol 1979;88:585-9.
2. McCabe BF. Autoimmune inner ear disease. In: Veldman JE, McCabe BF, Huizing EH, Mygind N, eds. Immunobiology, autoimmunity, and transplantation in otorhinolaryngology. Amsterdam, the Netherlands: Kugler, 1985:107-10.
3. Yoo TJ, Stuart JM, Kang AH, Townes AS, Tomoda K, Dixit S. Type II collagen autoimmunity in otosclerosis and Meniere's disease. Science 1982;217:1153-5.
4. Yoo TJ, Yazawa Y, Tomoda K, Floyd R. Type II collagen–induced autoimmune endolymphatic hydrops in guinea pig. Science 1983;222:65-7.
5. Tomiyama S, Harris JP. The endolymphatic sac: its importance in inner ear immune responses. Laryngoscope 1986;96: 685-91.
6. Arnold W, Pfaltz CR. Critical evaluation of the immunofluorescence microscopic test for identification of serum antibodies against human inner ear tissue. Acta Otolaryngol (Stockh) 1987;103:373-8.
7. Harris JP, Sharp PA. Inner ear autoantibodies in patients with rapidly progressive sensorineural hearing loss. Laryngoscope 1990;100:516-24.
8. Joliat T, Seyer J, Bernstein J, et al. Antibodies against a 30 kilodalton cochlear protein and type II and IX collagens in the serum of patients with inner ear disease. Ann Otol Rhinol Laryngol 1992;101:1000-6.
9. Helfgott SM, Moscicki RA, Martin JS, et al. Correlation between antibodies to type II collagen and treatment outcome in bilateral progressive sensorineural hearing loss. Lancet 1991; 337:387-9.
10. Cao MY, Gersdorff M, Deggouj N, Warny M, Tomasi JP. Detection of inner ear disease autoantibodies by immunoblotting. Mol Cell Biochem 1995;146:157-63.
11. Suzuki M, Krug MS, Cheng KC, Yazawa Y, Bernstein J, Yoo TJ. Antibodies against inner ear protein in the sera of patients with inner ear diseases. ORL J Otorhinolaryngol Relat Spec 1997;59:10-7.
12. Cheng K-C, Matsuoka H, Lee KM, et al. Proto-oncogene Raf-1 as an autoantigen in Meniere's disease. Ann Otol Rhinol Laryngol 2000;109:1093-8.
13. Yoo TJ, Tanaka H, Krug MS. β-Tubulin as an autoantigen in Meniere's disease. ARO Abstracts 1999: abstract 825.
14. Pearson BW, Brackmann DE. Committee on Hearing and Equilibrium guidelines for reporting treatment results in Meniere's disease. Otolaryngol Head Neck Surg 1985;93:579-81.
15. Terato K, Hasty KA, Cremer MA, Stuart JM, Townes AS, Kang AH. Collagen-induced arthritis in mice: localization of an arthritogenic determinant to a fragment of the type II collagen molecule. J Exp Med 1985;162:637-46.
16. Stuart JM, Cremer MA, Kang AH, Townes AS. Collagen-induced arthritis in rats: evaluation of early immunologic event. Arthritis Rheum 1979;22:1344-51.
17. Miller ED. Isolation and characterization of the cyanogen bromide peptides from the αI(II) chain of chick cartilage collagen. Biochemistry 1971;10:3030-5.
18. Reese LA, Mayne R. Minor collagens of chicken hyaline cartilage. Biochemistry 1981;20:5443-8.
19. Takeda T, Sudo N, Kitano H, Yoo TJ. Type II collagen-induced autoimmune ear disease in mice: a preliminary report on an epitope of the type II collagen molecule that induced inner ear lesions. Am J Otol 1996;17:69-75.
20. Yoo TJ, Tomoda K, Hernandez AD. Type II collagen–induced autoimmune inner ear lesions in guinea pigs. Ann Otol Rhinol Laryngol Suppl 1984;93(suppl 113):3-5.
21. Yoo TJ, Tomoda K, Stuart JM, Cremer MA, Townes AS, Kang AH. Type II collagen-induced autoimmune sensorineural hearing loss and vestibular dysfunction in rats. Ann Otol Rhinol Laryngol 1983;92:267-71.
22. Yoo TJ, Yazawa Y, Tomoda K, Floyd RA. Type II collagen induced autoimmune endolymphatic hydrops in guinea pig. Science 1983;222:65-7.
23. Soliman AM. Type II collagen induced inner ear disease: critical evaluation of the guinea pig model. Am J Otol 1990; 11:127-32.
24. Huang C, Saporta D, Abramson M. Immunologically in-

duced salpingitis in rats. Am J Otolaryngol 1985;6:368-72.

25. Huang C. Bone resorption in experimental otosclerosis in rats. Am J Otolaryngol 1987;8:332-41.

26. Cruz OLM, Miniti A, Cossermelli W, Oliveira RM. Autoimmune sensorineural hearing loss: a preliminary experimental study. Am J Otol 1990;11:342-6.

27. Tomoda K, Maeda N, Yamawaki T, Yamashita T, Kumazawa T, Ohashi T. Immunologically induced experimental hydrops: its mechanisms and pathology. In: Nadol JB, ed. 2nd International Symposium on Meniere's Disease. Amsterdam, the Netherlands: Kugler, 1989:165-72.

28. Tomoda K, Yamawaki T, Suzuka Y, Yamashita T, Kumazawa T. Inner ear immunology and the changes of charge barrier. Ear Res (Japan) 1988;19:356-8.

29. Yoo TJ, Tomoda K. Type II collagen distribution in rodents. Laryngoscope 1988;98:1255-60.

30. Slepecky NB, Savage JE, Yoo TJ. Localization of type II, IX and V collagen in the inner ear. Acta Otolaryngol (Stockh) 1992;112:611-7.

31. Slepecky NB, Cefaratti LK, Yoo TJ. Type II and type IX collagen form heterotypic fibers in the tectorial membrane of the inner ear. Matrix 1992;11:80-6.

32. Fattori B, Ghilardi PL, Gasani A. Immunological aspects of Meniere's disease. Rev Laryngol Otol Rhinol (Bord) 1991; 112:117-9.

33. Tomoda K, Suzuka Y, Iwai H, Yamashita T, Kumazawa T. Meniere's disease and autoimmunity: clinical study and survey. Acta Otolaryngol Suppl (Stockh) 1993(suppl 500):31-4.

34. Klein R, Timpl R, Zanetti FR, Plester D, Berg PA. High antibody levels against mouse laminin with specificity for galactosyl-(α1-3)galactose in patients with inner ear diseases. Ann Otol Rhinol Laryngol 1989;98:537-42.

35. Herdman RCD, Morgan K, Hold JL, Ramsden RT. Type II collagen autoimmunity and Meniere's disease. J Laryngol Otol 1993;107:994-8.

36. Guild SR. Observations upon the structure and normal contents of the ductus and saccus endolymphaticus in the guinea pig (*Cavia cobaby*). Am J Anat 1927;39:1-4.

37. Rask-Andersen H, Stahle J. Immunodefence of the inner ear? Lymphocyte-macrophage interaction in the endolymphatic sac. Acta Otolaryngol (Stockh) 1980;89:283-94.

38. Takahashi M, Harris JP. Anatomic distribution and localization of immunocompetent cells in normal mouse endolymphatic sacs. Acta Otolaryngol (Stockh) 1988;106:409-16.

39. Bui HT, Linthicum FH, Hofman FM, Bowman CA, House WF. An immunohistochemical study of the endolymphatic sac in patients with acoustic tumors. Laryngoscope 1989;89: 775-8.

40. Ichimiya I, Kawauchi H, Fujiyoshi T, Tanaka T, Mogi G. Distribution of immunocompetent cells in normal nasal mucosa: comparisons among germ-free, specific pathogen–free, and conventional mice. Ann Otol Rhinol Laryngol 1991;100:638-42.

41. Tomiyama S, Harris JP. The endolymphatic sac: its importance in inner ear immune response. Laryngoscope 1986;96:685-91.

42. Tomiyama S, Harris JP. The role of the endolymphatic sac in the inner ear immunology. Acta Otolaryngol (Stockh) 1987;103:182-8.

43. Kawauchi H, Ichimiya I, Kaneda N, Mogi G. Distribution of immunocompetent cells in the endolymphatic sac. Ann Otol Rhinol Laryngol Suppl 1992;101(suppl 157):39-47.

44. Yoo TJ, Lee MK, Min YS, et al. Epitope specificity and T cell receptor usage in type II collagen induced autoimmune ear disease. Cell Immunol 1994;157:249-62.

45. Rauch SD, SanMartin J, Moscicki RA. Bovine temporal bones as a source of inner ear antigen. Ann Otol Rhinol Laryngol 1992;101:688-90.

46. Yamanobe S, Harris J. Inner ear specific autoantibodies. Laryngoscope 1993;103:319-25.

47. Yamanobe S, Harris JP. Extraction of inner ear antigens for studies in inner ear autoimmunity. Ann Otol Rhinol Laryngol 1993;102:22-7.

48. Kosaka K, Yamanobe S, Tomiyama S, Yagi T. Inner ear autoantibodies in patients with sensorineural hearing loss. Acta Otolaryngol Suppl (Stockh) 1995(suppl 519):176-7.

49. Moscicki RA, Martin JES, Unintero CH, Rauch SD, Nadol JB Jr, Bloch KJ. Serum antibody to inner ear proteins in patients with progressive hearing loss, correlation with disease activity and response to corticosteroid treatment. JAMA 1994; 272:611-6.

50. Billings PB, Keithley EM, Harris JP. Evidence linking the 68 kilodalton antigen identified in progressive sensorineural hearing loss patient sera with heat shock protein 70. Ann Otol Rhinol Laryngol 1995;104:181-8.

51. Ramakrishnam A, Arts HA, Telian S, Carey TE. Assessing human sera for antibodies to the KHR1-3 inner ear antigen and HSP-70 protein. ARO Abstracts 1999: abstract 637.

52. Trune DR, Kempton RB, Mitchell CR, Hefeneiden SH. Failure of elevated heat shock protein 70 antibodies to alter cochlear function in mice. Hear Res 1998;116:65-70.

53. Cao MY, Deggouj N, Gersdorf M, Tomasi JP. Extraction of guinea pig inner ear antigens and its application for human autoimmune inner ear disease. Laryngoscope 1996;106:207-12.

54. Gottschlich S, Billings PB, Keithley EM, Weisman MH, Harris JP. Assessment of serum antibodies in patients with rapidly progressive sensorineural hearing loss and Meniere's disease. Laryngoscope 1995;105:1347-52.

55. Veldman JF, Hanada T, Meeuwsen F. Diagnostic and therapeutic dilemmas in rapidly progressive sensorineural hearing loss and sudden deafness. Acta Otolaryngol (Stockh) 1993;113: 303-6.

56. Blenis J. Signal transduction via the MAP kinase: proceed at your own RSK. Proc Natl Acad Sci U S A 1993;90:5889-92.

Ann Otol Rhinol Laryngol 110:2001

PERILYMPHATIC FISTULA AND MENIERE'S DISEASE

CLINICAL SERIES AND LITERATURE REVIEW

DENNIS C. FITZGERALD, MD
WASHINGTON, DC

There continues to be considerable confusion concerning the diagnosis and treatment of perilymphatic fistulas (PLFs) and Meniere's disease. This paper reports an 8-year experience with patients whose symptoms were compatible with Meniere's disease but who had some other element that raised the possibility of their having a PLF. This review is a retrospective report on 64 patients who had fluctuating hearing loss, vertigo, tinnitus, and aural fullness typical of Meniere's disease. However, they also had a positive fistula test and/or symptoms beginning immediately after head trauma. They all underwent at least a unilateral PLF repair, and some also underwent an endolymphatic sac–mastoid shunt operation. This report provides a literature review to help put this series' results into perspective. Of those 40 patients who underwent an initial PLF repair, 58% had a successful outcome. Of the 10 patients who underwent an initial PLF repair plus an endolymphatic sac–mastoid shunt, 70% had a successful outcome. Since it is often difficult to distinguish patients with PLFs and secondary endolymphatic hydrops (Meniere's syndrome) from patients with Meniere's disease (idiopathic endolymphatic hydrops), PLF repair is a reasonable first operation, reserving an endolymphatic sac–mastoid shunt operation as a secondary procedure if needed. The decision to consider a PLF repair is guided by a positive fistula test or an immediate onset of Meniere's disease symptom complex after head or ear trauma.

KEY WORDS — Meniere's disease, Meniere's syndrome, perilymphatic fistula, secondary endolymphatic hydrops.

INTRODUCTION

The relationship between a perilymphatic fistula (PLF) and Meniere's disease was first mentioned by H. P. House[1] in 1967. This paper discussed a possible disorder of the inner ear fluids in post-stapedectomy PLFs. In 1968, Fee[2] reported cases of presumed Meniere's disease that, at surgery, were found to be traumatic PLFs. In 1974, Arenberg et al[3] reported on a young girl who was thought to have Meniere's disease but had intraoperative evidence of a PLF. The preoperative hearing loss slowly improved over the 6-month postoperative observation period.[3] Lehrer et al[4] described their experience with positive glycerol tests (thought to indicate endolymphatic hydrops) in patients with posttraumatic PLFs. In 1983, Allen[5] described how an active PLF could lead to endolymphatic hydrops. Potter and Conner[6] expounded on the coexistence of Meniere's disease and PLFs after 2 of their patients with postoperative PLFs developed typical attacks of Meniere's disease. One patient was treated successfully with a labyrinthectomy, and the other with diuretic therapy.[6]

Following these reports on clinical experience with PLFs and Meniere's disease, experimental animal evidence showed the coexistence of these 2 disorders.[7-10] Electrocochleograms (ECochGs) were monitored by Gibson[11] during stapedectomies, and showed that when perilymph was suctioned from the vestibule, an abnormal ratio between the summating potential (SP) and the action potential (AP) resulted. Abnormal ECochGs had been reported as a reliable indicator of endolymphatic hydrops by several authors.[12-14]

This report concerns the clinical management of patients who, by their history and preoperative test results, were thought to have a PLF and secondary Meniere's syndrome.

SUBJECTS

This is a retrospective study of 64 patients who were seen over a span of 9 years. Entry into this study was limited to patients whose chief complaints included the full complement of "Meniere's disease" symptoms, ie, fluctuating hearing, episodic vertigo, tinnitus, and aural fullness. This set of symptoms will be referred to herein as Meniere's disease symptom complex (MDSC). These cases, however, had additional history or findings that seemed to separate them from "true" Meniere's disease, an *idiopathic* condition thought to have the pathological substrate of endolymphatic hydrops. These patients were a subset of patients with possible PLF seen from 1982 to 1991. The larger group of patients with unilateral PLF but without MDSC were reported earlier.[15]

The patients in this study had, in addition to MDSC, a history of trauma with the *immediate* onset of MDSC and/or a positive fistula test. Seventy-three percent (47/64) had a positive subjective fistula test, ie, Hen-

---

From the Department of Otology/Neurotology, Washington Hospital Center, Washington, DC.

CORRESPONDENCE — Dennis C. Fitzgerald, MD, Capital Ear Group, 106 Irving St NW, Suite 4600, Washington, DC 20010.

TABLE 1. PREOPERATIVE TEST RESULTS

Test	*Findings*	*No.*	*%*
Hearing	Normal hearing	8	12
	Mild sensorineural hearing loss	12	19
	Moderate sensorineural hearing loss	35	55
	Severe sensorineural hearing loss	9	14
Electronystagmography	Abnormal positional test findings	8	12
	Unilateral caloric weakness	21	33
	Abnormal positional test findings and reduced vestibular response	3	5
	Normal findings	26	41
	Did not test	6	9
Preoperative electrocochleography (extratympanic foam ear tips)	Abnormal (SP/AP >0.60)	23	46
	Borderline abnormal (SP/AP of 0.40-0.60)	11	22
	Normal (SP/AP <0.40)	16	32

SP/AP — ratio of summating potential to action potential.

nebert's symptom, and 63% (17/27) had a positive platform pressure test. Fifty-two percent (33/64) had a traumatic event; 48% (31/64) did not. The majority of the traumatic events were of the "mild head trauma" type. Other preoperative test results are shown in Table 1.

The ages of the patients ranged from 16 to 66 years. The median duration of time they had symptoms before seeing the author was 3 years. All patients had a follow-up period of at least 2 years.

METHODS

Patients' symptoms were assessed and categorized by the following chief complaints:

1. *Fluctuating hearing loss* — Audiograms show recurrent recovery and loss patterns on successive tests. This can be evident in both pure tone and speech audiometry. The patient also notices a fluctuation in hearing levels.
2. *Vertigo* — Any disturbance in spatial orientation resulting in the illusion of movement. These patients also may have noted a balance disturbance and motion intolerance.
3. *Tinnitus* — The perception of sound in the absence of an external stimulus.
4. *Aural fullness* — The subjective sensation of pressure, fullness, or stuffiness in the ear or temporal region of the head.

The combination of all 4 symptoms was present in all subjects. Because an underlying PLF was suspected in all patients who complained of the complete set of MDSC symptoms, we sought the distinguishing clinical characteristics to separate patients with PLF from patients with idiopathic endolymphatic hydrops. A detailed questionnaire was obtained from all patients, with particular emphasis on events just preceding the onset of symptoms. Care was taken to ask for events such as diving, air travel, head or ear trauma, and physical straining. The criteria used in advising a patient to have surgery were as follows:

1. Trauma (head, whiplash, barometric, increased intracranial pressure) resulting in MDSC.
2. Presence of MDSC with a positive "fistula test" (subjective or platform).

An office examination was routinely performed, including a subjective fistula test patterned after that of Thompson and Kohut,[16] performed as follows. The patient was seated in a chair, and a Bruening pneumatic otoscope (Storz-Bruening, Storz Instrument Co, St Louis, Mo) was placed into the ear canal with an airtight seal. The patient was asked to stare at an object on the opposite wall. Erratic increases and decreases in the external canal pressure were applied 6 to 10 times in each ear, never exceeding 120 mm Hg, and the response to the question, "Does that bother you?" was noted. A positive finding was recorded if the patient reported the object on the wall moving, a sensation of himself or herself moving, or nausea. A response of pain, pressure, or increased tinnitus was recorded as negative, as was a report of no sensation at all. A tandem Romberg test was routinely performed, with special attention to the side to which the patient fell when the eyes were shut.

All patients suspected of having a PLF had air-bone and speech audiometry, with tympanometry if possible. Most patients also had a standard electronystagmogram (ENG). When ECochG testing with extratympanic foam ear tips became available in our facility in 1985, this became a standard preoperative test, as did platform posturography with platform fistula testing when it became available. These platform tests were performed in a freestanding vestibular laboratory. The testing was performed on Neurocom Equitest A100100 equipment (Neurocom International, Clackamas, Ore). The software for the sensory and motor tests was Equitest 4.03; the platform fistula test software was Neurocom Pressure Test V1.12. The pressure test was similar to tests reported by Shepard et al.[17]

The patient was asked to stand on the force-plates with the eyes closed. The sway reference gain was set to 1.00. Ten trials of 0 pressure, –300 decapascals (dPa), and +300 dPa were conducted with the nonsuspect ear tested first. Pressure was applied through a hermetically sealed ear tip at a rate of 450 dPa/s. Once the selected pressure was achieved, it was immediately released.

The largest sway amplitude during 0 pressure for anteroposterior and lateral sway was selected, and its own standard deviation was added. The largest amplitude during the positive and negative pressure tests was chosen, and its own standard deviation subtracted. If the number from the positive or negative test was greater than the control number, the response was scored as positive, since it was greater by more than 2 standard deviations. Rotational chair testing was rarely used. Computed tomography scans of the temporal bones were ordered primarily in children and teenagers when a congenital malformation was suspected because of clinical setting or history. Gadolinium-enhanced magnetic resonance imaging of the head became part of the workup in July 1988 and, on occasion, showed interesting enhancement of the inner ear.[18] The only postoperative test performed on every patient was audiometry, but many patients had postoperative subjective fistula tests, especially in the later years of the study.

As would be expected, such problems as tympanic membrane perforations, trauma, and infections, along with financial limitations, prevented some patients from having all diagnostic tests. In the postoperative period, tests were repeated if the patient's symptoms persisted or recurred.

The PLF repair surgical procedure has been previously described.[15] Any endolymphatic sac–mastoid operations performed were patterned after the technique of Austin.[19]

Upon discharge, the patients were instructed to stay home for 3 days and were strictly warned against any lifting or physical exertion. After 3 days, they could leave home, but were advised to lift no more than 10 lb (4.5 kg) and not to engage in any sports. Flying was permitted after a week. One month after operation, the ear was cleaned, an audiogram was obtained, and a subjective fistula test was performed. At that time, the patients were advised to avoid contact sports, weight lifting, underwater diving, and skydiving. If symptoms persisted, care was extended for continued observation, revision surgery, or secondary treatment (eg, diuretics, vestibular therapy). Follow-up visits were performed at 6-month intervals for at least 2 years. The treatment was considered successful if the patient had undergone only a PLF repair and had no further symptoms for 2 months.

RESULTS

The first 24 patients seen during the time period of the study underwent both PLF repair and an endolymphatic sac–mastoid shunt operation as recommended by Lehrer et al.[20] Seventy-five percent (18/24) had a successful outcome. Twenty-nine percent (7/24) had improvement in their hearing level as shown by a comparison of the best preoperative test to the worst postoperative test (at least a 15-dB gain in the pure tone average [500 Hz, 1 kHz, 2 kHz, 3 kHz] or a greater than 15% improvement in the speech discrimination score). In those patients who did not have improvement in their vertigo, salvage was accomplished through vestibular neurectomy or labyrinthectomy. Eight percent of these patients (2/24) who underwent a PLF repair with a shunt developed immediate profound hearing loss of indeterminate cause. Of those 40 patients who underwent only an initial PLF repair, 58% (23/40) had a successful outcome, and 42% (17/40) needed further treatment, ie, an endolymphatic sac–mastoid shunt procedure. Of the 10 patients who elected to have a secondary shunt procedure, 70% (7/10) had a successful surgical outcome.

An abnormal preoperative ECochG did not predict failure for patients with PLF repair, as 70% (12/17) had a successful outcome with *only* a PLF repair. The overall pattern of outcome for all 64 patients is represented in the Figure.

DISCUSSION

Of the large body of literature that has accumulated regarding the association of Meniere's disease and PLF, one of the earliest, though probably unrecognized, connections was made by Prosper Meniere himself. As translated by Atkinson, Meniere describes patients with "cerebral congestion of apoplectic type,"[21(p22)] a symptom complex compatible with what we now call Meniere's disease. He describes the sudden onset of these symptoms as caused by "foreign bodies thrust into the ear."[21(p22)] In that same report, he describes clearly what most of us would recognize as an acute PLF caused by forceful nose blowing: "But one knows also there comes a moment when, on blowing the nose forcefully, on sneezing...air passes the obstruction and enters abruptly into the middle ear.....The phenomenon of sudden penetration of air into the cavity of the middle ear produces in some people an explosion accompanied

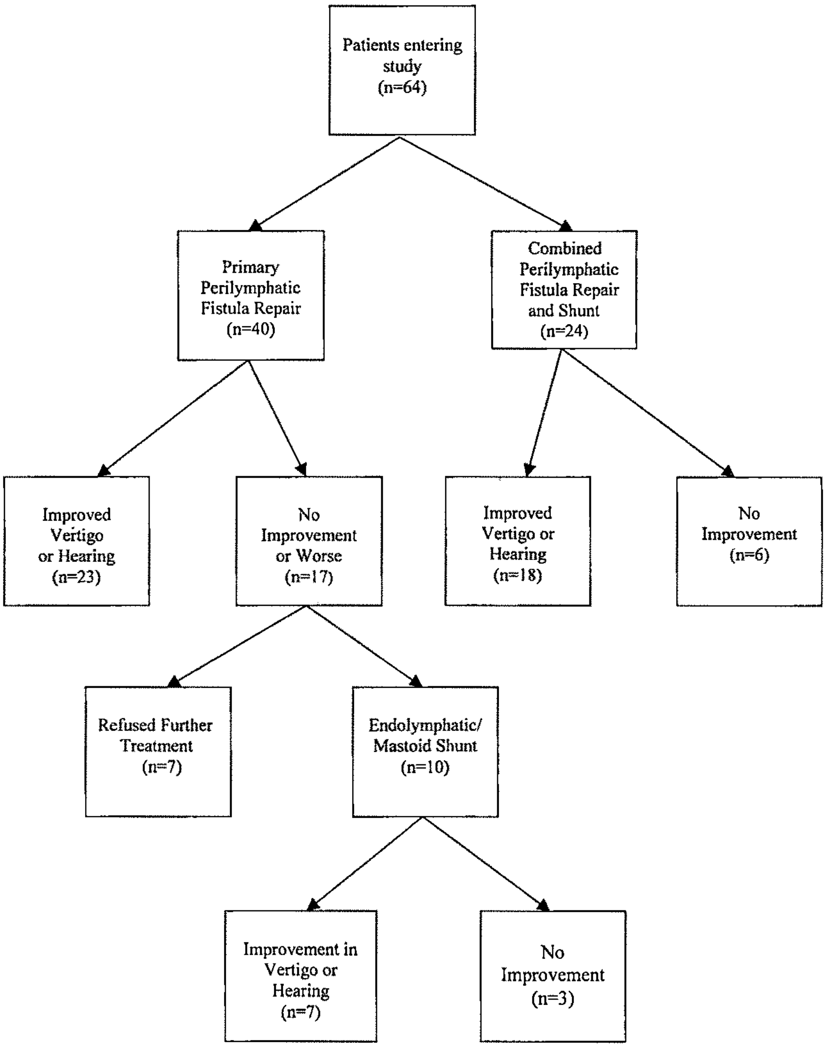
Patients entering study (n=64)
Primary Perilymphatic Fistula Repair (n=40)
Combined Perilymphatic Fistula Repair and Shunt (n=24)
Improved Vertigo or Hearing (n=23)
No Improvement or Worse (n=17)
Improved Vertigo or Hearing (n=18)
No Improvement (n=6)
Refused Further Treatment (n=7)
Endolymphatic/ Mastoid Shunt (n=10)
Improvement in Vertigo or Hearing (n=7)
No Improvement (n=3)

Surgical results of 64 patients in study.

by vertigo: if the patient is standing he reels, he is about to fall and needs several moments of rest to regain his balance."21(p24) This may have been only alternobaric vertigo, but also could have been an acute PLF.

H. P. House,[1] writing on post-stapedectomy PLFs in 1967, said, "In cases of PLF with a sensorineural hearing loss, the duration of symptoms and the inadequate patency of the perilymphatic duct may all be factors. The endolymphatic system can function normally if the pressure of the endolymphatic and perilymphatic fluid is the same. Any imbalance in the equalization over a period of time will result in dilation of the endolymphatic system, thereby producing an 'artificial' endolymphatic hydrops....This same phenomenon seems to occur in Meniere's disease."1(p1415)

This work, written decades ago, explains why we cannot always distinguish a PLF from Meniere's disease. The first known patients with PLF not related to surgery were described by Fee,[2] with symptoms quite compatible with those of Meniere's disease. In fact, Fee alluded to the concept that a PLF could lead to a dilated endolymphatic system.

Arenberg et al[3] later reported on a 10-year-old girl who had the classic history of Meniere's disease for 2 years but was found to have an oval window fistula. In 1977, Nadol[22] found a positive Hennebert's sign in 24 of 81 ears (30%) with "Meniere's disease." He interpreted this to mean that the test could be made positive by the disturbance of the saccule's being moved by pressure in the external ear canal or through vestibulofibrosis. I wonder whether the 24 patients with a positive Hennebert's sign and the diagnosis of Meniere's disease might not instead have had a PLF or even a combination of PLF and secondary Meniere's syndrome. In either case, Hennebert's test appears to be less specific for a PLF than previously thought. Another diagnostic test, the glycerol dehydration test, which had been thought to be specific for Meniere's disease, was found to be positive in a significant number of patients with posttraumatic PLFs.[4] In 1982, Simmons[23] very clearly expressed frustration in trying to differentiate PLF patients from those with Meniere's disease and wrote that the "atypical Meniere's disease" patient could very probably be a PLF patient instead. As evidence continued to mount for the possibility of a coexistence of PLF and Meniere's disease, Potter and Conner[6] reported that 2 of 15 PLF patients developed typical cases of Meniere's disease after having their PLFs repaired. Clinical evidence now seemed to indicate that a PLF repair could exacerbate an underlying secondary endolymphatic hydrops. In 1984, W. P. R. Gibson,[24] an early pioneer in ECochGs, reported a typical increase in the SP/AP ratio of PLF patients of about 25% to 35%, consistent with a mild endolymphatic hydrops. The University of Iowa (1986) reported on the largest series of PLF patients.[25] A significant part of the article dealt with differentiating a PLF from Meniere's disease. The authors raised the question of performing both endolymphatic shunt procedures and PLF repairs at the same time in cases in which there was not a clear differentiation between Meniere's disease and PLF.[25]

Up to this point, only a few authors who have written about PLFs have discussed how a leakage of perilymph could cause the myriad of symptoms seen with PLFs. In 1983, Fukaya and Nomura[26] ruptured the round window membrane in animals without even producing severe hearing loss. Nomura et al[10] questioned the idea that a mere fistula could be responsible for all of the reported symptoms of PLFs. They were the first to produce experimental PLFs in guinea pigs and describe morphological changes in their temporal bones. Typically, the round window membrane was ruptured (no oval window membranes ruptured) by a rapid increase in the cerebrospinal fluid (CSF) pressure in the posterior fossa. Massive bleeding was seen in the scala tympani and cochlear aqueduct. Many ears also showed signs of hydrops. In the vestibular system, the most common finding was the collapse of the ampullae of the semicircular canals. They also found that in the delayed-sacrifice animals there was no hydrops — a finding indicating that when the PLFs were allowed to heal, the hydrops was reversible. There were also areas of collapse of cochlear membranes.[10] These findings fit with Simmons'[27] findings of "double membrane breaks." The interpretation of this experiment by Nomura et al leads to the following conclusions.

1. Normalization of perilymph pressure is required before the distorted or ruptured membranous labyrinth can heal.
2. The closing of a PLF does not guarantee complete disappearance of all symptoms.
3. Rupture of the round window membrane itself may not produce the symptoms, but rather, the symptoms may be caused by damage to the inner ear membranes.

Following these early investigations, numerous clinical articles appeared that supported the concept that PLFs caused a secondary endolymphatic hydrops (Meniere's syndrome) and that the symptoms could be due to the hydrops itself rather than the leakage of perilymph. In addition, many reports on experimental PLFs in animals confirmed that active PLFs often resulted in hydrops and abnormal ECochGs.[7-10,28,29]

The reasons given for the development of a secondary endolymphatic hydrops in PLFs in all of the preceding articles related to a loss of perilymph volume causing compensatory endolymphatic hydrops or the same result on the basis of pressure differentials. One must remember that there are only about 0.34 mL of endolymph and 1.58 mL of perilymph in the human ear.[30] A loss of only a small part of the perilymph volume would have a large impact on the endolymph volume, quickly leading to endolymphatic hydrops. Overlooked so far is the protein concentration of perilymph and CSF. It has been generally accepted that approximately 25% of perilymph comes from CSF. If a PLF were to develop, there is the potential for a higher-than-normal percentage of PLF to be derived from the CSF. Perilymph has about 8 times as much protein as CSF.[31] If there were a PLF-related influx of CSF into the perilymphatic spaces, the perilymph would become hypotonic relative to the neighboring endolymph. This hypotonicity would produce diffusional forces and drive free water into the endolymphatic spaces, adding to the volumetric and pressure-related hydrops. This concept was discussed by Juhn et al[32] in 1982.

The 64 patients reported here presented with a symptom complex of episodic vertigo, fluctuating hearing loss, tinnitus, and aural fullness compatible with Meniere's disease. These patients, however, exhibited some particular historical event(s) or positive diagnostic test(s) that brought into question the diagnosis of a PLF. In the history, there might have been an inciting or exacerbating event(s) such as direct trauma, barotrauma, or increased intracranial pressure. As for diagnostic tests, some patients had a positive fistula test (subjective or platform) that kept them from receiving a diagnosis of "primary" Meniere's disease.

The first article to specifically address the issue of the timing and the advisability of combining a PLF repair with an endolymphatic shunt was published in 1987 by Lehrer et al.[20] They recommended this combined surgical approach in patients who had recurrent PLFs, attacks of spinning vertigo following PLF repairs, or clear PLFs with severe imbalance.

TABLE 2. SURGICAL OUTCOMES IN PATIENTS WITH HEARING LOSS

	Hearing Loss					
	Mild		*Moderate*		*Severe*	
	No.	*%*	*No.*	*%*	*No.*	*%*
Perilymphatic fistula repair (n = 35)						
+Surgical outcome	7/35	20%	14/35	40%	1/35	2%
−Surgical outcome	3/35	9%	8/35	23%	2/35	6%
Perilymphatic fistula repair + shunt (n = 21)						
+Surgical outcome	3/21	14%	8/21	38%	6/21	29%
−Surgical outcome			4/21	19%		

+Surgical outcome — improved hearing and/or vertigo; −surgical outcome — no change in or worsened hearing and/or vertigo.

One year later, Arenberg et al[8] found 14 of 23 patients with surgically confirmed PLFs to have an ECochG SP/AP ratio of greater than 0.50, indicating the coexistence of PLF and endolymphatic hydrops. Weider and Johnson[33] published a report in 1988 that suggested performing a PLF repair and shunt placement together when a PLF and endolymphatic hydrops coexisted in patients with "primary" Meniere's disease who had to undergo endolymphatic sac surgery anyway. However, they did not elaborate on how they knew when a PLF and hydrops coexisted. Meyerhoff and Yellin[34] found that 16 of 20 ears operated on for a suspected PLF that had an abnormal SP/AP ratio (greater than 0.37) were found to have a leak at surgery. They believed that a PLF would often have an abnormal SP/AP ratio. Our findings in 64 patients with the chief presenting complaints of fluctuating hearing, vertigo (often spinning), fullness, and tinnitus were called Meniere's disease symptom complex (MDSC) for this report. As can be seen from these results, 42% (17/40) of the patients who underwent a primary PLF repair required a secondary treatment, usually an endolymphatic shunt. Thirty-eight percent (24/64) had a combination PLF-shunt operation, our choice of operation for many years, when there appeared to be a PLF with secondary Meniere's syndrome or primary Meniere's disease with a traumatic event or a positive fistula test. This approach continued until 2 patients developed "dead ears" after this combination operation. These were the only 2 significant sensorineural hearing losses to develop as a result of surgery in the entire series of 64 patients. The incidence of severe hearing loss in endolymphatic sac surgery has generally run at less than 5%. Thus, it might not be out of line to have 2 "dead ears" in 24 operations. Still, I began to suspect that patients' ears with secondary Meniere's syndrome might somehow be more fragile than those with primary Meniere's disease, and thus more at risk for damage from a sac operation. Subsequently, the approach was altered to perform only a PLF repair and then wait to see whether a shunt was needed.

Analysis of my diagnostic testing revealed the high incidence of a borderline or abnormal ECochG in this group with MDSC (34/50 or 68%). This fits previous reports of Gibson,[24] Arenberg et al,[8] and Meyerhoff and Yellin.[34]

Only 41% of those patients who underwent only PLF repair and had abnormal preoperative ECochGs required secondary shunt surgery. This outcome indicates that secondary endolymphatic hydrops can resolve spontaneously if the PLF is surgically repaired.

J. Lehrer (personal communication, 1986) believes that patients with PLF and secondary endolymphatic hydrops and moderate or severe hearing loss will usually not do well with a PLF repair only. This idea was not borne out in this study, as only 29% of those patients who had a moderate or severe hearing loss had a negative surgical outcome with only a PLF repair (Table 2).

A few authors have reported problems in differentiating a positive surgical outcome from a placebo effect, as alluded to by Rizer and House[35] when evaluating the subjective symptoms of vestibular disorders. The placebo effect might certainly play some part in this series, but the high rate of good surgical outcomes and the duration of these subjective improvements weigh against the placebo effect's being a significant component of the successes.

Finally, the use of a positive fistula test to select a subset of MSDC patients suspected of having a PLF is still controversial. This distinguishing feature, a positive fistula test, in diagnostic testing was reaffirmed by Kohut et al[36] in 1995 and continues to guide the author in making the presumptive diagnosis of a PLF.

SUMMARY

The discussion now is not whether the patient with MDSC has a PLF or Meniere's disease, but rather whether the patient has primary Meniere's disease or a primary PLF with secondary Meniere's syndrome. By combining the history, fistula tests, and ECochGs, the appropriate medical and surgical treatments can be chosen and rendered. A PLF repair alone is successful in these patients almost 60% of the time. When a secondary endolymphatic sac–mastoid shunt procedure is performed at a second sitting, the success rate becomes almost 75%. This approach saves 60% of these patients an unnecessary shunt operation.

In 1982, Simmons wrote, "In brief, I know of no certain way to differentiate a Meniere's disease patient from all fistula patients and I strongly suspect that no one else does either."[23(p71)] I think we now can say that differentiation is often impossible, since both disorders coexist in the patient with an active PLF with secondary Meniere's syndrome.

I have concluded, therefore, that every active PLF has an element of endolymphatic hydrops, and that the hydrops is the cause of all symptoms except those related to inner ear membrane ruptures and scarring. Second, the resolution of symptoms after a PLF repair is dependent upon a self-healing process in the endolymphatic system that causes a resolution of the hydrops. Third, the exacerbation or change in character of the vestibular symptoms after a PLF repair, as is sometimes seen, is due to an exacerbation of the secondary endolymphatic hydrops and may require secondary medical or surgical treatment for the hydrops. Fourth, irreversible scarring probably occurs in some inner ears with PLFs, causing prolonged or permanent symptoms not relieved by a PLF repair.

REFERENCES

1. House HP. The fistula problem in otosclerosis surgery. Laryngoscope 1967;77:1410-26.
2. Fee GA. Traumatic perilymphatic fistulas. Arch Otolaryngol 1968;88:477-80.
3. Arenberg IK, May M, Stroud MH. Perilymphatic fistula: an unusual cause of Meniere's syndrome in a prepubertal child. Laryngoscope 1974;84:243-6.
4. Lehrer JF, Poole DC, Sigal B. Use of the glycerin test in the diagnosis of post-traumatic perilymphatic fistulas. Am J Otolaryngol 1980;1:207-10.
5. Allen GW. Clinical implications of experiments on alteration of the labyrinthine fluid pressure. Otolaryngol Clin North Am 1983;16:3-19.
6. Potter CR, Conner GH. Hydrops following perilymph fistula repair. Laryngoscope 1983;93:810-2.
7. Funai H, Hara M, Nomura Y. An electrophysiologic study of experimental perilymphatic fistula. Am J Otolaryngol 1988; 9:244-55.
8. Arenberg IK, Ackley RS, Ferraro J, Muchnik C. ECoG results in perilymphatic fistula: clinical and experimental studies. Otolaryngol Head Neck Surg 1988;99:435-43.
9. Campbell KCM, Parnes L. Electrocochleographic recordings in chronic and healed perilymphatic fistula. J Otolaryngol 1992;21:213-7.
10. Nomura Y, Hara M, Young Y-H, Okuno T. Inner ear morphology of experimental perilymphatic fistula. Am J Otol 1992; 13:32-7.
11. Gibson WPR. Electrocochleography in the diagnosis of perilymphatic fistula: intraoperative observations and assessment of a new diagnostic office procedure. Am J Otol 1992;13: 146-51.
12. Gibson WPR, Moffat DA, Ramsden RT. Clinical electrocochleography in the diagnosis and management of Meniere's disease. Audiology 1977;16:389-401.
13. Coats AC. The summating potential and Meniere's disease. I. Summating potential amplitude in Meniere and non-Meniere ears. Arch Otolaryngol 1981;107:109-208.
14. Ferraro JA, Arenberg IK, Hassanein RS. Electrocochleography and symptoms of inner ear dysfunction. Arch Otolaryngol 1985;111:71-4.
15. Fitzgerald DC, Getson P, Brasseux CO. Perilymphatic fistula: a Washington, DC, experience. Ann Otol Rhinol Laryngol 1997;106:830-7.
16. Thompson JN, Kohut RI. Perilymph fistulae: variability of symptoms and results of surgery. Otolaryngol Head Neck Surg 1979;87:898-903.
17. Shepard NT, Telian SA, Niparko JK, Kemink JL, Fujita S. Platform pressure test in identification of perilymphatic fistula. Am J Otol 1992;13:49-54.
18. Fitzgerald DC, Mark AS. Endolymphatic duct/sac enhancement on gadolinium magnetic resonance imaging of the inner ear: preliminary observations and case reports. Am J Otol 1996;17:603-6.
19. Austin DF. Endolymphatic fistulization. Ann Otol Rhinol Laryngol 1984;93:534-9.
20. Lehrer JF, Quraishi AU, Poole DC. The role of endolymphatic sac surgery in the management of secondary endolymphatic hydrops associated with perilymphatic fistulas: preliminary observations. Am J Otol 1987;8:93-5.
21. Atkinson M. Meniere's original papers. Acta Otolaryngol Suppl (Stockh) 1961(suppl 162).
22. Nadol JB Jr. Positive Hennebert's sign in Meniere's disease. Arch Otolaryngol 1977;103:524-30.
23. Simmons FB. Perilymph fistula: some diagnostic problems. Adv Otorhinolaryngol 1982;28:68-72.
24. Gibson WPR. Vertigo associated with trauma. In: Dix MR, Hood JD, eds. Vertigo. New York, NY: John Wiley & Sons, 1984:373-89.
25. Seltzer S, McCabe BF. Perilymph fistula: the Iowa experience. Laryngoscope 1986;96:37-49.
26. Fukaya T, Nomura Y. Experimental round window rupture with middle ear effusion. Acta Otolaryngol Suppl (Stockh) 1983(suppl 393):20-4.
27. Simmons FB. The double-membrane break syndrome in sudden hearing loss. Laryngoscope 1979;89:59-66.
28. Oshiro EM, Shelton C, Lusted HS. Role of perilymphatic fistula in sudden hearing loss: an animal model. Ann Otol Rhinol Laryngol 1989;98:491-5.
29. Bohmer A. Early alterations of cochlear function in experimental perilymph fistulas. Laryngoscope 1990;100:389-94.
30. Buckingham RA, Valvassori GE. Inner ear fluid volumes and the resolving power of magnetic resonance imaging: can it differentiate endolymphatic structures? Ann Otol Rhinol Laryngol 2001;110:113-7.
31. Juhn SK, Rybak LP, Prado S. Nature of blood-perilymph barrier in experimental conditions. Ann Otol Rhinol Laryngol 1981;90:135-41.
32. Juhn SK, Rybak LP, Fowlks WL. Transport characteristics of the blood-perilymph barrier. Am J Otolaryngol 1982;3: 392-6.
33. Weider DJ, Johnson GD. Perilymphatic fistula: a New Hampshire experience. Am J Otol 1988;9:184-96.
34. Meyerhoff WL, Yellin MW. Summating potential/action potential ratio in perilymph fistula. Otolaryngol Head Neck Surg 1990;102:678-82.
35. Rizer FM, House JW. Perilymph fistulas: the House Ear Clinic experience. Otolaryngol Head Neck Surg 1991;104:239-43.
36. Kohut RI, Hinojosa R, Thompson JN, Ryu JH. Idiopathic perilymphatic fistulas. A temporal bone histopathologic study with clinical, surgical, and histopathologic correlations. Arch Otolaryngol Head Neck Surg 1995;121:412-20.

Ann Otol Rhinol Laryngol 110:2001

BONE CONDUCTION IMPAIRMENT IN CHRONIC EAR DISEASE

CHRISTOPHER J. LINSTROM, MD
NEW YORK, NEW YORK
CAROL A. SILVERMAN, PHD
NEW YORK, NEW YORK
ARIE ROSEN, MD
EAST ORANGE, NEW JERSEY
LAWRENCE Z. MEITELES, MD
VALHALLA, NEW YORK

The preoperative and postoperative bone conduction (BC) thresholds were prospectively investigated in 24 patients with chronic ear disease in the form of cholesteatoma, chronic suppurative otitis media, or adhesive otitis media. All underwent tympanoplasty with mastoidectomy. Ossicular reconstruction was performed in 14, and the remaining 10 were still awaiting second-stage ossicular reconstruction at the time of this investigation. In each group, the postoperative results were compared with the preoperative results by the paired-samples *t*-test. In the ossicular reconstruction group, the results revealed a significant improvement in the postoperative BC thresholds, as compared with the preoperative BC thresholds, at 250, 1,000, and 2,000 Hz, with the largest mean improvement observed at 2,000 Hz. No significant improvement was observed at any frequency for the group without ossicular reconstruction. Postoperative improvement of at least 10 dB at 2 or more frequencies was observed in 71% of the ossicular reconstruction group, as compared with 0% of the group that did not undergo ossicular reconstruction. The results support the theory that the elevated BC thresholds of patients with chronic ear disease result from the elimination, due to disease, of the middle ear contribution (from the inertial ossicular component and ossicular resonance) to the BC response. The results also suggest that the middle ear contribution to the BC response is restored with ossicular reconstruction.

KEY WORDS — bone conduction threshold, Carhart effect, chronic ear disease, hearing, sensorineural hearing loss.

INTRODUCTION

Several investigators have reported the finding of elevated bone conduction (BC) thresholds in patients with chronic diseases of the middle ear (chronic suppurative otitis media, chronic otitis media, and cholesteatoma), despite the absence of symptoms of labyrinthitis.[1-14] The observed elevation in the BC thresholds has variously been ascribed to the elimination, due to the middle ear disease, of the contribution of BC to the middle ear mechanism of hearing[5,8] and/or cochlear dysfunction resulting from extension of inflammation in the middle ear cleft through the round window membrane.[2,3,14]

According to Tonndorf,[15] the outer ear, middle ear, and inner ear mechanisms that contribute to the total BC response include the following: 1) the response associated with radiation of sound energy from the external ear canal walls into the space of the external canal; 2) the inertial response of the ossicular chain (which is loosely coupled to the skull) and inner ear fluids; and 3) the compressional response of the inner ear spaces resulting from distortional vibration of the cochlea. Thus, the BC response is not a pure measure of the cochlear reserve.

Carhart[16] observed elevated BC thresholds in the frequency region around 2,000 Hz for patients with stapes ankylosis due to otosclerosis. This finding of a maximal loss at 2,000 Hz, which has been termed the Carhart notch, has been poorly understood. The maximal BC impairment at 2,000 Hz cannot be explained by the classic theory of BC; based on that theory, alteration of the low frequencies is predicted for patients with stapedial fixation. Tonndorf[15] demonstrated that the additional alteration at the higher frequencies and the observed maximal loss at 2,000 Hz resulted from the reduction or elimination of the resonance of the ossicular chain; in humans, the resonant frequency of the ossicular chain is 1,500 to 2,000 Hz. This effect has been substantiated for other disorders that affect the conductive mechanism.

Several approaches have been employed in the investigation of the BC hearing sensitivity in chronic ear disease. One approach has been based upon comparison of the BC thresholds for the diseased ear with those for the contralateral, nondiseased ear of persons with unilateral chronic ear disease.[4,8,10,12,13] With another approach, the BC thresholds for diseased ears have been contrasted with those for normal control ears.[1-3,8,9] A third approach has involved comparison of pretreatment BC thresholds with posttreatment BC thresholds.[4,7,11,14] Other approaches

---

From the Department of Otolaryngology–Head and Neck Surgery, Department of Veterans Affairs Medical Center, East Orange, New Jersey (Linstrom, Silverman, Rosen), and the Departments of Otolaryngology–Head and Neck Surgery (Linstrom, Silverman, Meiteles) and Communicative Sciences (Silverman), The New York Eye and Ear Infirmary, New York, New York. This work was supported by the Department of Veterans Affairs, New Jersey Health System, under contract No. V561P-2808.

CORRESPONDENCE — Christopher J. Linstrom, MD, Dept of Otolaryngology–Head and Neck Surgery, The New York Eye and Ear Infirmary, 310 E 14th St, New York, NY 10003.

have employed histopathologic analysis of the temporal bones of patients with chronic ear disease or animal studies involving injection of endotoxins into the perilymphatic space.[5,6]

Studies that are based on the comparison of pretreatment and posttreatment BC thresholds have the greatest bearing on improving our understanding of the middle ear contribution versus the inner ear contribution to the elevation of BC thresholds in chronic ear disease. In such studies, not only does the patient serve as his or her own control, but also, the affected ear serves as its own control. An observed improvement in the BC thresholds with treatment supports the role of the loss of the middle ear contribution in the elevated BC thresholds of patients with chronic ear disease. But the existing studies on the preoperative and postoperative BC thresholds[7,11,14] have methodological limitations similar to those of studies that have employed other approaches toward investigation of the BC thresholds in patients with chronic ear disease.

The methodological shortcomings have included retrospective analysis of the data; conservative criteria for improvement in BC hearing, such as at least 10-dB improvement in the BC thresholds over 2 or more frequencies together with the absence of statistical analysis of group data; and failure to control for ossicular reconstruction. If ears that did not undergo ossicular reconstruction are included in the data analysis with ears that underwent ossicular reconstruction, then the postoperative improvement in BC hearing sensitivity with treatment would be underestimated, as the middle ear contribution to the BC response would be at least partially restored in the latter, but not the former, condition.

Therefore, the aim of this investigation was to prospectively evaluate the preoperative and postoperative BC thresholds in adult patients with chronic ear disease in the form of chronic suppurative otitis media, cholesteatoma, or adhesive otitis media.

MATERIAL AND METHODS

Subjects. Twenty-four adult patients with chronic ear disease gave informed consent to participate in a prospective, endoscopic investigation to describe the status of the eustachian tube at the time of surgery. Of the 24 patients, 14 received ossicular reconstruction; the remaining 10 had not yet received ossicular reconstruction because they were still awaiting the second stage of staged surgery at the time of this study.

The ossicular reconstruction study sample with chronic ear disease comprised 8 men and 6 women (mean age, 42 years; range, 27 to 65 years). The disease was unilateral in 12 and bilateral in 2. The cause was chronic suppurative otitis media in 8, cholesteatoma in 3, and adhesive otitis media in 3. All received tympanoplasty with or without mastoidectomy, and all received ossicular reconstruction with an incus replacement prosthesis, partial ossicular replacement prosthesis, total ossicular replacement prosthesis, incus-stapes replacement prosthesis, or incus interposition.

The study sample with chronic ear disease that did not undergo ossicular reconstruction comprised 3 men and 7 women (mean age, 44 years; range, 23 to 56 years) who had undergone tympanoplasty with mastoidectomy. The disease was unilateral in 8 and bilateral in 2. The cause was chronic suppurative otitis media in 5 patients, cholesteatoma in 4 patients, and adhesive otitis media in 1 patient.

Subjects were excluded from the investigation if, at any frequency requiring masking in the opposite ear,[17] the BC or air conduction threshold failed to plateau with the Hood[18] procedure.

No subject had a positive history of head trauma, vertigo, or systemic ototoxic drugs. At surgery, no patient was found to have a labyrinthine fistula or an inner ear invasion. Also, at the time of surgery, notation was made regarding the mucosal status of the middle ear and the degree of ossicular involvement.

Procedure. A comprehensive audiological assessment, including the air conduction and BC thresholds, the speech recognition threshold, a suprathreshold speech recognition assessment, an uncomfortable loudness level measurement, tympanometry, and an acoustic reflex threshold measurement, was performed before and after operation on all subjects. The pure tone audiograms were completed with appropriate masking of the opposite ear[17] with narrowband noise, by a procedure based on the Hood[18] plateau. The audiological assessment was performed in 2-room, sound-treated audiometric suites by licensed and certified audiologists. The study was effectively double-blind, as neither the audiologist nor the patient was aware of the study hypothesis in relation to BC hearing sensitivity. Data were evaluated from the latest preoperative test, performed within the 2-week interval preceding surgery, and from the initial postoperative test, performed between 10 and 12 weeks after surgery.

RESULTS

The Shapiro-Wilk statistic[19] revealed that the sample data on the difference between the preoperative and postoperative BC thresholds were normally dis-

TABLE 1. STATISTICAL FINDINGS FOR DIFFERENCE BETWEEN PREOPERATIVE AND POSTOPERATIVE BONE CONDUCTION THRESHOLDS

	250 Hz	*500 Hz*	*1,000 Hz*	*2,000 Hz*	*3,000 Hz*	*4,000 Hz*
Ossicular reconstruction (n = 14)						
Mean preop BC threshold	13.9	15.7	16.4	26.4	23.6	25.4
Mean postop BC threshold	6.8	10.0	9.3	17.1	19.6	21.1
Mean BC difference (preop minus postop)	7.1	5.7	7.2	9.3	4.0	4.3
t Value	5.26	1.87	3.44	3.36	1.63	1.45
p Level	.0002*	.0836	.0044*	.0052*	.1274	.1711
No ossicular reconstruction (n = 10)						
Mean preop BC threshold	12.0	16.5	16.5	26.0	25.5	31.0
Mean postop BC threshold	11.5	15.0	18.5	28.0	29.5	35.5
Mean BC difference (preop minus postop)	0.5	1.5	−2.0	−2.0	−4.0	−4.5
t Value	0.16	0.71	0.69	1.12	1.92	2.38
p Level	.8793	.4961	.5086	.2695	.0868	.0414*

BC — bone conduction.
*Significant.

tributed in the group with ossicular reconstruction and the group without ossicular reconstruction. Therefore, the preoperative and postoperative BC thresholds for the operated ear were analyzed at 250, 500, 1,000, 2,000, 3,000, and 4,000 Hz with a paired-samples *t*-test.

For both groups, the preoperative and postoperative BC thresholds and the mean differences between the preoperative and postoperative BC thresholds are shown in Table 1. For the ossicular reconstruction group, the mean postoperative BC thresholds were significantly improved at 250, 1,000, and 2,000 Hz, in comparison with the mean preoperative BC thresholds, and a trend toward postoperative improvement was present at all other frequencies. The mean improvement was greatest at 2,000 Hz (9.3 dB). The range of improvement across subjects and frequencies was −10 to 30 dB. These findings support those of Browning and Gatehouse,[8] who reported a statistically significant contribution of disease (chronic suppurative otitis media) to the BC thresholds that was greatest at 2,000 Hz. Browning and Gatehouse attributed the elevated BC thresholds in the group with chronic suppurative otitis media, as compared with a normal control group, to the Carhart effect.

Further inspection of Table 1 reveals that in the group that did not undergo ossicular reconstruction, significant improvement in the mean postoperative BC thresholds, in comparison with the mean preoperative BC thresholds, failed to occur at any frequency. In fact, the mean postoperative BC threshold was slightly worse than the mean preoperative BC threshold at 4 of the 6 frequencies. At the other 2 frequencies, the improvement in the mean postoperative BC threshold as compared with the mean preoperative BC threshold was negligible and nonsignificant.

In the ossicular reconstruction group, an improvement of 10 dB or more over at least 2 frequencies was present for 71% of the 14 subjects. An improvement of 10 dB or more at a single frequency occurred for 7% of the 14 subjects. An improvement of at least 10 dB failed to occur at any frequency in 22% of the 14 subjects. In 2 of the 3 subjects with the least improvement in BC sensitivity, the middle ear mucosa was polypoid. None of the subjects with improvements of at least 10 dB over 4 or more frequencies had polypoid middle ear mucosa. The incus was eroded in all subjects, and inspection of the data revealed that the number of frequencies showing improvement was unrelated to the number of eroded ossicles.

In the group without reconstruction, an improvement of 10 dB or more over at least 2 frequencies was absent for 100% of the 10 subjects. An improvement of 10 dB or more at a single frequency was observed for 30% of the 10 subjects. For 90% of the 10 subjects, the postoperative BC threshold was worse than the preoperative BC threshold at 1 or more frequencies.

Table 2 shows the Pearson correlation coefficients for the relationship between the difference between the preoperative and postoperative BC thresholds at 2,000 Hz and the therapeutic efficiency (difference between preoperative and postoperative air conduction thresholds) in the ossicular reconstruction group. Inspection of this Table reveals significant correlations at 500 Hz, 1,000 Hz, 2,000 Hz, and 4,000 Hz. The correlation is very close to significance at 3,000 Hz. These findings reveal a moderately strong direct relationship between the magnitude of improvement in the 2,000-Hz BC threshold caused by surgery and the magnitude of improvement in the air conduction thresholds at 500, 1,000, 2,000, and 4,000 Hz caused by surgery.

TABLE 2. PEARSON CORRELATION COEFFICIENTS FOR RELATION BETWEEN BONE CONDUCTION IMPROVEMENT AT 2,000 HERTZ AND THERAPEUTIC EFFICIENCY OF OSSICULAR RECONSTRUCTION (N = 14)

	250 Hz	*500 Hz*	*1,000 Hz*	*2,000 Hz*	*3,000 Hz*	*4,000 Hz*	*8,000 Hz*
r Value	.51	.67	.74	.71	.53	.58	.45
p Level	.0658	.0090*	.0026*	.0045*	.0502	.0284*	.1108

*Significant.

DISCUSSION

The results of this prospective investigation on patients with chronic ear disease reveal significant improvement in the BC thresholds at 250, 1,000, and 2,000 Hz following ossicular reconstruction. The statistical findings are highly significant ($p < .01$), despite the small sample size. These findings resemble those of Carhart[16] for patients with otosclerosis, who showed poststapedectomy improvements in the BC thresholds at all frequencies, especially 2,000 Hz. No significant improvements in the BC thresholds were observed after operation in patients who did not undergo ossicular reconstruction.

The findings of a highly significant BC improvement for the reconstruction group and an absence of significant improvement in the group without reconstruction are buttressed by the results of individual data analysis indicating at least 10-dB improvement over 2 or more frequencies in 71% of the former group and 0% of the latter group. These findings present strong support for the theory that alteration in the mechanics of middle ear transmission accounts for the elevated BC thresholds in patients with chronic ear disease. Therefore, the mean observed difference between the postoperative and preoperative BC thresholds essentially represents the magnitude of the restoration of the middle ear contribution to the BC response that occurs with ossicular reconstruction. Thus, ossicular reconstruction, in these subjects, yielded a functional ossicular chain.

The absence of a postoperative improvement in the BC thresholds in the group without reconstruction suggests that the middle ear contribution to the BC response, which was eliminated because of disease, failed to be restored with surgery, since a functional ossicular chain had not been constructed. Had these ears been included in the group that received ossicular reconstruction, it is likely that significantly improved BC thresholds would not have been observed postoperatively — or, at the very least, the magnitude of the improvement would have been underestimated.

Polypoid middle ear mucosa was present in 2 of the 3 subjects with the least postoperative improvement in BC sensitivity and was absent in the subjects demonstrating the greatest postoperative improvement in BC sensitivity. Perhaps the presence of polypoid middle ear mucosa may reduce the ability of reconstruction to restore the middle ear contribution to the BC response. A large-sample investigation is needed to test this hypothesis.

The observed significant relationship between the magnitude of improvement in the BC threshold at 2,000 Hz and the therapeutic efficiency of ossicular reconstruction at 500, 1,000, 2,000, and 4,000 Hz provides further support for the theory that the elevated BC thresholds in conductive hearing impairment are mechanical. That is, the observed relationship between the magnitude of BC improvement and the therapeutic efficiency suggests that the mechanism underlying the postoperative improvement in the 2,000-Hz BC threshold is the same as that underlying the postoperative improvements in the air conduction thresholds measured between 500 and 4,000 Hz. The lack of a significant relationship between the postoperative improvement in the 2,000-Hz BC threshold and the therapeutic efficiency at 250 Hz may reflect increased variability in the air conduction threshold at 250 Hz and/or a smaller effect size at that frequency. Leakage of sound energy from under the earphones is greater at the lower frequencies than at the higher frequencies. The absence of a significant relationship between the postoperative improvement in the 2,000-Hz BC threshold and the therapeutic efficiency at 8,000 Hz may reflect a smaller effect size at the latter frequency.

ACKNOWLEDGMENTS — We thank Tina Presutti for her invaluable assistance in data collection and study setup, Dr Guopei Yu for his help with statistical analysis, Dr William Spencer for his assistance with endoscopic examination of the eustachian tube, and Mati Guzzo-Crocomo for her help with data reduction.

REFERENCES

1. Bluvshtein GM. The audiological characteristics of chronic suppurative otitis media. Vestn Otorinolaringol 1963;25:64-72.

2. Paparella MM, Brady DR, Hoel R. Sensorineural hearing loss in chronic otitis media and mastoiditis. Trans Am Acad Ophthalmol Otolaryngol 1970;74:108-15.

3. English GM, Northern JL, Fria TJ. Chronic otitis media as a cause of sensorineural hearing loss. Arch Otolaryngol 1973; 98:18-22.

4. Dumich PS, Harner S. Cochlear function in chronic otitis media. Laryngoscope 1983;93:583-6.

5. Walby AP, Barrera A, Schuknecht HF. Cochlear pathol-

ogy in chronic suppurative otitis media. Ann Otol Rhinol Laryngol Suppl 1983;92(suppl 103).

6. Paparella MM, Morizono T, Le CT, et al. Sensorineural hearing loss in otitis media. Ann Otol Rhinol Laryngol 1984;93: 623-9.

7. Papastavros T, Varlejides S. Reversible and permanent bone conduction threshold shift in cases of chronic suppurative otitis media. Am J Otol 1986;7:338-46.

8. Browning GG, Gatehouse S. Hearing in chronic suppurative otitis media. Ann Otol Rhinol Laryngol 1989;98:245-50.

9. Cusimano F, Cocita VC, D'Amica A. Sensorineural hearing loss in chronic otitis media. J Laryngol Otol 1989;103:158-63.

10. Levine BA, Shelton C, Berliner KI, Sheehy JL. Sensorineural loss in chronic otitis media: is it clinically significant? Arch Otolaryngol Head Neck Surg 1989;115:814-6.

11. Vartianen E, Seppa J. Results of bone conduction following surgery for chronic ear disease. Eur Arch Otorhinolaryngol 1997;254:384-6.

12. Blakeley BW, Kim S. Does chronic otitis media cause sensorineural hearing loss? J Otolaryngol 1998;27:17-20.

13. Eisenman DJ, Parisier SC. Is chronic otitis media with cholesteatoma associated with neurosensory hearing loss? Am J Otol 1998;19:20-5.

14. El-Sayed Y. Bone conduction impairment in uncomplicated chronic suppurative otitis media. Am J Otol 1998;19:149-53.

15. Tonndorf J. Bone conduction: studies in experimental animals. Acta Otolaryngol Suppl (Stockh) 1966(suppl 213).

16. Carhart R. Clinical application of bone conduction audiometry. Arch Otolaryngol 1950;51:798-808.

17. Silman S, Silverman CA. Auditory diagnosis: principles and applications. San Diego, Calif: Singular Publishing Group, 1991.

18. Hood JD. The principles and practice of bone conduction audiometry. Laryngoscope 1960;70:1211-28.

19. Riffenburgh RH. Common tests on the distribution shape of continuous data. In: Riffenburgh RH, ed. Statistics in medicine. San Diego, Calif: Academic Press, 1993:337-9.

≈

INTERNATIONAL HEARING AID CONFERENCE

International Hearing Aid Conference VI. Novel Processing and Fitting Strategies will be held in Iowa City, Iowa, June 7-9, 2001. For information, see web site www.medicine.uiowa.edu/otolaryngology/news/news, or contact Rich Tyler by telephone (319-356-2471) or e-mail (rich-tyler@uiowa.edu).

Ann Otol Rhinol Laryngol 110:2001

DETECTION OF INTRACYTOPLASMIC CYTOKINES BY FLOW CYTOMETRY IN ADENOIDS AND PERIPHERAL BLOOD LYMPHOCYTES OF CHILDREN

JOEL M. BERNSTEIN, MD, PHD
MARK BALLOW, MD
GARY RICH
BUFFALO, NEW YORK

Cytokine flow cytometry at the single-cell level has never been utilized in the study of adenoidal lymphocytes. We describe the multiparameter capability of flow cytometry to simultaneously detect an antigen on the surface of the adenoidal and peripheral blood lymphocytes and detect Th1 and Th2 cytokines within the cytoplasm of these lymphocytes. The data suggest that the percentage of cells producing interferon (IFN)–γ are decreased in adenoidal as compared to peripheral blood lymphocytes, confirming our previous studies. The new findings show that the CD8 subset of adenoidal lymphocytes produces lower amounts of IFN-γ as compared to peripheral blood CD8 cells. The intracytoplasmic synthesis of interleukin (IL)–2, however, appears to be similar in both adenoidal and peripheral blood lymphocytes. The CD4 subset of lymphocytes in the adenoid produces more IL-2, whereas the CD8 subset produces more IFN-γ. Finally, as shown in our previous studies, the Th2 cytokines appear to be produced in similar quantities in both adenoidal and peripheral blood lymphocytes.

KEY WORDS — adenoid, cytokine, flow cytometry.

INTRODUCTION

The adenoid is a lymphoepithelial organ situated in a critical position in the upper respiratory tract. It lies directly adjacent to the eustachian tube, which is the major entrance for bacterial or viral antigens entering the middle ear space. The adenoid also is situated very close to the natural ostia of the paranasal sinuses, so the bacteria and viral agents that predispose to sinusitis may also originate from the adenoid. Finally, the major pathogens that are responsible for chronic bronchitis and pneumonia most likely originate from the nasopharyngeal microflora.

It is therefore important to understand the immunologic events that take place in the adenoid, as these events may determine the outcome of infectious diseases of the upper and lower respiratory tract. Lymphocytes, as well as other immunocompetent cells of the adenoid, exert their effector function in part through the synthesis and release of cytokines. In the literature, very little information is available on lymphocyte function and cytokine production in the adenoid, although much is known about these molecules in the palatine tonsil, as well as in other lymphoid structures in the body.[1-3] We previously reported that adenoidal T lymphocytes appear to support synthesis of either adenoidal B cells or peripheral blood B cells less well than peripheral blood T cells.[4] Using an enzyme-linked immunosorbent assay, we also described decreased Th1 cytokine release by adenoidal lymphocytes as compared to autologous peripheral blood lymphocytes both in children with recurrent otitis media and in children without otitis media.[5] We concluded that Th1 cells (lymphocytes that produce mainly interferon [IFN]–γ and interleukin [IL]–2) may demonstrate an alteration or modulation of immunologic function. In contrast, Th2 cytokine production (IL-4, IL-5, IL-10) appeared to be approximately the same in the adenoidal lymphocytes and peripheral blood lymphocytes.[5]

Both IFN-γ and IL-2 are classic Th1 cytokines. These cytokines are primarily involved in cell-mediated immune responses and, as such, are important in the elimination of intracellular pathogens and in the eradication of virus-infected cells. Th2 cytokines such as IL-4 and IL-5 are primarily involved in the terminal synthesis of immunoglobulins, particularly IgE. Furthermore, IL-5 is a principal cytokine responsible for the survival of eosinophils, and thus, upregulation of Th2 cytokines appears to be important in the development of allergy and tissue eosinophilia. Alterations in the balance of Th1 and Th2 cytokines in the adenoid, therefore, are of critical importance in the development in children of various diseases, such as otitis media and sinusitis. One of the goals of our laboratory has been to determine cytokine production by adenoidal lymphocytes in various disease

---

From the Departments of Otolaryngology and Pediatrics, School of Medicine and Biomedical Sciences (Bernstein), the Department of Communicative Disorders and Sciences (Bernstein), and the Department of Pediatrics, Division of Allergy/Immunology (Ballow, Rich), State University of New York at Buffalo, and the Division of Infectious Diseases (Bernstein) and the Immunobiology Laboratory (Ballow, Rich), Children's Hospital of Buffalo, Buffalo, New York.

CORRESPONDENCE — Joel M. Bernstein, MD, PhD, 2430 N Forest Rd, Getzville, NY 14068.

TABLE 1. DEMOGRAPHICS OF CHILDREN

Child	*Sex*	*Age (y)*	*Condition of Adenoid*	*Allergy Status*	*Otitis Media With Effusion*	*Procedure*
1	M	3	Hypertrophic	–	+*	Adenoidectomy with bilateral tubes
2	M	4	Hypertrophic	–	–	Adenoidectomy
3	M	6	Infected (small)	+	–	Adenoidectomy
4	F	8	Hypertrophic	–	–	Adenoidectomy
5	M	3	Infected (small)	+	+*	Adenoidectomy with bilateral tubes
6	F	5	Hypertrophic	+	+	Adenoidectomy with bilateral tubes
7	F	4	Hypertrophic	–	–	Adenoidectomy
8	F	6	Infected (small)	–	+	Adenoidectomy with bilateral tubes
9	M	7	Hypertrophic	–	–	Adenoidectomy
10	M	6	Infected (small)	+	–	Adenoidectomy
11	M	5	Hypertrophic	–	–	Adenoidectomy
12	F	4	Hypertrophic	–	–	Adenoidectomy

*Otitis-prone child.

conditions, such as otitis media and sinusitis, to determine whether alterations in cytokine production may play a role in these clinical entities.

To further dissect the immune response in the adenoidal lymphocytes, we present now the detection of intracytoplasmic cytokines using flow cytometry and directly conjugated monoclonal anti-cytokine antibodies in adenoidal and autologous peripheral blood lymphocytes.

MATERIALS AND METHODS

The adenoids and peripheral blood of 12 children whose ages ranged from 3 to 8 years of age were used in this study. Six of the 12 children were admitted to the hospital for hypertrophic adenoids causing nasal obstruction. Although some of these 6 children had a history of otitis media, none of these children could be considered as otitis-prone as defined by 4 episodes of otitis media in the first year of life or 6 episodes of acute otitis media in the first 2 years of life. Four children were allergic as defined by clinical history, physical examination, and the presence of positive intradermal prick skin tests or radioallergosorbent tests. Two children of the 12 in this study were considered otitis-prone as defined above.

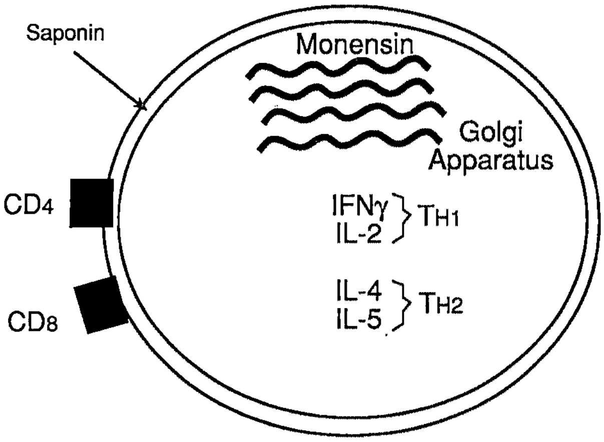

Diagrammatic representation of blood or adenoidal lymphocyte in technique of single-cell flow cytometry. Monoclonal antibody is directed against CD4 or CD8 with fluorescein-conjugated antibody producing green color. Saponin liquefies outer membrane of lymphocyte, allowing specific monoclonal antibody directed against Th1 and Th2 cytokines to enter cytoplasm. Monensin is bacterial-derived enzyme that disrupts Golgi apparatus, preventing efflux of cytokine from cell. Thus, cytokine synthesis remains within cell and can be measured. Monoclonal antibody directed against cytokine is stained with red stain so that 2-color flow cytometry is used to determine external antigen, as well as internal protein.

At the time of surgery, 4 children had otitis media with effusion and underwent adenoidectomy with installation of pressure-equalizing tubes. The other 8 children underwent adenoidectomy: 6 for hypertrophy alone and 2 because of a history of recurrent otitis media. (At the time of surgery, the middle ears were normal.) The demographics of the children are summarized in Table 1.

The homogenization of the adenoid and the separation of lymphocytes in both the adenoids and peripheral blood have been previously described.[4,5] The adenoid tissues were cut into small fragments and teased apart to disperse the cells into a single-cell suspension. Mononuclear cells were separated by Ficoll-Hypaque density gradient centrifugation. Peripheral blood lymphocytes were collected and washed in Hank's buffered salt solution (Gibco Laboratories, Grand Island, NY). Peripheral blood mononuclear cells were separated by Ficoll-Hypaque density gradient centrifugation. All cultures were carried out in medium RPMI 1640 (Gibco Laboratories) supplemented with 100-U/mL penicillin G, 50-µg/mL streptomycin, 2-mmol/L glutamine, 10-mmol/L Hepes buffer, and 15% heat-inactivated fetal calf serum (Flow Laboratories, McLean, Va). The technique for detection of intracytoplasmic cytokine using directly conjugated anti-cytokine antibodies and antibodies directed against the surface markers CD4 and CD8 is schematically summarized in the Figure. Briefly,

TABLE 2. PERCENTAGES OF CD4 AND CD8 LYMPHOCYTES IN PERIPHERAL BLOOD AND ADENOID (N = 12)

	Blood	*Adenoid*	*p*
CD4	45.4 ± 3.0	30.3 ± 4.3	.002
CD8	23.0 ± 2.2	10.9 ± 2.0	.006

TABLE 3. PERCENTAGES OF PERIPHERAL BLOOD LYMPHOCYTES AND ADENOIDAL LYMPHOCYTES PRODUCING CYTOKINES

	Blood	*Adenoid*	*p*
IFN-γ	16.9 ± 1.7	4.7 ± 0.61	<.001
IL-2	18.6 ± 2.3	14.9 ± 1.7	NS
IL-4	1.3 ± 0.2	2.75 ± 0.3	.001
IL-5	0.492 ± 0.20	1.7 ± 0.9	NS
CD4 IFN-γ	9.7 ± 1.26	9.8 ± 1.3	NS
CD4 IL-2	31.8 ± 3.58	37.1 ± 3.8	NS
CD4 IL-4	7.1 ± 3.4	5.36 ± 0.75	NS
CD4 IL-5	4.7 ± 3.2	1.7 ± 0.54	NS
CD8 IFN-γ	30.9 ± 3.3	21.13 ± 3.1	.016
CD8 IL-2	10.3 ± 1.5	14.1 ± 1.8	NS
CD8 IL-4	0.875 ± 0.16	2.75 ± 0.49	.001
CD8 IL-5	1.11 ± 0.71	1.99 ± 0.65	.067

IFN — interferon, IL — interleukin, NS — not significant.

cell activation with phorbol 12-myristate 13-acetate (PMA) and calcium ionophore was used to stimulate adenoidal and peripheral blood lymphocytes. Cells were cultured for 8 hours in the presence of monensin to accumulate the cytokine in the Golgi apparatus. Monensin is a lipophilic metabolite of *Streptomyces cinnamonensis* that binds Na^+, K^+, and H^+ ions, leading to a disruption of ion gradients and biological membranes.[6] This results in a perturbation of the Golgi complex and an interruption of transport to the cell membrane without influencing protein synthesis. Thus, monensin treatment results in an accumulation of a cytokine in the cell, leading to enhanced numbers of positively stained cells after a definite time period. Before cell preparation for flow cytometry, the Fc receptors on the lymphocytes were preblocked with an excess of irrelevant purified immunoglobulin. Cell surface antigens CD4 and CD8 were stained in a staining buffer consisting of approximately 0.5 μg of fluorescein-conjugated monoclonal antibodies specific for CD4 and CD8 obtained from Pharmingen (San Diego, Calif). The cells were then fixed with paraformaldehyde for 20 minutes at 4°C. The cells were kept overnight in fixation buffer at 4°C. Cell aggregation was avoided by pipetting and vortexing prior to fixation. After the cells were permeabilized with saponin, anti-cytokine antibody diluted to the appropriate concentration was incubated with the cells for 30 minutes at 4°C. Intracytoplasmic staining of 4 cytokines was performed with phycoerythrin (PE)–conjugated monoclonal anti–IL-2, IL-4, IL-5, and IFN-γ. In the initial studies, positive and negative controls were used in the following manner. Unlabeled monoclonal antibodies blocked the intracytoplasmic labeling of cytokines by means of non-labeled antibody controls, including cells that were not stimulated with PMA–calcium ionophore. Absence of cell stimulation resulted in no cytokine production inside the cell. Finally, monensin was cultured with the cells for 6 hours, which appears to be the ideal time for all 4 cytokines studied in this protocol.

The analysis of data was performed on a FACSCAN flow cytometer (Becton Dickinson Immunocytometry Systems, Palo Alto, Calif) with Lysis II software. Dead cells and monocytes were excluded by forward and side scatter gating. Typically, 20,000 to 100,000 events were acquired, depending on the cytokine being studied. Statistical markers were set with use of the negative control cells as a reference. Typically, 0.1% or fewer positive cells were allowed beyond the statistical marker in these controls.

Statistical analysis of the percentages of cytokine production by adenoidal lymphocytes and peripheral blood lymphocytes was performed by the Statistical Package for the Social Sciences (SPSS) with the paired Student's *t*-test. A p value of less than .05 was considered statistically significant.

Inasmuch as the palatine tonsils of the children were not studied because there was no clinical indication for their removal, a comparison between adenoidal T lymphocyte cytokine production and palatine tonsillar T lymphocyte cytokine production cannot be made in this study.

RESULTS

The results for the total study are given in Tables 2 and 3. The major findings demonstrate that there are more CD4 and CD8 cells in the peripheral blood than in the adenoid. The percentage of cells synthesizing IFN-γ in the peripheral blood is almost 4 times greater than that in the adenoid. The amounts of IL-2 production at both sites are approximately the same. In contrast, there is significantly more IL-4 being produced in the adenoid than in the peripheral blood lymphocytes. There is also more IL-5 in the adenoids than in the peripheral blood lymphocytes, but this finding does not reach statistical significance. In specifically dissecting the immune response, it appears that CD8 cells in the peripheral blood are producing significantly more IFN-γ than adenoidal CD8 cells, and this finding primarily accounts for the decreased production of IFN-γ in the adenoid. Finally, it is of interest to note that CD4 cells produce more IL-2 in both the peripheral blood and the adenoid and CD8 cells produce more IFN-γ in both the peripheral blood and the adenoid.

DISCUSSION

Cytokine flow cytometry differs from traditional cytokine assays in that the unit of data is the frequency of cytokine-producing cells. Such data may be meaningful. In this study, it has been demonstrated that the percentage of adenoidal lymphocytes producing IFN-γ is significantly less than the percentage of peripheral blood lymphocytes producing it. Furthermore, it appears that the CD8 subset of T lymphocytes is responsible for this decrease, because CD4 lymphocytes from both peripheral blood and adenoids appear to possess approximately the same percentage of cells producing IFN-γ.

Our studies also confirm previously reported findings in peripheral blood that IL-2 is the dominant cytokine produced by CD4 cells, whereas IFN-γ predominates in the CD8 response.[7] This is the first report of good correlations in the adenoid. Although IL-4 and IL-5 frequencies were generally slightly higher in the adenoid, the small numbers that were seen are again consistent with the previous published data, suggesting that the percentage of CD4 and CD8 cells producing Th2 cytokines is much smaller than the percentage of those producing Th1 cytokines.[8] In general, this study, detecting intracytoplasmic cytokines by using flow cytometry and directly conjugated anti-cytokine antibodies, confirms our previous studies demonstrating that adenoidal lymphocytes produce less IFN-γ than peripheral blood lymphocytes.[5] The significance of decreased amounts of IFN-γ in the adenoid as a part of the local immune system in the nasopharynx has yet to be established. However, it has been shown that IFN-γ enhances IgA production,[9] increases major histocompatibility complex antigen expression, and probably allows antigen presentation by different mucosal cells.[9] Interferon-γ also increases the expression of secretory component receptors on certain cells of the gastrointestinal tract and thus facilitates secretory IgA transport.[9] Furthermore, IFN-γ has been found to interfere with tight junction permeability between the intestinal epithelial cells, as well as with active electrolyte secretion by enterocytes in vitro.[10] Whether this interference occurs in the adenoid has yet to be determined. In addition, IFN-γ interferes with the receptivity of epithelial cells toward invasive pathogens in the gastrointestinal tract, such as *Shigella*, and stimulates infected epithelial cells and macrophages to produce nitric oxide, which is strongly bactericidal.[11] These functions of IFN-γ could possibly be playing a role at the level of the nasopharyngeal lymphoepithelial organ.

Viral infection is probably the most important trigger for the development of otitis media and sinusitis. The mechanisms are poorly known, but it has been suggested that viral infection enhances bacterial invasion of the middle ear and sinuses by decreasing mucociliary clearance[12] and decreasing neutrophil function.[13] Therefore, one of the most important consequences of diminished IFN-γ production in the adenoid is an increased susceptibility to viral infectious diseases of the upper respiratory tract, which may lead to increased bacterial replication in the adenoid.

In conclusion, the present studies confirm and extend our ideas on the pathogenesis of otitis media and sinusitis in relation to the adenoid. First, adenoidal T cells do not appear to support immunoglobulin synthesis, as compared with either homologous peripheral blood T cells or allogeneic T cells. Adenoidal B cells are able to synthesize immunoglobulins, particularly IgG, when stimulated either by the patient's own peripheral blood T cells or by allogeneic T cells; this finding suggests that it is the adenoidal T cells that exhibit perturbation in the support of immunoglobulin synthesis. In support of this concept of alteration of T cell function, there appears to be evidence that on enzyme-linked immunosorbent assay, IFN-γ production and IL-2 secretion are decreased in the adenoid as compared to peripheral blood lymphocytes. The present study has dissected the immune response somewhat further, in that we suggest that the alteration in the production of IFN-γ resides in the CD8 subset of T lymphocytes.

In analyzing the data in the study, it is important to emphasize that the numbers are relatively small. However, there were no differences between children with hypertrophic adenoids without otitis media and children with chronic adenoiditis and otitis media with effusion. Furthermore, the 2 otitis-prone children also had decreased production of IFN-γ by CD8 T cells. Thus, there was a uniformity in all patients regardless of their clinical disease or whether IgE-mediated hypersensitivity was present. At this time, no correlation can be made between the development of recurrent otitis media and perturbation of IFN-γ synthesis in the adenoidal lymphocytes. Although increased susceptibility to viral infection may be a leading candidate in the pathogenesis of recurrent otitis media, bacterial otitis media and bacterial rhinosinusitis are the result of many variables, including genetic predisposition as it relates to the synthesis of both IgA and IgG subclasses, anatomic variations of both the eustachian tube and the ostia of the sinuses, and epidemiological factors such as parental smoking, breast feeding, and socioeconomic conditions. The findings in this study present one important variable, however, and that is a consistent perturbation of T cell function in the adenoid in children undergoing adenoidectomy for either hypertrophy or otitis media with effusion. It remains to be determined whether this finding is an important predisposing factor in the development of upper respiratory tract viral and bacterial infection.

Cytokine flow cytometry has emerged in the past few years as the technique of choice for studying cytokine production at the single-cell level. By using 3-color flow cytometry, investigators will be able to identify novel subsets of adenoidal lymphocytes capable of producing specific cytokines. This ability will eventually permit detection of antigen-specific cytokine responses, an indispensable tool for the investigation of disease pathophysiology, immunomodulation, and vaccine development at the level of the nasopharynx.

REFERENCES

1. Agren K, Brauner A, Andersson J. *Haemophilus influenzae* and *Streptococcus pyogenase* group A challenge induce a $\mathrm{Th_1}$ type of cytokine response in cells obtained from tonsillar hypertrophy and recurrent tonsillitis. ORL J Otorhinolaryngol Relat Spec 1998;60:35-41.

2. Lisignoli G, Pozzi C, Toneguzzi S, Tomassetti M, Monaco MC, Facchini A. Different pattern of cytokine production and mRNA expression by lymphoid and non-lymphoid cells isolated from human palatine tonsil. Int J Clin Lab Res 1998;28:23-8.

3. Von Gaudecker B, Sticherling M, Sterry W. Immunohistochemical localization of cytokines and receptor-associated molecules in human tonsils and skin. Acta Otolaryngol Suppl (Stockh) 1996(suppl 523):71-4.

4. Bernstein JM, Rich GA, Odziemiec C, Ballow M. Are thymus-derived lymphocytes (T cells) defective in the nasopharyngeal and palatine tonsils of children? Otolaryngol Head Neck Surg 1993;109:693-700.

5. Bernstein JM, Ballow M, Xiang S, O'Neil K. $\mathrm{Th_1/Th_2}$ cytokine profiles in the nasopharyngeal lymphoid tissues of children with recurrent otitis media. Ann Otol Rhinol Laryngol 1998;107:22-7.

6. Prussin C. Cytokine flow cytometry: understanding cytokine biology at the single-cell level. J Clin Immunol 1997;17:195-204.

7. Prussin C, Metcalfe DD. Detection of intracytoplasmic cytokine using flow cytometry and directly conjugated anti-cytokine antibodies. J Immunol Methods 1995;188:117-28.

8. Harriman GR, Allison KC, Strober W. Expression of IL-5 receptors on B-cells: role in mucosal B-cell responses. Immunol Res 1991;10:413-7.

9. Madara JL, Stafford J. Interferon-gamma directly affects barrier function of cultured intestinal epithelial monolayers. J Clin Invest 1989;83:724-7.

10. Holmgren J, Fryklund J, Larsson H. Gamma-interferon–mediated down-regulation of electrolyte secretion by intestinal epithelial cells: a local immune mechanism? Scand J Immunol 1989;30:499-503.

11. Nussler AK, Billiar TR. Inflammation, immunoregulation, and inducible nitric oxide synthase. J Leukoc Biol 1993;54:171-8.

12. Bryson DG, Platten MF, McConnell S, McNulty MS. Ultrastructural features of lesions in bronchiolar epithelium in induced respiratory syncytial virus pneumonia of calves. Vet Pathol 1991;28:293-9.

13. Wang SZ, Xu H, Wraith A, Bowden JJ, Alpers JH, Forsyth KD. Neutrophils induce damage to respiratory epithelial cells infected with respiratory syncytial virus. Eur Respir J 1998;12:612-8.

Ann Otol Rhinol Laryngol 110:2001

IMMUNOPATHOLOGIC STUDY OF CHRONIC SINUSITIS: A PROPOSAL FOR ATOPIC AND NON-ATOPIC IGE-ACTIVATED MAST CELL ALLERGIC INFLAMMATION

LAWRENCE S. LOESEL, MD
TRAVERSE CITY, MICHIGAN

Paranasal sinus mucosa was examined in this study for mast cell membrane–bound IgE. The study material was from 54 patients identified in hospital records as having one of the following diagnoses: chronic sinusitis, chronic sinusitis with asthma, or chronic sinusitis with associated nasal polyps. Formalin-fixed tissue samples taken during endoscopic sinus surgery were routinely processed and examined with hematoxylin and eosin stains. Additional sectioned tissue was analyzed by fluorescence microscopy for mast cells after the use of anti-IgE and anti-tryptase antisera; 45% of the cases of chronic sinusitis, 50% of the cases of chronic sinusitis with polyposis, and 69% of the cases of chronic sinusitis with asthma exhibited 10 or more IgE-positive mast cells in the sinus mucosa. Significant numbers of individuals with chronic sinusitis have coexistent allergic disorders. Some individuals in this study who were not allergic by hospital record review also manifested IgE-positive mast cells in the sinus mucosa; a basis for this finding is proposed.

KEY WORDS — allergy, chromosome 5Q31.1, chronic sinusitis, IgE, interleukin-4, mast cell.

INTRODUCTION

My interest in upper airway allergy was initiated in 1980, with the immunofluorescence study of IgE-positive mast and plasma cells in adenoid tissue removed from 606 children.[1] That study and a subsequent analysis of additional cases for a total of 1,242 children revealed that 55% of the 259 children whose adenoid tissue demonstrated numerous fluorescent membrane–positive IgE mast cells had no evidence of clinical allergy.[2] In 1987, I proposed that some of the "false-positive," non-allergic children who manifested positive fluorescent IgE mast cells in their adenoid tissue might have been showing immune responses to viral or bacterial infections.[3]

A chance to examine sinus mucosa retrieved by endoscopic surgery afforded the opportunity to study upper respiratory tract mucosa in which multiple episodes of infection and/or inflammation had been clinically determined. Notably, functional endoscopic sinus surgery has been reported to ameliorate asthma in 90% of patients in long-term follow-up.[4] Newman et al[5] documented the surgically obtained culture results of 104 endoscopic sinus surgery patients with regard to aerobic and anaerobic bacteria and fungi; all cultures grew at least 1 aerobic organism, with coagulase-negative staphylococci being the most frequent.

MATERIALS

The cases were drawn from Munson Medical Center medical records and surgical pathology files for endoscopic sinus surgery procedures conducted in the years 1994 through 1996 inclusive. The clinical diagnoses and historical data for these cases were drawn solely from the medical records. Fifty-four cases were studied: 22 with chronic sinusitis alone, 16 with chronic sinusitis and asthma, and 16 with chronic sinusitis with associated nasal polyposis. The definition of chronic sinusitis used herein meets the working definition proposed by Lanza and Kennedy.[6] The site of the paranasal sinus is not further defined, because endoscopic surgical material from the ethmoid and maxillary sinuses was often jointly submitted in a single container for pathological examination.

The hospital records related to sinus surgery admission were inspected for specific mention of allergic rhinitis or hay fever and/or asthma. Asthma was well documented by physician admission history and the nurse's and anesthesiologist's preoperative notes. Allergic rhinitis, however, was not recorded in any of the 54 patients' records. The hospital records included a history of drug allergy or adverse drug reaction to 1 or more agents in 14 individuals: 6 men and 8 women. Eight cases had chronic sinusitis and asthma, 4 had chronic sinusitis alone, and 2 had chronic sinusitis and nasal polyposis. The majority of patients, 9, had had reactions to antibiotics, with penicillins and sulfonamides cited most frequently. One patient with chronic sinusitis, asthma, and nasal polyposis had asthma as a reaction to aspirin. This individual (case 35), later identified as hav-

---

From the Department of Pathology, Munson Medical Center, Traverse City, Michigan.
CORRESPONDENCE — Lawrence S. Loesel, MD, Dept of Pathology, Munson Medical Center, Traverse City, MI 49684.

ing Samter triad–type asthma, also had skin test–defined atopy that resulted in subsequent desensitization therapy.

METHODS

The examination of sinus tissue for mast cells and IgE was done in the context of an ongoing study of adenoid and lymphoid tissue that exceeded 3,000 cases during a 17-year period. Sensitivity, specificity, and sequential staining studies with anti-IgE and toluidine blue were carried out in initial studies.[1] The sensitivity of 200 IU/mL of IgE, a level that reflects appreciable elevation of that immunoglobulin, has been previously described in our work.[7] Addition of anti-tryptase antisera as a mast cell identifier was carried out in an investigation of mast cell participation in Hodgkin's disease.[7] The above antisera, and those described below, were used against positive and negative adenoid control tissue that manifested either numerous or rare mast cells. Specifically for this study, polyclonal rabbit anti-IgE was diluted 1:100 and followed by application of a 1:200 dilution of fluoresceinated goat anti-rabbit antiserum. Monoclonal mouse anti-tryptase was diluted 1:50 and followed by fluoresceinated goat anti-mouse diluted 1:20. Thirty-minute incubation periods at room temperature were carried out for both first- and second-set antibody applications. All dilutions and interval washes were carried out with phosphate-buffered saline solution, pH 7.2 (antisera from Dako Laboratories, Carpinteria, Calif). Microscopic examination was conducted with a Zeiss halogen epifluorescence microscope with excitation filters B-490 and EY-455 and barrier filters DM-500 and O-515. Photomicrographs were taken with a Nikon EFM system with Ilford 400 ASA film.

Immunofluorescence studies of sinus mucosa and stroma by the above technique revealed twofold variation in stromal mast cell counts in various areas of 14 cases, and threefold variation in 1 case. To moderate these variances in stromal sites, the 2 highest counts per high-power field (400×) were averaged. The single field of mucosal epithelium and subtendant stroma exhibiting the greatest visible number of mast cells per high-power field was similarly recorded.

Formalin-fixed, wax-embedded, and conventionally stained hematoxylin and eosin surgical pathology–accessioned slides were microscopically examined. An analysis of the dominant inflammatory cell type present was made. That is, if inspection of the glass slide revealed 75% or greater numbers of a particular cell type, it was so characterized, ie, eosinophilic, lymphocytic, or plasma cellular. If no cell type dominated and the inflammatory infiltrate was an admixture of variable proportions of eosinophils, lymphocytes, plasma cells, and neutrophils, the infiltrate was designated as mixed. For each case, the estimated area of inflammatory infiltrate on the hematoxylin and eosin–stained slide was microscopically determined and semiquantified as less than 10%, 10% to 40%, or greater than 40%. After examination of that single hematoxylin and eosin–stained slide that was most demonstrative of the above characterizations, the paraffin block from which the slide was prepared was further sectioned at 4 µm for immunofluorescence staining techniques to enumerate and localize mast cells.

RESULTS

Microscopic examination of the sinus mucosa and stroma by the immunofluorescence technique revealed readily identifiable fluorescent cells in the stroma and mucosa. By their larger size and convoluted appearance, mast cells seemed to be the most numerous, but in mucosal epithelium particularly, the distinction between mast cells and basophils is difficult. For reporting purposes and discussion in this study, the cells identified are tabulated as mast cells. Notably absent from the sinus tissue were immunofluorescent IgE plasma cells, except in 2 cases (cases 17 and 54), in which 1 plasma cell was identified in each.

Elevated numbers of IgE fluorescence–positive mast cells (10 or more per high-power field) in the sinus mucosa were noted in 29 of the 54 cases (54%). By disease category, 45% of the chronic sinusitis cases bore elevated numbers of IgE-positive cells (Table 1), as did 69% of the chronic sinusitis cases with asthma (Table 2) and 50% of the cases with chronic sinusitis with polyposis (Table 3). Anti-tryptase antisera detected significant numbers of mast cells in all 54 cases except 2 (cases 49 and 51), in which negligible numbers of mast cells were seen. Photomicrographs of IgE-positive mast cells and mast cells labeled with anti-tryptase are shown in Figs 1 and 2, respectively.

The predominant inflammatory cell infiltrate detected by hematoxylin and eosin correlated with immunofluorescence-detected mast cells is given in Table 4. In 2 of the 16 asthmatic cases, eosinophils predominated, whereas 11 cases, including the 2 that were eosinophilic-predominant, were detected by increased IgE-immunofluorescent mucosal mast cells (2/16 or 13%, versus 11/16 or 69%). Eighteen of the 38 nonasthmatic cases, or 47%, bore numerous IgE-immunofluorescent mucosal mast cells, and 11 of the 38, or 29%, showed predominant eosinophilic inflammation.

TABLE 1. CHRONIC SINUSITIS

				Anti-IgE MC/HPF		*Anti-Tryptase MC/HPF*	
Case	*Sex*	*Age (y)*	*Cell Type and Percent*	*Stroma*	*Mucosa*	*Stroma*	*Mucosa*
1	M	57	Mixed <10	0	0	17	24
2	F	30	Mixed <10	0	0	13	14
3	M	72	Mixed <10	6	0	23	16
4	M	52	Mixed <10	7	0	27	17
5	M	50	Mixed <10	25	14	44	40
6	M	31	Mixed <10	34	24	20	26
7	M	71	Mixed 10-40	0	0	15	14
8	F	40	Mixed 10-40	0	0	18	27
9	M	47	Mixed 10-40	0	0	20	42
10	F	44	Mixed 10-40	15	7	21	30
11	F	33	Mixed 10-40	15	14	11	8
12	F	24	EOS <10	0	0	18	15
13	M	40	EOS <10	13	12	21	19
14	M	69	EOS <10	23	42	9	43
15	M	33	EOS 10-40	12	23	17	45
16	M	66	EOS 10-40	21	52	18	53
17	M	42	EOS 10-40	24	21	21	29
18	F	61	EOS >40	16	0	29	26
19	F	57	LYMPH <10	0	0	23	19
20	F	31	LYMPH <10	8	12	14	20
21	F	71	LYMPH 10-40	8	2	24	22
22	M	48	PLASMA >40	4	36	15	16

MC/HPF — mast cells per high-power field, EOS — eosinophilic inflammation, LYMPH — lymphocytic inflammation, PLASMA — plasma cell inflammation.

DISCUSSION

In my original study[1] of adenoid tissue from children, the percentage of cases exhibiting fluorescence-positive IgE mast cells in stroma was 16%. Two percent of these children additionally revealed a transmucosal presence of 10 or more IgE-positive mast cells per high-power field in addition to numerous stromal mast cells.[1] The review by Brandtzaeg et al[8] of upper respiratory tract immunopathology noted that a shift of IgE-"armed" mast cells from the stroma into the mucosal epithelium signified allergen exposure. In this study of sinus mucosa from all clinical categories, 54% exhibited this feature of transmucosal inflammation. Among asthma cases, 69% displayed positive IgE mast cell mucosal involvement.

TABLE 2. CHRONIC SINUSITIS WITH ASTHMA

				Anti-IgE MC/HPF		*Anti-Tryptase MC/HPF*	
Case	*Sex*	*Age (y)*	*Cell Type and Percent*	*Stroma*	*Mucosa*	*Stroma*	*Mucosa*
23	F	64	Mixed <10	2	0	6	12
24	F	14	Mixed <10	9	3	12	20
25	F	29	Mixed <10	20	18	23	37
26	F	46	Mixed <10	15	22	10	20
27	F	59	Mixed 10-40	13	2	18	15
28	F	35	Mixed 10-40	10	10	33	30
29	F	45	Mixed 10-40	8	12	12	29
30	F	32	Mixed 10-40	21	18	29	22
31	F	49	Mixed 10-40	17	32	49	19
32	F	61	Mixed 10-40	32	33	30	24
33	F	63	Mixed 10-40	21	45	26	21
34	M	73	Mixed >40	5	0	18	19
35	M	44	Mixed >40	32	33	30	42
36	F	45	EOS 10-40	23	19	23	18
37	M	49	EOS >40	19	12	15	9
38	M	54	LYMPH 10-40	0	0	20	22

TABLE 3. CHRONIC SINUSITIS WITH POLYPOSIS

Case	Sex	Age (y)	Cell Type and Percent	Anti-IgE MC/HPF Stroma	Anti-IgE MC/HPF Mucosa	Anti-Tryptase MC/HPF Stroma	Anti-Tryptase MC/HPF Mucosa
39	M	44	Mixed <10	0	0	15	30
40	M	26	Mixed <10	13	9	11	25
41	M	38	Mixed <10	14	15	13	14
42	M	70	Mixed 10-40	4	1	16	18
43	M	58	Mixed 10-40	8	5	20	10
44	F	43	Mixed 10-40	70	45	57	27
45	M	55	Mixed 10-40	38	52	19	39
46	F	48	Mixed 10-40	37	59	46	55
47	M	75	Mixed >40	0	0	14	15
48	M	59	Mixed >40	12	22	16	8
49	M	55	EOS >10	0	0	2	0
50	F	53	EOS >10	2	6	13	24
51	M	75	EOS >10	12	19	2	3
52	M	58	EOS 10-40	18	31	16	27
53	M	60	LYMPH >40	17	24	38	26
54	M	31	PLASMA >10	0	0	27	23

As noted in a previous study[2] from our laboratory, 55% of children who had numerous stromal fluorescent IgE-positive mast cells in adenoid tissue had no clinical evidence of allergy. A follow-up of 39 non-allergic children performed 13 years later by mailed questionnaire (20 mast cell membrane IgE-positive and 19 IgE-negative) revealed that none had symptoms of allergy and that their personal physician had made no diagnosis of airway allergic disease (unpublished observations).

Newman et al,[5] in their study of chronic sinusitis by computed tomography (CT), immunoassays for IgE, and peripheral tissue eosinophilia, noted that

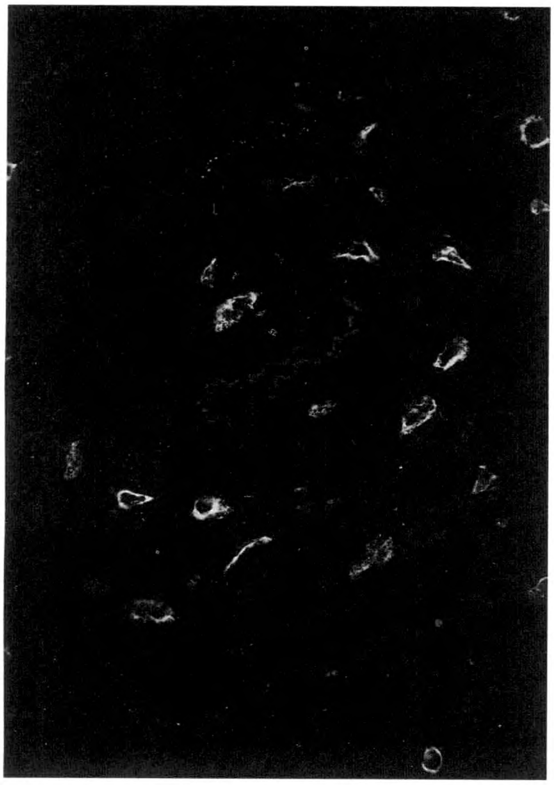

Fig 1. (Case 36) Mast cells distributed in stroma about coiled, partly autofluorescent elastica in blood vessel (anti-IgE/anti-rabbit fluorescein, original ×200).

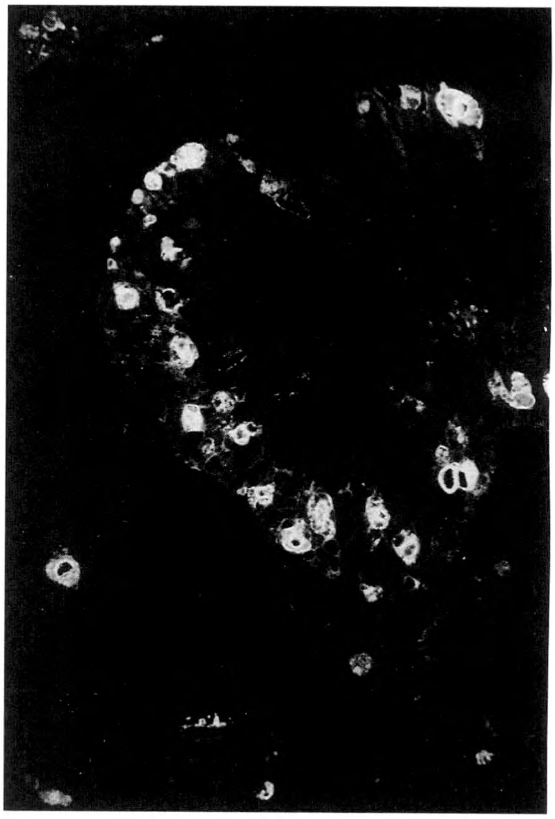

Fig 2. (Case 14) Mast cells principally resident in mucosal glandular epithelium and few in subtendant stroma (anti-tryptase/anti-mouse fluorescein; original ×200).

TABLE 4. DISTRIBUTION OF IGE MAST CELLS BY INFLAMMATORY CELL TYPE

	IgE-Positive (>10 MC/HPF)	*IgE-Negative (<10 MC/HPF)*
Asthmatic cases (n = 16)	11	5
Mixed	9	4
EOS	2	
LYMPH		1
Non-asthmatic cases (n = 38)	18	20
Mixed	8	13
EOS	7	4
LYMPH	2	2
PLASMA	1	1

IgE antibodies were associated with severe chronic sinusitis. The majority of patients with extensive sinus disease had a negative radioallergosorbent test (RAST) result. A subsequent study of an additional 80 patients by this group revealed atopy, as defined by an elevated IgE level and/or a positive RAST score, in 40% of patients.[9]

Baroody et al[10] analyzed the relationship between total IgE serum levels and sinus mucosal thickness on CT scans. Their study of 86 patients revealed a significant correlation between the extent of sinus disease as determined by CT scan and serum levels of IgE. They suggest that inflammatory responses to precipitating events such as viral or bacterial infections or IgE-mediated allergic reactions could be contributing factors. A smaller study by the same group[11] revealed sinus mucosal abnormalities by CT in 6 of 10 adults with ragweed allergic rhinitis. In discussion of hypotheses that may link chronic sinusitis and allergic rhinitis, they note that the character of inflammation in subjects with allergies differs from that in subjects without allergies. They cite the work of Hamilos et al,[12] which demonstrated similar eosinophilic leukocytic infiltrates in allergic and nonallergic hyperplastic sinusitis. The work of Hamilos et al would indicate that eosinophilic infiltrates cannot signify allergic inflammation unless fully characterized clinically with appropriate allergy skin testing or, as in their analysis, a broad panel of cytokine measurement.

Burrows et al,[13] in their study of 2,657 subjects in Tucson, Arizona, for asthma and allergic rhinitis, found the prevalence of asthma to be closely related to serum IgE level. Atopy was defined in this study by skin tests employing a variety of allergens common to the Tucson area. The prevalence of asthma followed the serum IgE level more closely than the degree of atopy. Slavin[14] reported, in his study of 80 adults who had sinusitis and asthma, that two thirds were non-atopic on the basis of history and skin tests.

Ponikau et al[15] recently made a novel contribution to the study and understanding of chronic rhinosinusitis. They contend that allergic (eosinophilic) fungal sinusitis was present in 93% of their 101 surgical chronic rhinosinusitis cases. They believe that type 1 hypersensitivity is not the common denominator in chronic rhinosinusitis. In the absence of a study of mast cells in sinus mucosa in their work, they cite Jankowski et al,[16] who state that mast cells are not increased in the nasal mucosa in chronic sinusitis.

Marsh et al[17,18] have proposed, in their genetic research of Amish families, an explanation for elevated IgE that does not have a basis in allergen-driven IgE production. They propose that a generalized up-regulation of interleukin 4 (IL-4) resident on chromosome 5Q31.1 leads to B-cell switching to production of IgE instead of IgG. This polyclonal increase in IgE would not be detected by multiallergen testing. Furthermore, they note that mast cells and basophils may constitute a source of IL-4 throughout life. Galli[19] suggests that the function of mast cells may be to initiate and orchestrate an early host response to microbial infection that in the context of immune activation equips the mast cell to function as a strategically located, highly reactive, and potent effector cell against invading pathogens. Umetsu and DeKruyff[20] suggest that it is likely that allergic individuals produce Th2 cytokines against many encountered antigens, including infectious agents, as well as allergens.

In summary, I identify a substantial number of individuals with chronic sinusitis who manifest numerous IgE-positive mast cells in the sinus mucosa. Many of these cases, particularly those associated with asthma, have an IgE origin through an atopic, allergen-driven, HLA-D encoded sequence of IgE formation. In non-allergic cases, significant amounts of mast cell–bound antibody identified in sinus mucosa mast cells may originate from previously committed plasma cell–generated IgG antibody against microbial organisms now re-emergent as IgE. I consider the IgE-positive mast cells in sinus mucosa to reflect a variety of antigenic experience, including allergens and infectious agents.

ACKNOWLEDGMENTS — The author thanks the personnel of the Munson Medical Center Department of Medical Records, Health Science Library, and Department of Histopathology for their contribution to this work.

REFERENCES

1. Loesel LS. Detection of allergic disease in adenoid tissue. Am J Clin Pathol 1984;81:170-5.
2. Loesel LS. An immunohistologic study of upper airway allergy in children: a proposed genetic relationship [Abstract]. Lab Invest 1986;54:38.
3. Loesel LS. The role of immunoglobulins in allergic dis-

ease: IgE and IgG4 immunofluorescent study of adenoid tissue. Semin Diagn Pathol 1987;4:153-6.

4. Senior BA, Kennedy DW, Tanabodee J. Long-term results of functional endoscopic sinus surgery. Laryngoscope 1998; 108:151-7.

5. Newman LJ, Platts-Mills TA, Phillips CD, Hazen KC, Gross CW. Chronic sinusitis. Relationship of computed tomographic findings to allergy, asthma, and eosinophilia. JAMA 1994;271:363-7.

6. Lanza DC, Kennedy DW. Adult rhinosinusitis defined. Otolaryngol Head Neck Surg 1997;117(suppl):S1-S7.

7. Loesel LS. IgE immunopathologic findings in Hodgkin's disease. Appl Immunohistochem 1994;2:123-9.

8. Brandtzaeg P, Jahnsen FL, Farstad IN. Immune functions and immunopathology of the mucosa of the upper respiratory pathways. Acta Otolaryngol (Stockh) 1996;116:149-59.

9. Hoover GE, Newman LJ, Platts-Mills TA, Phillips CD, Gross CW, Wheatley LM. Chronic sinusitis: risk factors for extensive disease. J Allergy Clin Immunol 1997;100:185-91.

10. Baroody FM, Su SH, Naclerio RM. Total IgE serum levels correlate with sinus mucosal thickness on computerized tomography scans. J Allergy Clin Immunol 1997;100:563-8.

11. Naclerio RM, deTineo ML, Baroody FM. Ragweed allergic rhinitis and the paranasal sinuses: a computerized tomographic study. Arch Otolaryngol Head Neck Surg 1997;123:193-6.

12. Hamilos DL, Leung DY, Wood R, et al. Evidence for distinct cytokine expression in allergic versus nonallergic sinusitis. J Allergy Clin Immunol 1995;96:537-44.

13. Burrows B, Martinez FD, Halonen M, Barbee RA, Cline MG. Association of asthma with serum IgE levels and skin-test reactivity to allergens. N Engl J Med 1989;320:271-7.

14. Slavin RG. Sinusitis in adults and its relation to allergic rhinitis, asthma, and nasal polyps. J Allergy Clin Immunol 1988; 82:950-6.

15. Ponikau JU, Sherris DA, Kern EB, et al. The diagnosis and incidence of allergic fungal sinusitis. Mayo Clin Proc 1999; 74:877-84.

16. Jankowski R, Bene MC, Moneret-Vautrin AD, et al. Immunohistological characteristics of nasal polyps: a comparison with healthy mucosa and chronic sinusitis. Rhinol Suppl 1989; 8:51-8.

17. Marsh DG, Neely JD, Breazeale DR, et al. Linkage analysis of IL4 and other chromosome 5q31.1 markers and total serum immunoglobulin E concentrations. Science 1994;264: 1152-6.

18. Marsh DG, Neely JD, Breazeale DR, et al. Genetic basis of IgE responsiveness: relevance to the atopic diseases. Int Arch Allergy Immunol 1995;107:25-8.

19. Galli SJ. The mast cell: a versatile effector cell for a challenging world. Int Arch Allergy Immunol 1997;113:14-22.

20. Umetsu DT, DeKruyff RH. Th1 and Th2 CD4+ cells in human allergic diseases. J Allergy Clin Immunol 1997;100:1-6.

Ann Otol Rhinol Laryngol 110:2001

LUDWIG'S ANGINA: REPORT OF A CASE AND REVIEW OF MANAGEMENT ISSUES

MICHAEL S. BARAKATE, BSC(MED), MBBS
JONATHAN M. HEMLI, MBBS(HONS)
MICHAEL J. JENSEN, FRACS, FACS
ANTONY R. GRAHAM, FRACS, FRCS(ENG)
SYDNEY, AUSTRALIA

Ludwig's angina, although uncommon, remains a potentially life-threatening condition because of the risk of impending airway obstruction. Effective treatment is based on early recognition of the clinical process, with the appropriate use of parenteral antibiotics, airway protection techniques, and formal surgical drainage of the infection. We present a case of Ludwig's angina together with a brief review of the relevant literature.

KEY WORDS — drainage, Ludwig's angina, tracheotomy.

INTRODUCTION

Ludwig's angina is a potentially lethal, rapidly spreading cellulitis involving the submandibular, sublingual, and submental spaces. It often originates from an odontogenic infection. Despite a significant drop in the mortality rate from Ludwig's angina since the preantibiotic era, this condition remains a therapeutic emergency because of its inherent life-threatening complication of airway obstruction. Airway protection and aggressive antimicrobial therapy, instituted early, have improved outcomes. However, with established infection, control of local sepsis with adequate surgical drainage is essential.

We report a case of a previously healthy adolescent male with acute airway obstruction associated with Ludwig's angina that required tracheotomy and formal surgical drainage of the infection. The latter was finally achieved after extraction of carious teeth.

CASE REPORT

A 15-year-old boy presented to a provincial hospital with a 3-day history of fever and malaise accompanied by pain and swelling in his left submandibular zone. He complained of inability to open his mouth and of marked dysphagia. He had no significant medical comorbidity, was previously otherwise healthy, and denied any recent dental extraction or orofacial trauma. Upon admission, the patient was found to be in acute respiratory distress with a compromised airway from soft tissue edema.

He was subsequently intubated with great difficulty, at which time the larynx was noted to be considerably distorted in appearance, although not dramatically erythematous or edematous. A regimen of intravenous antibiotics was started, consisting of penicillin G (1.2 g every 4 hours), floxacillin (2 g every 4 hours), and metronidazole (500 mg every 8 hours). Microbiological culture identified a group G β-hemolytic *Streptococcus* as the primary pathogenic organism. In spite of these therapeutic measures, the patient's condition did not improve, and the edema of his neck and face worsened. He was transferred to St Vincent's Hospital for further management.

On arrival at our institution, the patient was septic (temperature, 38.1°C), with a tachycardia (110 beats per minute), and had a blood pressure of 115/50 mm Hg. He had an endotracheal tube in situ. Clinical examination demonstrated indurated, tender, erythematous swelling extensively involving the left submandibular space and extending inferiorly to the level of the hyoid bone. Severe trismus was recorded. A diagnosis of Ludwig's angina was made.

Duplex studies of the neck demonstrated diffuse soft tissue swelling and increased vascularity throughout the entire left side; 3 small abscesses were identified in the patient's left parotid gland. Computed tomography (CT) of the neck revealed extensive submandibular inflammation with extension both superiorly and inferiorly, together with loss of associated fat planes (see Figure).

The patient proceeded to surgical drainage with a deep incision in the submandibular triangle, through the mylohyoid muscle and into the sublingual region. However, despite the combination of high-dose antibiotics, apparently adequate neck incision, and drainage of parotid abscesses, sepsis persisted with little

---

From the Department of Surgery, St Vincent's Hospital, University of New South Wales (Barakate, Jensen, Graham), and the Northern Clinical School, University of Sydney (Hemli), Sydney, Australia.

CORRESPONDENCE — Michael S. Barakate, BSc(Med), MBBS, 6 Virginia St, Kensington, NSW 2033, Australia.

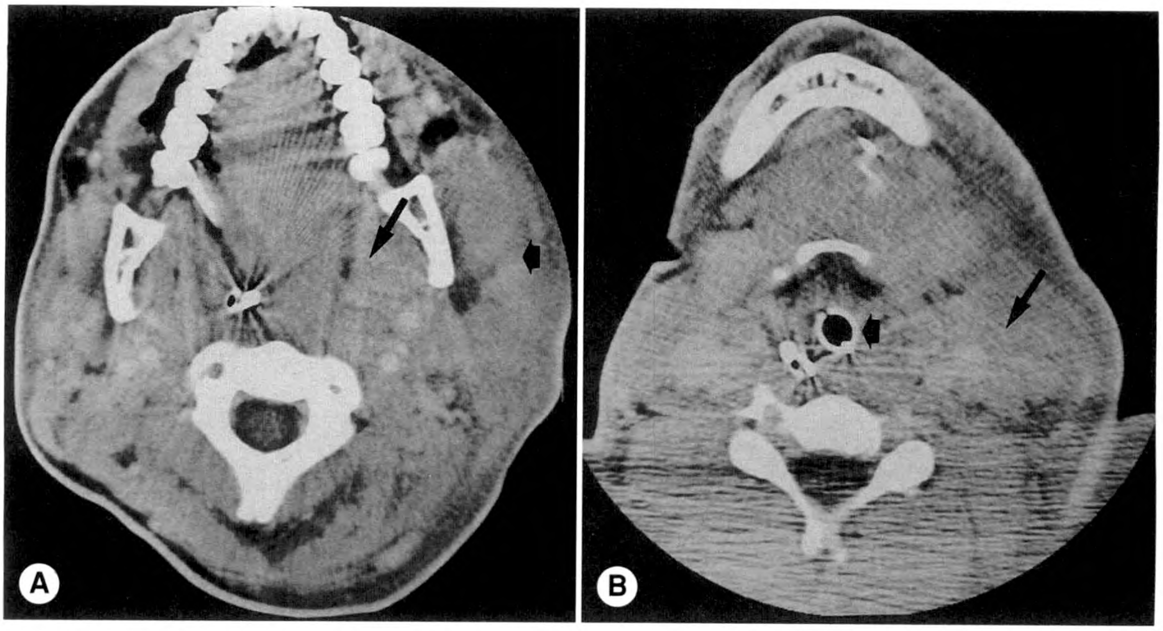

Computed tomographic scans of neck. **A**) Extensive submandibular inflammation and edema (long arrow) and associated airway compression are seen. Increased fascial streaking and compression of planes adjacent to left submandibular region are noted (broad arrow) as compared to right side of neck. **B**) At lower level than **A**. Extensive edema of left submandibular region is noted, extending inferiorly (long arrow) and displacing trachea to right (broad arrow).

clinical improvement. The patient was referred to the head and neck unit, where significantly carious lower left molars, mandibular percussion tenderness, a swollen alveolar margin, and a grossly edematous tongue were noted. Radiographic studies confirmed periodontal abscesses of the second and third lower left molar teeth. Only subsequent extraction of the 2 carious teeth and drainage of the associated periodontal abscesses resulted in ultimate resolution of the problem. A tracheotomy was performed to facilitate removal of the endotracheal tube, provide a secure definitive airway, and minimize laryngeal trauma.

There were no significant perioperative complications. The patient made an uneventful postoperative recovery, during which time the infection completely resolved.

DISCUSSION

Ludwig's angina most commonly originates from an odontogenic infection, classically located in the second and third lower molar teeth.[1] The apices of these teeth, in particular, are located just below the mylohyoid ridges, and are therefore in close anatomic proximity to the submandibular space. In the event of an infection of these molars, subsequent perforation of the lingual plate of the mandible will allow rapid direct spread of the septic process into the submandibular, sublingual, and submental tissue spaces,[1-3] with resultant clinical presentation as Ludwig's angina.

Although odontogenic infection is often the cause, accounting for more than 70% of cases,[4] a number of less common foci of infection have been reported as initiating Ludwig's angina, including quinsy,[4,5] sialadenitis,[6] epiglottitis, and an infected thyroglossal cyst. Ludwig's angina can also follow posttraumatic infection resulting from a compound fracture of the mandible, a penetrating injury to the floor of the mouth, or even trauma from endotracheal intubation or bronchoscopy.[2,3,5-7]

The majority of cases occur in previously healthy individuals.[6,8] However, certain underlying conditions may predispose patients to severe periodontal infection, including diabetes mellitus, neutropenia, aplastic anemia, and glomerulonephritis.[1,2,4-7] Other authors have documented an increased susceptibility to Ludwig's angina in the setting of immunodeficiency.[4,9,10]

Patients classically present with tooth pain, a history of recent dental extraction or poor dental hygiene, dysphagia and odynophagia, upper neck pain and swelling, and dysphonia and/or dysarthria.[2,5,6,8] The findings on physical examination are generally commensurate with those of an aggressive gangrenous cellulitis, and usually comprise fever, tachycardia, brawny induration and swelling of a tender submandibular space, and an elevated, protruding tongue.[1,2,5-8] Trismus is often present and indicates direct irritation of the masticatory muscles.[11] Dyspnea, tachypnea, inspiratory stridor, and cyanosis are signs of impending airway obstruction secondary to progressive supraglottic edema, and herald a medical emergency.[12] Acute laryngospasm secondary to aspiration, supine positioning of the patient, or attempted endotracheal intubation can precipitate the rapid onset of complete upper airway obstruction.[13]

The majority of patients with Ludwig's angina have mixed polymicrobial infections. The organisms most frequently responsible for the septic process are streptococci and staphylococci. Symbiotic infection with anaerobes is now known to be more significant than was previously appreciated.[2,4,6,11,14-17] A host of other bacteria may contribute to the infection, including various gram-negative rods[13,15,16] and other, more unusual organisms.[18]

Relatively unrestrained by anatomic barriers, infection in the floor of the mouth can spread readily to involve other tissues in the neck, the retropharyngeal fascial space, and, rarely, the mediastinum or subphrenic space. The reported complications of Ludwig's angina, in addition to airway compromise, include mediastinitis, subphrenic abscess formation, pericardial and/or pleural effusion, empyema, osteomyelitis of the mandible, infection of the carotid sheath and possible rupture of the carotid artery, and suppurative thrombophlebitis of the internal jugular vein.[7,11,13,16,17]

The initial assessment and treatment of Ludwig's angina is based primarily on clinical grounds, given the risk of airway obstruction that may occur with delayed investigation and therapy. A number of imaging methods are nevertheless useful in helping to define the severity of the infection. Plain radiographs of the neck and chest may demonstrate the extent of soft tissue swelling, as well as reveal gas in the tissues, particularly in the setting of anaerobic infection).[1,6,8] Plain chest radiography can also be used to look for intrathoracic extension of the infective process. Ultrasonography may highlight collections of pus, as well as reveal metastatic abscess formation. Computed tomography and magnetic resonance imaging may also be indicated, to confirm the presence of airway edema and to identify and localize any mediastinal fluid collections.[15]

Airway maintenance remains the most important immediate therapeutic goal in the management of Ludwig's angina. Airway obstruction as a result of swelling of the suprahyoid tissues and edema of the supraglottic larynx may be life-threatening. The most appropriate means of airway management deserves discussion, with tracheotomy favored when protracted soft tissue edema is anticipated.[1,3,6,13,15] Endotracheal intubation is difficult in these patients, and direct laryngoscopy may actually precipitate acute airway collapse.[13,15] The use of flexible fiberoptic endoscopy has facilitated the intubation of patients with difficult access.[8,19] In the emergency setting of severe swelling and trismus, in which intubation is not a viable option, formal tracheotomy remains the best solution to providing the patient with a definitive airway.[1,2,6,8,13,15,19]

Aggressive intravenous antibiotic administration is a cornerstone of therapy. The initial antibiotic cover is empiric, primarily targeted at gram-positive cocci, with penicillin the drug of choice.[2,3,6,7,11,15] Anaerobic cover should also be provided. Metronidazole is recommended because of the increasing emergence of penicillin-resistant strains of *Bacteroides* species.[10,11] An empiric combination of clindamycin, penicillin, and metronidazole is commonly recommended. Once bacteriologic studies have identified the specific pathogenic organisms responsible, the antibiotic therapy is adjusted accordingly.

Formal surgical drainage is indicated as an early procedure in the setting of suppurative infection. Absolute indications include fluctuance, crepitus, soft tissue air, and the presence of a purulent needle aspirate,[6-8,13] with a low threshold for routine incision and drainage in all severe soft tissue infections of the oropharynx.[3]

An incision is generally made parallel and 2 fingerbreadths inferior to the angle of the mandible. The location and size of the initial incision will depend on the specific anatomic spaces involved by the infection and, in severe cases, may need to extend to the midline below the chin. Multiple incisions may even be required. The superficial lobe of the submandibular gland is displaced, and the mylohyoid muscles are then divided to decompress the closed fascial spaces involved in the septic process. Blunt dissection should be carried out to completely explore the involved fascial compartments and to break up all loculations of suppurative material. Drains should be inserted into the fascial compartments to prevent reaccumulation of necrotic debris and pus. The goal of surgical drainage in this setting is thus twofold: the evacuation of pus, and decompression of all closed fascial spaces of the neck. If an infected tooth is present, it must be extracted to ensure complete drainage.

The described case demonstrates a number of the salient features of Ludwig's angina with respect to its causation and clinical presentation, highlighting the potentially fatal complication of airway obstruction. Formal surgical drainage to decompress all deep spaces (including, in our case, removal of carious lower molars) is essential to a successful outcome from Ludwig's angina.

REFERENCES

1. Spitalnic SJ, Sucov A. Ludwig's angina: case report and review. J Emerg Med 1995;13:499-503.

2. Moreland LW, Corey J, McKenzie R. Ludwig's angina. Report of a case and review of the literature. Arch Intern Med 1988;148:461-6.

3. Iwu CO. Ludwig's angina: report of seven cases and review of current concepts in management. Br J Oral Maxillofac Surg 1990;28:189-93.

4. Busch RF, Shah D. Ludwig's angina: improved treatment. Otolaryngol Head Neck Surg 1997;117:S172-S175.

5. Weisengreen HH. Ludwig's angina: historical review and reflections. Ear Nose Throat J 1986;65:457-61.

6. Lerner DN, Troost T. Submandibular sialadenitis presenting as Ludwig's angina. Ear Nose Throat J 1991;70:807-9.

7. Ferrera PC, Busino LJ, Snyder HS. Uncommon complications of odontogenic infections. Am J Emerg Med 1996;14: 317-22.

8. Patterson HC, Kelly JH, Strome M. Ludwig's angina: an update. Laryngoscope 1982;92:370-8.

9. Aden K, Nissen RL, Spaur C, Yonkers AJ. Ludwig's angina. Ear Nose Throat J 1985;64:168-72.

10. Finch RG, Snider GE, Sprinkle PM. Ludwig's angina. JAMA 1980;243:1171-3.

11. Horn J, Bender BS, Bartlett JG. Role of anaerobic bacteria in perimandibular space infections. Ann Otol Rhinol Laryngol Suppl 1991;100(suppl 154):34-9.

12. Marple BF. Ludwig angina. A review of current airway management. Arch Otolaryngol Head Neck Surg 1999;125:596-9.

13. Holland CS. The management of Ludwig's angina. Br J Oral Surg 1975;13:153-9.

14. Strauss HR, Tilghman DM, Hawkins J. Ludwig's angina, empyema, pulmonary infiltrate, and pericarditis secondary to extraction of a tooth. J Oral Surg 1980;38:223-9.

15. Meyers BR, Fawson W, Hirschman SZ. Ludwig's angina: a case report, with review of bacteriology and current therapy. Am J Med 1972;53:257-60.

16. Bounds GA. Subphrenic and mediastinal abscess formation: a complication of Ludwig's angina. Br J Oral Maxillofac Surg 1985;23:313-21.

17. van der Brempt X, Derue G, Severin DF, Colin L, Gilbeau JP, Heller F. Ludwig's angina and mediastinitis due to *Streptococcus milleri*: usefulness of computed tomography. Eur Respir J 1990;3:728-31.

18. Dryden MS, Dalgliesh D. *Pasteurella multocida* from a dog causing Ludwig's angina [Letter]. Lancet 1996;347:123.

19. Hart BT. Tracheotomy for Ludwig's angina. Oral Surg Oral Med Oral Pathol 1994;78:414-5.

Ann Otol Rhinol Laryngol 110:2001

EFFECT OF MACROLIDES ON THE EXPRESSION OF HLA-DR AND COSTIMULATORY MOLECULES ON ANTIGEN-PRESENTING CELLS IN NASAL POLYPS

YUKIKO IINO, MD, PHD
CHIE KOJIMA, MD, PHD
YUKAKO SASAKI, MD
TETSUO MIYAZAWA, MD
TOKYO, JAPAN

To clarify the basis of macrolide therapy for improvement of chronic sinusitis, we investigated the effect of macrolides on the expression of HLA-DR and costimulatory molecules such as CD54 and CD80 on macrophages in nasal polyps. Nasal polyps taken from 54 patients who had or had not been treated with macrolides were immunohistochemically studied. The percentages of CD68-positive macrophages expressing HLA-DR or CD54 were not significantly different between patients treated with macrolides and those not treated with macrolides. However, among patients exhibiting no atopic predisposition, the number of CD80-positive macrophages was higher in patients treated with macrolides than in those not treated. In addition, the percentage of CD80-positive macrophages was negatively correlated with the percentage of infiltrating eosinophils in the polyps. These results demonstrate that macrophages act as antigen-presenting cells, expressing both major histocompatibility complex II and costimulators, and that the expression of CD80 may play a key role in the immune responses occurring in a nasal polyp. Macrolides may modulate the mucosal immune responses through CD80 expression.

KEY WORDS — atopic predisposition, CD54, CD80, costimulatory molecule, HLA-DR, macrolide, macrophage, nasal polyp.

INTRODUCTION

Nasal polyps are usually associated with chronic sinusitis or allergic diseases such as allergic rhinitis and bronchial asthma, and the pathological features of nasal polyps vary significantly among individual cases. The mucosal surface of the nose and paranasal sinuses is continuously exposed to foreign bodies and, hence, is an important site of immunologic activity. Therefore, the pathogenesis and generation of nasal polyps may be closely related to the mucosal immune responses of each individual.

Immune responses against foreign bodies are initiated with the presentation of the antigen to T lymphocytes by antigen-presenting cells (APCs). Recent studies have shown that the proliferation of T cells requires recognition of the antigen/major histocompatibility complex (MHC) by a T cell receptor (TCR), as well as the delivery of other nonspecific costimulatory signals via molecules expressed on the surfaces of the APCs.[1-3] The costimulatory signals can be provided efficiently by costimulatory molecules such as CD54 (intercellular adhesion molecule–1; ICAM-1), CD80 (B7-1), and CD86 (B7-2). Activation of T cells only by the main signal in the absence of costimulatory signals would result in T cell unresponsiveness or anergy.

The mucosal immune response in the nasal and paranasal mucosa is still a controversial issue. In the nasal mucosa, Yoshimi et al[4] demonstrated that macrophages expressing HLA-DR, one of the MHC-II antigens, play the role of APCs and are responsible for the immune response under both normal and diseased conditions. In the paranasal mucosa and nasal polyps, however, there have been few studies concerning the APCs.

Macrolide therapy, that is, low-dose, long-term administration of 14-membered lactone ring macrolides, has recently been reported to be very effective for patients with chronic upper respiratory tract infections. Macrolide therapy was first reported by Kudoh et al.[5] They demonstrated a significant effect of erythromycin in patients with diffuse panbronchiolitis. Subsequently, the efficacy of macrolide therapy for patients with sinobronchial syndrome, chronic sinusitis, and otitis media with effusion has also been reported.[6-8] It is generally accepted that the effectiveness of macrolide therapy for chronic sinusitis is limited when patients have nasal polyposis, because the ostiomeatal complex is usually obstructed by the polyps, which prevent ventilation and drainage of the paranasal sinuses. However, in patients who receive macrolides, the size of nasal polyps is often reduced, and in addition, the inflammation of the paranasal sinus mucosa is decreased, and consequently, only min-

---

From the Department of Otolaryngology, Teikyo University School of Medicine, Tokyo, Japan. Supported by a grant-in-aid from the Ministry of Education, Science, Sports and Culture of Japan.

CORRESPONDENCE — Yukiko Iino, MD, PhD, Dept of Otolaryngology, Teikyo University School of Medicine, 2-11-1, Kaga, Itabashi-ku, Tokyo 173-8605, Japan.

EFFICACY OF MACROLIDES IN 41 PATIENTS WHO RECEIVED RXM OR CAM BEFORE ENDOSCOPIC NASAL SURGERY

		Efficacy Rate*	
	Drug	*No.*	*%*
Nonatopic	RXM	7/10	70
	CAM	7/12	58
Atopic	RXM	5/12	42
	CAM	3/7	43

RXM — roxithromycin, CAM — clarithromycin.

*Number of patients with excellent or good response per total number of patients.

imal bleeding occurs at the time of endoscopic nasal surgery. The effectiveness of macrolides on chronic respiratory infections is not due to an antimicrobial effect, but is attributable to anti-inflammatory effects or their regulation of immune response.[5] In this study, we identified APCs in nasal polyps and investigated the effect of macrolides on the expression of HLA-DR and costimulatory molecules on macrophages in the nasal polyps of patients with and without atopic predisposition. We demonstrated that the macrophages expressed both HLA-DR and costimulatory molecules, and that the polyps from patients who underwent macrolide therapy exhibited a higher rate of expression of the CD80 costimulatory molecule.

PATIENTS AND METHODS

Study Subjects. Nasal polyps taken from 54 patients (11 female and 43 male, 6 to 71 years old) were included in this study. Most of the patients had a history of nasal congestion and rhinorrhea, and had a diagnosis of chronic sinusitis that was made by rhinoscopy and computed tomography (CT) of the nose and paranasal sinuses. None of the patients had undergone a Caldwell-Luc operation. The allergic predisposition of the patients was determined on the basis of their radioallergosorbent test score, their serum IgE level, and the results of a skin test. Twenty-eight patients showed no predisposition to allergy (nonatopic group). Twenty-six patients had an allergic predisposition with positive results on at least 2 of the 3 tests described above (atopic group). Among them, 19 had perennial and/or seasonal nasal allergy without bronchial asthma. Seven patients were found by pulmonologists to have bronchial asthma. Patients with nonatopic bronchial asthma and those administered systemic or topical steroids within the 2 weeks prior to the endoscopic nasal surgery were excluded from the study. Forty-one patients (22 patients in the nonatopic group and 19 patients in the atopic group) had received low-dose macrolides — 150 mg/d of roxithromycin (RXM) or 200 mg/d of clarithromycin (CAM) — before the endoscopic nasal surgery; the period of administration ranged from 1 month to 1 year 6 months. In the nonatopic group, 10 patients received RXM, and 12 received CAM. In the atopic group, 14 patients were given RXM and 5 were given CAM. The efficacy of the macrolides was judged by 5 items of subjective symptoms (hyperrhinorrhea, nasal congestion, postnasal drip, headache, and olfactory disturbance), 4 items of rhinoscopic findings (injection and edema of the nasal mucosa, amount and character of rhinorrhea), and the findings of a CT scan of the nose and paranasal sinuses. One point was given for each item that improved after the administration of macrolides. A total score of 8 or more was regarded as excellent, a score of 7, 6, or 5 as good, a score of 4, 3, or 2 as fair, and a score of 1 or 0 as poor. The efficacy rate in each group is shown in the Table.

As controls, samples of the nasal mucosa of the inferior turbinate were obtained from 9 patients who had neither chronic sinusitis nor allergic diseases, including nasal allergy and bronchial asthma.

Tissue Preparation. The surgically resected polyps were immediately fixed in periodate–lysine–2% paraformaldehyde solution. They were immersed in a graded series of sucrose in phosphate-buffered saline solution, embedded in OCT compound (Sakura, Tokyo, Japan), and snap-frozen. The frozen samples were stored at −70°C until they were used. Cryosections of 6- to 8-μm thickness were prepared.

Immune Reagents. Mouse monoclonal antibodies were used for CD68 (DAKO, Glostrup, Denmark; a marker of macrophages), HLA-DR (DAKO; an MHC-II), CD54 (DAKO; ICAM-1 as a costimulatory molecule), and CD80 (Immunotech, Marseille, France; B7-1 as a costimulatory molecule). The antibodies were appropriately diluted in 0.01-mol/ L phosphate-buffered saline solution (pH 7.4) containing bovine serum albumin and used for immunohistochemical double staining.

Immunohistochemistry. To examine the distribution of HLA-DR and the costimulatory molecules on the macrophages in the nasal polyp specimens, an immunohistochemical double-staining method using a labeled streptavidin biotin kit (LSAB kit; DAKO) was used. Briefly, after blocking of endogenous peroxidases in 3% hydrogen peroxide and blocking with normal bovine IgG, the frozen sections were treated with one of the primary monoclonal antibodies. Each of these sections was incubated with a secondary antibody, biotinylated goat anti-mouse IgG, followed by a horseradish peroxidase (HRP)–labeled streptavidin complex, and stained with 3-amino-9-ethylcarbazole. After washing the sections in 0.1-mol/L glycine in hydrochloric acid solution (pH 2.2), we treated the sections further with another primary monoclonal antibody. Each of these sections was again incubated

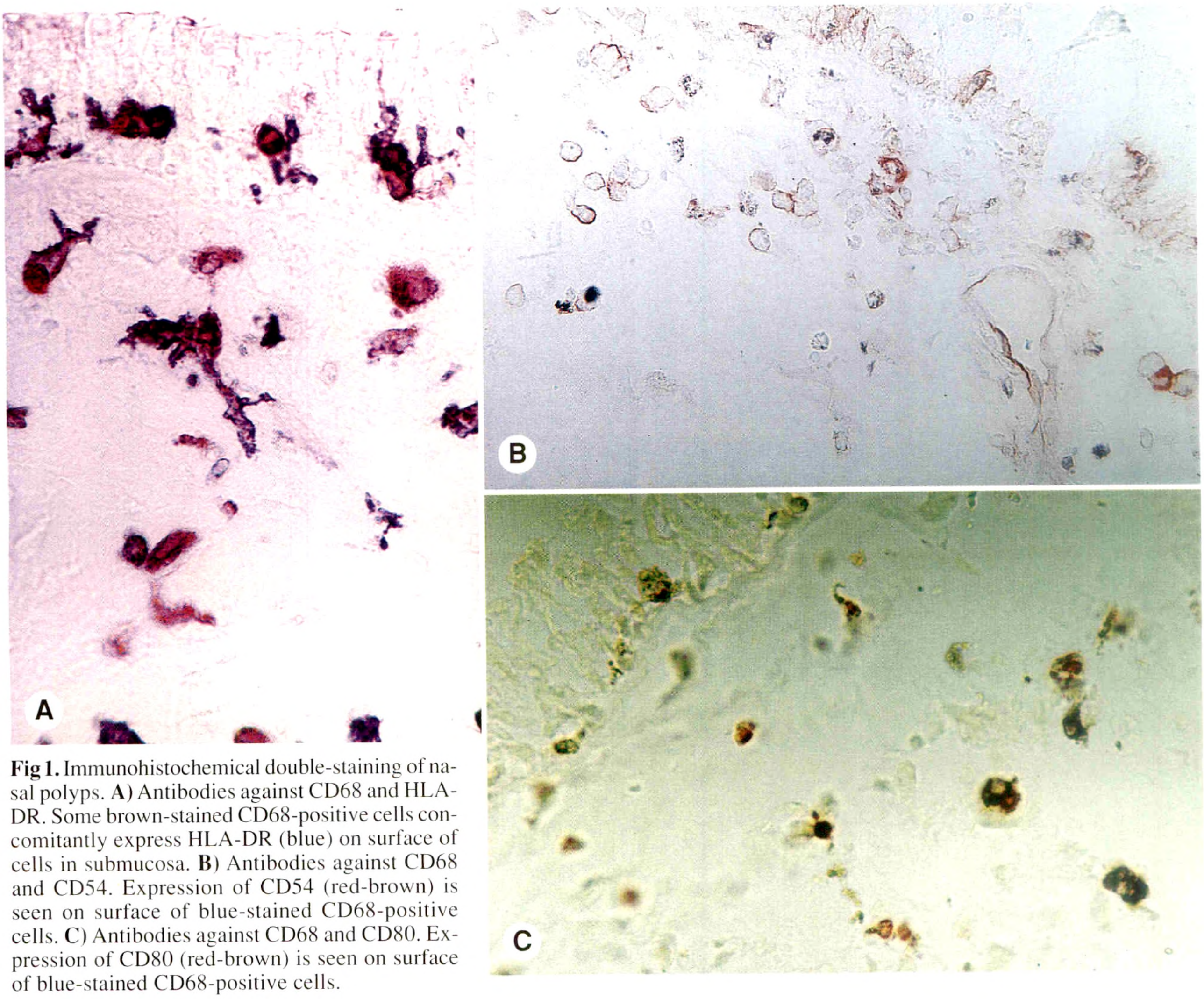

Fig 1. Immunohistochemical double-staining of nasal polyps. **A)** Antibodies against CD68 and HLA-DR. Some brown-stained CD68-positive cells concomitantly express HLA-DR (blue) on surface of cells in submucosa. **B)** Antibodies against CD68 and CD54. Expression of CD54 (red-brown) is seen on surface of blue-stained CD68-positive cells. **C)** Antibodies against CD68 and CD80. Expression of CD80 (red-brown) is seen on surface of blue-stained CD68-positive cells.

with biotinylated goat anti-mouse IgG, then incubated with an HRP-labeled streptavidin complex, and then stained with 4-chloro-1-naphthol hydrogen peroxide.

Evaluation. The sections were coded and evaluated independently by 2 individuals using a conventional light microscope at lower and higher magnifications, and the immunohistochemically stained cells in the submucosal layer were observed. We counted at least 200 CD68-positive cells, and among these, the number of cells that were also positive for HLA-DR, CD54, or CD80 were counted. Then, the ratio of the number of double-stained cells to that of cells positive for CD68 was calculated.

Simultaneously, the specimens were fixed in formalin, and the paraffin-embedded sections were prepared and stained with hematoxylin and eosin. The number of inflammatory cells infiltrating the submucosa was counted in 5 fields at 200× magnification, and the ratio of each cell type, including lymphocytes, plasma cells, neutrophils, and eosinophils, to the total number of inflammatory cells was determined.

Statistical analysis was carried out with an unpaired Student's *t*-test or Welch's *t*-test. Two-tailed p values of less than .05 were considered significant.

RESULTS

Immunohistochemically Double-Stained Cells in Submucosa of Nasal Polyps. CD68-positive cells were observed in the submucosal layers in the normal nasal mucosa, as well as in the nasal polyps examined. A positive reaction was observed within the cytoplasm of the cells. Two types of CD68-positive cells were identified: one round, and the other large and dendritic.

Positive staining for HLA-DR was observed on the surface of some of the CD68-positive cells, and such cells were mostly large and irregularly shaped. They were noted in the submucosal layer, as well as within the epithelium. A relatively large number of cells double-stained for CD68 and HLA-DR were identified (Fig 1A).

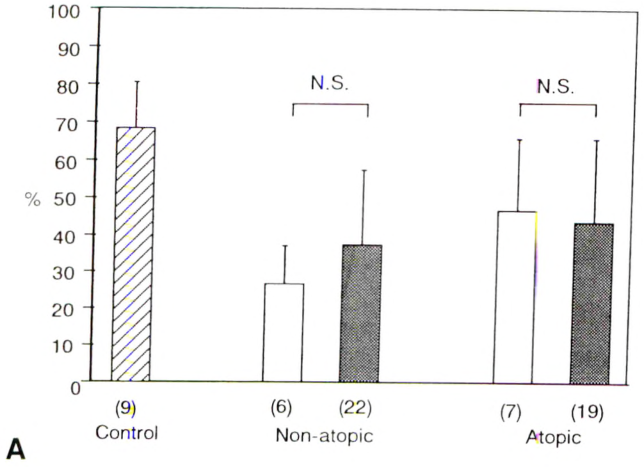

Fig 2. Expression of HLA-DR and costimulatory molecules on CD68-positive cells in nasal polyps. Open bar represents mean ± SD of percentages in patients who did not have macrolide therapy, and closed bar represents mean ± SD of percentages in patients who had macrolide therapy. Numbers of patients are in parentheses. N.S. — not significant. **A)** Percentages of cells that were positive for both CD68 and HLA-DR relative to total number of CD68-positive cells. **B)** Percentages of cells that were positive for both CD68 and CD54 relative to total number of CD68-positive cells. **C)** Percentages of cells that were positive for both CD68 and CD80 relative to total number of CD68-positive cells.

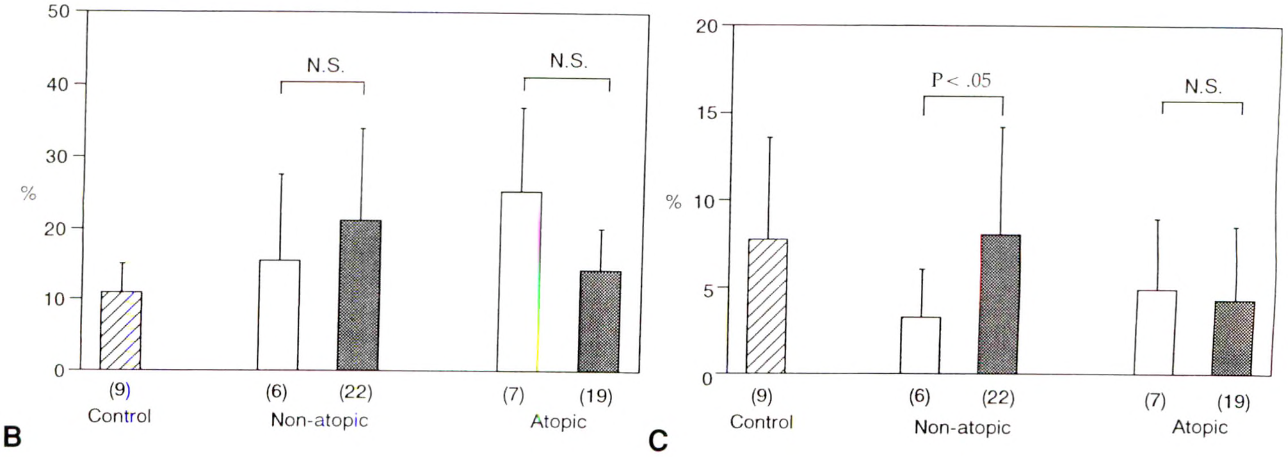

Figure 1B shows a nasal polyp immunohistochemically double-stained for CD68 and the costimulatory molecule CD54. Numerous CD54-positive cells were present in the submucosal layer. In addition, some basal cells of the ciliated epithelium, as well as the endothelial cells of the blood vessels, showed a positive reaction for CD54. Some of the CD68-positive cells were also positive for CD54.

Figure 1C shows a nasal polyp stained for both CD68 and CD80. Double-positive cells were observed in the submucosa, but the number of CD80-positive cells among the CD68-positive cells was low compared with those also positive for HLA-DR or CD54 in both the normal nasal mucosa and the nasal polyps.

HLA-DR Expression on CD68-Positive Cells in Nasal Polyp Specimens. The percentages of cells that were positive for both CD68 and HLA-DR in each group are shown in Fig 2A. In the normal nasal mucosa, approximately two thirds of CD68-positive cells simultaneously expressed HLA-DR. However, in the nasal polyps resected from patients, only 30% to 40% of the CD68-positive cells also expressed HLA-DR. Treatment with macrolides did not influence the percentage of HLA-DR–positive cells relative to the number of CD68-positive cells, either in the nonatopic group or in the atopic group.

CD54 Expression on CD68-Positive Cells in Nasal Polyp Specimens. The percentages of cells that were positive for both CD68 and CD54 in each group are shown in Fig 2B. The number of CD54-positive cells was higher in the nasal polyp specimens than in specimens of the normal nasal mucosa. In the atopic patients, after the administration of macrolides, the percentage of CD54-positive cells was reduced, but the decrease was not statistically significant.

CD80 Expression on CD68-Positive Cells in Nasal Polyp Specimens. The percentages of cells that were positive for both CD68 and CD80 in each group are shown in Fig 2C. The number of CD80-positive cells in the nasal polyp specimens was relatively small compared with that in the normal nasal mucosa. However, the expression of CD80 was significantly increased in the case of nonatopic patients who received macrolides ($p < .05$). On the other hand, in the case of atopic patients, macrolides had no effect on the expression of CD80 on cells in nasal polyps.

Histologic Characteristics of Nasal Polyps and Expression of HLA-DR and Costimulatory Molecules

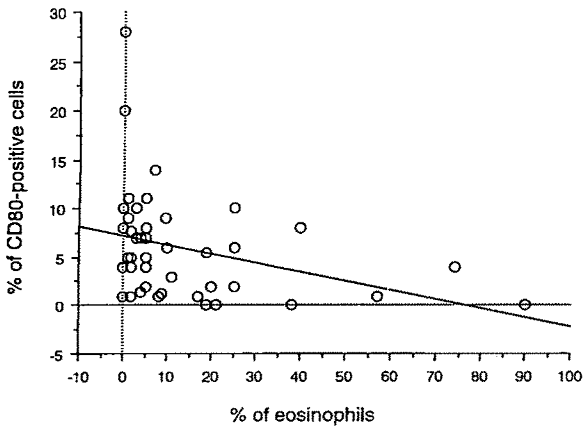

Fig 3. Correlation between percentage of CD80-positive cells in CD68-positive cells and percentage of eosinophils relative to total number of infiltrating cells in nasal polyps. Line indicates simple regression curve: $y = 7.254 - 0.094x$; $R^2 = .112$; $p < .05$.

on Macrophages. The composition of the cellular infiltrate in the submucosa varied significantly among patients. Lymphocytes, plasma cells, and macrophages were observed in all the patients. On the other hand, eosinophils and neutrophils were not consistently detected in the submucosa. In some patients, however, large numbers of eosinophils and neutrophils were observed. The percentages of eosinophils and neutrophils in the total number of infiltrating cells ranged between 0% and 90% (mean ± SD, 20.1% ± 25.8%) and 0% and 71% (mean ± SD, 10.1% ± 14.2%), respectively.

The correlation between the percentage of lymphocytes, plasma cells, or neutrophils in the submucosa and the expression levels of the HLA-DR and costimulatory molecules was investigated, but no significant correlation was noted. However, in the case of eosinophils, the expression of CD80 on CD68-positive macrophages and the percentage of eosinophils in relation to the total number of infiltrating cells were significantly negatively correlated with each other ($p < .05$; Fig 3).

DISCUSSION

Nasal polyps usually arise from the paranasal sinuses in patients with chronic infectious or allergic inflammation, and cause nasal obstruction. Chronic inflammatory responses within the mucosa of the paranasal sinuses may be closely related to the development of nasal polyps. However, the pathophysiological mechanisms underlying this benign tissue proliferation have not yet been determined in detail. The mucosal immune response is primarily a self-defense against foreign antigens. However, the immune response may also be responsible for perpetuating inflammation by promoting excessive production of inflammatory mediators.

One of the most critical events in the initiation of the immune response is the activation of T helper (Th) cells by APCs. The activated Th cells produce cytokines and express receptors for these cytokines, thereby promoting Th cell proliferation. In the nasal mucosa, Yoshimi et al[4] reported that macrophages expressing HLA-DR, one of the MHC-II antigens, may act as the APCs. However, in the paranasal mucosa and nasal polyps, the presence of APCs has not been confirmed. Stoop et al[9] showed that many HLA-DR–positive cells were present in the epithelium and submucosa of nasal polyps and in the mucosa of the middle turbinates, suggesting that these cells may be B-lymphocytes, activated T cells, and activated macrophages. The expression of MHC-II molecules is primarily limited to "professional" APCs such as macrophages, dendritic cells, and B cells. For effective T lymphocyte activation, MHC-II presentation (signal 1) along with costimulatory signals (signal 2) is required. The present study, using an immunohistochemical double-staining technique, demonstrated for the first time that one of the APCs in nasal polyps is a CD68-positive macrophage expressing both an MHC-II (HLA-DR) and costimulators (CD54 and CD80).

Fourteen-membered lactone ring macrolides such as erythromycin, RXM, and CAM have been reported to be very effective for patients with sinobronchial syndrome and chronic sinusitis,[6-8] and low-dose, long-term administration of macrolides (macrolide therapy) is now the therapy of first choice for the treatment of chronic sinusitis in Japan. In the present study, 41 patients received macrolides before endoscopic nasal surgery, and the efficacy rate was relatively high in the nonatopic group. The efficacy was not significantly different between the patients who received CAM and those who received RXM. Although little is known about the real mechanism underlying the clinical efficacy, the effectiveness of macrolides in chronic sinusitis may be related not to their antimicrobial actions, but to their anti-inflammatory or immunoregulatory actions.[5] Studies have demonstrated that the macrolides exhibit various biological and immunologic effects on immunocompetent cells such as macrophages, lymphocytes, and neutrophils, and also on respiratory epithelial cells, fibroblasts, endothelial cells, and glandular cells.[10-14] The effects on immunocompetent cells include suppression or enhancement of cytokine production, proliferative activities, and chemotactic activities.[10-14]

In our previous immunohistochemical study,[15] we reported that in the nasal polyps of patients who underwent macrolide therapy, the number of CD4-positive cells was decreased compared with that in patients who did not undergo the therapy. However, the fact that the number of HLA-DR–positive cells was not significantly different between the two groups indicates that the macrolides may modulate the APC–T cell interaction. Therefore, we investigated the expression of HLA-DR and costimulatory molecules on macrophages, one of the candidate APCs in nasal polyps.

Some examples of the costimulatory molecules expressed on APCs are CD54 (ICAM-1), CD80 (B7-1), CD86 (B7-2), vascular cell adhesion molecule–1 (VCAM-1), and CD58 (lymphocyte function–associated antigen–3; LFA-3). The corresponding receptors expressed on T cells are LFA-1, CD28, cytolytic T-lymphocyte–associated receptor (CTLA-4), and CD2. The presence of signal 1, in the absence of costimulatory signals, results in, instead of T-cell activation, an unresponsive state termed clonal anergy.

In the present study, we divided the patients into 2 groups according to the presence or absence of allergic predisposition, because there have been some reports that the cytokine profiles in nasal polyps were significantly different in atopic and nonatopic patients. Th lymphocytes have been categorized into 2 major functional phenotypes, Th1 and Th2, which produce distinct arrays of cytokines and are both thought to arise from a pluripotential precursor cell termed Th0. Type I allergy, the atopic type, is considered to be the result of Th2-dominant activation.

The present study demonstrated that large numbers of macrophages proliferating in the submucosa of the nasal polyps expressed HLA-DR. However, the number of HLA-DR–positive cells in the nasal polyps was lower than that in the normal inferior turbinate mucosa. Tissue macrophages are usually divided into 2 types based on the main role in tissues: the antigen-presenting macrophage and the phagocytotic one.[16,17] In nasal polyps, some macrophages may play a phagocytotic role rather than be involved in immune responses upon exposure to foreign bodies. In addition, macrolides had little effect on the expression of HLA-DR on macrophages.

It is generally accepted that in inflammation, expression of adhesion molecules such as CD54, VCAM-1, and E-selectin on endothelial cells is increased for the recruitment of leukocytes. Consistent with this notion, a large number of CD54-positive cells on macrophages was observed in the nasal polyps compared with that in the control turbinates. It has been reported that CD54 and VCAM-1 act on APCs as costimulators to activate resting T cells in the early stages of the immune response.[18,19] Concerning the effect of macrolides on the expression of adhesion molecules, in vitro and in vivo studies have shown that the expression of ICAM-1 and E-selectin on endothelial cells or neutrophils was suppressed after the administration of macrolides.[20,21] However, the present study revealed that the expression level of CD54 on the macrophages in nasal polyps was similar in patients who had and patients who had not undergone macrolide therapy. Therefore, the effect of macrolides may vary significantly, depending on the target cells.

CD80 is a costimulatory molecule in restimulating activated T cells in the late stage of the immune response.[22] The present study demonstrated that the number of macrophages expressing CD80 was relatively small. However, in nasal polyps from nonatopic patients, the number of CD80-positive macrophages was significantly higher in patients who had undergone macrolide therapy than in those who had not undergone the therapy. The mechanism underlying the increased expression of CD80 is not known. A clinical study showed that macrolide therapy is effective for patients with infectious sinusitis rather than allergic sinusitis.[23] The present study also exhibited that the efficacy rate of the macrolide therapy was higher in the nonatopic patients than in the atopic patients. Therefore, the increase in CD80 expression following macrolide therapy may be closely related to its clinical efficacy against nonallergic sinusitis. One study showed that in the absence of CD80-CD28 interaction, clonal anergy is induced characteristically in Th1 clones that normally produce interleukin (IL)–2 and interferon-γ, whereas Th2 clones proliferate even in the absence of CD80 expression on APCs.[24] In other words, Th0 clones can differentiate into Th2 clones to produce cytokines such as IL-4, IL-5, and IL-10 without signals from a CD80-CD28 interaction. These results suggest that HLA-DR and CD54 are always involved at the site of mucosal immune response in nasal polyps, but the subsequent immune reactions and immune response characteristics may be controlled by CD80 expression. Macrolides may normalize the Th1-Th2 balance and reduce the inflammation under the nonatopic condition, controlling the expression of CD80 on the APCs.

The activation of eosinophils and release of eosinophil granule mediators in the airway mucosa is an essential process in respiratory inflammations such as bronchial asthma, allergic rhinitis, and nasal polyps. Although eosinophils are proinflammatory cells that normally reside in the circulation, they are induced to extravasate into tissue by a diverse array of chemoattractants and viability-enhancing factors. These include eotaxins, granulocyte-macrophage colony-stimulating factors, IL-2, IL-5, RANTES ("regulated on activation, normal T cells expressed and secreted"), monocyte chemotactic peptides, and so on, which are produced by various inflammatory cells, epithelial cells, and fibroblasts. Therefore, eosinophilic infiltration does not always result from IgE-mediated hypersensitivity. One investigation[25] suggests that the eosinophil is the major cell type that synthesizes transforming growth factors and induces nasal polyposis. It has been shown that IL-5 plays an important role in the pathophysiology of eosinophilic nasal polyps, as a high concentration of IL-5 was also detected in nasal polyps from both allergic and nonallergic patients.[26] However, the extent of infiltration by eosinophils varies significantly among individuals. In the present study, eosinophilic infiltration was sparse in about one third of the polyps examined. We also showed that CD80 expression on macrophages and eosinophilic infiltration were negatively correlated. Therefore, the costimulatory signal of CD80 in nasal polyps may play a key role in the mucosal inflammatory response of nasal polyps, and macrolides may modulate the CD80 expression on APCs.

ACKNOWLEDGMENTS — The authors thank Prof Jun-Ichi Suzuki, chairman of the Department of Otolaryngology, Teikyo University School of Medicine, for his valuable comments on the study, and Reiko Sekiguchi and Yoshiko Kadoki for their technical help in preparing the specimens.

REFERENCES

1. Janeway CA Jr, Bottomly K. Signals and signs for lymphocyte responses. Cell 1994;76:275-85.
2. Guinan EC, Gribben JG, Boussiotis VA, Freeman GJ, Nadler LM. Pivotal role of the B7:CD28 pathway in transplantation tolerance and tumor immunity. Blood 1994;84:3261-82.
3. Kuchroo VK, Das MP, Brown JA, et al. B7-1 and B7-2 costimulatory molecules activate differentially the Th1/Th2 developmental pathways: application to autoimmune disease therapy. Cell 1995;80:707-18.
4. Yoshimi R, Takamura H, Takasaki K. Antigen presenting cells in nasal mucosa [in Japanese]. J Jpn Soc Immunol Allergol Otolaryngol 1994;12:144-5.
5. Kudoh S, Uetake T, Hagiwara K, et al. Clinical effects of low-dose long-term erythromycin chemotherapy on diffuse panbronchiolitis [in Japanese]. Jpn J Thorac Dis 1987;25:632-42.
6. Kikuchi S, Suzaki H, Aoki A, Ito O, Nomura Y. Clinical effect of long-term low-dose erythromycin therapy for chronic sinusitis [in Japanese]. Pract Otol (Kyoto) 1991;84:41-7.
7. Takagita S, Kitamura H, Nishikawa A, et al. Clinical effect of low-dose erythromycin chemotherapy on chronic sinusitis [in Japanese]. Pract Otol (Kyoto) 1991;84:489-98.
8. Iino Y, Sugita K, Toriyama M, Kudo K. Erythromycin therapy for otitis media with effusion in sinobronchial syndrome. Arch Otolaryngol Head Neck Surg 1993;119:648-51.
9. Stoop AE, van der Heijden HAMD, Biewenga J, van der Baan S. Lymphocytes and nonlymphoid cells in human nasal polyps. J Allergy Clin Immunol 1991;87:470-5.
10. Iino Y, Toriyama M, Kudo K, Natori Y, Yuo A. Erythromycin inhibition of lipopolysaccharide-stimulated tumor necrosis factor alpha production by human monocytes in vitro. Ann Otol Rhinol Laryngol Suppl 1992;101(suppl 157):16-20.
11. Takeshita K, Yamagishi I, Harada M, Otomo S, Nakagawa T, Mizushima Y. Immunological and anti-inflammatory effects of clarithromycin: inhibition of interleukin 1 production of murine peritoneal macrophages. Drugs Exp Clin Res 1989;15:527-33.
12. Anderson R, Fernandes AC, Eftychis HE. Studies on the effects of ingestion of a single 500 mg oral dose of erythromycin stearate on leucocyte motility and transformation and on release in vitro of prostaglandin E2 by stimulated leucocytes. J Antimicrob Chemother 1984;14:41-50.
13. Anderson R. Erythromycin and roxithromycin potentiate human neutrophil locomotion in vitro by inhibition of leukoattractant-activated superoxide generation and autooxidation. J Infect Dis 1989;159:966-73.
14. Roche Y, Gougerot-Pocidalo MA, Fay M, Forest N, Pocidalo JJ. Macrolides and immunity: effects of erythromycin and spiramycin on human mononuclear cell proliferation. J Antimicrob Chemother 1986;17:195-203.
15. Miyazawa T, Iino Y. Cell surface antigens on inflammatory cells in the paranasal mucosa of patients after macrolide therapy [in Japanese]. J Otolaryngol Jpn 1997;100:671-7.
16. Hamilos DL, Leung DYM, Wood R, et al. Evidence for distinct cytokine expression in allergic versus nonallergic chronic sinusitis. J Allergy Clin Immunol 1995;96:537-44.
17. Poulter LW, Campbell DA, Munro C, Janossy G. Discrimination of human macrophages and dendritic cells by means of monoclonal antibodies. Scand J Immunol 1986;24:351-7.
18. Damle NK, Klussman K, Linsley PS, Aruffo A. Differential costimulatory effects of adhesion molecules B7, ICAM-1, LFA-3, and VCAM-1 on resting and antigen-primed CD4+ T lymphocytes. J Immunol 1992;148:1985-92.
19. Damle NK, Klussman K, Linsley PS, Aruffo A, Ledbetter JA. Differential regulatory effects of intercellular adhesion molecule–1 on costimulation by the CD28 counter-receptor B7. J Immunol 1992;149:2541-8.
20. Enomoto F, Ichikawa G, Nagaoka I, Yamashita Y. Effect of erythromycin on otitis media with effusion in experimental rat model. Acta Otolaryngol Suppl (Stockh) 1998(suppl 539):57-60.
21. Okubo Y. Macrolides reduce the expression of surface Mac-1 molecule on neutrophil. Kurume Med J 1997;44:115-23.
22. Damle NK, Klussman K, Leytze G, et al. Costimulation of T lymphocytes with integrin ligands intercellular adhesion molecule–1 or vascular cell adhesion molecule–1 induces functional expression of CTLA-4, a second receptor for B7. J Immunol 1994;152:2686-97.
23. Iino Y, Okura S, Shiga J, Toriyama M, Kudo K. Histopathological studies on paranasal mucosa from patients treated with erythromycin [in Japanese]. J Otolaryngol Jpn 1994;97:1070-8.
24. Gajewski TF, Lancki DW, Stack R, Fitch FW. "Anergy" of Th0 helper T lymphocytes induces downregulation of Th1 characteristics and a transition to a Th2-like phenotype. J Exp Med 1994;179:481-91.
25. Ohno I, Lea R, Finotto S, et al. Granulocyte/macrophage colony-stimulating factor (GM-CSF) gene expression by eosinophils in nasal polyposis. Am J Respir Cell Mol Biol 1991;5:505-10.
26. Bachert C. Cytokines: comparison between polyp tissue, diseased sinus mucosa and normal nasal tissue. In: Mygind N, Lildholdt T, eds. Nasal polyposis: an inflammatory disease and its treatment. Copenhagen, Denmark: Munksgaard, 1997:98-104.

Ann Otol Rhinol Laryngol 110:2001

HISTOPATHOLOGY OF SUBMANDIBULAR GLANDS REMOVED FOR SIALOLITHIASIS

FRANCIS MARCHAL, MD   ANNE-MARIE KURT, MD   PAVEL DULGUEROV, MD
MINERVA BECKER, MD   MICHAELA OEDMAN, BS   WILLY LEHMANN, MD
GENEVA, SWITZERLAND

We reviewed the clinical history of 48 consecutive patients who underwent submandibular gland removal for radiologically proven sialolithiasis. The specimens were examined by a pathologist blinded to the clinical data. A histopathologic classification into 1 of 3 grades was established by evaluating the degrees of atrophy, fibrosis, and inflammation. A correlation between the clinical and pathological variables was sought in order to define clinical variables that would predict abnormal submandibular glands that required extirpation. A significant percentage of the submandibular glands exhibited normal histologic findings. The patients with normal submandibular glands had a clinical evolution similar to that of other patients with severely damaged glands. The only clinical variable that correlated with increased histopathologic alteration was the patient's age. In view of the newly available diagnostic and therapeutic techniques for sialolithiasis, a conservative attitude to submandibular gland resection appears justified.

KEY WORDS — classification, correlation, pathology; salivary gland, sialolithiasis, surgery.

INTRODUCTION

Sialolithiasis results in a mechanical obstruction of the salivary duct, causing recurrent glandular swelling during meals, which can remain transitory or be complicated by bacterial infections.[1,2] The classic response to sialolithiasis is antibiotic and anti-inflammatory treatment in hope of a spontaneous stone expression through the papilla.[3] When the submandibular stone is located close to the Wharton's duct opening, a marsupialization of the papilla (sialodochoplasty) can be performed and the stone extracted.[4] For posteriorly located stones, the gland is extirpated in most cases.[2,4]

The main indications for submandibular gland removal are sialolithiasis and sialadenitis,[5-7] which represent 69%[5] to 89%[7] of all indications. Although submandibular gland excision is a frequent operation, several reports demonstrate a rather high rate of complications.[6-11] According to Hald and Koks-Andreassen,[6] short-term complications are experienced by 37% of patients and include, among others, temporary marginal mandibular branch paresis (18%), infection (14%), and lingual nerve deficit (5%). In the same series, long-term complications are described in 35% of patients and include scar problems (17%), reduced salivation (14%), and alterations in sensation (13%). Paresis of the marginal mandibular branch is not rare, and an incidence of definitive paralysis of 7% is cited in one report.[12]

Since submandibular gland resection is not innocuous, and since a large percentage of these operations are performed for sialolithiasis, it is surprising that the indications for submandibular gland resection for sialolithiasis remain vague. While only a few studies have examined the function of salivary glands with sialolithiasis, it is believed that the glands are no longer functional.[13] Moreover, repeated infections, posteriorly located stones, and recurrent inflammatory swelling are thought to be directly proportional to glandular dysfunction.[14]

Even if there is no proven link between histopathology and function, it seems reasonable to assume that salivary glands exhibiting marked histopathologic alterations are not functional, and that morphologically normal glands could be functional. Few studies have examined the histopathology of removed submandibular glands. Histopathologic criteria have been proposed, such as inflammation, atrophy, or fibrosis.[13,15] The exact role of inflammation in salivary function is unknown. Regarding fibrosis and atrophy and their correlation to the function of the gland, it seems reasonable to assume that if glandular acini are replaced by fibrosis, or if diffuse atrophy is present, the glandular function is impaired.

The purpose of this study was to examine and classify the histopathologic changes found in submandibular glands removed for sialolithiasis, and to correlate these histologic changes to the patient's clinical history.

From the Division of Head and Neck Surgery (Marchal, Dulguerov, Oedman, Lehmann) and the Departments of Pathology (Kurt) and Radiology (Becker), Geneva University Hospital, Geneva, Switzerland.

Presented at the meeting of the American Academy of Otolaryngology–Head and Neck Surgery, New Orleans, Louisiana, September 26-29, 1999.

CORRESPONDENCE — Francis Marchal, MD, 16, Cours de Rive, 1204 Geneva, Switzerland.

TABLE 1. DISTRIBUTION OF PATIENTS BY GRADING OF SUBMANDIBULAR GLANDS ACCORDING TO DEGREE OF ATROPHY, FIBROSIS, AND INFLAMMATION

		Fibrosis		
Atrophy	*Inflammation*	*0*	*I*	*II*
0	0	4	0	0
	I	6	3	0
	II	0	0	0
I	0	0	0	0
	I	0	11	1
	II	0	4	4
II	0	0	0	0
	I	0	2	5
	II	0	0	8

See text for grading systems.

□ — Grade A, ▨ — Grade B, ■ — Grade C.

METHODS

Included in this series were 48 consecutive patients who underwent removal of their submandibular glands for sialolithiasis. The diagnosis of sialolithiasis was confirmed in all patients by conventional radiography, sialography, or ultrasound.

The indication for submandibular gland removal was 1) recurrent infections lasting more than 6 months or 2) chronic infection with symptoms lasting longer than 1 month despite antibiotic therapy. The surgery was performed under general anesthesia by standard techniques. For all patients, the following clinical data were noted: age, duration of symptoms, number of infectious episodes, time since the previous infection, and the surgery performed. By duration of symptoms, we mean the delay between the first episode of inflammation of the gland and the operation. By number of infectious episodes, we mean only the swelling episodes treated with antibiotics, excluding transitory episodes of inflammatory swelling.

The removed submandibular glands were fixed in formalin before examination by the pathologist. For each gland, 8 slides were stained with hematoxylin and eosin. For each specimen, the degrees of inflammation, fibrosis, and atrophy were staged by the same pathologist (A.-M.K.) without knowledge of the clinical data. The degree of inflammation was classified into 1 of 3 grades (0 = absent, 1 = moderate, 2 = important). The degree of fibrosis underwent similar staging (from 0 to 2), and the location of the fibrosis was recorded (pericanalar or intralobular). The atrophy was classified as focal or diffuse and scored similarly (0 = no atrophy, 1 = focal atrophy, 2 = diffuse atrophy). Other pathological findings recorded include ectasia of intercalated ducts, granulomas, abscesses, presence of caliciform cells, and squamous metaplasia of the ductal epithelium.

From these pathological findings, a new classification was established (Table 1 and Fig 1):

1. Grade A: no atrophy and no fibrosis (score 0), and absent or moderate inflammation (score 0 or 1).
2. Grade B: moderate atrophy (score 1) and/or fibrosis (score 1) with any stage of inflammation (score 0 to 2).
3. Grade C: important atrophy and/or fibrosis (score 2) with any stage of inflammation (score 0 to 2).

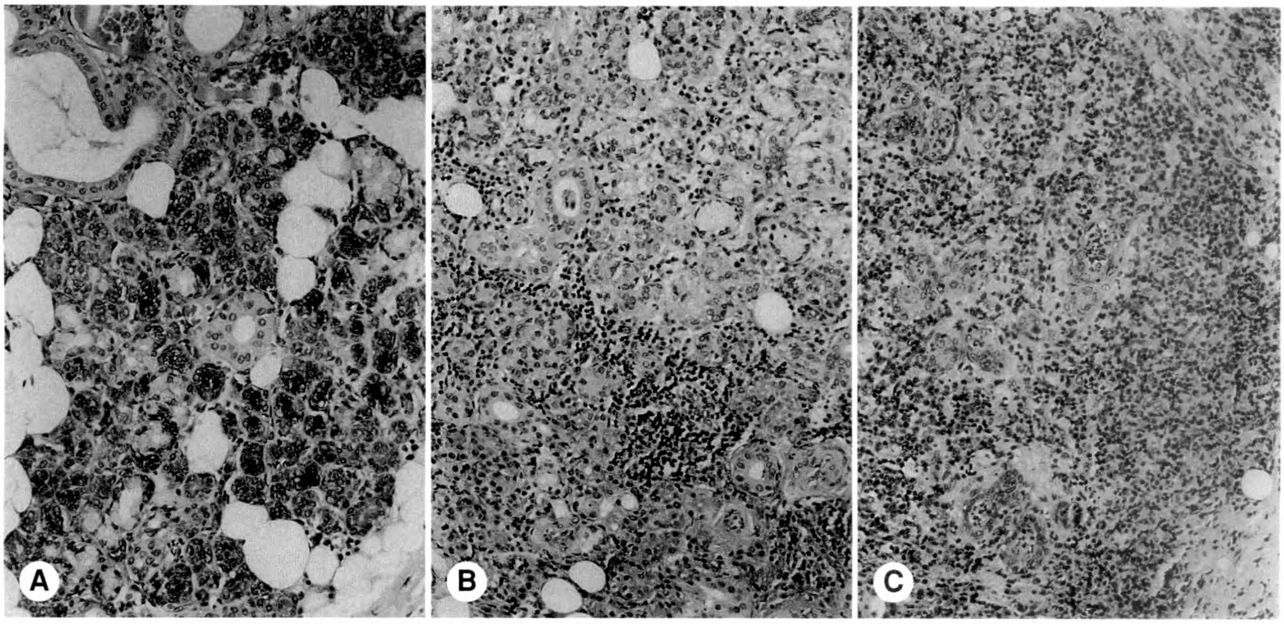

Fig 1. Histopathology of 3 pathological grades (H & E, original ×200). **A**) Grade A. Normal glandular parenchyma. Absence of inflammation or atrophy. **B**) Grade B. Salivary gland shows moderate inflammatory infiltrate without significant atrophy. **C**) Grade C. Severely inflamed glandular parenchyma with microabscesses and diffuse atrophy.

TABLE 2. COMPARISON OF CLINICAL DATA OF PATIENTS BY HISTOLOGIC GRADE

Clinical Parameters	*Grade A*	*Grade B*	*Grade C*	*p*	*Total*
No. of patients	10	18	20		48
Age (y)	35.2 ± 16.6	36.7 ± 10.4	54.3 ± 17.6	.001	43.8 ± 17.3
No. of infectious episodes	3.4 ± 1.8	3.4 ± 1.7	3.4 ± 2.3	.99	3.4 ± 1.9
Duration of symptoms (y)	2.4 ± 1.4	3.4 ± 4.8	2.5 ± 4.1	.72	2.8 ± 3.4
Time between last episode and surgery (d)	64.5 ± 26.5	74.8 ± 89.3	73.8 ± 86.7	.94	72.2 ± 77.9

Data are mean values ± SD. See text for definition of grades.

The statistical association between pathological variables and clinical data was performed by 1-way analysis of variance.

RESULTS

The mean age of the 48 patients was 43.8 ± 17.3 (SD) years. On average, these patients experienced symptoms for 2.8 ± 3.4 years, the number of infectious episodes was 3.4 ± 1.9, and the frequency of episodes per year was 3.2 ± 3.6 (Table 2).

The histopathologic grading classified the submandibular gland specimens as grade A (n = 10), grade B (n = 18), or grade C (n = 20). The distribution of the averages of patient age and duration and number of infectious episodes according to histopathologic grade is shown in Table 2. Only the patient's age was significantly related to a more pathologically altered gland. The numbers of infectious episodes presented by the patient before the extirpation of the gland were similar (mean, 3.4) in all 3 groups. There was no significant difference in duration of symptoms among the 3 pathological groups. Similarly, there was no difference in the delay between the last infection and the surgery.

The statistical relationship between individual histopathologic variables and the clinical data is shown in Table 3. None of the clinical data were significantly correlated to the pathological findings, except the patient's age. In particular, the 2 pathological variables most probably related to an impaired gland function, namely, diffuse atrophy and intralobular fibrosis, were associated with a similar number of infectious episodes and a similar duration of symptoms (Fig 2) as found in the cases without diffuse atrophy or intralobular fibrosis.

TABLE 3. STATISTICAL CORRELATION BETWEEN CLINICAL COURSE AND DIFFERENT PATHOLOGICAL VARIABLES

Pathological Variable	*Age*	*No. of Episodes*	*Duration of Symptoms*	*Time Between Last Episode and Surgery*
Atrophy score	.01*	.46	.71	.46
Fibrosis score	.001*	.84	.97	.85
Inflammation score	.04*	.92	.32	.62
Focal atrophy	.55	.71	.49	.84
Diffuse atrophy	.02*	.78	.50	.47
Local fibrosis	.046*	.31	.39	.33
Periductal fibrosis	.041*	.93	.74	.49
Abscess	.55	.73	.32	.01*
Metaplasia	.10*	.16	.11	.02*

Data are p values.

*$p \leq 0.1$.

The delay between the last infectious episode and the surgery was inversely related ($p < .02$) to the presence of abscesses and metaplasia (Table 3). When a delay of 30 days was used to subdivide patients into 2 groups (18 patients with a delay of less than 30 days as compared with the 30 remaining patients), the 18 patients with a shorter delay had a statistically ($p < .05$) higher degree of inflammation (1.56 ± 0.5 versus 1.07 ± 0.22).

DISCUSSION

The same pathologist analyzed 48 submandibular glands removed for radiologically proven sialolithiasis. A classification into 1 of 3 histopathologic grades was established. Submandibular glands classified as grade A had normal histologic findings and were found in 10 of 48 cases. Grade C, corresponding to markedly altered histologic findings with extensive atrophy and fibrosis, was found in 20 glands. Grade B was a group of 18 cases with intermediate histologic alterations.

Although the patients in group A had normal histologic findings, they presented a clinical evolution similar to that of the patients in the other groups. In particular, their number of infectious episodes and their duration of symptoms were similar to those of the remaining patients, who had histologically altered glands. Therefore, on the basis of clinical symptoms, their submandibular gland removal was completely justified, considering that no precise criteria for submandibular gland removal in cases of sialolithiasis are available.

The only other pathological classification of submandibular glands affected by sialolithiasis was proposed by Seifert[16] and modified by Isacsson et al.[14] Their grading was based mainly on the degree of in-

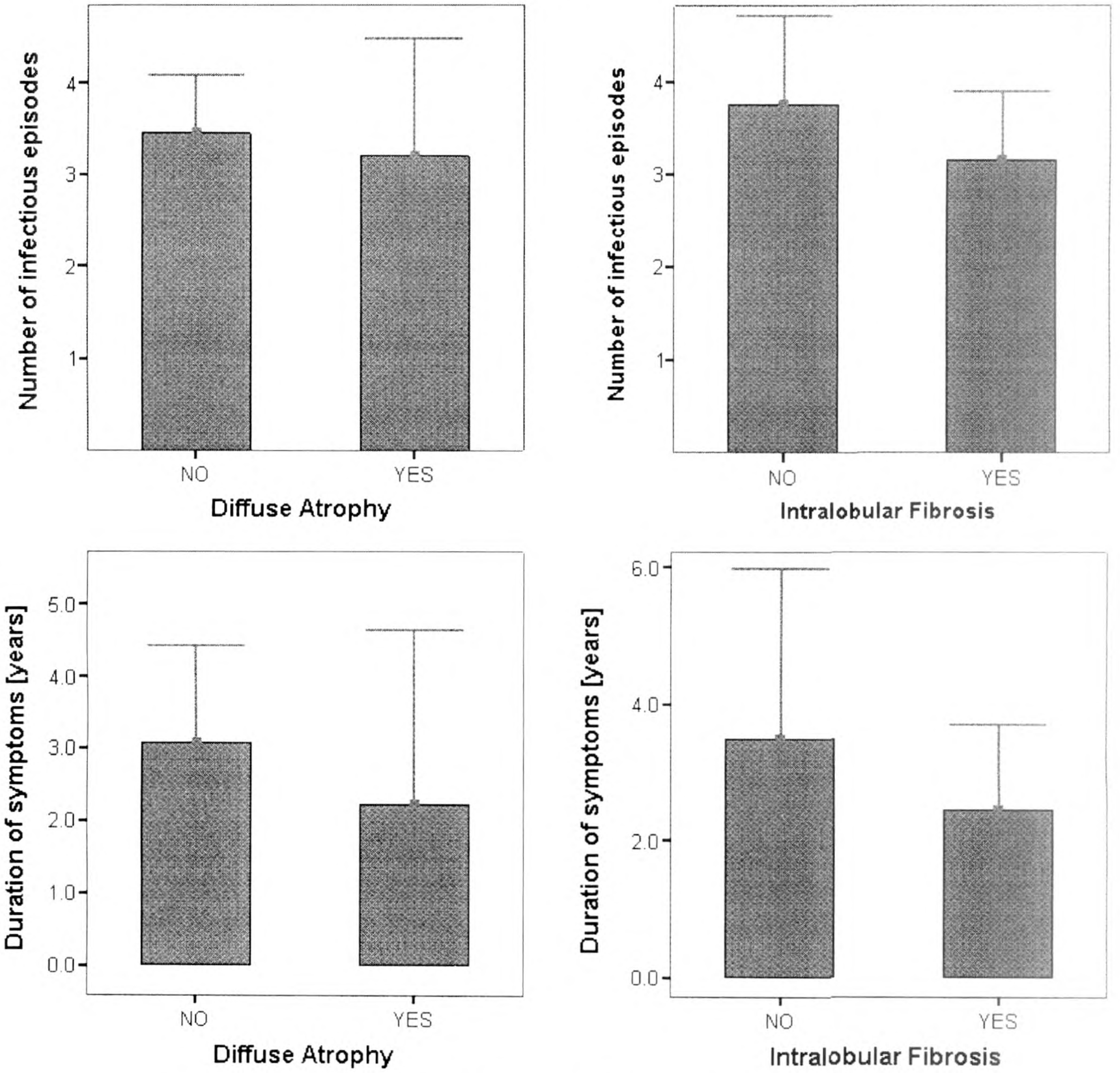

Fig 2. Presence or absence of fibrosis and atrophy correlated to clinical course.

flammation. In our study, the degree of inflammation was correlated to the delay between the last infectious episode and the surgery. Patients who suffered from chronic infectious processes and were operated on early had a significantly greater degree of inflammation than the remaining patients. Therefore, inflammation could be partially reversible, and does not obligatorily entail a permanent glandular dysfunction. Fibrosis and atrophy, such as considered in our grading, might be better predictors of the function of the gland. In the normal group (grade A), the glandular structure is completely conserved, and thus, we tend to assume that the function of the gland is normal. In the pathological group (grade C), most glandular acini were replaced by atrophy and/or fibrosis, and it is logical to postulate that the function of such glands is impaired. In the intermediate group (group B), there were no definitive signs by which to evaluate the associated salivary function.

In our study, the clinical history in terms of number of infectious episodes and duration of symptoms was not correlated to the histopathologic grade. Therefore, numerous infectious episodes or a long duration of symptoms cannot be used to predict the histologic alteration of submandibular glands removed for sialolithiasis. Although there is no proof of a direct correlation between histologic findings and function, the common opinion that submandibular glands with sialolithiasis should be removed because they are nonfunctional should be revised.

Despite an abundant literature on the role of saliva,[17] few specific tests of the function of an individual salivary gland are available. One possible approach is to evaluate the salivary flow. Van den Akker and Busemann-Sokole[4] performed scintigraphic and salivary secretion tests on patients after unilateral transoral removal of sialolithiasis. In their study, the majority of operated submandibular glands exhibited an output comparable to that of the normal contralateral submandibular gland. Already, in 1983, they had concluded that "the presence of a stone at the knee of the submandibular duct does not necessarily warrant excision of the submandibular gland."[4(p356)]

The only clinical variable that was correlated with the histopathologic grading was the patient's age. Scott[18] analyzed the histologic changes in submandibular glands obtained at necropsy of patients from 16 to 95 years old. Glands retrieved from young patients had a compact parenchyma, interrupted with thin fibrous bands, whereas older glands exhibited acinar atrophy and increased pericanalar fibrosis. Although a correlation to the commonly observed decrease of salivary function in elderly patients remains speculative, Scott's results are similar to our observations.

All of our patients had a lithiasis, proven not only by conventional radiologic techniques but also by ultrasound and magnetic resonance sialography.[19] Seifert and Donath,[20] in 1977, in a survey of 349 extirpated glands with sialadenitis, found only 41% of stones by conventional radiology. Isacsson et al[14] found 84% of stones by pathology in their series of submandibular glands resected for sialadenitis. The exact pathogenesis of sialadenitis remains unclear.[2] Recent advances in diagnostic imaging[19] and diagnostic sialendoscopy[21-23] make us favor sialolithiasis as the main cause of nonspecific sialadenitis. Conservative techniques for removal of sialolithiasis, such as external lithotripsy[24-26] and intraductal lithotripsy,[27-29] have already proven their efficacy. New endoscopic techniques, such as endoscopic-assisted stone removal, are being developed and may be of interest in the near future.[21-23]

CONCLUSIONS

1. A new histopathologic grading of submandibular glands removed for sialolithiasis is proposed.
2. A significant percentage of submandibular glands removed for sialolithiasis exhibit normal histologic characteristics.
3. The patients with normal submandibular glands have a clinical evolution similar to that of other patients with severely damaged glands.
4. In view of the newly available diagnostic and therapeutic techniques for sialolithiasis, a conservative attitude to submandibular gland resection appears justified.

REFERENCES

1. Lustmann J, Regev E, Melamed Y. Sialolithiasis. A survey on 245 patients and a review of the literature. Int J Oral Maxillofac Surg 1990;19:135-8.

2. Cawson RA, Gleeson MJ, Eveson JW. Sialadenitis. In: Cawson RA, Gleeson MJ, Eveson JW, eds. Pathology and surgery of the salivary glands. Oxford, England: Isis Medical Media, 1997:33-63.

3. Rice DH. Diseases of the salivary glands — non-neoplastic. In: Bailey B, Pillsbury HC, eds. Head and neck surgery–otolaryngology. Philadelphia, Pa: JB Lippincott, 1993:475-84.

4. van den Akker HP, Busemann-Sokole E. Submandibular gland function following transoral sialolithectomy. Oral Surg Oral Med Oral Pathol 1983;56:351-6.

5. Crabtree GM, Yarington CT. Submandibular gland excision. Laryngoscope 1988;98:1044-5.

6. Hald J, Koks-Andreassen U. Submandibular gland excision: short- and long-term complications. ORL J Otorhinolaryngol Relat Spec 1994;56:87-91.

7. Goh YH, Sethi DS. Submandibular gland excision: a five-year review. J Laryngol Otol 1998;112:269-73.

8. Smith WP, Peters WJ, Markus AF. Submandibular gland surgery: an audit of clinical findings, pathology and postoperative morbidity. Ann R Coll Surg Engl 1993;75:164-7.

9. Berini-Aytes L, Gay-Escoda C. Morbidity associated with removal of the submandibular gland. J Craniomaxillofac Surg 1992;20:216-9.

10. Coumel C, Vesse M, Perrin L, Rouaux JP. 50 Sous-maxillectomies. Rev Stomatol Chir Maxillofac 1979;80:344-8.

11. Panzoni E, Marchesi A, Lippi L. Sialoadenectomia sottomandibolare: tecniche chirurgiche, casistica operatoria ed esiti a distanza. Riv Ital Stomatol 1984;53:121-30.

12. Milton CM, Thomas BM, Bickerton RC. Morbidity study of submandibular gland excision. Ann R Coll Surg Engl 1986;68:148-50.

13. Isacsson G, Lundquist PG. Salivary calculi as an aetiological factor in chronic sialadenitis of the submandibular gland. Clin Otolaryngol 1982;7:231-6.

14. Isacsson G, Ahlner B, Lundquist PG. Chronic sialadenitis of the submandibular gland. A retrospective study of 108 cases. Arch Otorhinolaryngol 1981;232:91-100.

15. Shinohara M, Oka M, Yamada K, Hashimura K, Yuba K, Mori M. Immunohistochemical and electronmicroscopic studies of obstructive lesions in submandibular glands. J Oral Pathol Med 1992;21:370-5.

16. Seifert G. Klinische Pathologie der Sialadenitis und Sialadenose. HNO 1971;19:1-9.

17. Batsakis JG. Salivary glands. Physiology. In: Cummings CW, Fredrickson JM, Harker LA, Krause CJ, Schuller DE, eds. Otolaryngology–head and neck surgery. St Louis, Mo: Mosby, 1993:986-1007.

18. Scott J. Degenerative changes in the histology of the human submandibular salivary gland occurring with age. J Biol Buccale 1977;5:311-9.

19. Becker M, Marchal F, Becker CD, et al. Sialolithiasis and salivary ductal stenosis: diagnostic accuracy of MR sialography with a three-dimensional extended-phase conjugate-sym-

metry rapid spin-echo sequence. Radiology 2000;217:347-58.

20. Seifert G, Donath K. Zur Pathogenese des Kutter-Tumors der Submandibularis. Analyse von 349 Fallen mit chronischer Sialadenitis der Submandibularis. HNO 1977;25:81-92.

21. Marchal F, Becker M, Dulguerov P, Lehmann W. Interventional sialendoscopy. Laryngoscope 2000;110:318-20.

22. Marchal F, Dulguerov P, Becker M, Lehmann W. Interventional sialendoscopy. In: Wackym PA, Rice DH, Schaefer SD, eds. Minimally invasive surgery of the head, neck and cranial base. Philadelphia, Pa: Lippincott, Williams & Wilkins (in press).

23. Marchal F, Dulguerov P, Lehmann W. Interventional sialendoscopy. N Engl J Med 1999;341:1242-3.

24. Katz P. Thérapeutiques non chirurgicales des lithiases salivaires. Endoscopie et lithotrypsie extra-corporelle. Rev Off Soc Fr ORL 1997;45:47-52.

25. Iro H, Schneider HT, Fodra C, et al. Shockwave lithotripsy of salivary duct stones. Lancet 1992;339:1333-6.

26. Kater W, Meyer WW, Wehrmann T, Hurst A, Buhne P, Schlick R. Efficacy, risks, and limits of extracorporeal shock wave lithotripsy for salivary gland stones. J Endourol 1994;8:21-4.

27. Gundlach P, Scherer H, Hopf J, et al. Die endoskopisch kontrollierte Laserlithotripsie von Speichelsteinen. In-vitro-Untersuchungen und erster klinischer Einsatz. HNO 1990;38:247-50.

28. Arzoz E, Santiago A, Esnal F, Palomero R. Endoscopic intracorporeal lithotripsy for sialolithiasis. J Oral Maxillofac Surg 1996;54:847-52.

29. Ito H, Baba S. Pulsed dye laser lithotripsy of submandibular gland salivary calculus. J Laryngol Otol 1996;110:942-6.

≈

MANAGEMENT OF THE TINNITUS PATIENT

The Ninth Annual Conference on the Management of the Tinnitus Patient, for professionals and tinnitus patients, will be held in Iowa City, Iowa, October 4-6, 2001. For information, see web site www.medicine.uiowa.edu/otolaryngology/news/news or contact Rich Tyler by telephone (319-356-2471) or e-mail (rich-tyler@uiowa.edu).

Ann Otol Rhinol Laryngol 110:2001

CHARACTERIZATION OF THE MEDIAL SURFACE OF THE VOCAL FOLDS

DAVID A. BERRY, PHD
LOS ANGELES, CALIFORNIA
DOUGLAS W. MONTEQUIN, MA
IOWA CITY, IOWA
MARTYN J. O. CLARK, MS
IOWA CITY, IOWA
INGO R. TITZE, PHD
IOWA CITY, IOWA

A method is developed for the quantification of the medial surface of the vocal folds in excised larynges. Lead molds were constructed from the glottal airway of a canine larynx for 3 distinct glottal configurations corresponding to "pressed" folds, just barely adducted folds, and 1-mm-abducted folds as measured between the vocal processes. With a high-resolution laser striping system, the 3-dimensional molds were digitally scanned. Low-order polynomials were fitted to the data, and goodness-of-fit statistics were reported. For all glottal configurations, a linear variation (flat surface) approximated the data with a coefficient of determination of 90%. This coefficient increased to roughly 95% when a quadratic variation (curvature) was included along the vertical dimension. If more than the top 5 mm or so of the folds was included (the portion usually corresponding to vibration), a cubic variation along the vertical dimension was necessary to explain a change in concavity at the conus elasticus. These findings suggest the utility of a model based on a convergence coefficient and a bulging coefficient. For all glottal configurations, the convergence coefficients and bulging coefficients can be computed. Because pre-phonatory conditions have a profound influence on vocal fold vibration and on the quality of phonation, such shaping parameters are highly significant. With the viability of this method substantiated, it is envisioned that future studies will characterize greater quantities of glottal shapes, including those of human vocal folds.

KEY WORDS — glottis, larynx, vocal fold.

INTRODUCTION

Initial conditions and boundary conditions have a profound impact on many nonlinear dynamic systems. In vocal fold vibration, which represents such a nonlinear system, a small change in the pre-phonatory shape of the medial surface of the vocal folds can mean the difference between chest-like, falsetto-like, and fry-like vibration patterns, or it can mean the difference between periodic and aperiodic oscillations.[1] For phonosurgeons, who alter the glottal geometry in reconstructive procedures, pre-phonatory vocal fold shape is increasingly understood as a critical variable. For example, measurement of the angle of glottal opening and precise positioning of the arytenoid cartilage are becoming more and more common in phonosurgery.[2-4]

Several simulation models of vocal fold vibration have been used to quantify the subtleties of vocal fold shape.[5-7] These models solve second-order partial differential equations to describe the resultant vibrations. In such models, the specification of initial conditions, or pre-phonatory shape, is essential in making a reasonable prediction of the oscillations. A series of normal mode studies on the vocal folds has shown that phonation frequency has a remarkable correspondence with the lowest resonance frequency of the folds, as measured immediately before phonation.[8,9] Such resonance frequencies are known to be strongly influenced by glottal geometry.[10] However, to date, no quantitative data exist on these pre-phonatory shapes. In particular, previous magnetic resonance and computed tomographic images obtained from the vocal tract and laryngeal regions have not yielded the resolution needed for modeling the medial surface of the folds (on the order of 0.1 mm).

The focus of this report is the development of a method for high-precision quantification of the medial shape of the vocal folds in excised larynges. Once the methodological study is presented, future studies are envisioned in which greater numbers of molds will be analyzed, with more decisive conclusions drawn. The following questions will be probed. What order of polynomial must be used to approximate the vocal fold shape across a variety of glottal configurations? Does the theoretical model proposed by Titze,[11] which assumes a linear variation of vocal fold shape along the anterior-posterior length and a quadratic variation along the vertical depth, provide

---

From the Department of Speech Pathology and Audiology, National Center for Voice and Speech, The University of Iowa, Iowa City, Iowa. This work was supported by grant R29 DC03072 from the National Institutes of Health/National Institute on Deafness and Other Communication Disorders. This study was performed in accordance with the PHS Policy on Humane Care and Use of Laboratory Animals, the NIH *Guide for the Care and Use of Laboratory Animals*, and the Animal Welfare Act (7 U.S.C. et seq.); the animal use protocol was approved by the Institutional Animal Care and Use Committee (IACUC) of the University of Iowa (October 22, 1993).

CORRESPONDENCE — David A. Berry, PhD, UCLA School of Medicine, Division of Head and Neck Surgery, 31-24 Rehab Center, Los Angeles, CA 90095-1794.

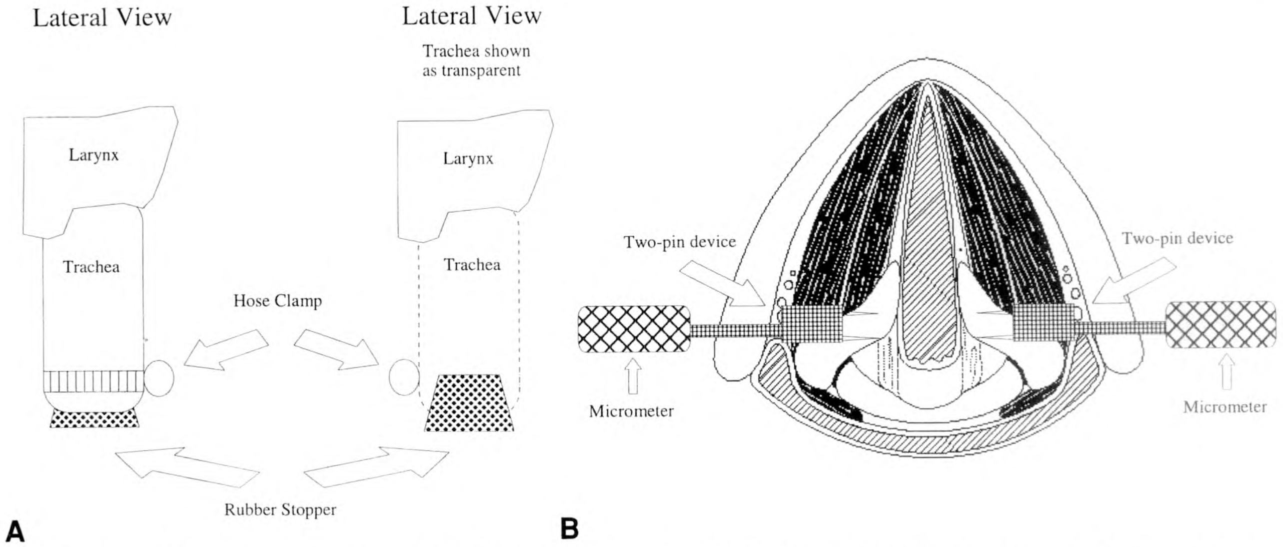

Fig 1. Views of larynx. **A)** Lateral view depicts stopper that was placed at base of trachea to prevent wax leakage during molding process. **B)** Superior view depicts 2-pin micrometer device used to control arytenoid adduction.

an adequate description of the molds? If so, what are the convergence coefficients and bulging coefficients of each of the molds, and how do these constants change as a function of glottal adduction?

METHODS

A canine larynx was obtained postmortem from an experimental animal weighing approximately 20 kg. Before molding the airway, we dissected the excised larynx to remove the epiglottis, the ventricular folds, and all but a short section (0.5 to 1 inch) of the trachea. The interior of the larynx was coated with a silicone gel to allow easy removal of the mold. A stopper, held in place with a hose clamp, was used to block the trachea (Fig 1A). The larynx was then mounted in a vertical orientation, and the vocal folds were adducted with 2-pin micrometer devices, as shown in Fig 1B. Once a desired level of adduction was achieved, molten wax (Tissueprep histologic wax) was injected into the glottal airway and left to harden.

In order to make a more permanent mold of the airway, we removed the wax mold and placed it in dental plaster so that the tracheal end of the wax mold broke the surface of the plaster (so that the wax could be removed later). After the plaster hardened, the wax was removed by placing the plaster-wax compound into a kiln and slowly heating the kiln to at least 327.5°C, which is the melting point of lead. The wax was burned away and was replaced with liquid lead. The lead mold was allowed to cool for 1 hour. Subsequently, the plaster was cracked away, leaving a 3-dimensional (3-D) lead mold of the glottal and subglottal airway, as well as a 3-D representation of the medial surface of the vocal folds. The molds appeared to yield a good representation of the glottal airway. There was no evidence of tissue deformation during the wax injection, or during hardening of the plaster or the reverse lead mold.

Three molds were obtained from the larynx, each mold corresponding to a unique glottal configuration: 1) an open larynx (a glottal width of approximately 1 mm, with no micrometer-adduction devices applied); 2) the arytenoids just barely adducted; and 3) the arytenoids pressed to the point of 1 mm beyond "just touching." Measurements of glottal width were taken between the anterior points of the vocal processes.

In preparation for analysis of the molds, it was necessary to digitize the surfaces. The physical orientation used throughout this report is as follows: z direction, the vertical dimension; y direction, the anterior-posterior length; and x direction, the medial-lateral dimension of the folds. The metallic composition of the lead molds facilitated digitization with a 3-D laser striping system. In particular, we used the IMAGINE2 laser striper, built by the Department of Artificial Intelligence at the University of Edinburgh, to digitize the molds.[12,13] The system measured the x coordinate with an error of approximately 0.1 mm, and scanned the surfaces in increments of 0.5 mm in the y and z directions. Scans were taken of all of the molds from 3 different orientations: the left, the top, and the right, as shown in Fig 2. Because the molds appeared to be predominantly symmetric, symmetry was assumed, and only the left view was analyzed. However, if one desired to analyze the geometric asymmetries between the left and right folds, the present technique could accommodate such a study (ie, both left and right views could be analyzed).

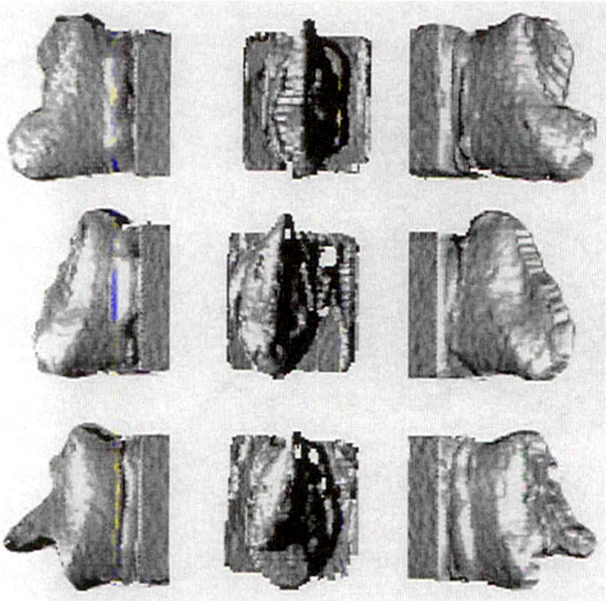

Fig 2. Surface rendering of 3-dimensional (3-D) data obtained with laser striper for larynx 1. Left, superior, and right views are shown from left to right in pictures, respectively. From top to bottom, open larynx, arytenoids just touching, and pressed arytenoid configurations are shown.

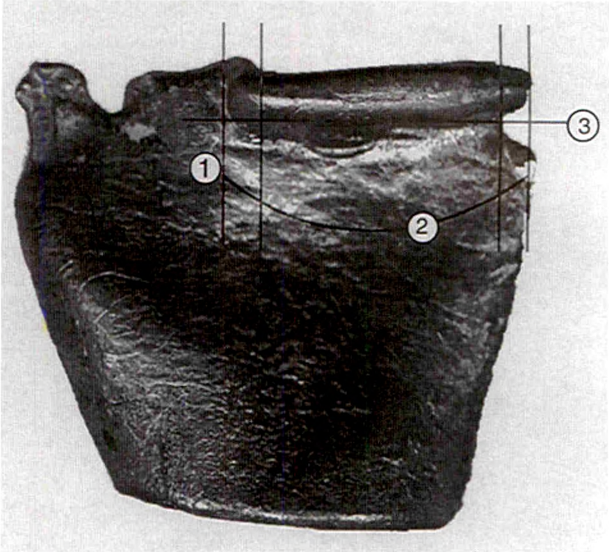

Fig 3. Side view of sample lead mold of glottal airway. Line 3 indicates superior edge of vocal fold, 2 indicates inferior edge on which tissue vibration is possible, and 1 indicates plausible choices for anterior-posterior boundaries. Although most extreme markers give more accurate indication of true vocal fold length, more interior markers were often used in this investigation in order to avoid noisy data near end points.

In modeling the medial surface of the folds, it was of particular interest to know which regions of the molds corresponded to vibrating tissues. Indeed, the focus of this investigation was the pre-phonatory shape of tissue regions in which oscillations might occur. Such data directly impact our computer models of vocal fold vibration and are also of interest in phonosurgery. Although the non-oscillating tissue regions were not the focus of this study, they could be useful for modeling subglottal airflow.

The region in which tissue vibration was possible is depicted on the lead mold shown in Fig 3, which illustrates a medial view of the mold. The numeral 3 delineates the superior surface of the folds, which appears as a clear indentation on the mold. Above this line, the molding material spilled over the top of the glottal airway. The numeral 2 marks the inferior boundary of vibrating tissue. Palpation of the subglottal wall on the original larynx (ie, not the mold) revealed that the depth to which tissue vibration could occur varied along the length of the folds. The depth was smaller at the anterior and posterior extremities than midway along the length. The inferior boundary was roughly symmetric about the midpoint of the membranous fold, curving upward anteriorly and posteriorly, as shown in Fig 3. The maximal depth of the region of vibration was approximately 5.6 mm on this mold.

The 4 vertical lines marked with a numeral 1 show 2 possible choices for the anterior and posterior boundaries of the vocal fold. Presumably, the most extreme positions give the most accurate estimate of vocal fold length. This is because the most extreme positions of the mold made contact with the structures typically used to measure vocal fold length, eg, the vocal process and the anterior commissure. However, noisy data at the extremes sometimes necessitated a small reduction of this region to facilitate data analysis.

DATA ANALYSIS, RESULTS, AND DISCUSSION

The first step of the analysis consisted of fitting low-order polynomials to the medial surface of the molds. Polynomials were expressed in the following general form:

$$X(y,z) = \sum_{i=0}^{M} \sum_{j=0}^{N} A_{ij} y^i z^j \qquad (1)$$

where A_{ij} are coefficients determined by computing a best-fit polynomial to the image data by Gaussian elimination.

Best-fit polynomials were computed for each mold. For each glottal configuration, the values of M and N were systematically modified, thus altering the degree of the polynomials in y and z (see equation 1). For every polynomial, the coefficient of determination (COD) was computed to assess its goodness of fit with the data. The COD is a standard statistical term used to assess the goodness of fit of linear and nonlinear models to empirical data. It is

TABLE 1. COEFFICIENT OF DETERMINATION PERCENTAGES FOR THREE MOLDS OF LARYNX ONE

	Open Larynx				*Just Barely Adducted*				*Pressed Arytenoids*			
	Maximum Power in y (M)				*Maximum Power in y (M)*				*Maximum Power in y (M)*			
Maximum Power in z (N)	*0*	*1*	*2*	*3*	*0*	*1*	*2*	*3*	*0*	*1*	*2*	*3*
0		31				23				10		
1	54	89	93		56	92	92		61	83	83	
2		92	93	94		95	96	96.0		95	95	95
3		93	95	96		96	96	96.9		95	95	95
4		93				96				95		

See text for definitions.

defined as follows:

$$(2)\qquad \mathrm{COD} = 1 - \frac{\sum_{i} (xi - yi)^2}{\sum_{i} (xi - \bar{x})^2}$$

where yi refers to predictions from the model, xi refers to the empirical data, and $\bar{x}$ refers to the average value of the empirical data. The value of the COD could range between 0 and 1. A value of 0 did not capture any of the variance of the data (ie, the model was no better than an average value estimate), and a value of 1 gave a perfect match between the model and the data. With a computed table of COD percentages for various values of M and N, one could objectively assess the order of polynomial necessary to fit the data. The results for the 3 molds are shown in Table 1.

For all of the glottal configurations, the data strongly suggested that the N = M = 1 condition was a satisfactory condition. If either N or M was lowered, the COD dropped dramatically, indicating that the model could no longer adequately explain the data. For N = M = 1, the COD ranged between 83% and 92%. An additional 3% to 8% gain could be obtained by increasing N to 2, suggesting that a quadratic variation in z might also be important in explaining the curvature of the folds. For the most part, only small gains were achieved by further increasing the values of M and N.

Using N = 2 and M = 1, a visual portrayal of the polynomial fit to the data is shown for the adducted and "pressed" conditions, as shown in Fig 4A,B. Notice that for the adducted mold, no data points were available for the superior-anterior portion of the mold. This illustrates a general limitation of the molding procedure: in order for the mold to exist in a particular region, the glottal airway needs to have a finite width (on the order of 0.1 mm). Thus, the mold did not exist (the molding material simply broke off) in any region in which the glottal airway had a width of less than 0.1 mm. For the purpose of data analysis, such regions were zero-padded. While this was a limitation of the procedure, given that the accuracy of the measurements was on the order of 0.1 mm, this was not viewed as a serious limitation, and zero-padding these regions yielded a reasonable estimate of the "missing" data. For the "pressed" mold as shown in Fig 4B, the entire top 5 mm of the data were missing.

For the separated folds, there were no missing data. Figure 4C shows the results of a cubic fit of the z curvature (M = 3 and N = 1) for the top 13 mm of the glottal airway. Although the cubic polynomial (COD = 93.9%) was not a great deal better than the quadratic polynomial (COD = 92.5%) according to the data in Table 1, physically, the cubic yielded a much better representation of the mold over this entire 13-mm region. As can be seen in Fig 4C, the convexity of the folds changed from top to bottom (ie, from concave to convex). A cubic polynomial was necessary to capture this variation in curvature.

However, as already noted, the focus of this study is on the medial surface of the folds, which may correspond to vibration. Traditionally, it is understood that only the top 3 to 5 mm of the folds is important in terms of vocal fold vibration. For the case of the cubic polynomial, the vertical inflection point was calculated to isolate just the "upper" curvature. The inflection point was 7.61 mm from the top anteriorly, and 8.23 mm from the top posteriorly. Midway along the vocal fold length, the inflection point was calculated to be 7.9 mm from the top. For simplicity, the inflection point was rounded off to 8 mm even. Because the mold captured the top 13 mm of the glottal airway, this inflection point corresponded to roughly the top 5 mm of the mold.

In Table 2, the COD percentages were calculated again with only the data corresponding to the vibrating portion of the molds (the upper 5 mm). With this taken into account, across all glottal configurations, the data suggest that a linear function in y and a quadratic function in z are sufficient to capture the curvature of the folds. This is a preliminary confirmation of the hypothesis proposed earlier by Titze[11] that the y curvature of the pre-phonatory glottis is linear

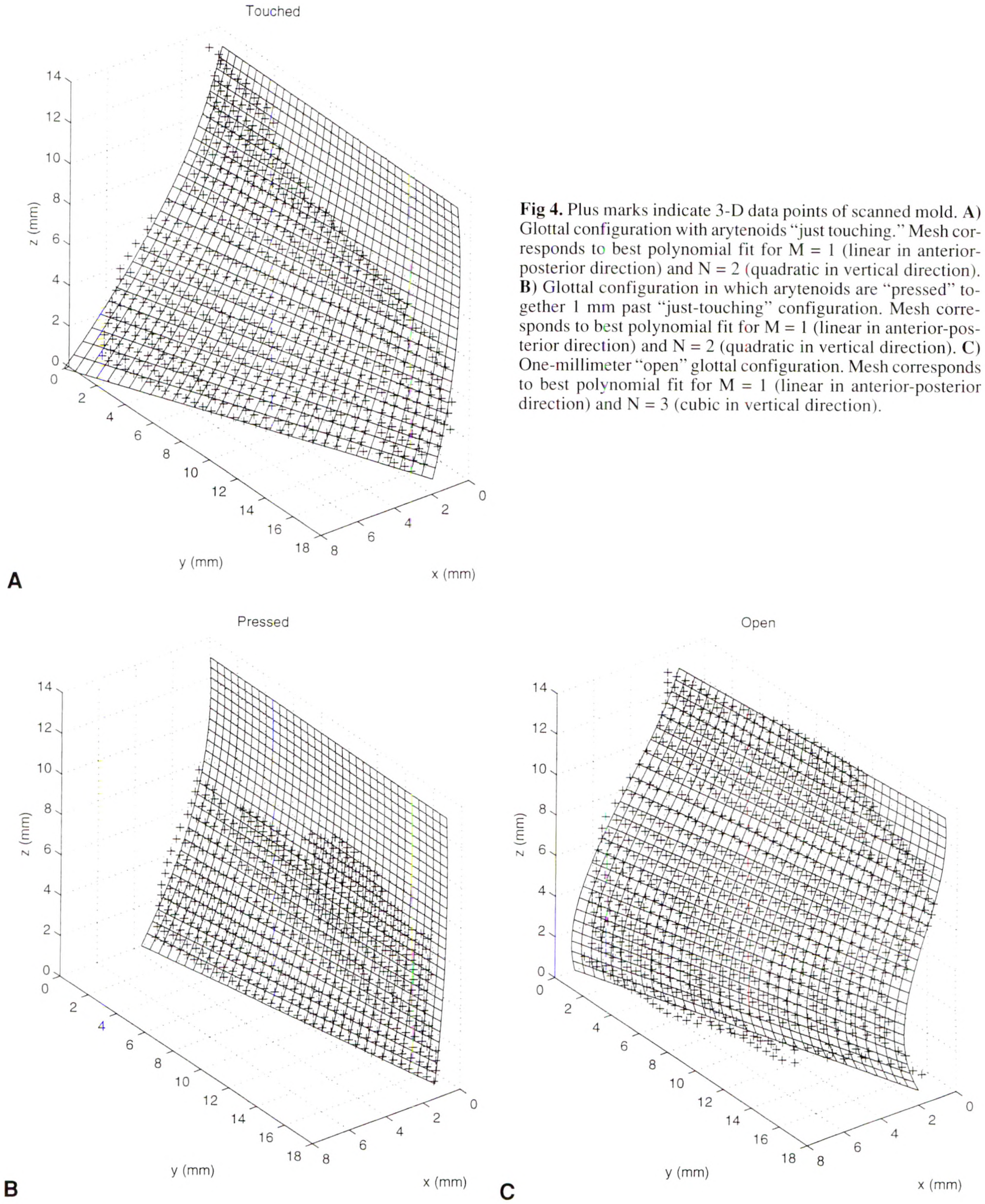

Fig 4. Plus marks indicate 3-D data points of scanned mold. **A)** Glottal configuration with arytenoids "just touching." Mesh corresponds to best polynomial fit for M = 1 (linear in anterior-posterior direction) and N = 2 (quadratic in vertical direction). **B)** Glottal configuration in which arytenoids are "pressed" together 1 mm past "just-touching" configuration. Mesh corresponds to best polynomial fit for M = 1 (linear in anterior-posterior direction) and N = 2 (quadratic in vertical direction). **C)** One-millimeter "open" glottal configuration. Mesh corresponds to best polynomial fit for M = 1 (linear in anterior-posterior direction) and N = 3 (cubic in vertical direction).

and that the z curvature is quadratic. Specifically, he hypothesized that the pre-phonatory glottis could be characterized as follows:

$$(3)\quad X(y,z) = \left(1 - \frac{y}{L}\right)\left[\xi_0 + \left(\xi_c - 4\xi_b \frac{z}{T}\right)\left(1 - \frac{z}{T}\right)\right]$$

where L is the anterior-posterior length of the folds, T is the vertical thickness, ξ_0 is the superior glottal half-width, ξ_c is the convergence coefficient describing the linear variation in z, and ξ_b is the bulging coefficient describing the quadratic variation in z. The physical meaning of these coefficients is further

TABLE 2. RECALCULATION OF COEFFICIENT OF DETERMINATION PERCENTAGES FOR OPEN LARYNX USING JUST UPPER FIVE MILLIMETERS OF MOLD

	Maximum Power in y (M)		
Maximum Power in z (N)	*0*	*1*	*2*
0	0.0	44.3	
1	29.1	89.7	90.8
2		96.4	98.0
3		96.6	

See text for definitions.

TABLE 3. SHAPING PARAMETERS (IN MILLIMETERS) FROM EQUATION THREE AND COD PERCENTAGES FOR THREE MOLDS OF LARYNX ONE

	ξ_o	ξ_c	ξ_b	*L*	*T*	*COD (%)*
Open larynx	1.71	2.75	1.03	20.0	5.00	94.4
Just barely adducted	0.01	1.65	0.16	18.7	4.12	94.7
Pressed arytenoids	0.00	0.26	0.18	20.0	5.07	95.2

L — length; T — thickness; COD — coefficient of determination. See text for other definitions.

illustrated in Fig 5.[11]

Although the polynomial of equation 3 is linear in y and quadratic in z, it is obviously more restrictive than the general polynomial of equation 1. However, one advantage of the more restrictive definition is that each parameter has a precise physical interpretation. Of course, the usefulness of this characterization must be judged by how well it matches the empirical data. To perform this evaluation, equation 3 was fitted to the same data as equation 1. In every case, the z = 0 level was set 5 mm below the assumed top of the folds. The results of this optimization procedure are shown in Table 3.

By comparing Tables 1 and 3 (Tables 2 and 3, for the case of the open larynx), one can see that the COD percentages drop anywhere from 0.1% to 2.0%. The values of Table 1 (Table 2, for the open larynx) that correspond to Table 3 are found in the column in which M = 1 and in the row in which N = 2. This slight drop in the goodness of fit did not appear to be significant. Although the fit of either equation was acceptable, the direct physical interpretation of the shaping parameters from equation 3 seemed to outweigh the slight loss in goodness of fit. An illustration of how the "optimized" polynomial (for equation 3) fit the "open" mold is shown in Fig 6.

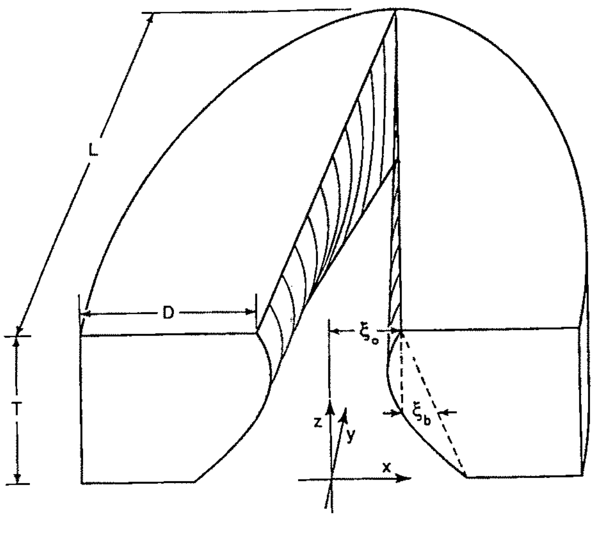

$$g(y,z) = \left(1-\frac{y}{L}\right)\left[\xi_o + \left(\xi_c - 4\xi_b\frac{z}{T}\right)\left(1-\frac{z}{T}\right)\right]$$

Fig 5. Drawing of pre-phonatory shaping function previously proposed by Titze,[11] illustrating coefficients introduced in equation 3.

The shaping parameters of Table 3 appeared to be quite descriptive of the molds, at least for the upper portions of the molds corresponding to the vibrating folds. The open larynx had the greatest glottal half-width ξ_o, the greatest linear convergence ξ_c (the surfaces converged medially when traversing the surfaces in a superior direction), and the greatest quadratic bulging ξ_b. For both the adducted and pressed molds, the glottal half-width was essentially 0, as expected. The glottal convergence of the adducted mold was only 60% of that of the open larynx, and the glottal convergence of the pressed mold was less than 10%. In terms of glottal bulging, both the adducted folds and the pressed folds had small values, ie, less than 20% of that of the open larynx.

One might argue whether the vocal fold length L and the thickness T should have been allowed to vary in the optimization procedure. Certainly, if the model gave large deviations from measured values, the technique would be suspect. There are several reasons why it was thought valid to allow such an optimization here. One reason is that the vocal fold length and effective thickness of the folds might truly vary as a function of glottal adduction. Another reason was that the data did not necessarily extend all the way to the anterior commissure as the model assumes. For example, as indicated in our earlier description of Fig 3, sometimes the length had to be trimmed posteriorly or anteriorly because of noisy data near these end points. By allowing the geometric dimensions L and T to vary, an optimum alignment between model and data was allowed, while still retaining the basic form of the equation. Finally, to compare the optimization results of equations 1 and 3, equation 1 had 6 parameters to vary (for the case in which M equals 1 and N equals 2), whereas equation 3 would have only 3 parameters if the values of L and T were fixed. By allowing a variation in

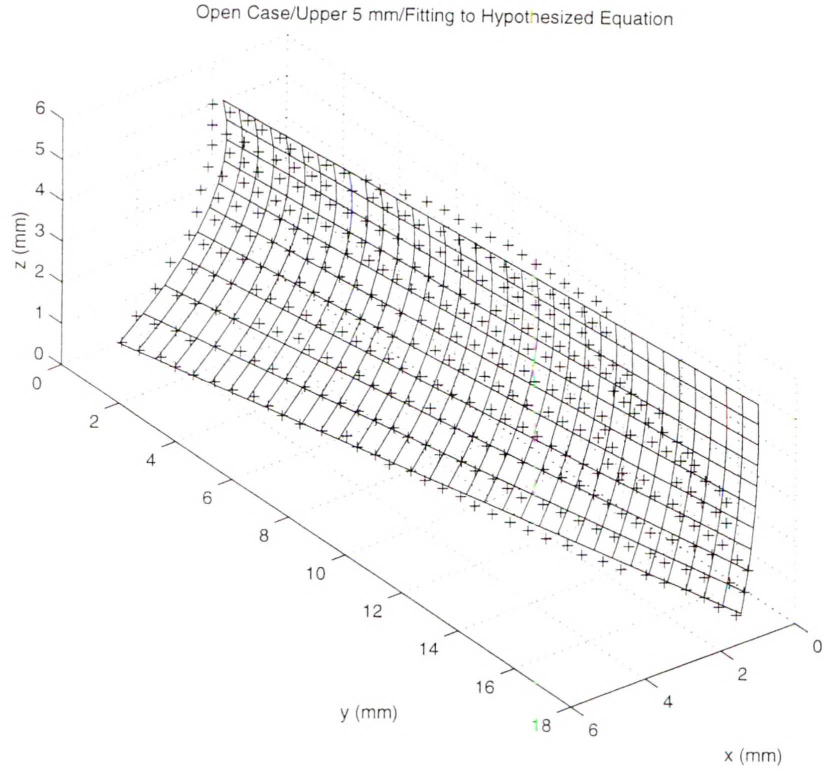

Fig 6. Plus marks indicate 3-D data points of scanned mold corresponding to 1-mm "open" glottal configuration, focusing approximately on top 5 mm, in which most tissue vibration would occur. Mesh corresponds to best polynomial fit to equation 3, using optimized shaping coefficients presented in Table 3.

L and T for equation 3, both equations 1 and 3 had a similar number of parameters to optimize. Optimization results yielded comparable goodness-of-fit statistics for the 2 equations.

SUMMARY AND CONCLUSIONS

A technique was presented for quantifying the prephonatory shape of the vocal folds mathematically on excised larynges. A primary limitation of this method is that the thyroarytenoid muscle is not activated in an excised larynx. However, this is a limitation that can only be overcome with imaging at higher levels of precision than are currently available on human subjects. Thus, a molding procedure was used to capture the shape of the excised larynges. Ultimately, a lead mold was generated, which was subsequently digitized with a 3-D laser striping system with a precision of 0.1 mm. Three molds were created, digitized, and fitted to low-order polynomials.

Through analysis of the COD for various polynomial models of glottal shape, it was argued that minimally, a linear variation in y and z was needed to capture the curvature of the folds. Further modest gains were achieved by allowing a quadratic variation in z. However, any further increase in the order of the polynomial did little to improve the correspondence between model and data. Consequently, on the basis of the 3 molds analyzed in this preliminary study, it was argued that a linear variation in y and a quadratic variation in z was sufficient to capture the curvature of the folds across a range of glottal adductions.

This result is a preliminary confirmation of an earlier hypothesis by Titze,[11] in which he presented an equation (equation 3) to describe the pre-phonatory shape of the folds on the basis of glottal convergence and bulging coefficients. In this study, the coefficients were optimized for each of the 3 molds, and are enumerated in Table 3. These coefficients provided a useful description of the pre-phonatory shape of the vocal folds, and could be directly inserted into our models of vocal fold vibration.

Our technique has been shown to capture the prephonatory glottal shape with a precision on the order of 0.1 mm. With the technique and results presented in this study, we now have the confidence to proceed with further studies in which greater numbers of molds will be generated, digitized, and analyzed. Such investigations are of extreme importance, because initial conditions and boundary conditions are known to have a profound impact on vocal fold vibration, just as they do on many other nonlinear dynamic systems.

ACKNOWLEDGMENTS — Special acknowledgment is given to the Department of Artificial Intelligence of the University of Edinburgh for use of their laser striping system. The authors also thank Karin Titze Cox, whose earlier investigations (K. A. Titze and I. R. Titze, unpublished manuscript) yielded fruitful insights into the present study, and to Cindy Steffensmeier, who manually digitized one of our initial molds using a 3-dimensional micrometer.

REFERENCES

1. Berry DA, Herzel H, Titze IR, Story BH. Bifurcations in excised larynx experiments. J Voice 1996;10:129-38.

2. Inagi K, Khidr AA, Ford CN, Bless DM, Heisey DM. Correlation between vocal functions and glottal measurements in patients with unilateral vocal fold paralysis. Laryngoscope 1997;107:782-91.

3. Woodson GE, Hengesteg A, Rosen CA, Yeung D, Chen N. Changes in length and spatial orientation of the vocal fold with arytenoid adduction in cadaver larynges. Ann Otol Rhinol Laryngol 1997;106:552-5.

4. Woodson GE, Murray T. Glottic configuration after arytenoid adduction. Laryngoscope 1994;104:965-9.

5. Titze IR, Talkin DT. A theoretical study of the effects of various laryngeal configurations on the acoustics of phonation. J Acoust Soc Am 1979;66:60-74.

6. Alipour-Haghighi F, Titze IR. Simulation of particle trajectories of vocal fold tissue during phonation. In: Titze IR, Scherer RC, eds. Vocal fold physiology: biomechanics, acoustics, and phonatory control. Denver, Colo: Denver Center for the Performing Arts, 1983:183-90.

7. Berry DA, Herzel H, Titze IR, Krischer K. Interpretation of biomechanical simulations of normal and chaotic vocal fold oscillations with empirical eigenfunctions. J Acoust Soc Am 1994;95:3595-604.

8. Kaneko T, Uchida K, Suzuki H, et al. Ultrasonic observations of vocal fold vibration. In: Stevens KN, Hirano M, eds. Vocal fold physiology. Tokyo, Japan: University of Tokyo Press, 1981:107-18.

9. Kaneko T, Komatsu K, Suzuki H, et al. Mechanical properties of the human vocal fold: resonance characteristics in living humans and in excised larynges. In: Titze IR, Scherer RC, eds. Vocal fold physiology: biomechanics, acoustics, and phonatory control. Denver, Colo: Denver Center for the Performing Arts, 1983:304-17.

10. Berry DA, Titze IR. Normal modes in a continuum model of vocal fold tissues. J Acoust Soc Am 1996;100:3345-54.

11. Titze IR. A four-parameter model of the glottis and vocal fold contact area. Speech Commun 1989;8:191-201.

12. Fisher R, Trucco E, Fitzgibbon A, Waite M, Orr M. Image: a 3-D vision system. Sensor Rev 1993;13:23-6.

13. Trucco E, Fisher R, Fitzgibbon A, Naidu DK. Calibration, data consistency and model acquisition with a 3-D laser striper. Int J Comput Integrated Manufacturing 1998;11:292-310.

Ann Otol Rhinol Laryngol 110:2001

MASS LOADING ON THE OSSICLES AND MIDDLE EAR FUNCTION

RONG Z. GAN, PHD
MARK W. WOOD, MD
ROBERT K. DYER, MD
KENNETH J. DORMER, PHD
OKLAHOMA CITY, OKLAHOMA

The middle ear as a levered vibrating system for sound transmission from the external to the inner ear is affected by changes in ossicular chain mass. Mass loading of the ossicles may impair ossicular dynamics and sound transmission to the inner ear. It is incumbent on otologic surgeons and researchers of middle ear mechanics to consider the mass loading effect on middle ear function in clinical and physiological applications. The residual hearing and frequency response can change after surgery or implantation of middle ear prostheses. We conducted experiments on mass loading effects on the middle ear transfer functions by using laser Doppler interferometry and a human temporal bone model. Two implant mass loading conditions were tested on 17 fresh or fresh-frozen temporal bones and compared with the unloaded condition for the frequencies 250 to 8,000 Hz. The results show that the linearity of the middle ear function did not change, although displacement of the stapes footplate decreased after the increased masses were placed on the incudostapedial joint. The greater the mass of the implant, the less displacement was measured at the stapes footplate. We conclude that there is a quantitative limit to increased mass on the ossicular chain above which the mass will remarkably impair hearing thresholds.

KEY WORDS — implantable hearing device, laser Doppler interferometry, mass loading, middle ear, ossicle, temporal bone.

INTRODUCTION

The emerging technology of implantable middle ear hearing devices (IMEHDs) has inherent limitations related to the placement of any mass load on the ossicular chain. There are actually 2 types of IMEHDs that add loading to an intact ossicular chain. The first type involves placement of a vibrating probe fixed to a transducer in contact with an ossicle. The second type places a free mass on the ossicular chain.[1,2] The former places a force load, while the latter, as seen in electromagnetic IMEHDs, places an inertial load in the middle ear. Mass loading is the topic of this study, in which we used laser Doppler interferometry (LDI) to measure the effects of loading on middle ear mechanics.

Since Newton's law of mass action is inviolate, any additional load on the ossicular chain will increase inertia and change its transfer function. Thus, the mass of an implant, its size, and its location on the ossicular chain all relate to the higher-frequency performance of IMEHDs. The earliest study on mass loading involved the mass of a middle ear replacement prosthesis for the incus. Lawrence[3] added 25 mg (an incus replacement) to the feline middle ear and found improved cochlear microphonic potentials at selected frequencies. However, the consensus of all loading studies to date is that additional mass is detrimental to middle ear function.[4-14]

Nishihara et al[9] were the first to use LDI to measure ossicular displacements at different sites on the tympanic membrane and ossicles in human temporal bones with and without the addition of masses. The addition of 3 to 5 mg of mass to the malleus head, incus long process, or stapes head produced a minimal loss in umbo displacement. Since 1993, laser interferometry has become a reliable means of evaluating middle ear mechanics with temporal bones and was proposed by Dormer et al[15] to be considered as an international standard for evaluating IMEHD performance.

This study specifically evaluated mass loading of an IMEHD, similar to the type currently in phase II clinical trials as the Soundtec Direct Drive Hearing System (DDHS; Soundtec, Inc, Oklahoma City, Okla). Two masses (magnet implants onto ossicles) were tested on 17 fresh or fresh-frozen temporal bones, and stapes displacements were compared with the (control) unloaded condition for frequencies of 250 to 8,000 Hz. The results show that the higher the implant mass, the greater the deficit in stapes footplate displacement.

MATERIALS AND METHODS

Implant Masses. Two experimental middle ear implants, model 1 (weight, 37.5 mg) and model 2 (weight, 22.5 mg), were used for the study (Fig 1).

From the Hough Ear Institute (all authors) and the Department of Physiology, University of Oklahoma Health Sciences Center (Dormer), Oklahoma City, and the School of Aerospace and Mechanical Engineering, University of Oklahoma, Norman (Gan), Oklahoma. Supported by the Oklahoma Center for the Advancement of Science and Technology and The Whitaker Foundation.

Presented at the Symposium on Middle Ear Mechanics in Research and Otosurgery, Boston, Massachusetts, October 21-24, 1999.

CORRESPONDENCE — Rong Z. Gan, PhD, Hough Ear Institute, 3400 NW 56th St, Oklahoma City, OK 73112.

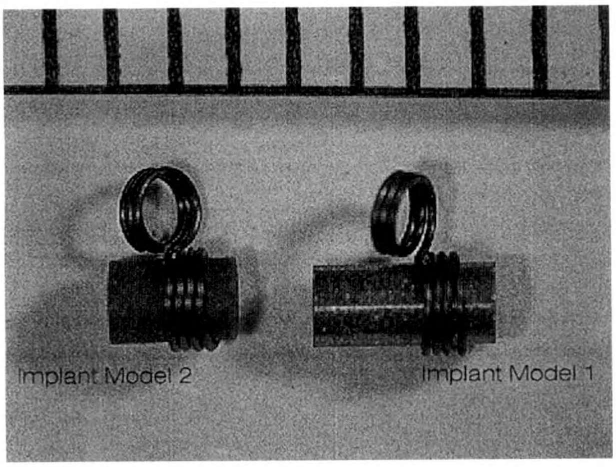

Fig 1. Picture of two implant models used in study. Implant model 1 was made of samarium-cobalt with wireform attachment at 45° angle with respect to longitudinal axis of magnet. Implant model 2 was made of neodymium-iron-boron with wireform attachment at 30° angle with respect to axis of magnet. Ruler is in millimeters.

These two implants were made of similar rare earth magnetic materials in a cylindrical configuration, including a titanium wireform for ossicular attachment. Both implants were 1.5 mm in diameter, but model 2 (2 mm) was 1 mm shorter than model 1. The wireform attachment ring for positioning the cylinders in the incudostapedial joint was 1.5 mm in diameter and contributed to the overall mass.

Human Temporal Bone Preparation. Eight whole fresh or fresh-frozen cadaveric temporal bones (group A, 6 fresh and 2 fresh-frozen) were obtained through the Donor Program, University of Oklahoma Health Sciences Center, and used in the study of model 1 implant mass. The donors' average age was 78.5 years (range, 57 to 85 years; 5 male and 3 female). Group B consisted of 9 temporal bones (average age, 64 years; range, 32 to 96 years; 8 male and 1 female; 6 fresh and 3 fresh-frozen) that were used for the model 2 implant study. To maintain soft tissue compliance and hydration upon receipt and after thawing, the bones were stored in 1:10,000 merthiolate in 0.9% saline solution at 5°C until use. The experiments were performed within 6 days.[10,16] Before acceptance into the study, each temporal bone was visually inspected under an operating microscope (Zeiss, OPMI-1) to confirm an intact tympanic membrane. If, during mastoidectomy for exposure of the middle ear, there was evidence of disease, the temporal bone was not used.

A canal wall–up mastoidectomy with an extended facial recess approach was performed to provide laser beam access to the middle ear ossicles. The bony external ear canal remained totally intact. In the facial recess and middle ear, the segment of the facial nerve and surrounding bone that forms the medial boundary of the facial recess was removed to improve optical access to the stapes footplate. A small piece of reflective tape, 0.5 mm^2, weighing 0.04 mg (3M Co, St Paul, Minn) was placed on the center of the stapes footplate as the reflective laser target. The bone was wrapped in wet (normal saline solution) gauze to prevent desiccation of the specimen during the experiment.

Temporal Bone Experimental Setup. Schematics of the temporal bone setup are shown for the control study (Fig 2) without an implant mass and for the experimental study (Fig 3) with an implant mass added to the incudostapedial joint. Each temporal bone was placed in a weighted temporal bone holder on a vibration isolation table, and each was studied consecutively for both the control and experimental interventions of mass loading.

The sound delivery system was identical for both control and experimental studies, as shown in Figs 2 and 3. Pure tone, narrowband, filtered sound signals from a calibrated clinical audiometer (Beltone, model 2000) were presented to the tympanic membrane by an insert earphone (model ER-2, Etymotic Research, Elk Grove Village, Ill). A stiff plastic tube (3 mm diameter and 15 mm length) was attached to the insert phone, which was sealed into the middle ear space with dental silicone polymer (Reprosil, DDI Inc, Milford, Del) around the bony rim of the ear canal. A probe microphone (model ER-7, Etymotic Research) was used for monitoring the input sound pressure level (SPL). The probe microphone tube was

Fig 2. Schematic of human temporal bone setup for control study.

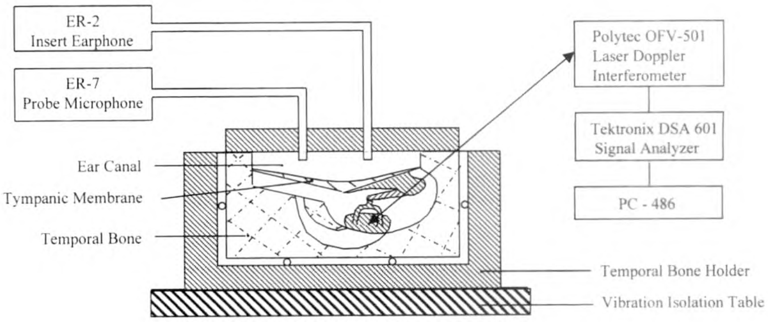

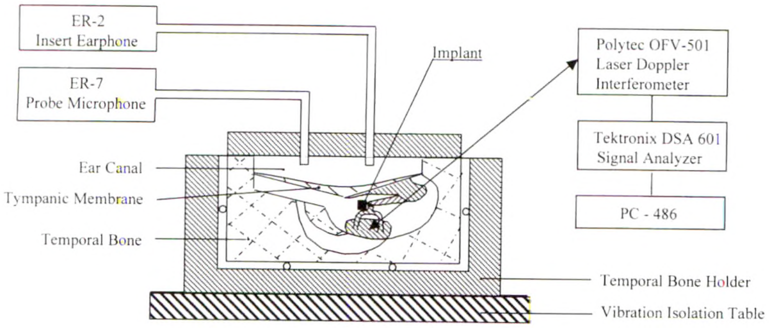

Fig 3. Schematic of human temporal bone setup for experimental study with implant.

secured parallel to the sound delivery tube, and the tip of the probe tube was positioned 2 mm from the tympanic membrane.

A single-point laser Doppler interferometer (Polytec PI, Costa Mesa, Calif, Vibrometer model OFV-501) with a controller (model OFV-3000) and a fiberoptic cable with a Nikon 50-mm focusing lens was used to measure the velocity and displacement of the stapes footplate caused by acoustic vibrations of the tympanic membrane. The vibrometer had a displacement resolution of 1×10^{-6} µm over the frequency range of 0 to 150 kHz in the velocity decoder of the hardware (minimum detectable velocity, 0.5 µm/s). Displacement measurements were derived independently of the velocity output by a separate fringe counter decoder, whose output was absolutely calibrated to the laser wavelength (minimum detectable displacement, 0.0008 µm).[17]

The light source (helium-neon single laser) was modulated at 40 MHz and focused onto the reflective tape on the center of the stapes footplate. We used a 3-dimensional micromanipulator (model UMM-3C, Narishige International, New York, NY) for positioning the laser fiberoptic cable and beam with respect to the reflective tape. The deviation of the laser beam with respect to the direction of vibration of the stapes varied from 30° to 50° off perpendicular to the footplate. The velocity or displacement measures with LDI were acquired in the frequency domain by back-weighted averaging of a live fast Fourier transform (FFT). The spectral magnitude and phase information were obtained by a fast-acquisition, multichannel, digitizing signal analyzer (model DSA 601 Tektronix, Beaverton, Ore) and then recorded on a personal computer for further analysis. The signal analyzer can also store waveforms and FFT settings for permanent storage and archiving. We accepted only data with a total harmonic distortion of less than 10% of pure tone signals according to the distortion index shown on the signal analyzer.

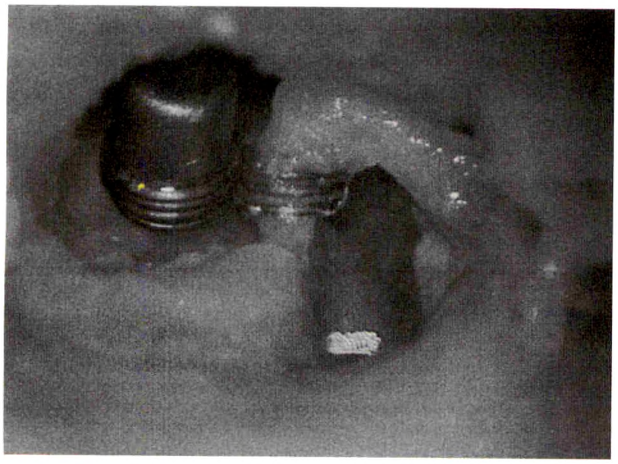

Fig 4. Picture of implant (model 2) placed on incudostapedial joint of left ear temporal bone. Joint was reattached and joint healing was simulated by means of cyanoacrylate glue.

The peak-to-peak displacement ($d_{p\text{-}p}$) of the footplate of the stapes was directly calculated from the voltage output of the LDI displacement decoder or converted from the output of the velocity decoder by the formula shown below[17]:

$$(1) \qquad d_{p\text{-}p} = k(A_{volt}/\pi f)$$

where A_{volt} is voltage amplitude in millivolts, f is frequency in kilohertz, and k is a constant related to the selected scale and a calibration factor in micrometers per millivolt per second. For instance, $k = 5 \times 10^{-3}$ µm/mV per second, if the scale factor 5 mm/s per volt is used.

Temporal Bone Experiment Protocols. The control study was performed first, to establish the normal middle ear transfer function. Displacements of the stapes footplate were measured in the frequency range of 250 to 8,000 Hz with input pure tone SPLs of 80, 90, and 100 dB, respectively. After obtaining control data, we cut the incudostapedial joint with a joint knife and placed the implant at the joint, which reclosed by natural tissue elasticity. Thus, each middle ear served as its own control. To simulate the in vivo soft tissue growth and healing that would normally occur at the incudostapedial joint, we secured the implant to the reattached joint with a drop of cyanoacrylate glue. Figure 4 shows the left ear temporal bone with the implant model 2 placed on the incudostapedial joint and the joint reattached with cy-

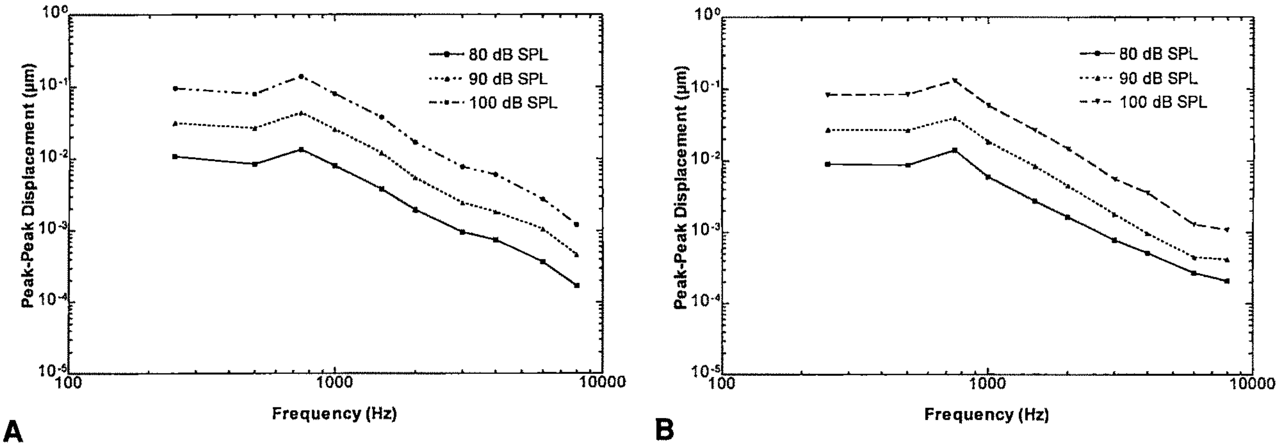

Fig 5. Mean peak-to-peak displacements measured at stapes footplate in group A (N = 8) with acoustic inputs of 80, 90, and 100 dB sound pressure level (SPL) at tympanic membrane. **A)** Displacements obtained from control study. **B)** Displacements obtained from experimental study with implant mass model 1 (weight, 37.5 mg).

anoacrylate glue. To exclude the effect of the surgical preparation on the temporal bones and the stiffness of the middle ear, we performed a separate surgical control study on 2 bones. By cutting and then gluing the incudostapedial joint, but without added mass, we repeated the control study protocol and did not find significant differences in stapes displacement as compared with the main control study.

In the experimental study, movement of the ossicles with the added implant mass was generated by the same sound pressures at the tympanic membrane as in the control study. Displacements of the stapes footplate were measured in the frequency range of 250 to 8,000 Hz with input SPLs of 80, 90, and 100 dB, respectively.

RESULTS

Figure 5A shows the mean peak-to-peak displacements of the stapes footplate measured from 8 bones (group A, control study) over a frequency range of 250 to 8,000 Hz, and Fig 6A shows the mean displacements of the stapes footplate measured from 9 bones (group B, control study). The frequency response curves of stapes footplate displacements in groups A and B are relatively flat at low frequencies (250 to 1,000 Hz) and decline at high frequencies. The response curves shown in Figs 5A and 6A agree with previously published data.[16,18] When the sound level was increased from 80 dB to 90 and 100 dB, the frequency response curves had upward parallel shifts. The increase of the footplate displacements for every 10-dB SPL change is equal to 10 dB over the whole frequency range. This finding demonstrates the linearity of middle ear function, in agreement with the umbo displacement curves obtained in a human subject by Goode et al.[19]

Figures 5B and 6B show the mean frequency response curves of stapes footplate displacements in the experimental studies, measured from the same 8 bones in group A and the same 9 bones in group B, respectively. Notice that the frequency response of the stapes with an added implant mass is similar to

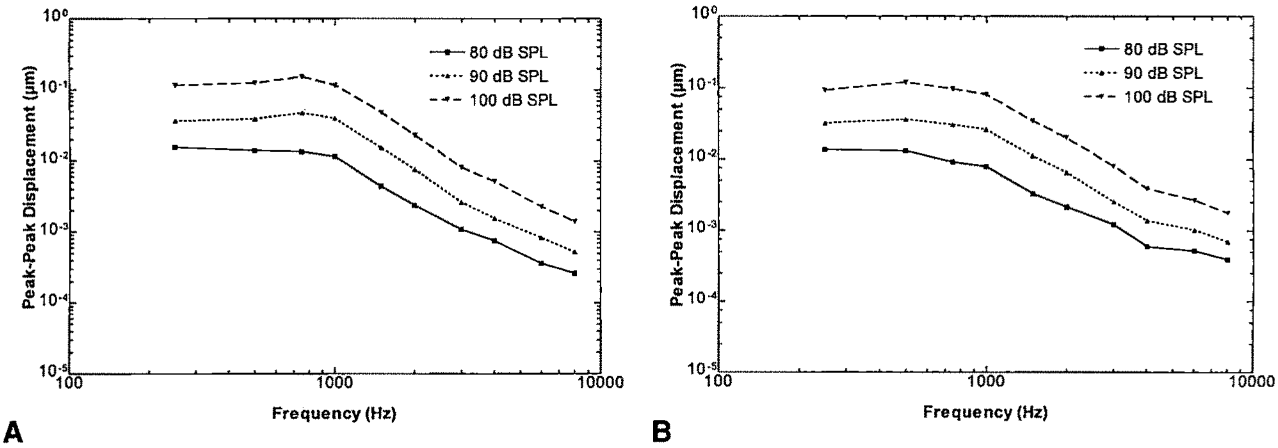

Fig 6. Mean peak-to-peak displacements measured at stapes footplate in group B (N = 9) with acoustic inputs of 80, 90, and 100 dB SPL at tympanic membrane. **A)** Displacements obtained from control study. **B)** Displacements obtained from experimental study with implant mass model 2 (weight, 22.5 mg).

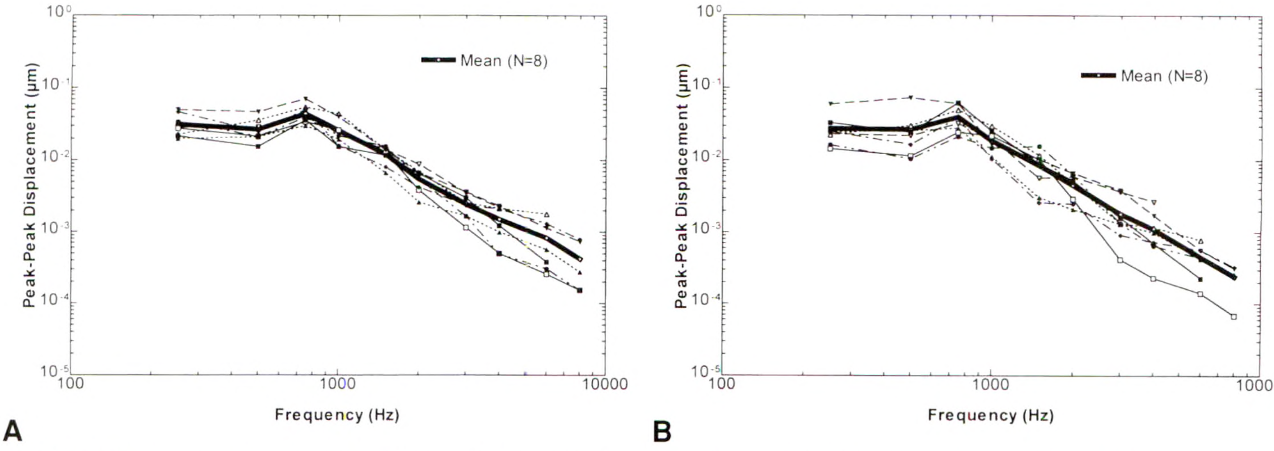

Fig 7. Frequency response curves of stapes footplate displacements measured in 8 bones (group A) with pure tone acoustic signals of 90 dB SPL at tympanic membrane. **A**) Control data. **B**) Experimental data from implant model 1.

that of the controls (Fig 5B compared with Fig 5A and Fig 6B compared with Fig 6A). The transfer function of the middle ear with an implant mass shows the same linearity as that in control temporal bones.

In the individual experiments, we selected the 90-dB SPL stimuli for a comparison study of the effect of different implant masses on the stapes displacement. Figure 7A shows the control data obtained from 8 bones of group A, and Fig 7B shows the experimental data obtained from the same 8 bones implanted with model 1. The mean frequency response curves of the stapes footplate from control and experimental studies are also included in Figs 7A and 7B, respectively. Similarly, the control data from 9 temporal bones of group B are given in Fig 8A, and the experimental data are given in Fig 8B. Some data points are missing in Figs 7 and 8 because of high distortion (noise floor) of the interferometer outputs measured at those frequencies. We did not accept any data with a total harmonic distortion of more than 10% of pure tone signals. Figure 9 compares all mean frequency response curves of stapes displacements at 90 dB SPL at the tympanic membrane. The control versus experimental data from implant model 1 are shown in Fig 9A with standard error bars. The control versus experimental data from implant model 2 are shown in Fig 9B. A gap between the solid line (control) and the broken line (experimental) depicts the effect of implant mass on stapes footplate displacement. As can be seen in Fig 9, the greater mass (model 1) resulted in a decrease of stapes displacement over the whole frequency range of 250 to 8,000 Hz (Fig 9A), and the attenuation induced by the model 2 implant in stapes displacement mainly occurred at frequencies of 750 to 2,000 Hz (Fig 9B).

To calculate the changes in decibels of the stapes displacement due to mass loading, we used

(2-1) $\delta dB = 20 \log(d_{exp}/d_{ref}) - 20 \log(d_{control}/d_{ref})$

or

(2-2) $\delta dB = 20 \log(d_{exp}/d_{control})$

Here, δdB is the change in decibels of the stapes displacement that occurred after the implant was placed

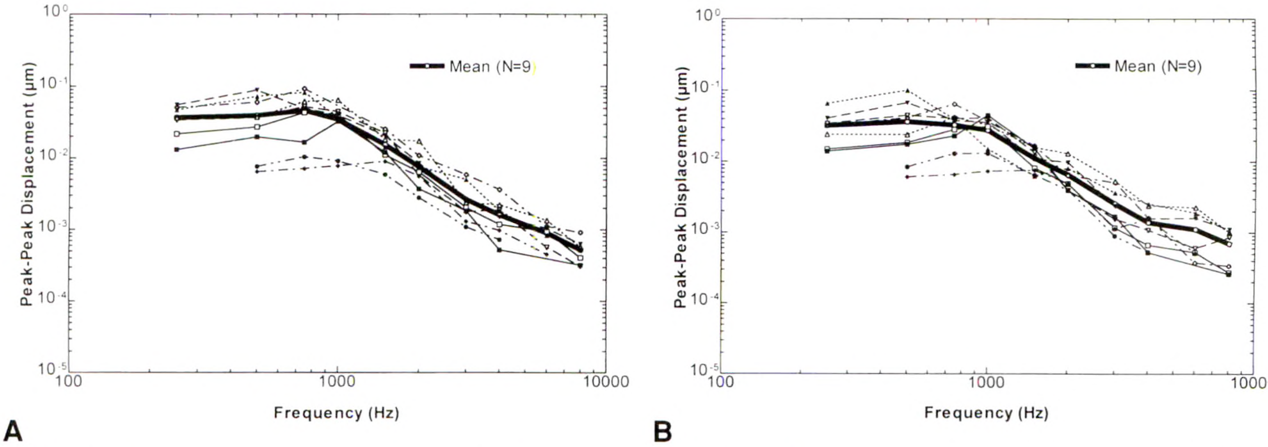

Fig 8. Frequency response curves of stapes footplate displacements measured in 9 bones (group B) with pure tone acoustic signals of 90 dB SPL at tympanic membrane. **A**) Control data. **B**) Experimental data from implant model 2.

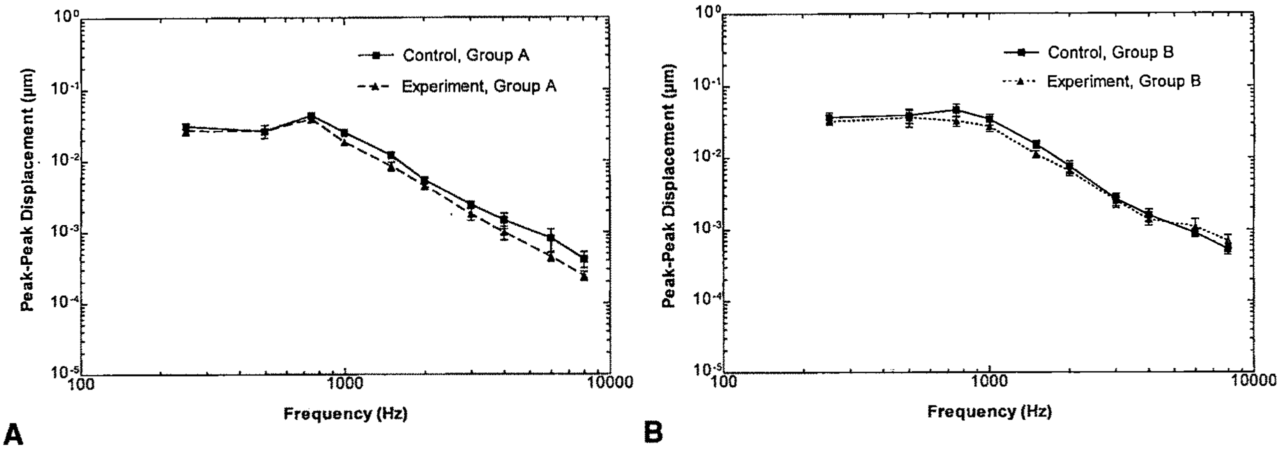

Fig 9. Comparison of mean (±SE) peak-to-peak displacements measured at stapes footplate in control and experimental studies in groups A and B with two implant masses. **A)** Group A (N = 8), implant mass model 1. **B)** Group B (N = 9), implant mass model 2.

on the ossicles; d_{exp} and $d_{control}$ are stapes displacements measured in the experimental and control studies, respectively; and d_{ref} is the reference displacement.

Using equation 2, we calculated decibel changes in footplate displacement due to implant mass loading on the incudostapedial joint. Figure 10 compares the mean decibel changes in stapes displacement that occurred with implant models 1 and 2 when the SPL at the tympanic membrane was 90 dB Standard error bars are not shown, so as not to obscure the mean data. The maximal drop in stapes displacement (5 dB) was observed at 1,500 Hz, or 6,000 Hz for bones with an implant mass of 37.5 mg (model 1). The implant mass of 22.5 mg in the group B bones resulted in a maximum drop of 3 dB at 1,500 Hz (model 2). There is no obvious difference between the two tested implants at low frequencies (250 to 750 Hz). However, the lower-mass implant (model 2) showed less attenuation of stapes displacement at high frequencies (above 1,000 Hz) than did model 1. The average effect of the lighter implant, model 2, on stapes displacement was decreased by 2.6 dB across the frequency range of 1,000 to 8,000 Hz.

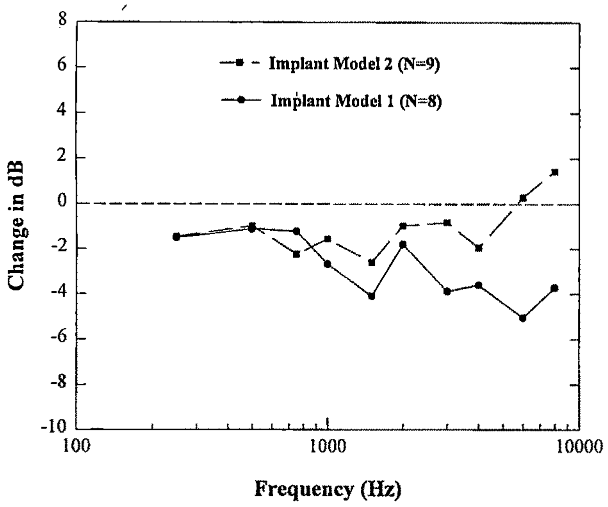

Fig 10. Comparison of changes, with respect to control, in stapes footplate displacement in human temporal bones after implantation with two types of implants, models 1 and 2.

DISCUSSION

The effects of changes in ossicular mass on middle ear transfer function have been studied in cats, humans, and human temporal bones by a variety of methods, including the most recent technology, LDI.[7,9,20-23] The effect of mass loading of middle ear prostheses, including total ossicular replacement prostheses (TORPs) and partial ossicular replacement prostheses (PORPs), on sound transmission has also been reported. Nishihara and Goode[10] used human temporal bones and LDI to study incus replacement prostheses and found that displacement of the stapes footplate was decreased above the resonance frequency (1,000 Hz) by additional mass fixed to the middle ear prostheses. Rosowski and Merchant,[24] using simulations based on electrical circuit models, showed that the addition of masses to middle ear prostheses caused a high-frequency loss in the middle ear. Recently, Meister et al[25] examined several TORPs and PORPs using a standardized measurement system and reported that the implant prostheses with the highest mass showed the lowest sensitivity in the high-frequency area. In this study, we did not replace the ossicles by middle ear prostheses. The middle ear remained intact, and the implant mass, a component of the middle ear implantable device, was added to the ossicular chain. We measured stapes displacement before and after ossicular implantation in mechanically normal temporal bones. Thus, our data provide important information for predicting the effect of implant mass loading on residual hearing in human subjects after implantation.

Our results show the linearity of the normal middle ear transfer function as frequency response curves of the stapes footplate displacement in response to the sound input levels at the tympanic membrane. That linearity did not change in ears with added implant masses. As shown in Figs 5 and 6, when the input SPL varied from 80 dB to 90 and 100 dB, the corresponding increase of the footplate displacement for each 10–dB SPL change was equal to 10 dB over the frequencies of 250 to 8,000 Hz. The curves displayed in Figs 5 and 6 may not show perfect linearity at higher frequencies (>2,000 Hz) because of the limited number of data points, especially at the 80-dB sound input level. For the same reason, not all data points are shown across the whole frequency range in Figs 7 and 8. However, the linearity of the middle ear transfer function in terms of frequency response curves of stapes displacement is clearly shown for most auditory frequencies, especially at the input levels of 90 and 100 dB SPL.

In general, adding mass to the ossicular chain interferes with sound transmission because of the mechanical loading effect, which results in reduced stapedial movement. The degree of attenuation in stapes displacement depends on the additional mass load on the ossicles and the stiffness of the middle ear structure. In our study, each bone served as its own control, and thus, the effect of individual ear stiffness was eliminated from the results.

Our results show that mass loading on the ossicles has a detrimental effect on movement of the stapes footplate. An average decrease of 1.6 dB at low frequencies (250 to 750 Hz) was observed in 8 bones with an implant mass of 37.5 mg, and a 1.3-dB decrease in 9 bones with an implant mass of 22.5 mg. The maximum decrease occurred at frequencies above 1,000 Hz. Our results agree with data obtained by Nishihara and Goode[10] and others regarding the effect of additional mass on the ossicles on middle ear dynamics. A comparison of the data obtained from the 2 types of implant masses in Fig 10 further indicates that the greater the implant mass, the greater the decrease of stapes displacement, particularly at high frequencies. Therefore, the passive mass loading on the ossicles is a critical factor influencing sound transmission through the middle ear and must be considered in the design of middle ear implantable devices.

CONCLUSIONS

These data suggest that residual hearing will be affected if a person undergoes implantation of additional mass on the middle ear ossicles. One of the likely reasons for residual hearing loss would be implant mass loading on the middle ear mechanics. Our studies provide important data for evaluating the potential effect of an implant at the incudostapedial joint on the footplate movement and the frequency response. The higher the implant mass, the higher the effect on residual hearing as observed through our temporal bone studies. These results may lead to further investigations of the quantitative relationships between ossicular mechanics and implant mass. It is also expected that the mass loading effect on residual hearing predicted in this study will be confirmed in clinical trials of IMEHDs in which mass loading of the ossicles occurs.

ACKNOWLEDGMENTS — The technical assistance of Don Nakmali, BSEE, and the surgical directions of J. V. D. Hough, MD, and Martin Schneider, MD, are gratefully recognized.

REFERENCES

1. Ball GR, Huber A, Goode RL. Scanning laser Doppler vibrometry of the middle ear ossicles. Ear Nose Throat J 1997; 76:213-8, 220, 222.

2. Dormer KJ, Gan RZ. Biomaterials for implantable middle ear hearing devices. Otolaryngol Clin North Am (in press).

3. Lawrence M. Acoustic effects of middle ear substitution. Trans Am Acad Ophthalmol Otolaryngol 1960;64:235-47.

4. Goode RL. An implantable hearing aid. State of the art. Trans Am Acad Ophthalmol Otolaryngol 1970;74:128-39.

5. Goode RL, Glattke TJ. Audition via electromagnetic induction. Arch Otolaryngol 1973;98:23-6.

6. Goode RL. Implantable hearing aids. Otolaryngol Clin North Am 1978;11:155-61.

7. Tonndorf J, Pastaci H. Middle ear sound transmission: a field of early interest to Merle Lawrence. Am J Otolaryngol 1986;7:120-9.

8. Goode R, Aritomo H, Gonzales J. The implantable hearing aid. In: Van Stenberghe D, ed. Tissue integration in oral and maxillo-facial reconstruction. Amsterdam, the Netherlands: Excerpta Medica, 1986:199-208.

9. Nishihara S, Aritomo H, Goode RL. Effect of changes in mass on middle ear function. Otolaryngol Head Neck Surg 1993; 109:899-910.

10. Nishihara S, Goode RL. Experimental study of the acoustic properties of incus replacement prostheses in a human temporal bone model. Am J Otol 1994;15:485-94.

11. Goode RL, Rosenbaum ML, Maniglia AJ. The history and development of the implantable hearing aid. Otolaryngol Clin North Am 1995;28:1-16.

12. Kartush JM, Tos M. Electromagnetic ossicular augmentation device. Otolaryngol Clin North Am 1995;28:155-72.

13. Maniglia AJ, Ko WH, Rosenbaum M, et al. Contactless semi-implantable electromagnetic middle ear device for the treatment of sensorineural hearing loss. Short-term and long-term experiments. Otolaryngol Clin North Am 1995;28:121-40.

14. Goode R. The ideal middle ear prosthesis. In: Hüttenbrink K-B, ed. Middle ear mechanics in research and otosurgery: pro-

ceedings of the International Workshop on Middle Ear Mechanics in Research and Otosurgery, Dresden, Germany, September 19-22, 1996:169-73.

15. Dormer KJ, Ball GR, Dietz T, Gan RZ. Laser Doppler interferometry. A standard for evaluating implantable hearing device. 2nd International Symposium on Electronic Implants in Otology and Conventional Hearing Aids, Sweden, 1996:4.

16. Kurokawa H, Goode RL. Sound pressure gain produced by the human middle ear. Otolaryngol Head Neck Surg 1995; 113:349-55.

17. Gan RZ, Wood MW, Ball GR, Dietz TG, Dormer KJ. Implantable hearing device performance measured by laser Doppler interferometry. Ear Nose Throat J 1997;76:297-9, 302, 305-9.

18. Goode RL, Killion M, Nakamura K, Nishihara S. New knowledge about the function of the human middle ear: development of an improved analog model. Am J Otol 1994;15:145-54.

19. Goode RL, Ball G, Nishihara S. Measurement of umbo vibration in human subjects — method and possible clinical applications. Am J Otol 1993;14:247-51.

20. Lawrence M. Acoustic effects of middle ear substitution. Trans Am Acad Ophthalmol Otolaryngol 1960;64:235-47.

21. Allen GW, Fernandez C. The mechanism of bone conduction. Ann Otol Rhinol Laryngol 1960;69:5-28.

22. Cottle RD, Tonndorf J. Mechanical aspects of stapedial substitution. An experimental study. Arch Otolaryngol 1966;83: 547-53.

23. Brenkman CJ, Grote JJ, Rutten WL. Acoustic transfer characteristics in human middle ears studied by a SQUID magnetometer method. J Acoust Soc Am 1987;82:1646-54.

24. Rosowski JJ, Merchant SN. Mechanical and acoustic analysis of middle ear reconstruction. Am J Otol 1995;16:486-97.

25. Meister H, Walger M, Mickenhagen A, von Wedel H, Stennert E. Standardized measurements of the sound transmission of middle ear implants using a mechanical middle ear model. Eur Arch Otorhinolaryngol 1999;256:122-7.

Ann Otol Rhinol Laryngol 110:2001

VOLUME OF MASTOID PNEUMATIZATION: THREE-DIMENSIONAL RECONSTRUCTION WITH ULTRAHIGH-RESOLUTION COMPUTED TOMOGRAPHY

MICHAL LUNTZ, MD

SHELTON MALATSKEY, MD
ELISHA BAR-MEIR, MD

MARK TAN, MD
DAVID RUIMI, PHD

HAIFA, ISRAEL

The volume of the mastoid air cell system was measured in 69 patients with normal middle ears. All patients underwent axial ultrahigh-resolution computed tomography. Mastoid pneumatization was marked on each axial slice, and 3-dimensional reconstruction was performed. The volumes were measured with a volumetric algorithm. A polyethylene tubing phantom with a density similar to that of bone on computed tomography was devised. The polyethylene tubing was tied in a particular fashion so as to create interconnecting air spaces with a known volume. The phantom was scanned with the imaging parameters used for scanning the temporal bone. The air in the tubing was marked, and 3-dimensional reconstruction for the marked phantom air was performed. The volume of the interconnecting air spaces was measured and found to be identical to its known volume, thereby verifying the accuracy of the method used. The mean mastoid volume was 6.61 cm^3. The smallest volume measured was 1.3 cm^3, and the largest was 12.7 cm^3. The importance of this technique lies in its high accuracy, ease of use, and ability to directly correlate mastoid size and clinical findings.

KEY WORDS — eustachian tube, mastoid pneumatization, measurement of mastoid pneumatization, middle ear aeration.

INTRODUCTION

The total amount of gas found in the middle ear (ME) is determined by the gas exchange between the ME and the nasopharynx, through the eustachian tube (ET), and the exchange between the ME and the blood-tissue compartment surrounding it, across the ME mucosa. Compromised ME aeration is a situation in which the amount of gas leaving the ME cavity exceeds the amount of gas entering the ME cavity, thereby creating a gas deficit in the ME.

More important than the gas deficit is the negative pressure that accompanies it, for it is the negative pressure that is responsible for the adverse biological effects of imbalanced ME aeration. The best clinical example of ME underaeration is the atelectatic ear. Because of a failure of the ME aeration mechanism, a gas deficit develops in the ME, and a negative pressure is built there. When this negative pressure is high enough to overcome the internal rigidity of the tympanic membrane (TM), the TM leans inward.[1]

It is possible to have a ME gas deficit without a significant negative pressure and without a significant TM atelectasis. This can be achieved if the deficit occurs in a ME with a very large cavity, ie, if the deficit occurs in a ME that is connected to a large mastoid air cell system. The following example clarifies this principle: when a certain amount of gas — 1 mL, for example — is withdrawn from the ME cleft, some negative pressure is expected to develop there. But whereas a 1-mL gas loss from a 2-cm^3 ME cleft (50% of what exists there) will result in a high negative pressure, the same 1 mL of gas lost from a 20-cm^3 ME cleft (only 5% of what exists there) will cause a much smaller decrease in pressure. Therefore, in the case of the small mastoid process (the 2-cm^3 ME cleft), a severe TM atelectasis is expected to develop, while in the case of the large mastoid process (the 20-cm^3 ME cleft), probably no atelectasis will be seen. Thus, the degree of ME negative pressure depends on gas gain and loss through the ET and through the mucosa, and on the size of mastoid pneumatization.[2,3]

In this study we focused on the total volume of mastoid pneumatization and endeavored to come up with as accurate a value as possible after measuring a large number of temporal bones, so that we would be confident that a correct normal distribution would be achieved.

MATERIALS AND METHODS

The present study consists of patients referred for

From the Departments of Otolaryngology–Head and Neck Surgery (Luntz, Malatskey) and Imaging and Radiology (Tan, Bar-Meir), Bnai Zion Medical Center, Faculty of Medicine, Technion-Israel Institute of Technology, Haifa, Israel. This research was supported by the VPR Fund–Hedson Fund for Medical Research.

CORRESPONDENCE — Michal Luntz, MD, Dept of Otolaryngology–Head and Neck Surgery, Bnai Zion Medical Center, POB 4940, 31048 Haifa, Israel.

TABLE 1. IMAGING PARAMETERS OF ULTRAHIGH-RESOLUTION COMPUTED TOMOGRAPHY OF TEMPORAL BONE

Patient position	Head in, face up
Scan diameter	250 mm
Slice thickness	1.1 mm
Slice increment	0.5 mm
Table speed	1.5 mm/s
Voltage	120 kV
Sequence length	70 mm
Sequence time	33 s
Milliampere seconds	117
Scan angle	360°
Resolution	Ultrahigh
Slices per scan	Dual
Angle of sampling	High
Filter	45% ied
Image matrix	512 × 512
Rotation angle	0°
Center x,y	0,0
Recording zoom	×1.5
Image zoom	×1.5
Tilt	0°
Swivel	0°
Scan protocol	Helix

a computed tomography (CT) scan of the temporal bone for various reasons other than disease of the ME cavity. Inclusion of a scan was based on the referral note of the referring physician stating that the ME was normal. The patients were not exposed to any excess radiation other than that necessary for investigating their underlying disease, which in most cases was suspicion of a space-occupying lesion in the internal auditory canal.

Altogether, 69 adults (138 ears) were scanned. All patients underwent a CT scan of the temporal bone. The axial scans were of 1.1-mm thickness, with increments of 0.5 mm. The scans were done with a Turbo Twin Flash Helical CT scanner supplied by Elscint, Haifa, Israel. The images were transmitted to an Indy Silicon Graphics (Mountain View, Calif) workstation and processed 3-dimensionally and semiautomatically with Omnipro 2.3 software provided by Algotech, Ra'anana, Israel. Table 1 shows the imaging parameters used. The parameters were examined together with a software applications engineer from Elscint (author D.R.) in order to ascertain the mathematical accuracy of the system and to evaluate the potential for improving on the system accuracy by upgrading the parameters.

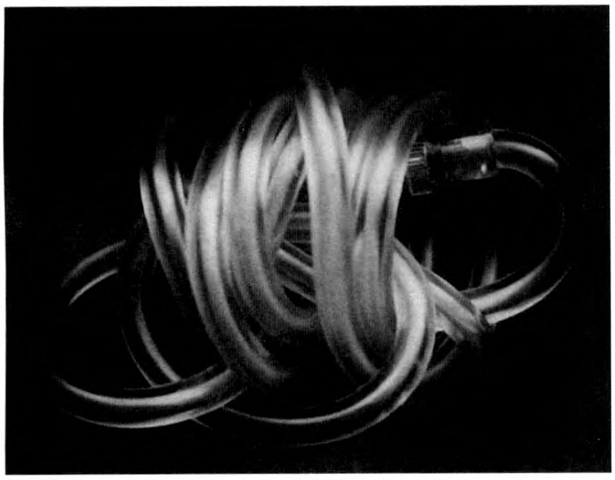

Fig 1. Phantom air cell system used to mimic structure of mastoid air cell system. Phantom consisted of polyethylene tubing, whose density on computed tomography (CT) is similar to that of bone (500 Hounsfield units), tied in particular fashion so as to create interconnecting air spaces with known volume of air.

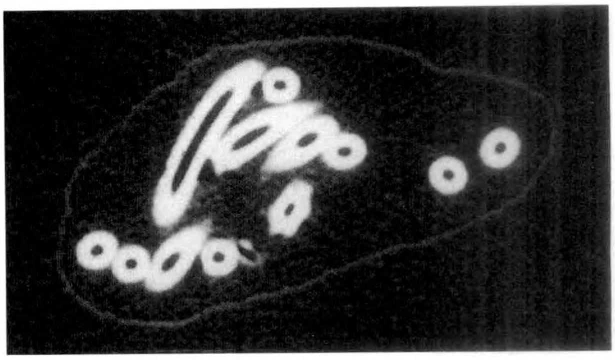

Fig 2. Axial CT scan of phantom air cell system, with boundaries of air-containing spaces marked. CT scan was done with same imaging parameters used for temporal bone (mastoid) scanning.

In order to check the calculated accuracy of the system, we created a phantom model. The phantom consisted of a polyethylene tube of which the density was found to be similar to that of bone on CT: 500 Hounsfield units. The tubing contained air, as does the mastoid air cell system. The phantom model was tied in a particular fashion so as to create interconnecting air spaces (Fig 1). In this way, the phantom model indeed mimicked the mastoid air cell system. The volume of air contained in the interconnecting air spaces in the phantom model was known to be 3.6 cm^3. We could now use the phantom model to check the accuracy of the system that was aimed at measuring the mastoid pneumatization, since we had a structure similar to the mastoid air cell system in densities and in structure. The phantom was immersed entirely in a water bath to make sure that the only air to be found in the system was that contained in its interconnecting spaces. The phantom system was then scanned by the imaging parameters presented in Table 1 (the same imaging parameters that were intended to be used for mastoid pneumatization measurement). The air in the phantom system was then identified and marked on each slice of the phantom scan (Fig 2). A 3-dimensional (3-D) recon-

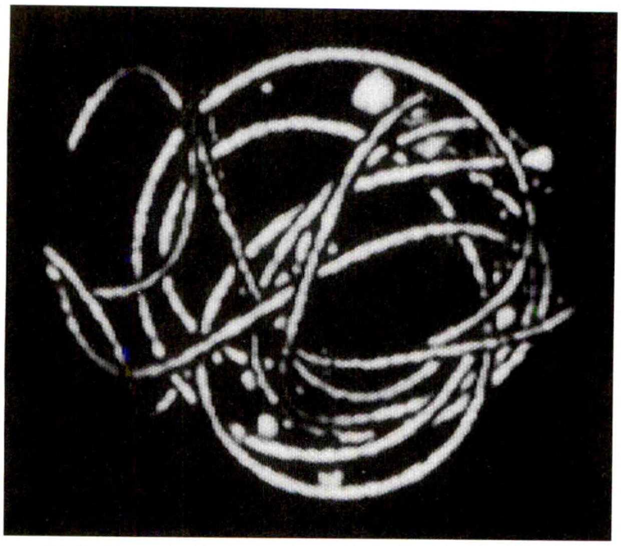

Fig 3. Three-dimensional reconstruction of air-containing spaces of phantom air cell system, made in order to check accuracy of measuring system.

struction (Fig 3) of the marked air was performed, and the resulting volume, which was the air contained in the phantom system, was measured to be 3.6 ± 0.7 cm^3, identical to its known true volume.

The accuracy obtainable when making 3-D measurements of a scanned object depends on a number of variables: the maximal system resolution of the scanner, the maximal resolution of the display (matrix resolution), and the software used (accuracy of the software as pertains to its algorithm for 3-D volumetric measurements) — in this case, Omnipro 2.3. The maximal system resolution of the scanner is obtainable by using a D-type filter (the smallest type available) and scanning in ultrahigh-resolution mode, as was done with all of our patients. With these parameters, the cutoff point for the scanner is 20 line pairs per centimeter; in other words, the scanner can be calculated to differentiate between lines 0.25 mm thick. The matrix resolution with the imaging parameters used is less than that — 0.32 mm — and is the maximal degree of accuracy for our system. The mean standard deviation of the 3-D algorithm for volume measurement of all the temporal bones measured was 13.2% (0.85 cm^3).

On the scanner screen, each axial slice of every temporal bone was examined, and gas in the ME and mastoid process was identified and marked. Air in the external ear canal was excluded. All air cells were meticulously checked to be certain that they were included, from the most inferior to the most superior, including petrous apex cells wherever they were found to exist (Fig 4). A 3-D reconstruction was performed (Fig 5) from the 3-D algorithm, and the resulting volume was measured and recorded. Each volume was measured 3 times to ensure that identification of the mastoid air cells' boundaries had been consistent.

Statistical analysis comparing the sexes and comparing left and right mastoid cavities was done with Student's *t*-test for independent variables. Analysis

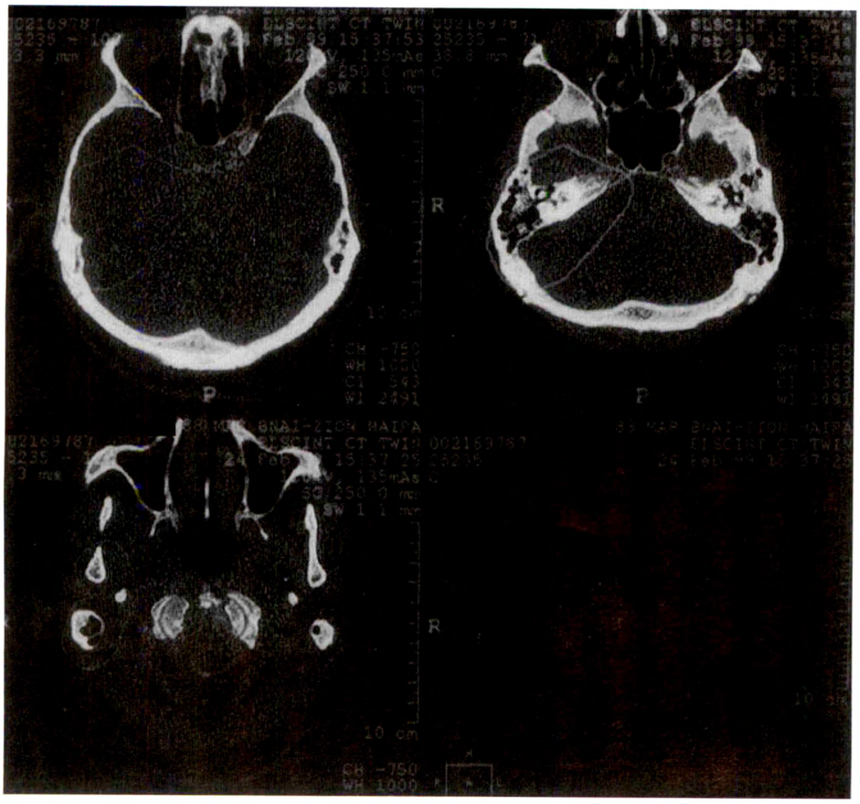

Fig 4. Axial CT scan of temporal bone: superiormost slice of mastoid air cell system (upper left quadrant), inferiormost slice (lower left quadrant), and axial slice with air in mastoid marked (upper right quadrant).

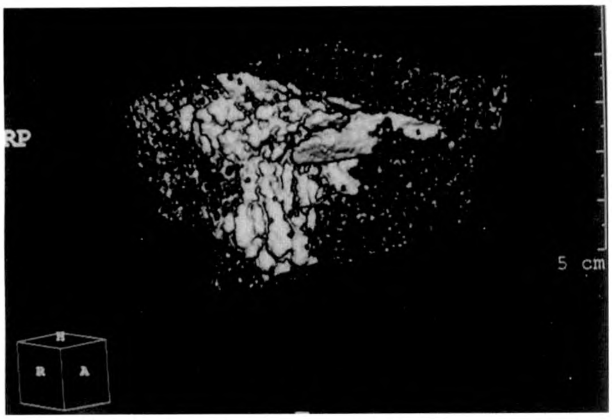

Fig 5. Three-dimensional reconstruction of gas contained in mastoid air cell system, as reconstructed with Omnipro 2.3 three-dimensional algorithm.

of the variance was performed with the Levern test. Two-tailed p values of .05 were considered to be statistically significant.

RESULTS

Altogether, 69 patients were included in the study (30 men and 39 women). The average ages were similar for the sexes: 54.6 years for the men and 51.5 years for the women. The age range was from 26 years to 88 years for the men, and 18 years to 88 years for the women. The average (±SD) mastoid volume was 6.61 ± 2.7 cm^3 overall (Table 2). The mastoid volumes ranged from 1.3 to 12.7 cm^3.

A cumulative bar chart depicting all of the mastoid processes measured resembles a gaussian-type curve that can be assumed to be representative of the normal adult population (Fig 6).

The average mastoid volume for men was 7.22 ± 2.92 cm^3 (7.22 ± 2.95 cm^3 for the left-sided mastoid processes and 7.22 ± 2.89 cm^3 for the right-sided mastoid processes). For women, the average mastoid volume was 6.13 ± 2.48 cm^3 (6.10 ± 2.53 cm^3 for the left side and 6.17 ± 2.43 cm^3 for the right side). No statistically significant difference was found between men and women (Table 2) or between left and right sides.

TABLE 2. MEAN VALUES OF MASTOID VOLUME ACCORDING TO SEX AND SIDE

	Mean Mastoid Volume (cm^3)		
	Left	*Right*	*Total*
Men	7.22 ± 2.95	7.22 ± 2.89	7.22 ± 2.92
Women	6.10 ± 2.53	6.17 ± 2.43	6.13 ± 2.48
Total	6.59 ± 2.76	6.63 ± 2.67	6.61 ± 2.70

DISCUSSION

Several measurements of mastoid pneumatization have been performed over the past 40 years, with use of planimetry,[4,5] impedance audiometry,[6] the principles of the gas laws,[7] and also CT,[8] but without 3-D reconstruction. The last authors[8] made use of axial CT. They calculated the area, which was then multiplied by the thickness of the axial slice for the third dimension. The study was performed in 1987, and computerized 3-D reconstruction was not used. Therefore, their method was impractical for measuring large numbers of temporal bones. Also, the system itself was not checked for accuracy, and ultrahigh-resolution CT was not used — a pitfall that might reduce that method's value for measurement of very small mastoid processes, which is our eventual target.

The claim that gas loss from a small mastoid process is expected to create a severe TM atelectasis, and that the same gas deficit in a ME with a large mastoid process will probably not create any atelectasis (since the negative pressure will not be large enough to overcome the internal rigidity of the TM), was proven experimentally by Yokobori et al.[9] Using a model of a ME with different mastoid sizes, they showed that the same gas deficit created a much more significant retraction of an artificial TM when no mastoid process existed, as compared to a mastoid process of 60 cm^3. The artificial TM of their

Fig 6. Bar chart of mastoid volume in cubic centimeters according to incidence of volume, divided into groups by 1-cm^3 increments.

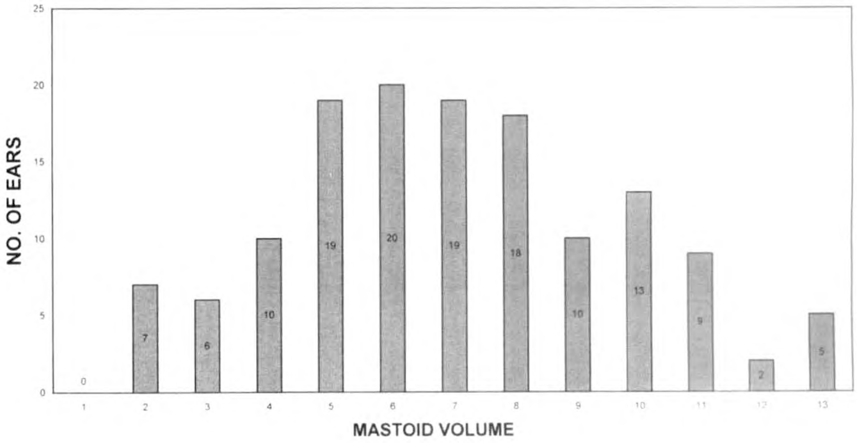

ME model was made of purified fibrous atelocollagen from bovine derma. They judged the severity of the retraction by the degree of tension that resulted in each of these artificial TMs. The degree of tension was evaluated under a magnification of view of 100× with light-green staining. When the retraction of the artificial TM was severe, as happened in the model with no mastoid process, the degree of tension on the artificial TM was high, and so the structure of the collagen membrane became rough because of the destruction and disorientation of the collagen fibers. In the ME model with a large mastoid process, the degree of tension on the artificial TM was low, and so very little deformation was present in the collagen membrane of the artificial TM.[9] This principle was demonstrated clinically by Sadé et al,[2] who showed that the severity of pars flaccida atelectasis was inversely correlated with the size of mastoid pneumatization. The same principle is expected to work also when gas is added to the ME. Elam et al[3] found that the rate at which positive pressure builds in the ME during nitrous oxide anesthesia is much higher in patients with small mastoid processes than in patients with large mastoid processes.

The individual variation of mastoid size is very significant, and the extent of mastoid pneumatization is a continuum. Also, the size of the various mastoid cells in each individual subject might be of importance when one tries to quantify the role played by the mastoid process as a ME pressure buffer.[10] The volume of each cell in the mastoid processes measured was not addressed in the present study.

We are all aware that a small mastoid process is linked with chronic ME disease, but we also know that normal aeration can exist in ears with small mastoid processes. This can probably happen if all other factors involved in the aeration mechanism of the ME are functioning optimally. But what is the minimal volume of the mastoid process that can overcome failures of other aeration mechanisms? Is there an optimal volume? What is the exact volume at which one would be very likely to encounter a chronic ME aeration problem with even a minute failure of other aeration mechanisms? Or, more clinically, what is the volume of mastoid process with which the chance of performing a successful tympanoplasty in a young child is significantly low (a question that has not been satisfactorily answered in studies that have regarded only ET function as a variable)?[11,12]

The importance of the method devised in the present study is its high accuracy, its relative ease of use, and the fact that by using modifications of the method, we can directly correlate the clinical picture to the volume of mastoid pneumatization. We hope that our data will be of use in concert with physiological data gathered in various clinics and laboratories in drawing a full picture of the aeration mechanism of the ME and in establishing a general theory for it. The general theory should explain as many as possible of the clinical phenomena related to ME aeration, especially those that are seemingly contradictory at this time.

ACKNOWLEDGMENT — We thank Shai Zur and his team of technicians for their invaluable assistance in checking the system accuracy and recording the computed tomography films.

REFERENCES

1. Luntz M, Fuchs C, Sadé J. Correlation between retractions of the pars flaccida and the pars tensa. J Laryngol Otol 1997;111:322-4.

2. Sadé J, Fuchs C, Luntz M. Shrapnell membrane and mastoid pneumatization. Arch Otolaryngol Head Neck Surg 1997; 123:584-8.

3. Elam M, Harell M, Luntz M, Fuchs C, Sadé J. Middle ear pressure variations during 50% N_2O anesthesia as a function of mastoid pneumatization. Am J Otol 1998;19:709-11.

4. Diamant M. Otitis and pneumatization of the mastoid bone. A clinical-statistical analysis. Acta Otolaryngol Suppl (Stockh) 1940(suppl 40).

5. Lindeman P, Haglund M. Size of the mastoid air cell system obtained with two types of X-ray equipment. Acta Otolaryngol (Stockh) 1983;95:101-4.

6. Lindeman P, Holmquist J. Measurement of middle ear volume using the impedance audiometer. Am J Otol 1981;2: 301-3.

7. Andreasson L, Ingelstedt S, Ivarsson A, Jonson B, Tjernstrom O. Pressure-dependent variation in volume of mucosal lining of the middle ear. Acta Otolaryngol (Stockh) 1976;81:442-9.

8. Todd NW, Pitts RB, Braun IF, Heindel H. Mastoid size determined with lateral radiographs and computerized tomography. Acta Otolaryngol (Stockh) 1987;103:226-31.

9. Yokobori AT Jr, Yoshinari H, Kowata I. Mechanical test methods of biomedical membranes such as used for otolaryngology. Biomed Mater Eng 1991;1:137-42.

10. Sadé J. The correlation of middle ear aeration with mastoid pneumatization. The mastoid as a pressure buffer. Eur Arch Otorhinolaryngol 1992;249:301-4.

11. Holmquist J. Eustachian tube function and tympanoplasty. Acta Otorhinolaryngol Belg 1991;45:67-9.

12. Sato H, Nakamura H, Honjo I, Hayashi M. Eustachian tube function in tympanoplasty. Acta Otolaryngol Suppl (Stockh) 1990(suppl 471):9-12.

IMAGING CASE STUDY OF THE MONTH

PETROUS INTERNAL CAROTID ARTERY PSEUDOANEURYSM DUE TO GUNSHOT INJURY

JUHA-PEKKA VASAMA, MD

HANS RAMSAY, MD ANTTI MARKKOLA, MD

HELSINKI, FINLAND

INTRODUCTION

Posttraumatic pseudoaneurysms of the internal carotid artery (ICA) are uncommon. However, a severe head injury associated with a skull base fracture may give rise to such lesions, which often present as delayed massive bleeding with potentially fatal consequences.[1,2] Pseudoaneurysms are pulsating hematomas and occur after injury to all layers of the arterial wall. The center of the hematoma liquefies and contains flowing blood that communicates with the arterial lumen, while the periphery of the hematoma clots, forming the wall of the aneurysm.[3] The majority of traumatic ICA pseudoaneurysms are based in the cavernous segment, and those in petrous bone are extremely rare.[2]

We report a case of posttraumatic tympanic petrous ICA pseudoaneurysm due to gunshot injury and present computed tomography (CT), magnetic resonance angiography (MRA), and carotid angiography findings. To our knowledge, such a lesion has not been previously reported.

CASE REPORT

A 5-year-old patient was referred to the Department of Otolaryngology, Helsinki University Hospital, from an outside hospital for evaluation of a sudden episode of vigorous epistaxis. The bleeding had been severe enough to result in loss of consciousness. The epistaxis had stopped spontaneously, and the patient's condition was stabilized by blood transfusion.

The young patient's history was tragic. Before his current presentation, he had been the victim of a shooting incident 1.5 years earlier. The handgun bullet had entered his skull via the right ear canal, had traveled obliquely through the retropharyngeal space, and finally had come out just below the left mandible. Amazingly, the patient had made a full recovery, except for the right ear, which developed a chronic middle ear infection with conductive hearing loss.

A contrast-enhanced CT scan demonstrated a dehiscence and a fracture of the right bony hypotympanic wall covering the ICA and an enhanced mass anterior to the ICA, protruding into the hypotympanum (Fig 1). The CT scan raised the suspicion of ICA pseudoaneurysm, and therefore, 3-dimensional time-of-flight MRA was performed (Fig 2). The MRA confirmed the diagnosis by showing a petrous ICA pseudoaneurysm with a narrow isthmus connecting it to the ICA. The location of the pseudoaneurysm on MRA matched that of the enhanced hypotympanic

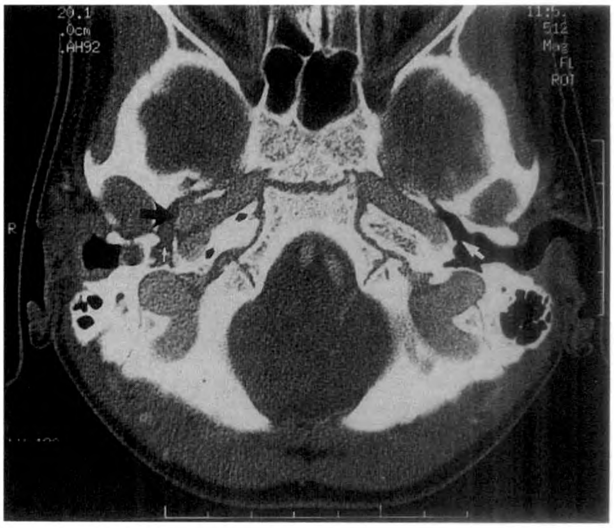

Fig 1. Contrast-enhanced computed tomography scan at level of hypotympanum shows dehiscence and fracture of right bony hypotympanum wall (compare to normal left side; large white arrow) and contrast-enhanced lesion (large black arrow), anterior to internal carotid artery (ICA; small black arrows), protruding into hypotympanum. Right hypotympanum is filled with blood (small white arrow).

From the Departments of Otolaryngology (Vasama, Ramsay) and Radiology (Markkola), Helsinki University Central Hospital, Helsinki, Finland.

CORRESPONDENCE — Juha-Pekka Vasama, MD, Dept of Otolaryngology, Helsinki University Central Hospital, Haartmaninkatu 4 E, 00290 Helsinki, Finland.

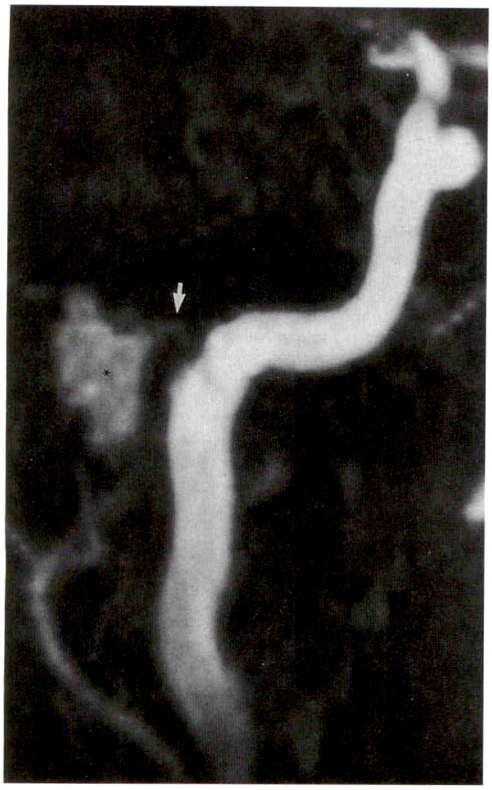

Fig 2. Three-dimensional time-of-flight magnetic resonance angiography in anterior-posterior projection shows pseudoaneurysm (asterisk) in petrous ICA. Narrow isthmus connects ICA to pseudoaneurysm (arrow).

mass on the CT scan. A decision was made to embolize the pseudoaneurysm with an endovascular detachable coil. Carotid angiography verified a contrast-filled pseudoaneurysm in the petrous ICA just before the coil installation (Fig 3). After the procedure, the pseudoaneurysm was obliterated and was not distinguishable on follow-up angiography (Fig 4). The treatment was successful, and the patient has not had any further episodes of epistaxis.

DISCUSSION

Epistaxis caused by a traumatic ICA pseudoaneurysm usually occurs within 3 weeks after the initial injury. However, massive hemorrhage may be delayed by months or even years.[4,5] This observation is in line with our case, in which vigorous bleeding took place 1.5 years after the head trauma. The delay is possibly explained by the time necessary for the traumatic event to weaken the ICA wall. Pseudoaneurysms located in the cavernous segment of the ICA may rupture into the sphenoid sinus, and cervical ICA pseudoaneurysms may rupture into the eustachian tube or the posterior nasopharynx.[2,4,5] In our case, the rupture and ICA bleeding were into the nasopharynx and eustachian tube.

Carotid angiography is a traditional tool for diagnosing suspected vascular injuries. In the case of a pseudoaneurysm, it typically shows an outpouching from the ICA, which is the wall of the pseudoaneurysm. The lumen is generally radiopaque and fills with contrast material. However, MRA provides excellent noninvasive visualization of vascular injuries of the temporal bone without the risk of complications associated with carotid angiography.[6] On the other hand, high-resolution CT is commonly performed after head trauma to evaluate possible brain and bone damage. Certain findings on CT suggest the possibility of a tympanic ICA pseudoaneurysm and should prompt MRA or carotid angiography for further evaluation. For example, a fracture or dehiscence of the bony hypotympanic wall and a mass adjacent to the petrous ICA should increase suspicion of a pseudoaneurysm.

Treatment of ICA pseudoaneurysms is aimed at maintaining normal vessel flow and preserving neu-

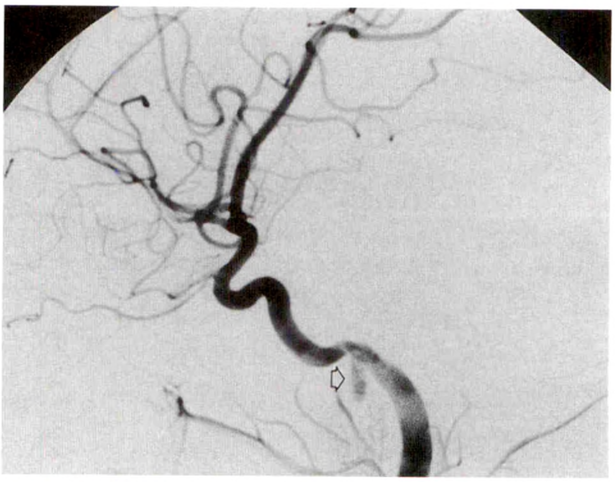

Fig 3. Digital subtraction ICA angiography in side projection, performed before endovascular coil embolization, demonstrates contrast-filled pseudoaneurysm in petrous ICA (arrow).

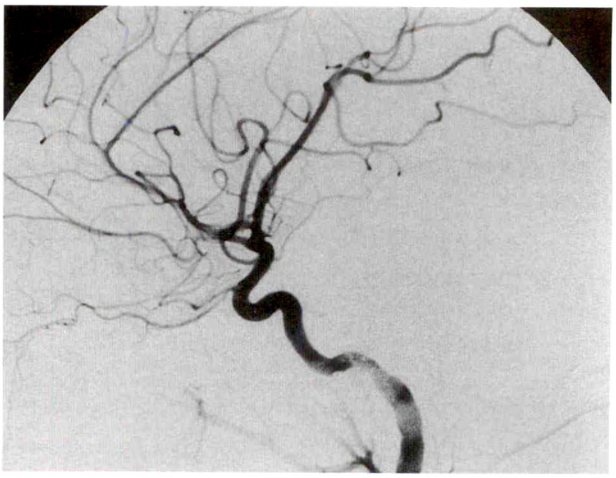

Fig 4. Digital subtraction ICA angiography in side projection, performed after endovascular coil embolization. Pseudoaneurysm is obliterated, and blood flow through ICA is preserved.

rologic function. Endovascular embolization with a detachable coil and/or detachable balloon occlusion is an effective treatment with many advantages.[2] It preserves the normal artery function, is easier to accomplish than surgical ligation or clipping, and may be used in areas that are relatively inaccessible by surgical alternatives. In our case, endovascular embolization with a detachable coil was successfully used.

Posttraumatic ICA pseudoaneurysm with secondary epistaxis is a rare and potentially fatal complication of head trauma. That the diagnosis is often delayed significantly contributes to the high mortality rate — as high as 50%.[7] Therefore, any patient with epistaxis and a history of prior serious head injury should be examined for a possible ICA pseudoaneurysm.

REFERENCES

1. Hern JD, Coley SC, Hollis LJ, Jayaraj SM. Delayed massive epistaxis due to traumatic intracavernous carotid artery pseudoaneurysm. J Laryngol Otol 1998;112:396-8.
2. Chen D, Concus AP, Halbach VV, Cheung SW. Epistaxis originating from traumatic pseudoaneurysm of the internal carotid artery: diagnosis and endovascular therapy. Laryngoscope 1998;108:326-31.
3. Batten TF, Heeneman H. Traumatic pseudoaneurysm of floor of mouth treated with selective embolization: a case report. J Otolaryngol 1994;23:423-5.
4. Chambers EF, Rosenbaum AE, Norman D, Newton TH. Traumatic aneurysms of cavernous internal carotid artery with secondary epistaxis. AJNR Am J Neuroradiol 1981;2:405-9.
5. Simpson RK Jr, Harper RL, Bryan RN. Emergency balloon occlusion for massive epistaxis due to traumatic carotid-cavernous aneurysm. Case report. J Neurosurg 1988;68:142-4.
6. Bold EL, Wanamaker HH, Hughes GB, et al. Magnetic resonance angiography of vascular anomalies of the middle ear. Laryngoscope 1994;104:1404-11.
7. Wang AN, Winfield JA, Gucer G. Traumatic internal carotid artery aneurysm with rupture into the sphenoid sinus. Surg Neurol 1986;25:77-81.

LETTER TO THE EDITOR

To the Editor:

In the past 2 years I have been aware of a puzzling movement-induced transient tinnitus for which no definite explanation has yet been found. Accordingly, I seek possible answers from some of your readers. The acoustic effect is readily and consistently evoked by abrupt voluntary head rotation to either side through an arc of 20° to 30° and consists of a soft tone. It lasts perhaps a half-second or so, is not lateralized, and is matched on audiometry at approximately 750 Hz. I have found among acquaintances 2 individuals with similar responses to this kind of head jolt; both were unaware of this effect in themselves until they carried out the motion on instruction. The age range in this group of 3, all males, is 53 to 85; possibly relevant, all of us have moderate presbycusis.

In a year's search of the medical literature, including Medline, I have found no mention of this specific variety of tinnitus, nor has any of the half-dozen research otologists whom I have contacted heard of it. I believe it can easily be overlooked, for it is so fleeting and soft and dependent on a type of sudden head motion unlikely to occur in ordinary activities. I speculate that this response to brief angular acceleration in ampullae of the horizontal semicircular canals is inappropriately transferred from vestibular to acoustic pathways at some level within the central nervous system, in the brain stem or above. Such a process is comparable to examples of anomalous transmodal activation in other sensory systems as described in the past 2 decades. It is possible also that the presbycusis in the herementioned subjects, by its partial "deafferentation" effect, permits or enhances the evoked tinnitus.

It is evident to me, a neurologist and no otologist, that much more data and sounder suggestions are needed to explain this intriguing benign noise.

E. Charles Kunkle, MD
PO Box 17
South Freeport, ME 04078-0017

BOOK REVIEW

Salivary Gland Tumours

Jerzy Klijanienko and Philippe Vielh. Hard cover, illustrated, indexed, 141 pages, 2000. Karger AG, Basel, Switzerland, $172.25.

As stated in the introduction to this segment, volume 15, of *Monographs in Clinical Cytology*, "This volume is designed to describe the cytological diagnostic criteria of salivary gland tumours, to demonstrate that fine-needle aspiration cytology can be a simple and reliable method of diagnosis, and to dispel a number of common misconceptions related to fine-needle aspiration cytology in this area" (page 1). Its primary focus is therefore directed toward clinical cytologists, rather than the surgical community. Because fine-needle aspiration cytology has become an increasingly common and important diagnostic tool in the management of head and neck tumors, it is appropriate to review this text from the point of view of otolaryngology–head and neck surgery.

The monograph makes use of the extensive and well-documented clinical experience of the Institut Curie, Paris, where a multispecialty approach to salivary gland cytology has been used since 1954. It first presents a review of the history of salivary gland cytology, along with the current indications and the accuracy of the technique as delineated by the recent medical literature. It then goes on to review the steps of obtaining fine-needle aspirate specimens and the basic and ancillary techniques that can be used to evaluate them. After giving several examples of imaging of salivary gland tumors, the volume approaches its main goal of illustrating and comparing the cytologic appearance of the normal components of salivary glands, benign and malignant tumors, lymphomas, and a collection of tumorlike lesions.

The bulk of this work consists of illustrations and descriptions of representative cytology as described above. Several of the illustrations are complemented by comparable histologic photomicrographs with which the head and neck surgeon might be more familiar. The preparation and stain quality of these photos, as well as their print quality, is no less than spectacular. They are arranged in a logical manner, and a single type of tumor with its differential can be found easily. The work appears to be all-inclusive. This section is liberally sprinkled with tables reporting the correlation from the literature between cytologic and histologic diagnosis. All in all, this monograph amply fulfills its stated goals and is aesthetically pleasing in its execution.

Cytology is becoming increasingly important in the diagnosis of head and neck masses, and certainly one of the most challenging areas of head and neck surgery is the identification of salivary tissue pathology. With more and more head and neck surgeons performing fine-needle aspiration and producing the smears for the cytologist to read, it behooves our specialty to expand our historical strength in regional histology to include cytology. On the other hand, this volume provides more than an individual head and neck surgeon is likely to want on this topic, and it comes at a stiff, if justifiable, price. I would think this would be an essential volume for an academic department library, or for a multispecialty clinic dealing with head and neck tumors. It will undoubtedly become required reading for anyone with whom the diagnostic buck stops.

Richard W. Babin, MD
Covington, Tennessee

ANNALS SUPPLEMENTS

Still-in-Stock — Quantities Limited — Order Now!

Supplement 177 (April 1999)
Clinical Results with the CLARION® Multi-Strategy™ Cochlear Implant
Price $23.00 (128 pages; Osberger & Koch)

Supplement 179 (Sept 1999)
Universal Modular Glottiscope System: The Evolution of a Century of Design and Technique for Direct Laryngoscopy
Price $6.50 (24 pages; Zeitels)

Supplement 180 (Nov 1999)
Laser Surgery for Allergic and Hypertrophic Rhinitis
Price $8.50 (20 pages; Inouye et al)

Supplement 181 (May 2000)
Temporal Bone Studies of the Human Peripheral Vestibular System
Price $9.50 (32 pages; Merchant et al)

Supplement 182 (May 2000)
Medical Management of Acute Bacterial Sinusitis
Price $6.50 (20 pages; Brook et al)

Supplement 183 (August 2000)
Controversies in the Medical Management of Persistent and Recurrent Acute Otitis Media. Recommendations of a Clinical Advisory Committee
Price $4.00 (12 pages; Pichichero et al)

Supplement 184 (October 2000)
24-Hour Ambulatory pH Monitoring for Patients With Suspected Extraesophageal Complications of Gastroesophageal Reflux: Indications and Interpretations
Price $7.50 (28 pages; Sasaki & Toohill, eds)

Supplement 185 (December 2000)
Seventh Symposium on Cochlear Implants in Children
Price $21.00 (128 pages; Gantz, Tyler, & Rubinstein, eds)

Supplement 186 (May 2001)
Analysis of the Suprabullar and Retrobullar Recesses for Endoscopic Sinus Surgery
Price $7.50 (16 pages; Bolger & Mawn)

Supplements Desired: # ________ ________ ________ ________ ________

Send to: ______________________________
____
____
____

Order from:

Annals Publishing Company
4507 Laclede Avenue
St Louis, MO 63108

Payment must be enclosed with order.
Checks (US funds only),Mastercard,
Visa, or American Express

11/00 Copyright ©2000 by Daiichi Pharmaceutical Corporation. All rights reserved.

Please see our full ad on pages 416a-d.

SUPPLEMENT 186 — MAY 2001
Volume 110, Number 5, Part 2

ANALYSIS OF THE SUPRABULLAR AND RETROBULLAR RECESSES FOR ENDOSCOPIC SINUS SURGERY

WILLIAM E. BOLGER, MD
LCDR CHRISTOPHER B. MAWN, MC, USN

ANNALS
OF OTOLOGY,
RHINOLOGY &
LARYNGOLOGY

ANALYSIS OF THE SUPRABULLAR AND RETROBULLAR RECESSES FOR ENDOSCOPIC SINUS SURGERY

WILLIAM E. BOLGER, MD
LCDR CHRISTOPHER B. MAWN, MC, USN

We gratefully acknowledge the support of Karl Storz Endoscopy,
which has made possible the publication of this supplement.

Calcutta University College of Medicine C.U.
LIBRARY

Additional copies may be purchased from Annals Publishing Company, 4507 Laclede Ave, St Louis, MO 63108.

COPYRIGHT© 2001, ANNALS PUBLISHING COMPANY

Ann Otol Rhinol Laryngol 110:2001

ANALYSIS OF THE SUPRABULLAR AND RETROBULLAR RECESSES FOR ENDOSCOPIC SINUS SURGERY

WILLIAM E. BOLGER, MD
PHILADELPHIA, PENNSYLVANIA

LCDR CHRISTOPHER B. MAWN, MC, USN
BETHESDA, MARYLAND

Presently, the basic structures and spaces of the paranasal sinuses are more clearly understood by otolaryngologists than ever before. Yet, the more subtle and complex ethmoid features, especially of the ethmoidal pre-recesses and recesses, still elude many otolaryngologists. One of the most nebulous, elusive, and difficult-to-understand recesses is the sinus lateralis, or as it is more correctly called, the retrobullar and suprabullar recesses. The primary purpose of this investigation was to ascertain the prevalence of the sinus lateralis in humans. The secondary purpose was to better characterize this subtle feature of ethmoid anatomy. Human cadaver sinonasal complexes were meticulously dissected by both gross and endoscopic techniques. The hiatus semilunaris superior and sinus lateralis were present in all specimens. A separate and discrete retrobullar recess was present in 93.8%. Typically, a crestlike projection from the basal lamella to the lamina papyracea was noted within the posterior aspect of the retrobullar recess. A single, discrete, well-developed suprabullar recess was present in 70.9%, and a rudimentary suprabullar recess was present in 22.9%. In 7.2%, a single large cleft collectively excavated the retrobullar and suprabullar recess areas; separate retrobullar and suprabullar tracts were not present in this subgroup. Typically, the suprabullar recess was separate from and did not communicate with the frontal recess. The data from this investigation indicate that the separate terms retrobullar recess and suprabullar recess more accurately designate the anatomy and are recommended over the term sinus lateralis.

KEY WORDS — endoscopic sinus surgery, paranasal sinuses, retrobullar recess, sinus lateralis, suprabullar recess.

INTRODUCTION

The modern rhinologic surgeon is continuously challenged to maintain precise orientation during ethmoid dissection, as the surgical field is replete with anatomic variations. Each patient's ethmoid sinus is unique; like fingerprints, no two ethmoid sinuses are exactly the same. In this light, it is easy to understand why the ethmoid sinus has been traditionally referred to as the labyrinth.

Surgeons can meet the challenge of performing safe and accurate ethmoid surgery by recognizing subtle but consistent anatomic features present in nearly all patients. Until recently, these structures and spaces were not well appreciated by most modern-day otolaryngologists. However, after the introduction of the sinus endoscope, interest in and appreciation of sinonasal anatomy increased. At first, "new" structures and spaces were superficially appreciated. Later, with continued exposure and study, select rhinologists gained a deeper appreciation of the complex regional anatomy. These rhinologists presented the newly rediscovered anatomic concepts to a large number of practicing otolaryngologists. The concepts were challenged initially, then superficially understood, explored, accepted, and finally understood on a deeper level by many otolaryngologists. Clearly, the ethmoid sinus is a complex 3-dimensional space with highly variable structures and subspaces. Mastery is not possible on first contact. Rather, a true understanding evolves over years of study.

Although the basic sinonasal structures and spaces are more clearly understood by otolaryngologists than ever before, the more subtle and complex ethmoid features still elude many surgeons. One of the most nebulous and difficult-to-understand ethmoid features is the sinus lateralis (or, as it is more correctly called, the retrobullar and suprabullar recesses). Few informative resources are available to illuminate its nature. Standard otolaryngology textbooks and journal articles provide limited information, and a dedicated comprehensive analysis of the sinus lateralis has not been conducted. Even studies to provide the most basic information, such as the prevalence of the recess, have not been undertaken. The paucity of information in this regard hinders otolaryngologists' understanding of this region and thereby limits the level of sophistication of surgical care. Improving our understanding of this important space is therefore clinically relevant. With an improved comprehension, surgeons can expect to localize their precise position within the ethmoid cavity better, perform more complete ethmoid surgery, and, of importance, approach the frontal recess in a more anatomically sound fashion.

From the Division of Rhinology and Sinus Surgery, Department of Otorhinolaryngology, University of Pennsylvania Health System, Philadelphia, Pennsylvania (Bolger), and the Department of Otolaryngology, National Naval Medical Center, Bethesda, Maryland (Mawn). The views expressed herein are those of the authors and do not necessarily reflect the views of the US Navy or the US Department of Defense.

CORRESPONDENCE — William E. Bolger, MD, Dept of Otorhinolaryngology, University of Pennsylvania Health System, 3400 Spruce St, 5 Silverstein, Philadelphia, PA 19104.

The term sinus lateralis appears to have been first introduced by Grunwald[1,2] to describe a deepening or a broadening of the hiatus semilunaris superior. This broadening developed laterally, inferiorly, and superiorly from the hiatus semilunaris superior. In 13% of specimens, there were 2 or 3 deepenings. He claimed that humans were the first to evolve this space and that it was not present in other primates. Grunwald also appears to have been the first to use the term hiatus semilunaris superior to identify the deepening or cleft behind the bulla in distinction from that anterior to the bulla, the hiatus semilunaris inferior. Information on the prevalence of the hiatus semilunaris superior or the sinus lateralis was not provided. The term sinus lateralis was conspicuously absent from the English-language literature until recently. In the modern endoscopic era, Stammberger,[3] in his exceptional anatomic and clinical treatise, refers to the sinus lateralis as a cleft that "when present" may extensively pneumatize and extend above and beyond the ethmoid bulla. He adds that the sinus lateralis is not a constant feature of ethmoid anatomy.[3] These comments suggest that the sinus lateralis is not present in all patients. In 1995, the Consensus Group on Anatomic Terminology and Nomenclature addressed the nomenclature by stating, "Grunwald's term, sinus lateralis, is suitable anatomically, but the complete term, sinus lateralis sinus ethmoidalis is necessary to differentiate it from the lateral sinus in the brain."[4(p10)] As the latter term is impractical, the group recommended that the terms suprabullar recess and retrobullar recess be used.[4] Despite their suggestions, the term sinus lateralis is still used liberally by otolaryngologists and otolaryngology educators.

The primary purpose of this investigation was to ascertain the prevalence of the sinus lateralis (that is, the retrobullar and suprabullar recesses) in humans. The secondary purpose was to better characterize this subtle feature of ethmoid anatomy.

MATERIALS AND METHODS

Phase 1. Ten adult human cadaver heads were used in this phase of the investigation. The specimens were randomly chosen and were not previously chemically treated or dissected. All specimens initially underwent a standard computed tomography (CT) evaluation on a GE HiSpeed Advantage CT scanner, with bone (window, 4,000; level, 600) and soft tissue (window, 350; level, 50) images with 1-second scan time, at 280 mA and 120 kV. Direct coronal images were obtained in 3-mm increments with 3-mm thickness, from the anterior limit of the frontal sinuses to the posterior limit of the sphenoid sinus. Direct axial images were obtained in 5-mm increments with 5-mm thickness, from the palate to the superior limit of the frontal sinuses. The CT scans were then evaluated by an individual highly experienced in interpreting paranasal sinus CT scan anatomic data (W.E.B.). The scans were evaluated for the presence or absence of a sinus lateralis on each side. The sinus lateralis was defined as a variable cleft that is located above and behind the ethmoid bulla. Its borders include the lamina papyracea laterally, the roof of the ethmoid (sinus) superiorly, the basal lamella of the middle turbinate posteriorly, and the roof and posterior wall of the ethmoid bulla anteriorly and inferiorly.[3] An attempt was made to appreciate and record the extent and character of each sinus lateralis.

After the CT evaluation, bilateral endoscopic dissection of the paranasal sinuses was conducted. The procedure consisted of uncinectomy, anterior and posterior ethmoidectomy, sphenoidotomy, and complete frontal recess dissection. The presence of the hiatus semilunaris superior and sinus lateralis was noted, and an attempt was made to appreciate and record the extent and character of the sinus lateralis when present. Dissection was performed with a 0° and 30° 4-mm nasal endoscope (Karl Storz Endoscopy–America, Inc, Culver City, Calif).

Phase 2. Thirteen adult human cadaver heads were used in this phase of the investigation. The specimens were chosen randomly and were not previously dissected or chemically treated. The cadaver heads were sectioned in the midline to create sagittal specimens for study (Fig 1A). If a sinonasal complex was violated or disrupted during sectioning, it was eliminated from the investigation. All dissections were conducted in a standardized fashion. The middle turbinate was reflected superiorly, and the hiatus semilunaris superior was identified (Fig 1B). Dissection was initiated at the hiatus semilunaris superior and extended from this central point. The bulbous lower portion of the middle turbinate was trimmed to allow unimpeded access to the middle meatal structures; however, the basal lamella was carefully preserved and marked with blue acrylic paint to maintain clearly its identity and integrity throughout the dissection (Fig 2A). The dissection was conducted in a meticulous fashion to delineate fully the sinus lateralis while preserving its boundary structures. The specific relationship of the sinus lateralis to the frontal recess was ascertained in all specimens. All "pneumatization tracts" were carefully identified and followed (Fig 2B-D). A complete sphenoethmoidectomy and frontal recess dissection was performed, and the dissection was photodocumented and sketched to create an accurate reference source.

Phase 3. Twenty-four sinonasal-ethmoid complexes were evaluated in this phase of the investigation.

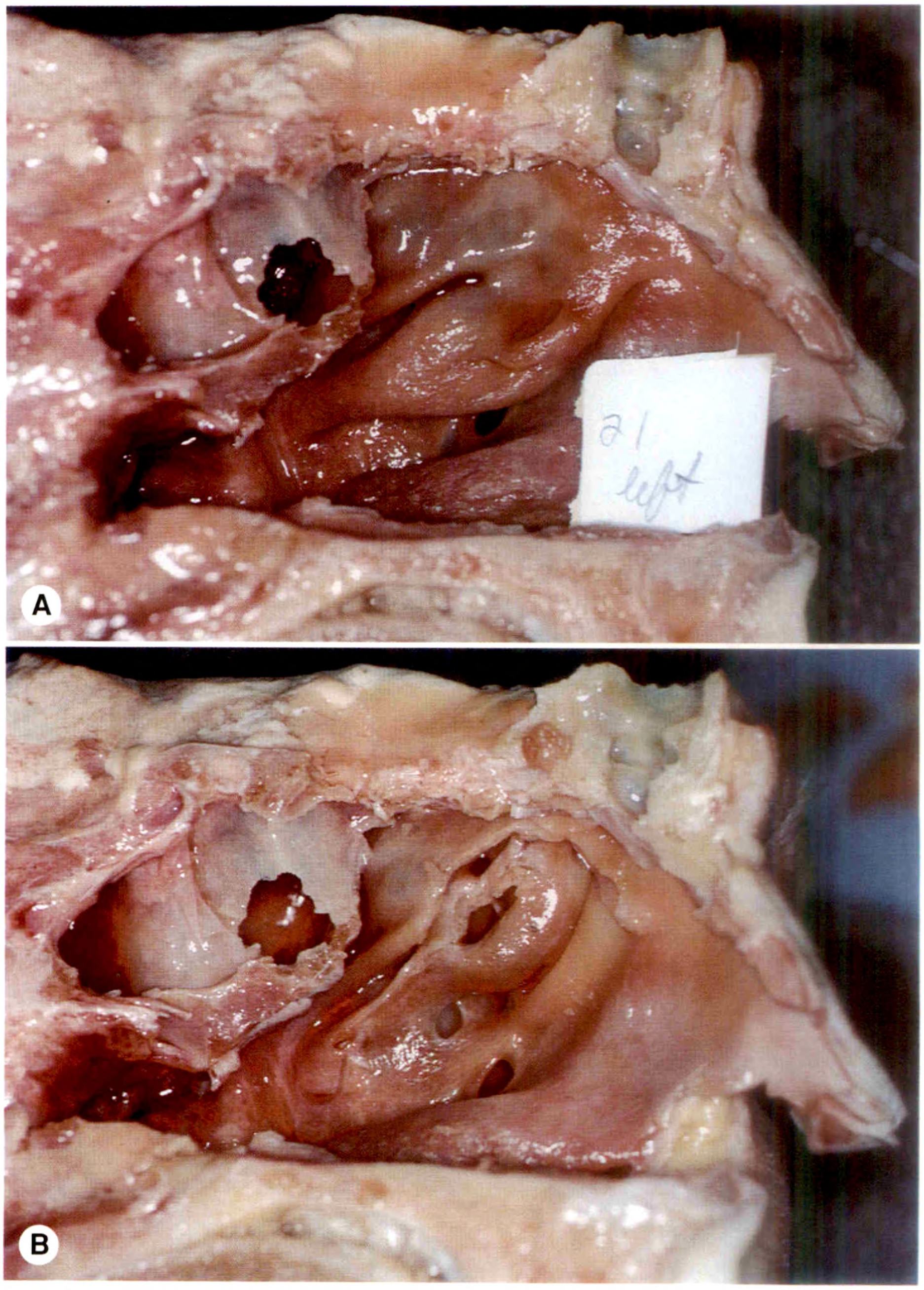

Fig 1. Left lateral nasal wall specimen. **A)** Ready for dissection. **B)** With middle turbinate resected to demonstrate middle meatal anatomic structures.

The specimens were obtained from 12 randomly chosen human cadaver heads that had not been previously chemically treated or dissected. The endoscope was advanced into the middle meatus to identify the hiatus semilunaris superior. The presence of the sinus lateralis was ascertained, and anatomic characteristics were noted. Using a 0° and 30° nasal endoscope, we conducted an endoscopic dissection in a standardized fashion to ascertain the presence, extent, and character of each sinus lateralis (Fig 3). The dissection was initiated by resecting the uncinate process. Next, a 3 × 3-mm window was created in the anterior face of the ethmoid bulla. Under viewing through the bullar window, the curved ball-tipped seeker was placed through the hiatus semilunaris superior and the retrobullar cleft. In this way, the pneumatization tracts from the retrobullar cleft could be visualized and followed. Next, cutting forceps were used to resect the medial aspect of the bulla. The major course of the basal lamella through the ethmoid cells and its attachment to the lamina papyracea was examined. Next, the suprabullar recess was identified and its pneumatization tract was carefully followed. Care was taken to correctly identify contiguous spaces and structures such as the recessus terminalis, the agger nasi cell, the entire uncinate process with special attention to its superior aspect, the frontal recess, the infundibulum, and any frontal cells.

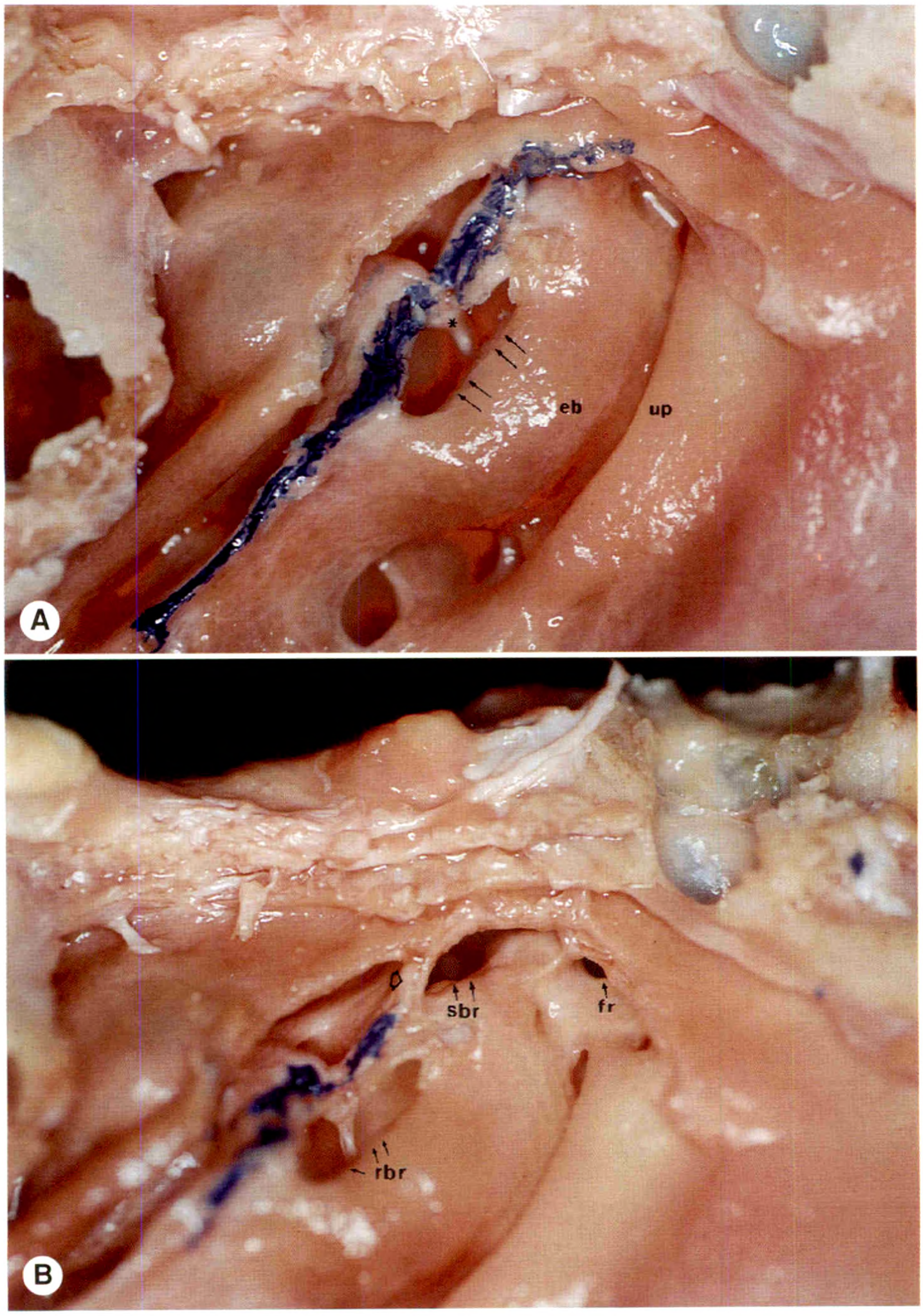

Fig 2. Dissection findings. **A)** Close-up view of ethmoid bulla (eb), uncinate process (up), retrobullar recess (arrows), and projection of basal lamella of middle turbinate to lamina papyracea with retrobullar recess (asterisk). Note that basal lamella of middle turbinate has been highlighted with blue acrylic paint to delineate clearly anterior and posterior ethmoid regions. **B)** Parasagittal view demonstrates separate retrobullar recess (rbr), suprabullar recess (sbr), and frontal recess (fr). Projection of middle turbinate lamella to bulla is evident between retrobullar and suprabullar recesses (open arrow). **(Continued on next page.)**

To ensure accurate delineation of the frontal recess, the corresponding frontal sinus was trephinated and a malleable probe was carefully passed through the outflow tract into the nose. The entire bulla lamella was carefully dissected superiorly to identify its attachment to the skull base, when present. The presence and origin of supraorbital pneumatization were ascertained, and the presence and location of the anterior ethmoid artery were identified. The dissection was conducted meticulously so as to fully delineate the sinus lateralis and preserve its boundary structures. All "pneumatization tracts" were carefully identified and followed. The dissection was photodocumented and sketched to create an accurate reference source.

RESULTS

Phase 1. Twenty ethmoid sinus complexes were evaluated in 10 cadaver heads. Both CT scanning and endoscopic dissection revealed that the hiatus semilunaris superior was present in all specimens. Both CT and endoscopic dissection revealed that a variable cleft, the sinus lateralis, was present, behind and/or above the bulla in all cases. However, additional accurate and reliable assessments as to the extent and character of the sinus lateralis were not pos-

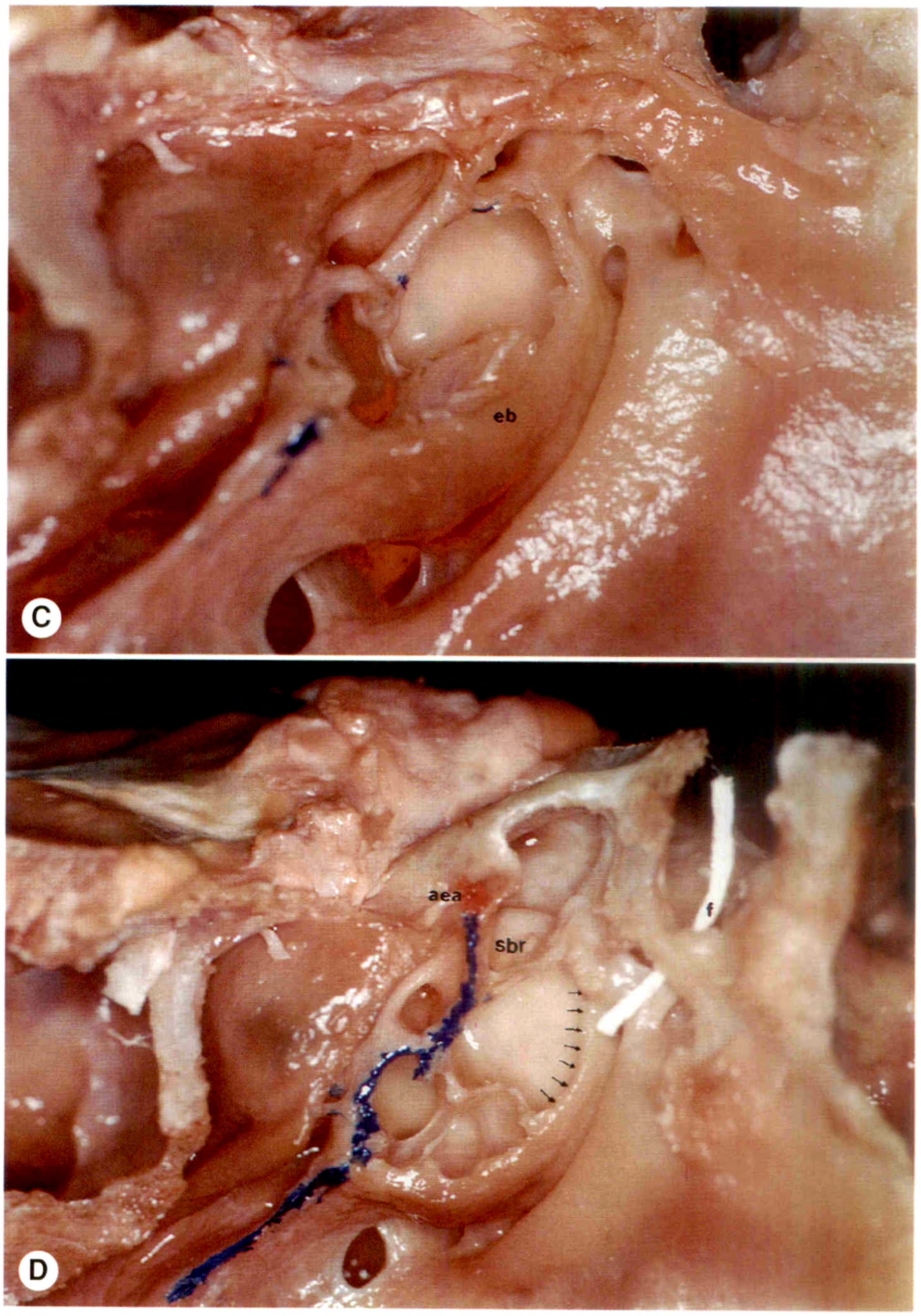

Fig 2, continued. C) Extent of retrobullar recess pneumatization is realized as medial surface of ethmoid bulla (eb) is removed. **D)** Dissection reveals attachment of bulla lamella and basal lamella of middle turbinate to skull base (arrows). Suprabullar recess (sbr) is extensive and pneumatizes above orbit. Frontal recess drainage pathway is clearly demonstrated by probe that descends from frontal sinus (f). Note that frontal recess and suprabullar recess are separate pneumatization tracts that do not communicate. In fact, thick bone separates them in this specimen. Anterior ethmoid artery (aea) is highlighted in red within its skull base canal, in this specimen, just anterior to ground lamella's connection with skull base. Basal lamella of middle turbinate has been highlighted in blue to show more clearly its important course.

sible with these study methods. Regarding CT, it was evident that the full extent and character of the sinus lateralis, a small variable cleft, was difficult to appreciate with incremental slice-type data. Incremental data did not permit accurate delineation of the sinus lateralis from adjacent spaces, recesses, cells, etc. Information for which a high degree of confidence could be assigned was not evident regarding the extent, variability, and character of the sinus lateralis air space by this method. Endoscopic dissection offered no better information in this regard. In providing exposure during the dissection, border structures of the sinus lateralis were necessarily removed, and their removal led to ambiguity regarding the actual limit and character of the space. Therefore, assessments were restricted to sinus lateralis prevalence.

Phase 2. Twenty-four sinonasal complexes were fully evaluated, and 2 specimens were eliminated because of artifact sustained during sagittal sectioning. Gross anatomic dissection revealed that a hiatus semilunaris superior and a sinus lateralis were present in all specimens. Typically, each sinus lateralis region comprised separate retrobullar and suprabullar pneumatization tracts. However, variability was evident.

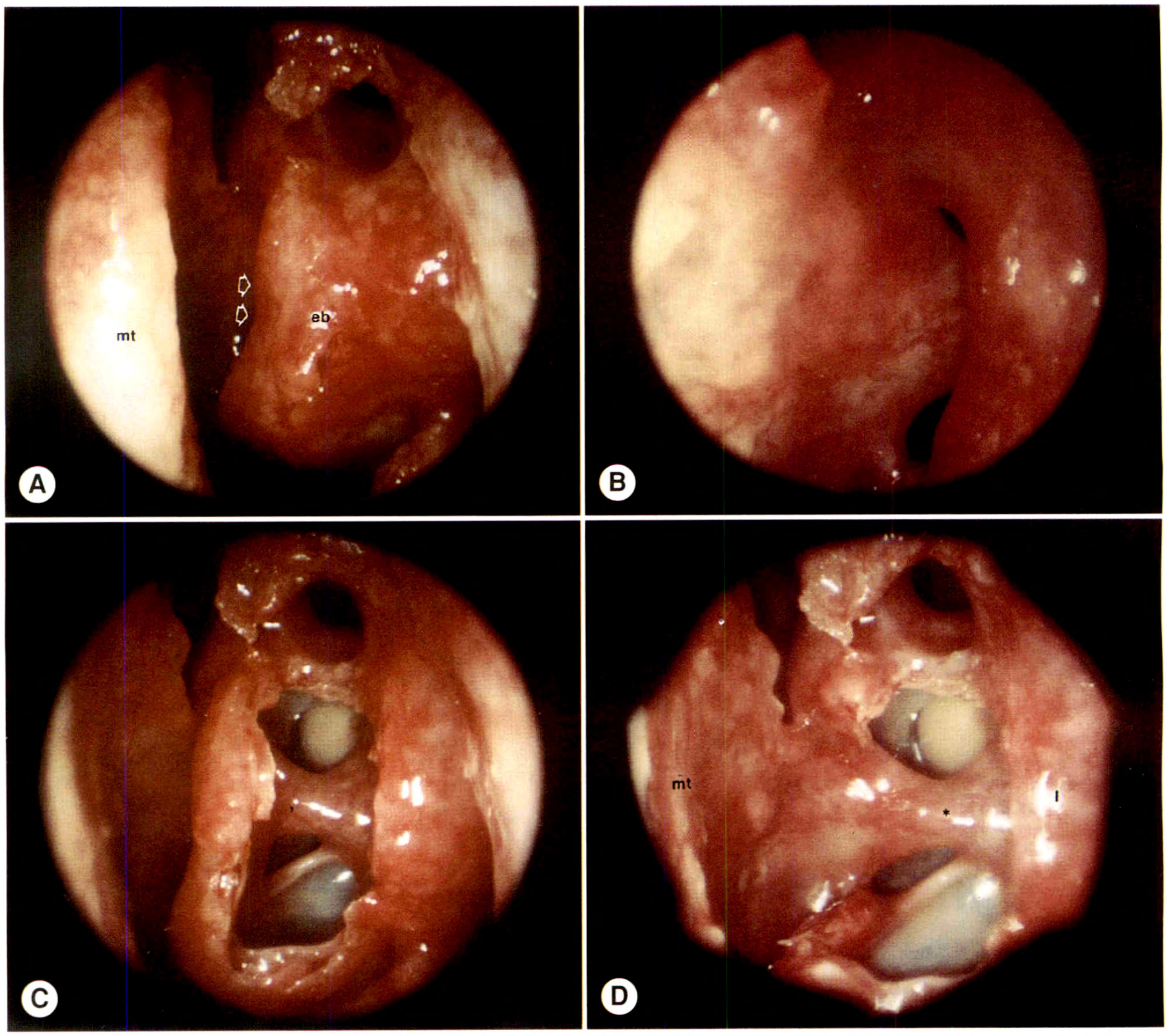

Fig 3. Endoscopic findings. **A)** View of ethmoid bulla within middle meatus after resection of uncinate process shows ethmoid bulla (eb), middle turbinate (mt), and area of hiatus semilunaris superior leading to sinus lateralis, specifically retrobullar recess (arrows). **B)** View through hiatus semilunaris superior into retrobullar recess. **C)** Portion of anterior wall of ethmoid bulla has been resected to create window allowing visualization of pneumatization tract emanating from retrobullar recess. **D)** Medial wall of ethmoid bulla is removed to demonstrate well-developed projection of middle turbinate's (mt) basal lamella (asterisk), which divides retrobullar recess and extends to attach on lamina papyracea (l).

With regard to the retrobullar recess, a separate and discrete retrobullar recess was present in 23 of 24 specimens. In 1 specimen, a single large cleft was present, rather than separate suprabullar and retrobullar recesses. With regard to the suprabullar recess, a separate suprabullar recess with a corresponding pneumatization tract developed above the bulla and extended to the lamina papyracea and skull base in 17 of the 24 specimens. In 5 of the 24 specimens, the suprabullar recess was rudimentary and did not fully develop. It was represented only as a small pouch, mucosal indentation, or cleft, rather than a true recess. In 1 specimen, the suprabullar recess pneumatization tract progressed to pneumatize the orbital plate of the frontal bone and frontal sinus. The frontal recess therefore opened into and through the suprabullar recess. As previously mentioned, a single large, diffuse cleft occupied the suprabullar and retrobullar regions collectively in 1 specimen. In the 17 specimens with a well-developed suprabullar recess, further observation revealed that a single discrete recess with a single corresponding pneumatization tract was present in 15 specimens, whereas in 2 specimens, the suprabullar recess subdivided into 2 pneumatization tracts. Additionally, in 5 specimens, the suprabullar pneumatization tracts were extensive and extended above the orbit to form supraorbital pneumatization, or a supraorbital ethmoid cell.

The suprabullar recess and frontal recess were noted to be separate pneumatization tracts without direct communications in 23 of the 24 specimens. The bulla lamella was noted to extend and attach to the skull base, separating the frontal recess from the suprabullar recess in 23 specimens. However, in 1 case, as previously mentioned, the frontal sinus was pneumatized from the suprabullar recess. In this case, the bulla lamella did not reach the skull base.

Two consistent projections from the basal lamella were observed in this investigation. Within the retrobullar recess, a small eminence of basal lamella projected to the lamina papyracea in all cases (Fig 2A). A second projection of the basal lamella joined the bulla lamella and typically divided the retrobullar and suprabullar recesses (Fig 2B). This projection extended laterally from the middle meatus to the lamina papyracea in the 17 of the 24 specimens that had a well-developed, discrete suprabullar recess.

Phase 3. Endoscopic dissection revealed that the hiatus semilunaris superior was present in all specimens. Endoscopic dissection also revealed that a variable cleft, the sinus lateralis, was present behind and/or above the bulla in all cases. Typically, each sinus lateralis region comprised separate retrobullar and suprabullar pneumatization tracts; however, variability was evident. With regard to the retrobullar recess, a separate and discrete retrobullar recess was present in 22 of the 24 specimens. In 2 specimens, a single large cleft was present, rather than separate suprabullar and retrobullar recesses.

With regard to the suprabullar recess, a single discrete recess with a single corresponding pneumatization tract developed above the bulla and extended to the lamina papyracea and skull base in 15 of the 24 specimens. In 6 specimens, the suprabullar recess was rudimentary and did not fully develop. It was represented only as a small pouch, mucosal indentation, or cleft, rather than a true recess. In 2 specimens, a single large cleft was present, rather than separate suprabullar and retrobullar recesses. In 1 specimen, the suprabullar recess pneumatization tract progressed to pneumatize the orbital plate of the frontal bone and frontal sinus. The frontal recess therefore opened into and through the suprabullar recess. Among the 15 specimens with a well-developed suprabullar recess, 8 displayed supraorbital pneumatization, or a supraorbital ethmoid cell, associated with extensive suprabullar pneumatization above the orbit. The suprabullar recess and frontal recess were noted to be separate pneumatization tracts without direct communications in 23 specimens.

The bulla lamella was noted to extend and attach to the skull base, separating the frontal recess from the suprabullar recess in 23 specimens (Fig 2C,D). However, in 1 case, as previously mentioned, the frontal sinus was pneumatized from the suprabullar recess. In this case, the bulla lamella was pneumatized from the upper aspect of the infundibulum. This configuration had the effect of indenting or splitting the bulla lamella.

Two consistent projections from the basal lamella were observed in this investigation. Within the retrobullar recess, a small eminence of basal lamella projected to the lamina papyracea in 22 specimens (Figs 2A and 3D). A second projection of the basal lamella joined the bulla lamella and typically divided the retrobullar and suprabullar recesses (Fig 2B). This projection extended laterally from the middle meatus to the lamina papyracea in all 17 specimens with a well-developed, discrete suprabullar recess.

DISCUSSION

This study was initiated in response to the question of how often the sinus lateralis is present, asked of the senior author (W.E.B.) by practicing otolaryngologists participating in endoscopic sinus surgery dissection courses. Our investigation revealed that the sinus lateralis was present in all specimens. Specifically, the hiatus semilunaris superior was present in all specimens, the retrobullar recess was present in nearly all specimens, and the suprabullar recess was present in most specimens. Typically, the suprabullar and retrobullar recesses are separate, and each has a corresponding pneumatization that does not connect with neighboring cells or structures (Figs 2B,D and 4). The two recesses are separated by a small but consistent tissue bridge that projects from the basal lamella to the superior aspect of the ethmoid bulla and lamina papyracea (Figs 2B and 4). An additional projection from the basal lamella within the retrobullar recess projects to the lamina papyracea (Figs 2 and 3). The consistency with which these anatomic features occur suggests that they represent normal sinonasal anatomy rather than anomalies. That these normal anatomic characteristics have not previously been fully characterized is significant. In this investigation, we sought not only to determine the prevalence of the sinus lateralis, but also to characterize this aspect of sinonasal anatomy. Accordingly, our observations regarding the retrobullar recess, the suprabullar recess, and their anatomic relationship to relevant surrounding structures and spaces are herein highlighted.

Important anatomic characteristics of the retrobullar recess were evident in this study. Pneumatization from the retrobullar recess typically developed anteriorly into the inferior and middle aspect of the bulla lamella. In some cases, 1 large pneumatization

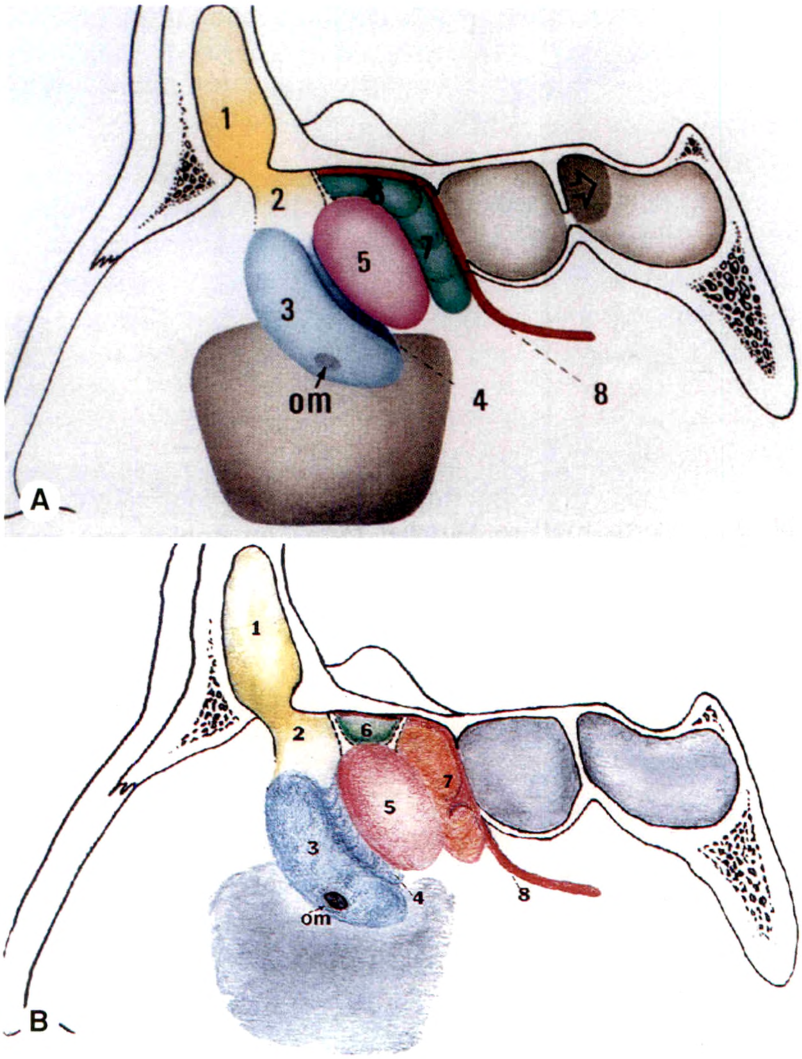

Fig 4. A) Illustration of lateral nasal wall shows region of retrobullar and suprabullar recesses and their central and key location within ethmoid sinus. 1 — frontal sinus; 2 — frontal recess; 3 — uncinate process; 4 — hiatus semilunaris inferior; 5 — ethmoid bulla; 6 — suprabullar recess; 7 — retrobullar recess; 8 — basal lamella of middle turbinate; om — ostium of maxillary sinus (behind and deep to uncinate process). Open arrow — area of potential sphenoethmoid or Onodi cell pneumatization. (Reprinted with permission from Stammberger H, Hosemann W, Draf W. Anatomische Terminologie und Nomenklatur fur die Nasennebenhohlenchirurgie. Laryngorhinootologie 1997; 76: 435-49.) **B)** Illustration of lateral nasal wall modified to reflect findings of this study. Suprabullar (6) and retrobullar (7) recesses were most often noted to be separate pneumatization tracts.

tract was evident, whereas in other instances, multiple tracts, partial septations, or even discrete cells were present (Fig 2). Variably, the inferior aspect of the retrobullar recess pneumatized posteriorly to indent the basal lamella. Pneumatization from the superior aspect of the retrobullar recess usually progressed posterior and lateral to the lamina papyracea, often to the skull base. In our experience, this area of pneumatization is what most otolaryngologists designate as the sinus lateralis. We began this investigation with the same understanding; however, as our study progressed, we came to appreciate the additional aforementioned characteristics of the sinus lateralis. Surprisingly, a frequent but consistent anatomic feature that previously had not been described was noted in this investigation. A crest projecting from the basal lamella to the lamina papyracea was present within the retrobullar recess in nearly all cases (Figs 2A and 3D).

Important characteristics of the suprabullar recess were also evident in this study. At the superior aspect of the retrobullar recess, a projection of the basal lamella blends with the bulla to form the superior border of the retrobullar cleft (Fig 2B). Just anterior to this tissue bridge, the suprabullar recess characteristically forms as an oval or slitlike opening approximately 2 to 3 mm in size. From the suprabullar recess, a single pneumatization tract emanates most commonly. This tract extends laterally to the lamina papyracea and to the skull base. It also can pneumatize the orbital plate of the frontal bone to form a supraorbital ethmoid cell. Typically, the suprabullar pneumatization tract does not communicate with the frontal recess or retrobullar recess. The bulla lamella, the anterior wall of the suprabullar recess, typically extends to the skull base. The location of the lamella's attachment to the skull base varies depending on the size of neighboring pneumatization tracts, such as the frontal recess, the retrobullar recess, and the clefts or cells from the superior infundibulum. The appearance of the bulla lamella also varies if pneumatization from the superior infundibulum develops posteriorly into the bulla lamella. If this occurs, a complete lamella or plate is not evident; rather, the lamella is indented or "split" by the pneumatization. However, even with this variation, we observed the medial and lateral aspects of the lamella to ascend and attach to the skull base in most cases.

The suprabullar recess bears an important relationship to the frontal recess. Understanding this relationship may be important for practicing surgeons, as endoscopic surgery in the frontal recess is among the most challenging of all otolaryngological surgeries. Stammberger[3] points out that the sinus lateralis is separated from the frontal recess only when the bulla lamella reaches the skull base; otherwise, the suprabullar recess opens into the frontal recess. We found the bulla lamella attached to the skull base in most specimens, although the precise point of attachment varied. Typically, the bulla lamella separated the suprabullar pneumatization tract from the frontal recess. However, we also observed the pattern noted by Stammberger in which the bulla lamella did not attach to the skull base over any appreciable distance. In 2 specimens, the bulla lamella joined the posterior wall of the invading frontal cell. The suprabullar recess pneumatized widely to the skull base and lamina papyracea, the orbital plate of the frontal bone, and then into the frontal bone proper. The suprabullar pneumatization "won out" over the suprainfundibular-frontal recess to pneumatize the dominant portion of the frontal bone. In these specimens, a small pneumatization tract from the area that normally develops into the frontal sinus, from the suprainfundibular region, extended superiorly but abruptly terminated, thereby forming a medially based cell similar to an invading frontal cell as described by Van Alyea.[5,6] In summary, in the majority of cases we studied, the suprabullar recess was located in close proximity to the frontal recess; however, the two recesses did not communicate.

Accurate nomenclature is essential in describing complex anatomy, and nowhere is this more important than in the intricate and varied ethmoid anatomy. Given the importance of standard nomenclature, it is interesting that in our review of the literature the term sinus lateralis is used primarily by Grunwald,[1,2] and by Stammberger[3] in his earlier works only. Although the term sinus lateralis may not have been universally adopted and used throughout the century, many investigators have made reference to the anatomy and apparently ascribed different terminology. Killian[7] did not use the term sinus lateralis or the term hiatus semilunaris superior. However, his 1903 anatomic drawings illustrate pneumatization arising from the retrobullar recess that he labels "upper intermediate cell of middle meatus," "cell of the ethmoidal bulla," or "middle ethmoid cell."[7] These annotations correspond to the retrobullar recess and its pneumatization tract into the bulla lamella. Zuckerkandl[8] did not use the term sinus lateralis or the term hiatus semilunaris superior; however, he used the term "sinus or fissure of the ethmoidal bulla" when referring to what we herein denote the retrobullar recess. Mouret[9,10] spoke of the *gouttiere retro-bullaire* or the "retrobullar gutter" and described the orifice of the ethmoid bulla as opening into this gutter. Van Alyea[5,6] also did not use the term sinus lateralis, but rather, used the term "hiatus semilunaris superior of Grunwald." He described "bullar cells" that arose from a "bullar groove." His descriptions and illustrations are strikingly similar to the pneumatization that we observed from the retrobullar recess and its corresponding pneumatization tracts. His eloquent description of the anatomy is noteworthy: "The normal bullar ostium, or groove, is a large crescentic opening, which lies superior, posterior and parallel to the hiatus semilunaris. Its resemblance to the hiatus semilunaris is marked, and because of this it has been designated, by Grunwald, the superior hiatus semilunaris."[5(p897)] He also wrote, "The bullar group frequently gives the impression of being one large cell containing various septums, which divide the cavity into compartments. When bullar cells communicate with each other it is generally through a wide opening which is often nearly as large as the cavities themselves."[5(p897)]

Over the years, pneumatization observed above the ethmoid bulla also led to corresponding anatomic terminology. Stammberger et al[3,4] helped us to understand the origin of the suprabullar nomenclature, pointing out the term "recessus suprabullaris," introduced by Hajek, and the term "susbullar cell," introduced by Mouret. The work of Mouret[9,10] is particularly germane to this investigation. When we began our investigation, we initially focused our literature review on Grunwald's descriptions of the sinus lateralis. It soon became clear that the anatomy had been amazingly and superbly described by Mouret with slightly different nomenclature. In 1898, Mouret addressed the French Society of Laryngology and reported his observations in 30 gross ethmoid dissections. Mouret spoke of 2 types of pneumatization, or cells, arising posterior to the infundibulum, and referred to these as retroinfundibular cells.[9,10] One opened into the posterior superior part of the infundibulum, but the other opened into an independent opening located at the superior aspect of the retrobullar gutter. He referred to this cell as the true retroinfundibular cell or, as he preferred, the *sus-bullaire* cell, meaning the cell over and above the bulla. The anatomic description and illustration match the appearance of the suprabullar recess and corresponding pneumatization tract in our investigation. Years after Mouret and Hajek, Mosher[11] wrote of this region and applied slightly different terminology. He also did not use the term sinus lateralis or the term hiatus semilunaris superior; however, he made reference to "an upper cell of the bulla which may grow forward towards and even over the rim of the orbit and make an accessory frontal sinus."[11(p393)] He referred to such a cell as a fronto-orbital cell. This cell appears similar to the suprabullar recess and its corresponding pneumatization tract noted in our dissections. We also noted the propensity of this cell for pneumatizing the orbital plate of the frontal bone.

Regardless of the terminology, it is clear that many investigators over the years have noted this area of pneumatization located above and behind the bulla. However, in the modern era, this area has been discussed infrequently and superficially. We hope our investigation serves to call attention to this important area of ethmoid anatomy and to provide more detail regarding the prevalence, extent, and character of this interesting and important space. We also hope that increased knowledge regarding the various pneumatization tracts in the superior-anterior ethmoid sinus will facilitate frontal recess surgery.

Accurate nomenclature for the sinus lateralis is desirable but challenging to attain. The terminology used to date to describe this space varies widely and includes groove, cleft, gutter, recess, cell, and sinus.[1-11] Stammberger[3] writes that the term "cell" is not a particularly good term for this space, since it is really only a cleft between the roof of the ethmoid, basal lamella, and bulla, with surface communication to the middle meatus through the hiatus semilunaris and anteriorly to the frontal recess. He adds that the sinus lateralis has not a single opening, but multiple openings, and therefore does not satisfy the criterion of a cell. We agree that the term "cell" is not the optimal term to characterize this space. However, we hesitate to accept that the sinus lateralis communicates with the middle meatus via both the hiatus semilunaris and the frontal recess, on the basis of our study. Our study revealed that in most cases, separate pneumatization "tracts" arise from the suprabullar and retrobullar recesses and drain into the middle meatus. Typically, the suprabullar recess is a single tract emanating from an ostium or slit-like opening and, therefore, does fit the criterion of a cell. However, the pneumatization emanating from the retrobullar recess was more varied and usually arose from a broad, often semilunar-shaped cleft, rather than a round or oval ostium. In some cases, 1 large pneumatization tract was evident; in others, multiple pneumatization tracts emerged with partial septations. In yet others, discrete cells were present within the bulla. Therefore, with respect to the retrobullar recess, our data support Stammberger's assessment that the sinus lateralis, especially the retrobullar recess, more closely represents a cleft rather than a cell. However, on the basis of the anatomic evidence we encountered, we prefer the descriptive term "pneumatization tracts."

Our observations of separate pneumatization tracts emanating from the suprabullar, retrobullar, and frontal recesses accord with the well-accepted theory of sinonasal embryological development. In this theory, the nasal mucosa invaginates at a specific point on the lateral nasal wall, forming the anlage of a sinus or ethmoid cell. The mesenchyme resorbs around the invagination, allowing progressive development of a sinus cavity. The embryological point at which the initial invagination occurs forms the future ostium of the sinus. Cilia develop and orient toward this ostium, allowing mucus to flow to and through the ostium.

On the basis of the evidence noted in this study, we recommend the separate terms retrobullar recess and suprabullar recess as the preferred nomenclature, rather than the term sinus lateralis. The term sinus lateralis is more general, whereas the separate terms retrobullar recess and suprabullar recess are more precise and descriptive. The latter terms identify the origin of each pneumatization tract and allude to the separate pneumatization arising from each recess. Using the two discrete terms, retrobullar recess and suprabullar recess, reduces the chance for miscommunication and increases precision and accuracy in documenting disease location. Again, our observations accord with the well-accepted principles of sinus embryology and mucociliary physiology. Each recess has a single point of embryological development and, hence, a single mucociliary drainage pathway to the middle meatus, rather than multiple drainage tracts through both the frontal recess and the middle meatus.

Our anatomic findings strongly support the recommendation of the Consensus Group on Anatomic Terminology and Nomenclature to use the separate terms suprabullar recess and retrobullar recess.[4]

Although we do recommend the separate terms retrobullar recess and suprabullar recess, we refrain from making any additional recommendations for nomenclature. Certainly, the projections from the basal lamella we describe might qualify for naming. However, we prefer in this article to focus on accurate description of our anatomic observations. We also prefer that an international gathering of otolaryngologists recommend sinonasal terminology, believing this to be the appropriate forum for introduction of new nomenclature. In that setting, a better chance might exist for widespread acceptance of the new terms.

The particular method of analysis used to study the sinus lateralis is noteworthy, as is the regional anatomic research experience of the investigators. Although endoscopic and CT analysis quickly provided the answer to our original question of prevalence, we found that endoscopic and CT analyses were not optimal for analyzing fully the extent and character of the sinus lateralis. Data were presented in a way that left much room for interpretation and interobserver error. A different method of analysis, highly detailed gross anatomic investigation, proved to be a far better method of characterizing this space. Gross dissection permits all pneumatization tracts to be followed with minimal disruption to the contiguous structures. Probes can easily be placed from the larger sinuses through the ethmoidal pre-recesses to demonstrate clearly the origin and fate of nearby pneumatization tracts. For research purposes, gross dissection provides the most accurate characterization of the sinus lateralis. Studies that do not incorporate this method into their design should be viewed skeptically. We acknowledge that CT analysis using "fly-through" technology, as opposed to incremental data, may allow accurate analysis of the sinus lateralis. We chose to use incremental data, as this method is what is currently available to the vast majority of practicing otolaryngologists. It is interesting that initially, endoscopic dissection was not considered reliable; however, after dedicated gross anatomic analysis, our impression changed. This outcome speaks to the humbling nature of studying sinonasal anatomy, especially through the endoscope. The subtleties of the sinus lateralis were not apparent to the primary author (W.E.B.) even after a decade of dedicated anatomic study and surgery. Only after systematic study of the sinus lateralis and many gross anatomic dissections were the subtleties and varied anatomic features accurately appreciated on endoscopy. It is therefore recommended that in future studies of the sinus lateralis, researchers perform a series of gross anatomic dissections before endoscopic analysis. It is also recommended that cutting forceps and a precise mucosal sparing technique be used in conducting endoscopic dissections. With cutting forceps, delicate ethmoid structures can be dissected and pneumatization tracts followed. In this way, boundary structures can be preserved while demonstrating the recesses. The dissection must be conducted with the greatest care to yield accurate, reliable information.

We hope that the anatomic features of the sinus lateralis detailed in this communication will reduce the number of dissections needed for future researchers to make reliable assessments of the gross and endoscopic anatomy. We submit our findings as an initial comprehensive exploration into a specific region of the ethmoid labyrinth, rather than as the final word on the subject. Additional studies will certainly enrich our collective understanding of this complex region. The sinus lateralis is no less complex or varied than the frontal recess or the posterior ethmoid sinus. A single study cannot realistically characterize all the possible variations and themes. Just as with fingerprint analysis or HLA typing, there are general categories but individual differences with the sinus lateralis. The general theme is that of separate suprabullar and retrobullar recesses, with pneumatization tracts emanating from each recess. The two major anatomic variations on this theme appear to be, first, a rudimentary suprabullar recess with a dominant retrobullar recess, and second, a dominant suprabullar recess that progresses to become the frontal recess and to pneumatize the frontal bone or sinus.

Delineating the anatomic features of the retrobullar and suprabullar recesses leads to a more complete understanding of the complex anatomic relationships within the ethmoid sinus, thereby demystifying the ethmoid "labyrinth." Neighboring spaces such as the frontal recess become easier to understand. It follows that surgeons who invest the time to appreciate more fully this regional anatomy will prepare themselves better for the challenges that await them in operating in the frontal recess and the superior aspect of the ethmoid sinus.

ACKNOWLEDGMENTS — The authors acknowledge the kind assistance of Dr Peter Hechl in translating the German reference sources, and of Karen E. Liese in translating the French reference materials. We also thank George Holborow of the Uniformed Services University of the Health Sciences, Anatomic Teaching Laboratory, for his kind and exceptional support with anatomic study material.

REFERENCES

1. Grunwald L. Deskriptive und topographische Anatomie der Nase und ihrer Nasenhohlen. In: Denker A, Kahler O, eds. Handbuch der Hals-Nasen-Ohrenheilkunde. Vol 1. Berlin: Springer-Bergmann, 1925:1-95.

2. Grunwald L. Die Lehre von den Naseneiterungen. Munich: Lehmann, 1896.

3. Stammberger H. Functional endoscopic sinus surgery: the Messerklinger technique. Philadelphia, Pa: BC Decker, 1991.

4. Stammberger HR, Kennedy DW, Bolger WE, et al. Paranasal sinuses: anatomic terminology and nomenclature. Ann Otol Rhinol Laryngol Suppl 1995;104(suppl 167):7-16.

5. Van Alyea OE. Ethmoid labyrinth: anatomic study, with consideration of the clinical significance of its structural characteristics. Arch Otolaryngol 1939;29:881-901.

6. Van Alyea OE. Frontal cells. Arch Otolaryngol 1941;34: 11-23.

7. Killian GJ. Die Nebenhohlen der Nase in ihren Lageziehungen zu den Nachbarorganen. Jena: Fischer, 1903.

8. Zuckerkandl E. Anatomie normale et pathologie des fosses nasales et de leurs annexes pneumatiques. Paris: G. Masson, 1895.

9. Mouret J. Anatomie des cellules ethmoidales. Rev Hebdo Laryngol Otol Rhinol 1889;31:913-24.

10. Mouret J. Rapport du sinus frontale avec le cellules ethmoidales. Rev Hebdo Laryngol Otol Rhinol 1901;46:577-95.

11. Mosher HP. Symposium on the ethmoid: the surgical anatomy of the ethmoidal labyrinth. Trans Am Acad Ophthalmol Otolaryngol 1929;34:376-410.

Expertise and Experience in Functional Endoscopic Paranasal Surgery

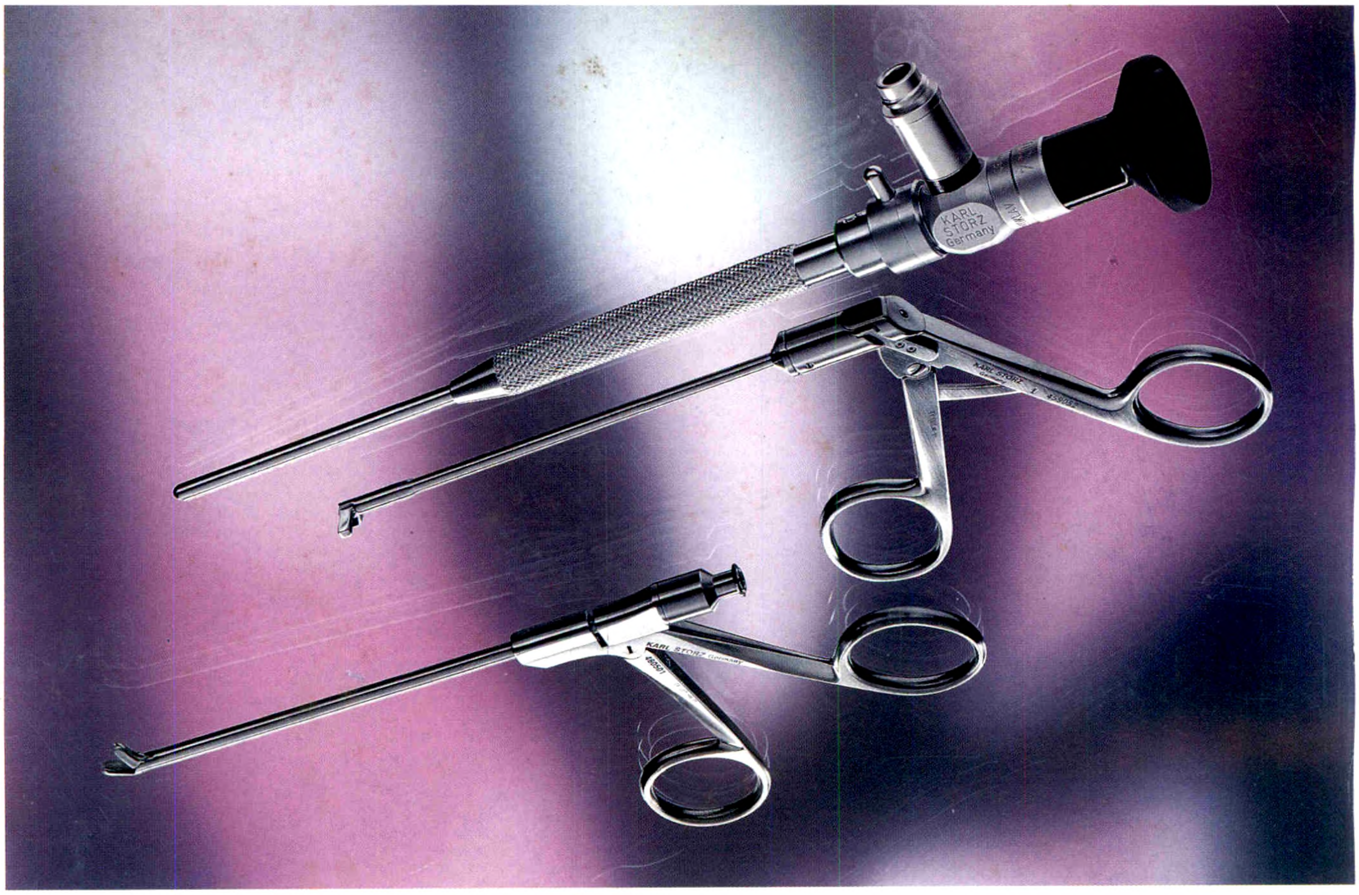

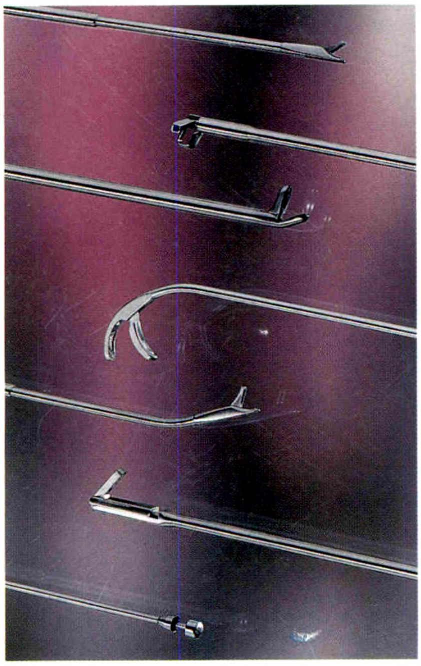

Count on Karl Storz to deliver the expertise that has made functional endoscopic paranasal surgery a precise, reliable technique the world over.

Nearly 20 years after introducing the first dedicated instruments for functional endoscopic paranasal surgery, Karl Storz remains the leading choice. Each instrument is the result of active collaboration with renowned practitioners. So surgeons can turn to Karl Storz with confidence for slender, ergonomically balanced instruments, which allow precise dissection. And HOPKINS® rod lens optics ensure brighter images, wider viewing angles and superior image sharpness over the entire field of view.

To learn more, call Karl Storz at **(800) 421-0837** or contact your local Karl Storz representative.

KARL STORZ GmbH & Co.
Mittelstraße 8, D-78532 Tuttlingen, Germany
Postfach 230, D-78503 Tuttlingen, Germany
Telefon: (07461) 70 80
Telefax: (07461) 70 81 05

KARL STORZ Endoscopy-America, Inc.
600 Corporate Pointe
Culver City, CA 90230-7600
Telephone: (310) 338-8100
(800) 421-0837
Telefax: (310) 410-5530

KARL STORZ Endoscopy-Canada, Inc.
438 University Avenue, Suite 1800
Toronto, Ontario, Canada M5G 2K8
Telephone: (416) 596-9900
(800) 268-4880 (English)
(800) 361-7388 (Francais)
Telefax: (416) 596-9333

KARL STORZ Endoscopia Latino America
815 N.W. 57th Ave., Ste. No. 480
Miami, FL 33126-2042, USA
Telefono: (305) 262-8980
Telefax: (305) 262-8986

E-mail: karlstorz-marketing@karlstorz.de
Internet: http://www.karlstorz.de
http://www.karlstorz.com

STORZ
KARL STORZ ENDOSCOPY

THE DIAMOND STANDARD

© 2000 Karl Storz Endoscopy-America, Inc.

VOLUME 110 (6) — JUNE 2001

— Founded in 1892 —

ANNALS

OF OTOLOGY, RHINOLOGY & LARYNGOLOGY

Official Organ of the
AMERICAN LARYNGOLOGICAL ASSOCIATION
AMERICAN BRONCHO-ESOPHAGOLOGICAL ASSOCIATION

LARYNGEAL REINNERVATION WITH THE HYPOGLOSSAL NERVE

APPING OF BRAIN STEM NEURONAL CIRCUITRY ACTIVE DURING SWALLOWING

COMBINED BUCCAL MUCOSA ISLAND AND STERNOHYOID FLAPS: A NEW TECHNIQUE OF HEMILARYNGEAL RECONSTRUCTION

AVAILABLE ON OUR WEB SITE ONLY:
TERNET RESOURCES FOR OTOLARYNGOLOGISTS

ANNALS
PUBLISHING CO

Superior results in less time.

The Montgomery® Thyroplasty Implant System

A complete system including implants, measuring devices, and 13-piece surgical instrument set.

Learn About Our Success – Listen to Our Patients

The Montgomery® Thyroplasty Implant System has successfully improved the communication abilities of thousands of patients with unilateral vocal cord paralysis. Surgeons appreciate the system's superior quality, standardization and simplified implantation procedure. Call us toll-free to learn more about how your patients can benefit from this exciting new system.

- **Reduced trauma and surgery time**
- **Reversible**
- **Proven clinical success**
- **Complete standardized system**
- **No need to hand-fashion implants**
- **Self-retaining implant design**

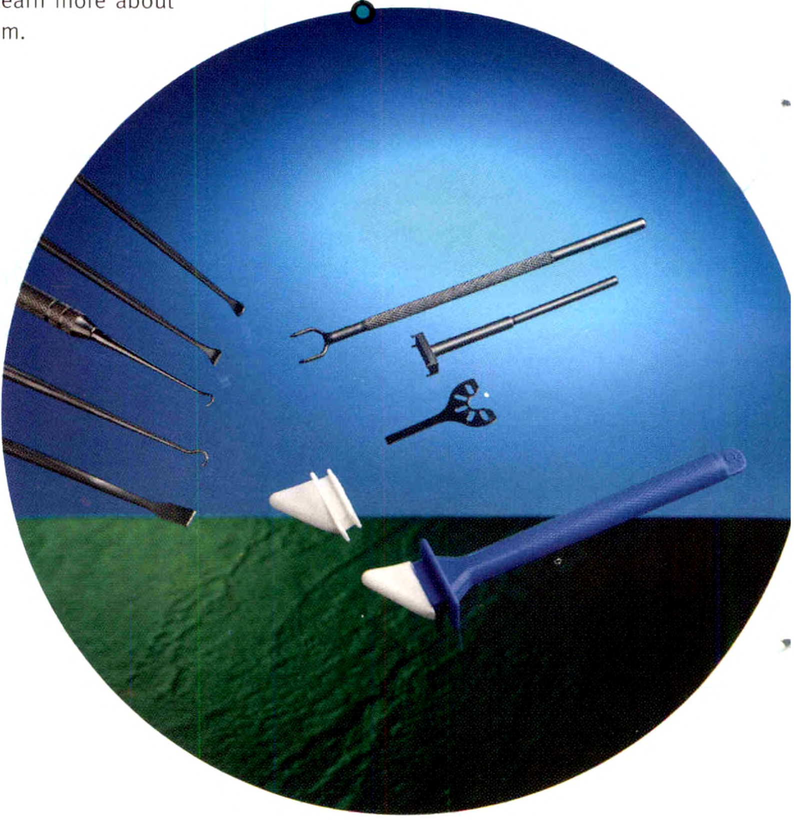

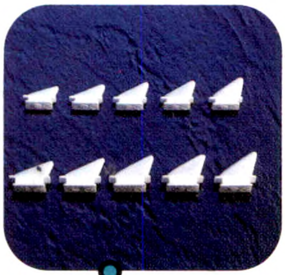

Male and female standardized implants, no need to hand-fashion implants.

Measuring devices simulate implant to determine optimum voice prior to implant insertion

Call us toll-free today for your
FREE INFORMATION PACKAGE
Including video and manual for use!
1-800-433-BMPI (2674)

Boston
Medical
Products

ANNALS OF OTOLOGY, RHINOLOGY & LARYNGOLOGY

VOLUME 110 JUNE 2001 NUMBER 6

CONTENTS

FROM THE AMERICAN BRONCHO-ESOPHAGOLOGICAL ASSOCIATION

Unique Presentation of a Bronchial Foreign Body in an Asymptomatic Child
Michael A. Freiman, MD; J. Scott McMurray, MD 495

Open Zenker's Diverticulectomy Using Stapling Techniques
Nicolas Y. Busaba, MD; Edwin Ishoo, MD; David Kieff, MD 498

Mapping of Brain Stem Neuronal Circuitry Active During Swallowing
Asif Amirali, MD; Greg Tsai, MD; Nicole Schrader, MD;
Donald Weisz, PhD; Ira Sanders, MD 502

FROM THE AMERICAN LARYNGOLOGICAL ASSOCIATION

Hemicricoidectomy for Voice Rehabilitation Following Hemilaryngectomy With Ipsilateral Arytenoid Removal
Milan R. Amin, MD; James A. Koufman, MD 514

Anterior Window Laryngoplasty: A New Anatomic Approach For Posterior Glottic and Subglottic Stenosis
Tulio A. Valdez, MD; Zhi Wang, MD; Roman Schumann, MD; Stanley M. Shapshay, MD 519

Intraoperative Pediatric Laryngeal Electromyography: Experience and Caveats With Monopolar Electrodes
Daniel L. Wohl, MD; Jefferson K. Kilpatrick, MD; Robert T. Leshner, MD;
Wayne T. Shaia, MD 524

INDEPENDENT CONTRIBUTIONS

Laryngeal Reinnervation With the Hypoglossal Nerve. I. Physiology, Histochemistry, Electromyography, and Retrograde Labeling in a Canine Model
Randal C. Paniello, MD; Steven E. West, MD; Patty Lee, MD 532

Combined Buccal Mucosa Island and Sternohyoid Flaps: A New Technique of Hemilaryngeal Reconstruction Studied in a Canine Model
Robert J. Andrews, MD; Keith E. Blackwell, MD; Gerald S. Berke, MD;
Marilene B. Wang, MD; Thomas C. Calcaterra, MD; Joel A. Sercarz, MD 543

Aerodynamic Profiles of a Hemilarynx With a Vocal Tract
Fariborz Alipour, PhD; Douglas Montequin, MA; Niro Tayama, MD 550

Effects of Length and Depth of Vibration of the Vocal Folds on the Relationship Between Transglottal Pressure and Fundamental Frequency of Phonation in Canine Larynges
Kenichi Kataoka, MD; Kazutomo Kitajima, MD 556

Isolated Vestibular Areflexia After Blunt Head Trauma
Jean-Philippe Guyot, MD; Pierre Liard, MD; Kristina Thielen, MD; Izabel Kos, MD 562

Cochlear Microphonic Potentials: A New Recording Technique
Francisco Carricondo, PhD; Pablo Gil-Loyzaga, MD, PhD;
Julio Sanjuán-Juaristi, MD; Joaquín Poch-Broto, MD 565

Role of Interleukin-1β in a Murine Model of Otitis Media With Effusion
Tetsuo Watanabe, MD; Takashi Hirano, MD; Masashi Suzuki, MD;
Yuichi Kurono, MD; Goro Mogi, MD 574

Bell's Palsy: Electrodiagnostics Are Not Indicative of Cerebrospinal Fluid Abnormalities
Christiane Birkmann, MD; Stephan Bamborschke, MD; Marco Halber, MD;
Walter F. Haupt, MD 581

Topical Ascorbic Acid Reduces Myringosclerosis in Perforated Tympanic Membranes. A Study in the Rat
Jorge E. Spratley, MD; Sten O. Hellström, MD, PhD; Cecilia K. Mattsson, MD, PhD;
Manuel Pais-Clemente, MD, PhD 585

IMAGING CASE STUDY OF THE MONTH

Intracranial Complications of Ethmoiditis Evidenced by Magnetic Resonance Imaging
Rémi Marianowski, MD, PhD; Jérome Forcioli, MD; Murielle Bouhnik, MD;
Jean-Louis Aït Amer, MD; Francis Brunelle, MD; Yves Manach, MD 592

SOFTWARE REVIEW

Experience With StatView 5.0
Michael Reiss, MD; Gilfe Reiss, MD 596

MISCELLANEOUS

Book Reviews 598

Information for Subscribers 1a

Index to Advertisers 8a

AVAILABLE ON OUR WEB SITE ONLY

Internet Resources for Otolaryngologists
Dimitrios G. Balatsouras, MD; Antonis Kaberos, MD; Stavros G. Korres, MD;
Dimitrios Kandiloros, MD; Eleftherios Ferekidis, MD;
Constantinos Economou, MD .... http://www.Annals.com

CLINICAL AND RESEARCH FELLOWSHIP IN OTOLOGY AND NEUROTOLOGY

MASSACHUSETTS EYE AND EAR INFIRMARY

Fellowship training is offered for individuals who aspire to a full-time academic career. Two- and three-year fellowships are available. Three-year fellowships provide additional opportunities for basic research training, while the two-year fellowship will provide opportunities for clinical research. Board eligibility or certification is required.

For more information, contact:

Michael J. McKenna, MD
Dept of Otolaryngology
Massachusetts Eye and Ear Infirmary
243 Charles Street
Boston, MA 02114
(617) 573-3654

A2

Courses on the Lateral Approaches to the Skull Base
(In English)

Course Director:
Mario Sanna, MD

This cadaver hands-on workshop provides the individual opportunity to participate in:

- Video presentation of techniques and clinical cases
- Didactic presentations
- Performing the surgical procedures on specially prepared bones and half-heads
- Discussions

For additional information, contact:

Secretary Gruppo Otologico
Via Emmanueli n.42
29100 Piacenza - Italy
telephone: 0523/754362
fax: 0523/453708
E-mail: Corsi.Sanna@otologic.it

A161

Advances in Endoscopic Management of Nasal & Sinus Disorders

November 1-3, 2001
23 CME Credit Hours

Program Highlights

- **Hands-on Dissection**
- **Lecture only option**
- **Frontal Surgery**
- **Sphenoid Surgery**
- **Image-Guided Surgery**
- **Fungal Rhinosinusitis**
- **Powered Instrumentation**
- **Polyposis**
- **Comprehensive Medical Management**

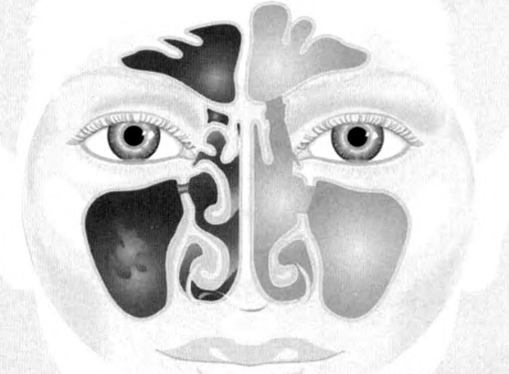

Course Directors

Martin J. Citardi, MD
Donald C. Lanza, MD

Honored Guest

David W. Kennedy, MD

Special Guest Faculty

Berrylin J. Ferguson, MD
Howard L. Levine, MD
Richard R. Orlandi, MD
Brent A. Senior, MD

Cynthia Kepp
Education Coordinator
Course No. 020116

216-444-4831
888-216-4012
Fax: 216-444-4830
keppc@ccf.org
www.ccf.org/misc

Department of Otolaryngology and Communicative Disorders
and The Minimally Invasive Surgery Center

The Cleveland Clinic Foundation, Cleveland, Ohio

ANNALS OF OTOLOGY, RHINOLOGY & LARYNGOLOGY

— Founded in 1892 —

Editor

BRIAN F. McCABE, MD
Iowa City, Iowa

Associate Editors

CHARLES D. BLUESTONE, MD
Pittsburgh, Pa

GEORGE A. GATES, MD
Seattle, Wash

OLLIVIER LACCOURREYE, MD
Paris, France

Board of Editors

JOHN G. BATSAKIS, MD	Houston, Tex; Kalkaska, Mich
JOEL M. BERNSTEIN, MD, PhD	Buffalo, NY
ANDREW BLITZER, MD, DDS	New York, NY
DERALD E. BRACKMANN, MD	Los Angeles, Calif
POUL BRETLAU, MD, DMSc	Copenhagen, Denmark
ITZHAK BROOK, MD	Washington, DC
RICHARD A. BUCKINGHAM, MD	Park Ridge, Ill
RICHARD A. CHOLE, MD, PhD	St. Louis, Mo
ROBIN T. COTTON, MD	Cincinnati, Ohio
ALFIO FERLITO, MD	Udine, Italy
UGO FISCH, MD	Zurich, Switzerland
IMRE FRIEDMANN, MD, ScD	Middlesex, England
BRUCE GANTZ, MD	Iowa City, Iowa
LEE A. HARKER, MD	Omaha, Neb
JEFFREY P. HARRIS, MD, PhD	San Diego, Calif
GERALD B. HEALY, MD	Boston, Mass
LAUREN D. HOLINGER, MD	Chicago, Ill
WILLIAM F. HOUSE, MD	Los Angeles, Calif
STEVEN K. JUHN, MD	Minneapolis, Minn
TIMOTHY T. K. JUNG, MD, PhD	Loma Linda, Calif
DAVID W. KENNEDY, MD	Philadelphia, Pa
FRANK E. LUCENTE, MD	New York, NY
WILLIAM L. MEYERHOFF, MD, PhD	Dallas, Tex
JOSEF MILLER, PhD	Ann Arbor, Mich
AAGE R. MØLLER, PhD	Dallas, Tex
WILLIAM W. MONTGOMERY, MD	Boston, Mass
EUGENE N. MYERS, MD	Pittsburgh, Pa
JOSEPH B. NADOL, Jr, MD	Boston, Mass
YASUYA NOMURA, MD	Tokyo, Japan
LORNE S. PARNES, MD	London, Canada
RANDALL L. PLANT, MD	Norfolk, Va
JAI H. RYU, PhD	Winston-Salem, NC
ISAMU SANDO, MD	Pittsburgh, Pa
CLARENCE T. SASAKI, MD	New Haven, Conn
ROBERT T. SATALOFF, MD, DMA	Philadelphia, Pa
RICHARD J. H. SMITH, MD	Iowa City, Iowa
HEINZ R. STAMMBERGER, MD	Graz, Austria
DEAN M. TORIUMI, MD	Chicago, Ill
JAN E. VELDMAN, MD, PhD	Utrecht, The Netherlands
BRUCE M. WENIG, MD	Bronx, NY
T. J. YOO, MD, PhD	Memphis, Tenn
STEVEN M. ZEITELS, MD	Boston, Mass

Software Review and Computer Applications Editor

KEVIN T. KAVANAGH, MS, MD .... Somerset, Ky

Imaging Editor and Book Review Editor

DENNIS G. PAPPAS, MD .... Birmingham, Ala

Emeritus Board Members

WESLEY H. BRADLEY, MD	Albany, NY
JACK D. CLEMIS, MD	Chicago, Ill
SEYMOUR COHEN, MD	Los Angeles, Calif
CHARLES W. CUMMINGS, MD	Baltimore, Md
PATRICK J. DOYLE, MD	Vancouver, Canada
ARNDT J. DUVALL III, MD	Minneapolis, Minn
JOHN M. FREDRICKSON, MD	St Louis, Mo
RICHARD R. GACEK, MD	Syracuse, NY
JEROME C. GOLDSTEIN, MD	Lake Worth, Fla
SIR DONALD F. N. HARRISON, MD PhD	London, England
SAM E. KINNEY, MD	Cleveland, Ohio
JOHN A. KIRCHNER, MD	New Haven, Conn
DAVID J. LIM, MD	Los Angeles, Calif
FRED H. LINTHICUM, Jr, MD	Los Angeles, Calif
MICHEL PORTMANN, MD	Bordeaux, France
LORING W. PRATT, MD	Waterville, Me
FRANK N. RITTER, MD	Ann Arbor, Mich
ROBERT J. RUBEN, MD	Bronx, NY
JACOB SADÉ, MD	Tel Aviv, Israel
WILLIAM H. SAUNDERS, MD	Columbus, Ohio
RUEDIGER THALMANN, MD	St Louis, Mo
HARVEY M. TUCKER, MD	Cleveland, Ohio
PAUL H. WARD, MD	Los Angeles, Calif

Ann Otol Rhinol Laryngol 110:2001

UNIQUE PRESENTATION OF A BRONCHIAL FOREIGN BODY IN AN ASYMPTOMATIC CHILD

MICHAEL A. FREIMAN, MD J. SCOTT MCMURRAY, MD

MADISON, WISCONSIN

A child who aspirates a foreign body may present in many ways. We present the case of an 8-year-old boy whose initial presentation consisted only of his preoccupation with his lost toy and his gesturing toward his oral cavity. There was no witnessed coughing or choking episode, and there were no initial physical examination findings of note, and no abnormalities on appropriate radiographic studies. The patient was transferred to our institution for further evaluation and management. Our careful examination revealed a slight wheeze at the left upper lobe. Endoscopy was immediately performed, and bronchoscopy revealed a yellow, tubular, plastic foreign body in the left main bronchus through which the patient was breathing freely. This was removed without incident by means of optical graspers. The physical characteristics of this foreign body, including its small size, relatively inert material, and large lumen, allowed this patient to present relatively asymptomatically. This case demonstrates the need for a high index of suspicion in the evaluation and management of foreign bodies in the aerodigestive tract.

KEY WORDS — aspiration, bronchus, foreign body.

INTRODUCTION

A child who aspirates a foreign body may present in many ways. There are usually 3 clinical phases of foreign body aspiration.[1] The first phase consists of coughing, choking, and/or gagging that occurs at the moment of aspiration and may lead to acute airway obstruction. If this first phase is not witnessed by the child's caregivers, the diagnosis of an aspirated foreign body is more challenging. The second phase is the asymptomatic phase, during which the foreign body becomes lodged and the airway's protective reflexes become fatigued. This phase may last from hours to weeks. The symptoms may vary in severity, depending on the object's size, the degree of obstruction, and the surrounding tissue reaction. The third phase is the complication phase, during which obstruction, erosion, or infection can lead to various manifestations of pulmonary disease. We present the case of an 8-year-old boy whose relatively asymptomatic presentation can be attributed to the physical characteristics and location of his aspirated foreign body.

CASE REPORT

An 8-year-old boy was seen at an outside institution for the evaluation of a potential aerodigestive tract foreign body. There was no witnessed coughing or choking episode or other presenting symptoms except for his concern about his lost toy and his gesturing toward his oral cavity. Reportedly, the findings of the physical examination were unremarkable. Anteroposterior and lateral radiographs of the neck did not reveal any laryngeal or tracheal foreign bodies. Inspiratory and expiratory chest radiographs failed to show any atelectasis, hyperinflation, or mediastinal shift. Interestingly, a computed tomography (CT) scan of the neck and chest was also performed and was negative. The patient was transferred to our institution for further evaluation and management upon the insistence of his parents.

Our careful examination revealed a slight wheeze at the left upper lobe in addition to the child's preoccupation and gesturing. The patient was taken immediately to the operating room for endoscopy. There was no foreign body identified in the oral cavity, oropharynx, hypopharynx, or larynx on microlaryngoscopy. Bronchoscopy revealed no foreign body in the trachea or right main bronchus. Examination of the left main bronchus, however, revealed a yellow, tubular, plastic foreign body through which the patient was breathing freely (Fig 1). It was removed without incident by means of optical graspers. The findings of repeat bronchoscopy and of esophagoscopy were normal. The patient tolerated the procedure well, there were no complications, and the patient was discharged on postoperative day 1 with no sequelae. The foreign body was a plastic toy part that was mainly cylindrical in shape; its length, outer diameter, proximal inner diameter, and distal inner diameter measured approximately 12.0 mm, 7.5 mm, 5.0 mm, and 3.0 mm, respectively (Fig 2).

DISCUSSION

This case illustrates many important features in

From the Department of Surgery, Division of Otolaryngology–Head and Neck Surgery, University of Wisconsin, Madison, Wisconsin.

Presented in poster form at the meeting of the American Broncho-Esophagological Association, Orlando, Florida, May 15-16, 2000.

CORRESPONDENCE — J. Scott McMurray, MD, Dept of Surgery, Division of Otolaryngology–Head and Neck Surgery, University of Wisconsin, 600 Highland Ave, Madison, WI 53972-3236.

University College of Medicine LIBRARY

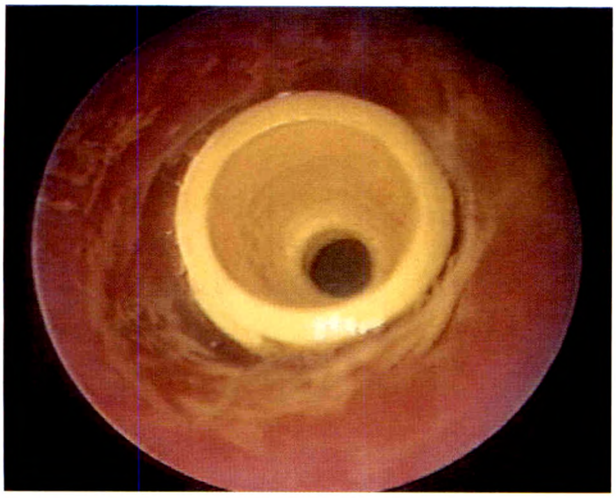

Fig 1. Tubular foreign body embedded in left main bronchus of 8-year-old boy. He was breathing comfortably through central lumen.

the evaluation and management of foreign bodies in the aerodigestive tract. The first important point is that as many as 50% of patients with foreign body aspiration do not have a witnessed episode of coughing, choking, or gagging.[2] Their absence can make the diagnosis more difficult, and therefore, a high index of suspicion is always necessary. Our patient's parents did not witness this first clinical phase, but their suspicion, as well as ours, was high. The second important point is that the physical examination findings may be relatively unremarkable. Of airway foreign bodies, approximately 80% to 90% are found in the bronchi.[3] Patients with bronchial foreign bodies will classically present with a triad of cough, wheezing, and decreased breath sounds. Sixty-five percent of patients present with the classic triad, according to a report of a large series,[4] and as many as 95% present with at least 1 finding.[5] At first, our patient reportedly had none of these symptoms or signs, but our careful examination did reveal a slight wheeze in the left upper lobe. The third important point is that plain film radiography is neither sensitive nor specific in the diagnosis of foreign body aspiration. One study reported that 35% of 400 patients with normal findings on radiographic studies were later found to have bronchial foreign bodies.[6] Our patient's radiographic studies, including a CT scan, were negative. The CT scan was performed at an outside institution, and this imaging modality is not part of our standard of practice. There are no clear indications for CT scans in patients suspected of having a foreign body within the airway, and they likely are not cost-effective in the evaluation, since these patients will need to undergo endoscopy anyway. The information from the CT scan would not alter the management of these patients, and the time necessary to perform this study may actually put the patient at increased risk. The fourth important point is that the physical characteristics of the aspirated foreign body play a large role in the development and manifestations of symptoms in the individual patient. Plastic objects constitute approximately 5% to 15% of airway foreign bodies and tend to remain longer, because they are inert and radiolucent.[7] The physical characteristics of the aspirated bronchial foreign body in our patient, including its small size, relatively inert material, and large lumen, allowed our patient to present in a relatively asymptomatic fashion.

This case illustrates that the history, physical examination findings, radiographic findings, and physical characteristics of the foreign body may make the diagnosis of an aspirated foreign body challenging. Foreign bodies account for approximately 3,000 deaths per year.[8] Chevalier Jackson's management techniques reduced the mortality rate to about 2%,[9]

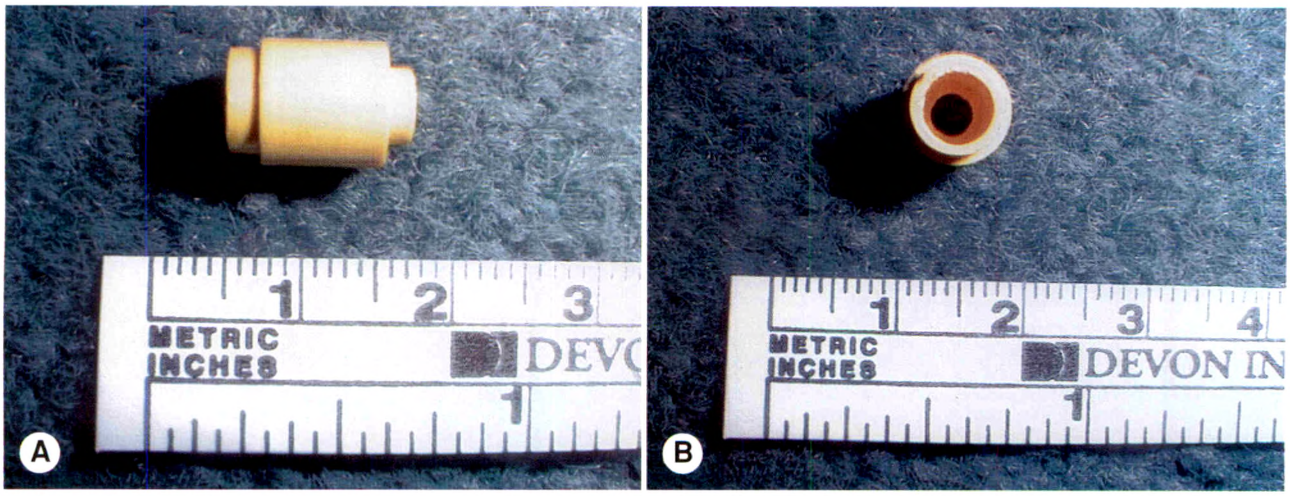

Fig 2. Tubular foreign body extracted from left main bronchus of 8-year-old boy. **A)** Length measured approximately 12.0 mm. **B)** Outer diameter, proximal inner diameter, and distal inner diameter measured approximately 7.5 mm, 5.0 mm, and 3.0 mm, respectively.

which is also the present rate.[4,5,10] Earlier diagnosis correlates with fewer complications, as most complications are the result of delayed diagnosis.[4] This case once again demonstrates the need for a high index of suspicion in the evaluation and management of foreign bodies in the aerodigestive tract.

REFERENCES

1. Darrow DH, Holinger LD. Foreign bodies of the larynx, trachea, and bronchi. In: Bluestone C, Stool S, eds. Pediatric otolaryngology. Philadelphia, Pa: WB Saunders, 1996:1390-401.
2. Friedman EM. Caustic ingestion and foreign bodies in the aerodigestive tract. In: Bailey BJ, ed. Head and neck surgery–otolaryngology. Philadelphia, Pa: Lippincott-Raven, 1998: 1159-67.
3. Esclamado RM, Richardson MA. Laryngotracheal foreign bodies in children. A comparison with bronchial foreign bodies. Am J Dis Child 1987;141:259-62.
4. Inglis AF Jr, Wagner DV. Lower complication rates associated with bronchial foreign bodies over the last 20 years. Ann Otol Rhinol Laryngol 1992;101:61-6.
5. Black RE, Johnson DG, Matlak ME. Bronchoscopic removal of aspirated foreign bodies in children. J Pediatr Surg 1994;29:682-4.
6. Mu L, He P, Sun D. Inhalation of foreign bodies in Chinese children: a review of 400 cases. Laryngoscope 1991;101: 657-60.
7. Murray AD, Mahoney EM, Holinger LD. Foreign bodies of the airway and esophagus. In: Cummings CW, ed. Pediatric otolaryngology–head and neck surgery. St Louis, Mo: Mosby, 1998:377-87.
8. Kramer TA, Riding KH, Salkeld LJ. Tracheobronchial and esophageal foreign bodies in the pediatric population. J Otolaryngol 1986;15:355-8.
9. Chatterji S, Chatterji P. The management of foreign bodies in air passages. Anaesthesia 1972;27:390-5.
10. Cohen SR, Herbert WI, Lewis GB Jr, Geller KA. Foreign bodies in the airway. Five-year retrospective study with special reference to management. Ann Otol Rhinol Laryngol 1980;89:437-42.

Ann Otol Rhinol Laryngol 110:2001

OPEN ZENKER'S DIVERTICULECTOMY USING STAPLING TECHNIQUES

NICOLAS Y. BUSABA, MD
BOSTON, MASSACHUSETTS

EDWIN ISHOO, MD
CINCINNATI, OHIO

DAVID KIEFF, MD
BOSTON, MASSACHUSETTS

This is a prospective review of patients who underwent Zenker's diverticulectomy, closure of the pharyngotomy with nonabsorbable staples, and cricopharyngeal myotomy through an open neck approach over a period of 2 years. The study group consisted of 9 men with a mean age of 67 years. The diagnosis of Zenker's diverticulum was based on a barium swallow esophagram. The mean operative time was 1.5 hours, with a mean estimated blood loss of 25 mL. Barium swallow esophagrams performed on the first postoperative day showed no pharyngeal fistulas. Oral feeding was started after the esophagram. One patient was discharged on postoperative day 1, 1 was discharged on postoperative day 3, and the remaining 7 were discharged on postoperative day 2. All patients were able to take oral feeding by postoperative day 1. There were no operative complications in this series. We conclude that stapling with nonabsorbable staples is a relatively safe and effective method for closing pharyngeal defects after Zenker's diverticulectomy. The technique leads to shortening of the operative time and hospital stay, and allows early resumption of oral feeding.

KEY WORDS — pharyngotomy, stapler, Zenker's diverticulum.

INTRODUCTION

Zenker's diverticulum is a herniation of the posterior mucosal wall of the hypopharynx through a weakened muscular layer located immediately above the esophageal inlet. Abraham Ludlow first described it in 1764.[1] The classic Zenker's diverticulum is readily diagnosed with a barium swallow esophagram (BaS).

The goals of the surgical treatment of Zenker's diverticulum are to reduce morbidity, shorten hospitalization, and ultimately achieve successful resolution of symptoms. Different surgical approaches and techniques have been described, ranging from the traditional diverticulectomy with cricopharyngeal myotomy through an open neck approach to the more recent endoscopic treatment.[1] Endoscopic treatment has steadily gained in popularity since Dohlman and Mattsson[2] reintroduced the procedure in 1960. The main advantages of the endoscopic treatment include short operative time, low morbidity, and quick resumption of oral feeding. On the other hand, the open neck approach allows for a more controlled and precise diverticulectomy, and allows for cricopharyngeal myotomy via improved exposure. However, it became less desirable because of the need to close a pharyngotomy defect and the resultant morbidity, delayed oral feeding, and longer hospital stay.

In-line nonabsorbable staples have been used relatively safely for alimentary tract division and anastomosis during bowel surgery for many years. Stapling techniques have also been described for Zenker's diverticulectomy.[3] It is generally recommended to delay oral feeding for at least 1 week after operations that involve a pharyngotomy. Closing the pharyngotomy with nonabsorbable material, such as titanium staples, could allow for earlier resumption of oral feeding. This subject, however, has not been adequately addressed previously.

The purpose of this study is to determine the safety and efficacy of using staples to close the pharyngotomy defect after diverticulectomy via an open neck approach, and to test the hypothesis that nonabsorbable staples allow earlier resumption of oral feeding.

MATERIALS AND METHODS

This is a prospective study of 9 patients who were operated on for Zenker's diverticulum over a 2-year period. The diagnosis of Zenker's diverticulum was based on BaS. All of the patients had significant symptoms relating to the diverticulum, including dysphagia and regurgitation of food particles.

The patients in our series underwent diverticulectomy via an open neck approach through a left ante-

---

From the Department of Otolaryngology–Head and Neck Surgery, Massachusetts Eye and Ear Infirmary and Harvard Medical School (Busaba), the Division of Otolaryngology, Boston Veterans Administration Health Care System (Busaba), and the Department of Otolaryngology–Head and Neck Surgery, Boston Medical Center and Boston University School of Medicine (Ishoo), Boston, Massachusetts.

Presented at the meeting of the American Broncho-Esophagological Association, Orlando, Florida, May 15-16, 2000.

CORRESPONDENCE — Nicolas Y. Busaba, MD, Dept of Otolaryngology–Head and Neck Surgery, Massachusetts Eye and Ear Infirmary, 243 Charles St, Boston, MA 02114; e-mail: nicolas_busaba@meei.harvard.edu.

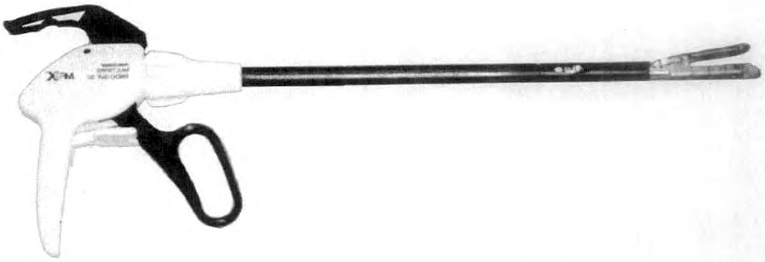

Fig 1. Endo-GIA 30 endosurgical stapler (US Surgical Corp, Norwalk, Conn).

rior-lateral incision. The diverticulum sac was identified, and the neck of the sac was skeletonized according to traditional surgical techniques. The sac was stapled at its neck with the Endo-GIA 30 endosurgical stapler (US Surgical Corp, Norwalk, Conn; Fig 1). The sac was then excised (Fig 2). A cricopharyngeal myotomy was performed. The surgical site was drained by closed-suction drainage.

Patients received 24 hours of perioperative intravenous antibiotics (cefazolin sodium) for surgical prophylaxis. A BaS was performed on postoperative day 1. The neck drain was removed and patients were started on oral feeding if the BaS revealed no leak in the hypopharynx at the site of the diverticulectomy. The patients were monitored for 12 to 24 hours after initiation of oral feeding and were discharged from the hospital once they tolerated adequate oral feeding.

The operative time, estimated blood loss, operative complications, time to resumption of oral feed-

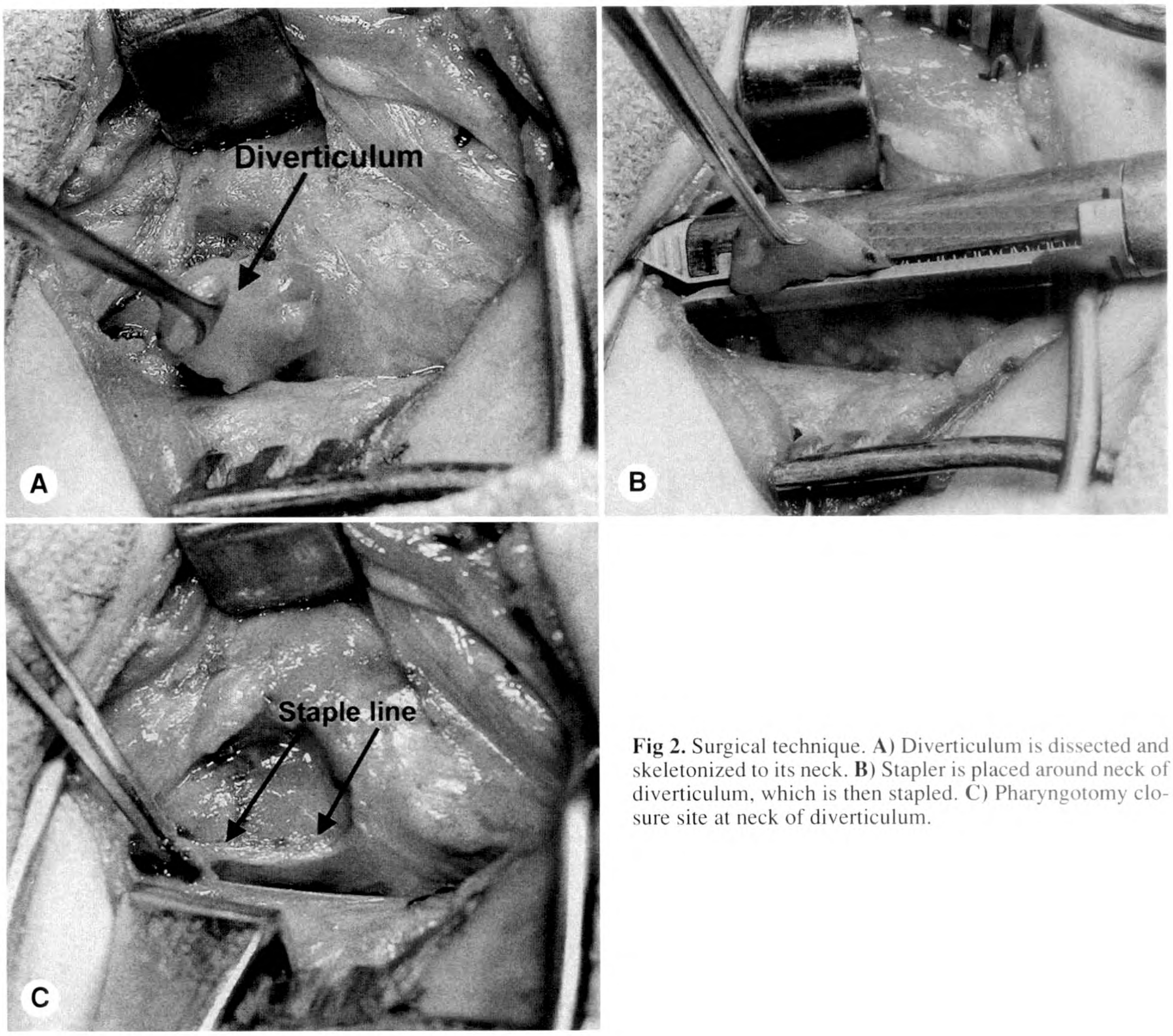

Fig 2. Surgical technique. **A**) Diverticulum is dissected and skeletonized to its neck. **B**) Stapler is placed around neck of diverticulum, which is then stapled. **C**) Pharyngotomy closure site at neck of diverticulum.

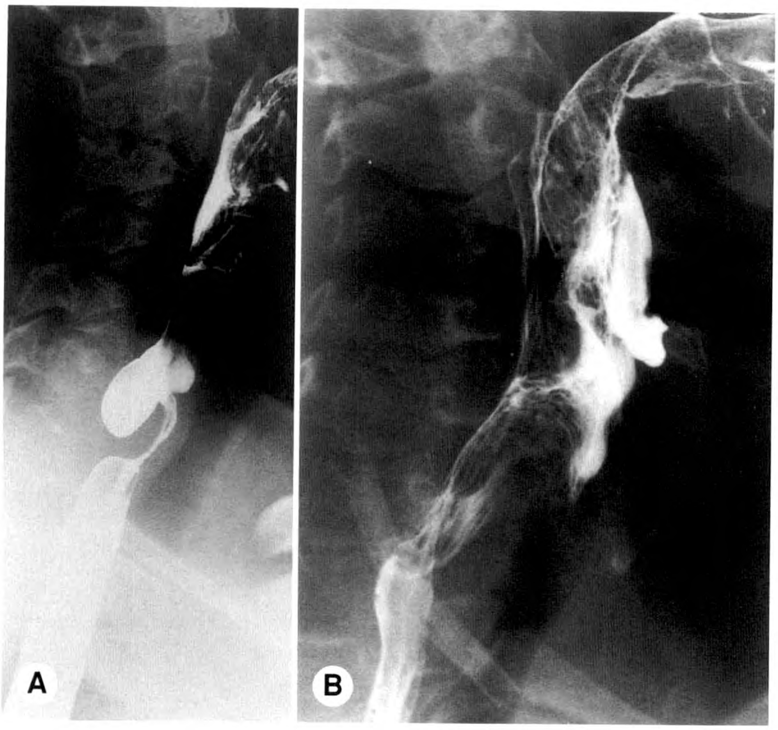

Fig 3. Barium swallow radiographs of subject from our series. **A)** Preoperative study demonstrates hypopharyngeal diverticulum. **B)** Postoperative study. Diverticulum is excised, and pharyngotomy site is sealed.

ing, and length of hospitalization were reviewed.

RESULTS

The study group comprised 9 patients who underwent surgical treatment for Zenker's diverticulum over the past 2 years. All patients were men. Their ages ranged between 62 and 75 years, with a mean of 67 years. The diagnosis was based on BaS. All of the patients in the series had symptoms relating to the diverticulum, including progressive dysphagia and regurgitation of food particles. The surgical technique used was as described above.

The average operative time was 1.5 hours (range, 1.2 to 2 hours). The mean estimated blood loss volume was 25 mL. A BaS was performed on postoperative day 1. The studies revealed no pharyngeal fistula at the site of diverticulectomy in any of the 9 patients (Fig 3). All patients were able to resume oral feeding on postoperative day 1, after the BaS. One patient was discharged around 12 hours after the initiation of oral feeding, and 7 patients were discharged from the hospital on postoperative day 2. One patient required hospitalization for 3 days because of slow oral intake despite evidence of adequate cricopharyngeal myotomy and a completely excised diverticulum on the postoperative BaS.

There were no operative complications. Eight of the patients in our series were regularly evaluated for a period of 6 months, and 1 patient for 2 months, after their operations. There were no instances of delayed pharyngeal fistula. All patients reported resolution of their symptoms.

DISCUSSION

Pharyngoesophageal diverticulum was first described by Abraham Ludlow in 1764. More than a century later, Von Zenker and Von Ziemssen reported on a collective series of 23 cases; this report led to the common eponym given to the diverticulum.[1] Zenker's diverticulum is a herniation of the posterior mucosal wall of the hypopharynx, most commonly through Killian's triangle. This is an area situated posteriorly between the lower pharyngeal constrictors and the most superior fibers of the cricopharyngeal muscle. The pathophysiology of formation of the diverticulum remains controversial and is thought to be multifactorial. Most theories on the development of Zenker's diverticulum have focused on structural or physiological abnormality of the cricopharyngeal muscle and its relationship to the remainder of pharyngeal and esophageal function.[4] Commonly reported predisposing factors include sustained high pharyngeal bolus pressure, congenital weakness in Killian's triangle, gastroesophageal reflux, and histologic abnormalities of the cricopharyngeal muscle.[5] However, subtle differences in the anatomy and pathophysiology of diverticula can affect the approach and type of surgical treatment.

There is a lack of consensus regarding the optimal surgery for Zenker's diverticulum. The surgical treatment needs to be tailored to variations in the pathophysiology and potential sites of the diverticular herniation. The ideal operation is one that leads to resolution of symptoms and early resumption of oral feeding in conjunction with low morbidity and short hospitalization. Described techniques include diverticulopexy, diverticulectomy through an open neck approach, and endoscopic division of the party wall between the diverticulum and hypopharynx.[1] Cricopharyngeal myotomy is generally considered to be the most important element in improving the surgical outcome and preventing relapse.

Endoscopic treatment became more popular after Dohlman and Mattsson[2] reintroduced this approach in 1960. The main advantages are a short operative time, a short hospital stay, and a low rate of morbidity. However, there are surgical risks and disadvantages inherent in this operation. Blind division of the party wall of the diverticulum through an endoscopic approach may injure the recurrent laryngeal nerve as it passes through the Killian-Jamieson dehiscence. It could also lead to hypopharyngeal perforation and incomplete cricopharyngeal myotomy.

The open neck approach, on the other hand, provides improved visualization and more direct access to the diverticulum. This leads to a more complete and controlled cricopharyngeal myotomy. Furthermore, variations in the site of the herniation can be identified and the surgery modified accordingly. A cricopharyngeal myotomy is not necessary if the sac has herniated through the Laimer-Haeckman space, located between the cricopharyngeal muscle superiorly and the most superior circular fibers of the esophageal wall muscle inferiorly. Performing a cricopharyngeal myotomy in this situation may in fact precipitate postoperative regurgitation. In addition, diverticulectomy through an open approach allows for histologic evaluation of the sac to rule out malignancy, the incidence of which is estimated to be as high as 3.7%.[6] Despite these advantages, the main drawback of diverticulectomy is the need to close the resultant pharyngotomy. Traditionally, this has been managed by suture closure. Patients are fed through a nasogastric tube for approximately a week until a BaS demonstrates a healed closure site. Dorion et al[3] described closing the pharyngotomy with nonabsorbable staples. This prevents contamination of the wound with saliva and pharyngeal flora, and shortens the operative time. Our study supports the benefits of using nonabsorbable staples. This technique shortens the operative time dramatically. The integrity of the pharyngeal closure is evaluated both by direct intraoperative inspection and by BaS soon after. Oral feeding can be relatively safely resumed within 24 hours of the surgery if the BaS reveals no leaks. Since the staples are made of nonabsorbable material (titanium), there is no need to wait for mucosal healing at the pharyngotomy site before initiation of oral feeding. Furthermore, the cricopharyngeal myotomy reduces the pressure generated by the food bolus at the pharyngotomy suture line in the immediate postoperative period.

Our data demonstrate the low rate of morbidity associated with this technique. Closing small pharyngotomies resulting from diverticulectomy with nonabsorbable staples is reliable and allows for early resumption of oral feeding. Further studies are needed to determine the feasibility of the technique's use in closing longer pharyngeal defects such as that following laryngectomy.

CONCLUSION

In conclusion, Zenker's diverticulectomy through an open neck approach using a stapling technique is a relatively safe and reliable technique. It is associated with a low rate of morbidity, a short operative time, and a short period of hospitalization. Pharyngeal closure with nonabsorbable staples usually allows resumption of oral feeding within 24 hours of surgery.

REFERENCES

1. Westrin KM, Ergun S, Carlsoo B. Zenker's diverticulum — a historical review and trends in therapy. Acta Otolaryngol (Stockh) 1996;116:351-60.

2. Dohlman G, Mattsson O. The endoscopic operation for hypopharyngeal diverticula. Arch Otolaryngol 1960;71:744-52.

3. Dorion D, Brown DH, Gullane PJ. Zenker's stapler diverticulectomy. J Otolaryngol 1994;23:145-7.

4. McConnel FMS, Hood D, Jackson K, O'Connor A. Analysis of intrabolus forces in patients with Zenker's diverticulum. Laryngoscope 1994;104:571-81.

5. Migliore M, Payne H, Jeyasingham K. Pathophysiologic basis for operation on Zenker's diverticulum. Ann Thorac Surg 1994;57:1616-21.

6. Feeley MA, Righi PD, Weisberger EC, et al. Zenker's diverticulum: analysis of surgical complications from diverticulectomy and cricopharyngeal myotomy. Laryngoscope 1999;109:858-61.

Ann Otol Rhinol Laryngol 110:2001

MAPPING OF BRAIN STEM NEURONAL CIRCUITRY ACTIVE DURING SWALLOWING

ASIF AMIRALI, MD
GREG TSAI, MD
DONALD WEISZ, PHD
NICOLE SCHRADER, MD
IRA SANDERS, MD
NEW YORK, NEW YORK

A poorly understood neural circuit in the brain stem controls swallowing. This experiment studied the swallowing circuit in the rat brain stem by means of *fos* immunocytochemistry. The *fos* protein is a marker of activated neurons, and under experimental conditions, repetition of a behavior causes the *fos* protein to be produced in the neurons involved in that behavior. The *fos* technique has been successfully used to delineate neural circuits involved in reflex glottic closure, cough, and vocalization; however, the technique has not been used to map the swallowing circuit. Nine rats were used in this study. Swallows were evoked in anesthetized rats for 1 hour, then, after a 4-hour delay to allow maximum *fos* production, the rats were painlessly sacrificed by perfusion. The brain stems were removed and sectioned in the frontal plane, and every fourth section was immunoreacted for *fos* protein. All sections were examined by light microscopy, and cells positive for *fos* were marked on drawings of brain stem structures for different levels throughout the brain stem. Control animals underwent sham experiments. After subtraction of the areas of *fos* labeling seen in controls, all experimental rats showed *fos*-labeled neurons in very discrete and localized areas, including practically all regions implicated by prior neurophysiology studies of swallowing. The distribution of labeled neurons was more dispersed through the brain stem than current theories of swallowing would suggest. Specifically, recent studies of swallowing control have focused on the nucleus of the solitary tract (NST) and the region surrounding the nucleus ambiguus (periambigual area) just *rostral* to the obex. These areas contained *fos*-labeled neurons, but unexpectedly, heavy labeling was found in the same areas *caudal* to the obex. Areas containing the heaviest labeling were specific subnuclei of the NST and surrounding reticular formation; the periambigual area; and the intermediate reticular zone in the pons and caudal medulla. Interestingly, none of these anatomic structures had uniform *fos* labeling; this finding suggests that the unlabeled areas are involved in other oromotor behaviors, or that the specific protocol did not activate the full population of swallowing-related neurons. A notable finding of this study is a candidate for the central pattern generator (CPG) of swallowing. Careful lesioning studies in cats strongly suggest that a region in the rostral-medial medulla contains the CPG for swallowing, although the exact location of the CPG was never pinpointed. In the homologous region of the rat brain stem, *fos* labeling was only found in a small group of neurons within the gigantocellular reticular formation that may be a candidate for the CPG. In summary, correlation with prior physiology experiments suggests that this experiment appears to have delineated many, if not all, of the components of the swallowing circuit for the first time in any mammal. In addition, other areas were found that might also be swallowing-related. One notable example is a small group of *fos*-labeled cells that may be the CPG for swallowing. Further studies are required to clarify the specific roles of the *fos*-labeled neurons seen in this study.

KEY WORDS — central pattern generator, *fos* immunocytochemistry, nucleus ambiguus, recurrent laryngeal nerve, reticular formation, solitary tract nucleus, swallowing.

Progress in the diagnosis and treatment of dysphagia requires an understanding of the central nervous system control of swallowing. Swallowing involves a sequence of well-coordinated contractions and relaxations of the muscles of the oral cavity, pharynx, and esophagus. Swallowing can be evoked by stimulation of either central (cortex and brain stem) or peripheral structures (glossopharyngeal nerve and superior laryngeal nerve [SLN]). It is a complex reflex that is controlled by interneurons organized into a functional circuit located in the brain stem; animals whose brain stems have been experimentally disconnected from the cortex are still capable of performing complete swallows.[1-3] In humans, the cortex usually initiates swallowing; however, normal swallows are performed by infants with severe cortical deficits, and by normal human fetuses before development of cortico-subcortical pathways.[4-6] Therefore, swallowing appears to be no different from a variety of repetitive oromotor acts, such as licking, suckling, and chewing, that have also been shown to have their control circuits in the brain stem.

The brain stem consists of 3 parts: the midbrain, the pons, and the medulla oblongata (Fig 1A). On the basis of lesion, stimulation, and microelectrode recording experiments, the swallowing circuit is believed to be located in the medulla oblongata.[1,3-5,7-12] The first neurons in the circuit receive and integrate afferent impulses from the cortex or the peripheral

---

From the Departments of Otolaryngology (Amirali, Tsai, Schrader, Sanders) and Neurosurgery (Weisz), Mount Sinai School of Medicine, New York, New York. This study was performed in accordance with the PHS Policy on Humane Care and Use of Laboratory Animals, the NIH *Guide for the Care and Use of Laboratory Animals*, and the Animal Welfare Act (7 U.S.C. et seq.); the animal use protocol was approved by the Institutional Animal Care and Use Committee (IACUC) of the Mount Sinai School of Medicine.

Presented at the meeting of the American Broncho-Esophagological Association, Orlando, Florida, May 15-16, 2000. Recipient of the Broyles-Maloney Award.

CORRESPONDENCE — Ira Sanders, MD, Dept of Otolaryngology, Box 1189, Mount Sinai School of Medicine, One Gustave L. Levy Place, New York, NY 10029.

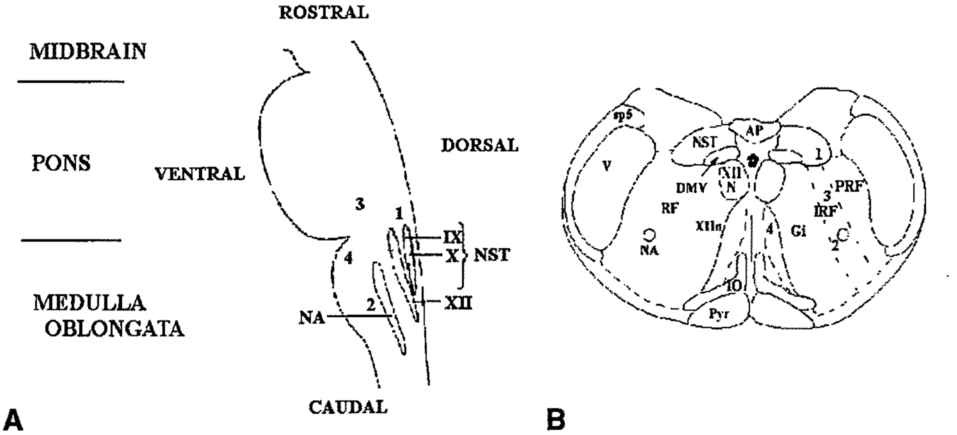

Fig 1. Parts of brain stem involved in swallowing. **A)** Three parts of brain stem are shown: midbrain, pons, and medulla oblongata. Swallowing center is believed to be located in medulla oblongata. Nucleus of solitary tract (NST) receives sensory input from both glossopharyngeal (IX) and vagus (X) nerves. **B)** Cross section at obex level in medulla oblongata. Diffuse area of neurons between dashed lines shown on left half of brain stem is called reticular formation (RF). RF itself is divided into intermediate reticular formation (IRF; commonly known as intermediate reticular zone), parvocellular reticular formation (PRF), and gigantocellular formation (Gi), shown on right. Four areas have been implicated in swallowing control by various investigators, depicted in A and B (right half) with numbers: 1 — NST and its surrounding reticular formation; 2 — RF neurons surrounding nucleus ambiguus (NA), also called periambigual area; 3 — neurons in caudal pons; 4 — neurons in medial part of RF in rostral medulla oblongata. AP — area postrema; CC — central canal; DMV — dorsal motor nucleus of vagus; IO — inferior olive; Pyr — pyramidal tract; V — trigeminal nucleus; sp5 — trigeminal nerve tract; XII N — hypoglossal nucleus; XIIn — hypoglossal nerve.

nerves, and then activate a second group of neurons that set the sequence and timing of the swallow. These neurons have been referred to as the swallowing center or the central pattern generator (CPG). The final stage of the circuit is the premotor neurons that directly control the activity of the motoneurons.

The locations of the neurons that receive sensory input and the motoneurons that directly control muscle contraction in swallowing are fairly well defined. In reflex swallowing evoked by stimulation of the pharynx, the neurons that receive and integrate sensory input are located in the nucleus of the solitary tract (NST; Fig 1B),[5] the principal sensory nucleus of the pharynx and esophagus. At the efferent or motor end of the circuit lie the motor nuclei: the nucleus ambiguus (NA), which controls the pharyngeal and esophageal muscles; the hypoglossal nucleus, which controls the tongue muscles; and the facial and trigeminal nuclei, which play a lesser role in swallowing. However, between these sensory and motor neurons, there is disagreement regarding the location of the other components of the swallowing circuit, and especially its key component, the swallowing center. Early neural tracing studies in cats by Holstege et al[13] and neurophysiological studies in rabbits by Sumi[14] suggested that part of the swallowing center lies in front of the medulla, in the caudal pons (Fig 1A), although later experiments suggest that this area is not essential for swallowing.[15] More recent studies have implicated the region of the reticular formation (RF) lying between the hypoglossal nucleus and the NA (Fig 1B). On the basis of lesion studies in various animal species, Doty et al[4,5] concluded that the control center lies in the medial part of the RF. In contrast, Barrett et al[16] have suggested that the control center may lie within the NST. After studying neurophysiological recordings from single neurons during evoked swallows, Kessler and Jean[15] and Amri et al[17] suggested that part of the swallowing circuit is also present below the NST and in the periambigual area, a poorly understood area surrounding the NA. In summary, the control of swallowing is currently thought to be divided between 2 areas: a dorsal part of the RF near the NST, and a ventral part surrounding the NA[15,17,18]; however, the issue remains controversial.

Physiological animal studies of swallowing have largely consisted of painstaking experiments in which electrodes are lowered into the brain stem to record the activity of individual neurons during reflex swallowing.[4-6,8,14,15,17-20] These experiments have been able to identify neurons corresponding to the different functional parts of the swallowing circuit alluded to above. However, the drawback to this technique is that each of these experiments samples just a few of the thousands of neurons that are active during the act of swallowing. In addition, it is difficult to accurately localize the position of the cell being recorded. The second major technique used to study swallowing is primarily anatomic. Retrograde tracing is done from swallowing-related muscles such as the esophagus by means of the transsynaptic neural tracer pseudorabies virus. Other experiments directly inject neural tract tracers such as horseradish peroxidase into motor nuclei to identify their premotor neurons. These studies have been extremely productive in showing the general patterns of neural connections in the brain stem. However, these traced connections are not specific to any single function. For example, the tongue is active during licking, chewing, suckling, respiration, vocalization, and swallowing. Different brain stem circuits control these activities, yet they share premotor and motor neurons that control tongue motions. The neurons involved in the oral and pharyngeal stages of swallowing apparently have no distinctive appearance and are intermixed among similar neurons controlling other functions. (One exception appears to be the reflex circuits modulating esophageal peristalsis. Direct connections have been identified between interneurons of the NST and esophageal motoneurons, and these interneurons are distinctive in their use of nitrous oxide as one of their neurotransmitters.)

A major problem in swallowing research has been the lack of a technique that identifies a functional network with resolution at the level of individual neurons. Previously, the only technique that could identify active neurons was radioactive glucose uptake, and the resolution of this method is very poor.[21] Recently, *fos* immunochemistry has been used as a high-resolution metabolic marker for functional networks in the brain and spinal cord[22] (for review, see additional references[21-25]). In the *fos* technique, the behavior to be studied is evoked repeatedly in an animal, to cause supraphysiologic stimulation of the neurons active during the behavior and trigger expression of the *fos* gene. The messenger RNA is translated into the *fos* protein in the cytoplasm that is transported back to the nucleus, where it acts as a promotor of protein expression. These proteins may be different in each particular type of neuron; however, the *fos* protein is common to all and can be detected by a specific antibody. Many experiments have used the *fos* technique to map functional central nervous connections. These experiments are often designed to use sensory stimulation[26-30] to evoke specific motor behaviors.[31-33] In the upper airway, *fos* immunocytochemistry has been used to study coughing,[34] reflex glottic closure,[35] and reflex modulation of vocalization.[29] It has also been used to study feeding regulation,[36-38] gustatory processing,[32,33,39] and conditioned taste aversion.[28,33,40]

Like any other technique, *fos* immunochemistry has its limitations. A common problem is false-positive *fos*-stained neurons resulting from anesthesia, surgery, or other technical aspects of the experimental protocol. Surgical stress, pain, anxiety, prolonged tachycardia, and tachypnea can all induce *fos* in cells regulating these activities.[21] For these reasons, proper controls are particularly important in *fos* experiments. In addition, motoneurons appear to stain poorly with this technique. The reason for this poor staining is not known. It is possible that the large motoneurons require more time to transport the *fos* protein back to the nucleus. However, locations of motoneurons involved in swallowing have already been defined, and they can be stained readily with special stains (see Materials and Methods).

The most important consideration in designing a *fos* experiment to study swallowing is to evoke only swallowing with the stimulus. Previous investigators who studied the neurophysiology of swallowing relied on stimulating the SLN to evoke a swallowing reflex. However, stimulation of the SLN also can cause cough, reflex glottic closure, and significant changes in cardiovascular and respiratory activity. The *fos* protein is expressed in the neurons involved in all these activities, and it would be impossible to distinguish them from neurons involved in swallowing. Recently, stimulation of the recurrent laryngeal nerve (RLN) was shown to evoke swallowing in rats without any other upper airway behavior (Tsai et al, unpublished observations). Therefore, it appeared that the combination of *fos* immunochemistry, which identifies activated neurons, and RLN stimulation, which evokes only swallowing, would be an ideal combination for studying the neurons that are active, and presumably participating, in the brain stem swallowing control circuit.

MATERIALS AND METHODS

A total of 9 adult male Sprague-Dawley rats weighing approximately 600 g were used in this experiment. The rats were divided into 2 groups, with 3 experimental rats and 3 controls in each group. Two more rats were used for Nissl staining (to identify brain stem landmarks[41]) and for immunocytochemical staining for calcitonin gene–related peptide (CGRP; the most reliable method for identifying motoneurons[42]). Another animal was required for testing various stimulation paradigms. To minimize background *fos* due to stress, we kept all animals on a 12-hour day-night cycle and deeply anesthetized with a combination of ketamine hydrochloride (85 mg/kg) and xylazine (12 mg/kg) given intraperitoneally soon after removal from their cages. Additional 0.15- to 0.2-mL intraperitoneal boluses were given periodically to maintain the anesthesia. All rats were maintained at normal body temperature with a heat lamp.

Reflex-Evoked Swallowing. A midline skin incision was made from the sternal notch upward to the mandible. The digastric muscle was retracted to expose the geniohyoid muscle. Dissection in the midline of the neck was performed to the trachea, the RLN was isolated in the tracheoesophageal groove, and its branches to the esophagus were severed as far down in the chest as possible to avoid any reflex activation of the RLN from the esophagus. The nerve was sectioned close to its entrance into the larynx,

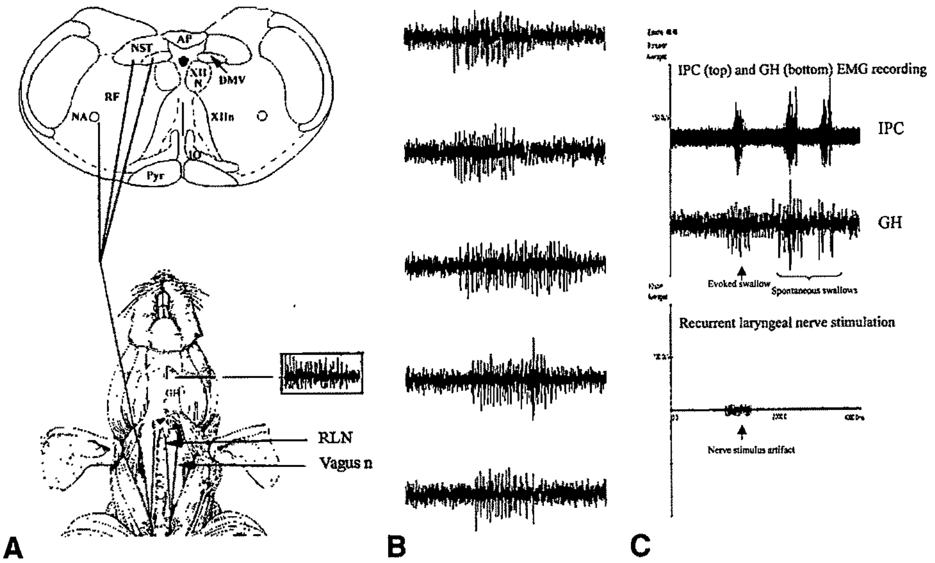

Fig 2. A) Schematic shows experimental preparation. Electrical stimulation was applied to recurrent laryngeal nerve (RLN) in rat, and excitation of sensory axons was transmitted to NST to elicit swallows. RLN also contains autonomic and motor axons that were stimulated. Autonomic axons originate from neurons in DMV, and motor axons originate from NA. Although motoneurons do not stain well with *fos*, DMV and NST were heavily stained on stimulated side. **B,C)** Electromyography (EMG) recordings were made from geniohyoid (GH) and inferior pharyngeal constrictor (IPC) muscles to confirm swallows. **B)** Geniohyoid EMG from 5 consecutive swallows. **C)** GH and IPC EMGs from evoked and spontaneous swallows. Evoked swallow corresponds to nerve stimulation seen at bottom of Figure. Note that evoked swallows are identical to spontaneous swallows.

and the proximal (central) end was placed on bipolar electrodes. Mineral oil was used to keep the nerve moistened. Electromyography (EMG) recording hook wire electrodes were inserted into the geniohyoid and inferior pharyngeal constrictor muscles, and surface electrodes were placed on the chest to monitor the heart rate. The swallows were confirmed on EMG, as well as by visual inspection, in which the larynx was seen to rise as it does during normal swallows. Additionally, EMG of the geniohyoid and inferior pharyngeal constrictor muscles was also recorded during spontaneous swallows in a separate experiment, and was found to be identical to swallows evoked during RLN stimulation (Fig 2C). The RLN was stimulated in the first rat in order to study the electrical parameters that would give a consistent response. This rat was not used in any other part of the experiment. Three rats were then used for stimulation in which the RLN was stimulated every 7 seconds with a pulse train of 500 ms at 60 Hz, each pulse having a 0.2-ms duration and a current of 0.2 mA. These parameters were found to give consistent swallows every time in all 3 rats. No other upper airway behavior was observed during the experiment. Swallowing was thus evoked for 1 hour, and the rats were then maintained under anesthesia for an additional 4-hour period so that the *fos* levels would reach their peak. The rats were then painlessly sacrificed by perfusion under anesthesia (as described below), and the brain stem was dissected out for *fos* immunocytochemistry. Three control rats underwent a sham operation identical to that of the experimental group, but without stimulation. Two more rats were sacrificed, and their brain stems were sectioned and used for Nissl staining,[41] a common histology stain that shows cell bodies, and CGRP staining (immunocytochemical method of identifying motoneurons[42]). These sections, along with the atlas of the rat brain published by Paxinos and Watson,[43] were used to identify brain stem structures.

Perfusion and Immunocytochemistry for Fos *and CGRP.* Similar perfusion and immunocytochemical procedures were followed for both *fos* and CGRP staining in different rats, as mentioned above. Under anesthesia, the rats were transcardially perfused with 250 to 300 mL of 0.1-mol/L phosphate-buffered saline solution (PBS; 37°C), followed by 500 mL of cold (4°C) 4% paraformaldehyde solution in 0.1-mol/L PBS, pH 7.4. The brain stem was removed and postfixed for 12 hours in the same solution. It was then transferred into a 20% sucrose solution and stored at 4°C overnight. The brain stem was removed from the sucrose solution, frozen, mounted in a cryostat, and serially sectioned at 40 μm in the frontal plane. The sections were numbered, and the distance from the obex was recorded for each section. Every fourth section was placed in a plastic well and rinsed in 0.1-mol/L PBS at 4°C and then processed for *fos* immunocytochemistry. The remaining sections were saved for use in case of technical problems with the immunocytochemical reaction. After rinsing, the sections were preincubated for 1 hour at room temperature in a blocking solution containing 1% normal bovine se-

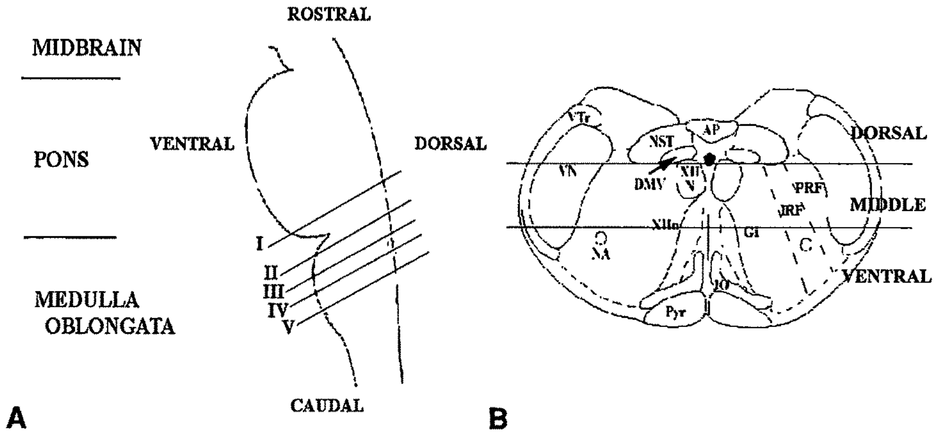

Fig 3. A) Diagram of brain stem shows where representative sections outlined in Results section were taken. Five levels were chosen to adequately represent all areas that have been implicated in swallowing control and those that were seen in our experiment: I — caudal pons; II — rostral medulla; III — mid-medullary region; IV — obex; V — caudal medulla. **B**) Each section was divided into 3 regions: dorsal, middle, ventral. Regions of interest (ROIs) were defined in each region based on Nissl and calcitonin gene–related peptide–stained sections and atlas of rat brain published by Paxinos and Watson.[43] ROIs are defined as follows. Dorsal region is NST, DMV, and hypoglossal nucleus (XII N). NST itself is divided into interstitial, intermediate, ventrolateral, dorsomedial, central, and commissural subnuclei. Each of these subnuclei were defined according to atlas.[43] Middle region is trigeminal nucleus (V); RF is divided into PRF, IRF, and medial gigantocellular area (Gi). Ventral region is NA; RF is divided into periambigual area, ventral gigantocellular formation (Gi), and IO.

rum albumin and 0.1% Triton X-100 in 0.1-mol/L PBS. The sections for *fos* immunocytochemistry were then transferred into primary *fos* antiserum (*fos* Ab-f, Calbiochem, San Diego, Calif: PC38-S, a rabbit polyclonal IgG, directed against residues 4 through 17 of *fos*).[21] The *fos* antiserum was diluted to a concentration of 1:10,000 with the above blocking solution. The sections for CGRP immunocytochemistry were incubated with rabbit anti-CGRP (Sigma, St Louis, Mo) diluted to 1:8,000 in the above blocking solution.[42] The sections were developed with a biotinylated second anti-rabbit IgG antibody (Vector Laboratories, Burlingame, Calif) diluted to 1:200 with 1% goat serum in 0.1-mol/L PBS and avidin-biotin horseradish peroxidase complex. These were then reacted with diaminobenzidine in the presence of hydrogen peroxide. The immunostained sections were rinsed, air-dried, and mounted. *Fos* protein appears dark brown with this method.

RESULTS

Stimulation of the RLN consistently evoked a swallow in all 3 experimental animals. This finding was confirmed by EMG of the geniohyoid and inferior pharyngeal constrictor muscles, as well as by visual inspection. Other upper airway behaviors, such as cough or gag, were not seen.

The sections were examined with a Zeiss Axiophot photomicroscope (Carl Zeiss, Inc, Thornwood, NY). The analysis included sections from the caudal (lower) pons to the caudal pole of the inferior olive (IO). The contralateral side of the brain stem was used for analysis, as the RLN contains motor and autonomic components whose neurons were also activated on the stimulated side. High-resolution digital photographs were taken of representative sections at 2.5×, which gives a photomicrograph of half a brain stem section. The hemisection was then photographed at 10× with 6 photographs, which overlapped slightly along their borders to allow for alignment. The Nissl and CGRP sections were photographed similarly. These, along with the atlas of the rat brain by Paxinos and Watson,[43] were used to identify the primary regions of interest (ROIs; see below and Fig 3): areas that have been implicated in swallowing. Blank outlines of the brain stem sections showing the major ROIs were then copied from the Paxinos and Watson atlas, and areas with *fos*-labeled cells on the photomicrographs were marked on these outlines. A similar set of outlines was created for the control cells as well. Representative sections are shown in Figs 4-8, comparing the swallowing and the control rats. The brain stem regions at these representative levels as defined in the Paxinos and Watson atlas are also shown. The distances shown are relative to the obex in the rostral-caudal axis. The obex is the point in the medulla at which the central canal opens into the fourth ventricle. This landmark is easily identified in most animals, including rats. As is common when reporting data in the brain stem, the obex has been designated as the zero mark; levels above the obex have a plus sign, and those below it have a minus sign.

Each brain stem hemisection was further divided into dorsal, middle, and ventral regions to aid in the analysis, and the primary ROIs were defined in each region. The primary ROIs in the dorsal region include the NST, the dorsal motor nucleus of the vagus nerve, and the hypoglossal nucleus. The NST

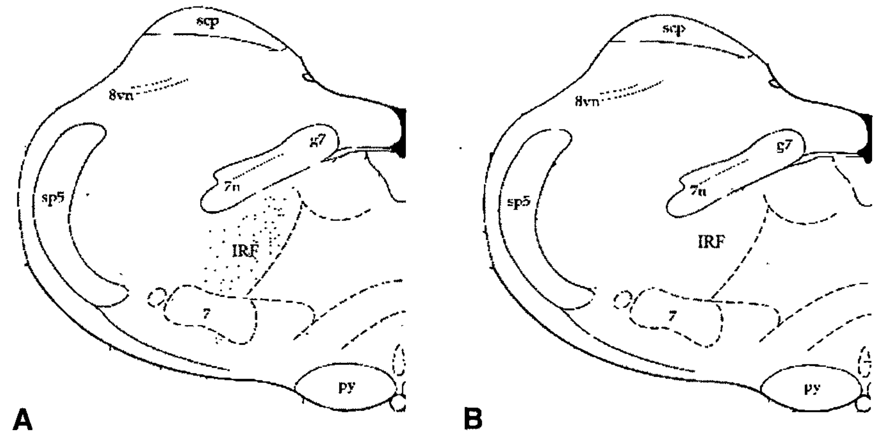

Fig 4. Level I: caudal pons (+3.2 mm). Figure shows outlines as defined in atlas of rat brain published by Paxinos and Watson.[43] ROIs labeled with *fos* were marked on these outlines for both experimental and control rats. *Fos*-labeled neurons are represented with dots. Number of dots does not correspond to actual number of *fos*-labeled neurons. **A)** Experimental rat. Notice areas of *fos*-labeled neurons localized to central zone in section just medial and ventral to facial nerve tract (7n). This area is defined as IRF in atlas. **B)** Control rat. No significant numbers of *fos*-labeled cells were identified in this region. Every section had few *fos*-labeled neurons located outside ROIs in both experimental and control rats that were not localized into groups. Those have been omitted from outlines for clarity. 7 — facial nucleus; 7n — facial nerve tract; g7 — genu of facial nerve; 8vn — vestibular root of eighth nerve; py — pyramidal tract; scp — superior cerebellar peduncle; sp5 — spinal trigeminal tract.

itself is divided into the interstitial, intermediate, ventrolateral, dorsomedial, central, and commissural subnuclei. Each of these subnuclei were defined according to the atlas of Paxinos and Watson.[43] The primary ROIs in the middle region include the trigeminal nucleus and the subdivisions of the RF, including the lateral parvocellular reticular formation (PRF), the intermediate reticular formation or zone (IRF), and the medial gigantocellular area. The primary ROIs in the ventral region include the NA, the IO, and the subdivisions of the RF, including the periambigual area and the ventral gigantocellular area.

Areas common to both the experimental and the control groups (Fig 9) included parts of the IO (Figs 9 and 10), the RF area ventral to the NA (respiratory area), and the central subnucleus of the NST (Figs 9 and 11). These areas were not considered to play a role in swallowing control. As to the areas specific to the experimental group, 5 representative levels were chosen to show the neurons labeled with *fos* (Fig 3). These include the caudal pons, the rostral medulla, the mid-medullary region, the obex, and the caudal medulla. The ROIs containing *fos*-labeled cells were marked on the outlines at each of these

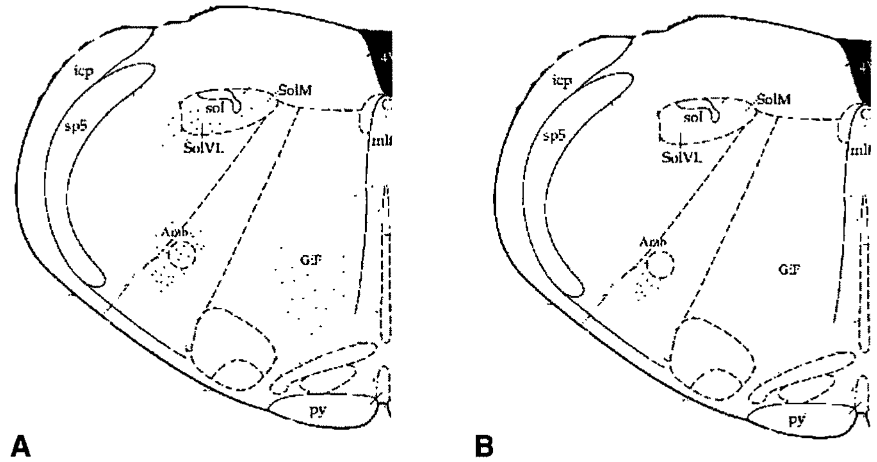

Fig 5. Level II: rostral medulla (+2.2 mm). Representative sections through rostral medulla. **A)** Experimental rat. *Fos*-labeled neurons were identified in NST and periambigual area. These 2 areas have been implicated in swallowing by other investigators. Surprisingly, *fos*-labeled neurons in these areas were fewer than in other areas that were identified as swallowing-related in experimental rats. In addition to these areas, medial part of RF called gigantocellular reticular formation (GiF) was identified as having large numbers of *fos*-labeled neurons, especially in its ventral aspect. This area has not traditionally been implicated in swallowing. **B)** Control rat. Note complete absence of *fos*-labeled neurons in NST and GiF. Some *fos*-labeled neurons were identified ventral to NA that are probably related to respiratory and cardiovascular function. icp — inferior cerebellar peduncle; py — pyramidal tract; sol — solitary tract; SolVL — ventrolateral subnucleus of NST; SolIM — intermediate nucleus of NST; sp5 — spinal trigeminal tract.

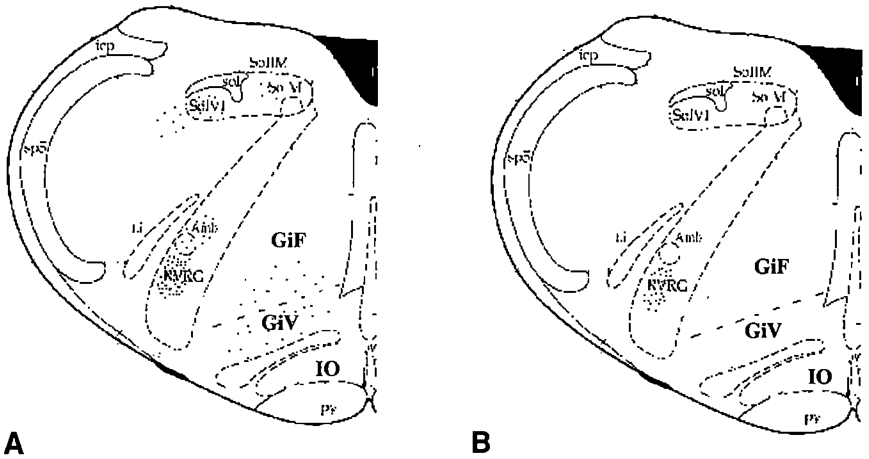

Fig 6. Level III: middle medulla (+1.0 mm). Representative sections through mid-level of medulla. **A)** Experimental rat. *Fos*-labeled neurons were identified in NST and periambigual area. Note that number of *fos*-labeled cells in these areas above obex was less than in these areas below obex and most other areas identified as swallowing-related in this study. In NST, these neurons were localized mostly in its SolVL and surrounding RF, with some neurons in SolIM. Neurons in periambigual area were identified dorsal as well as ventral to NA. Cells ventral to NA were mostly mixed with respiratory cells. RVRG — rostroventral respiratory group in atlas of Paxinos and Watson.[43] Probably more important are localized *fos*-labeled neurons, identified in medial part of RF, defined as gigantocellular reticular formation (GiF) and ventral gigantocellular formation (GiV). These areas have not traditionally been implicated in swallowing. **B)** Control rat. *Fos*-labeled cells were mostly identified ventral to NA in RVRG. Note also complete absence of *fos*-labeled neurons in IO above obex in both experimental and control rats. icp — inferior cerebellar peduncle; py — pyramidal tract; sol — solitary tract; sp5 — spinal trigeminal tract; Li — linear nucleus.

levels. The *fos*-labeled outlines are shown in Figs 4-8.

In the caudal pons (Fig 4), the dorsal region showed no significant labeling in any of the ROIs. In the middle region, *fos*-labeled cells were identified in the IRF (Figs 4 and 12). In the ventral region, no significant labeling was identified in any of the ROIs. In the rostral medulla (Fig 5), the dorsal region showed *fos* labeling in the NST with some surrounding RF laterally. The middle region showed *fos* labeling in a subset of the gigantocellular RF. The ventral region had labeling in the periambigual reticular area and the ventral gigantocellular area. In the mid-medullary level (Fig 6), the dorsal region showed *fos* labeling in the NST and surrounding RF laterally; the middle region had *fos* labeling in a subset of the gigantocellular RF; and the ventral region had *fos* labeling in the periambigual reticular area and ventral gigantocellular area. In the obex (Fig 7), the dorsal region

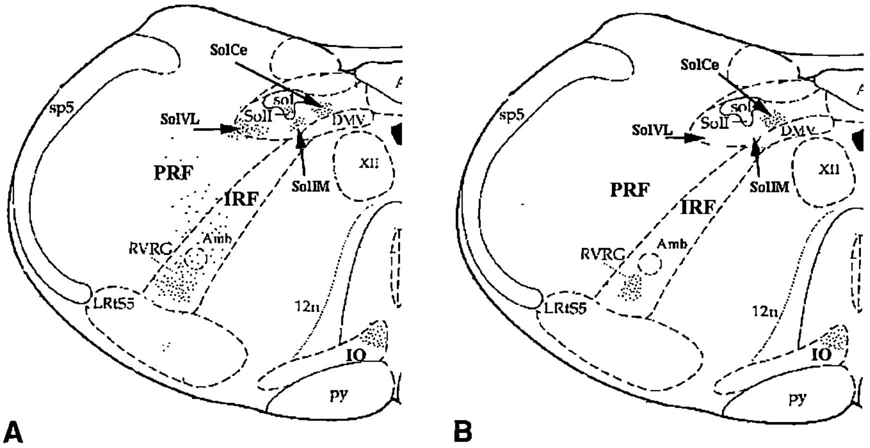

Fig 7. Level IV: obex (0 mm). Sections of brain stem through obex. Obex is most consistent and easily defined landmark in brain stem. All other sections were measured relative to obex, obex being 0 mm. **A)** Experimental rat. *Fos*-labeled neurons were identified in NST, periambigual area, and parts of IRF and PRF between them. In NST, *fos*-labeled neurons were localized to specific subnuclei as defined in atlas of Paxinos and Watson.[43] These are central subnucleus (SolCe), interstitial subnucleus (SolI), SolIM, and SolVL. Of these, SolI and SolIM are known to receive sensory afferents from pharynx and esophagus. SolVL, however, along with surrounding RF, is probably involved in swallowing. Note also that periambigual neurons are found all around NA, including ventrally, where they are mixed with neurons known to be involved with respiration (RVRG). However, experimental group contained far more *fos*-labeled neurons in this area than did control group. **B)** Control rat. *Fos*-labeled neurons were identified in SolCe, ventral to NA in RVRG, and in IO. These cells were not considered to be important in swallowing.

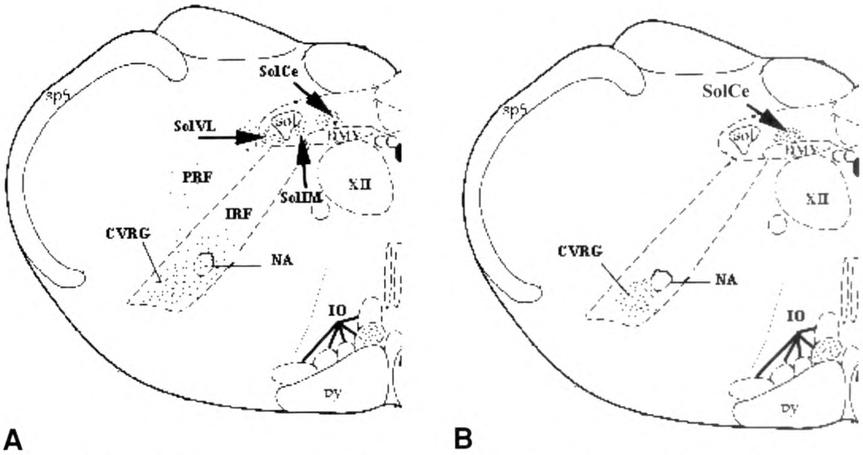

Fig 8. Level V: caudal medulla (–0.7 mm). Sections through caudal medulla, below obex. **A)** Experimental rat. *Fos*-labeled neurons are identified in NST, periambigual area, and IRF and PRF areas between them. Specific subnuclei within NST were labeled, including SolCe, SolIM, SolI, and SolVL. Cells in periambigual reticular area mostly belong to IRF and PRF. Note that *fos*-labeled neurons ventral to NA are mixed with those involved in respiration (CVRG in atlas of Paxinos and Watson[43]). Nevertheless, there are far more *fos*-labeled neurons ventral to NA compared to control. **B)** Control rat. Areas containing *fos*-labeled neurons include SolCe of NST, respiratory area ventral to NA (CVRG), and part of IO. These areas were not considered to be important in swallowing control. sp5 — spinal trigeminal tract; py — pyramidal tract.

showed *fos* labeling in the NST (interstitial, intermediate, and ventrolateral subnuclei) and the surrounding RF (Fig 13). The middle region showed labeling in the IRF (Fig 13) and the PRF. The ventral region had labeling in the periambigual reticular area. In the caudal medulla (Fig 8), the dorsal region had labeling in the NST (interstitial, intermediate, and ventrolateral subnuclei) and the surrounding RF (Fig 11); the middle region had *fos* labeling in the IRF and the PRF; and the ventral region had *fos* labeling in the periambigual reticular area.

DISCUSSION

The present study appears to have identified many, if not all, of the swallowing-related neurons within the brain stem for the first time in any mammal. After we subtracted areas of *fos* labeling seen in control areas, only a small fraction of the brain stem neurons were labeled with *fos*, and these were concentrated in discrete areas. As explained below, almost all areas that previously reporting neurophysiologists have identified as being related to swallowing were represented in the experimental animals. In addition, some novel areas that have not been reported to be swallowing-related were also seen. Whether these reflect unrecognized functional areas of the swallowing circuit or are merely artifacts requires further study to decide. The *fos* technique shows all neurons involved in an activity; however, it does not differentiate between activity patterns of different areas. Nevertheless, correlation with prior physiology experiments allows some inferences to be made regarding the functions of the components of the swallowing circuit outlined by the current experiment. One unexpected finding was that the area directly *rostral* to the obex that has been the focus of most research

Fig 9. Brain stem section of control rat at obex shows *fos*-labeled neurons. Note relative paucity of *fos*-labeled neurons in most ROIs. Labeled cells were localized to 3 areas in brain stem: SolCe, part of IO, and area ventral to NA defined as RVRG in atlas of Paxinos and Watson.[43] RVRG contains cells involved in respiratory control. None of areas implicated in swallowing were labeled. Localization of *fos* neurons to specific loci like RVRG shows ability of *fos* immunocytochemistry to mark specific systems. 12n — hypoglossal nerve tract; py — pyramidal tract; sol — solitary tract; sp5 —spinal trigeminal tract; XII — hypoglossal nucleus.

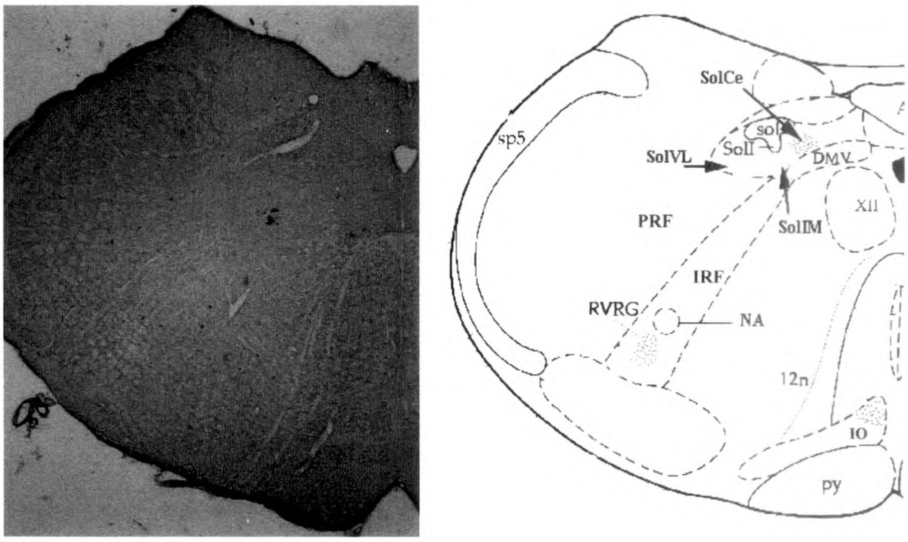

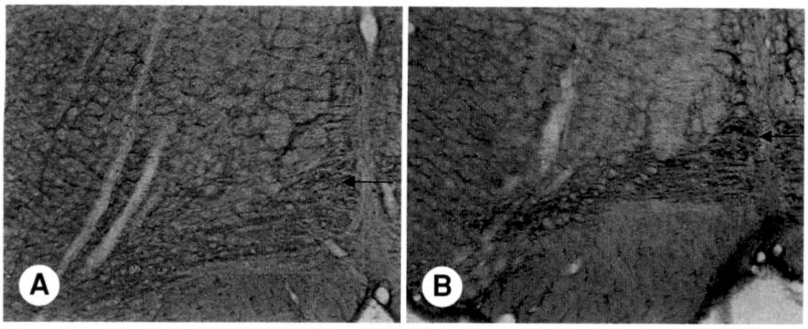

Fig 10. A) Section from caudal medulla shows IO in experimental rat. **B)** Section through caudal medulla shows IO in control rat. Note that discrete region is labeled within IO at exactly same location in both rats (arrows). This further shows ability of *fos* immunocytochemistry to highlight subset of neurons in given nucleus that may be specific to certain function.

had relatively few *fos*-labeled cells. In contrast, the caudal part of the pons, the gigantocellular RF and its ventral part, and especially the NST and the periambigual area *caudal* to the obex had many *fos*-labeled cells. Cell numbers do not translate into the importance of any given area, as in the nervous system, small numbers of cells can control the activity of large groups of neurons or even entire nuclei. However, the experimental results suggest that the swallowing circuit is distributed in a more balanced way in the brain stem than is currently believed.

A critical aspect of the experiment was the use of RLN stimulation to evoke swallows. In anesthetized rats, each stimulation of the RLN evoked a swallow for the entire hour of the experiment, and EMG of the geniohyoid muscle, as well as visual observation, confirmed this. Other upper airway behaviors, such as cough and gag, were not seen. It is not intuitive that RLN stimulation would result in swallowing. The sensory component of the RLN innervates the subglottis and trachea, and stimulation of these areas produces cough at low thresholds. However, the RLN also carries sensory innervation to the esophageal mucosa, and the stimulation may mimic the presence of a large food bolus to elicit swallowing. Investigators have noted that the swallowing reflex tends to override the respiratory reflexes, and this finding may explain why swallowing is produced instead of a cough. However, although the motor act of coughing was not seen, the sensory neurons originating from the trachea must have been activating interneurons in the NST related to respiratory function. In addition, the absence of cough suggests the activation of many inhibitory neurons. All these neurons would be expected to stain for *fos* and are no different in appearance from swallowing-related interneurons. This is the only source of false-positive labeling that is specific to the protocol and would not be reflected in the control animals.

Upon RLN stimulation, impulses are transmitted along the sensory component of the nerve to the caudal part of the NST on the stimulated side. The NST is the principal sensory nucleus for the upper airway structures and the cardiovascular system. These impulses are then transmitted to the neurons that initiate swallowing on both sides of the brain stem. (It is known that each side contains independent but coupled swallowing circuits.) Next, a poorly understood swallowing center (also called the CPG) then activates the premotor neurons in a sequential manner, which then stimulate the motoneurons. Therefore, except for the neurons stimulated by the anesthesia, the *fos* staining closely follows the specific neural circuitry involved in swallowing. This fact is supported by the concentration of localized groups of *fos*-positive neurons in specific areas of the brain stem that have been shown previously to be active in swallowing (by neurophysiology experiments that record individual neurons). The more obvious choice for eliciting swallows would seem to be the SLN, which most neurophysiology experiments have used. However, stimulation of this nerve also causes cough, reflex glottic closure, and significant changes in the neural control of cardiovascular and respiratory activity. *Fos* protein would be expressed in neurons involved in all these activities, and it would be impossible to discriminate them from those involved in swallowing.

One of the notable findings from this experiment was the presence of *fos*-labeled neurons in unexpected areas. For example, in cat experiments, Holstege et al[13] injected neural tracers into a small area

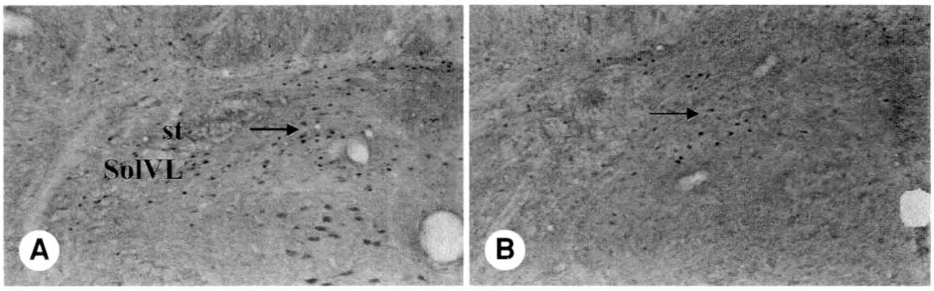

Fig 11. A) Section through caudal medulla shows NST in experimental rat. *Fos*-labeled cells were identified in SolI, SolIM, SolVL, and SolCE in experimental rats at various levels below obex. **B)** Section through caudal medulla shows NST in control rat. Note that SolCE was labeled in both experimental and control rats (arrows). st — solitary tract.

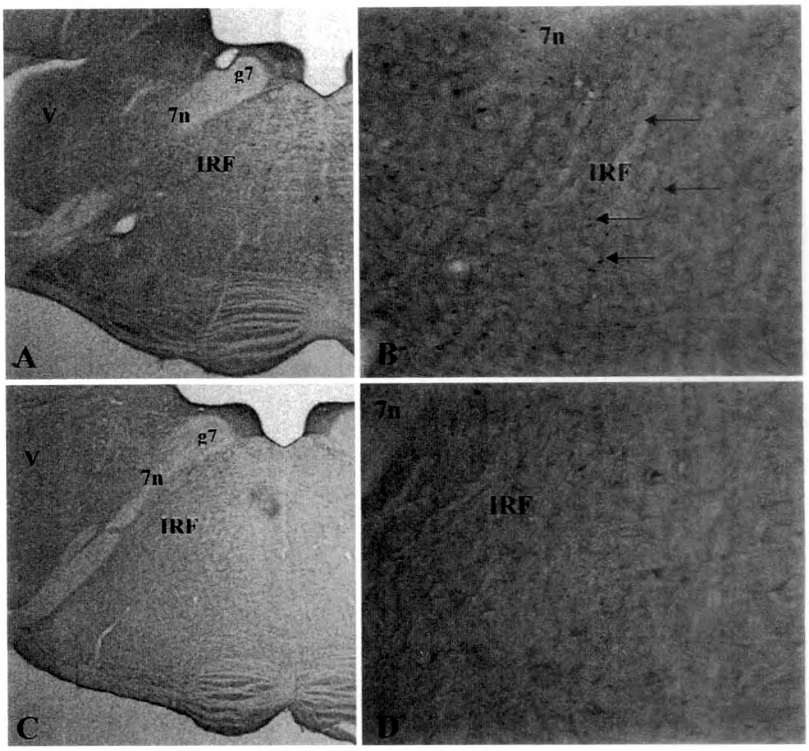

Fig 12. Photomicrographs of brain stem sections taken through caudal pons. **A)** Low-power view (original ×2.5) shows location of IRF adjacent to facial nerve tract (7n) in experimental rat. **B)** High-power view (original ×10) of IRF in A. Note large numbers of *fos*-labeled neurons in IRF (arrows). **C)** Low-power view (original ×2.5) of caudal pons shows IRF in control rat. **D)** High-power view (original ×10) of IRF in C. No significant numbers of *fos*-labeled cells were identified in IRF. g7 — genu of facial nerve; V — trigeminal nucleus.

of the pons just dorsal to the superior olive and demonstrated that it had axonal projections to all the motor nuclei active during swallowing. Sumi[14] was able to evoke swallowing by electrically stimulating a homologous area in the pons of rabbits. However, in rats, Kessler and Jean[15] methodically explored the pons with microstimulation, but were unable to evoke swallowing, and the attention of later researchers shifted to the medulla. Our results showed that a very localized area of the RF in the pons contained *fos*-labeled neurons (Fig 4). This area is defined as the IRF (Figs 4 and 12) in the Paxinos and Watson atlas,[43] and is quite rostral to the point at which the RLN sensory neurons terminate in the NST. The IRF is a recently described anatomic entity that extends from the NST to the NA and is present throughout

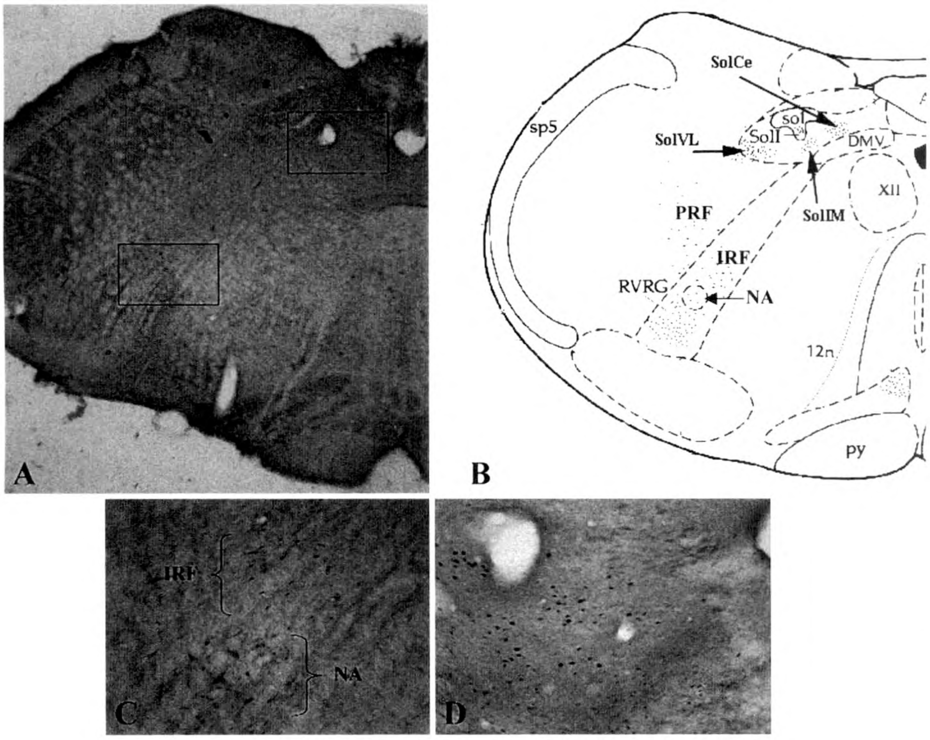

Fig 13. Brain stem section from experimental rat shows *fos*-labeled neurons on side opposite nerve stimulation. **A)** Low-power view of brain stem at level of obex (original ×3.2). **B)** Schematic of A shows locations of labeled neurons. Localized areas of labeled neurons were identified in NST, area surrounding NA, and parts of RF between these areas (IRF and PRF). *Fos*-labeled neurons were also identified in IO. **C,D)** Magnified boxes in A. **C)** High-power view of area surrounding NA (original ×20). Note *fos*-labeled cells above NA in IRF. IRF is subdivision of RF extending from NST to NA. **D)** High-power view of NST (original ×20). At different levels below obex, *fos*-labeled neurons were identified in SolI, SolIM, SolVL, and SolCE. SolCE and IO were also labeled in control rats and were not thought to be important in swallowing.

the length of the brain stem. The presence of *fos*-labeled cells in the pons may represent the premotor neurons for rostrally located motor nuclei such as the facial and trigeminal nuclei.

Another region that was labeled and has not received attention recently as having importance for swallowing is a relatively obscure region of the RF in the medial part of the brain stem. It appears to extend from the mid-level of the facial nucleus to the obex, although most cells were seen caudal to the facial nucleus and rostral to the obex. According to Paxinos and Watson,[43] this area probably lies in a subset of the gigantocellular RF and its ventral part (Fig 5). Doty[5] reported that lesions in this area eliminated reflex swallowing in a variety of species. He concluded that the swallowing center (CPG) lies in this area, approximately 1.5 mm lateral to the midline and between 1 and 3 mm dorsal to the rostral pole of the IO. The area described by Doty appears to be homologous to the general area in the rat containing the *fos*-labeled neurons of the gigantocellular RF and its ventral part. This area is a possible candidate for the CPG of swallowing.

Another notable finding was the heavy *fos* labeling *caudal* to the obex in the NST, its surrounding reticular area, and the periambigual area (Figs 7 and 8). Most neurophysiological studies have found little activity in the neurons below the obex during swallowing. Increased *fos* labeling in the NST can be caused by sensory feedback originating in the esophagus on the unstimulated side through its intact RLN. The sensory afferents from the RLN are known to localize to the cells in the NST below the obex. It is interesting to note that the sensory afferents from the SLN, which most previous investigators have used, localize in the NST rostral to the obex. It is possible that the swallowing center is distributed over a length of the medulla on either side of the obex, and that depending on the region of the NST being stimulated (rostral or caudal to the obex), the swallowing center is regionally activated. For this to be true, the swallowing center would have to be interconnected with most orofacial nuclei throughout its rostral-caudal length. However, such anatomic connections have not yet been defined. It appears that this caudal region has largely been ignored in most previous studies.

The *fos*-labeled cells in the NST below the obex appeared to be concentrated in specific locations within the nucleus. An area that was common to both the control and experimental animals was the central subnucleus of the NST (Figs 9 and 11). This area could be related to the respiratory or cardiovascular activity of the rats in either group. Most other cells in the experimental rats localized to the interstitial, intermediate, and ventrolateral subnuclei of the NST. Of these, the interstitial and the intermediate subnuclei are known to contain sensory neurons innervating the pharynx and the esophagus. These could have been activated during the swallow on the unstimulated side through its intact RLN. However, the ventrolateral nucleus is not known to contain sensory nuclei to either of these structures. It is possible that this part of the NST contains cells that play a role in swallowing control. Most investigators who have implicated the NST and surrounding RF rostral to the obex have implicated the lateral part of the NST. In fact, the lateral part of the NST, along with its surrounding RF, has been referred to as the lateral solitary complex by some investigators.

The periambigual area is an ill-defined zone consisting of the cells of the RF. The area covers cells mostly belonging to the IRF and the PRF. Examination of the sections made through the NA reveals that the location of the *fos*-labeled cells in and around the NA varies significantly over short distances. These cells are located medial, dorsal, lateral, and even ventral to the NA. The cells ventral to the NA are largely mixed with cells of the respiratory and cardiovascular group and are difficult to discriminate. Nevertheless, a simple comparison with the control rats shows far more labeled cells in the experimental rats.

Another important area below the obex that has not previously been implicated in swallowing but showed *fos*-labeled neurons was the RF area between the NST and the NA. These cells were distinct from the neurons immediately outside the NST or surrounding the NA (periambigual area). These cells were distributed over parts of the IRF and the PRF (Figs 7 and 8). There are no previous reports in the literature implicating these cells in swallowing control.

In addition to the above nuclei, there was a subset of neurons in the IO that was labeled in both the experimental and the control rats (Fig 10). These cells extended from the obex to the caudal part of the medulla. No activity was identified in the IO above the obex. Since they were identified in exactly the same locations in both the stimulated and the control rats, these were not considered to play an important role in swallowing. Although their function is not known, the fact that only a subset of neurons within the IO was labeled reinforces the validity of the *fos* technique in identifying discrete areas specific to a function.

CONCLUSION

In our experiment, RLN stimulation consistently evoked a reflex swallow. The experiment appears to have identified most areas in the brain stem involved in swallowing. Areas currently thought to be important in swallowing control were labeled. These included the NST with its surrounding RF and the periambigual reticular neurons *rostral* to the obex. In addition, novel areas not previously thought to be important in swallowing were labeled. These include areas in the caudal pons, the medial part of the RF in the rostral medulla, and the RF areas surrounding the NST, the NA, and the areas between them in the *caudal* medulla. Finally, a group of neurons were identified that may be the CPG for swallowing. The importance of these observations merits further experiments that specifically target the areas identified in this study.

REFERENCES

1. Meltzer SJ. On the causes of the orderly progress of the peristaltic movements in the oesophagus. Am J Physiol 1899; 2:266-72.
2. Meltzer SJ. Deglutition through an oesophagus partly deprived of its muscularis, with demonstration. Proc Soc Exp Biol Med 1907;4:40-3.
3. Miller FR, Sherrington CS. Some observations on the buccopharyngeal stage of reflex deglutition in the cat. Q J Exp Physiol 1916;9:147-86.
4. Doty RW, Richmond WH, Storey AT. Effect of medullary lesions on coordination of deglutition. Exp Neurol 1967;17: 91-106.
5. Doty RW. Neural organization of deglutition. In: Code CF, ed. Alimentary canal. Washington, DC: American Physiological Society, 1968:1861-902. (Handbook of physiology; vol 4.)
6. Sumi T. Neuronal mechanisms in swallowing. Pflugers Arch 1964;278:467-77.
7. Dubner R, Sessle BJ, Storey AT. The neural basis of oral and facial function. New York, NY: Plenum Press, 1978.
8. Jean A. Control of the central swallowing program by inputs from the peripheral receptors. A review. J Auton Nerv Syst 1984;10:225-33.
9. Miller AJ. Significance of sensory inflow to the swallowing reflex. Brain Res 1972;43:147-59.
10. Miller AJ. Characteristics of the swallowing reflex induced by peripheral nerve and brain stem stimulation. Exp Neurol 1972;34:210-22.
11. Miller AJ. Deglutition. Physiol Rev 1982;62:129-84.
12. Miller AJ. The search for the central swallowing pathway: the quest for clarity. Dysphagia 1993;8:185-94.
13. Holstege G, Graveland G, Bijker-Biemond C, Schuddeboom I. Location of motoneurons innervating soft palate, pharynx and upper esophagus. Anatomical evidence for a possible swallowing center in the pontine reticular formation. An HRP and autoradiographical tracing study. Brain Behav Evol 1983;23: 47-62.
14. Sumi T. Reticular ascending activation of frontal cortical neurons in rabbits, with special reference to the regulation of deglutition. Brain Res 1972;46:43-54.
15. Kessler JP, Jean A. Identification of the medullary swallowing regions in the rat. Exp Brain Res 1985;57:256-63.
16. Barrett RT, Bao X, Miselis RR, Altschuler SM. Brain stem localization of rodent esophageal premotor neurons revealed by transneuronal passage of pseudorabies virus. Gastroenterology 1994;107:728-37.
17. Amri M, Car A, Jean A. Medullary control of the pontine swallowing neurones in sheep. Exp Brain Res 1984;55:105-10.
18. Jean A. Localization and activity of medullary swallowing neurones [in French]. J Physiol (Paris) 1972;64:227-68.
19. Jean A. Localization and activity of oesophageal motoneurons in sheep [in French]. J Physiol (Paris) 1978;74:737-42.
20. Neya T, Watanabe K, Yamasoto T. Localization of potentials in medullary reticular formation relevant to swallowing. Rendic Gastroenterol 1974;6:107-10.
21. Dragunow M, Faull R. The use of c-fos as a metabolic marker in neuronal pathway tracing. J Neurosci Methods 1989; 29:261-5.
22. Sagar SM, Sharp FR, Curran T. Expression of c-fos protein in brain: metabolic mapping at the cellular level. Science 1988;240:1328-31.
23. Morgan JI, Curran T. Stimulus-transcription coupling in the nervous system: involvement of the inducible proto-oncogenes fos and jun. Annu Rev Neurosci 1991;14:421-51.
24. Onoda N. Odor-induced fos-like immunoreactivity in the rat olfactory bulb. Neurosci Lett 1992;137:157-60.
25. Smith MA, Banerjee S, Gold PW, Glowa J. Induction of c-fos mRNA in rat brain by conditioned and unconditioned stressors. Brain Res 1992;578:135-41.
26. Carstens E, Saxe I, Ralph R. Brainstem neurons expressing c-Fos immunoreactivity following irritant chemical stimulation of the rat's tongue. Neuroscience 1995;69:939-53.
27. Gieroba ZJ, Blessing WW. Fos-containing neurons in medulla and pons after unilateral stimulation of the afferent abdominal vagus in conscious rabbits. Neuroscience 1994;59:851-8.
28. Houpt TA, Philopena JM, Joh TH, Smith GP. c-Fos induction in the rat nucleus of the solitary tract correlates with the retention and forgetting of a conditioned taste aversion. Learn Mem 1996;3:25-30.
29. Jurgens U, Lu CL, Quondamatteo F. C-fos expression during vocal mobbing in the new world monkey *Saguinus fuscicollis*. Eur J Neurosci 1996;8:2-10.
30. Miller AD, Ruggiero DA. Emetic reflex arc revealed by expression of the immediate-early gene c-fos in the cat. J Neurosci 1994;14:871-88.
31. Barajon I, Gossard JP, Hultborn H. Induction of fos expression by activity in the spinal rhythm generator for scratching. Brain Res 1992;588:168-72.
32. Swank MW, Bernstein IL. c-Fos induction in response to a conditioned stimulus after single trial taste aversion learning. Brain Res 1994;636:202-8.
33. Swank MW, Schafe GE, Bernstein IL. c-Fos induction in response to taste stimuli previously paired with amphetamine or LiCl during taste aversion learning. Brain Res 1995;673:251-61.
34. Gestreau C, Bianchi AL, Grelot L. Differential brainstem Fos-like immunoreactivity after laryngeal-induced coughing and its reduction by codeine. J Neurosci 1997;17:9340-52.
35. Tanaka Y, Yoshida Y, Hirano M. Expression of Fos-protein activated by tactile stimulation on the laryngeal vestibulum in the cat's lower brain stem. J Laryngol Otol 1995;109:39-44.
36. Emond MH, Weingarten HP. Fos-like immunoreactivity in vagal and hypoglossal nuclei in different feeding states: a quantitative study. Physiol Behav 1995;58:459-65.
37. Fraser KA, Raizada E, Davison JS. Oral-pharyngeal-esophageal and gastric cues contribute to meal-induced c-fos expression. Am J Physiol 1995;268(suppl):R223-R230.
38. Rinaman L, Baker EA, Hoffman GE, Stricker EM, Verbalis JG. Medullary c-Fos activation in rats after ingestion of a satiating meal. Am J Physiol 1998;275(suppl):R262-R268.
39. Harrer MI, Travers SP. Topographic organization of Fos-like immunoreactivity in the rostral nucleus of the solitary tract evoked by gustatory stimulation with sucrose and quinine. Brain Res 1996;711:125-37.
40. Houpt TA, Philopena JM, Wessel TC, Joh TH, Smith GP. Increased c-fos expression in nucleus of the solitary tract correlated with conditioned taste aversion to sucrose in rats. Neurosci Lett 1994;172:1-5.
41. Clark G. Staining procedures. Baltimore, Md: Williams and Wilkins, 1981.
42. Skofitsch G, Jacobowitz DM. Calcitonin gene–related peptide: detailed immunohistochemical distribution in the central nervous system. Peptides 1985;6:721-45.
43. Paxinos G, Watson C. The rat brain in stereotaxic coordinates. San Diego, Calif: Academic Press, 1998.

Ann Otol Rhinol Laryngol 110:2001

HEMICRICOIDECTOMY FOR VOICE REHABILITATION FOLLOWING HEMILARYNGECTOMY WITH IPSILATERAL ARYTENOID REMOVAL

MILAN R. AMIN, MD
PHILADELPHIA, PENNSYLVANIA

JAMES A. KOUFMAN, MD
WINSTON-SALEM, NORTH CAROLINA

The purpose of this article is to describe an approach to reconstruction of the larynx after vertical partial laryngectomy with removal of the ipsilateral arytenoid cartilage. This method addresses the problem of postoperative posterior glottal incompetence (aphonia with or without aspiration). The technique involves resection of the ipsilateral half of the cricoid cartilage, use of an inferiorly based strap muscle flap for vocal fold reconstruction, and placement of a customized stent. This technique may be used at the time of the primary cancer extirpation or as a secondary rehabilitative procedure. Generally, patients who have undergone this procedure have had minimal postoperative breathiness with good phonatory and airway function. We recommend this reconstructive technique for patients with large posterior defects following hemilaryngectomy.

KEY WORDS — cricoid cartilage, hemicricoidectomy, hemilaryngectomy, laryngeal cancer, laryngeal carcinoma, laryngeal reconstruction, vocal cord cancer, vocal fold cancer, voice rehabilitation.

INTRODUCTION

This report presents the authors' approach to laryngeal reconstruction following vertical hemilaryngectomy with removal of the ipsilateral arytenoid cartilage. It specifically targets the problem of postoperative posterior glottal incompetence. The typical vertical hemilaryngectomy reconstruction involves the use of a pedicled muscle flap to fill the resection defect. However, when the ipsilateral arytenoid cartilage is removed, severe breathy dysphonia or aphonia usually results from posterior glottal incompetence. This outcome is due to profound air wasting due to the contralateral (healthy) vocal fold's inability to achieve posterior closure. We have employed ipsilateral hemicricoidectomy as a secondary rehabilitative procedure in such patients, and as a primary procedure at the time of hemilaryngectomy in patients who require arytenoid cartilage removal.

SURGICAL TECHNIQUE

A horizontal incision is made in a skin crease overlying the thyroid ala. The underlying tissue is dissected to expose the cricoid cartilage in the midline. Next, the soft tissue overlying the ipsilateral portion of the cricoid cartilage is dissected free, exposing the cartilage from the anterior midline to the posterior midline. Preserving the inner perichondrium and subglottic mucosa, the hemicricoidectomy is then carried out bluntly with a Freer or Herd elevator (Fig 1). An oscillating saw may also be used for this por-

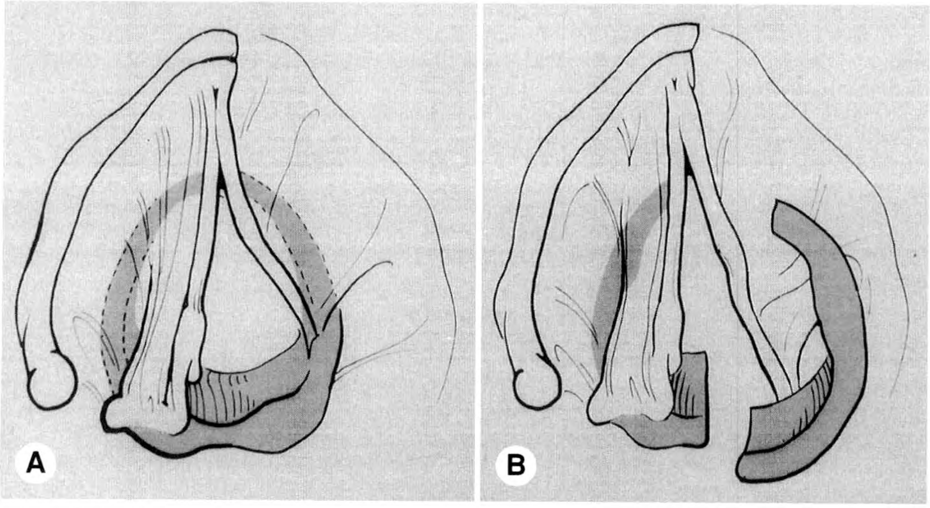

Fig 1. A) Problem: widely lateralized posterior neoglottis. **B)** Removal of ipsilateral half of cricoid cartilage.

From the Center for Voice Disorders of Wake Forest University, Winston-Salem, North Carolina (both authors), and the Department of Otolaryngology, Medical College of Pennsylvania/Hahnemann University School of Medicine, Philadelphia, Pennsylvania (Amin).

Presented at the meeting of the American Laryngological Association, Orlando, Florida, May 13-14, 2000.

CORRESPONDENCE — James A. Koufman, MD, Center for Voice Disorders, Dept of Otolaryngology, Wake Forest University School of Medicine, Medical Center Blvd, Winston-Salem, NC 27157-1034; e-mail: jkoufman@wfubmc.edu.

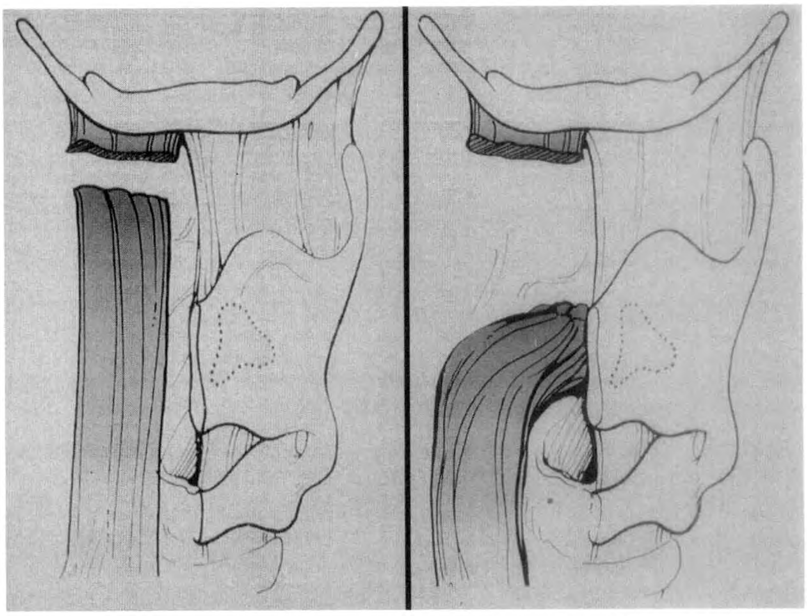

Fig 2. Reconstruction with strap muscle sutured to midline, filling gap left by removed arytenoid cartilage.

tion of the procedure. Care is taken not to cross the midline anteriorly or posteriorly. Excessive resection will lead to significant airway narrowing. Conversely, inadequate resection of the posterior portion of the cricoid cartilage leads to a poor postoperative outcome (due to a persistent glottal gap). The anterior cut is made at the midline, and the posterior cut is made 2 to 3 mm from the midline.

The vocal fold reconstruction is accomplished by the use of an inferiorly based portion of medial strap muscle, approximately 2 to 3 cm in thickness. The superior muscle detachment should be made just below the hyoid bone; care should be taken not to devitalize the neurovascular bundle below. The cut end of the strap muscle flap is sutured to the site of the previously removed arytenoid cartilage (Fig 2). Pyriform sinus mucosa is then mobilized and used to cover the muscle flap. The mucosal closure should be complete, particularly inferiorly. A Montgomery stent is then custom-tailored as a hemilaryngectomy mold (Fig 3A). Once the stent is placed into the larynx, the mucosa is closed in a standard fashion. The remaining strap muscles are closed in the midline. Finally, braided pacemaker wire is placed through the skin flap and the larynx, securing the stent. The wound is drained and closed in layers. Figure 3B shows the completed procedure. The stent is left in place 1 to 2 weeks and then removed endoscopically.

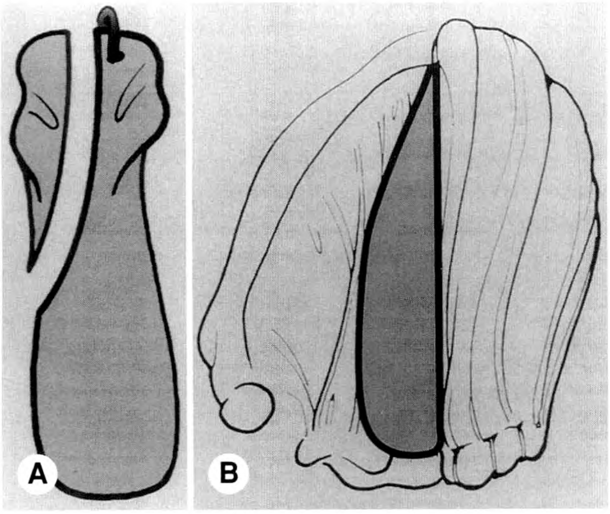

Fig 3. Modified Montgomery stent. **A)** Anterior view. **B)** Superior view of stent in place, against strap muscle reconstruction.

CASE REPORTS

CASE 1

A 30-year-old man with a history of T1N0 squamous cell carcinoma of the right true vocal fold had been initially treated with radiotherapy. Three years later, the tumor recurred, and he underwent a right vertical hemilaryngectomy with arytenoid cartilage removal. Afterward, the patient was aphonic. On examination, the patient demonstrated a wide-open posterior glottis during attempted phonation (Figure 4A,B). An attempt at improving the voice by augmenting the left vocal fold with lipoinjection was unsuccessful. The patient desired further voice rehabilitation and underwent hemicricoidectomy and reconstruction. The tracheotomy was removed 3 weeks after surgery. After the operation, the patient's voice was rated as class 2.0 (see Table). Figure 4C shows the appearance of the larynx during inspiration 1 year after reconstruction.

Comment. With the hemicricoidectomy procedure, the time to decannulation may vary from patient to patient, since the airway is significantly reconfigured

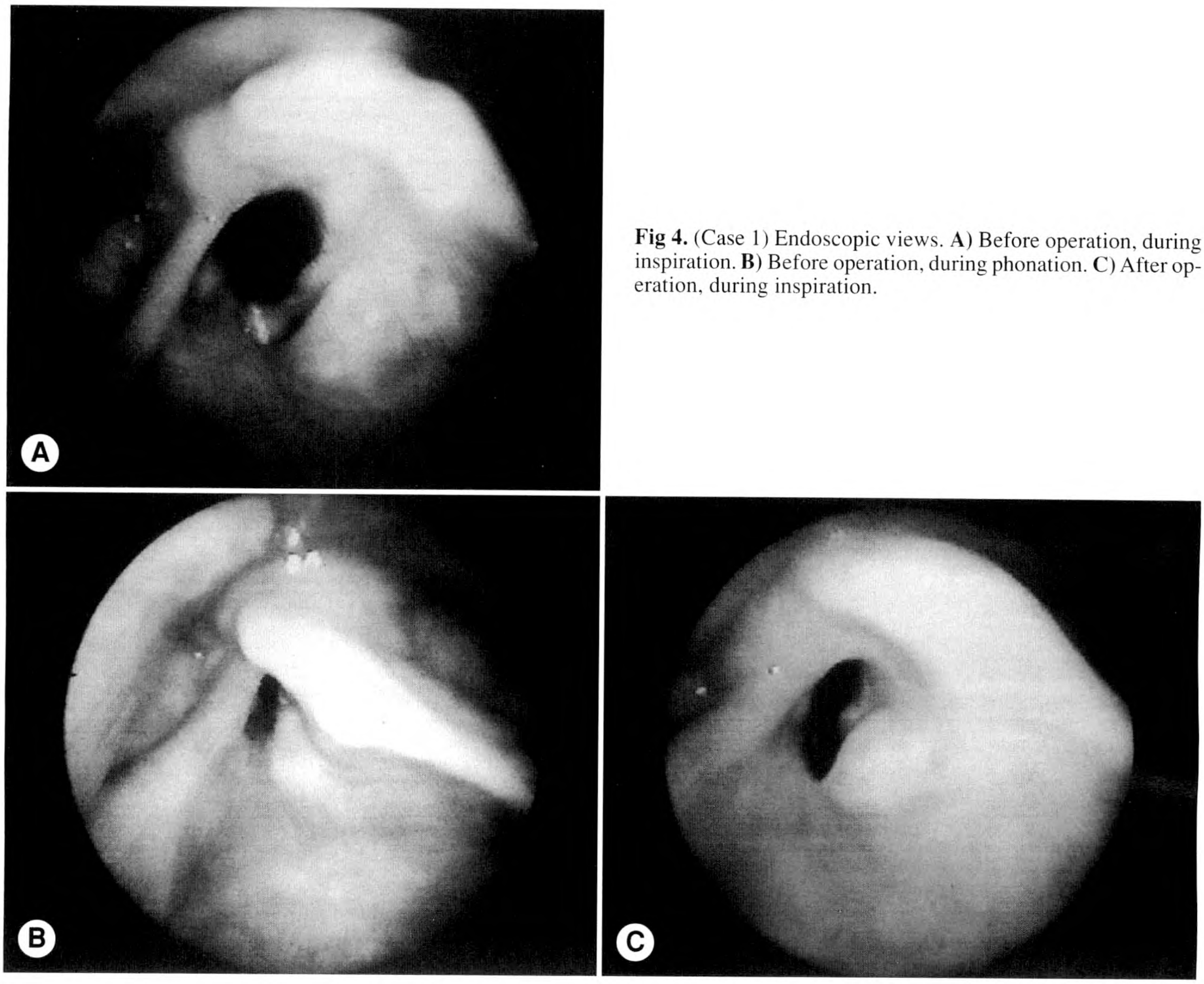

Fig 4. (Case 1) Endoscopic views. **A)** Before operation, during inspiration. **B)** Before operation, during phonation. **C)** After operation, during inspiration.

and reduced in size. In this patient, although Fig 4C shows that the airway was obviously narrowed, the patient was athletic and experienced no airway-related symptoms. Five years later, the patient's voice and airway were unchanged. In performing this procedure, the surgeon must avoid removing too much of the cricoid cartilage.

CASE 2

A 34-year-old woman was found to have a T2N0 squamous cell carcinoma of the left true vocal fold. The lesion was bulky and involved a portion of the ipsilateral arytenoid cartilage. The patient elected surgical therapy and underwent an extended left hemilaryngectomy with removal of the ipsilateral arytenoid cartilage. During the operation, the patient was left with a relatively large posterior defect. Therefore, she underwent hemicricoidectomy, followed by strap muscle reconstruction. She was decannulated 3 weeks after surgery. At the 2-year follow-up, the patient had no evidence of new or recurrent cancer, and her voice was rated as class 3.0; the patient was satisfied with the result.

VOICE RATING SYSTEM

Voice Rating	*Definition*
1.0	Normal voice
2.0	Near-normal voice (normal to layperson)
3.0	Moderate dysphonia
4.0	Severe dysphonia
5.0	Aphonia

Comment. Hemicricoidectomy as part of the primary oncological procedure may be indicated when the surgeon anticipates difficulty closing the posterior larynx with a traditional method of reconstruction.

DISCUSSION

Vertical partial laryngectomy has long been accepted as a form of conservation laryngeal surgery for the treatment of selected glottic tumors.[1-3] The procedure was initially designed to treat unilateral glottic malignancies, but has since been extended to include tumors involving the anterior commissure and/or the ipsilateral arytenoid mucosa.[4]

Although there has been little change in terms of the resection over the years, there have been many articles proposing different reconstructive techniques.[5-9] The goal of reconstructive techniques is mainly to provide better postoperative voice and deglutition by reconstructing the resected vocal fold. In his article on glottic reconstruction, Hirano[5] proposes three requirements for good phonatory function following this procedure: adequate glottic closure, proper alignment of the reconstructed fold at the glottic level, and a smooth lining for the reconstructed side. With standard hemilaryngectomies (not involving the resection of the arytenoid cartilage), the above criteria are achievable with the use of muscle flaps or other reconstructive techniques in most cases, since the surgical defect is relatively small. However, when the resection is extended to involve the arytenoid cartilage, a larger defect is created posteriorly. This posterior defect is usually difficult to fill with a pedicled muscle flap because of the height and bulk of the cricoid cartilage in this region. As a result, the patient undergoing reconstruction with a standard muscle flap often experiences profound air wasting due to a persistently open posterior glottis. The patient is also placed at an increased risk of aspiration, as he or she cannot occlude the glottis when swallowing.

Biller and Urken[10] recognized this problem and proposed hemicricoid collapse. This technique allowed the remaining arytenoid cartilage to better approximate the reconstructed side, resulting in elimination of aspiration in 3 of the 4 patients on whom they performed the procedure. Their procedure involved removing multiple small vertical segments of cricoid cartilage on the ipsilateral side and collapsing the cricoid ring. The segments were secured in the collapsed position with a suture.[10]

In addition to providing a novel reconstructive technique, Biller and Urken[10] demonstrated the relative safety of removing portions of the cricoid cartilage, which previously was thought to be injudicious. Unfortunately, the cricoid collapse procedure is quite technically complicated, as it entails making up to 9 cuts in the cricoid cartilage with a saw while avoiding injury to the inner perichondrium. We performed this procedure in 1 patient and found that it did not allow adequate medialization of the posterior portion of the glottis.

As an alternative, we propose removal of the ipsilateral half of the cricoid cartilage. This procedure has been used as an adjunct in reconstruction following hemilaryngectomy with resection of the ipsilateral arytenoid cartilage. The removal of half of the cricoid cartilage allows the muscle flap reconstruction to better approximate the midline, since it does not have to bend around the cricoid cartilage. Additionally, with removal of the bulky posterior portion of the cricoid cartilage, the muscle flap can more easily fill the posterior defect left by the removal of the arytenoid cartilage.

Because of the partial airway collapse, molds must be placed until the reconstructed side heals. A tracheotomy is therefore needed as part of the procedure. As mentioned, a modified endolaryngeal stent is placed; this is typically removed 1 to 3 weeks after the operation. After a period of observation, the patient is decannulated.

Hemicricoidectomy is infrequently indicated; we have performed this procedure in 6 patients. Unfortunately, follow-up in this group has been poor. Nevertheless, 5 of the patients were decannulated within 6 weeks. The other patient, who had long-standing suppurative chondritis before the operation, required prolonged tracheotomy. The average length of time to decannulation was 5 weeks. Long-term voice follow-up was possible for 3 patients: 1 had an excellent voice and 2 had fair voices. No patient in the series had significant postoperative aspiration.

One potential disadvantage of this procedure is the risk of causing airway narrowing. We did not encounter problems in decannulating these 6 patients. However, we recognize that we present only a small series of cases, and that these results may not hold up with continued use of this procedure.

CONCLUSIONS

Hemicricoidectomy with strap muscle reconstruction may be used to close the posterior larynx in patients requiring vertical hemilaryngectomy with removal of the ipsilateral arytenoid cartilage. We believe that this technique offers a viable method of vocal rehabilitation to patients who otherwise have no feasible alternatives. Although experience with this technique is limited, the procedure may provide excellent results in carefully selected cases.

REFERENCES

1. Ogura JH. Management of early cancer of the vocal cord — laryngofissure, hemilaryngectomy, irradiation. Trans Pac Coast Otoophthalmol Soc Annu Meet 1963;44:245-7.
2. Quinn HJ Jr. Hemilaryngectomy: indications and technique. J La State Med Soc 1968;120:316-20.
3. Leonard JR, Holt GP, Maran AG. Treatment of vocal cord carcinoma by vertical hemilaryngectomy. Ann Otol Rhinol Laryngol 1972;81:469-78.
4. Norris CM. Role and limitations of vertical hemilaryngectomy. Can J Otolaryngol 1975;4:426-31.
5. Hirano M. Technique for glottic reconstruction following vertical partial laryngectomy: a preliminary report. Ann Otol

Rhinol Laryngol 1976;85:25-31.

6. Bailey BJ. Glottic reconstruction after hemilaryngectomy: bipedicle muscle flap laryngoplasty. Laryngoscope 1975;85: 960-77.

7. Quinn HJ. Free muscle transplant method of glottic reconstruction after hemilaryngectomy. Laryngoscope 1975;85:985-6.

8. Kambic V, Radsel Z, Smid L. Laryngeal reconstruction with epiglottis after vertical hemilaryngectomy. J Laryngol Otol 1976;90:467-73.

9. Friedman M, Toriumi DM. Glottic reconstruction following hemilaryngectomy: false cord advancement flap. Laryngoscope 1987;97:882-4.

10. Biller HF, Urken M. Cricoid collapse. A new technique for management of glottic incompetence. Arch Otolaryngol 1985;111:740-1.

≈

NINTH INTERNATIONAL FACIAL NERVE SYMPOSIUM

The Ninth International Facial Nerve Symposium will be held July 29 to August 1, 2001, in San Francisco, California. For information, contact Office of Continuing Medical Education, University of California, San Francisco; telephone: (415) 476-5808; fax: (415) 502-1795; e-mail: info@ocme.ucsf.edu.

Ann Otol Rhinol Laryngol 110:2001

ANTERIOR WINDOW LARYNGOPLASTY: A NEW ANATOMIC APPROACH FOR POSTERIOR GLOTTIC AND SUBGLOTTIC STENOSIS

TULIO A. VALDEZ, MD
ROMAN SCHUMANN, MD
ZHI WANG, MD
STANLEY M. SHAPSHAY, MD
BOSTON, MASSACHUSETTS

This study explores the feasibility of an anterior thyroid window as a new approach for posterior glottic stenosis. An anterior window was made on the thyroid cartilage of human cadaver larynges, with its superior edge below the level of the vocal cords and an inferior pedicle composed of the inferior border of the thyroid cartilage attached to the cricothyroid membrane, which was left intact. By obtaining direct exposure of the posterior glottis and cricoarytenoid joints, mucosal graft suturing and exploration of the joints were easily achieved with an operating microscope. This study demonstrates the anatomic feasibility of an anterior window laryngoplasty as an alternative approach to treating posterior glottic stenosis while preserving the cartilage framework and avoiding the anterior commissure. This technique may improve endolaryngeal manipulation by providing a closer and more direct exposure than do endoscopic techniques, and by having fewer possible complications than traditional open techniques.

KEY WORDS — anterior thyroid window, anterior window laryngoplasty, posterior glottic stenosis.

INTRODUCTION

Treatment of posterior glottic stenosis constitutes a challenge for the head and neck surgeon. Airway compromise is the most common and severe manifestation of this condition dictating the rationale for therapy. In addition to improving the respiratory function, the surgeon should emphasize achieving good long-term voice quality and preserving normal swallowing.

Surgery performed to reestablish an adequate airway can be divided into endoscopic and open procedures. Both approaches offer a number of techniques, each with individual indications, advantages, and disadvantages. Careful assessment of the patient's overall condition and especially of the posterior commissure, including vocal cord mobility, cricoarytenoid joint function, and length of the stenosis, is key in selecting the best treatment.

"Window-type" laryngoplasties have provided access for the otolaryngologist to perform endolaryngeal procedures while minimally disrupting the cartilage framework. Good results have been obtained with window laryngoplasties in cases of vocal cord medialization[1,2] and, more recently, in treating glottic cancer involving the anterior commissure.[3] However, this technique has never been described in the treatment of laryngeal stenosis. This ex vivo study explores the anatomic feasibility of a new, less-invasive external approach for the treatment of posterior and subglottic stenosis using an anterior window access below the level of the vocal cords to preserve the anterior commissure and the integrity of the laryngeal framework. Our intention is to provide for a direct binocular approach to the posterior glottic and subglottic disorder with preservation of phonatory and swallowing function while reconstructing the stenotic airway.

METHODS

Five freshly harvested adult cadaver larynges with strap muscles were used in this study. The larynges were fixed and placed in a Plexiglas holder specially constructed for the project. The larynges were suspended to allow adequate endoscopic visualization with a large-bore Dedo-Jako design (Pilling Co, Philadelphia, Pa) laryngoscope. The operating microscope was used with a 250-mm lens, and ophthalmologic and otologic instruments were used in the dissection. Measurements were made with standard surgical calipers.

Open Procedure. The fascial layers of the sternohyoid and omohyoid muscles were separated in the

TABLE 1. DIMENSIONS OF SPECIMENS

Larynx	*Window Size Without Retractor (mm)*	*Window Size With Retractor (mm)*	*Distance From Window to Posterior Commissure (mm)*
1	14.0 × 15.0	16.0 × 23.0	40.0
2	14.0 × 5.5	15.0 × 24.0	39.0
3	13.0 × 13.0	14.0 × 21.0	37.0
4	13.0 × 14.5	15.0 × 22.0	38.0
5	14.0 × 15.0	15.0 × 22.0	42.0

From the Departments of Otolaryngology–Head and Neck Surgery (Valdez, Wang, Shapshay) and Anesthesia (Schumann), New England Medical Center, Tufts University School of Medicine, Boston, Massachusetts.

Presented at the meeting of the American Laryngological Association, Orlando, Florida, May 13-14, 2000.

CORRESPONDENCE — Tulio A. Valdez, MD, Dept of Otolaryngology, Tufts University School of Medicine, New England Medical Center, Otolaryngology Research Laboratory, 750 Washington St, Box 187, Boston, MA 02111.

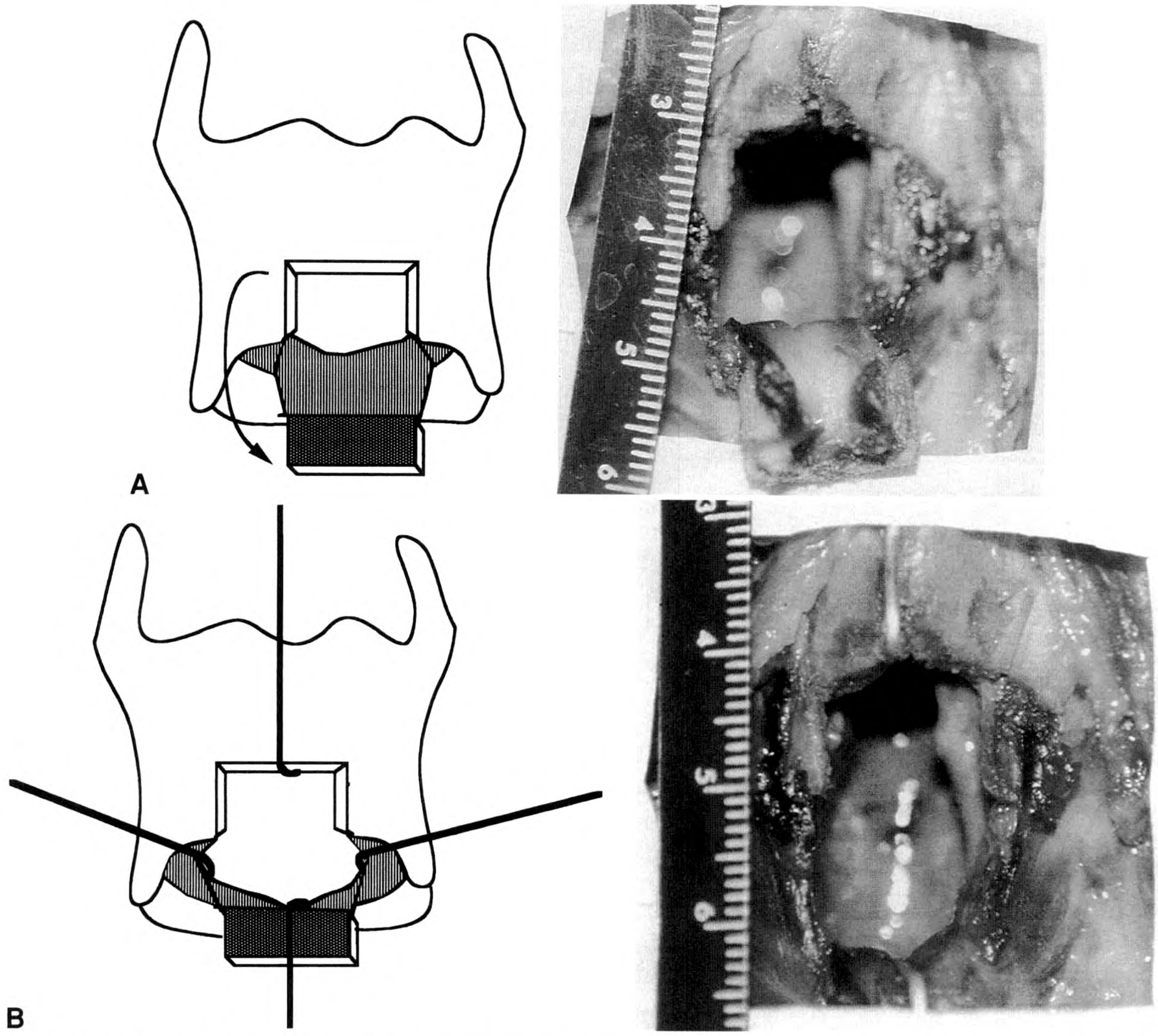

Fig 1. A) Everted anterior window with inferior pedicle composed of inferior border of thyroid cartilage attached to cricothyroid membrane (line drawing and photograph). **B)** Window after retraction of cricothyroid membrane. Note increase in size of window and direct exposure of posterior commissure and cricoarytenoid joint.

midline to expose the thyroid notch, the anterior aspect of the thyroid cartilage, the cricothyroid membrane, and the superior edge of the cricoid cartilage. A 22-gauge hypodermic needle was inserted through the middle third of the thyroid cartilage into the laryngeal lumen and viewed endoscopically to ensure the correct position of the intended window. Using a No. 10 surgical blade under endoscopic visual control, we created a window below the level of the vocal cords with an inferiorly based pedicle composed of the inferior border of the thyroid cartilage attached to the cricothyroid membrane, which was left intact. In cases in which the cartilage had undergone ossification, an oscillating saw was used to create the window. The distance between the cricothyroid muscles at their cricoid insertion dictated the width of the window. The external perichondrium was preserved to allow a complete closure after the procedure. After its completion, the window was everted with small skin hooks. After eversion of the cartilage from the window, a midline horizontal line was cauterized on the inner perichondrium with a bipolar cautery at a low power setting. This line was later incised to gain access to the airway lumen. Small self-retaining retractors were then placed in both vertical and horizontal axes to achieve wider exposure. The inferior vertical retractors were carefully placed between the medial insertions of the cricothyroid muscles to avoid any damage to these muscles. The size of the window was measured in all 5 larynges, as well as the distance from the window to the posterior commissure.

Intraluminal Procedures. The feasibility of various surgical and diagnostic procedures was explored through this new surgical approach. Under direct mag-

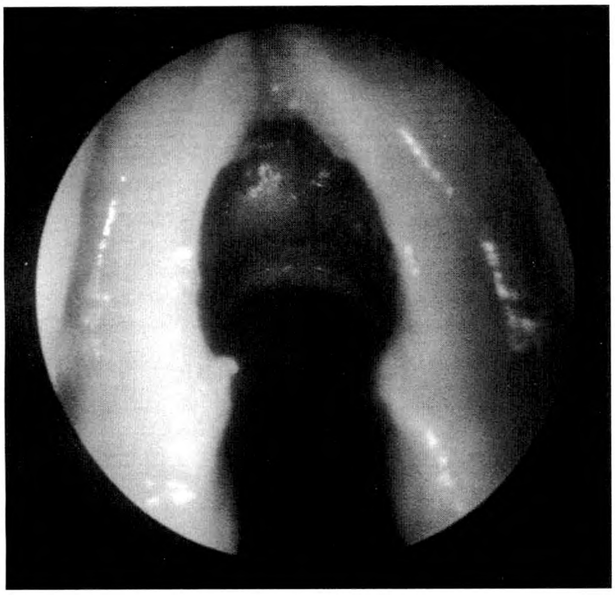

Fig 2. Endoscopic view of intact anterior commissure after anterior window laryngoplasty.

nified visualization with an operating microscope at 16× magnification, palpation and mobilization of the cricoarytenoid joint were performed. Incisions were made in the posterior commissure to create mucosal advancements flaps, mucosal grafts, and micro-trapdoor flaps, which were then sutured into place with 6-0 chromic sutures on non-cutting needles. A 3-dimensional scar model was made of silicone rubber and placed on the posterior glottis. Photodocumentation of the scar model was then done through the rigid laryngoscope and through the window laryngoplasty for comparison.

Closure. The inner perichondrium and mucosal lining were approximated with 4-0 chromic gut sutures. The cartilage window was then reapproximated along with the external perichondrium with uninterrupted 4-0 Dexon sutures in 2 specimens and with mini reconstruction plates[4] in the remaining larynges. The strap muscles were sutured into position with 2-0 chromic gut sutures.

RESULTS

The anterior window laryngoplasty provided an excellent direct exposure of the posterior commissure and the cricoarytenoid joints. Table 1 illustrates the dimensions of the windows and the distance from the anterior window to the posterior commissure in each specimen. The vertical dimensions of the window were increased significantly with the use of retractors without disrupting the cricothyroid membrane, allowing better exposure of the posterior commissure, cricoarytenoid joints, and posterior subglottis (Fig 1). No major vascular or nerve structures were disturbed through this approach. The anterior commissure (Fig 2) was spared, as well as the cricothyroid membrane and cricothyroid muscle.

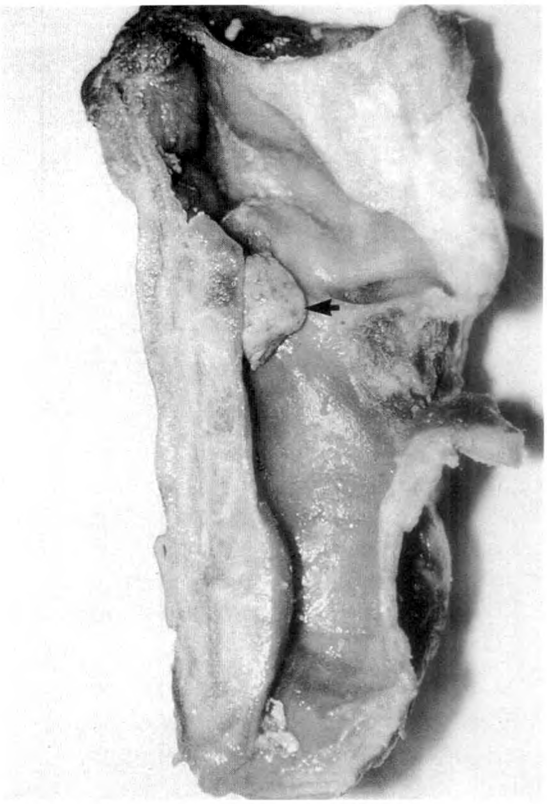

Fig 3. Sagittal cut through larynx and silicone scar model (arrow) on posterior glottis. Note window below vocal cords and access it provides to posterior glottis, subglottis, and cricoarytenoid joints.

In visualization of the scar model, significant differences were noted between the endoscopic approach and the window. Through the window, the scar model was seen in its entirety as a 3-dimensional structure, while the endoscopic view revealed only the superior aspect of the scar model, limiting assessment of the length and complexity of the lesion (Fig 3). Also by use of the window, the mobility of the cricoarytenoid joint was easily evaluated in its 3-dimensional range of movement.

The ability to use the microscope at a short operating distance allowed an improved endolaryngeal manipulation as compared to endoscopic techniques. By means of bimanual standard surgical techniques, creating mucosal flaps (mucosal advancement, micro-trapdoor flaps) and suturing them into place was achieved without difficulty. The use of readily available short–working length ophthalmologic and otologic instruments proved ideal for this purpose, facilitating the surgical procedures.

DISCUSSION

Posterior glottic stenosis is common and a major

TABLE 2. CLASSIFICATION OF POSTERIOR GLOTTIC STENOSIS

Type I	Interarytenoid scar with normal PC
Type II	PC scarring, no CA involvement
Type III	PC scarring with 1 CA involved
Type IV	PC scarring with both CAs involved

Classification system is from Bogdasarian and Olson.[7]

PC — posterior commissure, CA — cricoarytenoid joint.

cause of morbidity in patients who have undergone prolonged or traumatic endotracheal intubation. The incidence of posterior glottic stenosis has been reported to be as high as 14% in patients intubated for more than 10 days.[5] However, this condition is often overlooked, since patients with mild cases may present with a normal voice and minor respiratory symptoms, which are often misdiagnosed and attributed to other entities. Severe cases of posterior glottic stenosis, on the other hand, usually present with severe respiratory compromise that often requires a tracheotomy.

Distinguishing posterior glottic stenosis from other movement disorders of the vocal cords, such as vocal cord paralysis, is not easy.[6] Establishing a correct diagnosis normally requires laryngeal electromyography and visualization and palpation of the cricoarytenoid joints under direct laryngoscopy with assessment of the extent of the stenotic lesion. Bogdasarian and Olson[7] developed a classification system for posterior glottic stenosis that emphasizes the importance of cricoarytenoid joint mobility (Table 2). This classification is the most widely used today for this condition.

The most difficult challenge with this condition, however, is not diagnosis, but treatment. The goal of therapy, whenever possible, is to improve the patency of the respiratory glottis while preserving an adequate voice and avoiding aspiration and swallowing impairment. One factor that adds to the difficulty of treatment is stenosis that involves more than 1 anatomic site, such as combined subglottic and posterior glottic stenosis. Some studies have reported an incidence as high as 27% for cases of posterior glottic stenosis involving more than 1 anatomic site.[8]

The present treatment methods are divided into 2 groups, namely, endoscopic and open procedures. Endoscopic procedures comprise a number of techniques utilizing the laser or microlaryngeal instruments. Laser techniques have become popular over the past decade, and a number of procedures have been developed. Among these procedures, laser posterior cordotomy, laser partial and total arytenoidectomy, and micro-trapdoor flap techniques[9-12] are the most routinely used today for the treatment of posterior glottic stenosis. However, some limitations of endoscopic laser treatment have not been overcome, such as achieving good results in lesions with a vertical length greater than 1 cm or those involving more than 1 anatomic site.[13] Other limitations, such as the difficulty of achieving good endoscopic exposure, and the technical difficulties involved in elevating mucosal flaps or suturing or welding grafts, are also frequently present with the endoscopic approach.

The ideal exposure of posterior glottic and subglottic scarring can only be obtained through a direct external approach. The endoscopic line of vision is parallel to the scar site, rather than giving the preferred perpendicular access. The external exposure to the subglottic–posterior commissure area as designed in this study eliminates the long working distance inherent in the endoscopic approach. In addition, endoscopic treatment for posterior glottic stenosis often requires various procedures because of the high incidence of restenosis following scar resection. More recently, intraoperative use of topical mitomycin-C has been advocated to reduce scar formation after endoscopic laser procedures.[14] There are no data, however, to show that the use of mitomycin-C actually decreases the number of endoscopic procedures required to achieve an adequate airway.

Open surgical procedures such as laryngofissure and laryngotracheal reconstruction[15-17] are usually performed after failure of endoscopic procedures or when the area of stenosis is longer than 1 cm or involves multiple sites. Excellent exposure from a comfortable operating distance is obtained with these techniques; unfortunately, they violate the integrity of the cartilage framework and the anterior commissure, leading to changes in voice production. These procedures usually involve extensive surgical exposure and reconstruction, in many cases to treat lesions that are limited to only a few centimeters. Other surgical techniques, such as an anterior cricoid split with a midline thyrotomy, can also provide access to the posterior glottis while sparing the anterior commissure. However, this technique provides very limited exposure of the cricoarytenoid joints and therefore is best suited for early, membranous stenoses. A similar technique, involving an extended anterior cricoid split, has also been described for the treatment of membranous posterior glottic stenosis in pediatric patients.[18]

The rationale behind the anterior window laryngoplasty approach is obtaining an adequate exposure of the posterior commissure, cricoarytenoid joints, and subglottic region while minimally disrupting the cartilage framework, and preserving an intact anterior commissure, thereby preserving function. The anterior window laryngoplasty provides a direct exposure of the posterior glottis and the subglottic region, allowing the surgeon to assess joint mobility and the extent and complexity of the scar 3-dimensionally. Most important, it allows the surgeon to work bimanually under binocular magnification using an operating microscope, thereby improving endolaryngeal manipulation. Through the window laryngoplasty, we were able to perform endolaryngeal procedures technically difficult to perform through an endoscopic approach, such as raising mucosal flaps and suturing grafts into place.

The anterior window laryngoplasty spares important anatomic structures involved with voice production, such as the anterior commissure and the cricothyroid muscles, despite its midline location. At the same time, since the approach is midline, it does not violate any major vascular or nerve structure. The major anatomic advantage of this approach is provided by the possibility of retracting the cricothyroid membrane, significantly increasing the exposure and allowing the surgeon to use both hands. The size of the window after retraction of the cricothyroid membrane compares to that of the lumen of a large-bore rigid laryngosocope.

This ex vivo study validates the anatomic feasibility of this new approach to posterior glottic stenosis. It offers the possibility of a less-radical external approach to posterior glottic and subglottic stenosis, achieving exposure comparable to that of laryngofissure and preserving phonatory function. Additional procedures that may be performed through this approach are cricoarytenoid joint exploration, cordotomy, partial or complete arytenoidectomy, and posterior and anterior cricoid split with stent placement. Future clinical application of this technique is planned on the basis of this feasibility study. Ideal clinical candidates for this approach to posterior commissure and subglottic stenosis would be patients with preexisting tracheotomies, which would facilitate anesthesia and ventilation. Innovative ventilatory techniques are being discussed with our anesthesia colleagues for those patients without tracheotomies.

REFERENCES

1. Isshiki N, Morita H, Okamura H, Hiramoto M. Thyroplasty as a new phonosurgical technique. Acta Otolaryngol (Stockh) 1974;78:451-7.
2. Isshiki N. Mechanical and dynamic aspects of voice production as related to voice therapy and phonosurgery. J Voice 1998;12:125-37.
3. Rebeiz EE, Wang Z, Annino DJ, McGilligan JA, Shapshay SM. Preliminary clinical results of window partial laryngectomy: a combined endoscopic and open technique. Ann Otol Rhinol Laryngol 2000;109:123-7.
4. Woo P. Laryngeal framework reconstruction with miniplates. Ann Otol Rhinol Laryngol 1990;99:772-7.
5. Whited RE. A prospective study of laryngotracheal sequelae in long-term intubation. Laryngoscope 1984;94:367-77.
6. Cohen SR. Pseudolaryngeal paralysis: a postintubation complication. Ann Otol Rhinol Laryngol 1981;90:483-8.
7. Bogdasarian RS, Olson NR. Posterior glottic laryngeal stenosis. Otolaryngol Head Neck Surg 1980;88:765-72.
8. McCaffrey TV. Classification of laryngotracheal stenosis. Laryngoscope 1992;102:1335-40.
9. Kashima HK. Bilateral vocal fold motion impairment: pathophysiology and management by transverse cordotomy. Ann Otol Rhinol Laryngol 1991;100:717-21.
10. Dennis DP, Kashima H. Carbon dioxide laser posterior cordectomy for treatment of bilateral vocal cord paralysis. Ann Otol Rhinol Laryngol 1989;98:930-4.
11. Crumley RL. Endoscopic laser medial arytenoidectomy for airway management in bilateral laryngeal paralysis. Ann Otol Rhinol Laryngol 1993;102:81-4.
12. Dedo HH, Sooy CD. Endoscopic laser repair of posterior glottic, subglottic and tracheal stenosis by division or micro-trapdoor flap. Laryngoscope 1984;94:445-50.
13. Simpson GT, Strong MS, Healy GB, Shapshay SM, Vaughan CW. Predictive factors of success or failure in the endoscopic management of laryngeal and tracheal stenosis. Ann Otol Rhinol Laryngol 1982;91:384-8.
14. Rahbar R, Valdez TA, Shapshay SM. Preliminary results of intraoperative mitomycin-C in the treatment and prevention of glottic and subglottic stenosis. J Voice 2000;14:282-6.
15. McCaffrey TV. Management of subglottic stenosis in the adult. Ann Otol Rhinol Laryngol 1991;100:90-4.
16. Grillo HC. Primary reconstruction of airway after resection of subglottic laryngeal and upper tracheal stenosis. Ann Thorac Surg 1982;33:3-18.
17. Montgomery WW. Posterior and complete laryngeal (glottic) stenosis. Arch Otolaryngol 1973;98:170-5.
18. Fell WR, Brown OE. Membranous posterior glottic stenosis successfully treated by extended cricoid split procedure: a case report. Int J Pediatr Otorhinolaryngol 1996;37:269-75.

Ann Otol Rhinol Laryngol 110:2001

INTRAOPERATIVE PEDIATRIC LARYNGEAL ELECTROMYOGRAPHY: EXPERIENCE AND CAVEATS WITH MONOPOLAR ELECTRODES

DANIEL L. WOHL, MD
JACKSONVILLE, FLORIDA
ROBERT T. LESHNER, MD
RICHMOND, VIRGINIA
JEFFERSON K. KILPATRICK, MD
RICHMOND, VIRGINIA
WAYNE T. SHAIA, MD
RICHMOND, VIRGINIA

We report our experience with intraoperative laryngeal electromyography (L-EMG) using direct laryngoscopy and placement of monopolar electrodes under general anesthesia in the evaluation and management of laryngeal dysfunction in pediatric patients. In this series of case studies, we present clinical data on 30 pediatric patients with known or suspected anatomic or neurologic laryngotracheal disorders evaluated with placement of shielded monopolar electrodes into the thyroarytenoid muscles during direct laryngoscopy under general anesthesia. Diagnoses included congenital vocal fold paralysis (VFP), laryngotracheal stenosis, cerebral palsy, laryngeal tumors, traumatic vocal fold dysfunction, and postsurgical VFP. The impact of L-EMG on patient management was assessed. We found that L-EMG objectively supported clinical findings, but provided new objective data relevant toward management recommendations in only a few selected pediatric patients with new-onset vocal fold paralysis or paresis or infiltrative laryngeal tumors, and in selected postsurgical cases involving decannulation decisions. The prognostic utility of L-EMG in newborns with congenital VFP has not been established. A normal L-EMG recording indicates an intact neuromuscular axis, but does not guarantee vocal fold mobility or guarantee muscle function in a partially denervated or deconditioned muscle. The potential for false-negative recordings is the major limitation of this technique.

KEY WORDS — electromyography, insufflation anesthesia with spontaneous ventilation, motor unit action potentials, vocal fold paralysis.

INTRODUCTION

Electromyography (EMG) is an accepted methodology for evaluating neuromuscular diseases in children.[1] It provides diagnostic information on muscle function and innervation. It can aid in establishing the site of neural disease. It can distinguish between upper and lower motor dysfunction. Laryngeal EMG (L-EMG) is commonly performed on adults to differentiate myopathy from neuropathy and to distinguish between functional and organic disorders.[2,3] The application of L-EMG in the pediatric population is relatively recent. The clinical indications, as well as the most sensitive and specific technique, have not been established. It has been recommended for the evaluation of vocal fold paralysis (VFP) in children,[4,5] but its utility as a prognostic test for congenital VFP has been questioned.[6]

In this series of case studies, we report our experience with 30 pediatric patients who underwent direct rigid laryngoscopy and intraoperative shielded monopolar L-EMG. The preoperative diagnoses included congenital or acquired VFP and other known or suspected anatomic, physiological, and neuromuscular laryngotracheal disorders. We discuss the advantages and disadvantages of the clinical application of this technique in pediatric patients.

MATERIALS AND METHODS

PATIENT SELECTION

Between August 1993 and March 1998, the senior author (D.L.W.) selected 32 patients for L-EMG testing. All patients were evaluated in a tertiary care academic institution. When possible, both sides of the larynx were sampled. Patients who underwent L-EMG were placed into 3 categories based on their clinical diagnosis: 1) patients with congenital paralysis or paresis of the true vocal folds, 2) patients with anatomic, physiological, or neuromuscular laryngeal abnormalities other than congenital VFP, and 3) patients with normal vocal fold mobility according to clinical examination but with other laryngotracheal disorders warranting an endoscopic airway evaluation under general anesthesia.

TECHNIQUE

All recordings were obtained with either a Nicolet (Madison, Wis) or a Neuromax (Excel Technology Limited, Oakville, Canada) EMG unit. We used 37-,

---

From the Department of Otolaryngology–Head and Neck Surgery, Virginia Commonwealth University School of Medicine and Children's Hospital, Richmond, Virginia.

Presented in part at the meeting of the American Laryngological Association, Palm Beach, Florida, May 9-10, 1998.

CORRESPONDENCE — Daniel L. Wohl, MD, Division of Pediatric Otolaryngology–Head and Neck Surgery and Communication Sciences, Nemours Children's Clinic, 807 Nira St, Jacksonville, FL 32207.

48-, or 75-mm shielded TECA (Oxford Instruments, Hawthorne, NY) disposable monopolar needle EMG electrodes to assess for thyroarytenoid muscle motor unit action potential (MUAP) activation. The reference surface electrodes were placed immediately below the clavicle.

Under general insufflation anesthesia with spontaneous ventilations, each patient underwent flexible and rigid direct laryngoscopy. Assessments were made for vocal fold mobility in phase with the ventilatory cycle, and palpation was done to determine normal cricoarytenoid joint mobility. Suspension laryngoscopy with microscopic examination was used early in this series. Handheld laryngoscopy was judged to be more efficient and became our preferred technique for palpation and visualization of the supraglottis and glottis.

The electrodes were placed into the thyroarytenoid muscle with microlaryngeal forceps or, in small children, placed directly using the longer needles. Special care was taken to avoid stripping the Teflon coat during needle electrode placement. Correct placement was confirmed by direct vision or, in patients in whom direct visualization was difficult, by the use of a rigid 4.0-mm or 2.8-mm telescope. As many as 3 passes into each thyroarytenoid muscle were performed to ensure wide sampling of the thyroarytenoid muscles if action potentials were not identified despite vocal fold movement in phase with the ventilatory cycle.

Recordings were interpreted by 1 neurologist-electromyographer (R.T.L.), who was present throughout the procedure. Special attention was taken to make sure that recorded potentials were "near motor units" as defined by MUAP activation with a rapid rise time and a sharply contoured waveform configuration, and not "distant motor units" from the surrounding strap or intercostal musculature. The distinction between near units and distant motor unit potentials was deemed critical in defining the integrity of the recurrent laryngeal nerve–thyroarytenoid muscle axis. Clinical correlation between endoscopic findings and motor unit recruitment or spontaneous electrophysiological abnormalities was made. Characterization of motor unit configuration, especially long-duration or complex motor units, was made.

RESULTS

Between August 1993 and March 1998, we evaluated 30 pediatric patients with direct laryngoscopy and L-EMG. Nine patients were female, and 21 were male. Their ages ranged from 49 days to 17 years (median, 4 years). Two young children with hypoplastic mandibles (Nos. 16 and 32) were selected for this study, but L-EMG could not be performed because of anatomic constraints. No patient was admitted postoperatively as a direct result of his or her airway endoscopy.

The clinical diagnoses, endoscopic findings, and L-EMG results are presented in the Table. Patient-specific information is provided in the Discussion: Impact on Clinical Care section. In group 1, congenital bilateral VFP correlated with bilaterally absent MUAP recordings in 2 of the 5 children. Two children had absent MUAP activation on 1 side only, with inconclusive testing on the contralateral side. One child exhibited marked paresis; unilateral MUAP activation was identified. The L-EMG findings did not affect the clinical management in any patient in this group. In group 2, the L-EMG findings influenced the clinical management in 5 of the 20 patients by providing objective data supporting decannulation decisions (Nos. 1 and 3), additional surgery (No. 15), interventional testing (No. 22), or a recommendation against surgery (No. 4). The L-EMG data did not significantly alter the clinical management in the other 15 children. The objective data were provided during postoperative consultation to support the observed clinical characteristics of laryngotracheal stenosis (Nos. 6 and 21), laryngeal trauma (Nos. 12 and 18), or cerebral palsy with laryngeal incompetency (Nos. 13, 25, 29, and 30), or to assist with predicting the functional status after open laryngotracheal reconstruction (No. 18). One child (No. 4) had cricoarytenoid joint fixation. In group 3, positive bilateral MUAP activation was identified in 3 of the 5 patients; in 2 children, only unilateral MUAP activation was identified.

The L-EMG findings correlated with the endoscopic findings in 25 patients (83%). In group 1, 4 of the 5 children with congenital VFP did not exhibit MUAP activation. In groups 2 and 3, 14 of 17 patients with normal bilateral true vocal fold mobility had normal bilateral L-EMG recordings. Two (Nos. 19 and 24) exhibited only unilateral MUAP activation, and in 1 patient (No. 17) no MUAP activation was recorded bilaterally. Overall, normal MUAP activation was recorded in 34 of 38 vocal fold samplings with normal visualized vocal fold mobility (89%). All 4 patients with normal unilateral vocal fold mobility (Nos. 18, 21, 22, and 30) exhibited normal L-EMG findings on the mobile side and absent MUAP activation or fibrillation potentials on the contralateral side. Two of the 4 patients (Nos. 1 and 15) with noncongenital clinical bilateral VFP exhibited bilateral MUAP activation; in the other 2 patients (Nos. 3 and 4) bilateral MUAP activation was not recorded.

PATIENT DATA

Patient No.	*Sex*	*Age*	*Clinical Diagnosis*	*Flexible and Rigid Laryngoscopy Findings*	*Thyroarytenoid Electromyography Findings*
Group 1: Congenital vocal fold paralysis or paresis					
2	M	9 mo	Congenital B TVF paralysis	B TVF paralysis	Absent L MUAP
5	F	1 mo	Congenital B TVF paralysis	B TVF paralysis	Absent L and R MUAP
9	M	5 mo	Congenital B TVF paralysis	B TVF paralysis	Absent L and R MUAP
11	M	18 mo	Congenital B TVF paralysis	B TVF paralysis	Absent L MUAP
27	M	1 mo	Congenital B TVF paralysis	Marked B TVF paresis	Normal R MUAP, absent L MUAP
Group 2: Other neurologic or anatomic laryngeal abnormality					
1	M	3 y	B TVF paralysis, TEF	Paradoxical TVF mobility	Present, but sparse, L and R MUAP
3	F	15 y	B TVF paralysis, meningioma	B TVF paralysis	Absent L and R MUAP
4	M	3 y	Laryngotracheal stenosis	LTS/LTR, absent TVF mobility	Absent L and R MUAP
6	M	4 y	Laryngotracheal stenosis	LTS/LTR, normal TVF mobility	Normal EMG
7	M	8 mo	Recurrent croup, intubation history	Grade 1 LTS, normal TVF mobility	Normal EMG
10	M	2 mo	Obstructive laryngomalacia	Type 4 laryngomalacia, normal TVF mobility	Normal EMG
12	M	6 mo	Vocal fold paresis after MVA	Recovered TVF mobility	Normal EMG, except for low amplitude
13	M	2 y	Cerebral palsy, mild aspiration	Normal anatomy, normal TVF mobility	Normal EMG
15	F	1 y	Cervicofacial lymphangioma	Laryngeal lymphangioma, absent TVF mobility	Normal EMG
16	M	2 y	Chromosomal abnormality	Hypoplastic mandible, normal TVF mobility (flex)	Unable to assess
17	M	3 y	Laryngotracheal stenosis	LTS, normal TVF mobility	Absent L and R MUAP
18	M	17 y	Laryngeal trauma	Anterior web, normal L and absent R TVF mobility	Normal L MUAP, R fibrillations
20	M	9 mo	Subglottic hemangioma	Normal TVF mobility	Normal EMG
21	M	4 y	Laryngotracheal stenosis	Present L TVF mobility, absent R TVF mobility	Normal L MUAP, absent R MUAP
22	M	4 y	Skull base neurofibroma	Normal L TVF mobility, R TVF paresis	R fibrillations, normal L MUAP
23	F	2 y	Anterior cricoid decompression	Normal anatomy, normal TVF mobility	Normal EMG
25	M	5 y	Cerebral palsy, mild aspiration	Normal anatomy, normal TVF mobility	Normal EMG
28	M	4 y	Obstructive laryngomalacia	Type 3 laryngomalacia, normal TVF mobility	Normal EMG
29	M	4 mo	Cerebral palsy, mild aspiration	Normal anatomy, normal TVF mobility	Normal EMG
30	M	5 y	Cerebral palsy, moderate aspiration	Normal R TVF mobility, absent L TVF mobility	Normal R MUAP, absent L MUAP
31	F	4 y	Cerebral palsy, laryngotracheal stenosis	LTS/LTR, normal TVF mobility	Normal EMG
32	M	3 y	Goldenhar's syndrome	Hemifacial microsomia, normal TVF mobility (flex)	Unable to assess
Group 3: Normal clinical laryngeal findings					
8	M	5 y	Recurrent croup	Prominent innominate artery, normal TVF mobility	Normal EMG
14	F	7 y	Recurrent croup, Turner's syndrome	Normal anatomy, normal TVF mobility	Normal EMG
19	F	7 mo	Double aortic arch	Midtracheal compression, normal TVF mobility	Normal L MUAP, absent R MUAP
24	F	6 y	Hoarseness, intubation history	Reflux changes, normal TVF mobility	Normal L MUAP, absent R MUAP
26	M	2 y	Hoarseness, intubation history	Normal anatomy, normal TVF mobility	Normal EMG

B — bilateral, TVF — true vocal fold, MUAP — motor unit action potentials, TEF — tracheoesophageal fistula, LTS — laryngotracheal stenosis, LTR — laryngotracheal reconstruction, EMG — electromyography, MVA — motor vehicle accident, flex — flexible laryngoscopy.

Artifacts commonly encountered in the operating room included the volume-conducted electrocardiogram artifact and (rarely) 60-Hz electrical interference. Needle insertional abnormalities included fibrillations and positive waves.

DISCUSSION

BACKGROUND

Although L-EMG has been widely discussed in the adult otolaryngological literature,[2,3,7-10] only a few studies have delineated the best technique for pediatric patients and evaluated its clinical utility. In 1987, Koch et al[4] were the first to report on pediatric L-EMG. They used a wire endoscopically placed as a monopolar electrode under general endotracheal anesthesia in 12 pediatric patients with signs or symptoms of VFP. They concluded that L-EMG was valuable in determining vocal fold function in pediatric patients and that the monopolar technique was the most appropriate method for children. In 1993, Gartlan et al[5] reported the use of bipolar hooked wire electrodes passed transcutaneously under light anesthesia in 4 pediatric patients with VFP or vocal fold paresis. They summarized that L-EMG was useful in the pediatric population, that it offered some prognostic information, that general anesthesia was required, that electrode placement had to be verified by direct observation, and that the percutaneous method was reliable but subject to electrical interference. In 1996, Berkowitz[6] reported his experience using concentric needle electrodes placed endoscopically into the posterior cricoarytenoid and thyroarytenoid muscles under general anesthesia in 4 patients with congenital bilateral VFP. He concluded that congenital bilateral VFP was characterized by normal L-EMG findings, which did not have prognostic significance. He suggested that congenital VFP may result from laryngeal abductor and adductor muscle action imbalance and may not necessarily represent a true paralysis.

TECHNIQUE ANALYSIS

Our technique varied from previous techniques in several ways. Bipolar electrodes are limited to sampling activity between the wires. Theoretically, concentric needles shield the surrounding muscle fibers to 180°. In cases in which visualization is limited, it would be difficult to rotate a concentric needle once placed. Monopolar electrodes sample 360° of muscle fibers. Koch et al[4] used a 40-mm monopolar silver wire, with a bent tip, placed via direct laryngoscopy through a 28-gauge needle. We used monopolar needles, which are disposable and available in a variety of lengths. The theoretic disadvantage of sampling a large motor unit size when using a monopolar technique was not deemed clinically significant in our study.

The transcutaneous technique without general anesthesia that is used for diagnostic L-EMG in adults and for the treatment of spasmodic dysphonia is not easily translated to the pediatric arena. Smaller larynges compromise correct anatomic placement of the electrode. Volitional thyroarytenoid muscle activation during phonation is an unrealistic expectation in an infant. Gartlan et al[5] used general anesthesia for transcutaneous electrode placement. A modification of their technique using flexible endoscopic technology may be useful in children, in whom anatomic constraints limit the effectiveness of direct rigid laryngoscopy. Koch et al[4] also used general anesthesia. Unless there was a tracheotomy, their patients were ventilated through an endotracheal tube. We believe that direct, unimpeded visualization from a superior approach under general anesthesia with spontaneous ventilations is a logical method that is applicable in almost all children.

Even under direct vision, particularly in infants or in children with distorted anatomy, accurate placement of the monopolar electrode can be difficult. Other potential technical problems include short-circuiting the needle electrode by stripping the Teflon coating as it is placed. Use of atraumatic laryngeal forceps will reduce this possibility, but slippage may occur as the needle is being inserted.

The plane of anesthesia is crucial. In this series, spontaneous ventilations were maintained throughout the procedure, but in several cases, MUAP activation was not initially observed under deep planes of anesthesia. Activation of the MUAP was subsequently recorded as the plane of anesthesia lightened, and it correlated well with the return of stronger vocal fold motion in phase with the ventilatory cycle. If the anesthesia became light enough for the child to "awaken," motor unit sampling was limited to only 1 side (Nos. 19 and 24), unless sampling the second side was deemed critical for potential management decisions.

Similar to those described in other reports,[11-13] the current technique has limitations in sensitivity. We encountered several examples of "EMG silence" despite normal, strong true vocal fold mobility during endoscopy and accurate electrode placement. On occasion, brief adductor spasm without identification of MUAP activation was even encountered. Despite the extremely complex innervation of the thyroarytenoid muscle,[14] we theorize that needle electrode placement remote from activated muscle cells is a limiting factor with this technique. In several patients, reinsertion of the active electrode in a different location revealed "near motor unit" recruitment. Parallel orientation of individual muscle fibers within the thyroarytenoid muscle may play a role. We suggest using as many as 3 needle insertions at different distances from the lateral margin of the true vocal fold to increase the likelihood of sampling different motor units on repeated needle placements to minimize the potential for false-negative recordings.

Using visualized normal vocal fold mobility as a reference, we found that the clinical specificity of this technique is good; only 2 children (Nos. 1 and 15) had positive MUAP activation without normal vocal fold mobility. Reports from animal studies[15] support the hypothesis that stimulation of the recurrent laryngeal nerve correlates with intrinsic laryngeal muscle contraction. Our clinical experience, however, suggests that positive MUAP activation can only imply that there is at least partial continuity of the recurrent laryngeal nerve–thyroarytenoid muscle axis. It does not guarantee adequacy of contraction, power, or elimination of fatigue in a partially denervated or deconditioned thyroarytenoid muscle. Further, intact MUAP activation may also be identified in patients with clinical VFP secondary to cricoarytenoid joint fixation or with an infiltrative laryngeal mass. Flexible fiberoptic laryngoscopy in the awake child remains the most sensitive and specific technique for evaluating vocal fold mobility, limited primarily by patient (and parent) compliance and the interpretive skills of the endoscopist. Subtle laryngeal findings, however, particularly in children, may require repeat evaluations for diagnostic confirmation.

IMPACT ON CLINICAL CARE

The use of L-EMG directly influenced the management of several patients. One child (No. 1) with bilateral clinical VFP failed decannulation multiple times after tracheoesophageal fistula repair. At 3 years of age, he exhibited paradoxical vocal fold mobility without active in-phase vocal fold movement. Intraoperative endoscopy revealed normal laryngeal anatomy without thyroarytenoid muscle atrophy. He had bilateral sparse, but present, MUAP activation. The potential for developing normal vocal fold mobility was discussed with his parents, and more aggressive plugging trials were recommended.

One adolescent (No. 3) exhibited bilateral VFP 6 months after bilateral jugular foramen meningioma resection. By report, the vagal nerves were not visually resected. She was able to take food orally, but there was a recurrent aspiration history. She had a soft but adequate voice. She desired to speak more loudly, swallow without aspiration, and be decannulated. The patient and her mother wanted to make an informed decision based on reasonable expectations at that time rather than wait several additional months or more to fully acknowledge permanent VFP. The absence of positive MUAP activation objectively supported that diagnosis. The patient and her mother assessed their relative priorities and elected to maintain the use of tracheotomy with a speaking valve rather than pursue surgery to address VFP or aspiration.

One child (No. 22) had a large base-of-skull neurofibroma diagnosed in early childhood with no identifiable cranial nerve deficits. The findings of flexible fiberoptic laryngoscopy and L-EMG were initially normal. The surgical risk was deemed critically high. It was elected to follow the child's clinical course and initiate a second series of functional and diagnostic tests should cranial nerve deficit be subsequently identified. After 2 years of follow-up, serial office laryngoscopy identified bilaterally intact, but unilaterally weakened, in-phase vocal fold mobility. The surgical risk remained critically high, and the patient's mother desired objective documentation of clinical tumor progression. The new L-EMG finding of ipsilateral fibrillation potentials objectively established the diagnosis of new-onset unilateral vocal fold palsy with greater certainty than the subtle laryngoscopy findings had done, and a second wave of diagnostic imaging studies was initiated in consideration of surgical intervention.

One child (No. 4) failed to develop an adequate voice with a sufficiently patent conductive airway after laryngotracheal reconstruction. His disorder included bilateral cricoarytenoid fibrosis extending into and involving the lateral glottic structures. His reconstructive surgery predated our institutional implementation of pediatric L-EMG testing. Subsequent L-EMG did not identify positive MUAP activation on either side, and revision surgery was not recommended.

One child (No. 15) presented with an extensive cervicofacial lymphangioma with diffuse laryngeal involvement and absent visualized vocal fold mobility. The cervical portion of the tumor was debulked, and a tracheotomy was created. The presence of positive MUAP activation established the potential for normal vocal fold mobility. A recommendation was made for additional surgery designed to reduce the lateral glottic tumor bulk and to decrease supraglottic obstruction from epiglottic involvement, with the goal being the development of glottic speech.

Five children had congenital VFP (Nos. 2, 5, 9, 11, and 27). Only 1 exhibited MUAP activation. In 2 infants, we were able to obtain only unilateral recordings. There is a recognized tendency for spontaneous recovery of function with this disorder.[16,17] Normative L-EMG data on congenital VFP, however, are limited, and the significance of MUAP activation has not yet been determined. One child (No. 5) required a tracheotomy and has since moved out of town. One child (No. 2) had partial clinical return of right unilateral vocal fold mobility. A subsequent study revealed positive MUAP activation on that side. Long-term follow-up (minimum, 2 years) is available for 2 of the other 3 children. The fact that no functional return has been identified in the 1 child with initially positive MUAP activation (No. 27) further supports the idea that L-EMG has limited prognostic utility in congenital VFP. To date, we have not identified a child with congenital VFP and absent MUAP activation in whom positive MUAP activation was identified before visual return of vocal fold mobility. As a result of this study, new parents of infants with congenital VFP have been counseled that L-EMG data have not been demonstrated to be predictive of a return of vocal fold mobility.

Five children with laryngotracheal stenosis (Nos. 4, 6, 17, 21, and 31) were studied. Patient 4 has already been discussed. Three children (Nos. 6, 21, and 31) had consistent endoscopy and L-EMG findings. One was decannulated after endoscopic management. The other 2 subsequently underwent successful laryngotracheal reconstruction. If absent vocal fold mobility in these children was identified in association with absent MUAP activation at staging endoscopy, reconstructive surgery would not have been recommended. However, if absent vocal fold mobility *was* identified, but there was intact MUAP activation at staging endoscopy, then surgery would have been recommended. One child (No. 17) had intact vocal fold mobility with absent MUAP activation. At the time this child was studied, questions regarding technique sensitivity were raised. The observed endoscopy findings took clinical precedence over the technical recording.

Two patients with laryngeal trauma were studied. A 6-month-old (No. 12) developed a weak cry after blunt neck trauma. Office endoscopy was performed within 48 hours of the incident. There was no vocal fold mobility. There was no laryngeal ecchymosis, and the vocal fold levels and arytenoid processes were symmetrically normal. At the time of diagnostic endoscopy, $2^1/2$ weeks after the injury, the quality of her cry had improved and there was return of limited, but in-phase, vocal fold mobility. Positive MUAP activation was identified, although the amplitude was lower than that which would be normally expected. The follow-up endoscopy and L-EMG findings both served in counseling her parents after the operation that full return of function was a reasonable expectation.

The second trauma patient (No. 18) was an adult-sized teenager who sustained a complex laryngeal fracture during a street fight. He presented with a field-placed tracheotomy. There was gross laryngeal cartilage disruption. Normal left vocal fold mobility on endoscopy and positive MUAP activation were observed. There was no right vocal fold mobility, and fibrillation potentials were identified. The L-EMG findings were used in subsequent consultation to help establish reasonable expectations, particularly regarding voice, after his fracture reduction and reconstructive surgery.

Five children with cerebral palsy (Nos. 13, 25, 29, 30, and 31) were studied. These children presented with airway obstruction and aspiration histories of various severity. They would not tolerate an adequate office examination. One child (No. 31) presented with a tracheotomy. All exhibited normal vocal fold mobility and normal MUAP activation, except for the child (No. 30) with the most significant history of recurrent aspiration, who had unilateral paralysis that correlated with absent MUAP activation. The assessment of laryngeal competency is a clinical judgment based on the ability of the child to protect his or her airway under the various circumstances of everyday living, including eating, activity, and sleeping. The decision for medical or surgical intervention is often based on parental assessment of the anticipated post-treatment impact on the quality of life for their child. Complementary use of laryngeal motor and sensory testing, along with the traditional analysis of the clinical history and laryngoscopy, and fluoroscopy studies, may have the potential to provide parents with additional objective and specific clinical data that will help them arrive at an informed decision regarding management recommendations.

SUMMARY

The routine use of L-EMG in the evaluation of laryngeal dysfunction in children is not advocated. Awake flexible fiberoptic laryngoscopy in combination with intraoperative palpation of the cricoarytenoid joints and glottis provides the greatest clinical value when assessing children with vocal fold dysfunction. In our study, the clinical utility of L-EMG was limited to children with noncongenital abnormal vocal fold mobility, such as new-onset vocal fold paresis or paralysis or infiltrative laryngeal tumors with abnormal vocal fold mobility, and in selected post-surgical cases involving decannulation decisions. On the basis of these results and those of Berkowitz,[6] we do not recommend the routine use of L-EMG in children with congenital VFP. With further refinement in technique and continued study, L-EMG may have clinical utility in the preoperative assessment of children with laryngotracheal stenosis and abnormal vocal fold mobility who are being considered for laryngotracheal reconstruction.

Electrophysiological (EMG) testing is often used to differentiate upper motor neuron dysfunction, which occurs in disorders such as cerebral palsy, from lower motor unit dysfunction, such as that seen with disease of the anterior horn cells, peripheral nerve, or muscle cell. The application of these techniques to nerve-muscle axes of respiratory and airway motor units is relatively new in the pediatric population. If modifications of technique result in greater sensitivity, pediatric L-EMG has the potential to complement or augment traditional laryngeal testing in attempts to differentiate central from peripheral nervous system laryngeal mobility disorders, and may, therefore, have a valuable role in the assessment and management of selected chronic aspiration cases.

Use of long, shielded monopolar needles is a modification of a relatively new technique. Individuals attempting to duplicate this work should be cautious when initially learning to interpret the recorded electrical activity. A positive MUAP recording indicates an intact nerve-muscle axis, but is not an indicator of muscle function. One must resist the temptation to interpret distant respiratory muscle motor unit activation as an indication of continuity of the recurrent laryngeal nerve–thyroarytenoid muscle axis. The potential for brief-duration and low-amplitude MUAP activation under general anesthesia, and the difficulty in localizing near motor units within the thyroarytenoid muscle, may prove taxing and frustrating. Even with observed vocal fold mobility, the possibility of a "negative L-EMG" must be recognized. Given the anatomic constraints of pediatric L-EMG, this technique may represent state-of-the-art electrodiagnostic capability with the direct superior vision approach. A multi-lead needle electrode[18] would probably not increase the sensitivity of the recording capability.

CONCLUSIONS

Intraoperative pediatric L-EMG testing with endoscopically placed monopolar electrodes has limited utility. It can objectively support clinical findings, but in this study, it provided new objective data relevant to management recommendations in only a few selected pediatric patients with new-onset vocal fold paresis or paralysis or infiltrative laryngeal tumors, and in selected postsurgical cases involving decannulation decisions. The prognostic utility of L-EMG in newborns with congenital VFP has not been established. Use of L-EMG in children should not be considered a substitute for awake flexible fiberoptic laryngoscopy, which remains the single most specific and sensitive technique for evaluating vocal fold mobility.

One must be cautious in the interpretation of MUAP activation with endoscopically placed monopolar needle electrodes in pediatric patients under general anesthesia. A normal L-EMG recording indicates an intact neuromuscular axis, but does not guarantee vocal fold mobility or guarantee adequacy of contraction, power, or elimination of fatigue in a partially denervated or deconditioned thyroarytenoid muscle. There can be difficulties in obtaining normal L-EMG recordings even with observed vocal fold mobility. The possibility of false-negative EMG recordings must be recognized and remains the major limitation of this technique.

REFERENCES

1. Jones HR, Harmon RL, Harper CM, Bolton CF. An approach to pediatric electromyography. In: Jones HR, Bolton CF, Harper CM, eds. Pediatric clinical electromyography. Philadelphia, Pa: Lippincott-Raven, 1996:1-37.

2. Simpson DM, Sternman D, Graves-Wright J, Sanders I. Vocal cord paralysis: clinical and electrophysiologic features. Muscle Nerve 1993;16:952-7.

3. Miller RH, Rosenfield DB. The role of electromyography in clinical laryngology. Otolaryngol Head Neck Surg 1984; 92:287-91.

4. Koch BM, Milmoe G, Grundfast KM. Vocal cord paralysis in children studied by monopolar electromyography. Pediatr Neurol 1987;3:288-93.

5. Gartlan MG, Peterson KL, Hoffman HT, Luschei ES, Smith RJH. Bipolar hooked-wire electromyographic technique in the evaluation of pediatric vocal cord paralysis. Ann Otol Rhinol Laryngol 1993;102:695-700.

6. Berkowitz RG. Laryngeal electromyography findings in idiopathic congenital bilateral vocal cord paralysis. Ann Otol Rhinol Laryngol 1996;105:207-12.

7. Thumfart WF. Electrodiagnosis of laryngeal nerve disorders. Ear Nose Throat J 1988;67:380-4, 386-8, 390-3.

8. Yin SS, Qiu WW, Stucker FJ, Hoasjoe DK, Aarstad RF. Evaluation of bilateral vocal fold dysfunction: paralysis versus fixation, superior versus recurrent, and distal versus proximal to the laryngeal nerves. Am J Otolaryngol 1997;18:9-18.

9. Rontal E, Rontal M, Silverman B, Kilney PR. The clinical differentiation between vocal cord paralysis and vocal cord fixation using electromyography. Laryngoscope 1993;103:133-7.

10. Quiney RE. Laryngeal electromyography: a useful technique for the investigation of vocal cord palsy. Clin Otolaryngol 1989;14:305-16.

11. Ford CN. Laryngeal EMG in clinical neurolaryngology. Arch Otolaryngol Head Neck Surg 1998;124:476-7.

12. Woo P. Laryngeal electromyography is a cost-effective clinically useful tool in the evaluation of vocal fold function. Arch Otolaryngol Head Neck Surg 1998;124:472-5.

13. Woodson GE. Clinical value of laryngeal EMG is dependent on experience of the clinician. Arch Otolaryngol Head Neck

Surg 1998;124:476.

14. Sanders I, Wu BL, Mu L, Li Y, Biller HF. The innervation of the human larynx. Arch Otolaryngol Head Neck Surg 1993;119:934-9.

15. Nasri S, Dulguerov P, Damrose EJ, Ye M, Kreiman J, Berke GS. Relation of recurrent laryngeal nerve compound action potential to laryngeal biomechanics. Laryngoscope 1995; 105:639-43.

16. Cohen SR, Geller KA, Birns JW, Thompson JW. Laryngeal paralysis in children. A long-term retrospective study. Ann Otol Rhinol Laryngol 1982;91:417-24.

17. Rosin DF, Handler SD, Potsic WP, Wetmore RF, Tom LWC. Vocal cord paralysis in children. Laryngoscope 1990;100: 1174-9.

18. Rea JL, Templer JW, Davis WE. Design and testing of a new electrode for laryngeal electromyography. Arch Otolaryngol 1978;104:685-6.

≈

MANAGEMENT OF THE TINNITUS PATIENT

The Ninth Annual Conference on the Management of the Tinnitus Patient, for professionals and tinnitus patients, will be held in Iowa City, Iowa, October 4-6, 2001. For information, see web site www.medicine.uiowa.edu/otolaryngology/news/news or contact Rich Tyler by telephone (319-356-2471) or e-mail (rich-tyler@uiowa.edu).

Ann Otol Rhinol Laryngol 110:2001

LARYNGEAL REINNERVATION WITH THE HYPOGLOSSAL NERVE

I. PHYSIOLOGY, HISTOCHEMISTRY, ELECTROMYOGRAPHY, AND RETROGRADE LABELING IN A CANINE MODEL

RANDAL C. PANIELLO, MD

STEVEN E. WEST, MD PATTY LEE, MD

ST LOUIS, MISSOURI

This study was performed to determine whether the hypoglossal nerve (cranial nerve XII [XII]) would serve as a useful donor for laryngeal reinnervation by anastomosis to the recurrent laryngeal nerve (RLN). Twenty hemilarynges in 10 dogs were studied prospectively after XII-RLN anastomosis (group A; n = 5), split XII–RLN anastomosis (group B; n = 3), XII-RLN anastomosis with a 2-cm interposition graft (group C; n = 2), no treatment (group D; n = 5), RLN section (group E; n = 2), or ansa cervicalis–RLN anastomosis (group F; n = 3). Spontaneous activity was observed monthly by infraglottic examination through permanent tracheostomies and was recorded by electromyography. Laryngeal adductory pressure and induced phonation were obtained by stimulating the RLN while passing a pressure transducer balloon or humidified air through the glottis. At sacrifice, the laryngeal muscles were stained for adenosine triphosphatase to determine the ratio of type I to type II fibers. Retrograde labeling of the brain stem was performed with horseradish peroxidase. Infraglottic examination at 6 months showed a full range of adductory motion in groups A and B during the swallow reflex, comparable with that in group D. Groups C and F showed good bulk and tone, but little spontaneous motion. Group E remained paralyzed. Stimulation of the transferred nerves caused more activity in groups A and B than in the other groups; groups C and F partially adducted at high levels. The laryngeal adductory pressure responses of groups A and B were similar to those of group D. The XII-reinnervated larynges were capable of producing normal induced phonation. Retrograde labeling of the RLN showed that the reinnervating axons originated only in the hypoglossal nucleus. Electromyography of the reinnervated adductor muscles confirmed spontaneous activity in the dogs (awake). Histochemical analysis confirmed slow-to-fast transformation of both the posterior and lateral cricoarytenoid muscles, indicating that significant reinnervation occurred. We conclude that the hypoglossal nerve functions well as a donor for adductory reinnervation of the larynx.

KEY WORDS — dog, larynx, nerve, reinnervation, vocal fold paralysis.

INTRODUCTION

Unilateral vocal fold paralysis (UVFP) has several causes; the most common is traumatic injury to the recurrent laryngeal nerve (RLN).[1] The treatment for UVFP has interested researchers for decades, yet a completely satisfactory method has been elusive. The ideal treatment would restore normal physiologic movement to the vocal fold.[2]

Current treatments for UVFP fall into 2 general classes: static and dynamic. Static methods include vocal fold medialization by injection of Teflon, autologous fat, or collagen.[3,4] Laryngeal framework surgical methods include thyroplasty[5,6] and arytenoid adduction.[7,8] These procedures can be very effective, but do have some problems.[1,9] The implants are only effective for medializing the anterior half of the vocal fold, so that they are less useful in patients with aspiration problems or wide posterior glottic chinks.[10] They may cause permanent changes in the larynx, thus being essentially irreversible.[11,12] Implants may become less effective with time as a result of continued atrophy of the thyroarytenoid (TA) muscle — a problem that prompted Tucker[13] to recommend combined medialization and reinnervation.

Dynamic methods include laryngeal reinnervation and muscle transfers. Crumley[12,14] believes that reinnervation has the best potential for a normal voice, with restoration of muscle tone, a more normal compliance of the vocal fold, and stabilization of the arytenoid and vocal process. In addition, reinnervation techniques are reversible, and do not preclude the use of static methods if needed.

In this project, the use of the hypoglossal nerve (cranial nerve XII [XII]) for laryngeal reinnervation after UVFP was evaluated. The hypoglossal nerve was considered an ideal nerve for laryngeal reinnervation

---

From the Department of Otolaryngology–Head and Neck Surgery, Washington University School of Medicine, and the Department of Surgery, Veterans Affairs Medical Center, St Louis, Missouri. Supported by the Department of Otolaryngology–Head and Neck Surgery, Washington University. This study was performed in accordance with the PHS Policy on Humane Care and Use of Laboratory Animals, the NIH *Guide for the Care and Use of Laboratory Animals*, and the Animal Welfare Act (7 U.S.C. et seq.); the animal use protocol was approved by the Institutional Animal Care and Use Committee (IACUC) of the Veterans Affairs Medical Center, St Louis, Missouri.

Presented at the meeting of the American Laryngological, Rhinological and Otological Society, Palm Desert, California, April 26-28, 1999.

CORRESPONDENCE — Randal C. Paniello, MD, Dept of Otolaryngology–Head and Neck Surgery, 517 S Euclid Ave, Box 8115, St Louis, MO 63110.

because 1) it has many more motor axons than other available nerves, such as the ansa cervicalis; 2) its natural activity is temporally similar to the adductor function of the RLN, because it is normally active during speech and during swallowing; and 3) the rate of hypoglossal donor site morbidity has historically been low. The preliminary data from this project were previously given,[15] in the first known report on the use of XII for laryngeal reinnervation. Here, we describe the detailed neurophysiological data obtained from 20 hemilaryngeal preparations. The first use of this technique in humans with vocal fold paralysis has been previously reported.[16]

The initial experiments were carried out to determine whether XII would provide suitable neural input for the larynx to provide reanimation of the vocal fold and maintenance of tone. Additional studies determined whether the same level of activity could be obtained with a split hypoglossal nerve or with the use of an interpositional cable graft to bridge a small gap between the nerves.

For the physiological studies, reinnervation was assessed by stimulating the RLN and recording the strength of vocal fold adduction; maximal stimulation levels were used for relative comparisons. Previous studies showed that stimulation of the RLN at frequencies higher than 60 Hz results in graded levels of adduction; stimulation at low frequencies (lower than 30 Hz) causes abduction.[17] This finding is most likely due to the relative abundance of slow-twitch (type I) muscle fibers in the posterior cricoarytenoid (PCA) muscle and the relative abundance of fast-twitch (type II) muscle fibers in the adductor muscles. At constant high-frequency stimulation, there is a steady increase in adductor force with increasing current until the muscles reach tetany. At higher current levels, there is a plateau level of adductory strength, resulting in a sigmoid-shaped stimulation curve. In normal dogs, the pressure plateau at 80 Hz is about 60 to 70 mm Hg.[18]

At a constant current near maximum, variation of the stimulation frequency produces a linear relationship with a characteristic slope in the transition zone of 30 to 60 Hz. Changes in this slope reflect changes in the ratio of fast-twitch to slow-twitch fibers in the reinnervated muscle. The data from this curve indicate the degree of reinnervation (amplitude) and the muscle fiber type (slope). Faster muscles require higher levels of adenosine triphosphatase (ATPase) for rapid energy conversion. Histochemical stains for alkaline-stable ATPase appear dark on microscopy; the relative amounts of light and dark staining of a muscle reflect its fiber content.

Buller et al[19] demonstrated that when a slow-twitch muscle is reinnervated by a nerve from a fast-twitch muscle, it will undergo a histochemical transformation to take on the characteristics of the muscle formerly innervated by that nerve. Fast-twitch muscles can also be induced to transform to slow-twitch muscles; the nerve dictates the muscle fiber type, and muscles have the plasticity to change fiber type if their innervation changes. The data of Buller et al[19] showed this change occurring as early as 6 weeks after the nerve transfer procedure. In the present study, histochemical transformation of the intrinsic laryngeal muscles reinnervated by XII would also be predicted. Because the tongue muscles are fast-twitch, the expected change would be an increase in the percentage of dark fibers in the PCA muscle, and possibly in the adductor muscles as well.

Artificially induced phonation experiments can indicate the potential for the reinnervated vocal fold to participate in actual phonation. Induced phonation is obtained by forcing air through the trachea and larynx while approximating the vocal folds by stimulating the RLNs.[20]

The sectioned RLN has a strong tendency to regenerate some fibers.[21,22] A retrograde labeling experiment was performed to confirm the source of the reinnervating laryngeal motor neurons. Neural tracers injected into the muscle or the distal nerve stump are carried back to the nerve cell body by axonal flow.[23] Staining of the brain stem (hypoglossal or vagal nuclei) identifies the origin of the regenerating neurites.

MATERIALS AND METHODS

Ten purpose-bred, conditioned, female mongrel dogs weighing 20 to 25 kg were obtained and maintained in a facility approved by the American Association for Accreditation of Laboratory Animal Care. All experiments were performed according to a protocol approved by the Institutional Animal Care and Use Committee. When used, general anesthesia was induced with intravenous thiopental sodium and maintained with 2% halothane inhalant.

Surgery. A tracheostomy through rings 10 to 13 was performed according to a previously described method[24] and was allowed to mature for 2 weeks. The 3 experimental groups had neurorrhaphy between the RLN and the ipsilateral whole nerve XII (group A; 5 dogs), a split XII (group B; 3 dogs), or a whole XII with a 2.0-cm interposition nerve graft (group C; 2 dogs; Fig 1). On the contralateral side, the 3 control groups had no treatment (group D; 5 dogs), RLN section without repair (group E; 2 dogs), or ansa cervicalis–RLN neurorrhaphy (group F; 3 dogs; Fig 1). The experiments were allocated among the 10 dogs

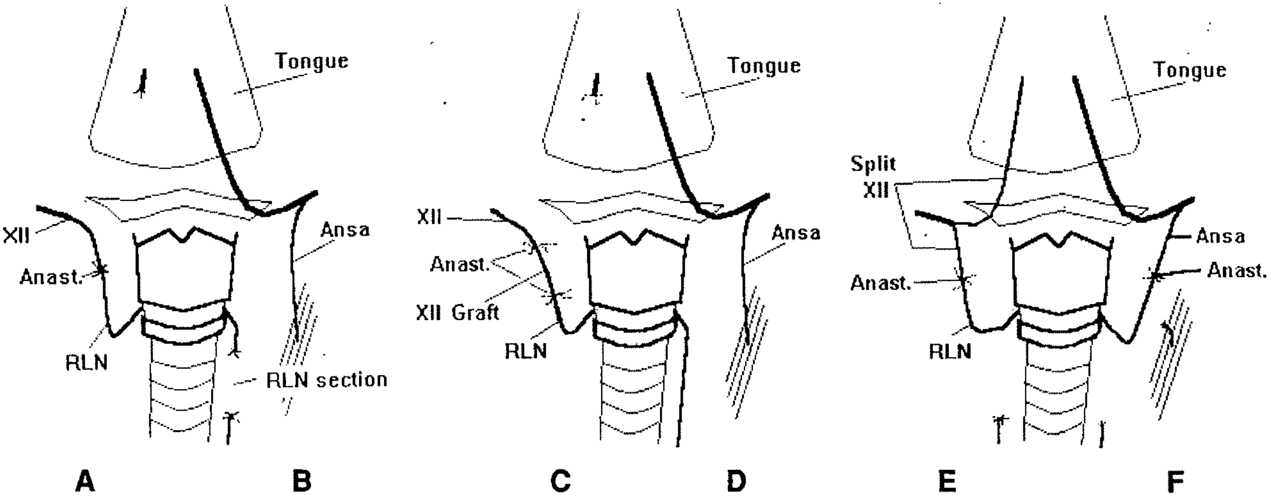

Fig 1. Canine experimental and control groups. At left is ventral view of dog 2 or 3, with whole hypoglossal nerve (XII)–recurrent laryngeal nerve (RLN) anastomosis on dog's right side (**A**) and RLN section on left (**B**). At center is dog 8 or 9, with XII-RLN anastomosis on dog's right (**C**) and normal control on left (**D**). At right is dog 6 or 10, with split XII–RLN anastomosis on dog's right (**E**) and ansa cervicalis–RLN anastomosis on left (**F**). Other dogs had different combinations of these 6 experiments (see text).

as shown in Table 1.

Surgery was performed under general anesthesia with aseptic technique, as follows. A midline incision was made from the suprastomal region to the submental region. The hypoglossal nerve was identified near the hyoid bone and dissected into the tongue. The ipsilateral RLN was identified and dissected inferiorly for 6 to 8 cm.

For the whole XII group (group A), XII was divided from the tongue, rotated, and directed inferiorly toward the larynx. The RLN was rotated superiorly at the cricothyroid joint. In all 5 dogs, there was ample nerve length to perform an end-to-end anastomosis between the whole XII and the RLN. The hypoglossal nerve was the same size as, or only slightly larger than, the RLN in all cases. The microneural anastomosis was performed with 4 to 6 epineural sutures of 8-0 or 9-0 nylon placed circumferentially. Excess nerve length was trimmed from the RLN before neurorrhaphy, leaving enough for a tension-free anastomosis. The skin was closed, and the dog was awakened from anesthesia.

TABLE 1. EXPERIMENTAL AND CONTROL GROUP ASSIGNMENTS

Dog No.	*Experimental Side (Group)*	*Control Side (Group)*
1	Whole XII–RLN (A)	Normal (D)
2	Whole XII–RLN (A)	Section RLN (E)
3	Whole XII–RLN (A)	Section RLN (E)
4	Whole XII–RLN (A)	Normal (D)
5	Whole XII–RLN (A)	Ansa cervicalis–RLN (F)
6	Split XII–RLN (B)	Ansa cervicalis–RLN (F)
7	Split XII–RLN (B)	Normal (D)
10	Split XII–RLN (B)	Ansa cervicalis–RLN (F)
8	Graft XII–RLN (C)	Normal (D)
9	Graft XII–RLN (C)	Normal (D)

XII — hypoglossal nerve, RLN — recurrent laryngeal nerve.

For the split XII group (group B), the nerves were dissected as described for group A, but the entire XII was not immediately separated from the tongue. Instead, the distal XII was dissected between major fascicles and divided so that about half of the nerve continued to innervate the tongue, while half was free for anastomosis. The fascicles were dissected in a distal-to-proximal direction until the nerve trunk began turning superiorly toward the skull base. The split segment was rotated inferiorly. In the 3 dogs, this split nerve was estimated to contain 40% to 50% of the total XII motor fibers. End-to-end neurorrhaphy was performed as described above (Fig 2A).

For the interposition graft group (group C), the whole XII and the RLN were dissected and positioned alongside one another as described for group A. The most distal 2.0 cm of the hypoglossal nerve was excised, rotated 180°, and anastomosed end-to-end to the RLN. The excess length of the remaining XII was excised, and a second anastomosis (between two segments of XII) was performed (Fig 2B). In this manner, the 2.0-cm segment formed an interposition graft between XII proximally and the RLN distally.

On the contralateral (control) side, the 5 normal dogs (group D) had no dissection or intervention. In the RLN section group (group E), a 4-cm segment of the RLN was excised and discarded; the two ends were tied off. In group F, end-to-end neurorrhaphy was performed between the ansa cervicalis and the RLN.

Follow-up. To determine the degree of functional

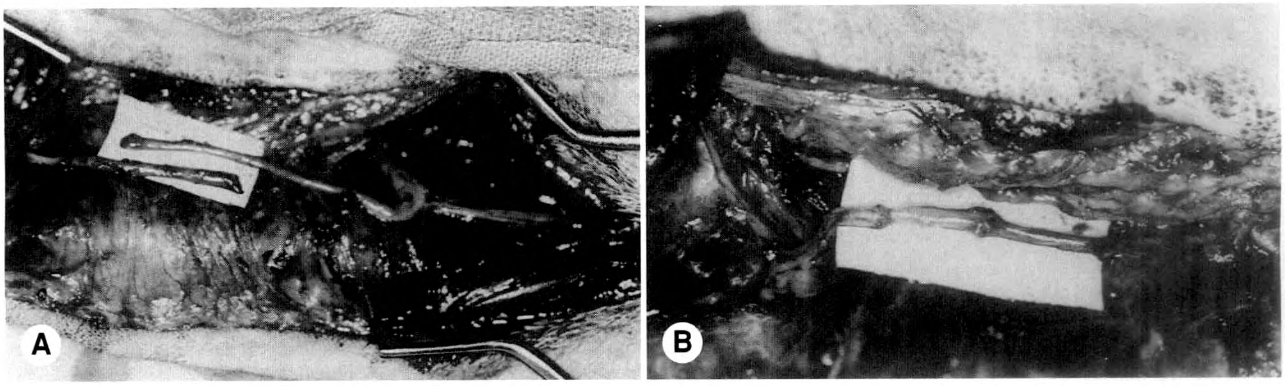

Fig 2. Intraoperative photographs from canine experiments. **A)** Split XII in position to anastomose to RLN (dog 6). Nerves are easily long enough for tensionless neurorrhaphy. **B)** Anastomosis of XII-RLN with 2-cm interposition graft has been completed on dog 8.

recovery of vocal fold adduction, monthly infraglottic examinations were performed. The awake animal was placed in a sitting position on the examination table; the neck was extended by an assistant.[11] A 0° telescope (Karl Storz, Tuttlingen, Germany) was inserted through the tracheostomy to view the inferior aspect of the vocal folds. Vocal fold motion was induced by stimulating a swallow reflex with 1 to 2 mL of water injected into the oral cavity. The vocal fold activity was recorded with a camera (Panasonic KS152, Matsushita Electric Corp, Secaucus, NJ) attached to the telescope and a video recorder (BV2000, Mitsubishi, Tokyo, Japan). This method allowed observation of awake, spontaneous laryngeal activity, including the range of motion during swallow. The resting position of the vocal folds and phasic respiratory activity were directly observed.

The laryngeal adductory pressure during swallowing was measured with the awake dog in the same position, although it was less well tolerated. The balloon catheter method[25,26] was found to be relatively simple and effective. A cuffed endotracheal tube filled with 10 mL of air was held against the neck skin and positioned so that the middle portion of the balloon corresponded to the vocal cord position. The position of the superior end of the stoma against the tube was marked. The tube was passed through the stoma superiorly so the mark was again aligned with the top of the stoma. This brought the balloon into position between the vocal folds. The pilot from the endotracheal tube was connected to a pressure transducer and a chart recorder. The contact of the balloon against the vocal folds immediately induced a series of swallow reflexes. The pressure from each squeeze on the balloon was recorded by the transducer. The squeezing motion occasionally caused the balloon position to change. Because the pressure reading is very sensitive to balloon position, the highest pressures recorded were used as the swallowing pressure.

Physiological Data. These experiments were carried out under general anesthesia on the planned day of sacrifice, before euthanasia.

The neck was explored, and a platinum wire and silicone elastomer electrode was placed around XII, proximal to the neurorrhaphy. On dog 10, a second electrode was placed on the ansa cervicalis. The electrode was connected to a custom constant-current laryngeal nerve stimulator (WR Medical Electronics, Stillwater, Minn) with adjustable current and frequency.

Induced laryngeal adductory pressure was measured with a previously described method[18] in which the RLN is stimulated while the balloon of an endotracheal tube is passed between the vocal folds. The RLN was stimulated for 3 to 5 seconds at a series of fixed-interval stimulation levels. The nerve was allowed to recover for at least 1 minute between stimulations.

The pressure-versus-current curve was determined by subtracting the baseline (resting) pressure from each measurement. The maximum-amplitude stimulation plateau level was determined, and the lowest-amplitude stimulation current that gave the plateau value was recorded. Holding this amplitude constant, we made a series of pressure measurements at different stimulating frequencies, from 10 to 100 Hz at 10-Hz intervals.

Induced Phonation. An endotracheal tube was directed rostrally into the tracheostomy and positioned with the balloon close to the stoma to maximize the distance between the tip and the vocal folds. Warmed, humidified air was passed through the larynx, with the flow controlled by a rotameter. Suspension laryngoscopy was performed. The vocal folds were observed as phonation was induced by activating one or both nerves with the laryngeal stimulator. Vocal fold motion was documented on videotape with the 0° telescope and camera. The acoustic output was recorded with a microphone and a digital audiotape re-

TABLE 2. HORSERADISH PEROXIDASE INJECTIONS

Dog No.	*Site*	*Horseradish Peroxidase Dose (mg)*	*Sacrifice Interval (d)*
0	L TA	2	5
	R BOT	2	
2	R TA	2	7
4	R TA	7	4
5	R TA	15	4
6	L RLN	4	3
7	R RLN	5	2

TA — thyroarytenoid muscle, BOT — base of tongue, RLN — recurrent laryngeal nerve.

corder and was later analyzed with a voice analysis computer (CSL 4300B, Kay Elemetrics, Lincoln Park, NJ). The parameters recorded included jitter, shimmer, and noise-to-harmonics ratio. In addition, a new parameter, the voice turbulence index, was included in the analysis of the induced voice samples. The voice turbulence index is defined by Kay Elemetrics as a measure of "the relative energy level of high frequency noise. It mostly correlates with the turbulence caused by incomplete or loose adduction of the vocal folds."[27(p17)]

Electrodes were placed around the dissected nerves. On the hypoglossal neurorrhaphy side, the electrode was placed several centimeters superior (proximal) to the anastomosis. Electrodes were also placed on the control side, on the normal RLN or on the ansa cervicalis. A trial of phonation involved stimulating the nerve(s) for 20 to 60 seconds. The nerves were allowed to recover for a minimum of 5 minutes before another trial.

It is often possible to induce phonation by stimulating just one of the nerves. However, this usually produces a more breathy or rough sound than that obtained with bilateral stimulation. This finding is similar to UVFP in the clinical setting.

Retrograde Labeling. This experiment was performed on dogs 2, 4, 5, 6, and 7 at the conclusion of the other planned experiments. One additional animal (dog 0) was used first, so we could gain experience with the method and the horseradish peroxidase (HRP) doses. The HRP crystals (Sigma Chemical, St Louis, Mo) were suspended in sterile water at the time of injection and used for the neural tracer.

Previous reports of retrograde labeling in large animals are sparse,[28-30] so the methods used in smaller animals were adapted.[31-33] Estimates of the time required for retrograde axonal transport (to concentrate the HRP in the brain stem) were based on reported flow rates and nerve lengths in smaller animals.[23] The HRP doses and sacrifice intervals for all dogs are shown in Table 2.

Direct laryngoscopy was performed under general anesthesia. The HRP (2 to 15 mg) was injected into the posterior TA muscle; dog 0 also had HRP injected into the right side of the tongue base. For dogs 6 and 7, instead of injection into the TA muscle, we used a technique in which the RLN was dissected about 1 to 2 cm from the larynx, the injection needle was inserted through the epineurium, and the sharp edge was used to lacerate some of the distal axons. The HRP was deposited within the epineurium, and the needle was withdrawn; the HRP was not seen leaking out.

After 2 to 7 days, the dog was returned to the operating room and anesthetized. The carotid arteries, vertebral arteries, and jugular veins were dissected; resection of the sternocleidomastoid muscles and manubrium was helpful. The arteries were cannulated distally and cross-clamped proximally. The jugular veins were cross-clamped inferiorly and cannulated superiorly to prevent the venous outflow from mixing with the systemic circulation. Perfusion of the brain and brain stem was performed with 1 to 4 L of normal saline solution over 30 to 60 minutes. This was followed by perfusion with 2 to 3 L of 1.25% glutaraldehyde/1.0% paraformaldehyde fixative over 30 to 60 minutes and with 700 mL of cold 10% sucrose in 0.1-mol/L phosphate buffer over 1 hour. In the prone position, a craniotomy was performed to remove the skull from the anterior fossa to the foramen magnum. The vertebral bodies of the first 3 cervical vertebrae were removed, and the spinal cord was divided. The brain and brain stem were removed and placed in additional sucrose buffer. For dog 7, the brain and brain stem were soaked in additional fixative for 45 minutes before transfer to the sucrose solution.

The brain stem was cut into 40- to 50-μm sections and processed for histologic examination. The slides were reacted with hydrogen peroxide according to the tetramethyl benzidine method of Mesulam.[34] Light microscopy was performed to identify cells stained with HRP, which stain dark after the peroxide reaction.

Histochemical Analysis. This experiment was conducted on dogs 8, 9, and 10. Immediately after the dog was sacrificed, the larynx was harvested and the TA, PCA, and lateral cricoarytenoid (LCA) muscles were harvested bilaterally. The 6 muscles were placed by an assistant in separate containers with coded labels; the key to these codes was kept secret until after the histochemical analysis was completed so as to keep the results blinded. The fresh muscle specimens were frozen in liquid nitrogen and sectioned at 50 μm. The sections were stained for actomyosin al-

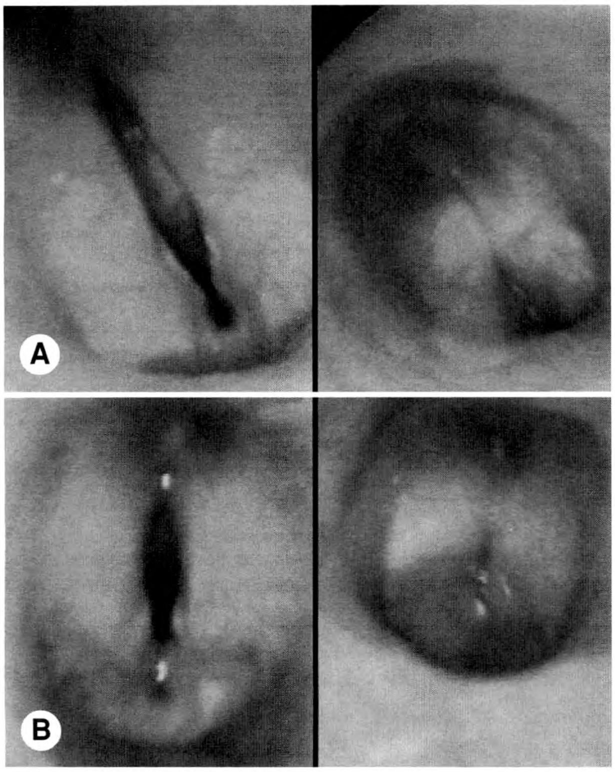

Fig 3. Infraglottic examinations: resting (left) and swallow closure (right) views. In each photograph, left vocal fold is on right, and anterior commissure is at top. **A**) (Dog 2) Whole XII–RLN reinnervated left vocal fold (VF) crosses midline to completely close glottic gap against paralyzed (nerve section) right VF. **B**) (Dog 10) Right VF (reinnervated by split XII–RLN) crosses to meet left VF (reinnervated by ansa cervicalis–RLN), which shows bulk but no motion.

kali-stable ATPase according to the method of Guth and Samaha.[35] Light microscopy was performed, and the light and dark fiber contents of each muscle were counted. The mean of 10 high-power fields was used for each muscle.

Electromyography. An electromyographic (EMG) differential amplifier became available only in time to collect data from the last dog (No. 10). After induction of general anesthesia, direct laryngoscopy was performed. A Teflon-coated monopolar EMG needle was inserted percutaneously into each TA muscle, with the position confirmed by visualizing the vocal fold while moving the needle. Ground and reference electrodes were connected, and the EMG output was filtered into digital recording software on a microprocessor. The dog was allowed to awaken from anesthesia. During this time, the vocal folds were observed through the laryngoscope, glottic activity was induced by stimulation of the tongue, and EMG activity was recorded.

RESULTS

Whole XII–RLN Group (A). The first dog had no motion of the reinnervated vocal fold at 3 months. Its neck was explored, and the anastomosis was found to be entrapped by scar to the skin. Subsequent dogs demonstrated that 3 months was probably too early to observe gross adductory motion. This dog was excluded from further analysis.

The remaining 4 dogs (Nos. 2, 3, 4, and 5) first showed evidence of partial adduction on swallowing at 3, 4, 4, and 2 months, respectively. A complete range of motion, as seen on infraglottic examination, developed 1 to 2 months later (Fig 3A). Coincidental motion of the reinnervated vocal fold and the tongue was sometimes observed. Two of the dogs exhibited normal spontaneous barking despite the presence of tracheostomies. The 4 dogs in this group were followed for 14 to 18 months after the operation. After the first 6 months, there was no additional progression in the range of motion, but the bulk of the TA muscle continued to increase until about the 12-month point. The final resting size was slightly larger than normal, suggesting muscle hypertrophy. In dog 4, hypertrophy continued longer than 1 year, so that its resting position was near the midline.

Split XII–RLN Group (B). The split XII dogs (Nos. 6, 7, and 10) showed initial movement at 3, 4, and 3 months, respectively. All 3 dogs achieved a full range of motion 1 to 2 months later (Fig 3B). The movement was not as brisk as in the group A dogs. The final bulk of the TA muscle (at 10 to 11 months) was less hypertrophied than that in group A. Activity was noted to be correlated with movement of the tongue. One dog in this group had spontaneous barking despite the tracheostomy.

Interposition Graft Group (C). The 2 interposition graft dogs (Nos. 8 and 9) showed restoration of some muscle tone. Both showed slight movement with incomplete glottic closure — one at 5 months and the other at 6 months. The tone and slight movement of the TA muscle allowed the contralateral normal vocal fold to close the glottic aperture completely on spontaneous swallows.

Controls. The normal group (group D; Nos. 1, 4, 7, 8, and 9) showed continued normal motion of the vocal folds. The RLN section dogs (group E; Nos. 2 and 3) had no evidence of recovery during the follow-up period (18 months). The vocal fold appeared to atrophy during the first 3 to 4 months and then remained stable (Fig 3A).

Ansa Cervicalis–RLN Group (F). In the ansa cervicalis–RLN group (Nos. 5, 6, and 10), no active adduction was observed. However, all 3 vocal folds gradually drifted medially, so that the contralateral side could close completely (Fig 3B). At rest, 2 of

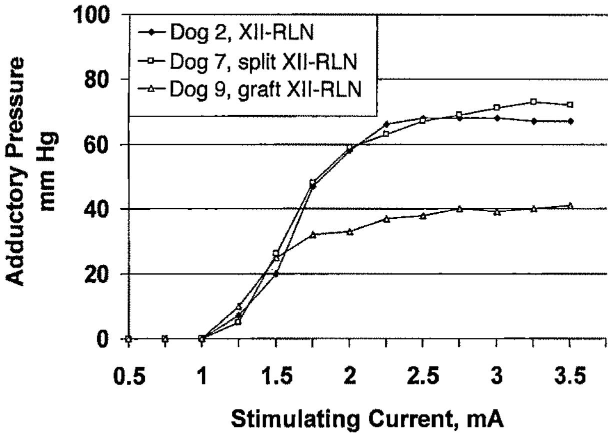

Fig 4. Pressure-versus-current curves. Tracings for dogs 2 and 7 have normal morphology and amplitude. All measurements were made with constant stimulating frequency of 80 Hz.

these dogs had occasional random twitches in the TA muscle. These twitches were not associated with motion of the opposite fold or of the tongue, and they did not move the vocal fold medially.

Physiological Data. The adductory pressure during swallowing (in awake dogs, induced by a water bolus into the oral cavity) approximated normal levels (about 100 to 130 mm Hg) in all dogs.

In dogs 3 and 4, a neurapraxic injury occurred during dissection for electrode placement, and the nerves could not be stimulated. Dog 5 had successful electrode placement, but the nerve required a very low stimulation level to reach its maximum plateau, and intermediate values could not be determined. The remaining dogs had successful electrode implantation. Thus, there were 6 dogs evaluable for the pressure-versus-current study, and 7 dogs evaluable for the pressure-versus-frequency study.

The pressure-versus-current curves demonstrated a normal sigmoid morphology for the whole XII–RLN dog and for the split XII–RLN dogs, reaching a normal pressure plateau of about 65 to 70 mm Hg (Fig 4). The other dogs had a partial recovery to about half the usual maximum stimulable pressure.

The pressure-versus-frequency curves for dogs 7 and 8 showed low pressures below 30 Hz, then linearly increasing pressures to 60 to 70 Hz, where the plateau was reached (Fig 5). This is similar to normal curves. Dogs 2, 5, 6, 9, and 10 had flatter-than-expected slopes in the transition range of 30 to 70 Hz. For dogs 5, 6, and 9, the flatter slopes were a function of the lower total motor axon recovery. For dogs 2 and 10, the flat slope was due to the higher-than-expected pressures at low frequencies. This last finding suggests an increased percentage of fast-twitch fibers in the reinnervated muscles.

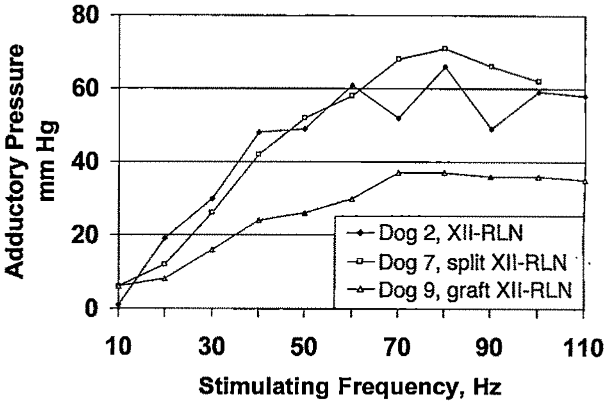

Fig 5. Pressure-versus-frequency curves. Tracing for dog 7 has normal morphology and amplitude. Each set of measurements was made with suprathreshold stimulating current.

In dog 10, the split XII–RLN side could be compared with the ansa cervicalis–RLN side. The waveform morphologies were similar for both sides. The amplitude of the plateau was normal on the split XII–RLN side, but was reduced by about 25% on the ansa cervicalis side.

Induced Phonation. This experiment was performed on 6 dogs (Nos. 2, 4, 5, 8, 9, and 10). In dog 2, the RLN section side demonstrated vocal fold atrophy, as well as immobility. The XII-RLN side had good movement and could approximate the anterior half of the opposite fold. This larynx did not phonate, because of a large persistent posterior glottic gap. A similar result was obtained with dog 10 (split XII–RLN and ansa cervicalis–RLN), in which there was good stimulated closure on both sides, but phonation did not occur because of a wide posterior chink. The posterior chink was not present during glottic closure with swallowing, but became evident as subglottic pressure increased and airflow passed through the vocal folds.

Dog 4 produced phonation using either the normal side alone or the whole XII–RLN neurorrhaphy side alone. It was also possible to find stimulation current levels that demonstrated the contributions of the neurorrhaphy side: with the normal side turned to a low level, applying stimulus to the XII-RLN side significantly increased the acoustic signal (Fig 6). In dog 5, the ansa cervicalis–RLN side showed no response to stimulation. The whole XII–RLN neurorrhaphy side moved well, and a strong phonation sample was obtained by stimulating the XII-RLN neurorrhaphy side alone.

Dog 8 was able to produce induced phonation with either the normal side or the grafted side independently. Phonation was better with both sides stimulated. The induced phonation sample from the graft

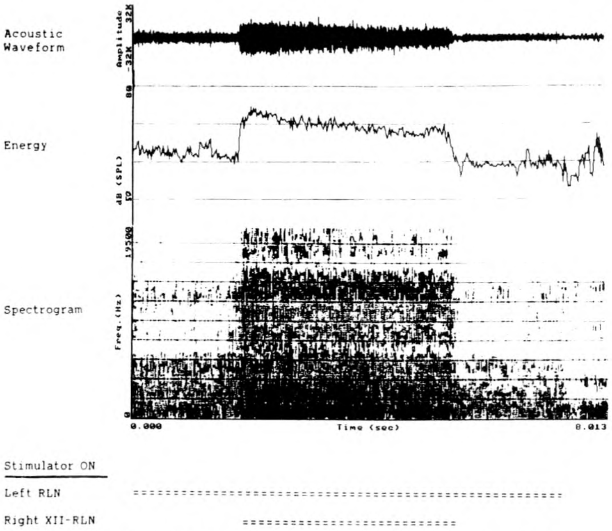

Fig 6. Induced phonation from dog 4. There is weak signal with unilateral stimulation of left (normal) RLN, and significant increase in acoustic waveform and energy when stimulation of right XII-RLN is added.

side had a subjective quality better than that of the normal side. Dog 9 also had a graft side and a normal side. The graft side activity was inadequate to close the posterior glottic chink, and phonation was not obtained with this side alone. The normal side produced typical phonation samples. When both nerves were stimulated, the voice quality could be altered by turning the grafted side on or off during the sample; this finding suggests there was some participation by this side in the process.

The results of the computer analysis of the phonation samples are given in Table 3. The samples from dog 4 could not be analyzed, because the recordings were excessively noisy. The voicing parameters for dog 8 were better for phonation with the grafted side alone than for phonation with the normal side alone — and even better when the two were used together.

TABLE 3. VOICE PARAMETERS FROM INDUCED PHONATIONS IN THREE DOGS

	Jitter (%)	*Shimmer (%)*	*NHR*	*VTI*	*Fo (Hz)*
Normal value	<1.04	<3.81	<0.19	0.061	
Dog 5					
Right (whole XII)	5.22	8.24	0.25	0.241	227
Dog 8					
Right (graft XII)	5.06	13.16	0.45	0.252	177
Left (normal)	7.27	19.29	0.66	0.300	156
Both	4.10	13.04	0.38	0.168	168
Dog 9					
Right (normal)	1.61	9.39	0.20	0.156	112
Both (with split XII)	1.03	9.33	0.35	0.277	115

Normal values given are for human phonations with sustained /a/.
NHR — noise-to-harmonics ratio, VTI — voice turbulence index, Fo — fundamental frequency.

TABLE 4. DATA FROM HISTOCHEMICAL EXPERIMENT

	Dog 8		*Dog 9*	
Muscle	*Normal L*	*Graft XII R*	*Normal R*	*Graft XII L*
TA	55	49	56	65
LCA	59	53	59	72*
PCA	39	56*	55	66*

Data shown are percentage of dark (type II, fast) muscle fibers.
L — left, R — right, TA — thyroarytenoid muscle, LCA — lateral cricoarytenoid muscle, PCA — posterior cricoarytenoid muscle.
$^*p < .05$.

In summary, induced phonation was tested in 6 dogs and was successful in 4. In 3 of the 4 dogs in which phonation was successful (2 whole XII–RLN and 1 XII-graft-RLN), the reinnervated side could adduct to produce phonation without activation of the other side. The fourth dog (XII-graft-RLN) could not close the folds tightly, but actively participated in the induced phonation. The one ansa cervicalis–XII side tested did not produce phonation.

Retrograde Labeling. The perfusion preparations improved with each iteration, with less red blood cell artifact each time. The number of stained cell bodies increased significantly when the RLN was injected directly in dogs 6 and 7. In all cases, HRP staining occurred only in the hypoglossal nucleus. Careful examination of the slides revealed some red cell artifact in other areas, but no HRP was found in the vagal nucleus or other sites.

Histochemical Analysis. Data were obtained from dogs 8 and 9; both dogs had a grafted XII and a normal opposite side. The staining of slides from dog 10 was unsuccessful; it was later discovered that the pH of one of the solutions was wrong. The ratios of dark to light fibers for these 2 dogs are given in Table 4; a sample slide is shown in Fig 7. There was a statistically significant increase in the number of dark fibers in the PCA muscle of both dogs, and in the LCA muscle of dog 9. Other changes were not significant. Some type grouping was also found.

Electromyography. Spontaneous EMG waveforms from the left TA muscle (reinnervated by a split XII) are shown in Fig 8A; those from the right TA (reinnervated by the ansa cervicalis) are shown in Fig 8B. Both sides had polyphasic action potentials, with evidence of recruitment, but much more EMG activity was observed on the split XII side.

DISCUSSION

Hemilarynges reinnervated with a whole or split XII regain full adduction during swallowing, as seen

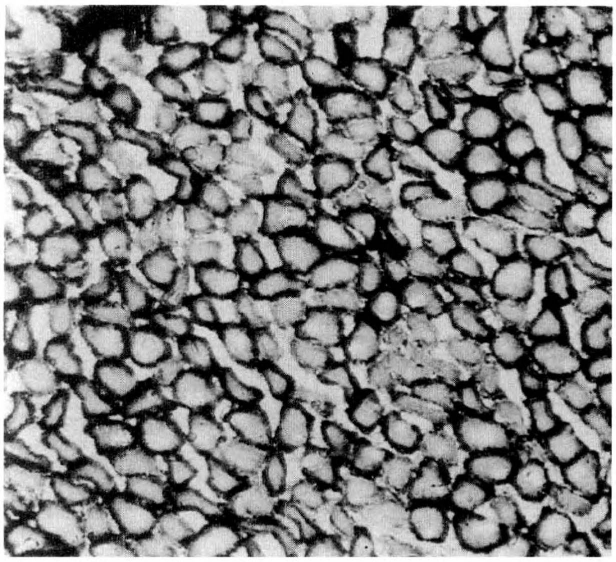

Fig 7. Alkaline-stable adenosine triphosphatase stain of posterior cricoarytenoid muscle from dog 9. Type II fibers, staining dark, are present in increased numbers compared with normal control side.

on awake infraglottic examination. It is likely that the amount of adduction is less during spontaneous phonation, because the hypoglossal nerve (like the RLN) is less active during phonation than it is during swallowing. However, the resting tone and medial vocal fold position, even without significant motion, are favorable for phonation.

After glottic closure during swallowing, the XII-reinnervated vocal folds snap back open to their resting position. This response is clearly not a function of the PCA muscle, because it is reinnervated by XII, like the adductor muscles. Instead, it likely represents recoil caused by the intrinsic elasticity of the cricoarytenoid ligaments.

The hypoglossal nerves with the interposition grafts gave results similar to those of the ansa cervicalis transfers. The grafted nerves developed some tone, but no functional motion. This outcome is likely due to the presence of 2 nerve anastomoses. Approximately 50% of motor neurons fail to cross *each* neurorrhaphy.[36] Thus, if the hypoglossal nerve will not reach the RLN to allow a tension-free primary anastomosis, it would *not* be advantageous to use XII with a nerve graft rather than the ansa cervicalis.

The normal swallowing adductory pressures were found because all 10 dogs had at least one side with a full range of motion (whole XII–RLN, split XII–RLN, or normal). The RLN section control dogs (group E) both had a whole XII–RLN procedure on the opposite side, which had enough adductory activity to reach the normal range. This finding suggests that reinnervation had occurred to a maximum level.

It should be noted that the reinnervation procedures were performed at the same time as the denervation procedure, in a clean operative field. Optimal conditions for reinnervation were present. In clinical situations, there is usually a delay of 6 to 12 months between RLN injury and reinnervation. A delay may reduce the amount of reinnervation because of scarring of the axonal tubules. Atrophy of the intrinsic laryngeal muscles may further reduce the potential for reinnervation after a delay.[22,37,38]

Physiological Data. The stimulated pressure curves confirmed that significant reinnervation occurred, and that normal activity levels were achieved in some dogs. The data also showed that in experimental nerve-muscle preparations, it is possible to produce, with direct electrical neural stimulation, responses that do not correspond with naturally occurring spontaneous activity. Green et al[39] reported similar canine experiments in which the ansa cervicalis was used to reinnervate the hemilarynx. They were able to electrically stimulate adduction through the ansa cervicalis, but did not observe any spontaneous vocal fold motion. The findings in the ansa cervicalis group in this study were similar.

Some of the dogs in this study showed electrophysiological evidence of an increase in the proportion of fast-twitch fibers. This finding indicates that the fast hypoglossal motor nerve has induced a histochemical change in the muscle (discussed below).

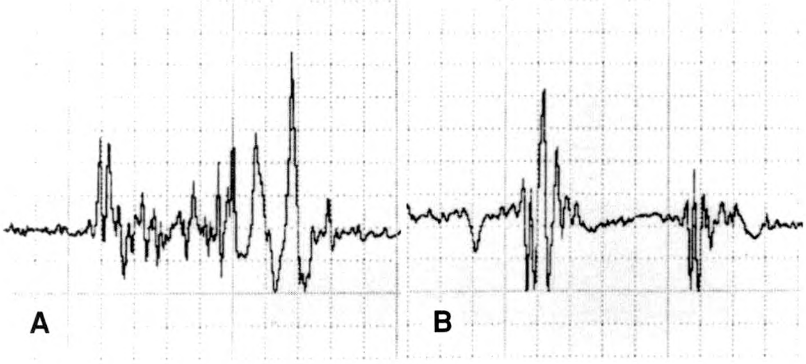

Fig 8. Electromyographic tracings from dog 10. **A)** Left thyroarytenoid muscle (split XII–RLN group). **B)** Right thyroarytenoid muscle (ansa cervicalis–RLN group).

Induced Phonation. The ability to induce phonation when passing air through the vocal folds while stimulating the appropriate motor nerves offers additional evidence of successful reinnervation. Induced phonation has been used by others to demonstrate the efficacy of the ansa cervicalis as a potential donor nerve.[39] The conditions used for induced phonation are not reproduced naturally by the dog, however. Induced phonation uses supramaximal stimulation levels that are not achieved naturally. Furthermore, stimulating the RLN (or XII or ansa cervicalis) causes simultaneous activation of both the PCA muscle and the adductor group, which does not naturally occur. The ability to artificially induce phonation does not guarantee that there will be spontaneous natural adduction, but the converse is probably true: if phonation cannot be induced electrically, it probably will not occur naturally. Thus, the induced phonation test was valuable in this study.

Retrograde Labeling. This study showed that the laryngeal reinnervation did indeed come from the hypoglossal nerve as expected. Other new brain stem connections, such as interneurons to the vagal nucleus, would not be expected to stain with this method. The temporal similarity between the natural activity of XII and that of the RLN may make such neural plasticity unnecessary.

Histochemical Analysis. The work of Buller et al[19] suggests there should be an increase in the ratio of dark to light fibers in the muscles innervated by the fast hypoglossal nerve. This increase was seen in both of the PCA muscles examined and in the LCA muscle of 1 dog. One explanation might be that the reinnervation pattern is most likely random, with variable numbers of axons going to each muscle, so that a variable pattern would be expected. Another possibility is that the laryngeal adductor muscles are already predominantly fast and have little room for becoming faster.

Because the PCA is the only intrinsic laryngeal muscle that is predominantly type I, it should undergo the greatest fiber type change after reinnervation by XII. When the PCA muscle is activated during adduction, it can help rock the arytenoid back on the cricoarytenoid joint and stabilize its position, thus allowing for better phonation and airway protection. Excessive PCA activity during adduction could be detrimental to laryngeal function, but this was not observed in any of these dogs.

Electromyography. The EMG evidence reaffirms that reinnervation occurred on both sides, but was greater on the split XII side than on the ansa cervicalis side. The EMG waveforms were generated by the reinnervated TA muscle of an awake dog and were not evoked electrically. It is interesting to note that the side with the greater EMG activity (split XII) had visible movement, whereas the ansa cervicalis side did not. The differences in spontaneous EMG activity may also reflect the activity of the animal at that time, rather than being a true indication of the level of reinnervation; but the split XII side showed more EMG activity than the ansa cervicalis side at all times.

CONCLUSIONS

The hypoglossal nerve is capable of providing dynamic activity to the unilateral paralyzed vocal fold. A split nerve provides this same result, although a bit weaker. The ansa cervicalis provide bulk and tone, but no active motion. If a cable graft is needed to allow the hypoglossal nerve to reach the RLN, it will probably not give a better result than a primary neurorrhaphy with the ansa cervicalis. There does not appear to be any vagal contribution at the brain stem level; the axons originate from the hypoglossal nucleus. Once achieved, reinnervation of the PCA muscle by XII may cause it to become more of a fast-twitch muscle and help stabilize the arytenoid on the cricoid during phonation. The hypoglossal nerve appears to be a very suitable donor for adductor reinnervation of the larynx, and may offer advantages over other donor nerves, such as the ansa cervicalis.

Part II of this work (submitted as a Candidate's Thesis to the American Laryngological, Rhinological and Otological Society, Inc), "Clinical Evaluation and Early Patient Experience," has already been published and supports these conclusions.[16]

ACKNOWLEDGMENTS — The authors thank Dr Richard Doyle and John Salmo for their diligent care of the animals, Dr John Fredrickson for the departmental bridge funding that supported this project, and Dr J. Gershon Spector and Dr Donald Sessions for their help and guidance as proposers and mentors throughout the thesis process.

REFERENCES

1. Benninger MS, Crumley RL, Ford CN, et al. Evaluation and treatment of the unilateral paralyzed vocal fold. Otolaryngol Head Neck Surg 1994;111:497-508.

2. Tucker HM, Rusnov M. Laryngeal reinnervation for unilateral vocal cord paralysis: long-term results. Ann Otol Rhinol Laryngol 1981;90:457-9.

3. Trapp TK, Berke GS, Bell TS, Hanson DG, Ward PH. Effect of vocal fold augmentation on laryngeal vibration in simulated recurrent laryngeal nerve paralysis: a study of Teflon and Phonogel. Ann Otol Rhinol Laryngol 1989;98:220-7.

4. Remacle M, Marbaix E, Hamoir M, Declaye X, van den Eeckhaut J. Initial long-term results of collagen injection for vocal and laryngeal rehabilitation. Arch Otorhinolaryngol 1989; 246:403-6.

5. Isshiki N, Okamura H, Ishiwaka T. Thyroplasty type I (lateral compression) for dysphonia due to vocal cord paralysis or atrophy. Acta Otolaryngol (Stockh) 1975;80:465-73.

6. Isshiki N, Taira T, Kojima H, Shoji K. Recent modifications in thyroplasty type I. Ann Otol Rhinol Laryngol 1989;98: 777-9.

7. Isshiki N, Masahiro T, Sawada M. Arytenoid adduction for unilateral vocal cord paralysis: a comparison. Laryngoscope 1988;98:1200-4.

8. Slavit DH, Maragos NE. Physiologic assessment of arytenoid adduction. Ann Otol Rhinol Laryngol 1992;101:321-7.

9. Crumley RL. Unilateral recurrent laryngeal nerve paralysis: a review. J Voice 1994;8:79-83.

10. Sasaki CT, Leder SB, Petcu L, Friedman CD. Longitudinal voice quality changes following Isshiki thyroplasty type I: the Yale experience. Laryngoscope 1990;100:849-52.

11. Paniello RC, Dahm JD. Reversibility of medialization laryngoplasty: an experimental study. Ann Otol Rhinol Laryngol 1997;106:902-8.

12. Crumley RL. Teflon versus thyroplasty versus nerve transfer: a comparison. Ann Otol Rhinol Laryngol 1990;99:759-63.

13. Tucker HM. Combined laryngeal framework medialization and reinnervation for unilateral vocal fold paralysis. Ann Otol Rhinol Laryngol 1990;99:778-81.

14. Crumley RL. Update: ansa cervicalis to recurrent laryngeal nerve anastomosis for unilateral laryngeal paralysis. Laryngoscope 1991;101:384-8.

15. Paniello RC, Lee P, Dahm JD. Hypoglossal nerve transfer for laryngeal reinnervation: a preliminary study. Ann Otol Rhinol Laryngol 1999;108:239-44.

16. Paniello RC. Laryngeal reinnervation with the hypoglossal nerve: II. Clinical evaluation and early patient experience. Laryngoscope 2000;110:739-48.

17. Sanders I, Aviv J, Biller HF. Transcutaneous electrical stimulation of the recurrent laryngeal nerve: a method of controlling vocal cord position. Otolaryngol Head Neck Surg 1986; 95:152-7.

18. Lee P, Paniello RC. Laryngeal chemodenervation: effects of injection site, dose, and volume. Ann Otol Rhinol Laryngol 1999;108:1140-5.

19. Buller AJ, Eccles JC, Eccles RM. Interactions between motoneurones and muscles in respect of the characteristic speeds of their responses. J Physiol (Lond) 1960;150:417-39.

20. Paniello RC, Dahm JD. Long-term model of induced canine phonation. Otolaryngol Head Neck Surg 1998;118:512-22.

21. Crumley RL, McCabe BF. Regeneration of the recurrent laryngeal nerve. Otolaryngol Head Neck Surg 1982;90:442-7.

22. Shindo ML, Herzon GD, Hanson DG, Cain DJ, Sahgal V. Effects of denervation on laryngeal muscles: a canine model. Laryngoscope 1992;102:663-9.

23. LaVail JH. The retrograde transport method. Fed Proc 1975;34:1618-24.

24. Dahm JD, Paniello RC. Tracheostomy for long-term laryngeal experimentation. Otolaryngol Head Neck Surg 1998; 118:376-80.

25. Hvidegaard T, Vase P, Dalsgaard SC, Jorgensen K. Endolaryngeal devices for perioperative identification and functional testing of the recurrent nerve. Otolaryngol Head Neck Surg 1984;92:292-4.

26. Lipton RJ, McCaffrey TV, Litchy WJ. Intraoperative electrophysiologic monitoring of laryngeal muscle during thyroid surgery. Laryngoscope 1988;98:1292-6.

27. Kay Elemetrics. Operations manual, multi-dimensional voice program (MDVP) model 4305. Pine Brook, NJ: Kay Elemetrics, 1993:17.

28. Henry C, Cazals Y, Gioux M, Didier A, Aran JM, Traissac L. Neuroanatomical study of Galen's anastomosis (nervus laryngeus) in the dog. Acta Anat (Basel) 1988;131:177-81.

29. Hisa Y, Toyoda K, Uno T, Murakami Y, Ibata Y. Localization of the sensory neurons in the canine nodose ganglion sending fibers into the internal branch of the superior laryngeal nerve. Eur Arch Otorhinolaryngol 1991;248:265-7.

30. Toyoda K, Hisa Y, Uno T, Tadaki N. Distribution of the afferent neurons from the canine recurrent laryngeal nerve. Eur Arch Otorhinolaryngol 1993;249:485-7.

31. Basterra J, Dilly PN, Chumbley CC. The hypoglossal nucleus of the guinea pig, labelled with horseradish peroxidase. Acta Otorhinolaryngol Belg 1987;41:589-95.

32. Kitamura S, Nishiguchi T, Sakai A. A horseradish peroxidase study of rat lingual motoneurons with axons passing through the cervical nerve. Exp Neurol 1985;87:20-34.

33. Thomander L, Aldskogius H, Grant G. A procedure for studying the organization of peripheral nerves with horseradish peroxidase demonstrated on the facial and hypoglossal nerves in the rat. ORL J Otorhinolaryngol Relat Spec 1984;46: 111-6.

34. Mesulam MM. A tetramethyl benzidine method for the light microscopic tracing of neural connections with horseradish peroxidase (HRP) neurohistochemistry. J Histochem Cytochem 1978;26:106-17.

35. Guth L, Samaha FJ. Procedure for the histochemical demonstration of actomyosin ATPase. Exp Neurol 1970;28:365-7.

36. Spector JG, Lee P. Axonal regeneration in severed peripheral facial nerve of the rabbit: relation of the number of axonal regenerates to behavioral and evoked muscle activity. Ann Otol Rhinol Laryngol 1998;107:141-8.

37. Nomoto M, Yoshihara T, Kanda T, Konno A, Kaneko T. Misdirected reinnervation in the feline intrinsic laryngeal muscles after long-term denervation. Acta Otolaryngol Suppl (Stockh) 1993(suppl 506):71-4.

38. Morledge DR, Lauvstad WA, Calcaterra TC. Delayed reinnervation of the paralyzed larynx. Arch Otolaryngol 1973;97: 291-3.

39. Green DC, Berke GS, Graves MC. A functional evaluation of ansa cervicalis nerve transfer for unilateral vocal cord paralysis: future directions for laryngeal reinnervation. Otolaryngol Head Neck Surg 1991;104:453-66.

Ann Otol Rhinol Laryngol 110:2001

COMBINED BUCCAL MUCOSA ISLAND AND STERNOHYOID FLAPS: A NEW TECHNIQUE OF HEMILARYNGEAL RECONSTRUCTION STUDIED IN A CANINE MODEL

ROBERT J. ANDREWS, MD KEITH E. BLACKWELL, MD GERALD S. BERKE, MD
MARILENE B. WANG, MD THOMAS C. CALCATERRA, MD JOEL A. SERCARZ, MD
LOS ANGELES, CALIFORNIA

No single method of reconstruction has proven ideal for all patients with defects following vertical hemilaryngectomy. In this report, we detail a new technique for hemilaryngeal reconstruction involving the use of a pedicled buccal mucosa island flap supplied by the facial artery and vein. The buccal flap was used to resurface a transversely oriented sternohyoid myofascial flap. The reconstructive outcome was analyzed in 4 animals, 3 of which survived the early postoperative period. Videoendoscopy and stroboscopy were performed to analyze the laryngeal configuration and vibration. Each subject was decannulated and had a competent airway free of aspiration. After sacrifice of the animals, whole organ axial sections were made at multiple levels. Endoscopic and histologic findings documented that this technique produced an appropriate neocord position. Laryngeal stroboscopy in each animal showed bilateral mucosal traveling waves, with entrainment of the reconstructed neocord mucosa and native vocal cord mucosa. We conclude that the layered reconstructive technique described, compared to traditional methods of reconstruction, more closely replicates the structure of the excised tissue in hemilaryngeal reconstruction, potentially resulting in an improved voice outcome.

KEY WORDS — larynx, mucosa flap, reconstruction.

INTRODUCTION

Reconstruction of the hemilaryngeal defect continues to challenge laryngologists. One of the most significant problems of traditional reconstructive methods using local flaps is that the resulting reconstructed neocord often lacks a suitable vibratory surface to oppose the remaining native vocal cord.

Our goal in this study was to develop an improved method of hemilaryngeal reconstruction, utilizing a pedicled buccal mucosa island flap rotated into the larynx to serve as a vibratory "cover" for the neocord. In the technique described in this study, a transversely oriented sternohyoid myofascial flap is positioned lateral to the buccal mucosa island flap to serve as a substitute for the excised thyroarytenoid muscle. Finally, a microplate and a thyroid perichondrial flap are used to provide rigidity to the laryngeal framework. This technique, while technically challenging, is theoretically sound compared to the myofascial and cartilage flaps that are most commonly used for clinical hemilaryngeal reconstruction today.

In a previous report by Andrews et al,[1] this technique was compared to other reconstructive methods in dogs, and it was found to be superior to other rotational flaps. Because of space limitations, it was not possible to describe the surgical technique nor the unique physiological aspects of this procedure in the previous study. In this report, we describe the technical details and the outcome of this new approach to laryngeal reconstruction, one that holds promise as a method for use in humans.

MATERIALS AND METHODS

SURGICAL TECHNIQUE

Institutional guidelines regarding humane animal experimentation were followed. Four mongrel dogs were premedicated with intramuscular acepromazine maleate (0.2 mg/kg) as a preoperative sedative. An intravenous line was placed in one of the hind legs, and pentobarbital sodium was administered to achieve corneal anesthesia. The subjects were placed supine on the operating table and intubated with a cuffed endotracheal tube. A mixture of 0.5% to 2.0% halothane and oxygen was administered to maintain anesthesia throughout the procedure. The dogs underwent identical procedures for left hemilaryngeal resection and reconstruction.

A faculty surgeon and a resident assistant per-

From the Division of Head and Neck Surgery, University of California, Los Angeles School of Medicine, Los Angeles (all authors), and the Division of Head and Neck Surgery, Harbor–University of California, Los Angeles Medical Center, Torrance (Sercarz), California. Supported by a Veterans Administration Merit Review Grant. This study was performed in accordance with the PHS Policy on Humane Care and Use of Laboratory Animals, the NIH *Guide for the Care and Use of Laboratory Animals*, and the Animal Welfare Act (7 U.S.C. et seq.); the animal use protocol was approved by the Institutional Animal Care and Use Committee (IACUC) of the University of California, Los Angeles.

CORRESPONDENCE — Joel A. Sercarz, MD, UCLA School of Medicine, Division of Head and Neck Surgery, 10833 Le Conte Ave, Room 62-132, Los Angeles, CA 90095.

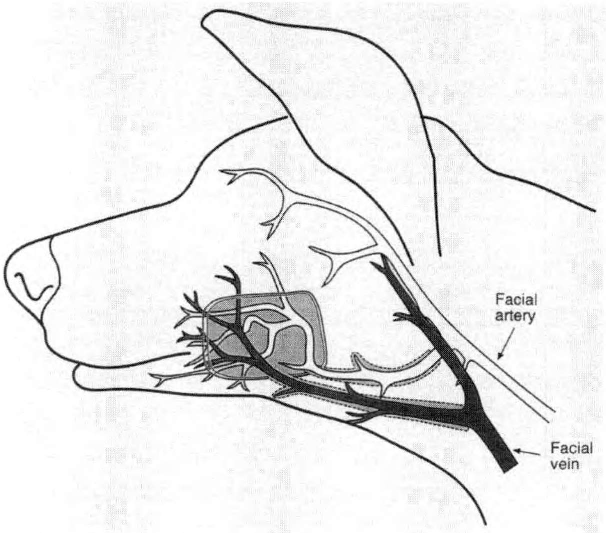

Fig 1. Illustration of buccal flap with vascular pedicle in dog.

formed the operation. A tracheotomy was performed at the fifth tracheal ring, and the dog was intubated through this site. The laryngeal framework was exposed by midline dissection and lateral retraction of the strap muscles. A posteriorly based left external thyroid perichondrial flap was developed. The perichondrium was incised vertically a few millimeters to the right of the midline and horizontally along the superior and inferior borders of the left thyroid ala. A scalpel was used to make the thyroid cartilage cuts in the midline and at the junction of the posterior one third and anterior two thirds of the left thyroid ala.

An incision was made in the anterior cricothyroid membrane, and the larynx was entered. A midline vertical thyrotomy was made, and then superior and inferior cuts were completed through the thyrohyoid and cricothyroid membranes. A mucosal incision was made in the midline of the posterior commissure. The specimen, which included the left true vocal cord, ventricle, false vocal cord, thyroarytenoid muscle, arytenoid cartilage, and anterior two thirds of the ipsilateral thyroid cartilage, was excised.

RECONSTRUCTION METHOD

A second skin incision was made in the left submandibular region, inferior and parallel to the mandible, to harvest the pedicled buccal mucosa island flap (Fig 1). The facial vein was located inferior to the submandibular gland and dissected superiorly through the gland to the inferior border of the mandible.

In this study, the ramus mandibularis of the facial nerve was cut to facilitate dissection of the flap; its cutting produced no functional disability or visible facial asymmetry in the dogs. For application of this flap to human patients, the marginal mandibular nerve would be preserved. Its preservation would require careful dissection of the nerve away from the underlying vascular pedicle to allow mobilization of the buccal flap beneath the nerve so it could reach the laryngeal defect.

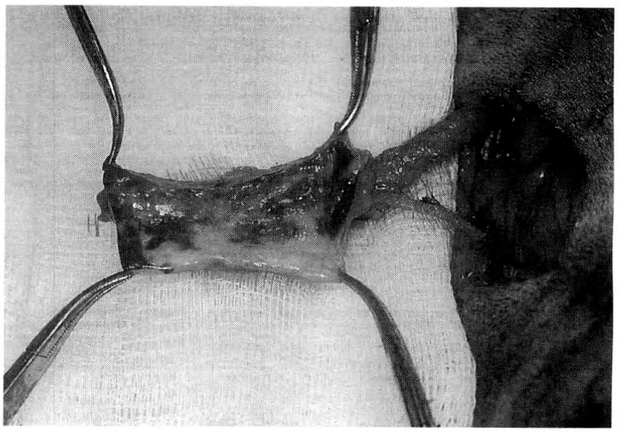

Fig 2. Buccal flap with vascular pedicle in submandibular wound. Dark areas are pigmentation of canine buccal mucosa.

A rectangular mucosal flap, measuring approximately 2 cm high by 3 cm wide, was incised in the buccal mucosa. The vascular pedicle was located in the center of the mucosal island flap. The inferior mucosal incision was placed several millimeters superior to the gingival-buccal sulcus, and the superior mucosal incision was located below Stensen's duct. The posterior mucosal incision was placed close to the ascending ramus of the mandible, and the anterior mucosal incision was several centimeters posterior to the oral commissure.

The distal facial artery and vein were ligated and divided at the superior edge of the buccal flap. The buccal flap was then carefully mobilized, with care taken to avoid injury to the vascular pedicle. In most cases, the flap was 0.5 to 1.0 cm thick and included buccal mucosa, submucosa, and a portion of the buccinator muscle. The flap was passed inferiorly into the neck, and proximal dissection of the artery and vein was continued to allow tension-free rotation of the buccal flap into the laryngeal lumen. In all cases, the arc of rotation of the vascular pedicle allowed it to reach the larynx without difficulty. The vascular integrity of the flap was then verified by observation of bleeding from the mucosal edges (Fig 2).

A superiorly based sternohyoid myofascial flap was raised as described by Hirano.[2] A 2-0 polyglactin suture was placed through the posterior aspect of the remaining hemilarynx, incorporating the remaining interarytenoid muscle and the inner perichondrium of the cricoid cartilage. This suture was used later in

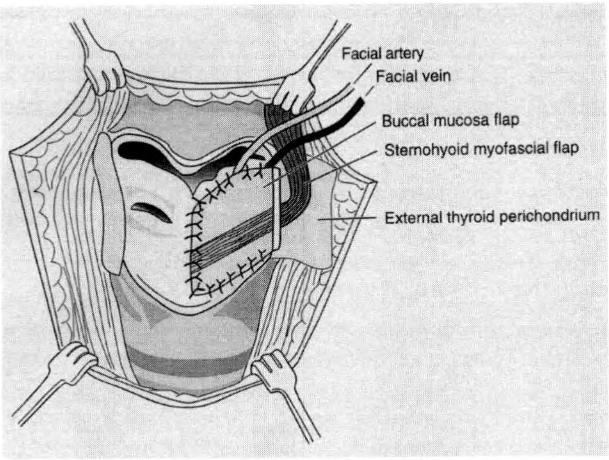

Fig 3. Illustration via laryngofissure of mucosal and myofascial flap placement.

the procedure to fix the sternohyoid myofascial flap to the posterior commissure.

The size of the laryngeal mucosal defect was assessed, and the mucosal edges of the buccal island flap were trimmed to approximate the size of the defect. The flap was then inset into the laryngeal defect. The buccal mucosa was approximated to the laryngeal mucosa with interrupted 5-0 polyglactin sutures.

The anterior mucosal edge of the intact right hemilarynx was sutured to the anterior edge of the right thyroid cartilage and inner perichondrium with interrupted 5-0 absorbable sutures placed superior and inferior to the true vocal cord. The larynx was then closed anteriorly with interrupted 5-0 polyglactin sutures to approximate the anterior edge of the buccal mucosa flap to the right laryngeal mucosa and the right thyroid cartilage inner perichondrium. These measures were taken to reconstruct a sharp anterior commissure and prevent web formation.

The superiorly based sternohyoid myofascial flap was then raised and sutured into the laryngeal defect as described by Hirano.[2] The flap was trimmed and folded approximately 90° at the level of the upper border of the cricoid cartilage to reach the posterior commissure without tension. The end of the myofascial flap was then sewn to the posterior commissure with the 2-0 polyglactin suture placed earlier. The myofascial flap was then sutured to the sternothyroid muscle and the remnant of the cricothyroid muscle to fix the position of the flap at the anterior commissure. Figure 3 is a schematic illustration of the first 2 steps of the reconstruction technique as viewed through a laryngofissure.

The reconstruction was completed with placement of a titanium microplate at the level of the neoglottis to bridge the defect in the left thyroid ala, followed by closure of the outer perichondrium anteriorly (Fig 4). The microplate was positioned before the resection and served to medialize the myofascial and buccal flaps at the level of the glottis and stabilize the laryngeal framework. The animals were given ampicillin and gentamicin sulfate for 1 week after surgery. The tracheostomy tube was removed 2 to 3 weeks after the operation.

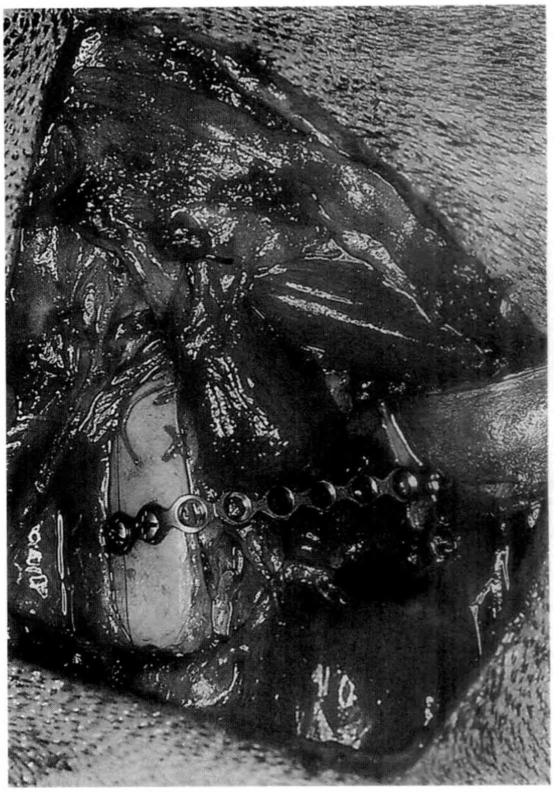

Fig 4. Appearance of larynx following placement of myofascial and muscle flaps and placement of microplate into thyroid lamina.

POSTOPERATIVE EVALUATION

Two months after the hemilaryngeal reconstruction, each dog underwent direct laryngoscopy. Endoscopy was performed and subglottic pressures were assessed in the live dog under anesthesia. The subjects were euthanized after data collection.

Laryngoscopy and Preparation. Each dog received acepromazine maleate (0.2 mg/kg) intramuscularly as a preoperative sedative. Pentobarbital was administered intravenously to a level of corneal anesthesia. The subject was placed supine on the operating table, and direct laryngoscopy was performed. The dog was intubated with a cuffed endotracheal tube for ventilator-assisted respiration. Dexamethasone (8 mg given intravenously) was administered to reduce laryngeal edema during phonation.

A midline vertical skin incision was made from the sternal notch to just below the cricoid cartilage.

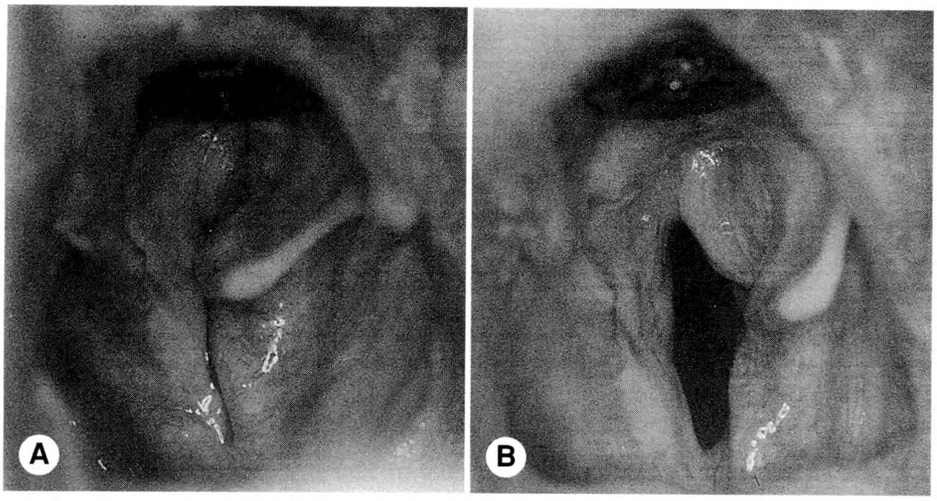

Fig 5. Postoperative endoscopy **A)** with and **B)** without recurrent laryngeal nerve stimulation, 2 months after left hemilaryngeal reconstruction using pedicled buccal mucosa flap.

Dissection was carried out in the midline, and the strap muscles were retracted laterally. A low tracheotomy was made at the level of the sternal notch, through which a cuffed endotracheal tube was passed for assisted ventilation. The oral endotracheal tube was then removed.

A second tracheotomy was placed 3 tracheal rings superior to the first, and a recurrent laryngeal nerve–stimulating endotracheal tube was inserted and directed superiorly so that its tip was located approximately 10 cm below the glottis. This tube had foil electrodes attached to the cuff so that the nerve could be stimulated through the tracheal cartilage.[3,4] The tube was positioned so that the electrodes on the cuff were oriented with the stimulating electrodes adjacent to the tracheal-esophageal groove. A ground electrode was positioned at the anterior tracheal wall.

Recurrent Laryngeal Nerve Stimulation. Stimulation was provided via a nerve stimulator (model 2SLH, WR Medical Electronics Co, St Paul, Minn) connected to the tracheal electrodes. The stimulus frequency was 80 Hz, with a 1.5-ms pulse duration and current of 3 to 5 mA.

Videolaryngoscopy and Videostroboscopy. Videolaryngoscopy was performed with a 0° endoscope (Karl Storz Endoscopy–America Inc, Culver City, Calif) connected to a halogen light source via a fluid-filled light cable. For videostroboscopy, a laryngostrobe (model 8000, Storz) was connected to the endoscope. Images were recorded with a charge-coupled device video camera (model IK-C30A, Toshiba, Buffalo Grove, Ill) and a 3/4-inch videotape recorder (model VO-9850, Sony, Park Ridge, NJ). Recorded images were viewed on a video monitor (model PVM-1341, Sony) for frame-by-frame analysis.

Whole Organ Sections. The excised larynges were fixed in formaldehyde, and whole organ axial sections were made at the levels of the supraglottis, ventricle, glottis, and subglottis for gross and histologic examination. The specimens were then embedded in paraffin, and hematoxylin and eosin slides were prepared from each axial section.

RESULTS

COMPLICATIONS

There was 1 postoperative death due to a plugged tracheostomy tube on postoperative day 8. A necropsy revealed no evidence of aspiration or pulmonary infection. There were no other complications identified in the series. The intraoral donor site of the buccal flap healed without stricture or contracture after primary closure of the defect.

AIRWAY AND SWALLOWING FUNCTION

There was no clinical evidence of aspiration with solids or liquids either before or after decannulation in any subject. All of the surviving dogs were decannulated between the second and third postoperative weeks. The first 2 subjects underwent direct laryngoscopy under sedation before decannulation. Each subject demonstrated an adequate airway. The dogs were decannulated when they tolerated a sustained period of exercise with the tracheostomy tubes removed and their stomas occluded with surgical tape. After decannulation, the stoma sites were allowed to heal by secondary intention.

ENDOSCOPY

On endoscopic examination, the mucosa was viable and well healed throughout the reconstructed hemilarynx. The suture lines healed without granulation tissue or stenosis. The anterior commissure was free of webbing. The anterior-posterior dimension of the larynx appeared to be normal. The flap was positioned in the midline posteriorly, with complete closure of the glottis on stimulation of the right recurrent laryngeal nerve (Fig 5). At rest, the glottic con-

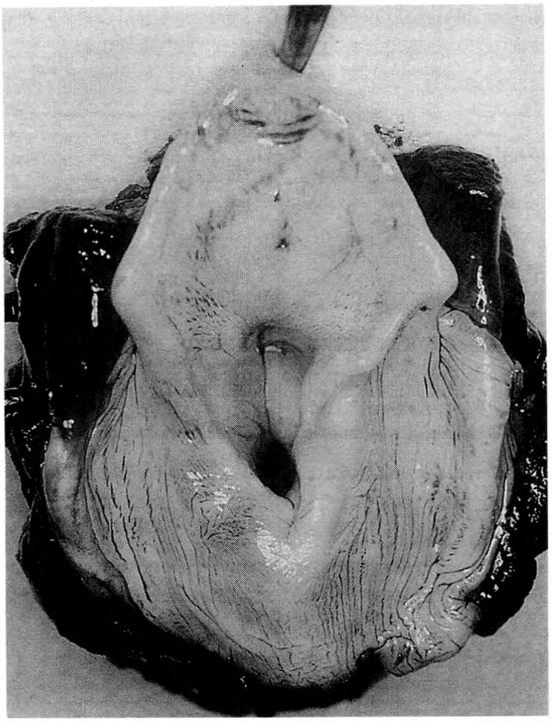

Fig 6. Laryngeal specimen, superior view, immediately after postoperative endoscopy.

figuration was similar to that which is seen after a paralyzed vocal cord has been medialized by a thyroplasty procedure.

STROBOSCOPIC EXAMINATION

All subjects in the study underwent videostroboscopic evaluation. When phonation was induced under anesthesia, a mucosal traveling wave was produced in the reconstructed left neocord that was synchronous with the wave in the native right vocal cord. The propagation of the mucosal wave in the reconstructed hemilarynx continued superiorly along the mucosal flap, above the level of the remaining right ventricle.

WHOLE ORGAN GROSS AND HISTOLOGIC AXIAL SECTIONS

Figure 6 is a photograph of the larynx made immediately after sacrifice of one of the dogs. A representative whole organ section through the level of the midglottis is shown in Fig 7. The whole organ sections demonstrate several important features of this reconstruction technique. New bone and cartilage growth was noted on the site at which the external thyroid perichondrial flap was placed over the microplate. In addition, the sections clearly demonstrated that the superiorly based sternohyoid muscle flap was fixed in the same orientation as the excised thyroarytenoid muscle. It was also noted that the myofascial flap was medialized by the bone and cartilage at the microplate site, and that it had maintained sufficient bulk to effectively medialize the neocord at the level of the glottis.

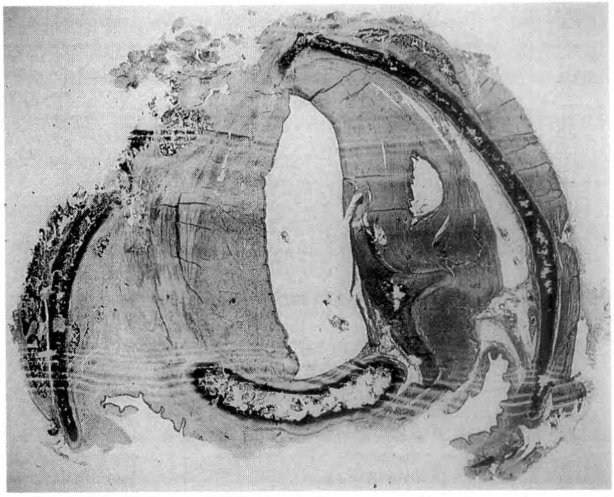

Fig 7. Whole organ axial section at level of mid-glottis.

DISCUSSION

The most common methods used for reconstruction of vertical hemilaryngectomy defects employ strap muscle myofascial flaps or rotational flaps from adjacent larynx or hypopharynx mucosa.[5-8] There are a number of disadvantages to these methods. When local mucosal rotational flaps are used alone, they may not provide adequate bulk for restoring volume to the laryngeal defect. This lack can result in breathy dysphonia or aspiration. Rotational mucosal flaps produce distortion of the donor sites in the pyriform sinus or epiglottis, which can also contribute to dysphagia or aspiration.

Local strap muscle flaps are used frequently for hemilaryngeal reconstruction, in the belief that the disadvantages of local rotational or free mucosal grafts outweigh their benefits. Many myofascial flaps have been described that can provide adequate bulk for replacing the excised hemilarynx. The primary disadvantage is that they result in an adynamic glottic surface lined by a thin mucosal layer that does not physiologically vibrate. Despite deficiencies related to vocal function, myofascial flaps are a very good option for partial laryngeal reconstruction, because they are versatile and produce consistent results.

An alternative approach to vocal cord reconstruction involves the use of the false vocal cord to reconstruct the true cord. In imbrication laryngectomy,[9] the false vocal cord and aryepiglottic folds are imbricated medially to allow the false cord to vibrate opposite the intact contralateral true cord. The false vocal cord flap[10] is another alternative, in which the false cord is unfolded and sutured to the inferior portion of the defect. Neither of these techniques is appropriate for the kind of complete hemilaryngeal defect described in this study.

When a mucosal island flap such as the buccal flap described herein is used, the mucosa and submucosa are transferred as a unit, producing a cover that closely replicates the excised vocal fold mucosa and lamina propria. We believe that the buccal mucosa island flap method is preferable to a thin free buccal graft, because the submucosal integrity is preserved in the former. In addition, the potential for graft necrosis and scar contracture is limited in this well-vascularized, axial-pattern mucosal flap as compared to a nonvascularized buccal graft. Unfortunately, *no* method is capable of precisely reproducing the normal layered structure of the vocal cord, including the extracellular matrix proteins of the lamina propria.

The canine experience with this method indicates that it is a promising approach to hemilaryngeal reconstruction. The ability to produce a mucosal wave in the reconstructed neocord is particularly noteworthy, because traditional methods of reconstruction are unable to provide such vibration. In the canine model, the larynx was competent and swallowing function was preserved. However, because the larynx is less upright in the dog than in the human, this model may not be sensitive in determining potential clinical problems with glottal competence in human laryngeal reconstruction. The airway was adequate to allow sustained periods of exercise after closure of the tracheostomy. Endoscopy indicated that the laryngeal airway was similar to that seen after a medialization procedure for unilateral vocal cord paralysis. The addition of a laryngeal framework reconstruction contributed to the technique by providing support at the anterior commissure and maintaining the anterior-posterior diameter of the glottis.

It is difficult to predict the anticipated human speech result from canine experiments. In the dogs, however, the phonatory result was subjectively very good. There was minimal breathiness, and each dog produced a loud bark that indicated that they were able to achieve complete closure of the glottis for generation of subglottic pressures substantial enough to drive phonation. Also, the mucosal wave seen on the reconstructed side during videostroboscopy suggests that a vascularized mucosal flap may provide a suitable substitute for the viscoelastic properties of the native laryngeal mucosa and lamina propria.

The new bone and cartilage that grew over the microplate scaffold acted to replicate the excised thyroid cartilage. The microplate placed at the level of the glottis maintained the structural integrity of the larynx and prevented the unresected thyroarytenoid muscle from pulling the anterior commissure to the contralateral side. In our previous experience in the canine model, it was found that there was shortening of the anterior-posterior dimension of the glottis when the laryngeal framework was not reconstructed. This shortening may prevent the remaining thyroarytenoid muscle from effectively tensing the intact vocal cord. We believe this limitation would have a significant effect on the resulting quality of vocal function following this reconstruction.

Our preliminary results indicate that this procedure is a relatively safe and effective method of hemilaryngeal reconstruction in the canine model. In order to advocate this procedure in a human subject with a hemilaryngeal defect, one would have to consider several factors. First, additional operative time would be necessary to raise the buccal mucosa island flap. The flap also would produce an additional surgical wound in the oral cavity. However, this donor site defect is usually well tolerated in patients who undergo nonvascularized buccal mucosa grafts and intraoral facial artery myomucosal flaps. Finally, there is a potential for injury to the marginal branch of the facial nerve, which is located adjacent to the vascular pedicle of the flap.

Sasaki et al[11,12] reported a full-thickness cheek flap based on the facial artery that included both cheek skin and buccal mucosa. This approach has been used for reconstruction of cervical esophageal strictures and limited pharyngeal defects in humans. The donor site morbidity was reported to be acceptable. A vascularized buccal mucosa island flap may prove to be a useful technique for human laryngeal reconstruction, if it can be performed with acceptable risk and demonstrate an improvement in vocal function compared to traditional methods of hemilaryngeal reconstruction.

In conclusion, we present a new technique for partial laryngeal reconstruction consisting of a vascularized buccal mucosa island flap, a transversely oriented sternohyoid muscle flap, and a microplate laryngeal framework repair. Our preliminary experience with this technique in the canine model has been encouraging. The primary advantage of this layered reconstruction is that it produces a functional, vibratory neocord offering a voice outcome potentially better than that achieved with traditional methods of hemilaryngeal reconstruction.

REFERENCES

1. Andrews RJ, Sercarz JA, Ye M, Kreiman J, Calcaterra TC, Berke GS. Vocal function following vertical hemilaryngectomy: comparison of four reconstruction techniques in the canine. Ann Otol Rhinol Laryngol 1997;106:261-70.

2. Hirano M. Technique for glottic reconstruction following vertical partial laryngectomy: a preliminary report. Ann Otol Rhinol Laryngol 1976;85:25-31.

3. Sercarz JA, Berke GS, Rothschiller J, Ming Y. Fabrication of a custom electrode endotracheal tube. Laryngoscope 1991;101:1024-5.

4. Berke GS, Moore DM, Gerratt B, Aly A, Tantisira J. Transtracheal stimulation of the recurrent laryngeal nerve. Am J Otolaryngol 1988;9:12-7.

5. Burgess LP. Laryngeal reconstruction following vertical partial laryngectomy. Laryngoscope 1993;103:109-32.

6. Bailey BJ. Glottic reconstruction after hemilaryngectomy: bipedicle muscle flap laryngoplasty. Laryngoscope 1975; 85:960-77.

7. Calcaterra TC. Sternohyoid myofascial flap reconstruction of the larynx for vertical partial laryngectomy. Laryngoscope 1983;93:422-4.

8. Calcaterra TC. Bilateral omohyoid muscle flap reconstruction for anterior commissure cancer. Laryngoscope 1987; 97:810-3.

9. Liu C, Ward PH, Pleet L. Imbrication reconstruction following partial laryngectomy. Ann Otol Rhinol Laryngol 1986; 95:567-71.

10. Brasnu D, Laccourreye O, Weinstein G, Fligny I, Chabardes E. False vocal cord reconstruction of the glottis following vertical partial laryngectomy: a preliminary analysis. Laryngoscope 1992;102:717-9.

11. Sasaki TM, Baker HW, McConnell DB, Yeager RA, Vetto RM. Cheek island flap for replacement of critical limited defects of the upper aerodigestive tract. Am J Surg 1986;152:435-7.

12. Sasaki TM, Taylor L, Martin L, Baker HW, McConnell DB, Vetto RM. Correction of cervical esophageal stricture using an axial island cheek flap. Head Neck Surg 1983;6:596-9.

Ann Otol Rhinol Laryngol 110:2001

AERODYNAMIC PROFILES OF A HEMILARYNX WITH A VOCAL TRACT

FARIBORZ ALIPOUR, PHD
DOUGLAS MONTEQUIN, MA
NIRO TAYAMA, MD
IOWA CITY, IOWA

The pressure-flow relationship was examined in excised canine and human larynges with and without a vocal tract. Canine and human larynges were prepared and cut in the midsagittal plane from the top to about 10 mm below the vocal folds. The right half was removed and replaced with an acrylic plate. The vocal tract was simulated initially with a 15-cm plastic tube and later with a vocal tract model with an area function resembling "ah." Simultaneous recordings were made of the glottal pressure, mean subglottal pressure, and average airflow at various levels of adduction. Preliminary data indicated that the pressure-flow relationships were similar to those of a full larynx and were almost linear. The addition of the vocal tract increased the glottal resistance by moving these pressure-flow lines to the lower-flow and higher-pressure region. The human larynx appears to phonate more easily than the canine larynx on the laboratory bench and has lower phonation threshold pressures.

KEY WORDS — canine hemilarynx, glottal adduction, intraglottal pressure, miniature transducer, pressure-flow relationship, vocal tract.

INTRODUCTION

The vocal fold dynamics of phonation depends on the tissue properties and pressure distribution within the glottis. While most tissue properties are almost constant during phonation, the pressure distribution is dynamically changing within the glottis. Also, the pressure distribution within the glottis is not uniform and has large variations both in the superior-inferior direction, parallel to the airflow, and in the anterior-posterior direction, perpendicular to the airflow.[1] Measuring these dynamic intraglottal pressures has been a difficult task in the past because of glottal space limitations present during vibration of the vocal folds. Recently, these measurements were made possible by the use of miniature pressure transducers in excised hemilarynx experiments.[1-3]

Excised canine hemilarynges were used by Jiang and Titze[2] to study contact pressure during phonation. They reported a method and data for contact pressures using a hemilarynx approach. Placing a single pressure transducer at various glottal locations, they found that the impact pressures on the vocal fold surfaces increased with subglottal pressure and adduction. Also, Alipour and Scherer,[1] in a similar protocol using canine hemilarynges, studied dynamic pressure within the glottis. Although their study was similar in technique, their focus was intraglottal pressure during a complete cycle of oscillation and was not limited to the portion of the cycle in which vocal fold contact occurred. They reported that the pressures in the glottis varied throughout the phonatory cycle, in both the superior-inferior and anterior-posterior directions. They also reported that the pressures varied most widely near the location of maximum vibratory amplitude, and that they can include negative pressures during a portion of the cycle. Kataoka and Kitajima[4] investigated the relationship between changes in the fundamental frequency of phonation and the subglottal pressure in 3 excised canine hemilarynges. They reported some correlations between the length and depth of the vibration and the fundamental frequency.

Much has been learned from the excised canine experiments so far, but there are some anatomic differences between canine and human larynges that could make the extrapolation of the canine data to human phonation a little difficult. Among the major anatomic differences is the lack of a vocal ligament in the canine vocal fold, which limits the range of fundamental frequency of phonation. Also, the excised larynx technique does not include a vocal tract, which has a major effect on acoustic output. The resonance of the vocal tract could also affect the dynamics of the vocal fold, since the vocal tract air column is an inertive and resistive load.[5]

The purpose of this study was to compare the aero-

From the Department of Speech Pathology and Audiology, The University of Iowa, Iowa City, Iowa. This work was supported by the National Institutes of Health/National Institute on Deafness and Other Communication Disorders (grant R01 DC03566-03). This study was performed in accordance with the PHS Policy on Humane Care and Use of Laboratory Animals, the NIH *Guide for the Care and Use of Laboratory Animals*, and the Animal Welfare Act (7 U.S.C. et seq.); the animal use protocol was approved by the Institutional Animal Care and Use Committee (IACUC) of The University of Iowa on October 25, 1996.

CORRESPONDENCE — Fariborz Alipour, PhD, Dept of Speech Pathology and Audiology, The University of Iowa, 334 WJSHC, Iowa City, IA 52242-1012.

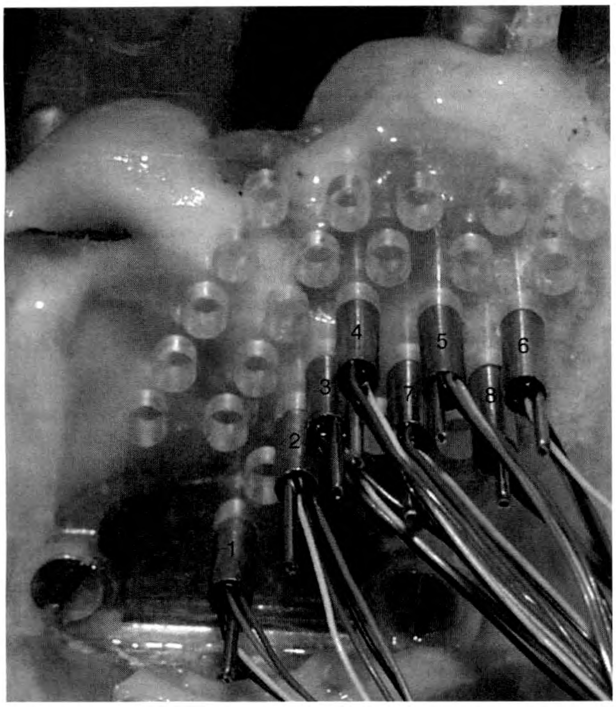

Fig 1. Side view of Plexiglas sheet with embedded pressure transducers (foreground) and mounted hemilarynx (on other side of Plexiglas). Pressure transducers are numbered 1 through 8 on Figure.

dynamics of human and canine hemilarynges with and without the presence of a simple vocal tract.

METHODS

Two human larynges were obtained from autopsy at the University of Iowa Hospitals and Clinics. These larynges were collected within 24 hours after death and after the stages of rigor mortis in the neck region. They were donated from 2 men ages 56 and 57 years. These individuals had no history of head or neck trauma or disease of the larynx. Six canine larynges were obtained after cardiovascular research experiments at the University of Iowa Hospitals and Clinics. No dogs were sacrificed for the purpose of this study. The canine specimens were obtained from large adult subjects with no evidence of trauma or head and neck disease. All larynges, both human and canine, were quick-frozen with liquid nitrogen and stored in a freezer (at −20°C) and slowly thawed in a refrigerator before use.

Each larynx was cut in half along the midsagittal plane. Excess tissue was removed, leaving 1 true vocal fold, 1 arytenoid cartilage, and the thyroid and cricoid cartilages on the retained side. The hemilarynx was mounted on a $^3/_4$-inch stainless steel tube mimicking the trachea so that the glottis was easily viewed by a camera and was accessible by equipment (Fig 1). A 60 × 60-mm $^1/_4$-inch sheet of clear acrylic had an array of holes drilled into it for later passage of pressure transducers. The acrylic sheet was mounted to the stainless steel tubing with screws after the trachea was positioned on the tube. The hemilarynx was glued to the acrylic plate at the thyroid and cricoid cartilage borders. The remaining spaces between the hemilarynx and the acrylic plate were sealed with rubber glue.

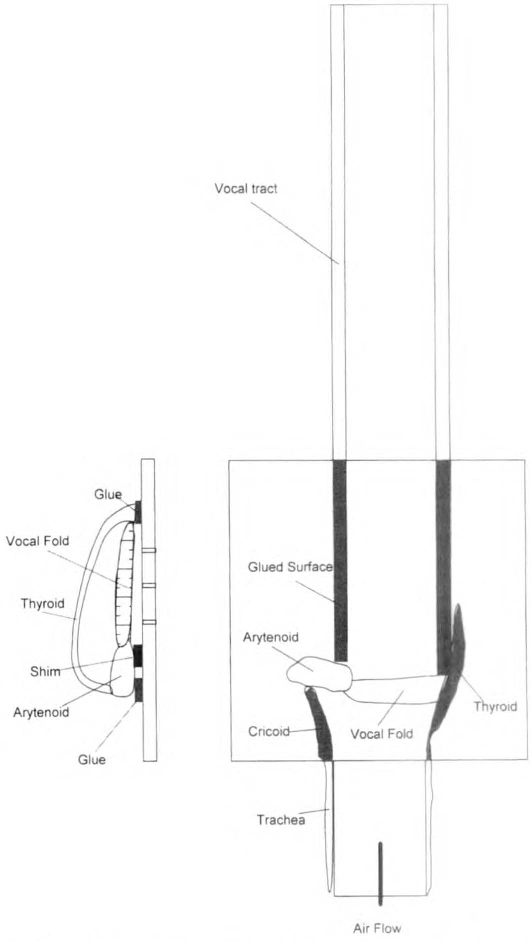

Fig 2. Schematic of hemilarynx mounting with vocal tract and measuring equipment.

Adduction was controlled by the placement of metal shims of various thicknesses (0.1 to 1.0 mm) between the arytenoid cartilage and the acrylic pane, posterior to the vocal process. A 2-pronged probe was used to adduct the arytenoid cartilages and keep each shim in place. Tension control and elongation was aided by sutures attached to the arytenoid cartilage at one end and a weight strung over a pulley at the other end. For each tension adjustment, first the 2-pronged probe was retracted to allow the length change, and then a shim was inserted for proper adduction.

The vocal tract model initially was made from a plastic hose with a diameter of 2.5 cm, a length of 15 cm, and a thickness of 0.25 cm. Later, a model was made from a hard rubber material in an attempt to mimic the area function of the vowel "ah." Later anal-

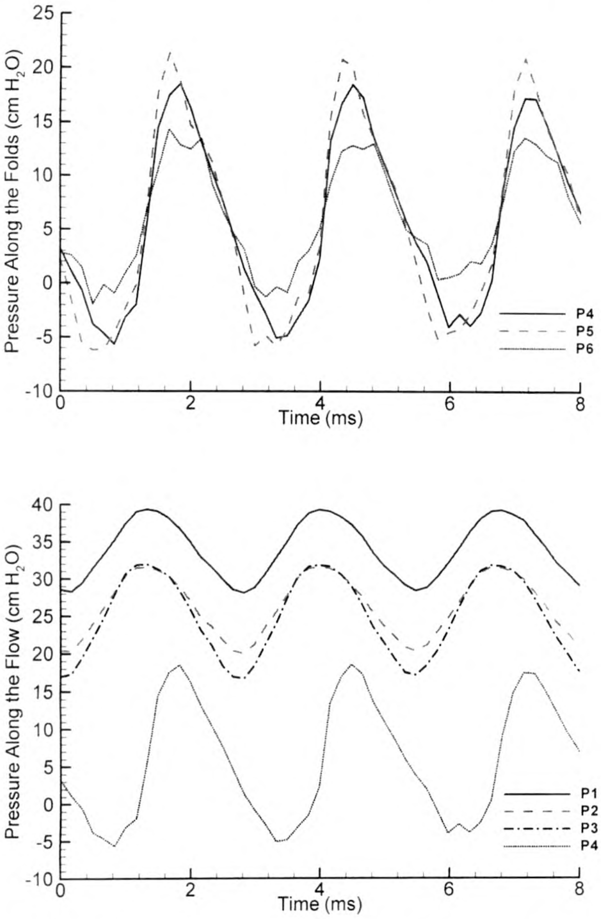

Fig 3. Pressure waveforms for 2 arrays of pressure transducers in glottis. Top traces refer to pressure taps in posterior-anterior direction (P4-P6). Bottom traces refer to pressure taps along flow direction (P1-P4).

ysis showed slight deviation from the targeted model. The vocal tract was glued to the acrylic plate just above the vocal folds and sealed with rubber glue to prevent air leakage (Fig 2).

Intraglottal air pressures were measured with miniature pressure transducers (Entran EPE-551). The mean subglottal pressure was monitored with a wall-mounted water manometer (Dwyer No. 1230-8) at a location 10 cm below the glottis. The time-varying subglottal pressure was recorded with a piezoresistive pressure sensor (Microswitch 136PC01G1) at the same location as the manometer tap. The mean flow rate was monitored with an in-line flowmeter (Gilmont model J197). An 8-channel Sony digital audiotape recorder was used to record the pressure signals. Selected signals were monitored on a 4-channel Data Precision digital oscilloscope. Analog signals from the digital audiotape recorder were digitized with a 12-bit analog-digital board and analyzed on a personal computer.

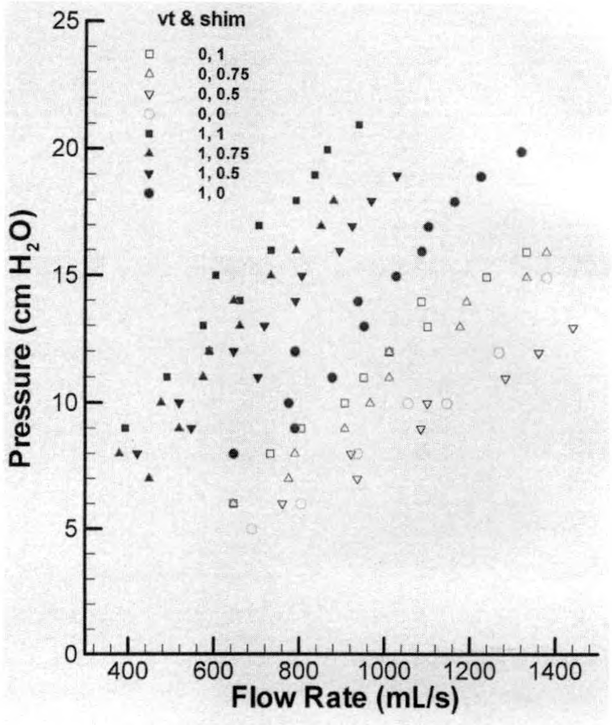

Fig 4. Typical pressure-flow relationship for human hemilarynx (HH01) during phonation, with and without vocal tract, at various adduction levels (shim sizes). Hollow and filled symbols refer to cases without and with vocal tract, respectively.

RESULTS

Figure 3 shows glottal pressure waveforms for canine hemilarynx HL62, obtained during phonation at a frequency of 370 Hz induced by vocal fold tension. The top traces represent the pressure variation in the posterior-anterior direction. These pressure taps are located about 1 to 2 mm below the vocal fold edge and are 5 mm apart. Tap 6 is about 2 mm from the anterior commissure, and tap 4 is about 3 mm from the vocal processes. The pressure readings of taps 4 and 5 show a negative component that corresponds to the time of maximum excursion of the vocal folds at those locations.[1] The bottom traces refer to the pressure waveforms along the flow. Subglottal pressures P1, P2, and P3 appear to be almost sinusoidal and in phase with each other, and have decreasing values as the location becomes closer to the vocal folds. This relationship may not hold at the time of closure, when they become maximum, at which time P2 and P3 take the same value, but P1 is still a higher value.

Figure 4 shows the pressure-flow relationship of human hemilarynx HH01 at various levels of adduction. The solid symbols represent data gathered with vocal tract 1 (the tube), and the hollow symbols are data gathered without the vocal tract. The general linear increasing pressure-flow trend that was reported by Alipour et al[6] and Alipour and Scherer[1] can be observed in both models with and without a

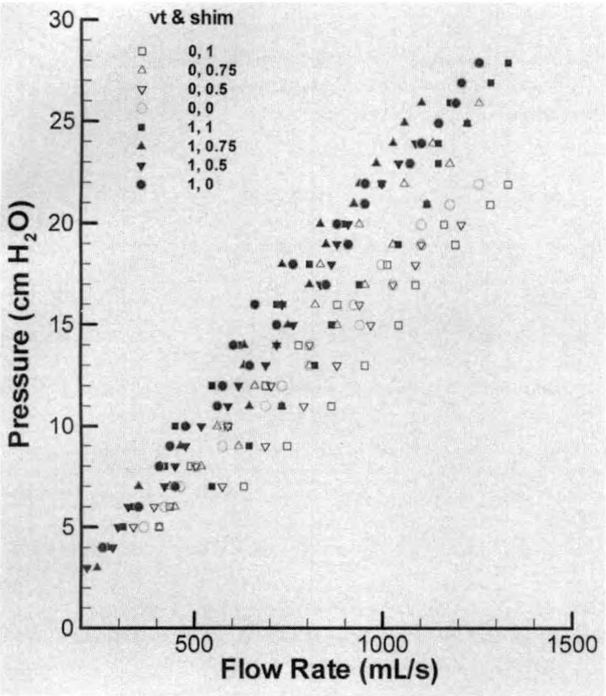

Fig 5. Another example of pressure-flow relationship for human hemilarynx (HH02) during phonation with and without vocal tract, at various adduction levels.

tract. For a given flow rate, the pressure values are higher for models with a tract than for models without a tract. Also, the model with a vocal tract has a lower flow rate, which indicates that the vocal tract causes some aerodynamic load on the larynx and increases the glottal resistance. The differential flow resistance[6] or slope resistance of the cases without the vocal tract ranges between 10.2 and 14.6 cm H_2O per liter per second (lps), with an average of 13.2 cm H_2O/lps. Use of the vocal tract makes the range of resistance 18.7 to 23 cm H_2O/lps, with an average of 20.7 H_2O/lps, ie, an increase of 57%.

Figure 5 demonstrates the same phenomena for human hemilarynx HH02. However, it is interesting to note that the phonation threshold pressure is lower with the vocal tract (3 cm H_2O) than without the vocal tract. The ranges of differential resistance in this larynx were 17.6 to 23.9 cm H_2O/lps without a vocal tract and 22 to 26.4 cm H_2O/lps with a vocal tract. The average resistance showed an increase of 23%, from 19.6 to 24.2 cm H_2O/lps. The smaller range of resistance is predictable from the lower scatter in data points for this larynx, which suggests a lower sensitivity of this larynx to adduction control.

Similar data are shown in Fig 6 for canine hemilarynx HL58. Again, the vocal tract has an increasing effect on the aerodynamic load that moves the pressure-flow line to the upper left of the graph (solid symbols). The range of resistance for this canine hemilarynx without a vocal tract was 17.9 to 38.1 cm H_2O/lps, with an average of 26.0 cm H_2O/lps. Use of a vocal tract model similar to "ah" increased the resistance to a range of 32 to 40.3 cm H_2O/lps and an average of 36.6 cm H_2O/lps, ie, a 41% increase. The phonation threshold pressure for this canine model ranges from 6 to 10 cm H_2O, which is higher than that for human larynx HH02. This finding confirms that the excised human larynx is a good instrument for phonation. Indeed, human larynx phonation on the laboratory bench is easier and more stable than canine phonation, even with larynges from elderly subjects.

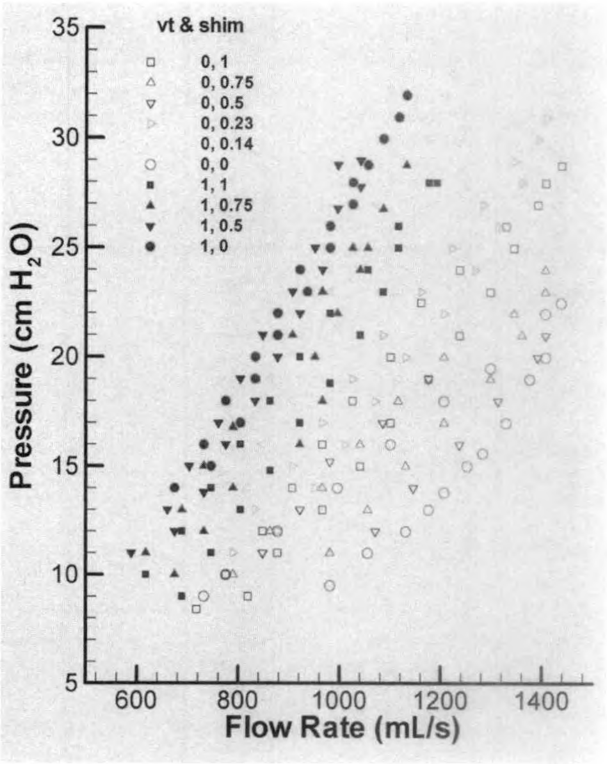

Fig 6. Pressure-flow relationship for canine hemilarynx (HL58) during phonation with and without vocal tract, at various adduction levels.

Figure 7 is the representation of the sound pressure level (SPL) in canine hemilarynx HL63 with and without a vocal tract. As subglottal pressure increases, the SPL increases in a nonlinear manner, with sharp increases at the beginning and a slower rise at the end. Increasing adduction or using smaller shims has pronounced effects on the SPL. In most cases, increasing adduction or using smaller shim sizes causes an increase in the SPL; however, this effect is not consistent and may require further investigation. On the other hand, the addition of the vocal tract consistently increases the SPL. In this experiment, the vocal tract resembling "ah" was used. The increase in SPL due to the presence of the vocal tract is probably caused by partial resonance effects.

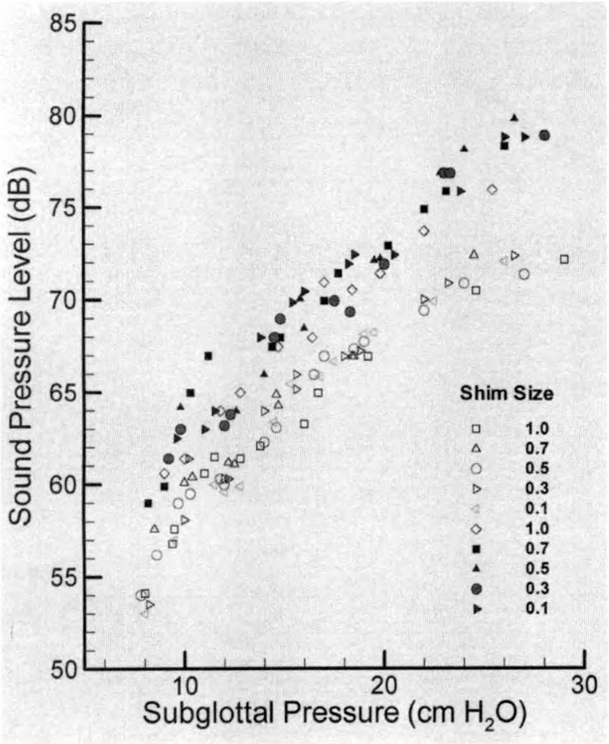

Fig 7. Effects of subglottal pressure on sound pressure level in canine hemilarynx (HL63) during phonation with and without vocal tract, at various adduction levels.

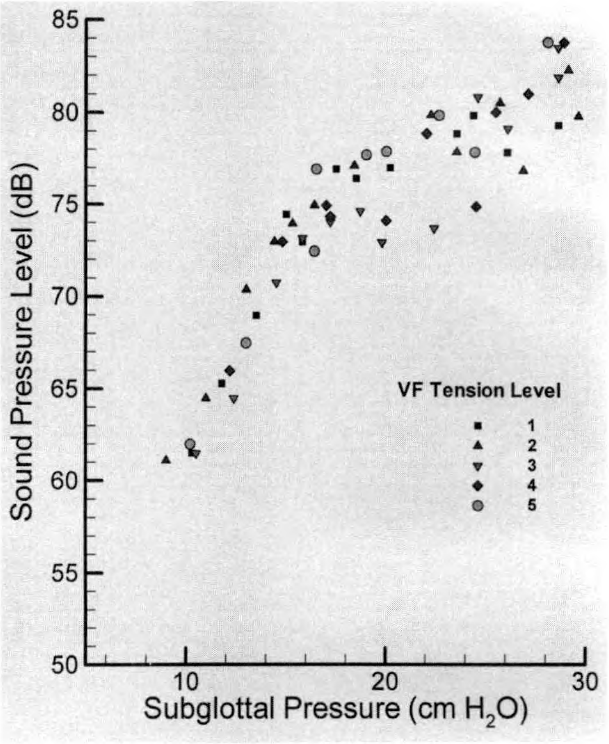

Fig 8. Effects of vocal fold tension on sound pressure level in canine hemilarynx (HL63) during phonation with vocal tract, at various tension levels.

To verify the resonance effects of the vocal tract, we increased the fundamental frequency of phonation by increasing the vocal fold tension. Figure 8 shows variations of SPL versus subglottal pressure for canine hemilarynx HL63. In this experiment, the vocal fold was elongated with a suture attached to the arytenoid cartilage. The tension level was identified with numbers in increasing order. The increase of frequency that is caused by tension has the effect of increasing the SPL.

DISCUSSION

The hemilarynx was chosen for this study of aerodynamics during phonation because of the difficulty in securing pressure transducers to the vocal folds in a whole larynx, and the ease of attaching a vocal tract and small pressure transducers within a rigid sheet against which the vocal fold could vibrate. In fact, the canine larynx model has been used frequently to study voice production, because of the ease of supply of canine larynges and their anatomic resemblance to the human larynx. The excised larynx has proved that vocal folds can oscillate in a sustained mode without any vocal tract. This study examined the effects of a vocal tract on excised larynx phonation, both in canine and human larynges.

An interesting finding in this study is that the intraglottal pressures near the location of maximum amplitude of vocal fold vibration reach some negative values compared to more anterior and posterior glottal locations. The negative pressure in pressure taps 4 and 5 corresponds to the time that subglottal pressure P1 is raised to its peak, which is the closing phase of oscillation. This generates a driving force that is opposite in phase with the tissue displacement, and is the basis for the mechanism of vocal fold self-oscillation suggested by Titze.[5]

An increase in differential flow resistance was intuitively predictable, and it was demonstrated in this study. The decrease in the phonation threshold pressure can be explained by the impedance of the vocal tract.[5] The inertive component of impedance has a positive effect on the self-oscillation of the larynx. The addition of the vocal tract to the hemilarynx setup had shown an increasing effect on sound intensity that was due to partial resonance effects. The overall objective of this study was fulfilled with these data.

When comparing the human and canine data and considering results with and without the vocal tract, one can extrapolate and revise the previous data from canine experiments for better human voice modeling. Once the vocal tract design is improved, future studies can investigate aerodynamic properties, as well as the tuning of vocal fold oscillations by means of various vocal tract shapes.

REFERENCES

1. Alipour F, Scherer RC. Dynamic glottal pressures in an excised hemilarynx model. J Voice 2000;14:443-54.

2. Jiang JJ, Titze IR. A methodological study of hemilaryngeal phonation. Laryngoscope 1993;103:872-82.

3. Jiang JJ, Titze IR. Measurement of vocal fold intraglottal pressure and impact stress. J Voice 1994;8:132-44.

4. Kataoka K, Kitajima K. Effects of length and depth of vibration of the vocal folds on the relationship between transglottal pressure and fundamental frequency of phonation in canine larynges. Ann Otol Rhinol Laryngol 2001;110:556-61.

5. Titze IR. The physics of small-amplitude oscillation of the vocal folds. J Acoust Soc Am 1988;83:1536-52.

6. Alipour F, Scherer RC, Finnegan E. Pressure-flow relationships during phonation as a function of adduction. J Voice 1997;11:187-94.

≈

COSMETIC FACIAL SURGERY

The Indian Society of Facial Plastic and Reconstructive Surgery Inaugural Conference and Workshop on Cosmetic Facial Surgery will be held December 7-9, 2001, in Indore, India. For information, please contact Dr Subramaniam Iyyer (subu@md3.vsnl.net.in) or Dr Brajendra Baser, 109 Trade House South Tukoganj Indore MP 452001, India (brajendrab11@hotmail.com, baser@vsnl.com).

Ann Otol Rhinol Laryngol 110:2001

EFFECTS OF LENGTH AND DEPTH OF VIBRATION OF THE VOCAL FOLDS ON THE RELATIONSHIP BETWEEN TRANSGLOTTAL PRESSURE AND FUNDAMENTAL FREQUENCY OF PHONATION IN CANINE LARYNGES

KENICHI KATAOKA, MD KAZUTOMO KITAJIMA, MD

OTSU, JAPAN

The relationship between fundamental frequency of phonation (F0) and the change in F0 per unit change of transglottal pressure (dF/dP) was investigated in 3 excised canine larynges. The effects of the length and depth of vocal fold vibration on the relationship between dF/dP and F0 were evaluated. A positive correlation between dF/dP and F0 was observed when an increase in F0 was accompanied by a decrease in the depth of vibration while the length of vibration reached a plateau. Although a negative correlation between dF/dP and F0 was observed in only 1 case, this relationship seemed relevant to the length of vibration. These results help to clarify the adjustments of length and depth of vibration involved in regulating F0.

KEY WORDS — fundamental frequency, phonation, transglottal pressure, vibration, vocal fold.

INTRODUCTION

Transglottal pressure influences the fundamental frequency of phonation (F0). Tanaka et al[1] reported that changes of F0 per unit change of transglottal pressure (dF/dP) vary with F0. For a graph in which dF/dP is the y-axis and F0 is the x-axis, dF/dP versus F0 exhibits a V-shape in the modal register. That is, the values for dF/dP decrease with an increase in F0 at a lower F0, and increase with F0 at a higher F0.[1] The mechanism underlying the effects of transglottal pressure on F0 has been evaluated theoretically and experimentally by Titze,[2] who stated that the value of dF/dP is determined by the magnitude of vocal fold stretching. Because the length of the vocal folds in humans increases as F0 increases,[3-5] the left side of the V-shaped curve results from the stretching of the vocal folds. However, the right half of the V requires explanation, because the values of dF/dP increase with an increase in F0. Titze[2] reported that the depth of vibration is another parameter for determining the values of dF/dP. Such values increase when the depth of vibration is limited to the edge of the vocal folds, as is typical of falsetto phonation. Hollien[3] studied the relationship between the thickness of the vocal folds and F0 and found that the thickness decreases as the F0 increases. We investigated the effects of the vibrating depth as well as the vibrating length of the vocal folds on the relationship between dF/dP and F0 using excised canine larynges.

METHODS

We obtained larynges that had been excised by total laryngectomy in 3 beagles (8 to 10 kg) that had undergone physiological study at the Department of pharmacology, Shiga University of Medical Science. None of the dogs had undergone endotracheal intubation. One larynx (larynx 1) had been stored frozen at −80°C and was used after having been defrosted at 10°C for 24 hours. The other 2 larynges (2 and 3) were freshly obtained 15 minutes after death, which was induced by the intravenous administration of pentobarbital sodium solution (100 mg/kg).

We developed a model of hemilaryngeal phonation as described by Jiang and Titze.[6] We trimmed any remaining muscles away from the thyroid cartilage of the excised canine larynges. The larynx was cut horizontally through the thyroid cartilage at the point about 4 mm above the level of the true vocal folds. The right vocal fold, the right arytenoid cartilage, and the right half of the thyroid cartilage were removed. The remaining left half of the larynx was fitted exactly to a transparent Plexiglas plate (7 × 7 cm) with epoxy resin glue and clay (Fig 1). A 2-pronged device was used to adjust the arytenoid cartilage. The cut edge of the thyroid cartilage was pulled anteriorly to control the length of the vocal folds.

To investigate the effects of the length of vibration and the depth of vibration on the relationship between dF/dP and F0, we analyzed 2-directional images of the vocal folds. A block diagram of the system is shown in Fig 2. The transparent Plexiglas plate enabled us to observe the vibration from the medial side (sagittal view), as well as from superior side (axial view). The larynx was forced to vibrate by de-

---

From the Department of Otolaryngology, Shiga University of Medical Science, Otsu, Japan. This work was funded by a Grant-in-Aid for Encouragement of Young Scientists (09771349) from the Ministry of Education, Science, Sports and Culture of Japan.

CORRESPONDENCE — Kazutomo Kitajima, MD, Dept of Otolaryngology, Shiga University of Medical Science, Seta, Otsu, 520-2192 Japan.

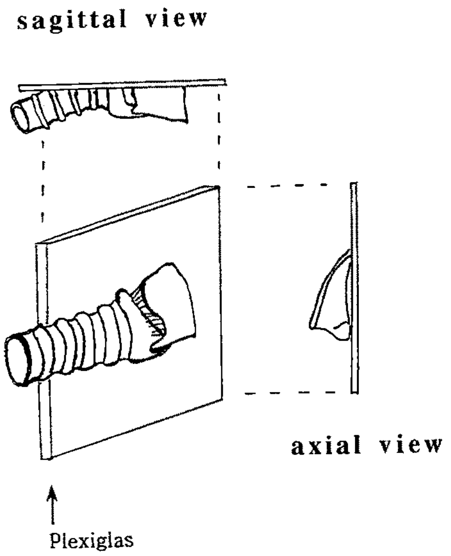

Fig 1. Left half of canine larynx was mounted on Plexiglas. Two views (sagittal and axial) of vocal fold were obtained.

livering an air stream conditioned to 38°C and 100% humidity. During stable vibration, the transglottal pressure was suddenly reduced by quickly closing the shutter valve mounted on the trachea. This valve consisted of a rotating cylinder with a hole for the passage of air (Nagashima Air Flow Interrupter NK 100, Tokyo, Japan). The cylinder was programmed to rotate 45° by a switch. The diameter of the airway inside the valve was reduced by one seventh (0.143), resulting in a reduction in the transglottal pressure during phonation. The rotated cylinder was kept in that position for 300 ms and was then rotated to the original position. The time required to rotate the cylinder was 25 ms. Intratracheal air pressure (Pt) was sensed through a tube mounted between the larynx and the shutter valve and was converted to an electrical signal (San-Ei Biophysiograph 180 System, Tokyo). The voice signal was picked up with a microphone. The air pressure and the voice signal were simultaneously stored on a digital audiotape recorder (TEAC RD-130TE, Tokyo) for later analysis.

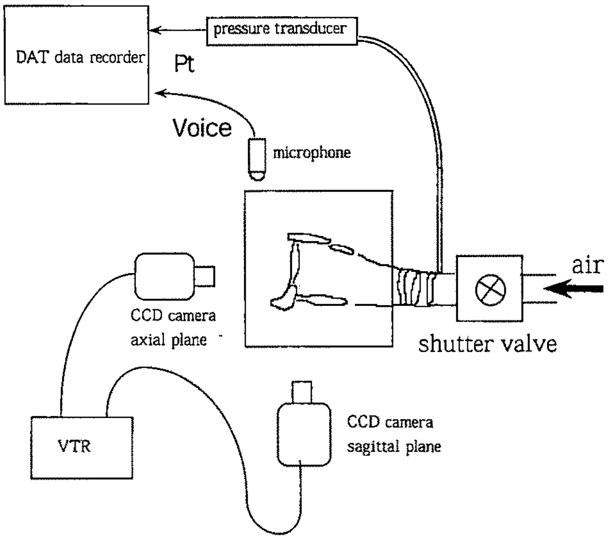

Fig 2. Diagram of system. Movement of vocal fold was observed through transparent Plexiglas (sagittal view) and from above vocal fold (axial view). Voice signal and intratracheal air pressure (Pt) were recorded during vibration. DAT — digital audiotape, CCD — charge-coupled device, VTR — videotape recorder.

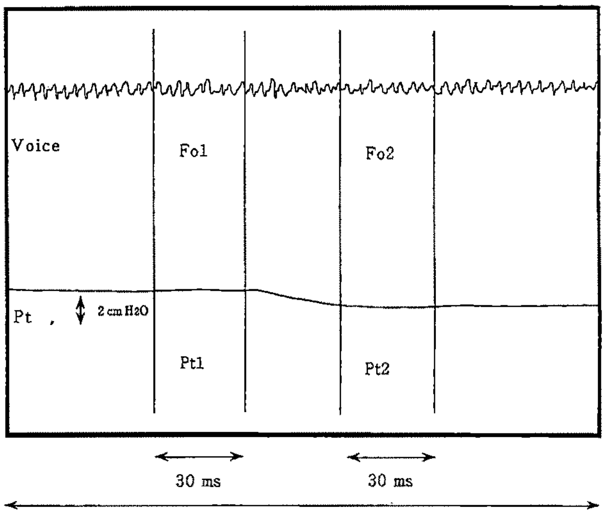

Fig 3. Computer display of signals and 4 vertical cursors. Values for 4 parameters — fundamental frequency of phonation (Fo) before reduction of intratracheal air pressure (Fo1), Fo after reduction of intratracheal air pressure (Fo2), intratracheal air pressure (Pt) before reduction (Pt1), and Pt after reduction (Pt2) — were calculated with 4 vertical cursors on display.

The length of the vocal folds was increased by pulling a nylon thread that was sutured to the anterior edge of the thyroid cartilage, parallel to the longitudinal direction of the vocal folds during vibration. Clay was used to seal the gap between the cut edge of the thyroid cartilage and the Plexiglas so as to prevent the escape of air during insufflation. Each time the thyroid cartilage was moved or pulled, we readjusted the clay seal. The action of the thyroarytenoid muscle was not simulated. The movements of the vocal folds in 2 directions, on the axial and sagittal planes, were monitored during vibration by 2 CCD cameras (ELMO CN42H, Tokyo) under 2 strobe lights (First Stroboscope FLS-100, Tokyo) and were projected on the same screen (Video Mixer, First MV-100 Multi Viewer, Tokyo). The strobe lights were projected on the axial and sagittal planes from the back of 2 cameras. The images were stored on videotape (Sony SVO-260, Tokyo) for analysis.

The voice signal and subglottal pressure (Pt) were analyzed with a signal processor (San-Ei 7T18). The computer program used was designed to register signals of 200 ms. The sampling frequency was 20 kHz. A typical computer display is illustrated in Fig 3.

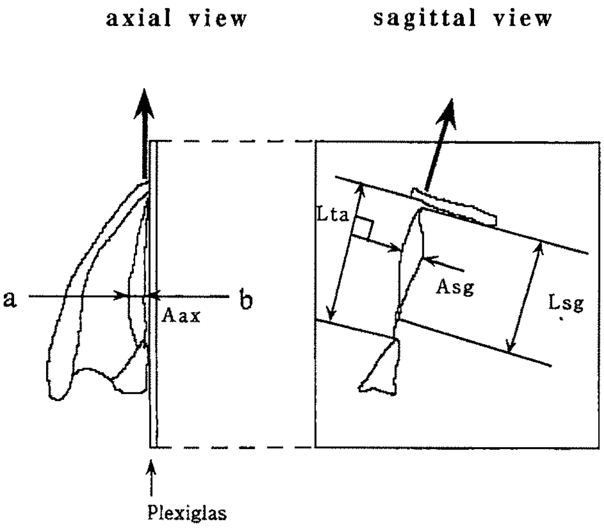

Fig 4. Definition of parameters as related to model. Lta — length of vocal fold, Lsg — length of vibration on sagittal plane, Asg — amplitude of vibration on sagittal plane, Aax — amplitude of vibration on axial plane.

With 4 vertical cursors on this display, the value of dF/dP was calculated by a computer as follows: dF/dP = (F01 – F02)/(Pt1 – Pt2), where F01 (hertz) is the F0 before the reduction of Pt calculated with fast Fourier transformation of a 30-ms time window; F02 (hertz) is the F0 after the reduction of Pt calculated with fast Fourier transformation of a 30-ms time window; Pt1 (centimeter of water) is the Pt before the reduction, averaged for the 30-ms time window corresponding to the F01; and Pt2 (centimeters of water) is the Pt after the reduction, averaged for the 30-ms time window corresponding to the F02. The calculation of dF/dP was done once for each F0.

Four parameters were defined on the videotape recorder display of the larynx. On the sagittal view (right side of Fig 4), the distance between the anterior commissure and the vocal process was defined as the length of the vocal fold (Lta). The vibrating edges of the vocal fold were traced on several frames involved in 1 cycle of vibration on the axial view (left side of Fig 4). We selected the most lateral and medial tracings. The greatest distance between these 2 tracings measured along the perpendicular line to the Plexiglas (line a-b) was defined as Aax, the amplitude of the vibration on the axial plane. On the sagittal view (right side of Fig 4), the crest of the traveling wave was traced on each cycle of vibration. The most cephalic and the most caudal tracings were selected. The greatest distance between these 2 tracings measured along a straight line perpendicular to that connecting the anterior commissure and the vocal process was defined as Asg, the amplitude of the traveling wave on the sagittal plane. The distance between the 2 points at which the 2 crest tracings used to define Asg met anteriorly and posteriorly was defined as Lsg, which was the length of vibration on the sagittal plane. We supposed that Aax was the depth of vibration on the axial plane, and Asg was the depth of vibration on the sagittal plane.

TABLE 1. RANGES OF LTA

Larynx	*Initial Lta (mm)*	*Maximum Lta (mm)*	*Maximum Lta/ Initial Lta (mm)*
1	15.3	19.3	1.26
2	14.8	20.3	1.37
3	12.3	17.6	1.43

Lta — length of vocal fold.

TABLE 2. RANGES OF LSG, AAX, AND ASG

Larynx	*Lsg (mm)*	*Aax (mm)*	*Asg (mm)*
1	14.1-15.3	0.25-0.56	0.62-1.16
2	14.6-16.1	0.28-0.80	1.05-1.80
3	12.2-15.3	0.30-1.19	1.30-2.58

Lsg — length of vibration on sagittal plane, Aax — amplitude of vibration on axial plane, Asg — amplitude of vibration on sagittal plane.

RESULTS

The initial and maximum values for Lta are shown in Table 1. The ratio of elongation (maximum Lta/initial Lta) ranged from 1.26 to 1.43. The ranges of Lsg, Aax, and Asg are shown in Table 2. The values for Asg were about twice those for Aax. Tables 3-5 show the values for dF/dP, F0, Aax, Asg, Lsg, and Lta for each larynx. To obtain a better understanding of the relationship between F0 and the other parameters, we plotted these values against F0 (Fig 5). Figure 5A shows the relationship between dF/dP and F0. Larynx 1 showed an almost linear relationship with F0. Larynx 3 showed a U- or V-shaped curve against F0 similar to our previous observations in hu-

TABLE 3. RESULTS IN CANINE LARYNX 1

F0	*dF/dP*	*Lta*	*Lsg*	*Aax*	*Asg*
205.4	6.2	15.3	15.3	0.53	1.16
215.4	5.7	15.9	14.7	0.49	0.95
222.4	6.3	16.2	14.8	0.53	0.95
227.6	7.2	16.3	15.0	0.56	1.13
234.5	6.3	16.7	14.1	0.56	0.96
235.5	5.7	16.7	14.7	0.53	0.86
235.6	9.0	16.8	14.2	0.50	0.85
250.9	7.3	17.3	14.3	0.39	0.92
252.9	7.8	17.4	14.5	0.42	1.06
267.2	10.1	17.9	14.1	0.49	0.91
277.3	11.0	18.1	14.1	0.50	0.95
284.3	8.3	18.2	14.8	0.46	1.03
286.6	10.0	18.3	14.6	0.32	0.67
288.1	14.4	18.4	14.4	0.32	0.62
310.0	9.3	19.3	15.0	0.25	0.70

F0 — fundamental frequency of phonation, dF/dP — change in transglottal pressure.

TABLE 4. RESULTS IN CANINE LARYNX 2

Fo	*dF/dP*	*Lta*	*Lsg*	*Aax*	*Asg*
210.4	4.4	14.8	14.6	0.83	1.80
220.8	5.1	15.6	14.9	0.80	1.77
232.8	4.7	16.4	15.4	0.78	1.78
244.2	3.9	17.0	15.5	0.69	1.61
254.8	4.1	17.4	15.6	0.71	1.55
264.0	6.2	18.4	15.2	0.64	1.48
275.2	6.1	18.8	15.7	0.53	1.40
288.9	9.4	19.5	16.1	0.30	1.30
306.2	9.9	20.3	15.8	0.28	1.05

TABLE 5. RESULTS IN CANINE LARYNX 3

Fo	*dF/dP*	*Lta*	*Lsg*	*Aax*	*Asg*
204.2	21.3	12.3	12.2	1.19	2.58
240.3	15.6	12.3	13.6	1.11	2.39
255.5	8.9	12.6	14.2	1.06	2.35
262.1	5.4	12.6	13.5	1.07	2.05
264.5	1.9	15.3	14.3	0.98	2.06
268.0	1.3	15.3	14.9	0.93	2.24
268.3	6.5	15.3	15.1	0.85	2.13
284.6	2.5	16.0	15.3	0.87	2.08
296.2	7.0	16.0	15.3	0.64	1.88
296.9	4.6	16.3	15.3	0.62	1.80
308.9	15.7	16.3	14.9	0.60	1.60
318.0	17.8	16.3	15.1	0.60	1.62
321.5	14.4	16.4	14.7	0.47	1.55
337.1	14.5	17.6	14.5	0.41	1.48
354.1	12.6	17.6	15.1	0.30	1.30

mans.[1] Larynx 2 showed a mixture of the patterns seen in larynges 1 and 3, resulting in a J-shaped curve. Because our objective was to investigate the effects of the length and depth of vibration on the relationship between dF/dP and F0, we divided the data into 2 groups: that with a lower F0 and that with a higher F0, at the smallest values for dF/dP. In larynx 2, we arbitrarily divided the data between 244.2 Hz (dF/dP = 3.9) and 254.8 Hz (dF/dP = 4.1), as is shown by the dotted line in Table 4. In larynx 3, we divided the data between 268.0 Hz (dF/dP = 1.3) and 268.3 Hz (dF/dP = 6.5), as is shown by the dotted line in Table 5. These 4 groups of data were designated 2a, 2b, 3a, and 3b. Because larynx 1 showed an almost linear trend, no classification was performed, and it was designated group 1. These classifications were done somewhat arbitrarily. But what we would like to know is how the length and depth of vibration relate to F0 when the values of dF/dP are decreasing or increasing with F0. Thus, we consider that the classification could be good for our purposes. The correlation coefficients between F0 and dF/dP for the 5 groups are shown in the top line of Table 6. Positive correlations were observed in groups 1, 2b, and 3b, with correlation coefficients being .774, .950, and .680, respectively. A negative correlation was observed in group 3a (–.952). No correlation was observed in group 2a.

The findings in the 3 groups that showed a positive correlation between F0 and dF/dP (groups 1, 2b, and 3b) were as follows: 1) there was a positive correlation of F0 with Lta (Table 6, second line: r = .993, .985, .938); 2) there was a negative correlation with Aax (Table 3, fourth line: r = –.786, –.963, –.957); 3) there was a negative correlation with Asg (Table 6, fifth line: r = –.651, –.984, –.971); and 4) there was no correlation between F0 and Lsg. These 4 findings mean that when a positive correlation exists between dF/dP and F0, the depth of vibration (Aax and Asg) is closely correlated with F0, whereas the length of vibration (Lsg) is not.

Only group 3a showed a negative correlation between F0 and dF/dP. What differed from observations from groups 1, 2b, and 3b was that Lsg showed a positive correlation with F0 (r = .902) and Lta showed no relationship to F0. The Lsg seemed relevant to the negative correlation between dF/dP and F0 in this group.

Group 2a showed no correlation between F0 and dF/dP. What differed from observations from groups 1, 2b, and 3b was that Lsg had a positive correlation with F0 (r = .974). The Lsg may be relevant to the flat relationship between dF/dP and F0 in this group.

DISCUSSION

We hypothesized that the length and depth of vibration of the vocal folds would each have a role in the determination of the V-shaped relationship between dF/dP and F0. A positive relationship was observed between dF/dP and F0 when the depth of vibration showed a negative correlation with F0 while the length of vibration did not change with F0. This observation supports our speculation that a reduction in the depth of vibration may explain the right side of the V-shaped relationship, and may confirm the theory of Titze[2] concerning the relationship between dF/dP and depth of vibration. The present study showed a negative relationship between dF/dP (left side of V shape) only in 1 group (3a), and therefore the present study could not confirm our hypothesis regarding the left side of the V shape. However, a positive correlation of Lsg against F0, observed in groups 3a and 2a, has encouraged us to pursue our study.

Confirmation of our hypothesis would require a model that showed a negative correlation between F0 and dF/dP. A negative correlation between dF/dP and F0 at a lower F0 has been consistently observed in humans.[1] In the present study, this relationship

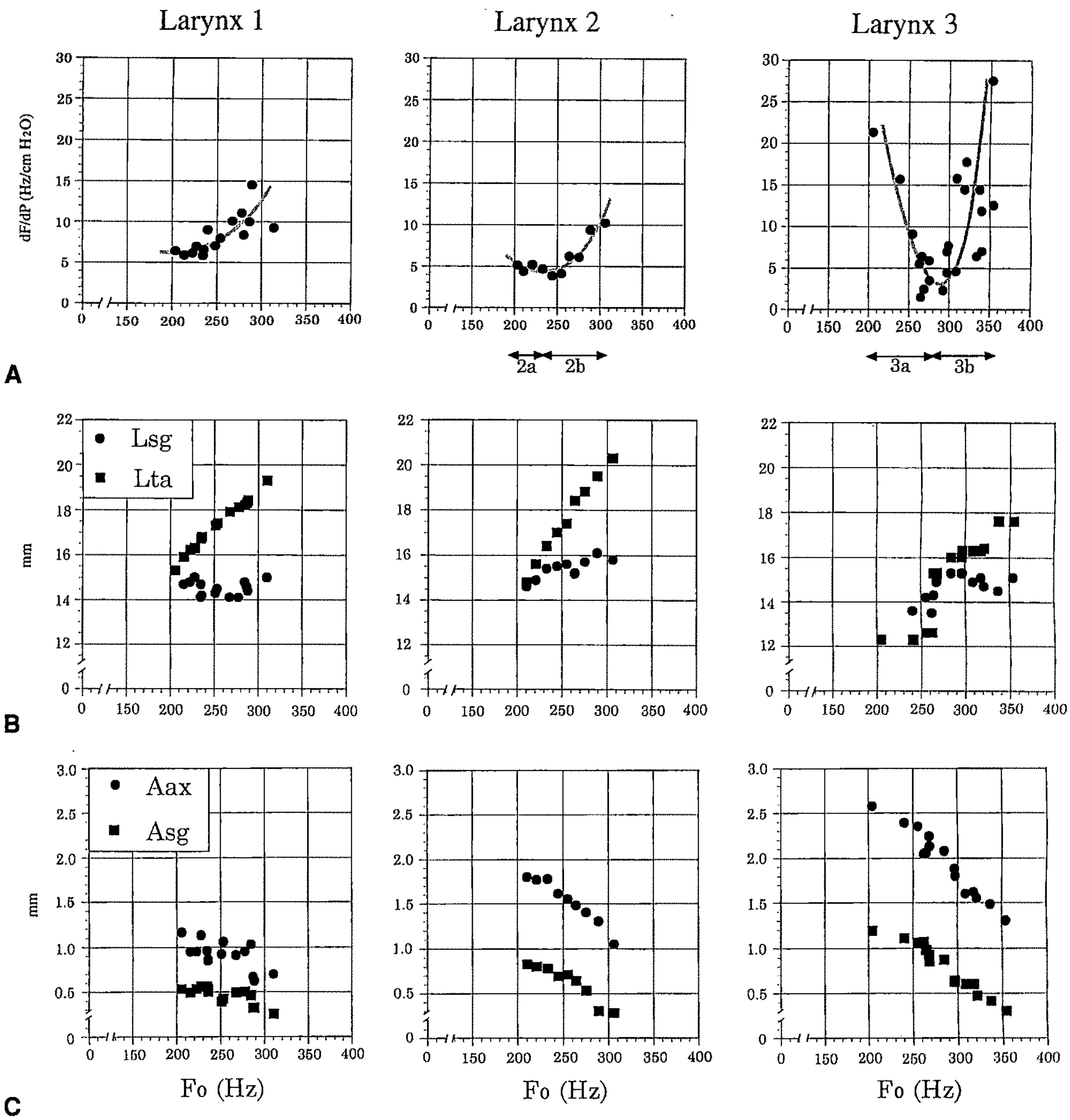

Fig 5. Values for **A**) change in transglottal pressure (dF/dP), **B**) Lta and Lsg, and **C**) Aax and Asg in 3 canine larynges plotted against F0.

was observed in only 1 of 3 animal larynges. There are 3 possible reasons for this discrepancy. The first reason is the absence of thyroarytenoid (TA) muscle activity. The activity of the TA and cricothyroid muscles increases in parallel with F0, at least within the modal register.[7-9] Concerning the length of the vocal folds, the TA muscle shortens the vocal fold length.[10] Thus, if such muscle activity were present, the change in the length of the vocal folds would have shifted to the shorter side, or to a lower F0 than that seen in the present study. At such a lower F0 region, a negative correlation would be expected between dF/dP and F0. The second reason is related to the activity of the TA muscle, which controls the thickness of the vocal fold. Hirano[11] stated that when the F0 is raised, the activity of the vocalis muscle (medial part of the TA muscle) is required to maintain phonation within the modal register or to prevent the depth of vibration from becoming too small for the modal register. Yumoto et al[12] reported that stimulation of the TA muscle increases the cross-sectional area of the canine vocal folds. Our present experiment did not include that effect, so that the depth of vibration decreased rather easily, even in response to a small de-

TABLE 6. CORRELATIONS BETWEEN Fo AND DF/DP, LTA, LSG, AAX, AND ASG IN FIVE GROUPS OF DATA (THREE LARYNGES)

	Group 1	*Group 2a (≤244.2 Hz)*	*Group 2b (≥254.8 Hz)*	*Group 3a (≤268.0 Hz)*	*Group 3b (≥268.3 Hz)*
Fo vs dF/dP	.744*	–.505	.950†	–.952*	.680†
Fo vs Lta	.993*	.997*	.985*	.610	.938*
Fo vs Lsg	–.218	.974†	.619	.902†	–.523
Fo vs Aax	–.786*	–.994	–.963*	–.884†	–.957*
Fo vs Asg	–.651*	–.828	–.984*	–.857†	–.971*

Data are correlation coefficients (r).
*$p < .01$.
†$p < .05$.

gree of elongation. The third reason is related to differences in the anatomy of the vocal folds among species. The lamina propria of canine vocal folds is thicker than that of humans.[13] In dogs, the effect of a change in depth may exceed that of a change in length.

As shown in Table 6, we observed a positive correlation between F0 and Lta in all groups except for group 3a. Between F0 and Lsg, however, there was no correlation, except for groups 2a and 3a. This finding shows that the Lsg reached a plateau near the maximum Lta in larynx 2 (group 2b) and larynx 3 (group 3b). Haji et al[14] reported that areas near the anterior commissure and the vocal process are stiffer than those in the middle of the membranous portion. In the presence of a large Lta, the area near the anterior commissure should be too stiff to vibrate, causing a plateau in the Lsg. Similar observations have been reported in humans by Tanabe et al.[15]

CONCLUSION

A positive relationship was observed between dF/dP and F0 when the depth of vibration showed a negative correlation with F0 while the length of vibration did not change with F0. Concerning a negative correlation between dF/dP and F0, the length of vibration seemed relevant to this relationship. Although our results in the canine larynx are preliminary, they suggest that the relationship between dF/dP and F0 would show the role of length and depth adjustments in raising the F0. Additional investigations are needed to clarify the factors involved in the regulation of F0.

REFERENCES

1. Tanaka K, Kitajima K, Kataoka H. Effects of transglottal pressure change on fundamental frequency of phonation: preliminary evaluation of the effect of intraoral pressure change. Folia Phoniatr Logop 1997;49:300-7.
2. Titze IR. On the relation between subglottal pressure and fundamental frequency in phonation. J Acoust Soc Am 1989;85:901-6.
3. Hollien H. On vocal registers. J Phonetics 1974;2:125-43.
4. Nishizawa N, Sawashima M, Yonemoto K. Vocal fold length in vocal pitch change. In: Fujimura O, ed. Voice production, mechanisms and function. New York, NY: Raven Press, 1988:75-82. (Vocal physiology; vol 2.)
5. Sonninen A, Hurme P, Vilkman E. Roentogenological observations on vocal fold length-changes with special reference to register transition and open/covered voice. Scand J Logop Phoniatr 1992;17:95-106.
6. Jiang JJ, Titze IR. A methodological study of hemilaryngeal phonation. Laryngoscope 1993;103:872-82.
7. Hirano M, Ohala J, Vennard W. The function of laryngeal muscles in regulating fundamental frequency and intensity of phonation. J Speech Hear Res 1969;12:616-28.
8. Shipp T, McGlone RE. Laryngeal dynamics associated with voice frequency change. J Speech Hear Res 1971;14:761-8.
9. Gay T, Hirose H, Strome M, Sawashima M. Electromyography of the intrinsic laryngeal muscles during phonation. Ann Otol Rhinol Laryngol 1972;81:401-9.
10. Titze IR. Control of fundamental frequency. In: Titze IR, ed. Principles of voice production. Englewood Cliffs, NJ: Prentice Hall, 1994:197-9.
11. Hirano M. Vocal mechanism in singing: laryngological and phoniatric aspects. J Voice 1988;2:51-69.
12. Yumoto E, Kadota Y, Kurokawa H, Sasaki Y. Effects of vocal fold tension and thyroarytenoid activity on the infraglottic aspect of vocal fold vibration and glottal source sound quality. In: Fujimura O, Hirano M, eds. Vocal fold physiology: voice quality control. San Diego, Calif: Singular Publishing Group, 1995:127-45.
13. Hirano M. Morphological structure of the vocal cord as a vibrator. In: Hirano M, ed. Phonosurgery: basic and clinical investigations. Otologia Fukuoka 1975;21(suppl 1):239-62.
14. Haji T, Mori K, Omori K, Isshiki N. Mechanical properties of the vocal fold. Stress-strain studies. Acta Otolaryngol (Stockh) 1992;112:559-65.
15. Tanabe M, Kitajima K, Gould WJ, Lambiase A. Analysis of high-speed motion pictures of the vocal folds. Folia Phoniatr (Basel) 1975;27:77-87.

Ann Otol Rhinol Laryngol 110:2001

ISOLATED VESTIBULAR AREFLEXIA AFTER BLUNT HEAD TRAUMA

JEAN-PHILIPPE GUYOT, MD
KRISTINA THIELEN, MD
PIERRE LIARD, MD
IZABEL KOS, MD
GENEVA, SWITZERLAND

The sudden unilateral loss of vestibular function is a frequent cause of vertigo. This condition is called vestibular neuronitis or vestibular neuritis. Its cause remains unknown, but many authors consider it to be a sequel of vestibular viral infection. We report the history and clinical findings of 5 patients in whom a unilateral vestibular loss occurred after head trauma. None of these patients complained of hearing loss. In all cases, the vertigo gradually subsided over days or weeks. The follow-up showed the partial recovery of vestibular function in 2 cases, while vestibular areflexia persisted in 3. The clinical course and findings were similar in every respect to those in patients with classic idiopathic vestibular neuronitis.

KEY WORDS — etiology, head trauma, vertigo, vestibular compensation, vestibular neuritis, vestibular neuronitis.

INTRODUCTION

The sudden unilateral loss of vestibular function is a frequent cause of vertigo.[1] Symptoms are characterized by an acute onset of vertigo without auditory or neurologic disorders. The vertigo gradually resolves within a few days. Most authors refer to this condition as vestibular neuritis[2] or vestibular neuronitis.[3] The cause of the disorder remains unknown, but some authors favor the possibility of a viral infection affecting the sensory neuroepithelium or nerve. However, studies supporting this hypothesis have suffered from flaws, and their results and conclusions are debatable. Schuknecht and Kitamura[4] reported that the postmortem findings in 4 temporal bones from patients with attacks of vertigo suggestive of vestibular neuritis were similar to those observed in well-documented viral disorders such as mumps or measles. Nadol,[5] who reexamined the same temporal bones, considered the anomalies as nonspecific for a viral infection. Baloh et al[6] examined a temporal bone of a patient who died of a myocardial infarction 9 years after a well-documented vestibular neuritis. Although the immunohistochemical stainings for antigens of many different viruses were negative and viral inclusion bodies were absent from the nuclei or cytoplasm of the vestibular neurons on light and electron microscopy, they estimated that "the many potential viruses implicated in vestibular neuritis were not ruled out"[6(p590)] and concluded that their findings were "most consistent with an isolated viral infection of Scarpa's ganglion"[6(p589)]! Other authors consider that other factors are implicated, such as a circulatory disturbance of the inner ear,[7] an immunologic cause,[8] or toxicity,[8] but no definite proof supports these assumptions, either.

In the past 20 years, 17,500 patients were investigated in our otoneurological unit. Among them, 5 presented with the history and the clinical findings of a sudden unilateral vestibular loss that occurred immediately after head trauma or a slap on the ear. We report these unusual cases and discuss some hypothetical physiopathologic mechanisms.

CASE REPORTS

Case 1. An 8-year-old boy was seen in the emergency room immediately after he was struck in the left parietotemporal area by a golf ball. He complained of acute pain and intense rotatory vertigo accompanied by profuse vomiting. The otoscopic examination revealed a discrete swelling of the tympanic membrane. The patient was severely unsteady, with a significant postural deviation to the left. There was a marked spontaneous nystagmus beating to the right that was not modified by caloric stimulation of the left ear (20 mL of water at 10°C in 20 seconds). The fistula test was negative. A complete neurologic evaluation failed to reveal any other dysfunction. A computed tomography (CT) scan of the head yielded normal findings. Three days after the trauma, a pure tone audiogram showed a slight high-frequency sensorineural hearing loss. The following day, the thresholds were normal (see Figure). The vertigo resolved spontaneously, and 3 weeks after the trauma, the child was asymptomatic.

The patient underwent a standardized otoneurologic workup with audiological tests and electronystagmography (ENG). The audiological tests included a pure tone audiogram, impedance audiometry with stapedial reflex threshold and decay measurements, and auditory brain stem response (ABR) testing. The ENG consisted of recording of spontaneous nystagmus with and without visual fixation, positional nystagmus, op-

---

From the Department of Otolaryngology–Head and Neck Surgery, University Hospital, Geneva, Switzerland.

Presented at the meeting of the International Otopathology Society (The Schuknecht Society), Boston, Massachusetts, June 17, 2000.

CORRESPONDENCE — Jean-Philippe Guyot, MD, Dept of Otolaryngology, University Hospital, 1211 Geneva 14, Switzerland.

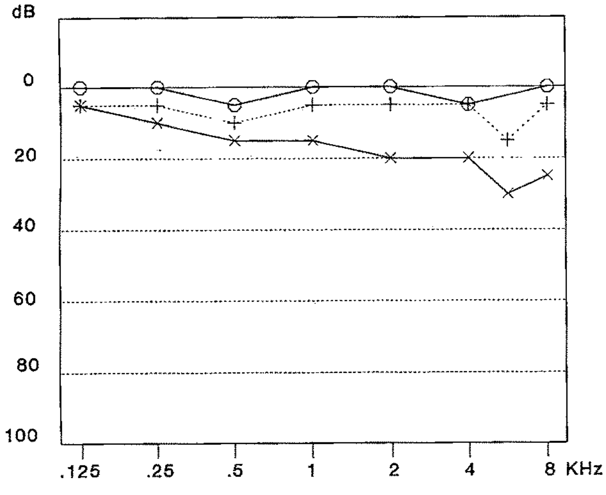

(Case 1) Audiogram. Two consecutive audiograms showed high-frequency temporary threshold shift. O — right air conduction; × — left air conduction, 3 days after trauma; + — left air conduction, 4 days after trauma.

tokinetic nystagmus, and smooth pursuit; a rotatory pendular test (undamped rotation of 360° in 20 seconds); and a caloric test (20 mL of water at 44°C, 28°C, and, if necessary, 10°C, in 20 seconds). A diagnosis of hyporeflexia is considered when the binaural difference of the nystagmus duration is greater than 40%. Areflexia refers to the absence of a response even at 10°C. The details of the testing procedure and criteria of abnormality used for evaluating otoneurologic tests have been reported previously.[9] In this case, the sole anomaly of the otoneurologic workup consisted of a persisting left areflexia on the caloric test.

Case 2. A previously healthy 30-year-old woman was referred to the otolaryngology department a few hours after head trauma consequent to a traffic accident. She complained of rotatory vertigo with nausea and vomiting. She denied any hearing loss or tinnitus. The otoscopic examination yielded normal findings. The Weber test (512 Hz) was not lateralized, and the Rinne test was positive on both sides. Normal hearing was confirmed by a pure tone audiogram. Postural tests revealed a deviation to the left. A spontaneous nystagmus was beating to the right, inhibited by visual fixation. The response to caloric stimulation of the left ear was markedly diminished (side difference, 75%). The symptoms spontaneously resolved in 5 to 6 days. The patient was seen again 2 years after the trauma, and ENG demonstrated a slight persisting left hyporeflexia on the caloric test (side difference, 40%).

Case 3. A previously healthy 20-year-old woman was seen 4 days after she received a slap on her left ear. She complained of an intense rotatory vertigo accompanied with nausea, vomiting, and deviation to the left when walking. The findings of an otoscopic examination, an audiogram, impedance audiometry, and ABR testing were normal. Right-beating nystagmus was found on ENG, and a left areflexia was found on pendular and caloric tests. A clinical fistula test (pneumomassage) was negative. One month later, the patient was free of symptoms. Vestibular testing showed a slight persisting left hyporeflexia on the caloric test (side difference, 40%).

Case 4. A 31-year-old man received several blows to the face and left ear. After a short loss of consciousness, he complained of rotatory vertigo associated with nausea and vomiting. He was admitted to the emergency department. The vertigo subsided spontaneously within a few days. He was referred to the otoneurology unit 6 weeks later and was free of symptoms. An otoscopic examination and a pure tone audiogram yielded normal findings. A vestibular evaluation revealed a left areflexia on the caloric test.

Case 5. A 37-year-old man was seen 3 months after a head injury associated with a short loss of consciousness. Immediately after recovery, he complained of rotatory vertigo, and he noticed a vertical diplopia that lasted several days. A CT scan of the head demonstrated a left parietal bone fracture. An otoneurologic workup performed 3 months after the accident did not reveal any spontaneous nystagmus, but showed a right areflexia on the caloric test. The nystagmic response on pendular testing was symmetric.

DISCUSSION

This report describes 5 cases of vestibular loss immediately following blunt head trauma. None of these patients complained of a concomitant hearing loss, although a slight temporary threshold shift was noticed in 1 case. Direct trauma to the labyrinth via the eardrum and ossicles seemed unlikely, as there was no sign of conductive hearing loss, and impedance audiometry results and ABR wave latencies were normal. Three patients were seen during the early stage of the disorder, and the typical symptoms and signs of an acute vestibular loss were present. Two patients were referred to us with delays of 6 and 12 weeks. The diagnosis was made on the basis of the clinical history and a persisting unilateral vestibular areflexia on caloric testing. In all patients, the vertigo and all of the associated signs and symptoms gradually subsided over days or weeks. The follow-up showed a partial recovery of vestibular function in 2 cases, while vestibular areflexia on the caloric test persisted in 3. The processes of vestibular compensation were sufficient to allow all of them to resume their normal daily activities. Therefore, the clinical course and findings were similar in every respect to those of patients with classic vestibular neuronitis.[10]

It has long been known that auditory and vestibular symptoms may follow head trauma. In 1934, Voss[11] introduced the name labyrinthine concussion to describe this condition. However, most patients reported with a labyrinthine concussion would be considered today as suffering from a cupulolithiasis or canalolithiasis,[12,13] which are more recent concepts.[14,15] Therefore, to our knowledge, these 5 cases represent the first description of an isolated sudden vestibular loss occurring after head injury.

Several hypotheses can be considered to explain these observations. First, the vestibular loss could result from a perilymphatic fistula.[16] This hypothesis is unlikely, since perilymphatic fistulas typically manifest as episodic vertigo precipitated by movements that place the damaged ear downward or by sneezing.[17,18] Moreover, perilymphatic fistulas generally occur in conjunction with hearing loss, tinnitus, and aural fullness.[17,19] Second, the deficit could result from a temporal bone fracture. However, otoscopic examination did not show any hematotympanum or laceration of the external ear canal roof. The only parietal bone fracture confirmed radiologically was contralateral to the affected ear. Third, the symptoms could result from a massive dislodgment of otoconia from the utricle or saccule. However, in none of the patients was the vertigo position-dependent. Fourth, the sudden vestibular loss could be caused by a latent neurotropic virus reactivated by the stress of the accident. Such a hypothesis is supported by a recent publication showing a high incidence of possibly virus-induced cell degeneration in the ganglia of the facial nerve and of the vestibular nerve.[20] Fifth, the symptoms could result from a contrecoup injury of the vestibular nerve.[21] Such a hypothesis is supported by case 5. On the impact side, the CT scan demonstrated a parietal bone fracture, while the vestibular deficit was on the contralateral side. Finally, the symptoms could be due to mechanical damage to the sensory neuroepithelium or vasculature of the vestibular system, similar to that observed at the level of the organ of Corti after acoustic trauma.[22] Some authors have reported subclinical disturbances of the vestibular system associated with sensorineural hearing loss in victims of intense impulse noises.[23,24] Our cases are unique, as none involved hearing loss. They may represent a particular and specific form of sudden vestibular loss that could be conveniently called "vestibular trauma" by analogy to the hearing loss resulting from acoustic trauma. Further research is necessary to explain the physiopathology of this disorder.

REFERENCES

1. Montandon PB, Häusler R. Relevance of otopathological findings in the treatment of dizzy patients. Ann Otol Rhinol Laryngol Suppl 1984;93(suppl 112):12-6.
2. Ashan G, Stahle J. Vestibular neuritis. A nystagmographical study. J Laryngol Otol 1956;70:61-6.
3. Dix MR, Hallpike CS. The pathology, symptomatology and diagnosis of certain common disorders of the vestibular system. Ann Otol Rhinol Laryngol 1952;61:987-1016.
4. Schuknecht HF, Kitamura K. Vestibular neuritis. Ann Otol Rhinol Laryngol Suppl 1981;90(suppl 78).
5. Nadol JB Jr. Vestibular neuritis. Otolaryngol Head Neck Surg 1995;112:162-72.
6. Baloh RW, Lopez I, Ishiyama A, Wackym PA, Honrubia V. Vestibular neuritis: clinical-pathologic correlation. Otolaryngol Head Neck Surg 1996;114:586-92.
7. Lindsay JR, Hemenway WG. Postural vertigo due to unilateral sudden partial loss of vestibular function. Ann Otol Rhinol Laryngol 1956;65:692-706.
8. Silvoniemi P. Vestibular neuronitis. An otoneurological evaluation. Acta Otolaryngol Suppl (Stockh) 1988(suppl 453).
9. Guyot JP, Hausler R, Reverdin A, Berney J, Montandon PB. Diagnosis of cerebellopontine angle tumors. ORL J Otorhinolaryngol Relat Spec 1992;54:139-43.
10. Coats AC. Vestibular neuronitis. Trans Am Acad Ophthalmol Otolaryngol 1969;73:395-408.
11. Voss O. Is there a labyrinthine concussion? [Letter]. JAMA 1934;103:1721-2.
12. Lumio JS, Aho J. Oto-neurological findings in post-traumatic encephalopathy. Acta Otolaryngol (Stockh) 1963;56:546-54.
13. Barber H. Positional nystagmus especially after head injury. Laryngoscope 1964;74:891-944.
14. Schuknecht HF. Cupulolithiasis. Arch Otolaryngol 1969;90:765-78.
15. Epley JM. The canalith repositioning procedure: for treatment of benign paroxysmal positional vertigo. Otolaryngol Head Neck Surg 1992;107:399-404.
16. Fee GA. Traumatic perilymphatic fistulas. Arch Otolaryngol 1968;88:477-80.
17. Singleton GT, Post KN, Karlan MS, Bock DG. Perilymph fistulas. Diagnostic criteria and therapy. Ann Otol Rhinol Laryngol 1978;87:797-803.
18. Legent F, Beauvillain C, Viale M, Korb G, Desson P, Bonnet J. Fistules péri-lymphatiques. Difficultés diagnostiques et thérapeutiques. Ann Otolaryngol Chir Cervicofac 1988;105:465-75.
19. Guyot J-P, ed. Perilymphatic fistula. A controversial issue. In: Oto-Rhino-Laryngologia Nova. Basel, Switzerland: Karger, 1998.
20. Gacek RR. The pathology of facial and vestibular neuronitis. Am J Otolaryngol 1999;20:202-10.
21. Ruan JS, Khalil T, King AI. Dynamic response of the human head to impact by three-dimensional finite element analysis. J Biomech Eng 1994;116:44-50.
22. Canlon B. The effect of acoustic trauma on the tectorial membrane, stereocilia, and hearing sensitivity: possible mechanisms underlying damage, recovery, and protection. Scand Audiol Suppl 1988(suppl 27).
23. Ylikoski J, Juntunen J, Matikainen E, Ylikoski M, Ojala M. Subclinical vestibular pathology in patients with noise-induced hearing loss from intense impulse noise. Acta Otolaryngol (Stockh) 1988;105:558-63.
24. Shupak A, Bar-El E, Podoshin L, et al. Vestibular function in acoustic trauma [in Hebrew]. Harefuah 1995;128:129-34, 200.

Ann Otol Rhinol Laryngol 110:2001

COCHLEAR MICROPHONIC POTENTIALS: A NEW RECORDING TECHNIQUE

FRANCISCO CARRICONDO, PHD
JULIO SANJUÁN-JUARISTI, MD
PABLO GIL-LOYZAGA, MD, PHD
JOAQUÍN POCH-BROTO, MD
MADRID, SPAIN

A new instrumentation and a particular method for detecting and recording cochlear microphonic potentials (CMPs) are described here. The CMPs were recorded in rats by means of pure tones (4,000, 2,000, 1,000, 500, and 250 Hz) and intraepidermic electrodes; the electrocochleography technique was avoided. An experimental design that included the use of a glutamatergic agonist (kainic acid [KA]) and an aminoglycoside antibiotic (kanamycin [KANA]) was carried out to demonstrate the origin of the recorded potential. Morphological studies showed that KA selectively eliminated the afferent type I dendrites of the spiral ganglion, while the administration of KANA resulted in the absence of outer hair cells. When CMPs were recorded after KA administration, no alterations were detected. In contrast, KANA administration resulted in the absence of any selective electrophysiological activity corresponding to CMPs. All these results were compared with the recording of the compound action potential of the eighth nerve obtained by electrocochleography. These findings and the great specificity of the reproduction of the sound stimulus confirm that the CMPs can be recorded by the new equipment.

KEY WORDS — cochlea, electrophysiology, microphonic potential, neurotoxicity, ototoxicity.

INTRODUCTION

The cochlear microphonic potential (CMP) was discovered by Wever and Bray.[1] It is one of the cochlear evoked potentials, and its main property is the reproduction of the waveform of the sound stimulus.[2] The CMP corresponds to the physiological activity of the outer hair cells (OHCs)[3,4]; therefore, it can be recorded in functional ears. When the CMP disappears, there are no responses to acoustic stimuli. It is the first potential produced in the cochlea after the sound stimulus, and its amplitude is lower than the amplitude of the cochlear compound action potential (CAP).[5]

The origin of the CMP has been largely analyzed by means of experimental models involving drug administration. Comparing the recordings of the CAP and the CMP can aid in the localization of the action sites of drugs. A decrease in the CAP without changes in the CMP could indicate damage to nerve endings without hair cell alterations.[6] Therefore, the administration of glutamate agonists (eg, glutamate, kainic acid, α-amino-3-hydroxy-5-methyl-4-isoxazole propionic acid [AMPA], *N*-methyl-D-aspartate [NMDA]),[6-14] which specifically affect the type I afferent dendrites of the spiral ganglion, altering the CAP, has no effect on the CMP.[12,13,15] On the other hand, the administration of aminoglycoside antibiotics, which affect the hair cells, produces changes in both the CMP[16] and the CAP.[17] For these reasons, the CMP can give reliable data about the cochlear status.

The main property of the CMP, the reproduction of the sound stimulus wave, constitutes, paradoxically, the main problem in its correct evaluation. The sound stimuli often used to evoke the cochlear potentials — clicks, tone pips, and tone bursts — are not well reproduced by earphones. The poor reproduction produces sounds that differ from the predetermined stimulus. This situation is graphically shown in the classic representation in Fig 1A. The CMP produced, which repeats the sound stimulus, lacks frequency specificity.[5] A cochlear frequency exploration can only be done, with this type of stimulus, by using a spectral analysis of the recorded responses. Thus, the easiest way to get reliable CMP recordings is by using pure tones as the sound stimulus, as they can be correctly reproduced by earphones (Fig 1B).

In human beings, the CMP is often registered by means of transtympanic electrodes together with the cochlear CAP.[18] The first reliable human CMP recordings, isolated from the CAP,[19] were registered with an electrode placed in the tympanic membrane to avoid the problems of the transtympanic technique. The results were obtained with continuous pure tones, not with transient stimuli, to induce a specific frequency response from the OHCs. The advantages shown by the use of surface electrodes and pure tonal

---

From the Laboratory of Hearing Neurobiology, Department of Surgery II (Otorhinolaryngology), Faculty of Medicine, Complutense University of Madrid, Madrid, Spain (Carricondo, Gil-Loyzaga, Poch-Broto). Supported by Spanish government grant FIS 98/0732 and Complutense University grants PR 156/97-7136 and PR 294/95-6187/95.

CORRESPONDENCE — Pablo Gil-Loyzaga, MD, PhD, Apartado de Correos 60075, 28080 Madrid, Spain.

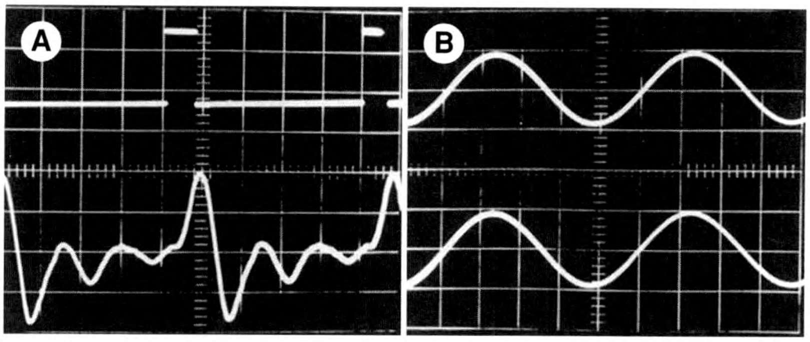

Fig 1. Electrical and acoustic comparisons between sound stimuli of **A**) click type and **B**) pure tone type, with both stimuli recorded with double-beam oscilloscope. In both A and B, upper wave represents electrical signal of sound stimulus and lower wave represents acoustic signal recorded with microphone at earphone. Electrical signal of sound stimulus click (**A**) faithfully represents square signal of click. However, earphone cannot reproduce stimulus, since earphone membrane has inertia that hinders correct reproduction of sudden rise and fall of electrical signal. In contrast, pure tone (**B**), which is sinusoidal electrical signal, is reproduced correctly by earphone and gives possibility of faithful tonal stimulation.

stimulation were the bases for the development of more advanced electronic equipment,[2,20] but to the present day, only a few reports exist on research on new methods to record the CMP.[5,21]

The aim of this report is to present a technique that allows reliable CMP responses to be recorded in animals by means of simple external contact electrodes. The results obtained, thanks to the technique's great selectivity and sensitivity, could be used in the diagnosis of cochlear disorders in animals or in humans.

MATERIALS AND METHODS

Three experimental protocols were designed for validation of the results obtained with the new CMP recording equipment and technique. These protocols allowed the localization of the recorded potentials in the auditory receptor, and allowed a comparison between these results and ones obtained in CAP recordings of the eighth nerve by means of the electrocochleography technique.

Neurotoxicity in Adult Rat Protocol. Four adult male rats were used. The animals were deeply anesthetized (chloral hydrate 8% intraperitoneally), and a CMP recording was carried out in an anechoic chamber. Three subcutaneous needle electrodes were placed: 2 of them in the mandibular muscles and a reference electrode at the vertex. The CMP screening was done at 5 frequencies — 4,000, 2,000, 1,000, 500, and 250 Hz — with pure tones (see CMP Recording Electronic Equipment, below). When the animals awoke from the deep anesthesia, a single intraperitoneal injection of kainic acid (KA; Sigma, St Louis, Mo), 5 mg/kg body weight, was administered to them. Twenty-four hours later, the animals were again anesthetized for CMP and CAP recordings. The CAP recording was done by the electrocochleography technique (see CAP Recording, below). The means and SEMs of the CMP and CAP thresholds and the CAP N1 wave latency and amplitude values were plotted and statistically compared by a one-way analysis of variance (ANOVA) with a Bonferroni post hoc test.

Ototoxicity in Adult Rat Protocol. Five adult male rats were used. The ototoxicity was produced by a daily intraperitoneal administration of kanamycin (KANA; Sigma), 300 mg/kg body weight, for 22 days. After this treatment, the CMP recording was null. The CMP recordings (see CMP Recording Electronic Equipment, below) were carried out before the treatment (day 0) and on days 3, 9, 13, 18, and 22, under deep anesthesia. The frequency CMP threshold, mean, and SEM for each exploration day were plotted to observe the evolution patterns of the CMP during the KANA treatment.

Ototoxicity in Developing Rat Protocol. Six 10-day-old male rats were used. They were treated daily with 300 mg/kg body weight of KANA from postnatal day 10 to postnatal day 13. When the animals reached adult age (postnatal day 45), they were deeply anesthetized and prepared for CMP and CAP recordings. The means and SEMs of the CMP and CAP thresholds and CAP N1 wave latency and amplitude values were plotted and statistically compared by a one-way ANOVA with a Bonferroni post hoc test.

CMP Recording Electronic Equipment. The electronic equipment (Fig 2A) for the CMP recording (PM/97, Electrónica General Española, Madrid, Spain) consists of 2 independent units. The first, which produces the recording, amplification, and average of the electrophysiological signal, includes the electrodes, a differential preamplifier, an amplifier, data collection equipment, and an averaging system. The second unit serves as a stimulus generator and a sound pressure controller.

The CMP is recorded by subcutaneous electrodes

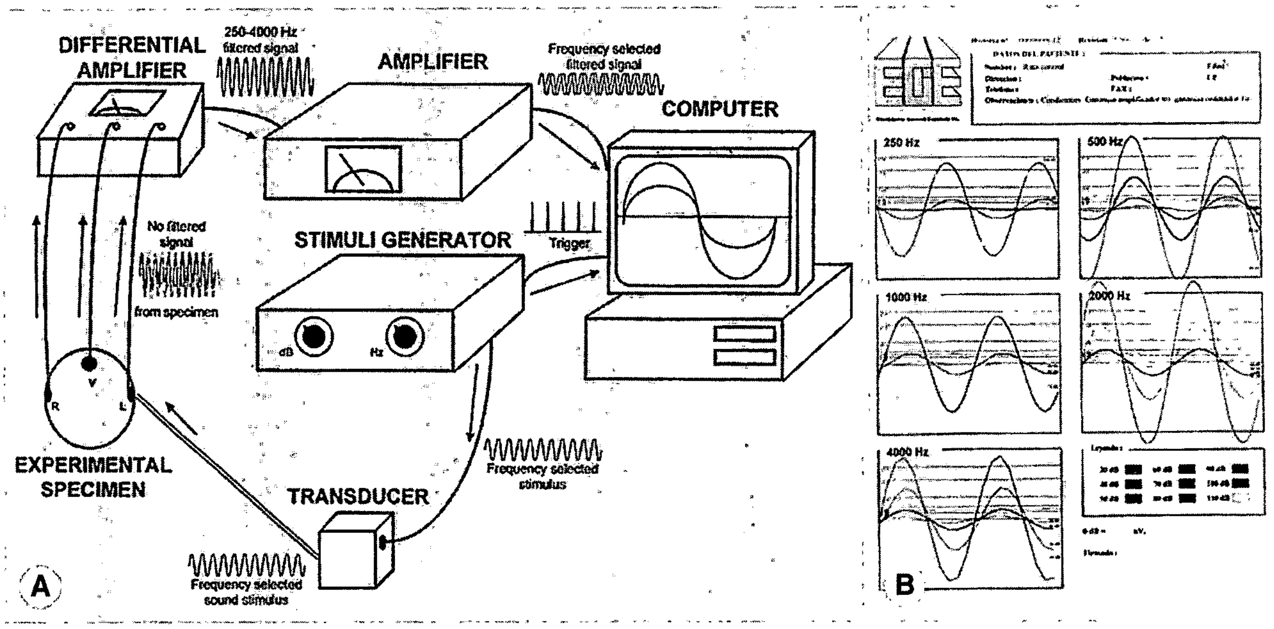

Fig 2. Cochlear microphonic potential (CMP) electronic equipment. A) Diagram of CMP electronic equipment. Bioelectrical signal from specimen is collected by 3 surface or intraepidermal electrodes (right and left sides and vertex). Then, it is sent to differential amplifier that filters signal among 250 and 4,000 Hz. This is connected to amplifier that amplifies and filters signal to selected stimulus frequency. Signal is finally processed in computer averaging card, combining filtered signal with trigger produced by stimulus generator to discriminate synchronized CMP from recorded signal. Stimulus generator produces pure tone signals (250, 500, 1,000, 2,000, and 4,000 Hz) that are converted to sound stimuli by transducer. Sound reaches ear via rubber tube. **B**) CMP data sheet shows results obtained after CMP recording of rat from control group. In this case, CMP thresholds obtained were 80 dB sound pressure level (SPL) at 250 Hz, 60 dB SPL at 500 Hz, 50 dB SPL at 1,000 Hz, 30 dB SPL at 2,000 Hz, and 30 dB SPL at 4,000 Hz.

in animals or by surface electrodes in humans, placed at both mandibular muscles and the vertex and connected to a differential amplifier. The differential amplifier collects the electrophysiological signal from the patient. It has the first bandpass filter, which filters the signal between 250 and 4,000 Hz, which are the limits of the exploration frequencies.

At this stage of the recording, the relationship between the CMP signal and noise is not good. Next, the signal is filtered to a frequency (stimulus frequencies 250, 500, 1,000, 2,000, and 4,000 Hz) with low and high bandpass filters, 90 dB per third of an octave on the low- and high-pass sides. The filter rejects the noise frequencies that differ from the stimulus frequency. In this way, the amplifier system filters the signal that comes from the differential amplifier.

The greatest problem is to identify the CMP potential in the filtered signal. It is obtained by averaging the recorded signals that are synchronized in phase with the sound stimuli. To locate it, the sound stimuli are marked with the beginning signal, a trigger, that is produced by the stimulus generator. In that way, the hair cell response is synchronized in phase with the stimulus. This synchronization allows the average of the signal to be obtained in a computer with an averager card and its software, and allows the discrimination of the CMP potential from the recorded signal.

The stimulus, a pure tone (250, 500, 1,000, 2,000, or 4,000 Hz), is produced as a function of the generator together with the trigger signal. At the output, a step attenuator allows decibel selection between 30 and 110 dB. This signal is converted to sound stimuli by a transducer.

The transducer is an electromagnetic element that produces a strong magnetic field. This magnetic field has the same stimulus frequency as, and is synchronous with, the trigger signal. This could introduce false effects in the CMP potential recordings. To avoid this problem, the transducer can be isolated and moved away from the patient. The sound stimulus reaches the patient through a 4-m-long plastic tube connected to the transducer at one end and to an adapter for the patient's ear at the other.

The CMP recordings can be plotted to study the exploration results (Fig 2B). The CMP result sheet (1 per ear) includes a record card (a rectangle in the upper part of the sheet) on which the operator can write the patient's personal data: name, age, address, telephone and fax numbers, and exploration observations. The main part of the sheet is occupied by 5 squares that show the results for each exploration frequency (250, 500, 1,000, 2,000, and 4,000 Hz). The

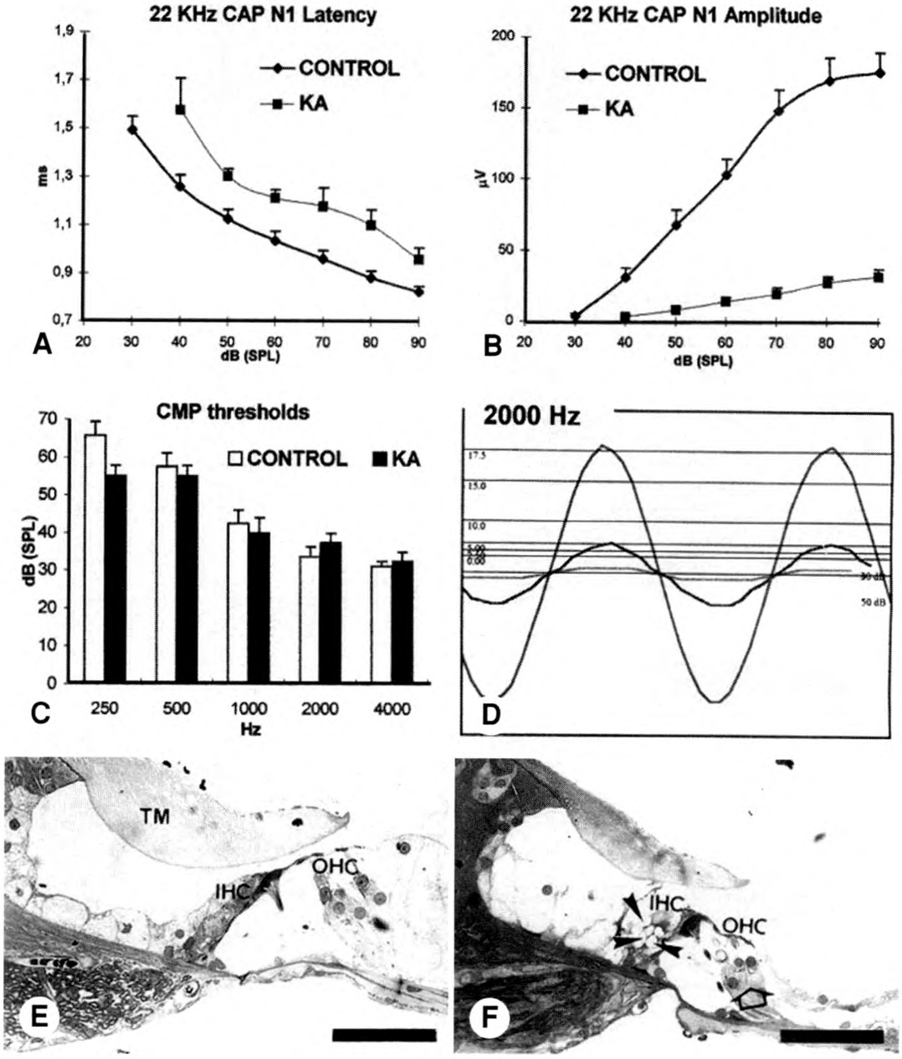

Fig 3. Neurotoxicity protocol results. **A,B**) Input-output functions of cochlear compound action potential (CAP) N1 wave **A**) latency and **B**) amplitude obtained with 22-kHz filtered clicks. Mean + SEM is shown at each stimulation level for each treatment group: control group and kainic acid (KA) group. **C**) Histogram of CMP thresholds obtained in these groups. Mean + SEM is presented for control group and KA group. **D**) Example of 2,000-Hz CMP recording of rat treated with KA. CMP threshold obtained in this case was 40 dB SPL, which was similar to control values. **E,F**) Low-magnification photographs of organ of Corti from cochleas obtained from **E**) control animal and **F**) KA-treated animal. Great swelling (arrowheads) of type I afferent dendrites, below inner hair cell (IHC) basal pole, can be observed. No damage was detected at outer hair cell (OHC) area (empty arrow). TM — tectorial membrane, scale bars — 50 µm.

results are expressed as curves that represent the CMP obtained at each sound intensity. A color code for the sound intensities, which can be seen in the lower part of the sheet, can help to identify the stimulus used and the auditory threshold at each frequency. Below the intensity color code, the equivalence between decibels (sound pressure level [SPL]) and nanovolts can be established. The equivalence here is 0 dB = 10 nV. To complete the CMP results sheet, the operator can sign the exploration.

CAP Recording. The CAP recording[9] was carried out, under general anesthesia, on both cochleas of each animal. The animals were artificially ventilated (small animal ventilator, 141 A, New England Medical Instruments Inc, Medway, Mass), and the rectal temperature was kept at 37°C with a heating pad. A hole made in the posterolateral wall of the tympanic bulla allowed the placement of a silver electrode, coated with Teflon except at the tip, on the cochlear round window. The reference electrode was placed subcutaneously on the mandibular muscle, and the ground electrode on the contralateral armpit.

The CAP recording was carried out in an anechoic chamber with an attenuation of 30 dB SPL over the external sound (Stock, Madrid). The bioelectrical signals were amplified, filtered, digitized, averaged, measured, and printed by a Mistral evoked potential compact unit (Medelec International, Woking, England). The sound stimuli used were 100-µs filtered clicks (22, 18, 16, 12, 8, and 4 kHz). The stimuli were generated from a waveform synthesizer (HP 8904 A, Hewlett-Packard, Spokane, Wash) and delivered through an earphone (Telephonics TDH39, Medelec International) placed close to the ear of the rat. The potentials recorded were averaged from 64 samples (repetition rate, 10 stimuli per second). The intensity of the stimulus was measured by a microphone (CLR-224, Promax, Barcelona, Spain) connected to a sound meter (SI-131 A, Promax), placed at the same distance from the earphone as the rat's ear, with the decibel SPL scale used for the sound level measurements. The ears were stimulated in a free field with

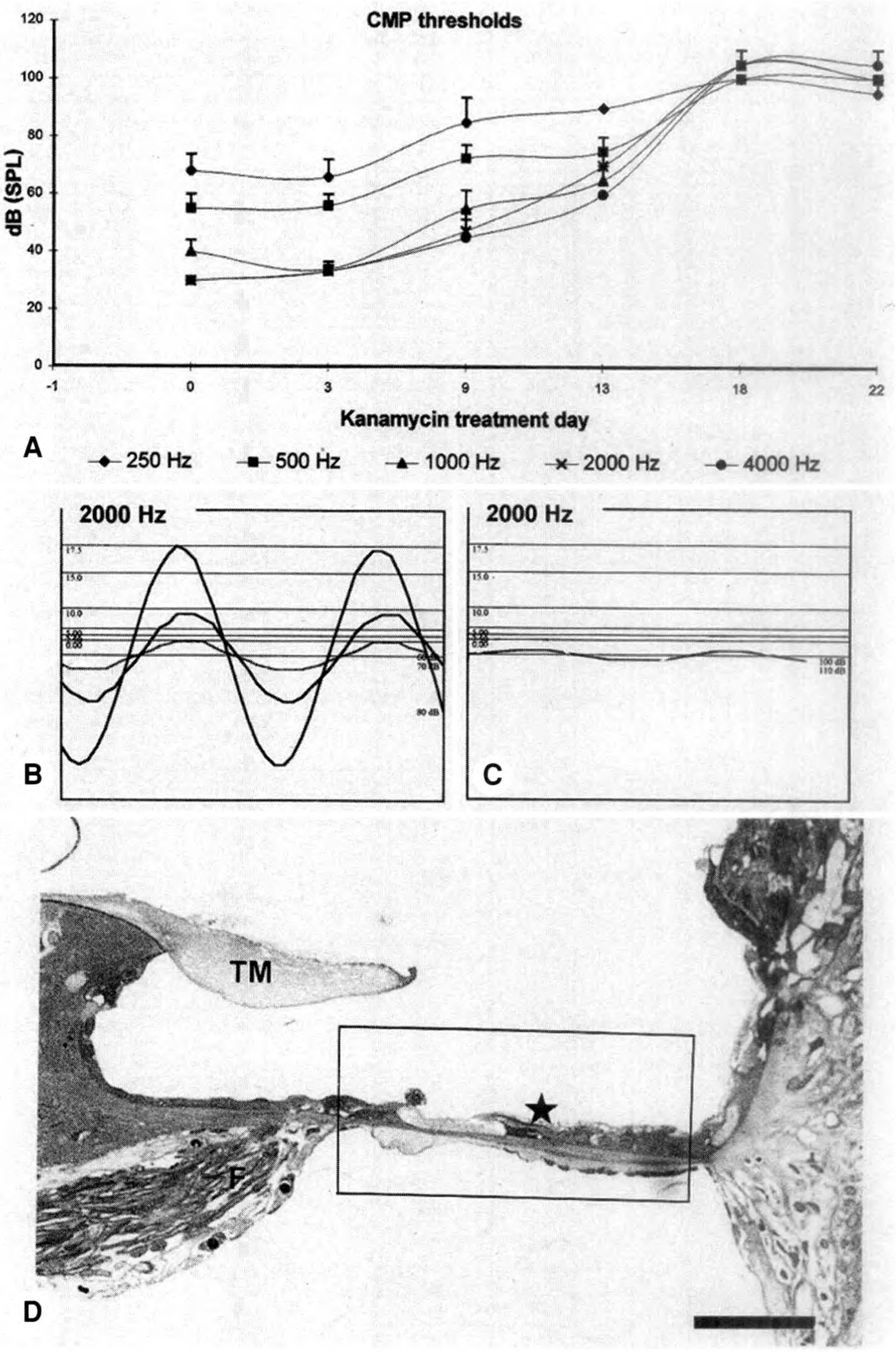

Fig 4. Results obtained from protocol of ototoxicity in adult rats. **A**) Evolution of CMP thresholds for each stimulus frequency recorded throughout kanamycin (KANA) treatment: day 0 (before KANA treatment) and treatment days 3, 9, 13, 18, and 22. Mean + SEM for each stimulation frequency is shown. **B,C**) Examples of CMP recordings at 2,000 Hz at 2 treatment days. **B**) Day 9, CMP threshold at 60 dB SPL. **C**) Day 22, CMP threshold at 100 dB SPL. **D**) Low-magnification photograph of organ of Corti obtained from animal treated with KANA for 22 days. Ototoxicity damage can be observed in organ of Corti area (rectangle). It resulted in total hair cell loss (star). No damage is detected in spiral ganglion type I dendrites (F). TM — tectorial membrane, scale bar — 50 μm.

intensities varying in 10–dB SPL steps from 100 to 30 dB SPL. The N1 wave latency and amplitude were determined as a function of the intensity of the stimulus.

Morphological Study. After the physiological recordings, while still under deep anesthesia, the animals were decapitated; the cochleas were then removed and fixed with 2.5% glutaraldehyde in 0.1-mol/L phosphate buffer (pH 7.4). Next, the cochleas were decalcified and postfixed in osmium tetroxide dissolved in a phosphate solution, and then embedded in Spurr resin. The samples were sectioned at 1 μm, stained with Richardson blue stain, and studied under a light microscope (Leica DM, Wetzlar, Germany).

RESULTS

Neurotoxicity in Adult Rats. In comparison to the control values, the administration of KA (Fig 3) produced marked modifications in the CAP (Fig 3A,B). These were a significant increase in the N1 wave latency (Fig 3A) and an important decrease of the N1 amplitude values (Fig 3B) at all the frequencies.

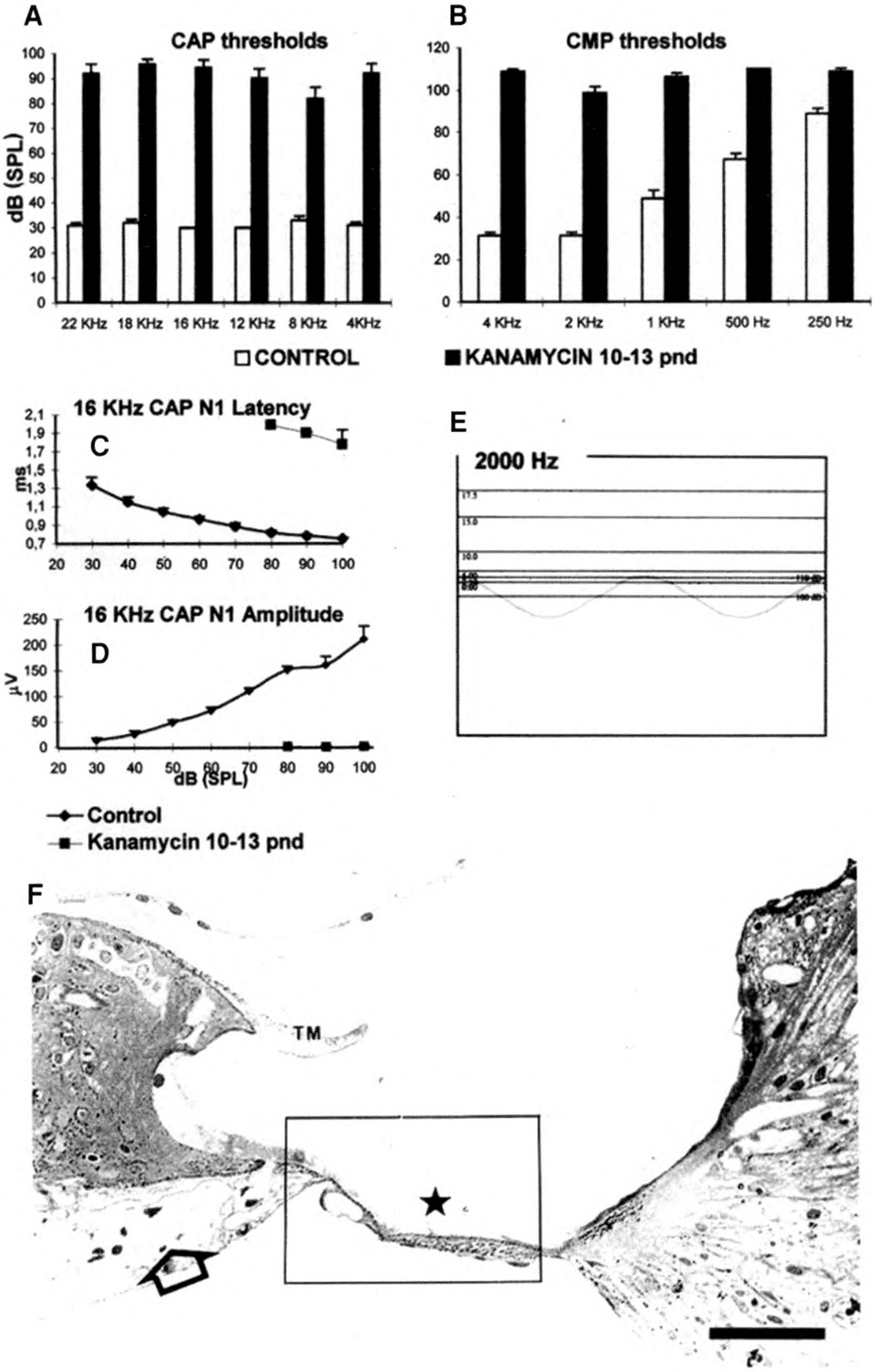

Fig 5. Results obtained from protocol of ototoxicity in developing rats. **A)** Histogram represents CAP thresholds obtained with filtered clicks at each stimulus frequency. Mean + SEM of each group is shown: control group (white bars) and group that received KANA at postnatal days (pnd) 10 to 13. **B)** Histogram represents CMP thresholds obtained with pure tones at each stimulus frequency. Mean + SEM of each group is shown: control group and group that received KANA at pnd 10 to 13. **C,D)** Input-output functions of CAP N1 wave **C)** latency and **D)** amplitude obtained with 16-kHz filtered clicks. Mean + SEM is shown at each stimulation level for each treatment group: control group and group that received KANA at pnd 10 to 13. **E)** Example of 2,000-Hz CMP recording obtained from rat that received KANA at pnd 10 to 13. In this case, CMP threshold was 110 dB SPL. **F)** Low-magnification photograph of organ of Corti obtained from KANA-treated rat. Organ of Corti area is shown inside rectangle. Total loss of hair cells (star), as well as degeneration of spiral ganglion fibers (empty arrow), can be observed. TM — tectorial membrane, scale bar — 50 µm.

Only the 22-kHz CAP recordings are presented as examples of the effects on the CAPs of KA-treated animals. The same effects were observed in the recordings of the other frequencies.

Otherwise, the CMP thresholds obtained in the KA administration group did not differ from the CMP control thresholds (Fig 3C). The CMP recordings of the animals that received KA (Fig 3D) looked like the control CMP recordings with the CMP threshold at 30 to 40 dB SPL. Only the 2,000-Hz CMP recording is presented as an example of the effects of KA administration on the CMP recordings.

In the morphological study (Fig 3E,F), the KA administration (Fig 3F) resulted in a complete swelling of the type I dendrites of the spiral ganglion, which could be observed under the inner hair cells (IHCs), as compared with a control organ of Corti (Fig 3E). No damage was detected in the IHCs or OHCs in these cochleas.

Ototoxicity in Adult Rats. The administration of KANA to adult rats (Fig 4) produced a progressive increase in the CMP thresholds starting with treatment day 3 (Fig 5A). The highest CMP threshold, 110 dB SPL, was reached at treatment day 19. The thresholds obtained in the CMP recording previous to the treatment with the stimulus frequencies 4,000, 2,000, and 1,000 Hz were lower than those obtained at 500 and 250 Hz. These differences were maintained during the treatment until treatment day 19, on which all the CMP thresholds reached 110 dB SPL.

Two examples of 2,000-Hz CMP recordings are presented (Fig 4B,C). In the CMP recording of treatment day 9 (Fig 4B), a low increment in the CMP threshold (60 dB SPL), can be observed with respect to the control values (30 dB SPL; Fig 3C). At treatment day 22 (Fig 4C), the CMP threshold was the highest reached (100 dB SPL).

Morphologically (Fig 4D), this treatment with KANA produced the elimination of the hair cells of the organ of Corti. No damage was observed in the fibers of the spiral ganglion.

Ototoxicity in Developing Rats. The KANA treatment from postnatal days 10 to 13 (Fig 5) produced a significant increase of the CAP thresholds with respect to control values (Fig 5A) at all of the studied frequencies. In addition, the CMP thresholds obtained from KANA-treated animals were higher than the control values (Fig 5B). The CMP threshold shift between KANA and the control values was lower when the exploration was carried out with low-frequency stimuli (500 and 250 Hz). An example of a 2,000-Hz CMP recording of a KANA-treated rat is presented in Fig 5E.

The CAP recordings of rats treated with KANA from postnatal days 10 to 13 showed, at all of the studied frequencies, a large increment in the N1 wave latency and a significant decrease of the N1 wave amplitude with respect to the control recordings. Figure 5C,D shows the 16-kHz CAP recordings.

The morphological study (Fig 5F) showed that treatment with KANA produced the loss of all of the hair cells of the organ of Corti, as well as the spiral ganglion neurons. The cochlear basal coil was the one most affected by the KANA treatment.

DISCUSSION

A new method for CMP recording has been tested. The CMP recording equipment has been tested with 3 experimental protocols aimed at showing the CMP identity of the recorded potentials. The ability of the new electronic equipment to record the CMP has been demonstrated by studying the pathophysiological effects of some drugs on the hypothetical CMP recordings. The results obtained will be discussed for each experimental protocol.

Neurotoxicity in Adult Rats. It is largely accepted that the origin of the CMP is the activity of the OHCs.[3,4] The neurotransmitter involved in synapses between OHCs and type II afferent dendrites remains unknown, but glutamate can be excluded.[22,23] Nowadays, it seems clear that glutamate is involved in neurotransmission in primary afferent synapses between IHCs and type I spiral ganglion neurons[6-11,14,24,25] and is not involved in the synapses between OHCs and type II cochlear afferent dendrites. Therefore, cochlear afferent type I neurotoxicity was selected for this experiment to eliminate the possibility that the potential recorded could have been derived from the activity of either IHCs or afferent type I dendrites.

It has been largely reported that the intraperitoneal administration of KA, a glutamatergic non-NMDA receptor agonist, produces an excitotoxic process both in the central nervous system[26,27] and in the cochlea.[7-9,11,24,25] As could be expected, KA treatment produced damage that consisted of swelling of most of the type I afferent dendrites, even when no damage was observed in the IHCs, OHCs, or type II afferent fibers. This damage is consistent with the excitotoxic process and is based on the entry of calcium (Ca^{2+}) and water into the fiber. In the electrophysiological recordings, these KA neurotoxic effects produced great alterations in the cochlear CAP, increasing the latencies and decreasing the amplitudes of the CAP N1 wave. These electrophysiological results reflect the excitotoxic effects of the KA administration, since the CAP reflects the synchronous discharge of the spiral ganglion neurons.[12]

The administration of KA did not induce any significant changes in the CMP thresholds compared with the control values. These results are in agreement with those of previous studies[12,13,15] that reported the lack of any effect of the glutamatergic agonists on CMP production. This finding demonstrates that the potential recorded by the new electronic equipment is not generated in the IHCs. With 250- and 500-Hz stimulus frequencies, the threshold of the CMP increased in both the control and KA groups. This CMP threshold increase could demonstrate a deficiency of CMP production by the OHCs at these frequencies. This effect could be related to the auditory spectrum of the rat. This CMP electronic equipment was designed for human screening, and it uses stimulus frequencies that are audible and useful for humans; however, these frequencies are probably too low for the rat cochlea.

Ototoxicity in Adult Rats. Aminoglycoside antibiotic ototoxicity was the second test selected to probe the CMP recording by the new equipment. The ototoxic properties of these antibiotics have been extensively studied and are well known.[23] Administration of these drugs produces changes in the CMP,[16,17] as well as lesions in the OHCs and other structures of the organ of Corti.[28]

The aminoglycoside antibiotic selected to produce ototoxicity in the present study was KANA. Its administration resulted in a significant increase in the CMP threshold values from the third treatment day on. The development of ototoxicity could be followed for the whole treatment, thanks to the capacity of the new CMP recording equipment to record the CMP with surface electrodes and without any surgical intervention. The progressive increase in the CMP thresholds recorded throughout the treatment indicates the great specificity of the CMP recorded. The KANA-induced ototoxicity observed was corroborated by the histologic images, in which damage to the hair cells was seen. In these cochleas, no signs of degeneration were detected in the spiral ganglion fibers, possibly because of a resistance of the adult animals to the KANA-induced damage. Alternatively, there may have been insufficient time between the treatment and the histologic processing of the cochleas for spiral ganglion degeneration to take place.

The CMP recordings made before the KANA treatment (day 0) showed some differences between frequencies. The lowest CMP threshold values corresponded to 4,000, 2,000, and 1,000 Hz, whereas the 500- and 250-Hz frequencies produced higher CMP threshold values. This result confirms the data obtained in the neurotoxicity protocol. It demonstrates that the low frequencies explored by the CMP recording equipment are at the limit of the auditory spectrum of the rat.

This protocol allowed us to demonstrate that the CMPs obtained by the new recording equipment have their origin in the activity of the OHCs.

Ototoxicity in Developing Rats. As a complement to the previous ototoxicity protocol, we designed a study of the electrophysiological effects of the aminoglycoside antibiotic KANA in developing animals. This protocol allowed us to compare the results of cochlear CAP recordings and CMP recordings obtained with the new equipment. Postnatal days 10 to 13 were selected as the administration period, because the period of maturation of the cochlear potentials and the final cochlear structure is the period with the greatest sensitivity to aminoglycoside ototoxicity.[29] In this period, the administration of aminoglycoside antibiotics in low doses that do not affect the adult cochlea produces great damage in the developing cochlea.[23]

The KANA treatment produced the expected ototoxic effects in the developing rats. The effects on the CAP N1 wave, at all of the studied frequencies, consisted of a highly significant increase in latency and a reduction of amplitude, as well as a large increase in the CAP auditory thresholds, with respect to the control values. These electrophysiological findings were produced by the ototoxic process that induced a complete loss of the hair cells of the organ of Corti and the later degeneration of the spiral ganglion fibers. Morphologically, the greatest damage was observed in the cochlear basal coil. This is a characteristic effect of treatment with aminoglycoside antibiotics, since immunoreactivity to amikacin is mainly located at the OHCs of the cochlear basal coil.[30] In addition, aminoglycoside treatment significantly increased the CMP thresholds in comparison to the control values. This is a consequence of the hair cell loss reported. Again, little difference was observed between the control and KANA-treated animals in the CMP thresholds obtained with 250- and 500-Hz sound stimuli; this finding corroborates the inability of the rat cochlea to generate a normal CMP at these stimulating frequencies.

In conclusion, the results obtained in the experimental protocols designed for the validation of the new electronic equipment for CMP recording are in agreement with previous findings.[23] This technique has demonstrated a great specificity in cochlear tonal screening, thanks to its bandpass filters and its amplification system. The pure tones used as the sound stimuli allow a reliable tonal exploration of the cochlear hair cell function, overcoming the lack of frequency specificity of the click stimulus. This equipment, designed as a screening method for human CMP recordings, was able to detect 500- and 250-Hz hypoacusis in the rat cochlea; this outcome demonstrates the ability of the system to explore the hair cell status. In newborn human screening,[5,21] the results have also been interesting, showing the normal patterns of CMP recording thresholds. In short, this new CMP recording equipment, combined with other, previously established tests, such as those of the brain stem auditory evoked potentials and the CAP of the eighth nerve, can give much valuable information on cochlear physiology and pathology.

ACKNOWLEDGMENTS — The authors are grateful to Prof Jochen Schacht (Kresge Institute, Ann Arbor, Mich) for helpful comments made during the experimental process, to Dr M. Angeles Vicente-Torres for criticisms of the manuscript, to David Doig for correction of the English version, and to Jesús San Román, Esther Hernández, and Teresa Rodríguez for help given during the experimentation and technical work.

REFERENCES

1. Wever EG, Bray CW. The nature of acoustic response: the relation between sound frequency of impulses in the auditory nerve. J Exp Psychol 1930;13:373-87.

2. Sohmer H, Pratt H. Recording of the cochlear microphonic potential with surface electrodes. Electroencephalogr Clin Neurophysiol 1976;40:253-60.

3. Davis H. A mechano-electrical theory of cochlear action. Ann Otol Rhinol Laryngol 1958;67:789-801.

4. Russell IJ, Sellick PM. Low-frequency characteristics of intracellularly recorded receptor potentials in guinea-pig cochlear hair cells. J Physiol (Lond) 1983;338:179-206.

5. De Los Santos G, Sanjuán J, Gavilán J. New method for recording human cochlear microphonic potentials [in Spanish]. Acta Otorrinolaringol Esp 1998;49:341-5.

6. Puel JL. Chemical synaptic transmission in the cochlea. Prog Neurobiol 1995;47:449-76.

7. Gil-Loyzaga P, Hernández-Ortiz MJ, Rodríguez-Benito T, Lasso de la Vega ML. Diltiazem protects against neurotoxicity induced by excitotoxic amino acids on cochlear afferent fibers. ORL J Otorhinolaryngol Relat Spec 1993;55:211-5.

8. Gil-Loyzaga P, San Román J, Carricondo F, Vicente-Torres MA, Bartolomé MV. Effects of dopamine agonists on the compound action potential of the auditory nerve [Abstract]. 35th Workshop on Inner Ear Biology, Innsbruck, Austria, 1998:88.

9. Gil-Loyzaga P, Hernández E, Carricondo F, Simón F, Poch-Broto J. Trimetazidine prevents cochlear lesions induced by intraperitoneal and perilymphatic administration of kainic acid. Brain Res 1999;826:95-103.

10. Janssen R. Glutamate neurotoxicity in the developing rat cochlea is antagonized by kynurenic acid and MK-801. Brain Res 1992;590:201-6.

11. Juiz JM, Rueda J, Merchán JA, Sala ML. The effects of kainic acid on the cochlear ganglion of the rat. Hear Res 1989; 40:65-74.

12. Puel JL, Ladrech S, Chabert R, Pujol R, Eybalin M. Electrophysiological evidence for the presence of NMDA receptors in the guinea pig cochlea. Hear Res 1991;51:255-64.

13. Puel JL, Pujol R, Ladrech S, Eybalin M. Alpha-amino-3-hydroxy-5-methyl-4-isoxazole propionic acid electrophysiological and neurotoxic effects in the guinea-pig cochlea. Neuroscience 1991;45:63-72.

14. Simón F, Gil-Loyzaga P, Hernández E, Carricondo FJ. Monosodium glutamate affects cochlear function in adult rats [Abstract]. 31st Workshop on Inner Ear Biology, Montpellier, France, 1994:7.

15. Jenison GL, Winbery S, Bobbin RP. Comparative actions of quisqualate and *N*-methyl-D-aspartate, excitatory amino acids agonists, on guinea-pig cochlear potentials. Comp Biochem Physiol C 1986;84:385-9.

16. Nuttall AL, Marques DM, Lawrence M. Effects of perilymphatic perfusion with neomycin on the cochlear microphonic potential in the guinea pig. Acta Otolaryngol (Stockh) 1977;83: 393-400.

17. Dumas G, Charachon R. Ototoxicity of kanamycin in developing guinea pigs. An electrophysiological study. Acta Otolaryngol (Stockh) 1982;94:203-12.

18. Kumagami H, Miyazaki M. Reliability of cochlear microphonics in clinical electrocochleography. ORL J Otorhinolaryngol Relat Spec 1987;49:93-8.

19. Gavilán C, Sanjuán J. Microphonic potential picked up from the human tympanic membrane. Ann Otol Rhinol Laryngol 1964;73:101-9.

20. Pratt H, Sohmer H, Barazani N. Surface-recorded cochlear microphonic potentials during temporary threshold shifts in man. Audiology 1978;17:204-12.

21. Sanjuán-Juaristi J. Study of hearing in premature infants. Evoked cochlear microphonics. Acta Otorrinolaringol Esp 1998; 49:525-31.

22. Gil-Loyzaga PE. Neurotransmitters of the olivocochlear lateral efferent system: with an emphasis on dopamine. Acta Otolaryngol (Stockh) 1995;115:222-6.

23. Eybalin M. Neurotransmitters and neuromodulators of the mammalian cochlea. Physiol Rev 1993;73:309-73.

24. Gil-Loyzaga P, Pujol R. Neurotoxicity of kainic acid in the rat cochlea during early developmental stages. Eur Arch Otorhinolaryngol 1990;248:40-8.

25. Gil-Loyzaga P, Pujol R. Kainic acid toxicity on cochlear type I neurons. Proceedings of the 14th World Congress of Otorhinolaryngology and Head and Neck Surgery, Madrid, Spain, 1989:37-9.

26. Rothman SM, Olney JW. Excitotoxicity and the NMDA receptor. Trends Neurosci 1987;10:299-302.

27. Choi DW. Glutamate neurotoxicity and diseases of the nervous system. Neuron 1988;1:623-34.

28. Bartolomé MV, Vago P, Gil-Loyzaga P, et al. Sequential changes in anti–GAL-1 staining of the rat organ of Corti following amikacin exposure. Brain Res 1999;822:43-51.

29. Pujol R. Periods of sensitivity to antibiotic treatment. Acta Otolaryngol Suppl (Stockh) 1986(suppl 429):29-33.

30. Hayashida T. An immunohistochemical method for the study of aminoglycoside ototoxicity in the guinea pig cochlea using decalcified frozen sections. Arch Otorhinolaryngol 1989; 246:161-4.

Ann Otol Rhinol Laryngol 110:2001

ROLE OF INTERLEUKIN-1β IN A MURINE MODEL OF OTITIS MEDIA WITH EFFUSION

TETSUO WATANABE, MD
OITA, JAPAN

TAKASHI HIRANO, MD
OITA, JAPAN

MASASHI SUZUKI, MD
OITA, JAPAN

YUICHI KURONO, MD
KAGOSHIMA, JAPAN

GORO MOGI, MD
OITA, JAPAN

To clarify the role of interleukin-1β (IL-1β) in the pathogenesis of otitis media with effusion (OME), we developed and investigated a murine model of this disease. Specific pathogen–free male BALB/c mice received intratympanic injections of 20 μg of endotoxin derived from nontypeable *Haemophilus influenzae*. Three days after injection, middle ear effusions were observed through the eardrum. Similar pathological changes were observed after inoculation with 100 ng of recombinant IL-1β. Anti–IL-1 receptor antibodies inhibited the pathological changes induced by the endotoxin. In situ hybridization showed expression of IL-1β messenger RNA in the epithelium of the middle ear mucosa. These results suggest that IL-1β might be associated with endotoxin-induced inflammation in the middle ear and might play an important role in the induction of otitis media with effusion.

KEY WORDS — endotoxin, interleukin-1β, mouse, otitis media with effusion.

INTRODUCTION

Endotoxin is detected frequently in middle ear effusion (MEE)[1-3] and is thought to be involved in the pathogenesis of otitis media with effusion (OME). In recent studies, endotoxin or lipopolysaccharides have been used to induce MEE in animal models,[4-6] and lipopolysaccharide-induced inflammation has been shown to be regulated by a complex network of inflammatory mediators, particularly cytokines.[7,8] Among the cytokines, interleukin-1β (IL-1β), one of the proinflammatory cytokines, is thought to contribute to the acute phase of the inflammatory response and promote the release of other cytokines.

There have been many reports indicating the presence of IL-1β in MEE. Yellon et al[9] first demonstrated the presence of IL-1β in MEE. They analyzed 95 human MEE samples and found high levels of IL-1β in 51% of the samples. Juhn et al[10] analyzed 74 human MEE samples classified by age and type of effusion (serous, mucoid, or purulent) and found that IL-1β levels were highest in purulent MEE. Himi et al[11] analyzed 144 human MEE samples classified by gross appearance and cytologic findings and also found significantly higher IL-1β concentrations in purulent or neutrophil-rich MEE than in other types of MEE. These findings suggest that IL-1β contributes to infiltration of neutrophils into the middle ear. Maxwell et al[12] demonstrated that IL-8 was consistently present in the MEE of children with OME and was strongly correlated with levels of IL-1β. They also showed the level of IL-1β, as well as that of IL-8, to be correlated significantly with several clinical variables. Expression of IL-8 is enhanced by IL-1β and is associated with neutrophil infiltration. Recently, Willett et al[13] reported significant correlations between concentrations of endotoxin and IL-1β. These findings suggest that IL-1β is associated with the pathophysiology of OME.

In the present study, a murine model of OME was developed by intratympanic inoculation with endotoxin or murine recombinant IL-1β (rIL-1β), and the responses were compared by immunologic and histologic analysis. Further, the effects of anti–IL-1 receptor antibodies on endotoxin-induced OME were investigated in order to clarify the role of IL-1β in the pathogenesis of OME.

MATERIALS AND METHODS

Animals. Eighty-five specific pathogen–free male BALB/c mice between 6 and 10 weeks of age were used in this study. All animals were purchased from Seac Yoshitomi, Ltd (Fukuoka, Japan).

Endotoxin. Endotoxin was isolated in our laboratory from nontypeable *Haemophilus influenzae* cultured from the nasopharynx of a patient with OME according to the method of Westphal and Jann.[14]

From the Department of Otolaryngology, Oita Medical University, Oita, Japan. Supported by Grants-in-Aid for Scientific Research (B) from the Ministry of Education, Science and Culture of Japan (Nos. 09470374, 1157126, and 10307040).

CORRESPONDENCE — Goro Mogi, MD, Dept of Otolaryngology, Oita Medical University, 1-1 Idaigaoka, Hasama-machi, Oita, 879-5593 Japan.

Induction of OME. The animals were anesthetized by intraperitoneal injection with ketamine hydrochloride (0.6 mg/g), and the following procedure was performed under a surgical microscope. An initial incision was made in the retromandibular area along the angle of the mandible. Blunt dissection was performed to expose the tympanic bulla. With a 27-gauge needle, 2 small holes were made in the tympanic bulla. One hole was used for injection of 10 μL (2 mg/mL) of endotoxin, 10 μL (10 μg/mL) of rIL-1β (Pharmingen, San Diego, Calif), or 10 μL of phosphate-buffered saline solution (PBS). The other hole allowed equilibration of middle ear pressure. After injection, the holes were packed with bone wax. Upon completion of the procedure, the skin incision was closed with 4-0 nylon sutures. The animals were observed during recovery and were allowed ample food and water. The procedure was performed on the right ear, and the left ear served as a control.

MEE Collection. Three days after intratympanic inoculation with endotoxin or PBS, a microscope was used to observe the presence of MEE through the eardrum, and the findings were classified into 3 categories, as follows: no effusion, effusion with bubbles, and effusion without bubbles. The MEEs were collected through the eardrum by washing with 50 μL of PBS. The effusions were immediately centrifuged at 150*g* for 10 minutes and divided into liquid and cellular components. The liquid components were frozen and stored at –80°C until analysis. The cellular components were diluted in 200 μL of PBS and centrifuged at 1,000 rpm for 10 minutes for cytologic study by staining with hematoxylin-eosin.

Bacteriologic Study of MEE. The MEEs from 5 mice were cultured immediately after collection. Samples were inoculated on chocolate agar plates with sterile cotton-tipped swabs. The plates were incubated for 48 hours at 37°C in a humidified atmosphere containing 5% carbon dioxide.

Histologic Preparation. After the MEE samples were collected, the mice were perfused with 10% buffered formaldehyde and killed painlessly. For light microscopy, the temporal bones were immersed in 10% buffered formaldehyde, decalcified with ethylenediaminetetraacetic acid, dehydrated through a graded ethanol series, and embedded in paraffin. Paraffin sections of each 6 μm were stained with hematoxylin-eosin or periodic acid–Schiff stain. For in situ hybridization, the temporal bones were fixed with 10% buffered formaldehyde, decalcified with ethylenediaminetetraacetic acid, washed with 0.01-mol/L PBS (pH 7.4) containing 30% sucrose, and embedded in Tissue-Tek OCT compound (Sakura Finetek USA, Torrance, Calif).

Enzyme-Linked Immunosorbent Assay. The concentrations of IL-1β in the MEE samples were determined with the InterTest-1β enzyme-linked immunosorbent assay kit (Genzyme Corp, Cambridge, Mass).

Inhibition of OME by Anti–IL-1 Receptor Antibodies. The influence of IL-1 receptor antibodies on the production of MEE was examined by intratympanic injection of anti–IL-1 receptor antibodies together with endotoxin. Purified rat anti-mouse IL-1 receptor antibodies type I/p80 and type II/p68 (both from Pharmingen) were injected together with endotoxin, and the presence of MEE was examined 3 days after injection as described above.

Histologic Evaluation. The temporal bone tissue sections were examined microscopically in the anterior portion, the posterior portion, the inner side of the tympanic orifice of the eustachian tube, and the outer side of the tympanic orifice of the eustachian tube (Fig 1). The experimental and control ears were examined for epithelial thickness with the image processor Nexus 6800 (Kashiwagi Research Co, Tokyo, Japan). The cellular components of MEE samples were examined microscopically. The numbers of leukocytes were counted at 400× magnification. The averages of counts from 4 fields were classified into 4 grades: 0 to 10, 10 to 100, 100 to 200, and 200 or more cells per field. All histologic evaluations were performed in a double-blind fashion.

In Situ Hybridization. A fluorescein isothiocyanate–labeled oligonucleotide complementary RNA probe for IL-1β and a control probe were purchased from Biognostick GmbH (Gottingen, Germany). Ten-micrometer frozen sections were placed on gelatin-formalin slides and rehydrated in water. The slides were placed on an incubation tray, covered with 100 μL of 1-mg/mL proteinase K in 0.05-mol/L Tris-buffered saline solution, pH 7.6, and incubated for 30 minutes at 37°C. The slides were then immersed in water, dehydrated in 99% ethanol, and air dried. The IL-1β probe or the control probe (50 pmol/mL each) in HybriBuffer ISH (Biognostick GmbH) was heated to 95°C for 3 minutes, chilled on ice, and placed on the sections. The sections were covered with a coverslip and hybridized in a humidified chamber for 12 to 24 hours at 30°C. The coverslips were removed carefully, and the slides were washed 3 times for 3 minutes each in Tris-buffered saline solution containing 0.1% Triton X-100. The sections were then covered with blocking solution and incubated for 10 minutes. The blocking solution was removed, and rabbit F(ab') anti–fluorescein isothiocyanate–AP (Universal ISH Detection Kit, Novocastra Laboratories Ltd, Newcastle, England) was added to the slides. The slides were incubated for 30 minutes;

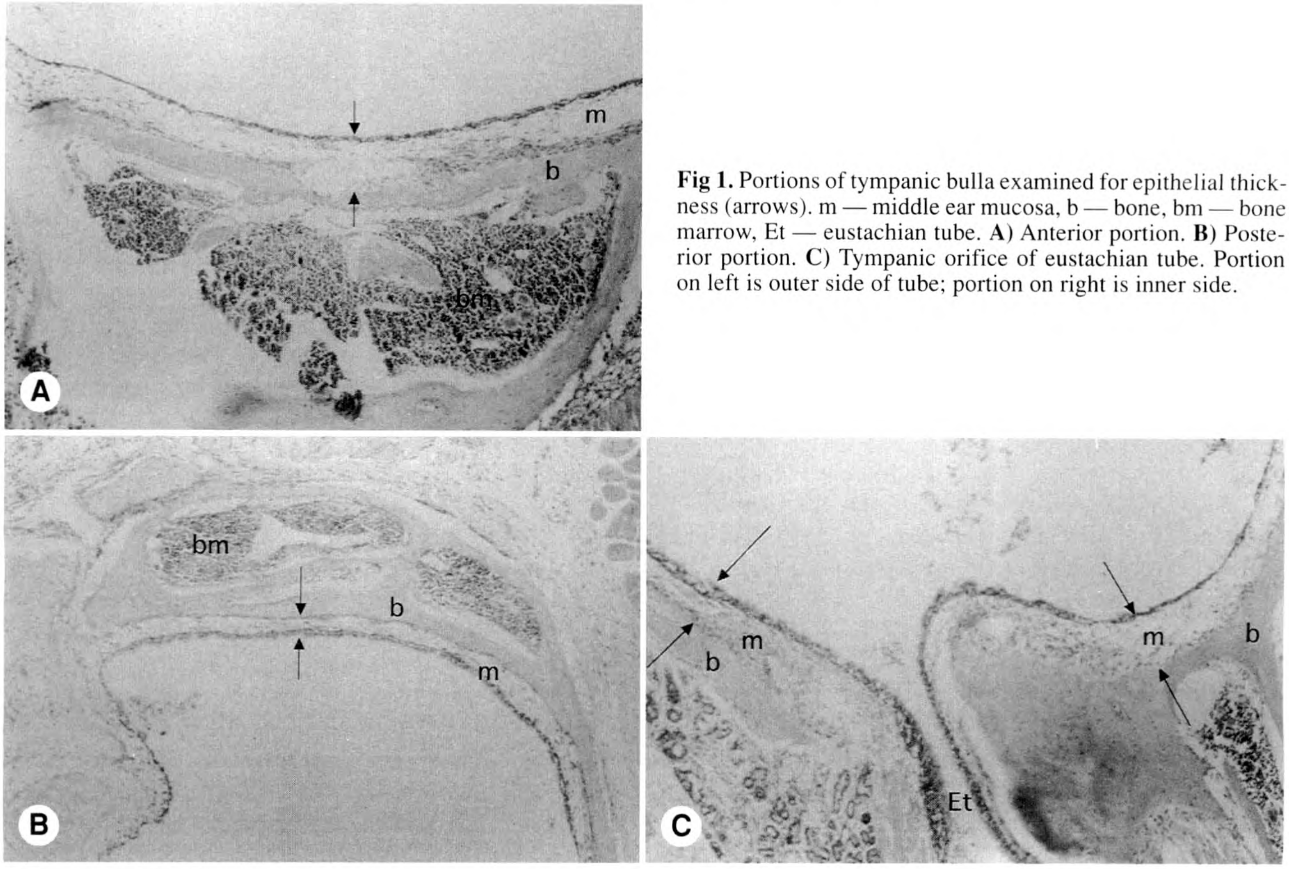

Fig 1. Portions of tympanic bulla examined for epithelial thickness (arrows). m — middle ear mucosa, b — bone, bm — bone marrow, Et — eustachian tube. **A**) Anterior portion. **B**) Posterior portion. **C**) Tympanic orifice of eustachian tube. Portion on left is outer side of tube; portion on right is inner side.

washed 2 times for 3 minutes each in Tris-buffered saline solution, and washed for 5 minutes in phosphate substrate buffer, pH 9.0. The sections were incubated sequentially with 5-bromo-4-chloro-3-indolylphosphate and nitroblue tetrazolium for 30 minutes at room temperature. The sections were then counterstained with methyl green, mounted in crystal mounting solution (Biomeda, Foster City, Calif), and analyzed by light microscopy. Spleen tissues incubated with endotoxin from normal mice were used as a positive control.

Statistical Analysis. Statistical analyses were performed with Student's *t*-test, χ^2 test, or the Mann-Whitney U test as appropriate. A p value of less than .05 was considered significant.

RESULTS

Endotoxin-Induced OME. Microscopic examination of the eardrum showed the presence of MEE in 4 of 5 mice by 3 days after the injection with endotoxin. Histologic examination of the middle ear revealed significant edema, infiltration of inflammatory cells into the submucosa or middle ear cavity, and increased numbers of goblet cells (Fig 2A). These changes were observed in all ears injected with endotoxin. Cytologic examination of MEEs showed infiltration of neutrophils and macrophages (Fig 3A). Neither MEE nor these histologic changes were observed in PBS-injected mice (n = 5).

IL-1β–Induced OME. Microscopic examination through the eardrum revealed MEE in 7 of 12 mice. The histologic findings of the middle ear mucosa and the cytologic findings of the MEEs were similar to those found in the mice with endotoxin-induced OME (Figs 2B and 3B).

Bacteriologic Study of MEE. No colonies were observed in the culture.

Enzyme-Linked Immunosorbent Assay. The mean concentrations of IL-1β in MEE were 201 ± 12 pg/mL (n = 10) in endotoxin-injected ears and 18 ± 12 pg/mL (n = 4) in PBS-injected ears. The concentration of IL-1β in MEE was significantly higher in endotoxin-injected ears than it was in PBS-injected ears ($p < .01$, Student's *t*-test).

Inhibition of Endotoxin-Induced OME With Anti–IL-1 Receptor Antibodies. Production of MEE was observed in all ears injected with endotoxin (n = 14) and was not observed in any ears injected with PBS (n = 10). We found MEE in 6 of 12 ears injected with 1 μg of type I IL-1 receptor antibody and 2.5 μg of type II IL-1 receptor antibody together with endotoxin. The incidence of MEE in ears inoculated with endotoxin together with type I and type II receptor antibodies was significantly lower than that

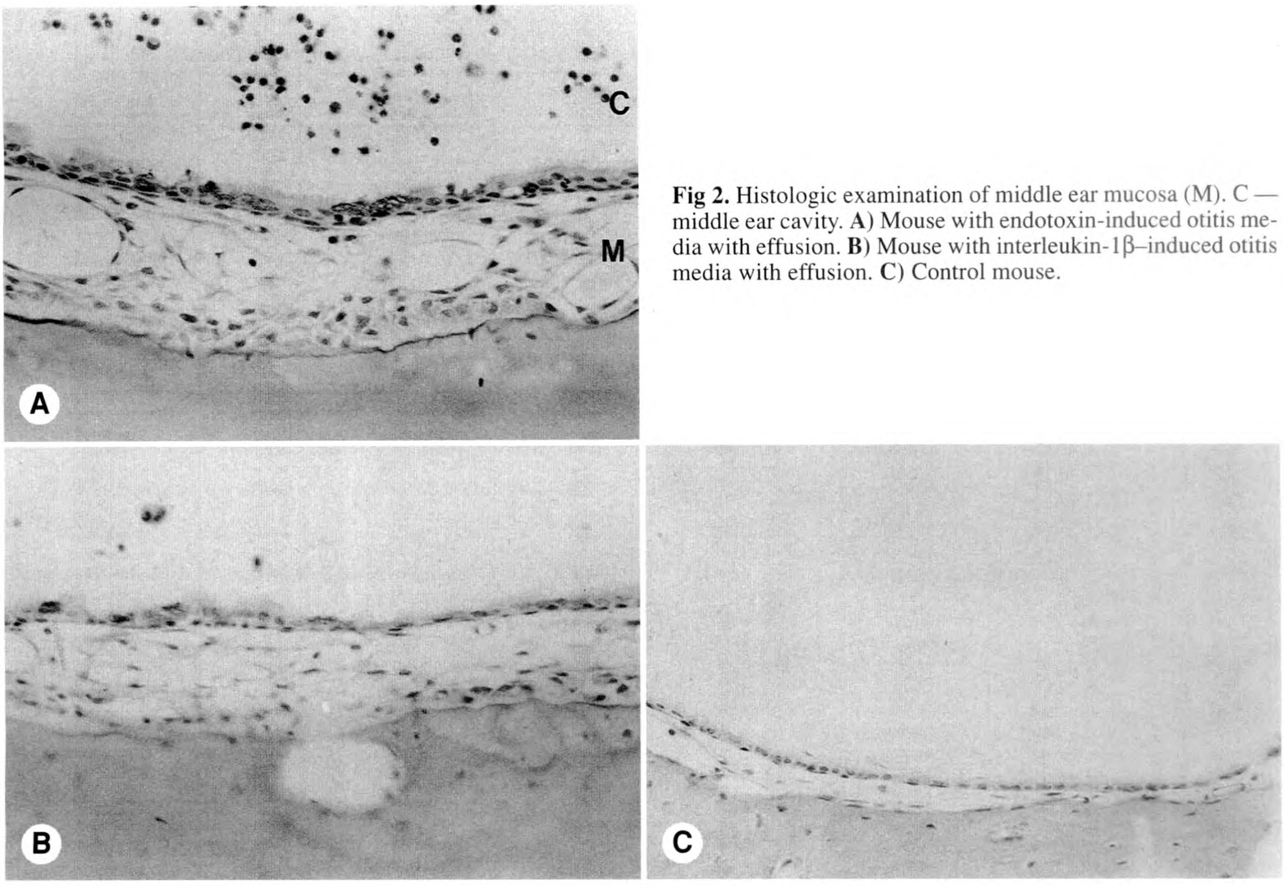

Fig 2. Histologic examination of middle ear mucosa (M). C — middle ear cavity. **A**) Mouse with endotoxin-induced otitis media with effusion. **B**) Mouse with interleukin-1β–induced otitis media with effusion. **C**) Control mouse.

in ears inoculated with endotoxin alone ($p < .01$).

The mucosal thickness of the anterior part of the tympanic bulla (Fig 1A) was 81.4 ± 12.8 µm in the endotoxin-injected group, 70.1 ± 16.8 µm in the group injected with endotoxin and receptor antibody, and 38.6 ± 16.6 µm in the group injected with PBS. The mucosal thickness of the posterior part of the tympanic bulla (Fig 1B) was 66.7 ± 11.7 µm in the endotoxin-injected group, 43.4 ± 14.4 µm in the endotoxin-plus-receptor-antibody–injected group, and 29.9 ± 2.3 µm in the PBS-injected group. At the inner tympanic orifice of the eustachian tube (Fig 1C), the mucosal thickness was 97.5 ± 11.3 µm in the endotoxin-injected group, 84.2 ± 21.1 µm in the endotoxin-plus-receptor-antibody–injected group, and 45.5 ± 11.0 µm in the PBS-injected group. The mucosal thickness of the outer tympanic orifice (Fig 1C) was 75.5 ± 4.6 µm in the endotoxin-injected group, 54.8 ± 11.6 µm in the endotoxin-plus-receptor-antibody–injected group, and 29.3 ± 10.3 µm in the PBS-injected group. The epithelial and subepithelial thicknesses were also decreased in the middle ear mucosa of ears inoculated with endotoxin together with

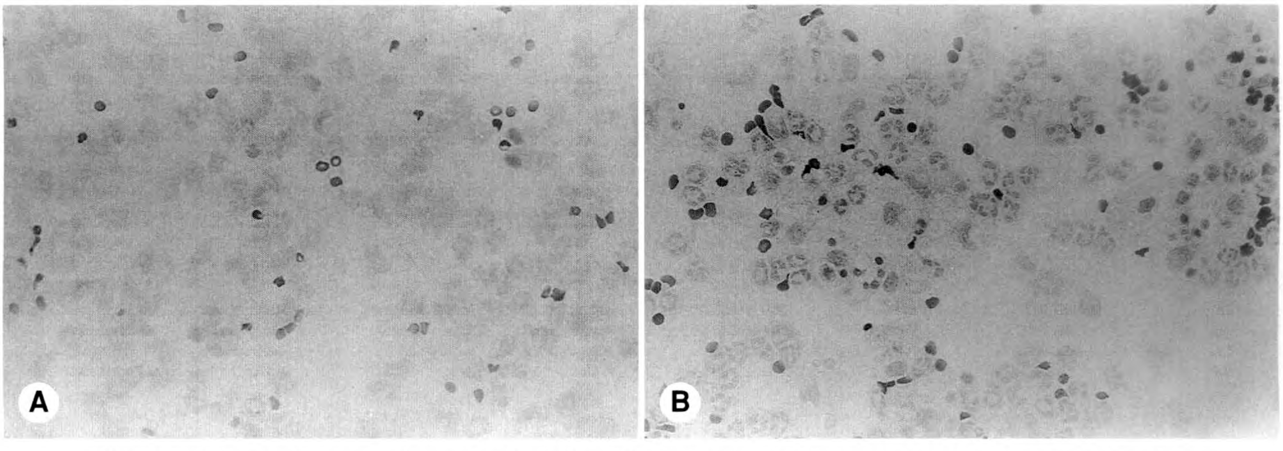

Fig 3. Cells in middle ear effusions of otitis media with effusion induced by **A**) endotoxin or **B**) interleukin-1β.

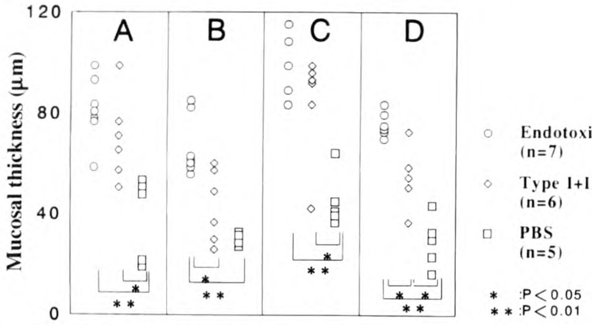

Fig 4. Mucosal thickness. **A)** Anterior portion of tympanic bulla. **B)** Posterior portion of tympanic bulla. **C)** Inner side of tympanic orifice of eustachian tube. **D)** Outer side of tympanic orifice of eustachian tube. Endotoxin — middle ear mucosa from ears inoculated with endotoxin only; Type I+II — middle ear mucosa from ears inoculated with endotoxin plus type I and type II receptor antibodies; PBS — middle ear mucosa from ears inoculated with phosphate-buffered saline solution only; n — number of mice. Statistical analysis was performed with Mann-Whitney U test.

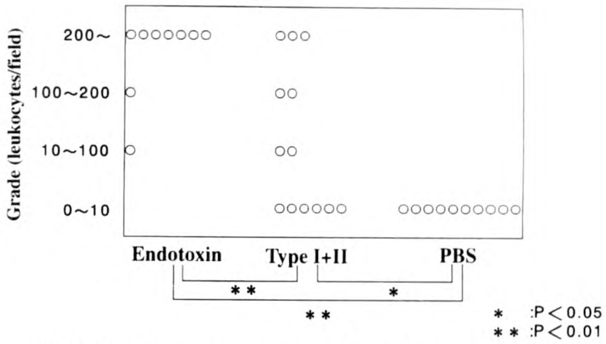

Fig 5. Number of neutrophils in MEE. Endotoxin — effusion from ears inoculated with endotoxin only; Type I+II — effusion from ears inoculated with endotoxin plus type I and type II receptor antibodies; PBS — effusion from ears inoculated with phosphate-buffered saline solution only. Statistical analysis was performed with Mann-Whitney U test.

type I and type II receptor antibodies in comparison to thicknesses in mucosa from ears inoculated with endotoxin alone (Fig 4).

The numbers of neutrophils were higher in MEEs collected from ears inoculated with endotoxin alone than in MEEs collected from ears inoculated with endotoxin plus type I and type II receptor antibodies (Fig 5).

In Situ Hybridization. Expression of IL-1β messenger RNA (mRNA) was observed in the epithelium of the middle ear mucosa of mice inoculated with endotoxin (Fig 6). No IL-1β mRNA was detected in

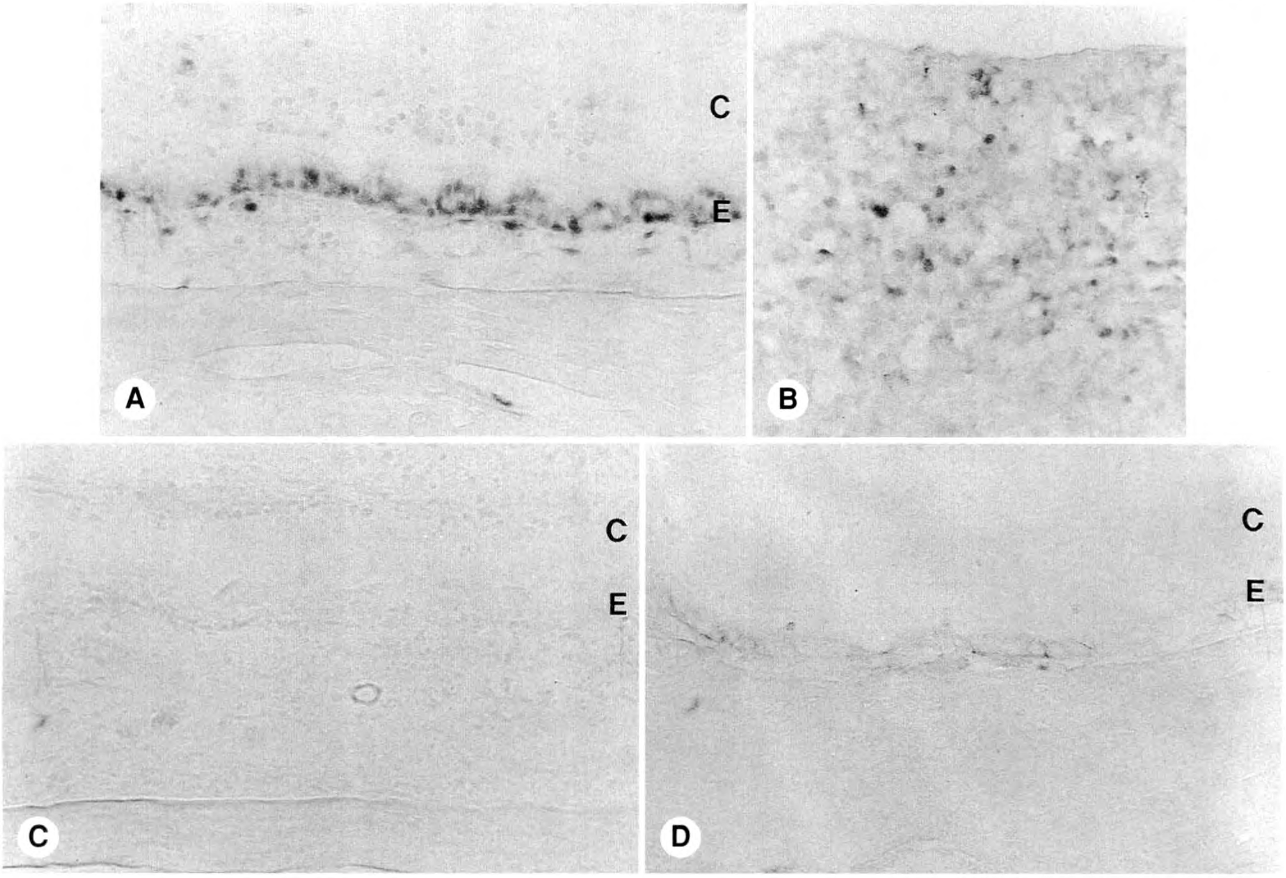

Fig 6. Interleukin-1β messenger RNA expression in middle ear mucosa. **A)** Mouse with endotoxin-induced otitis media with effusion. **B)** Positive control. **C)** Negative control (negative probe). **D)** Mouse with injection of phosphate-buffered saline solution. C — middle ear cavity, E — epithelium of middle ear mucosa.

the epithelia of the middle ear mucosa of PBS-injected ears or untreated ears.

DISCUSSION

In the present study, mice were used as the experimental animals, and the induction of OME was demonstrated by intratympanic injection with endotoxin isolated from nontypeable *H influenzae*. Further, OME was induced by intratympanic injection with rIL-1β, and the histologic and cytologic findings were similar to those in ears with endotoxin-induced OME. Mice are more suitable for immunologic and molecular biological analyses than other animals, because many immunologic agents for them are available commercially. Johnson et al[15] also developed a murine model of OME by eustachian tube blockage and immunohistochemically demonstrated IL-1α expression in the middle ear.

The effects of IL-1β on the induction of MEE have been investigated in animals other than mice. Johnson et al[16] used a chinchilla model of otitis media induced by injection of heat-killed *Streptococcus pneumoniae* after surgical blockage of the eustachian tube. They demonstrated a significant correlation between IL-1β and the presence of MEE. On the other hand, Catanzaro et al[17] injected human rIL-1β into the middle ear of guinea pigs transtympanically, but they did not succeed in inducing otitis media. They hypothesized that human rIL-1 does not activate IL-1 receptors in guinea pigs. Thus, the role of IL-1β in animal models of OME is still controversial.

In order to investigate the role of IL-1β in endotoxin-induced OME, we injected anti–IL-1 receptor antibodies with endotoxin. The results showed that anti–IL-1 receptor antibodies reduced the incidence of OME and pathological changes of the middle ear mucosa. However, the dose of IL-1β injected into the middle ears of the mice was much higher than that detected in the human MEE, and the inhibition of endotoxin-induced OME by anti–IL-1 receptor antibody was not complete. Ball et al[18] investigated the role of IL-1 by injecting IL-1β receptor antagonist in rats with endotoxin-induced OME. Since IL-1 receptor antagonist did not significantly alter the production of MEE, they suggested that IL-1 was not associated with the production of MEE in this model of OME. Those findings suggest that inflammatory factors other than IL-1β might be associated with the induction of OME. For example, DeMaria and Murwin[19] reported that endotoxin induced tumor necrosis factor production locally in the middle ear of chinchillas. The production and action of IL-1 could be regulated by multiple pathways, although IL-1β might be one of the factors that participate in the pathogenesis of MEE.

That the concentration of IL-1β in MEE was elevated in the endotoxin-injected ears suggests that IL-1β was produced locally in the middle ear cavity. In order to clarify which cells are responsible for the production of IL-1β, we applied in situ hybridization. The results showed the expression of IL-1β mRNA in the middle ear epithelia. This is the first study to demonstrate the expression of IL-1β mRNA in the middle ear mucosa of an animal model of OME. Previous studies have demonstrated that airway epithelium can be the source of production of IL-1β.[20,21] Those findings suggest that IL-1β could be produced by inflamed middle ear mucosa, as well as macrophages and monocytes, by stimulation with endotoxin.

In summary, OME was induced in mice by injection with endotoxin isolated from nontypeable *H influenzae* in mice. In this animal model, the concentration of IL-1β in MEE was elevated, and IL-1β mRNA was detected in the middle ear epithelium by in situ hybridization. Further, OME was induced by intratympanic injection of murine rIL-1β and was partially inhibited by injection of anti–IL-1 receptor antibodies. The findings suggest that IL-1β might be associated with the pathogenesis of OME. Further, a new strategy targeting cytokines such as IL-1β might be applicable to the treatment of OME.

REFERENCES

1. Bernstein JM, Praino MD, Neter E. Detection of endotoxin in ear specimens from patients with chronic otitis media by means of the limulus amebocyte lysate test. Can J Microbiol 1980;26:546-8.

2. DeMaria TF, Prior RB, Briggs BR, Lim DJ, Birck HG. Endotoxin in middle-ear effusions from patients with chronic otitis media with effusion. J Clin Microbiol 1984;20:15-7.

3. Iino Y, Kaneko Y, Takasaka T. Endotoxin in middle ear effusions tested with *Limulus* assay. Acta Otolaryngol (Stockh) 1985;100:42-50.

4. DeMaria TF, Briggs BR, Lim DJ, Okazaki N. Experimental otitis media with effusion following middle ear inoculation of nonviable *H influenzae*. Ann Otol Rhinol Laryngol 1984;93:52-6.

5. Nonomura N, Nakano Y, Satoh Y, Fujioka O, Niijima H, Fujita M. Otitis media with effusion following inoculation of *Haemophilus influenzae* type b endotoxin. Arch Otorhinolaryngol 1986;243:31-5.

6. Ohashi Y, Nakai Y, Ikeoka H, Esaki Y, Ikeoka H, Kato S, Kato M. Experimental otitis media with effusion induced by lipopolysaccharide from *Klebsiella pneumoniae*: mucociliary pathology of the middle ear. Am J Otolaryngol 1988;9:83-9.

7. Kilian PL, Otterness IG. Cytokines and inflammation. In: Lewis AJ, Doherty NS, Ackerman NR, eds. Therapeutic approaches to inflammatory disease. New York, NY: Elsevier, 1989:14-7.

8. Shaw RJ, Clark RA. Interleukins and their interactions in inflammation. In: Heusen PM, Murphy RC, eds. Handbook of inflammation. Vol 6. New York, NY: Elsevier, 1989:245-67.

9. Yellon RF, Leonard G, Marucha PT, et al. Characterization of cytokines present in middle ear effusions. Laryngoscope 1991;101:165-9.

10. Juhn SK, Tolan CT, Garvis WJ, Cross DS, Giebink GS. The levels of IL-1β in human middle ear effusions. Acta Otolaryngol Suppl (Stockh) 1992(suppl 493):37-42.

11. Himi T, Suzuki T, Kodama H, Takezawa H, Kataura A. Immunologic characteristics of cytokines in otitis media with effusion. Ann Otol Rhinol Laryngol Suppl 1992;101(suppl 157): 21-5.

12. Maxwell KS, Fitzgerald JE, Burleson JA, Leonard G, Carpenter R, Kreutzer DL. Interleukin-8 expression in otitis media. Laryngoscope 1994;104:989-95.

13. Willett DN, Rezaee RP, Billy JM, Tighe MB, DeMaria TF. Relationship of endotoxin to tumor necrosis factor–α and interleukin-1β in children with otitis media with effusion. Ann Otol Rhinol Laryngol 1998;107:28-33.

14. Westphal O, Jann K. Bacterial lipopolysaccharides. In: Whisler RL, ed. Methods in carbohydrate chemistry. Vol 15. San Diego, Calif: Academic Press, 1965:83-91.

15. Johnson MD, Contrino A, Contrino J, Maxwell K, Leonard G, Kreutzer DL. Murine model of otitis media with effusion: immunohistochemical demonstration of IL-1α antigen expression. Laryngoscope 1994;104:1143-9.

16. Johnson MD, Fitzgerald JE, Leonard G, Burleson JA, Kreutzer DL. Cytokines in experimental otitis media with effusion. Laryngoscope 1994;104:191-6.

17. Catanzaro A, Ryan A, Batscher S, Wasserman SI. The response to human rIL-1, rIL-2, and rTNF in the middle ear of guinea pigs. Laryngoscope 1991;101:271-5.

18. Ball SS, Prazma J, Dais CGD, Triana RJ, Pillsbury HC. Role of tumor necrosis factor and interleukin-1 in endotoxin-induced middle ear effusions. Ann Otol Rhinol Laryngol 1997; 106:633-9.

19. DeMaria TF, Murwin DM. Tumor necrosis factor during experimental lipopolysaccharide-induced otitis media. Laryngoscope 1997;107:369-72.

20. Devalia JL, Campbell AM, Sapford RJ, et al. Effect of nitrogen dioxide on synthesis of inflammatory cytokines expressed by human bronchial epithelial cells in vitro. Am J Respir Cell Mol Biol 1993;9:271-8.

21. Lindberg K, Rynnel-Dagöö B, Sundqvist KG. Cytokines in nasopharyngeal secretions; evidence for defective IL-1β production in children with recurrent episodes of acute otitis media. Clin Exp Immunol 1994;97:396-402.

Ann Otol Rhinol Laryngol 110:2001

BELL'S PALSY: ELECTRODIAGNOSTICS ARE NOT INDICATIVE OF CEREBROSPINAL FLUID ABNORMALITIES

CHRISTIANE BIRKMANN, MD
STEPHAN BAMBORSCHKE, MD
MARCO HALBER, MD
WALTER F. HAUPT, MD
COLOGNE, GERMANY

Electrodiagnostic testing (electromyography, electroneuronography, and blink reflex) and cerebrospinal fluid (CSF) examination (cell count, immunoglobulins, and antigen-specific intrathecal immunoglobulin G synthesis against herpes simplex virus, varicella zoster virus, cytomegalovirus, and *Borrelia burgdorferi sensu latu*) were performed in 56 patients with Bell's palsy. The CSF was normal in 45 patients and abnormal in 11 patients. Acute borreliosis was the most common specific pathological CSF finding (4 of 11). Electromyography revealed abolished volitional activity in 22% of patients with normal CSF and in 36% with pathological CSF. Electroneuronographic tests with an amplitude decrease of more than 90% on the affected side or abolished responses were found in 20% of patients with normal CSF and in 18% with pathological CSF. Abolished orbicularis oculi reflexes were seen in 67% of patients with normal CSF and in 82% with pathological CSF. Concerning electrodiagnostic testing, no statistically significant difference between patients with normal and abnormal CSF was found, so we conclude that electrodiagnostic testing has no indicative value for abnormal CSF in Bell's palsy.

KEY WORDS — Bell's palsy, cerebrospinal fluid, electrodiagnostics.

INTRODUCTION

With an incidence of 0.2 per 1,000 inhabitants in northern Europe, Bell's palsy is a common disease of all ages.[1] Although the cause is still unknown, viral infections, in particular of the herpes virus group, are discussed.[2-8] In recent years, *Borrelia burgdorferi* has also been found to be a causative agent.[9-12] A correct diagnosis is important, since treatment differs with the various causes and early treatment provides the best chance of a favorable outcome. The purpose of this study was to establish 1) to what extent patients with Bell's palsy have abnormal cerebrospinal fluid (CSF) findings indicating inflammatory nervous system involvement and 2) whether patients with pathological CSF findings show any differences in their clinical or electrodiagnostic findings from patients with normal CSF.

MATERIAL AND METHODS

We examined 56 consecutive adult patients with Bell's palsy between 1995 and 1997. We included only patients with acute, isolated, unilateral facial palsy in whom a lumbar puncture and electrodiagnostic testing were performed within 14 days after onset of disease. Patients with symptomatic facial palsy, such as trauma, tumor, a middle ear cause, Ramsay-Hunt syndrome, or herpes zoster infection, were excluded. Patients with diseases such as diabetes mellitus, malignancies, or chronic inflammatory disease were excluded.

The following features were recorded: side and number of days between the onset of palsy and the examination, retroauricular pain, and diminished taste sense. All patients underwent clinical examination for neurological status and examination of eyes and ears; herpes vesicles were sought. Computed tomography or magnetic resonance imaging of the brain was performed in all patients. The grade of the facial palsy was assessed with Stennert's grading scale and was scored as mild, moderate, or severe or total.[13]

A CSF cell count was performed with phase contrast microscopy and the Fuchs-Rosenthal chamber. Albumin and immunoglobulins G, M, and A were measured in unconcentrated CSF and serum by laser nephelometry. The function of the blood-CSF barrier and the amount of intrathecally synthesized immunoglobulins were determined with CSF and serum ratios of albumin and immunoglobulins according to Reiber and Felgenhauer.[14] Intrathecal IgG synthesis was also determined by isoelectric focusing of CSF and serum with polyacrylamide electrophoresis and silver staining for detection of oligoclonal bands. Antigen-specific intrathecal IgG synthesis against herpes simplex virus, varicella zoster virus, cytomegalovirus, and *Borrelia burgdorferi sensu latu* was determined by a standard enzyme-linked immunosorbent assay (ELISA) in corresponding CSF and serum samples that were diluted to identical IgG concentrations of 1

From the Department of Neurology, University of Cologne, Cologne, Germany.

CORRESPONDENCE — Christiane Birkmann, MD, Dept of Neurology, University of Cologne, Joseph-Stelzmann-Str 9, D 50924 Cologne, Germany.

mg/dL. Specific IgM antibodies against *B burgdorferi sensu latu* were only detected in blood sera by ELISA, and positive results were checked by Western blot.

Standard electromyography (EMG) was performed in the frontalis and orbicularis oris muscles of the affected side.[15] The facial nerve was electrically stimulated with supramaximal-intensity electroneuronography (ENoG) at the stylomastoid foramen. The compound muscle action potential (CMAP) was recorded from a surface electrode placed on the orbicularis oris and frontalis muscles in order to calculate the ratio between the amplitude of the CMAP on the affected side and that on the normal side.[16] The blink reflex was examined with percutaneous electrical stimulation at the supraorbital foramen and surface EMG recording at both orbicularis oculi muscles.[17,18] The electrodiagnostic results were classified as normal, pathological, or abolished responses. Electroneuronography tests with an amplitude decrease of more than 90% were graded as abolished responses.

The Mann-Whitney 2-tailed rank test was used for comparison between groups.

RESULTS

We studied 56 adult patients (32 men and 24 women). The palsy was mild in 7 patients (13%), moderate in 18 (32%), and severe or total in 31 (55%). Thirty-nine patients had retroauricular pain, and the taste sense was impaired in 33 patients. Cerebral computed tomography and magnetic resonance imaging disclosed no disorders related to the facial palsy.

CSF Findings. The CSF was normal in 45 patients (80%) and abnormal in 11 patients (20%). Six patients demonstrated an isolated mononuclear pleocytosis ranging from 5 to 31 cells per microliter (median, 15 cells per microliter). In 2 patients, we detected a mild pleocytosis (4 and 5 cells per microliter) in CSF in combination with positive IgM antibodies against *B burgdorferi* in blood serum. Two patients showed a combination of CSF pleocytosis (10 and 38 cells per microliter), intrathecal IgG synthesis according to laser nephelometry, and a specific intrathecal IgG synthesis against *B burgdorferi*. One patient revealed specific intrathecal IgG synthesis against herpes zoster virus. All patients with mild palsy showed normal CSF, 2 patients (11%) with moderate palsy showed pathological CSF, and 9 patients (29%) with severe or total palsy had pathological CSF. There was no statistically significant difference between the groups concerning the incidence of retroauricular pain (71% normal CSF, 64% pathological CSF) or of taste sense impairment (60% normal CSF, 55% pathological CSF).

Electrodiagnostic Testing. Seven patients demonstrated normal EMG results (6 with normal CSF, 1 with pathological CSF). Thirty-five patients showed pathological EMG findings (29 with normal CSF, 6 with pathological CSF), and 14 patients showed abolished volitional acitivity (10 with normal CSF, 4 with pathological CSF). Electroneuronography with an amplitude decrease of less than 50% on the affected side was found in 6 patients (all normal CSF), an amplitude decrease between 50% and 90% was found in 39 patients (30 with normal CSF, 9 with pathological CSF), and an amplitude decrease of more than 90% or an abolished response was found in 11 patients (9 with normal CSF, 2 with pathological CSF). No patient had a normal blink reflex. Seventeen patients showed a pathological reflex response (15 with normal CSF, 2 with pathological CSF), and abolished blink reflexes were seen in 39 patients (30 with normal CSF, 9 with pathological CSF). There were no statistically significant differences between the patients with normal CSF and those with pathological CSF concerning electrodiagnostic testing.

DISCUSSION

Electrodiagnostic testing and CSF examination were performed in 56 patients with Bell's palsy. We examined only patients whose clinical data, ie, history and examination, suggested an "idiopathic" facial palsy. In 80% of these patients, the CSF was normal; however, 20% had pathological CSF findings. For the 11 abnormal CSF results, an explanation could be found in 5 cases, and 6 cases remained unexplained.

In a study of 230 patients with idiopathic facial palsy, Kohler et al[19] reported abnormal CSF in 11% of the cases. An explanation could be found in 5 of these 29 cases, while 24 of the 29 remained unexplained.[19] Roberg et al[20] examined 56 patients with Bell's palsy and found CSF pleocytosis in 15% and an elevation of intrathecal immunoglobulins in 30% of their cases. Weber et al,[21] who examined 62 patients with Bell's palsy, noted abnormal CSF in 25%. The most common pathological finding was a slightly impaired blood-CSF barrier, and pleocytosis was found in 7 of the 62 patients.[21]

In our study, Lyme disease was the most common specific pathological CSF finding. Four of 11 patients had an acute infection with *Borrelia*, with mononuclear CSF pleocytosis and serum *Borrelia* IgM antibodies in 2 cases, and intrathecal antibody synthesis in another 2 patients. Isolated facial palsy in Lyme disease is a difficult problem. Often, the facial paresis is accompanied by more diffuse symptoms, such as arthralgia or meningoradiculitis.[22] If a peripheral facial palsy is the only symptom, the diagnosis can be missed. Furthermore, positive serology for *Borrelia* does not necessarily imply that the palsy is due to Lyme disease, since a high percentage of the population in high-risk areas demonstrates positive serology.[23] Nevertheless, diagnosis of underlying borreliosis is important, because a specific treatment is necessary for fast recovery and to avoid other manifestations. Jonsson et al[12] note that CSF examination gives earlier results than serologic blood tests in borreliosis and recommend CSF examination if borreliosis is suspected. Hydén et al[5] reported 3 patients with isolated facial palsy and normal serology who demonstrated elevated CSF titers to *Borrelia*. Similar findings were noted by Roberg et al[20] in a group of 56 patients with acute facial paresis in which 2 cases were due to borreliosis and showed normal serum parameters. Neither patient had a history of a tick bite or erythema migrans, and without a CSF examination, the diagnosis would have been missed.[20]

One patient in our series demonstrated intrathecal herpes zoster antibody synthesis without showing any vesicles in the course of the disease. Serology is often not useful at the beginning of the paresis, but rapid diagnosis is important, since early treatment with acyclovir and prednisone is effective.[19,24]

Concerning electrodiagnostic testing (EMG, ENoG, and blink reflex), we investigated whether there are any differences between patients with normal CSF and those with pathological CSF to indicate a probable symptomatic palsy. No statistically significant difference between the two groups was found, so we conclude that electrodiagnostic testing has no indicative value for abnormal CSF in Bell's palsy. Transcranial magnetic stimulation within the canalicular portion of the facial nerve and on the contralateral motor cortex in combination with ENoG seems to be more specific in separating different causes.[25,26] As it is a relatively new approach, it was not used in our series. Concerning clinical features, neither retroauricular pain nor taste sense impairment showed any significant differences between the two groups of patients.

CONCLUSION

Twenty percent of our patients with Bell's palsy had abnormal CSF, as did 29% of patients with severe or total paresis. The leading symptomatic cause was acute borreliosis. Electrodiagnostic testing had no indicative value for abnormal CSF. A CSF examination in Bell's palsy is necessary for early detection of symptomatic forms, which require fast and specific treatment.

REFERENCES

1. Devriese PP, Schumacher T, Scheide A, de Jongh RH, Houtkooper JM. Incidence, prognosis, and recovery of Bell's palsy: a survey of about 1000 patients (1974-1983). Clin Otolaryngol 1990;15:15-27.
2. Adour KK, Bell DN, Hilsinger PL. Herpes simplex virus in idiopathic facial paralysis (Bell's palsy). JAMA 1975;233:527-30.
3. Schirm J, Mulkens PS. Bell's palsy and herpes simplex virus. APMIS 1997;105:815-23.
4. Murakami S, Mizobuchi M, Nakashiro Y, Doi T, Hato N, Yanagihara N. Bell's palsy and herpes simplex virus: identification of viral DNA in endoneurial fluid and muscle. Ann Intern Med 1996;124:27-30.
5. Hydén D, Roberg M, Forsberg P, et al. Acute "idiopathic" peripheral facial palsy: clinical, serological, and cerebrospinal fluid findings and effects of corticosteroids. Am J Otolaryngol 1993;14:179-86.
6. Adour KK. Otological complications of herpes zoster. Ann Neurol 1994;35(suppl):S62-S64.
7. Djupesland G, Berdal P, Johannessen TA, Degré M, Stien R, Skrede S. Viral infection as a cause of acute peripheral palsy. Arch Otolaryngol 1976;102:403-6.
8. Hadar T, Tovi F, Sidi J, Sarov B, Sarov I. Specific IgG and IgA antibodies to herpes simplex virus and varicella zoster virus in acute peripheral facial palsy. J Med Virol 1983;12:237-45.
9. Kuiper H, Devriese PP, de Jongh BM, Vos K, Dankert J. Absence of Lyme borreliosis among patients with presumed Bell's palsy. Arch Neurol 1992;49:940-3.
10. Clark JR, Carlsson RD, Sasaki CT, Pachner AR, Steere AC. Facial palsy in Lyme disease. Laryngoscope 1985;95:1341-5.
11. Jonsson L, Stiernstedt G, Thomander L. Tick-borne *Borrelia* infection in patients with Bell's palsy. Arch Otolaryngol Head Neck Surg 1987;113:303-6.
12. Jonsson L, Stiernstedt G, Carlson J, Stromberg A, Sjoberg O, Larsson A. Serum and cerebrospinal fluid examinations in the diagnosis of *Borrelia* infection in Bell's palsy. Acta Otolaryngol (Stockh) 1990;110:421-6.
13. Stennert E, Limberg CH, Frentrup KF. Parese- und Defektheilungsindex. Ein leicht anwendbares Schema zur objektiven Bewertung von Therapieerfolgen bei Fazialisparesen. HNO 1977;25:238-45.
14. Reiber H, Felgenhauer K. Protein transfer at the blood cerebrospinal fluid barrier and the quantitation of the humoral immune response within the central nervous system. Clin Chim Acta 1987;163:319.
15. Malin JP. Neurologische Diagnostik des Nervus facialis. In: Hopf HC, Poeck K, Schliack H, eds. Neurologie in Klinik und Praxis. Vol 3. Stuttgart, Germany: Thieme, 1993:109-12.
16. Vogel P, Bahlmann W. Zur Elektroneurographie des N. facialis. Akt Neurol 1990;17:150-7.
17. Ghonim MR, Gavilan C. Blink reflex: prognostic value in acute peripheral facial palsy. ORL J Otorhinolaryngol Relat Spec 1990;52:75-9.
18. Heath JP, Cull RE, Smith IM, Murray JAM. The neurophysiological investigation of Bell's palsy and the predictive value of the blink reflex. Clin Otolaryngol 1988;13:85-92.

Ann Otol Rhinol Laryngol 110:2001

TOPICAL ASCORBIC ACID REDUCES MYRINGOSCLEROSIS IN PERFORATED TYMPANIC MEMBRANES

A STUDY IN THE RAT

JORGE E. SPRATLEY, MD
PORTO, PORTUGAL

STEN O. HELLSTRÖM, MD, PHD
UMEÅ, SWEDEN

CECILIA K. MATTSSON, MD, PHD
UMEÅ, SWEDEN

MANUEL PAIS-CLEMENTE, MD, PHD
PORTO, PORTUGAL

Myringosclerosis, a common finding after myringotomy, has been recently associated with an increased production of oxygen free radicals. Ascorbic acid's proposed actions include collagen synthesis, antioxidation, and free radical scavenging. The effects of topical ascorbic acid on healing tympanic membranes were studied. Particular attention was given to detecting the presence of myringosclerosis. Twelve Sprague-Dawley rats were bilaterally myringotomized. Their ears were randomized into group A, which received topical ascorbic acid in Gelfoam, group B, which received topical saline solution in Gelfoam, and group C, which received no treatment. The tympanic membranes were harvested on day 13, after routine otomicroscopy. Under light microscopy, the connective tissue layer of the untouched side of the pars tensa was distinctly thicker in group A than in group B or group C. At this level, the extent of sclerotic lesions was significantly less in the ascorbic acid–treated group. It is inferred that topical ascorbic acid reduces the occurrence of myringosclerosis following tympanic membrane perforations in the rat.

KEY WORDS — ascorbic acid, myringosclerosis, myringotomy, rat, tympanic membrane, vitamin C.

INTRODUCTION

An intact and vibrating tympanic membrane (TM) is of the utmost importance for the normal physiology of hearing. Its movement is hampered by lesions of sclerotic material, as seen after ventilation tube placement. Previous animal experiments suggest an intimate relationship between the formation of myringosclerosis (MyS) and an increased concentration of oxygen in the environment of the wound following myringotomy.[1] Further, the development of sclerotic lesions could be prevented by topical application of oxygen free radical scavengers.[2]

Ascorbic acid (AscA), synonymous with vitamin C, participates in roles in health maintenance as diverse as leukocyte activity,[3,4] nonheme iron absorption,[5] eye defense from ultraviolet light,[6] and possible protection against cancer.[7] The ability of this molecule to protect against free radical–mediated tissue damage is well acknowledged.[8,9] Furthermore, the effect of AscA on wound healing has been extensively studied in different structures — for example, the colon,[10] cornea,[11] skin,[12] and gingiva.[13] Ascorbic acid seems to actively participate in different steps of the synthesis and formation of connective tissue, such as collagen gene expression and hydroxylation with an increased secretion of collagen in parallel with an augmented production of some of the matrix glycoproteins.[14]

In recent years, an increasing interest has focused on the possibility of interfering with the healing of TM perforations through topical application of bioactive substances.[15-17] Although a few studies were published in the Japanese literature regarding the metabolism of AscA in the ear during chronic inflammation,[18,19] to our knowledge there is a lack of reports focusing on the use of AscA on the healing TM.

The purpose of the present investigation was to study the effects of topical application of AscA after myringotomy, with particular attention to the development of MyS.

MATERIAL AND METHODS

Twelve healthy male Sprague-Dawley rats, of the same age and weighing 250 to 300 g, were used for the study. All animals were kept under standard laboratory conditions and were given pellets and water ad libitum without any vitamin restriction. The research protocol was in compliance with the Institutional Committee for the Care and Use of Labora-

---

From the Department of Otorhinolaryngology, University Hospital of Umeå, Umeå, Sweden (Spratley, Hellström, Mattsson), and the Department of Otorhinolaryngology, University of Porto Medical School, Porto, Portugal (Spratley, Pais-Clemente). Supported in part by grants from the Swedish Medical Research Council No. 06758, the Swedish Society for Medical Research, the Medical Faculty of Umeå University, and the Comissão de Fomento da Investigação em Cuidados de Saúde do Ministério da Saúde de Portugal.

CORRESPONDENCE — Jorge E. Spratley, MD, Dept of Otorhinolaryngology, University of Porto Medical School, Hospital de S. João, 4200 Porto, Portugal.

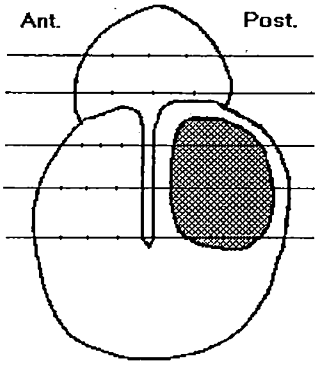

Fig 1. Schematic drawing represents rat tympanic membrane and standardized area of perforation (shaded), levels of sectioning (horizontal lines), and spots selected for measurements (intersections).

tory Animals of the University of Umeå. For all of the procedures, the rats were anesthetized intravenously with a short-acting barbiturate, methohexital sodium (Brietal; Eli-Lilly and Company, Indianapolis, Ind), via a tail vein. Under the otomicroscope, a perforation, standardized in size, occupying almost the entire superior rear quadrant of the TM, was made with a myringotomy lancet through an ear speculum.

Each ear was randomized to receive one of the following topical treatments immediately after the myringotomy (day 0): 1) group A (9 ears), which had covering of the perforation with a rounded pledget of Gelfoam (The Upjohn Co, Kalamazoo, Mich) soaked in a solution of 28-mmol/L AscA ($C_6H_8O_6$) in sterile water (pH 3); 2) group B (9 ears), in which the perforation was covered with Gelfoam soaked in sodium chloride 9 g/L; and 3) group C (6 ears), in which the perforation was left untouched.

The TM status was routinely evaluated under the otomicroscope by 2 observers simultaneously on days 1, 3, 5, 7, 10, and 13. The findings were documented on standardized protocol sheets. On days 1 and 3, group A and B ears received an additional topical treatment, through instillation of drops containing AscA and saline solution, respectively, over the residues of Gelfoam, through an ear speculum. Thirteen days after the myringotomy, the animals were painlessly sacrificed with an intraperitoneal overdose of pentobarbital sodium (Pentobarbitalnatrium, Apoteksbolaget, Stockholm, Sweden) and decapitated. The tympanic bulla was immediately dissected free, opened, and filled with a fixative solution containing 3% glutaraldehyde in 75-mmol/L sodium cacodylate buffer (pH 7.4) with 4% polyvinylpyrrolidone and 2-mmol/L calcium chloride added. After immersion in the fixative at 4°C for 24 hours, the TMs were dissected out in toto in continuity with the adjacent external ear canal skin under a stereomicroscope. After a brief rinsing in cacodylate buffer, the pars tensa and pars flaccida were separated from each other with a sharp scalpel and post-fixed overnight in 1% osmium tetroxide. The specimens were then dehydrated in increasing concentrations of ethanol and embedded in an epoxy resin (Polybed; Polysciences Inc, Warrington, Pa). For light microscopy, semithin sections (1 μm) were cut perpendicular to the handle of the malleus, collected, and stained with toluidine blue. Sections were prepared from 3 standardized levels of the upper quadrants of the pars tensa and from 2 levels of the pars flaccida. Under a light microscope equipped with an eyepiece micrometer scale, the distance from the handle of the malleus to the annulus was divided into 4 equal parts, in which the pars tensa thickness was measured (Fig 1). Each section of the pars flaccida was also divided into 4 parts, and the thickness was measured. A semiquantitative analysis of myringosclerotic deposits was performed on each section in a blinded manner with a 4-point scale: no visible MyS, occasional MyS, moderate MyS, and severe MyS. For transmission electron microscopic observations, ultrathin sections were cut and contrasted with uranyl acetate and lead citrate. The statistical significance of the results was tested with the χ^2 test, and with the 2-tailed Fisher exact test (2 groups) or the Kruskal-Wallis test (more than 2 groups) for unpaired samples.

RESULTS

Otomicroscopy. On day 1 after myringotomy, dilated vessels in the annular region, in the anterior and posterior tympanomalleolar folds, and extending along the handle of the malleus were noticed in all TMs. The vascular reaction was most intense in group A. White, chalky spots in the pars tensa could be distinguished in most of the nontreated controls and in a few of the saline-treated TMs. The sclerosis pattern occurred mainly on the noninjured side of the region around the umbo.

On day 3, an increase in vessel caliber was observed to be still more enhanced in the group A, AscA-treated TMs. A bulging yellow pars flaccida, representing the presence of effusion in the epitympanum, affected 2 of 3, 1 of 3, and 1 of 3 cases in groups A, B, and C, respectively. In 1 TM of group A, faint, whitish deposits of MyS were detected, and in all cases in groups B and C, whitish lesions were seen extending along the handle of the malleus.

On day 5, reactions at the borders of the perforations were observed. On TMs devoid of scaffolding, a spur of keratin, originating from the anterior-superior region of the myringotomy rim, was noticed. Two TMs of group A had spontaneously lost the Gelfoam pledget, and their perforation rims showed intense signs of keratin production together with a dark yel-

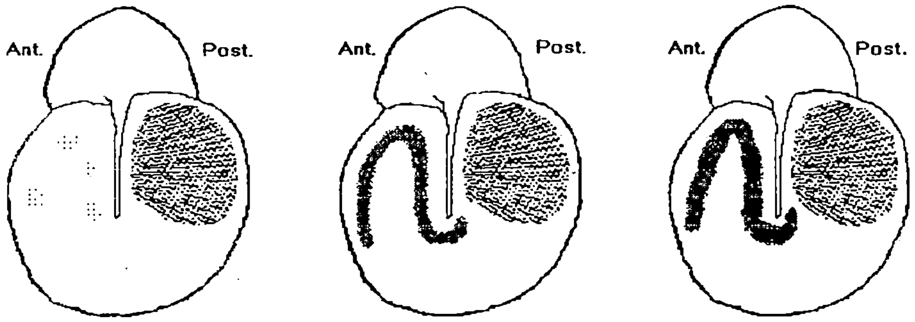

Ascorbic Acid (2/9)
Group A

Saline Solution (9/9)
Group B

No Treatment (6/6)
Group C

Fig 2. Schematic drawing depicts otomicroscopic distribution of myringosclerotic deposits on day 13, according to different treatment methods (groups A, B, and C). Note that myringosclerosis is located in anterior quadrant, and area of healed perforation is represented in posterior-superior quadrant. Numbers show number of eardrums with myringosclerosis per number of eardrums in group.

low color to this area. In groups B and C, the sclerotic lesions continued to increase in intensity and became more widespread along the handle of the malleus and also in the annulus region, still preferentially in the nonperforated quadrant. Two cases in group A were now also affected by MyS.

Postmyringotomy day 7 was characterized by a peak of vascular exuberance. For the first time, very thin capillaries, originating as branches from the annular and malleolar vessels, were noticed reaching the border of the perforation. The intensity of this vascular pattern was more evident in group A than in groups B and C. All perforations were reduced to less than half of their original size. An elevated circular rim of keratin was present in those cases without Gelfoam, and in the remaining cases, the gelatin sponge seemed to be deeply incorporated in the TM tissue.

On day 10, the numbers of closed perforations were 7 of 9, 6 of 9, and 3 of 6 in groups A, B, and C, respectively. The differences were not significant.

By day 13, all TMs were closed except for 1 in group A. This particular case was less than 10% of its initial size and exhibited an intense keratinization. In all other TMs, the area of the healed perforation was opaque — more markedly in groups A and B than in group C. The vascular reaction had almost vanished, although some capillaries could yet be detected in the vicinity of the traumatized area. The MyS deposits in group C, the nontreated cases, were confluent, forming a horseshoe-shaped pattern. This feature was less intense in the saline group and faint or nonexistent in the AscA-treated TMs (Fig 2). Only 2 cases in group A showed any signs of MyS, and then in small amounts. In the pars flaccida, no MyS could be observed with the otomicroscope.

TABLE 1. LIGHT MICROSCOPIC EVIDENCE OF MYRINGOSCLEROSIS IN PARS TENSA

	Myringosclerosis			
Group	*None*	*Occasional*	*Moderate*	*Severe*
A (ascorbic acid; n = 9)	6	1	2	
B (saline solution; n = 9)		1	5	3
C (no treatment; n = 6)			1	5

Light Microscopy. The amount of MyS in the pars tensa is depicted in Table 1. The most extensive MyS in the pars tensa specimens was found in the untreated ears (Fig 3). The MyS occurred predominantly in the region adjacent to the handle of the malleus, but also near the annular region. The MyS deposits were sometimes confluent and could be observed in the middle layer on both sides of the handle of the malleus, although they were more pronounced on the noninjured side. Similar findings were present in the TMs of the saline group (Fig 4). In contrast, only 3 specimens treated with AscA showed any light microscopic evidence of MyS, and then with few and scattered deposits. The occurrence of MyS deposits was significantly different between groups A (3/6) and B (9/0; $p < .01$) and between groups A (3/6) and C (9/0; $p < .03$), but the difference between groups B and C was not significant.

A significant variability in the TM thickness of the anterior-superior quadrants could also be distinguished (Table 2). The AscA-treated TMs were the most thickened (Fig 5). The thickening of the AscA TMs seemed mainly to be due to a swollen middle connective tissue layer. This layer showed an increased number of fibroblasts characterized by an increased nucleus-cytoplasm ratio, suggesting augmented metabolic activity. The reaction in the middle layer was slight in the saline group and negligible in the nontreated TMs.

The epithelial layers, both keratinizing and mucosal, appeared normal, except in the area previously perforated, in which single or double layers of keratinocytes with signs of an increased production of keratin, visible nuclei, and "pseudopodia" facing the basal lamina could be observed. An increased amount

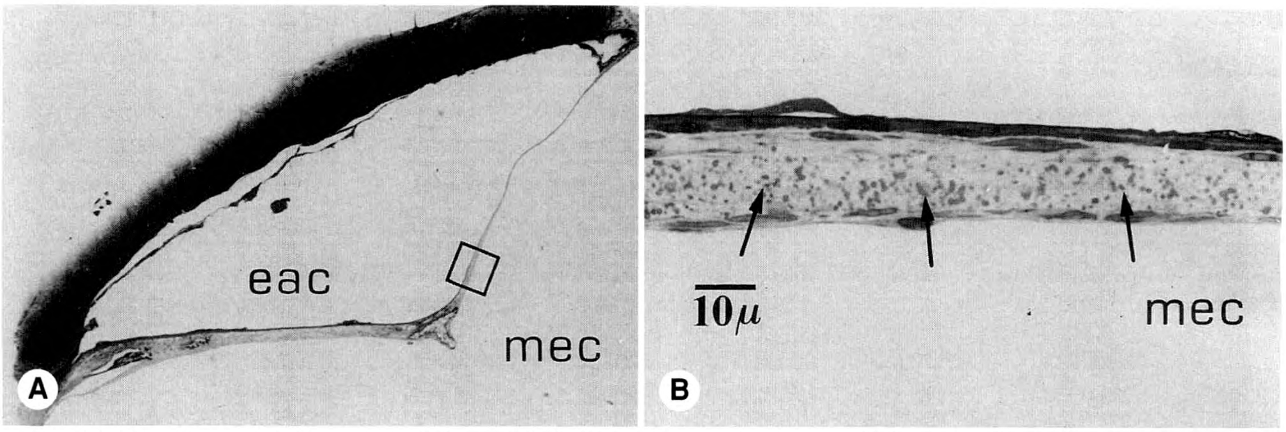

Fig 3. Light micrographs of pars tensa left untouched after myringotomy. mec — middle ear cavity. **A)** Survey micrograph (toluidine blue, original ×30). eac — External auditory canal. **B)** Detail of boxed area in A (toluidine blue, original ×550). Note extensive sclerotic lesions in lamina propria (arrows).

of keratin debris was detected inside the external auditory canal in group A.

In the majority of group A and B cases, islands of Gelfoam still persisted on the TM, undergoing a process of degradation. This process was accompanied by a foreign body–type reaction in which a glossy, structureless substance was being digested in the presence of macrophages, giant multinucleated cells, some mast cells, and fibroblasts, along with increased vascular proliferation. The inner mucosal layer cells were flat and, in some cases, slightly cuboidal.

The pars flaccida was quite similar in appearance in all groups. The outer keratinocyte layer looked thicker than in the pars tensa. The lamina propria was well developed, with a random distribution of collagen and elastic fibers in between fibroblasts and rare macrophages. Adjacent to the epidermal layer, mast cells could be seen in proximity to the capillaries and nerve fibers. Occasional MyS lesions were noticed in 3 of 9, 7 of 9, and 4 of 6 cases in groups A, B, and C, respectively. The sclerotic deposits were predominantly located close to the inner epithelial layer. The inner epithelium was flat, but was sometimes interrupted by ciliated mucosal cells. No intergroup differences could be detected in the thickness of the pars flaccida (Table 2).

Electron Microscopy. The MyS lesions in the pars tensa were localized in between the collagen fibers of the lamina propria. They were distributed among both fiber layers: the inner layer with circular fibers and the outer layer with radiating fibers. The majority of deposits were, however, in the latter layer. These lesions varied from granular, electron-dense deposits with an irregular surface to confluences of more rounded, globular, multilamellar structures (Fig 6).

In the pars flaccida, the MyS lesions, mostly of the round, multilamellar type, were predominantly located in the submucosal region.

DISCUSSION

In the present investigation, topical AscA application to the perforated TM of the rat was associated with a significant reduction of MyS in the pars tensa.

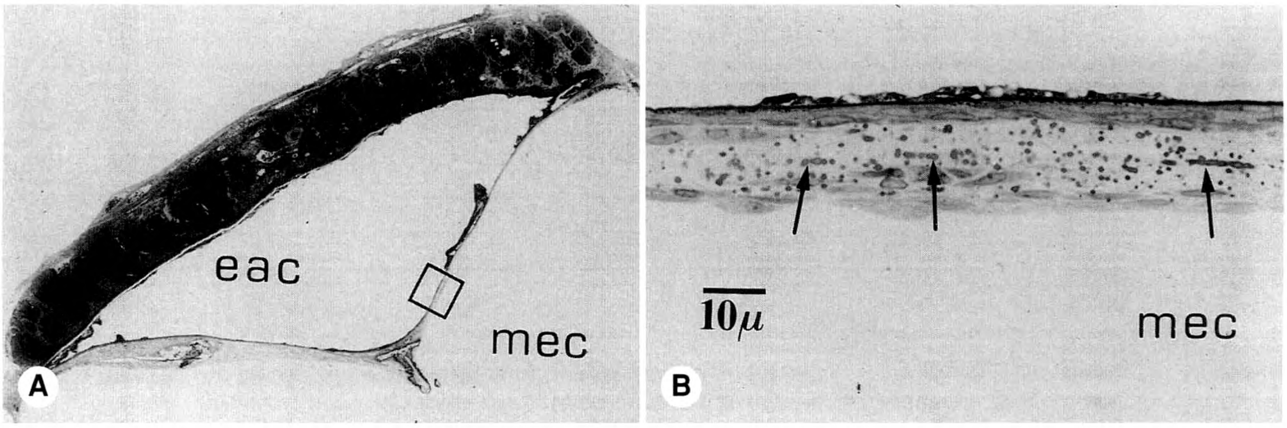

Fig 4. Light micrographs of pars tensa treated with topical application of saline solution after myringotomy. **A)** Survey micrograph (toluidine blue, original ×30). **B)** Detail of boxed area in A (toluidine blue, original ×550). Note abundant sclerotic lesions in lamina propria (arrows).

TABLE 2. TYMPANIC MEMBRANE THICKNESS AT DIFFERENT LEVELS OF ANTERIOR-SUPERIOR QUADRANT OF PARS TENSA AND OF PARS FLACCIDA

	Anterior-Superior Quadrant of Pars Tensa			*Pars Flaccida*	
Group	*1st Level*	*2nd Level*	*3rd Level*	*1st Level*	*2nd Level*
A (ascorbic acid; n = 9)	22.6 ± 9.3	27.6 ± 13.2	36.1 ± 14.6	67.4 ± 19.3	57.8 ± 15.5
B (saline solution; n = 9)	10.3 ± 4.0	10.7 ± 3.0	11.8 ± 2.7	62.3 ± 14.8	49.3 ± 11.1
C (no treatment; n = 6)	7.4 ± 2.0	10.2 ± 3.7	10.8 ± 2.4	66.2 ± 15.3	51.7 ± 9.0
	p = .0007	p = .0012	p = .0002	p = .898	p = .426

Data are mean ± SD in micrometers.

There are several explanations as to how AscA could prevent MyS. In the absence of adequate endogenous AscA, hydroxylated collagen tends not to accumulate within the cytoplasmic vacuoles of cells, consequently becoming more sensitive to degradation.[20] However, this degradation did not seem to occur in the present study, as increased extracellular connective tissue was detected, along with signs of an enhanced fibroblastic activity. Previous studies[21,22] suggested that sclerosis preferentially occurred in areas in which the connective tissue was more dense. Our results in part seem to confirm this hypothesis, as the MyS deposits in the pars tensa predominated in the saline-treated and nontreated cases that showed a thinner connective tissue layer. However, in the pars flaccida, where the connective tissue is typically more lax, we could still find MyS deposits in all groups. That the 2 distinct effects of AscA — increase of collagen and reduction of MyS — are coincidental cannot be excluded.

A connection between the low pH of the AscA solution used and the reduction of MyS deposits might also be considered. In an earlier report,[23] an acidic environment was associated with a reduction of sclerotic deposits in the TM.

An increased oxygen concentration in ears with traumatized TMs has been shown to increase the extent of MyS deposits.[1] Furthermore, data strongly support the importance of inflammation with production of oxygen free radicals in the pathogenesis of MyS.[24] This sequence was shown to be arrested in the presence of free radical scavengers in the injured tissue. Thus, the role of AscA as an antioxidant in the prevention of MyS is the most attractive hypothesis of all. However, a synergistic effect of the Gelfoam scaffolding on the prevention of MyS has to be considered, as this might protect the middle ear from an increased oxygen tension. This effect is likely, as the noncovered TMs showed the most intense deposits.

Also, according to Monboisse and Borel,[25] superoxide anion is capable of fragmenting collagen with secondary liberation of small peptides containing hydroxyproline. Ascorbic acid could play a role in preventing this sequence by protecting collagen from hydroxyl radicals in the presence of oxygen.[14]

In the present study, the regions in the vicinity of the annulus and along the malleus handle were the preferential sites of MyS deposits. One may speculate that this localization might be due to a higher saturation of soluble oxygen in these richly vascularized areas, which, together with the shear stresses created on the fibers by myringotomy,[26] could lead to increased production of oxygen free radicals.

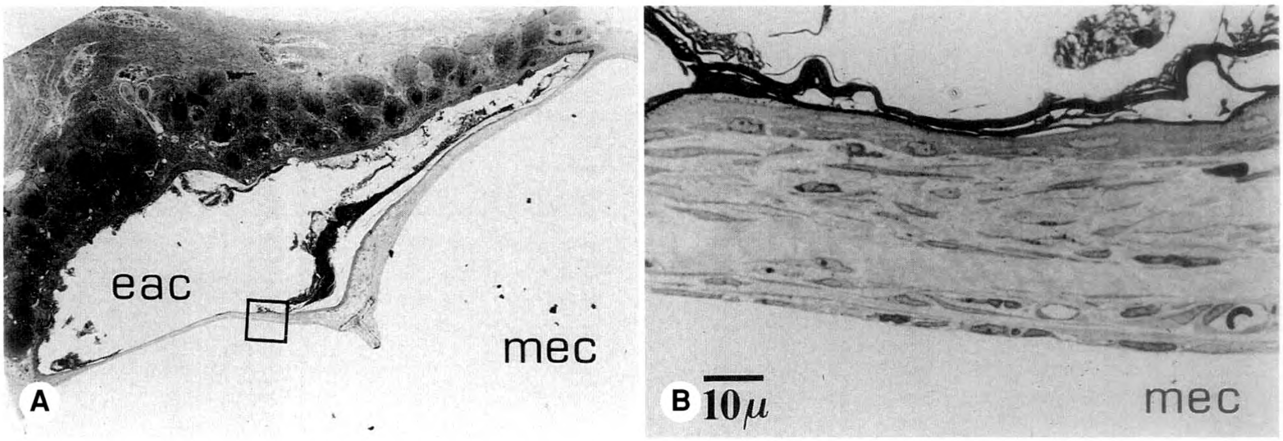

Fig 5. Light micrographs of pars tensa treated with topical application of ascorbic acid after myringotomy. **A**) Survey micrograph (toluidine blue, original ×30). **B**) Detail of boxed area in A (toluidine blue, original ×550). Note increased thickness of lamina propria and absence of sclerotic lesions.

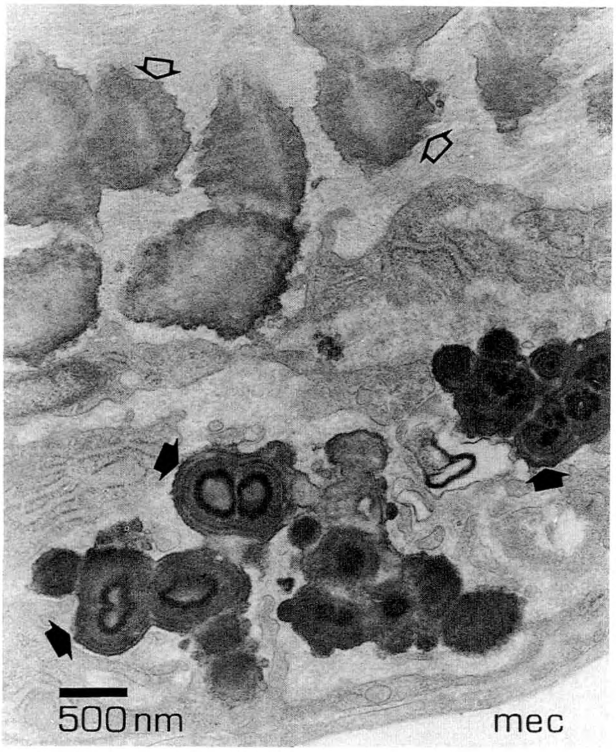

Fig 6. Electron micrograph of pars tensa from specimen treated with saline solution depicts 2 different types of myringosclerotic lesions encountered: rounded, multilamellar lesions with confluent characteristics (dark arrows) and granular, electron-dense structures with spiked surface (open arrows). mec — middle ear cavity.

During wound healing, an excess of iron ions acts negatively,[27] apparently through the activation of free radicals that interact with fibroblast cell membranes, impairing the synthesis of collagen. According to Vaxman et al,[28] reporting the healing of skin sutures in humans, the supplementation of AscA leads to a decreased iron content in the tissue and a subsequent improvement in healing. Mattsson et al[2] obtained a reduction of MyS with the iron chelator desferrioxamine. Consequently, the decrease in iron ions affecting the free radical cascade may also be another beneficial effect of AscA in the present model.

Nitric oxide promotes endothelium-dependent vasodilation. The bioactivity of this molecule is partially dependent on its interaction with superoxide. Ascorbic acid and superoxide dismutase, acting as scavengers of superoxide radicals, indirectly preserve the activity of nitric oxide.[29] Recently, the potentiation of nitric oxide synthesis in endothelial cells by the action of L-AscA was also demonstrated.[30] Both effects might be related to the enhanced vascularity observed otomicroscopically in the AscA-treated TMs compared to the saline-treated and nontreated TMs.

The noninjured anterior quadrant reacted consistently, like a mirror image of the injured side, to the various treatment methods. The decision to restrict the measurements of thickness to the nonperforated side of the TM was justified by the presence of remaining Gelfoam in the area previously perforated, creating unreliable measurements.

In the present study, the rat was used to investigate the influence of AscA on healing TM perforations. Unlike humans, rats are able to endogenously synthesize AscA. Thus, no dietary variations of the AscA content should influence the results. This allowed us to conclude that topical supplementation of AscA was responsible for the effects noted. That AscA exerts effects in nondeprived animals has been shown in rabbits kept under standard nutrition, in which an additional administration of AscA was associated with increased tensile strength of a colonic anastomosis.[10] Similarly, oral lesions in guinea pigs showed enhanced healing following daily intake of AscA above the standard requirements, in comparison to controls fed a standard, nondeprived diet.[13]

From this investigation, it is concluded that AscA strongly diminishes the occurrence of MyS in the healed TM after a myringotomy. These observations open different avenues for future studies to evaluate the possible mechanisms involved, long-term effects, and clinical applications of AscA.

ACKNOWLEDGMENTS — The skillful technical assistance of Cathrine Johansson and Ann-Louise Grehn is gratefully acknowledged. Statistical analyses were performed by Claudia Silva, Department of Epidemiology, University of Porto Medical School.

REFERENCES

1. Hellström S, Goldie P, Magnuson K, Fall C. Oxygen level influences the middle ear tissue reaction in ears with perforated tympanic membranes. In: Lim DJ, Bluestone CD, Klein JO, Nelson JD, Ogra PL, eds. Proceedings of the Fifth International Symposium on Recent Advances in Otitis Media. Toronto, Canada: Decker Periodicals, 1993:334-5.

2. Mattsson C, Marklund SL, Hellström S. Application of oxygen free radical scavengers to diminish the occurrence of myringosclerosis. Ann Otol Rhinol Laryngol 1997;106:513-8.

3. Goldschmidt MC. Reduced bactericidal activity in neutrophils from scorbutic animals and the effect of ascorbic acid on these target bacteria in vivo and in vitro. Am J Clin Nutr 1991; 54(suppl):1214S-1220S.

4. Del Rio M, Ruedas G, Medina S, Victor VM, De la Fuente M. Improvement by several antioxidants of macrophage function in vitro. Life Sci 1998;63:871-81.

5. Hallberg L, Brune M, Rossander L. The role of vitamin C in iron absorption. Int J Vitam Nutr Res Suppl 1989;30(suppl): 103S-108S.

6. Reddy VN, Giblin FJ, Lin LR, Chakrapani B. The effect of aqueous humor ascorbate on ultraviolet-B–induced DNA damage in lens epithelium. Invest Ophthalmol Vis Sci 1998;39: 344-50.

7. Block G. Epidemiologic evidence regarding vitamin C and cancer. Am J Clin Nutr 1991;54(suppl):1310S-1314S.

8. Bendich A, Machlin L, Scandurra O, Burton G, Wayner D. The antioxidant role of vitamin C. Adv Free Radic Biol Med 1986;2:419-44.

9. Halliwell B, Gutterridge J. Free radicals in biology and medicine. 2nd ed. Oxford, England: Clarendon Press, 1989:123-6.

10. Vaxman F, Chalkiadakis G, Olender S, et al. Amélioration de la cicatrisation des anastomoses coliques par une supplémentation en vitamines B5 et C: étude expérimentale chez le lapin. Ann Chir 1990;44:512-20.

11. Saika S, Uenoyama K, Hiroi K, Tanioka H, Takase K, Hikita M. Ascorbic acid phosphate ester and wound healing in rabbit corneal alkali burns: epithelial basement membrane and stroma. Graefes Arch Clin Exp Ophthalmol 1993;231:221-7.

12. Kim M, Otsuka M, Yu R, Kurata T, Arakawa N. The distribution of ascorbic acid and dehydroascorbic acid during tissue regeneration in wounded dorsal skin of guinea pigs. Int J Vitam Nutr Res 1994;64:56-9.

13. Collins CK, Lewis AE, Ringsdorf WM Jr, Cheraskin E. Effect of ascorbic acid on oral healing of guinea pigs. Int J Vitam Nutr Res 1967;37:492-5.

14. Pasquali-Ronchetti I, Quaglino D, Bergamini G. Ascorbic acid and connective tissue. In: Harris JR, ed. Subcellular biochemistry. Vol 25. New York, NY: Plenum Press, 1996:249-64.

15. Laurent C, Hellström S, Fellenius E. Hyaluronan improves the healing of experimental tympanic membrane perforations. A comparison of preparations with different rheologic properties. Arch Otolaryngol Head Neck Surg 1988;114:1435-41.

16. Fina M, Baird A, Ryan A. Direct application of fibroblast growth factor improves tympanic membrane perforation healing. Laryngoscope 1993;103:804-9.

17. Hellström S, Spandow O. Exogenous heparin, topically administered, aids the remodelling of connective tissue in the healing of experimental tympanic membrane perforations. ORL J Otorhinolaryngol Relat Spec 1994;56:45-50.

18. Yamaguchi M, Asaga H, Hasegawa S, Shimada S. Vitamin C metabolism in the tympanic membrane in chronic inflammation [in Japanese]. South Med J 1970;63(suppl):956-7.

19. Yamaguchi T. Pathology of the tympanic mucosa with chronic inflammation with reference to vitamin C metabolism [in Japanese]. Nippon Jibiinkoka Gakkai Kaiho 1972;75:905-7.

20. Olsen BR, Prockop DJ. Ferritin-conjugated antibodies used for labeling of organelles involved in the cellular synthesis and transport of procollagen. Proc Natl Acad Sci U S A 1974; 71:2033-7.

21. Kinney SE. Post-inflammatory ossicular fixation in tympanoplasty. Laryngoscope 1978;88:821-38.

22. Bhaya MH, Schachern PA, Morizono T, Paparella MM. Pathogenesis of tympanosclerosis. Otolaryngol Head Neck Surg 1993;109:413-20.

23. Hellström S, Fall C, Goldie P, Magnuson K, Spandow O. Factors influencing the development of tympanosclerosis: an experimental study. In: McCabe BF, Mogi G, eds. Immunobiology in otology, rhinology and laryngology. Amsterdam, the Netherlands: Kugler Publications, 1992:159-62.

24. Mattson C. Myringosclerosis. An experimental basis for a theory of its etiology [Dissertation]. Umeå, Sweden: Umeå University, 1997:34-51.

25. Monboisse J, Borel J. Oxidative damage to collagen. In: Emerit J, Chance B, eds. Free radicals and aging. Basel, Switzerland: Birkhauser Verlag, 1992:323-7.

26. Lesser TH, Williams KR, Skinner DW. Tympanosclerosis, grommets and shear stresses. Clin Otolaryngol 1988;13:375-80.

27. Ackerman Z, Seidenbaum M, Loewenthal E, Rubinow A. Overload of iron in the skin of patients with varicose ulcers. Possible contributing role of iron accumulation in progression of the disease. Arch Dermatol 1988;124:1376-8.

28. Vaxman F, Olender S, Lambert A, Nisand G, Grenier JF. Can the wound healing process be improved by vitamin supplementation? Experimental study on humans. Eur Surg Res 1996; 28:306-14.

29. Jackson TS, Xu A, Vita JA, Keaney JF Jr. Ascorbate prevents the interaction of superoxide and nitric oxide only at very high physiological concentrations. Circ Res 1998;83:916-22.

30. Heller R, Munscher-Paulig F, Grabner R, Till U. L-Ascorbic acid potentiates nitric oxide synthesis in endothelial cells. J Biol Chem 1999;274:8254-60.

Ann Otol Rhinol Laryngol 110:2001

IMAGING CASE STUDY OF THE MONTH

INTRACRANIAL COMPLICATIONS OF ETHMOIDITIS EVIDENCED BY MAGNETIC RESONANCE IMAGING

RÉMI MARIANOWSKI, MD, PHD
JEAN-LOUIS AÏT AMER, MD
JÉROME FORCIOLI, MD
FRANCIS BRUNELLE, MD
MURIELLE BOUHNIK, MD
YVES MANACH, MD
PARIS, FRANCE

INTRODUCTION

In children, sinusitis is usually a mild illness involving often the ethmoid sinus but sometimes also the frontal sinus. The most common complication of ethmoiditis is orbital infection, and that of frontal sinusitis is intracranial invasion, which may be life-threatening.[1,2] The clinical expression of ethmoiditis and of frontal sinusitis in children is inflammatory eyelid edema. The treatment lies in antibiotics and steroids, which may mask neurologic symptoms of intracranial invasion. Correct diagnosis and knowledge of underlying sinusitis are essential for proper patient management. Therefore, imaging techniques are highly important. Computed tomography (CT) scans have traditionally been used, but magnetic resonance imaging (MRI) is more efficient for the detection of endocranial complications of sinusitis in children.[3-5]

Ethmoiditis occurring in children over 6 years old carries a risk of frontal sinus involvement. The variability of development of the frontal sinuses is well known.[6] They begin as outpouchings of the anterior ethmoid cells at about 1 year of age, but usually cannot be radiographically distinguished until 5 or 6 years. The sinus grows vertically until 18 years of age, when the average adult volume of 6 to 7 cm^3 is obtained. The thin inner plate of the frontal sinus is almost all compact bone, while the outer plate is composed of both cancellous and compact bone.[6] Since the early initial growth of the sinus is over the inner plate, the frontal recess becomes tortuous and may be prone to obstruction in children.[2] Valveless veins extending through the bony frontal sinus wall afford direct communication from the sinus mucosa to veins in the dura mater; hence, septic thrombi can easily induce intracranial complications.[7]

CASE REPORT

On June 24, 1999, an 11-year-old boy was examined in the emergency room of our department for fever, rhinopharyngitis, and right superior eyelid edema. The symptoms had started 8 days before admission and had increased slowly since. The ophthalmological examination revealed a right chemosis and ophthalmoplegia. No exophthalmia had been noted. The peripheral white blood cell count was 12,000/mL (9,000 neutrophils), the erythrocyte sedimentation rate was 76 mm/h, and the C-reactive protein level was normal. An MRI scan showed a right orbital abscess with right pansinusitis and enhancement of the meninges (Figs 1-3). The treatment consisted of surgical drainage of the abscess (external ethmoidectomy) and intravenous antibiotic therapy (amoxicillin-clavulanate and amikacin). The frontal sinus was not irrigated after the drainage. A Gram stain from the abscess pus identified *Porphyromonas* and *Streptococcus*. The patient left our department on July 3 with a persistent right superior eyelid edema. The treatment at home consisted of oral amoxicillin-clavulanate for 15 days.

On July 29, clinical examination findings were normal, except for persistent right superior eyelid edema. A CT scan showed a slight hypodensity of the right frontal lobe, evoking cerebritis. An MRI scan showed an increased signal of the right frontal lobe without brain edema on T2-weighted images (Fig 4). The findings of angiographic MRI were normal. Intravenous antibiotic therapy was started in our department. It included ceftriaxone, metronidazole, and amikacin. After 5 days of evolution, the clinical examination findings remained identical. Intravenous steroids were added to the antibiotic therapy and continued for 5 days, and the patient left our department

---

From the Departments of Pediatric Otorhinolaryngology (Marianowski, Forcioli, Aït Amer, Manach) and Pediatric Radiology (Bouhnik, Brunelle), Hôpital Necker, Paris, France.

CORRESPONDENCE — Rémi Marianowski, MD, PhD, 11 av Franco-Russe, 75007 Paris, France.

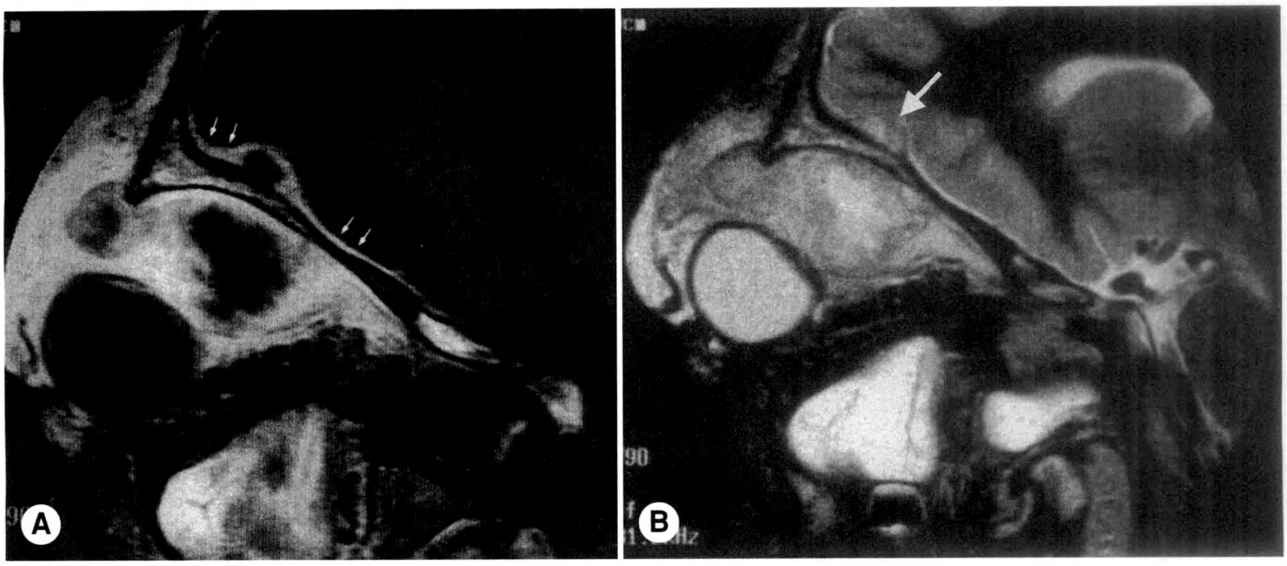

Fig 1. Sagittal magnetic resonance images show preseptal orbital abscess. **A**) T1-weighted fast spin echo image shows enhancement of frontal meninges (arrows) without contrast injection. **B**) T2-weighted image shows localized cortical edema (arrow).

on August 10. He completed a 10-day course of oral steroids and amoxicillin-clavulanate at home. No anticoagulation treatment was ordered. On September 13, the findings of clinical examination and MRI were normal.

DISCUSSION

Although the usual management of ethmoiditis does not include imaging procedures, it might be important to use such procedures when the frontal sinuses are involved. Much attention should be paid to the age of the child and whether a frontal sinus already exists. This case confirms that MRI is a useful tool in the detection of endocranial complications of sinusitis in children. Precise determination of the sinusitis site and its relationship to adjacent structures is essential, since it influences the therapeutic strategy. Septic thrombosis of the frontal cortical veins was presumed to be the cause of our radiologic findings.

The frontal sinus is located in a supraorbital position by the age of 4 years, but is not radiographically distinguishable from the ethmoid sinus until 5 to 6 years of age. It grows progressively for another 8 to 10 years before reaching full adult size.[8] The vascular supply of the frontal sinus originates in the dura mater for the inner table, in the periorbita for the orbital plate, and in the cranial periosteum for the outer table. Venous mucosal drainage occurs through the diploic veins extending through the bony sinus wall.[9] The extensive nature of this diploic venous system affords direct communication from the sinus mucosa to the marrow spaces of the frontal bone, to veins in

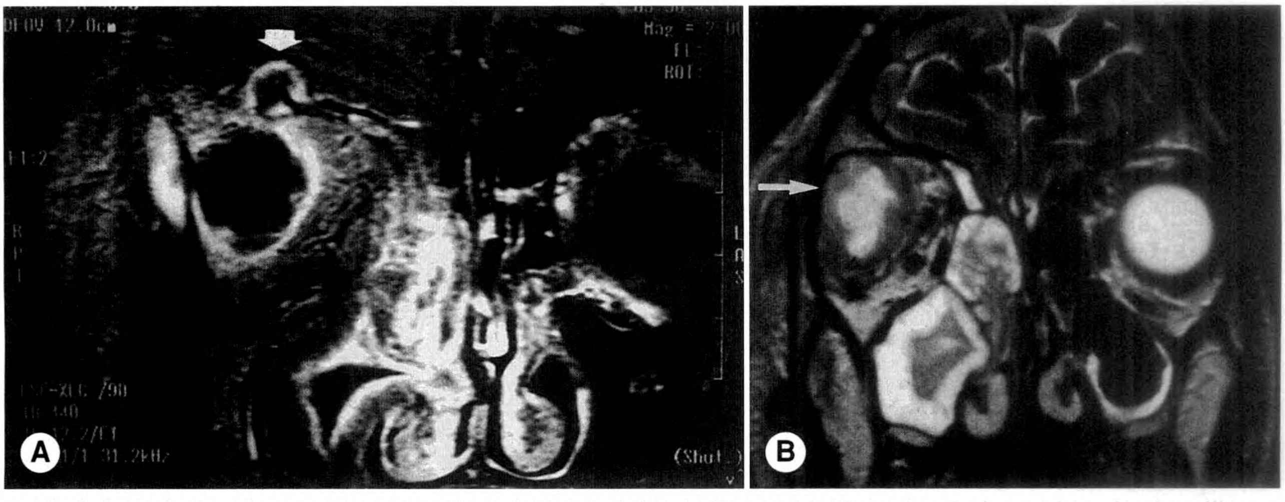

Fig 2. Frontal magnetic resonance images show right ethmoiditis. **A**) T1-weighted fast spin echo image shows local swelling of cortex of right frontal lobe (arrow). **B**) T2-weighted image shows orbital abscess (arrow). Note thickening of mucosa of right maxillary sinus.

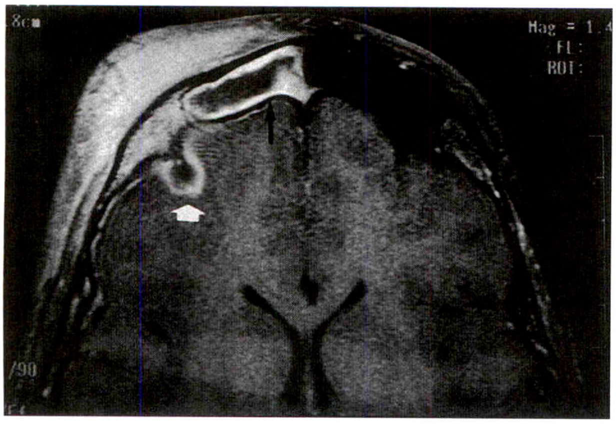

Fig 3. T1 fast spin echo axial magnetic resonance image shows right frontal sinusitis (black arrow) with local swelling of cortex of right frontal lobe (white arrow) and edema of soft tissues of upper eyelid.

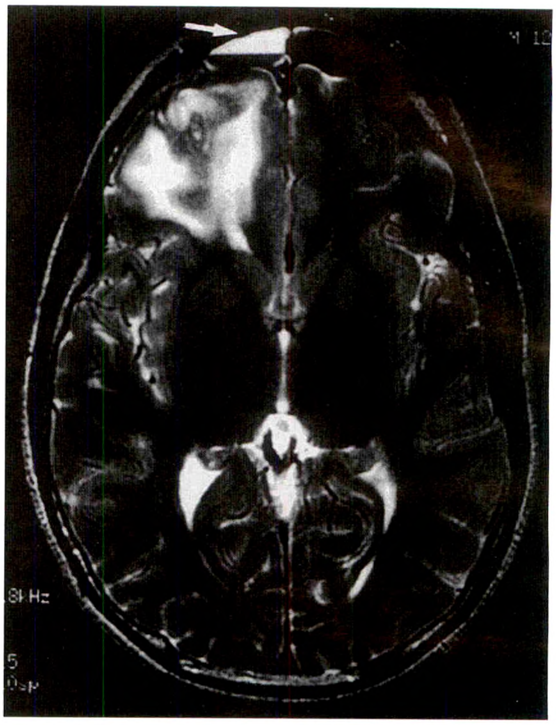

Fig 4. T2 axial magnetic resonance image shows cerebritis extending to whole right frontal lobe without brain edema, with fluid remaining in right frontal sinus (arrow).

the dura mater, to the superior sagittal sinus, and through the cortical veins to distant parts of the skull and cerebrum.[10] The lack of valves within these diploic veins allows for blood flow in any direction and accounts for the propagation of septic thrombi from the vessels of the mucosa to bone, dura, and brain. The dura mater acts as a barrier to bacterial invasion, being relatively impermeable to infecting agents.[9] This barrier effect explains the rarity of bacterial meningitis complicating frontal sinusitis. The frontal lobes are typically a neurologically silent area, and abscess formation may not produce any focal signs.

Orbital complications are most often due to ethmoid sinusitis, but frontal sinusitis may progress to the development of subperiosteal and/or orbital abscesses.[1,11] A series of 6 children with orbital abscesses has been presented.[12] Those with frontal sinusitis developed abscesses in the superolateral location, as shown here. In addition to thrombophlebitis and septic microemboli, it was suggested that direct extension through congenital bony dehiscences posterior to the trochlear fossa at the supraorbital notch and at the junction of the middle and outer thirds of the frontal sinus floor, would explain the preponderance in this location.[12]

The most common symptoms of frontal sinusitis are headaches, rhinitis, local tenderness, and pressure sensations. Nasal obstruction, fever, and fatigue are less common. Patients with intracranial complications present mostly headache and fever, but these signs are not specific.[7] When patients with sinusitis are assessed to exclude intracranial complications, the signs sought are nuchal rigidity, localizing neurologic signs, and alteration of consciousness. If these are absent, it is assumed that the patient does not have an intracranial lesion. This is not necessarily true. Cerebritis may occur in children without the classic signs and symptoms referable to an intracranial lesion.[13]

For unknown reasons, intracranial complications of frontal sinusitis have been predominantly described in male patients, with a peak in the second and third decades.[14] In a retrospective study of intracranial infections secondary to paranasal sinusitis occurring over a 12-year period, the median age was 14 years, with 89% of patients over 9 years, and 78% of the patients were male.[14] In our case, the persistence of eyelid edema in an adolescent male patient was a sign of high importance, prompting us to look for intracranial infection.

A routine CT scan may be an inadequate initial study in patients with intracranial sepsis associated with sinusitis. It has been recommended that contiguous 10-mm-thick semiaxial slices through the cranium should be imaged before and after administration of intravenous contrast medium and followed by thin axial slices (3 to 5 mm) through the frontal and ethmoid sinuses. These should be viewed with a bone window (minimum window width, 3,000 Hounsfield units) to demonstrate the presence and full extent of sinus disease.[15] Subdural empyemas are seen without intravenous contrast enhancement, but contrast medium is necessary for outlining small epidural abscesses and for differentiating cerebritis from brain abscesses. A nonenhancing hypodense area suggesting cerebritis can evolve into a ring-enhancing lesion with surrounding edema. Infection in the sinuses is more likely to extend intracranially along the valveless diploic veins. Thrombophlebitis that occurs in small cortical veins is difficult to diagnose. It may cause necrosis and is a common precursor of brain abscess.[10,16] Intracranial complications include meningitis, epidural or subdural empyema, cerebral empyema, and cavernous sinus thrombosis. Subdural empyema has been considered to be the most frequent intracranial complication of sinusitis.[17-19] However, frontal lobe abscess was suggested as the most frequent by a combined institutional review.[7]

A CT scan may not be the radiologic study of choice for the diagnosis of sinusitis and its complications. An MRI scan is more sensitive in delineating the extent of cerebral edema and inflammation associated with the infectious process. Use of MRI has been proved useful in distinguishing malignant tissue from inflammatory disease.[20] It can also distinguish intrasinus hemorrhage and fungal sinusitis from other causes of sinus opacification more accurately than CT.[21,22] Routine MRI images of the head performed because of suspected intracranial disease are usually obtained in the axial plane and therefore include views of all 4 sinuses. Normal sinus mucosa is very thin and is beyond the spatial resolution of MRI. The majority of infections and chronic inflammatory diseases of the sinuses have bright signal intensities on T2-weighted images, caused by increased water content. Fungal masses in allergic fungal sinusitis represent an exception, since they show no or little resonance on T2-weighted images.[22] The MRI appearance of inflammatory processes on T1-weighted images is more variable and is related to protein content. Serous secretions yield low signal intensities that rise as the percentage of proteinaceous material in the fluid increases.[20] Neither air nor cortical bone produces a signal on any MRI sequence.

Intracranial complications may occur in sinusitis involving the frontal sinuses in young children without clinical neurologic signs. Magnetic resonance imaging is more sensitive than CT in diagnosing intracranial sepsis at an early point in its development and should therefore be used in the first place.

REFERENCES

1. Wald ER, Pang D, Milmoe GJ, Schramm VL Jr. Sinusitis and its complications in the pediatric patient. Pediatr Clin North Am 1981;28:777-96.

2. Wenig BL, Goldstein MN, Abramson AL. Frontal sinusitis and its intracranial complications. Int J Pediatr Otorhinolaryngol 1983;5:285-302.

3. Rosenblum ML, Hoff JT, Norman D, Weinstein PR, Pitts L. Decreased mortality from brain abscesses since advent of computerized tomography. J Neurosurg 1978;49:658-68.

4. Whelan MA, Hilal SK. Computed tomography as a guide in the diagnosis and follow-up of brain abscesses. Radiology 1980;135:663-71.

5. Lloyd GA, Lund VJ, Phelps PD, Howard DJ. Magnetic resonance imaging in the evaluation of nose and paranasal sinus disease. Br J Radiol 1987;60:957-68.

6. Fairbanks DNF. Embryology and anatomy. In: Bluestone CD, Stool SE, eds. Pediatric otolaryngology. Vol 1. Philadelphia, Pa: WB Saunders, 1990:647-78.

7. Clayman GL, Adams GL, Paugh DR, Koopmann CF Jr. Intracranial complications of paranasal sinusitis: a combined institutional review. Laryngoscope 1991;101:234-9.

8. Sadler TW. Langman's medical embryology. 6th ed. Baltimore, Md: Williams & Wilkins, 1990.

9. Patrick CC, Kaplan SL. Current conception in the pathogenesis and management of brain abscesses in children. Pediatr Clin North Am 1988;35:625-36.

10. Remmler D, Boles R. Intracranial complications of frontal sinusitis. Laryngoscope 1980;90:1814-24.

11. Arjmand EM, Lusk RP, Muntz HR. Pediatric sinusitis and subperiosteal orbital abscess formation: diagnosis and treatment. Otolaryngol Head Neck Surg 1993;109:886-94.

12. Garcia CE, Cunningham MJ, Clary RA, Joseph MP. The etiologic role of frontal sinusitis in pediatric orbital abscesses. Am J Otolaryngol 1993;14:449-52.

13. Johnson DL, Markle BM, Wiedermann BL, Hanahan L. Treatment of intracranial abscesses associated with sinusitis in children and adolescents. J Pediatr 1988;113:15-23.

14. Rosenfeld EA, Rowley AH. Infectious intracranial complications of sinusitis, other than meningitis in children: 12-year review. Clin Infect Dis 1994;18:750-4.

15. Saxton VJ, Boldt DW, Shield LK. Sinusitis and intracranial sepsis: the CT imaging and clinical presentation. Pediatr Radiol 1995;25(suppl 1):S212-S217.

16. Dolan RW, Chowdhury K. Diagnosis and treatment of intracranial complications of paranasal sinus infections. J Oral Maxillofac Surg 1995;53:1080-7.

17. Jones RL, Violaris NS, Chavda SV, Pahor AL. Intracranial complications of sinusitis: the need for aggressive management. J Laryngol Otol 1995;109:1061-2.

18. Courville CB. Subdural empyema secondary to purulent frontal sinusitis: a clinicopathologic study of forty-two cases verified at autopsy. Arch Otolaryngol 1944;39:211-30.

19. Singh B, Van Dellen J, Ramjettan S, Maharaj TJ. Sinogenic intracranial complications. J Laryngol Otol 1995;109:945-50.

20. Som PM, Shapiro MD, Biller HF, Sasaki C, Lawson W. Sinonasal tumors and inflammatory tissues: differentiation with MR imaging. Radiology 1988;167:803-8.

21. Som PM, Shugar JM, Troy KM, Sacher M, Stollman AL. The use of magnetic resonance and computed tomography in the management of a patient with intrasinus hemorrhage. Arch Otolaryngol Head Neck Surg 1988;114:200-2.

22. Zinreich SJ, Kennedy DW, Malat J, et al. Fungal sinusitis: diagnosis with CT and MR imaging. Radiology 1988;169:439-44.

SOFTWARE REVIEW

EXPERIENCE WITH STATVIEW 5.0

Company: SAS Institute Inc, SAS Campus Dr, Cary NC 27513; www.statview.com.

Hardware requirements: Operating systems: Microsoft Windows 3X, Windows 95, or Windows NT. Minimum RAM, 8 Mb for Windows 3X or 95, and 12 Mb for Windows NT. Hard disk space required, 18 Mb. Macintosh and Power Macintosh, minimum CPU, any Macintosh or Power Macintosh, 68040 or better recommended. Minimum system version, 7.1. Minimum RAM, 4 Mb free (11 Mb for Power Macintosh with Virtual Memory turned off).

The choice of platforms and software data analysis involves considerations of computational power, graphic display, ease of transfer to other platforms and applications, and ease of use.[1,2] Research involving large sets of data used to be labor-intensive.[3] We use the personal computer for most of our scientific work, not only for data management and graphics, but also for statistical analysis. There are many computer programs, but very few stand out as truly useful, time-saving, and work-enhancing. One of them is StatView. StatView software is designed for scientific and medical researchers, analysts, and anyone who needs to analyze data and present their results.[4-6] The functions and the use of the software package StatView for Windows are described here.

StatView may be installed from a CD. It comes with 2 manuals, *Using StatView* and *StatView Reference*. Both manuals are well written.

A good way to get started with StatView is by going through the tutorial, which takes about 1 to 2 hours. There are several places to look for help. The help menu gives general advice and instructions for several tasks. The manuals provide more detailed instructions and also a useful introduction to the statistical analyses. When a data set is opened, it appears as a spreadsheet in the Data Set Window. An attributes pane may be opened at the top of the data window. One enters data into the databases through an edit window, tabbing from field to field as one provides the required information. Scrolling down the pane reveals summary statistics of the columns, which are automatically updated. This is very impor-

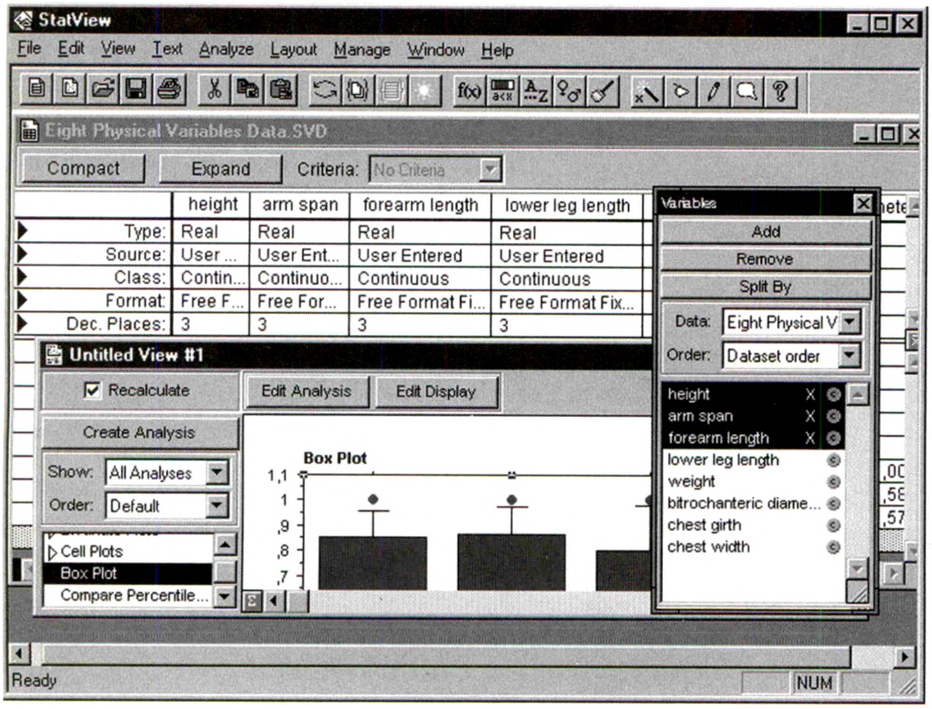

Criteria: No Criteria

	height	arm span	forearm length	lower leg length
Type:	Real	Real	Real	Real
Source:	User ...	User Ent...	User Entered	User Entered
Class:	Contin...	Continuo...	Continuous	Continuous
Format:	Free F...	Free For...	Free Format Fi...	Free Format Fix...
Dec. Places:	3	3	3	3

☑ Recalculate

Show: All Analyses

Order: Default

Data: Eight Physical V

Order: Dataset order

Display of study data in Data Set Window and Analysis Browser.

tant when checking the data quality.

When a view window is opened, the Analysis Browser appears that lists the analytical methods and graphs. Summary statistics shown in the spreadsheet update automatically whenever the data change (see Figure).

StatView can import plain text or Excel files along with SAS Transport and SAS data set files. One can also enter data into the databases through an edit window, tabbing from field to field to provide the required information. There are fields for classes (nominal or continuous variables), analysis stage, and decimal places.

The functions available in StatView include comprehensive statistics (descriptive statistics, frequency distribution, percentiles, *t*-tests, confidence intervals, variance tests, correlation and covariance, regression, ANOVA, cross-tabulation tables), survival analysis (nonparametric methods, regression models), quality control (subgroup measurement, individual measurement, Pareto analysis), and presentation graphics.

When requesting descriptive statistics, the user may select "basic" or "complete," which give exactly what the words imply. Percentiles and frequency tables are available as separate analysis options. The ANOVA button of the Analysis Browser offers univariate and multivariate analyses of 1-way and factorial designs, as well as analyses of repeated measures designs. As displays, StatView offers summary statistics and interaction bar or line charts. The Regression button allows the user to select an ANOVA table, a regression summary table, or a table of regression coefficients. Various regression plots and diagnostics may be added and residuals or fitted values may be saved as new variables in the data set.

StatView offers a variety of graphs for displaying categorical and continuous variables.

StatView has an incredibly intuitive interface. Analyses, variables, and results all appear in "browsers" that sit on the desktop. There are no commands or scripts to memorize. With built-in hints and a complete Windows help system, help is only a click away.

StatView is a clear and clean program. It is relatively easy to use. Altogether, StatView provides an excellent combination of features and ease of use. It is an excellent program. A word of caution, however, is needed. The aforementioned features may induce inappropriate use of statistics and thus may result in false conclusions.[1,2] Therefore, a qualified statistician is indispensable for advice on the choice of appropriate tests and complex statistical analyses.

MICHAEL REISS, MD
GILFE REISS, MD
Dept of Ear, Nose and Throat
Klinikum Görlitz
James von Moltkestrasse 52
D-02827 Görlitz
Germany

REFERENCES

1. Siegrist RB Jr. Knowledge is power: comparative analysis software is a powerful tool for healthcare. Ambul Outreach 1998(spring):25-6.

2. Weitzman EA. Analyzing qualitative data with computer software. Health Serv Res 1999;34(suppl):1241-63.

3. Wright TL, Takahashi TJ. Hawaii Bibliographic Database. Bull Volcanol 1998;59:276-80.

4. Goldfarb M. Two-dimensional electrophoresis and computer imaging: quantitation of human milk casein. Electrophoresis 1999;20:870-4.

5. Parker LP, Parker JR, Bodurka-Bevers D, et al. Paget's disease of the vulva: pathology, pattern of involvement, and prognosis. Gynecol Oncol 2000;77:183-9.

6. Bermingham M, Brock K, Tran D, Yau J, Tran-Dinh H. Smoking and lipid cardiovascular risk factors in Vietnamese refugees in Australia. Prev Med 1999;28:378-85.

BOOK REVIEWS

Surgical Solutions for Conductive Hearing Loss

Mirko Tos. Hard cover, illustrated, indexed, 269 pages, 2000. Thieme, Stuttgart, Germany, $149.

Purpose: Described and discussed in detail are surgical solutions for a conductive hearing loss due to ossicular fixation.

Contents: The book contains 4 sections: tympanosclerosis and postinflammatory, posttraumatic, and postoperative bony fixations of the ossicular chain. Three sections concern otosclerosis (13 chapters) and congenital ossicular fixations and defects, along with classifications and embryology (3 chapters).

Attributes and Limitations: All aspects of fixation of the tympanic membrane and ossicular chain are discussed. Although tympanic membrane fixation by tympanosclerosis is rare, Dr Tos deals with the pathogenesis and pathology of all surgical methods used for myringosclerosis. Surgery of tympanosclerotic stapes fixation may be treated with stapes mobilization after removal of the plaques. Stapedectomy is more commonly recommended when there is a defective or absent malleus and incus. Statistics on mobilization results for such cases would be of benefit.

The preferred treatment for malleus head fixation is an extensive atticotomy with removal, of course, of the lesion and leaving the ossicular chain intact. The defect is then treated with cartilage reconstruction. Dr Tos prefers this method, rather than the bypass ossicular chain technique.

In the section on otosclerosis, the author has chosen to give a review of almost every author from the literature and diagrammatically shows their techniques. This portion is an excellent historical review of past techniques and complications. Perhaps every prosthesis that has ever been manufactured is shown diagrammatically. Dr Tos himself, at the present time, recommends stapedectomy and gives excellent reasons for his arguments in favor of this method.

There are excellent reviews throughout the book of various classifications according to the condition or anomaly of the ear, and the review in the last part, on minor congenital malformations, is very worthy. Dr Tos recommends surgery at no younger than 10 years of age, because of concern for middle ear infection. Patients with congenital ankylosis tend to have maximum conductive hearing loss and typically are identified early in life and should have amplification with hearing aids. As one who deals with such cases, I disagree with that age (10 years), feeling that it is late, and would rather the patient have normal natural hearing through surgery before school begins at age 6.

Applicability: Certainly, everyone who practices otology should have this volume, in that it well summarizes various and conclusive surgical solutions for conductive hearing loss. To make it easier for the reader, Dr Tos could consider omitting some of the descriptions throughout the book and some of the repetition (though not great), to form an atlas. He has a good start for such a book through the 576 illustrations.

Dennis G. Pappas, MD
Birmingham, Alabama

Teaching Atlas of Head and Neck Imaging

Robert Lufkin, Alexandra Borges, and Pablo Villablanca. Hard cover, illustrated, indexed, 470 pages, 2000. Thieme, New York, NY, $99.

Purpose: Crafted to be a casebook, this was written by radiologists and geared to give the radiologist a more thorough knowledge of head and neck pathology. The authors feel there is a need for this, since they see patients referred for head and neck imaging who have not been previously evaluated in this area. This is a result of modern medical care, in which workup of patients has been streamlined through a number of mechanisms that have ultimately resulted in less access to medical resources and expertise. In essence, patients have only a limited clinical workup. Patients are being sent directly to a radiology department for examination and triage. Thus, the radiologist must have a more thorough knowledge of the head and neck and the conditions thereof. All aspects of the head and neck are covered in the book. Within each section there are radiographic studies followed by radiographic findings, differential diagnoses, and discussion, which is broken down into features such as epidemiology, pathophysiology, clinical findings, imaging findings, and management. Highlighted are pearls and pitfalls. Suggested readings are included.

Attributes and Limitations: Reading case studies like those presented in this text is somewhat stimulating, compared to a textbook on radiology, which tends to put one to sleep. The authors have reviewed current information on the mechanisms and preferred treatment of the disorders, all of which are otolaryngological. They give accurate descriptions in their presentations. Although the radiographic prints are readable, they could have been better in quality.

Applicability: The book provides pertinent and applicable material for clinicians of the otolaryngology–head and neck specialties, as well as radiologists.

Dennis G. Pappas, MD
Birmingham, Alabama

ANNALS SUPPLEMENTS

Still-in-Stock — Quantities Limited — Order Now!

Supplement 177 (April 1999)
Clinical Results with the CLARION® Multi-Strategy™ Cochlear Implant
Price $23.00 (128 pages; Osberger & Koch)

Supplement 179 (Sept 1999)
Universal Modular Glottiscope System: The Evolution of a Century of Design and Technique for Direct Laryngoscopy
Price $6.50 (24 pages; Zeitels)

Supplement 180 (Nov 1999)
Laser Surgery for Allergic and Hypertrophic Rhinitis
Price $8.50 (20 pages; Inouye et al)

Supplement 181 (May 2000)
Temporal Bone Studies of the Human Peripheral Vestibular System
Price $9.50 (32 pages; Merchant et al)

Supplement 182 (May 2000)
Medical Management of Acute Bacterial Sinusitis
Price $6.50 (20 pages; Brook et al)

Supplement 183 (August 2000)
Controversies in the Medical Management of Persistent and Recurrent Acute Otitis Media. Recommendations of a Clinical Advisory Committee
Price $4.00 (12 pages; Pichichero et al)

Supplement 184 (October 2000)
24-Hour Ambulatory pH Monitoring for Patients With Suspected Extraesophageal Complications of Gastroesophageal Reflux: Indications and Interpretations
Price $7.50 (28 pages; Sasaki & Toohill, eds)

Supplement 185 (December 2000)
Seventh Symposium on Cochlear Implants in Children
Price $21.00 (128 pages; Gantz, Tyler, & Rubinstein, eds)

Supplement 186 (May 2001)
Analysis of the Suprabullar and Retrobullar Recesses for Endoscopic Sinus Surgery
Price $7.50 (16 pages; Bolger & Mawn)

Supplements Desired: # ________ ________ ________ ________ ________

Send to: ______________________________
____
____
____

Order from:

Annals Publishing Company
4507 Laclede Avenue
St Louis, MO 63108

Payment must be enclosed with order.
Checks (US funds only),Mastercard,
Visa, or American Express

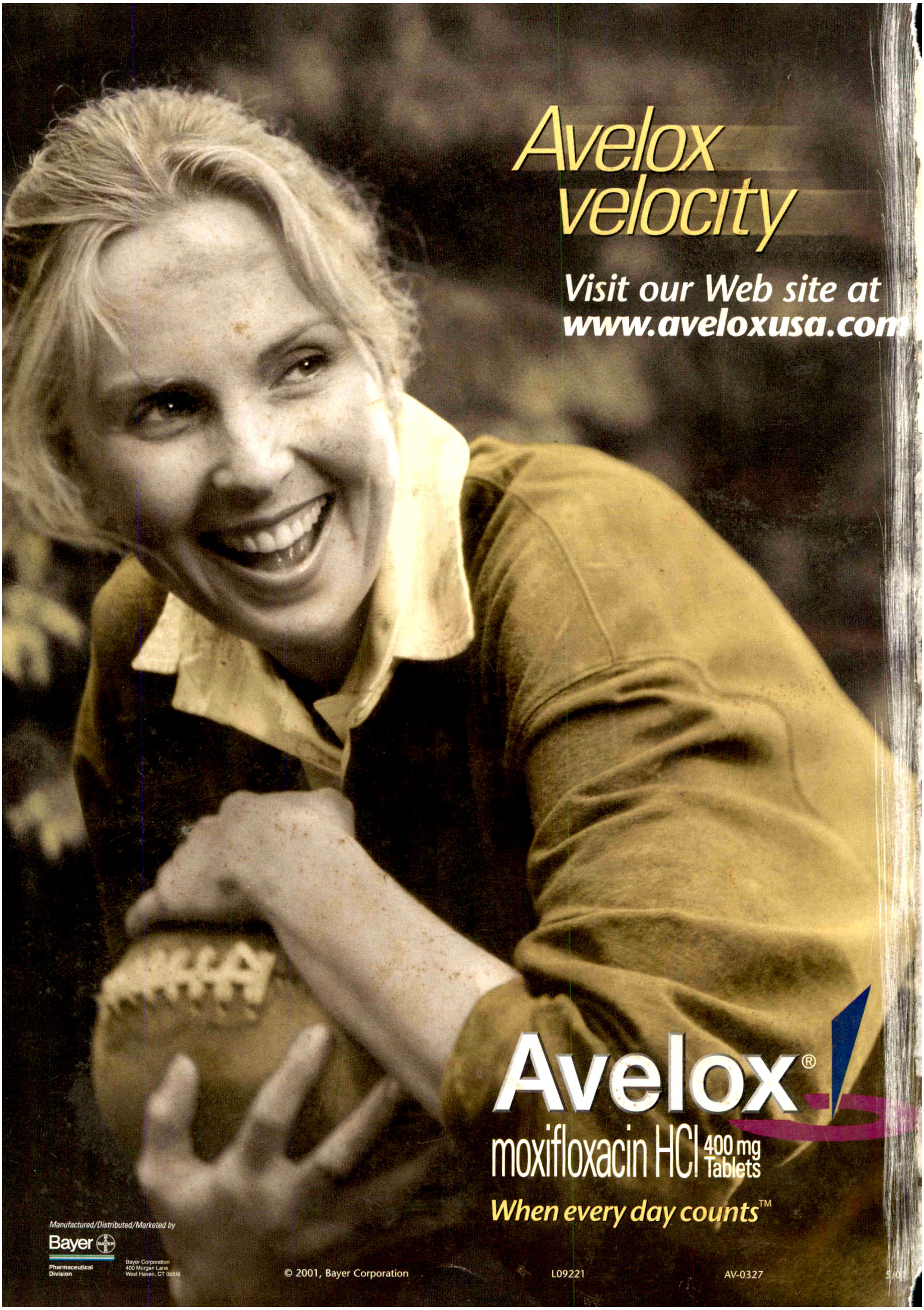

Avelox velocity

Visit our Web site at
www.aveloxusa.com

Avelox®
moxifloxacin HCl 400 mg Tablets

When every day counts™

Manufactured/Distributed/Marketed by
Bayer
Pharmaceutical Division

Bayer Corporation
400 Morgan Lane
West Haven, CT 06516

© 2001, Bayer Corporation L09221 AV-0327 5/0